International Baltic Earth Secretariat Publication No. 13, June 2018

2nd Baltic Earth Conference

The Baltic Sea in Transition

Helsingør, Denmark, 11 to 15 June 2018

Conference Proceedings

Edited by
Silke Köppen and
Marcus Reckermann

Danmarks Meteorologiske Institut

Baltic Earth
Earth System Science for the Baltic Sea Region

Impressum

International Baltic Earth Secretariat Publications
ISSN 2198-4247

International Baltic Earth Secretariat
Helmholtz-Zentrum Geesthacht GmbH
Max-Planck-Str. 1
D-21502 Geesthacht, Germany

www.baltic.earth
balticearth@hzg.de

Front page photo: Kronborg Castle, Helsingør, Denmark
(Marcus Reckermann)

Conference Organizers and Sponsors

Danish Meteorological Institute
Denmark

Helmholtz-Zentrum Geesthacht
Germany

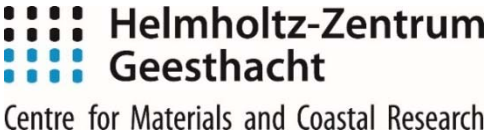

Leibniz Institute for Baltic Sea Research Warnemünde
Germany

Uppsala University
Sweden

Swedish Meteorological and Hydrological Institute
Sweden

Merge
Modelling the Regional and Global Earth System
A joint initiative of Lund University, University of Gothenburg, Rossby Centre/SMHI, Linnaeus University, Chalmers University of Technology and Royal Institute of Technology

Conference Committee

Juris Aigars, Latvia
Franz Berger, Germany
Inga Dailidienė, Lithuania
Irina Danilovich, Belarus
Matthias Gröger, Sweden
Jari Haapala, Finland
Karol Kulinski, Poland
Andreas Lehmann, Germany
H. E. Markus Meier, Germany (Chair)
Kai Myrberg, Finland
Piia Post, Estonia
Marcus Reckermann, Germany
Gregor Rehder, Germany
Anna Rutgersson, Sweden
Corinna Schrum, Germany
Benjamin Smith, Sweden
Tarmo Soomere, Estonia
Martin Stendel, Denmark
Ralf Weisse, Germany
Sergey Zhuravlev, Russia

Organisation Committee

Martin Stendel, Denmark
Silke Köppen, Germany
H. E. Markus Meier, Germany
Marcus Reckermann, Germany

Acknowledgments

We thank our local partner institution Danish Meteorological Institution (DMI), for co-organizing this conference. We would like to specifically thank Martin Stendel of DMI for a dedicated and efficient collaboration in preparing the conference, and Silke Köppen of the International Baltic Earth Secretariat at Helmholtz-Zentrum Geesthacht for putting together this abstract volume and the programme booklet, next to taking care of the hundreds of other things necessary to make this concerence a success. Moreover, we would like to thank Gitte Winberg of Konventum in helping with the local organization, and Sabine Billerbeck and Sabine Hartmann for helping during the conference.

Preface

The scope of this second Baltic Earth Conference is “The Baltic Sea region in transition”. This refers to the geographical location of the conference, as Helsingør is located in the transitional waters between the North Sea and the Baltic Sea, but the title of the conference also refers to the environmental changes, which currently take place in the region, due to climate change and other anthropogenic pressures. Consequently, a major focus for Baltic Earth research in the coming years will be on the impact of multiple drivers of Earth system changes in the region, to estimate and describe the various individual pressures, and assess their dependencies and interrelations.

Baltic Earth has existed now for 5 years. What have we achieved? We could name the numerous workshops, outreach events, summer schools and conferences, as well as research projects and publications, which Baltic Earth has initiated or organized together with partner institutions in the region, and which are available at the Baltic Earth website. An envisaged initiative for the next future is the production of dedicated assessment reports on the Grand Challenges, including climate change and its impacts as overarching topic.

The sessions of this conference reflect the Baltic Earth Grand Challenges and topics:

- Salinity dynamics
- Land-Sea-Atmosphere biogeochemical linkages
- Natural hazards and high impact events
- Sea level dynamics, coastal morphology and erosion
- Regional variability of water and energy exchanges
- Multiple and interrelated drivers of environmental changes
- Regional climate system modeling

130 participants from 14 countries have registered for this second Baltic Earth conference, among them also countries outside the Baltic Sea region, and 126 presentations will be given (65 orals, 61 posters). We are happy to be able to avoid parallel sessions, allowing for a true interdisciplinary exchange between scientists. This has been the principle from the very beginning of the BALTEX era. As usual, no discrimination is made in this volume regarding poster or oral presentation; they are all sorted alphabetically within topics.

We sincerely hope that this conference will be a fruitful and joyful experience for all participants, and that it may foster the international and interdisciplinary scientific exchange in the Baltic Sea region.

Markus Meier and Marcus Reckermann

On behalf of the Conference Committee and the Baltic Earth Science Steering Group

Contents

Contributions are sorted alphabetically within topics.

Keynotes and special talks

Topic A: Salinity dynamics

Topic B:
Land-sea-atmosphere biogeochemical feedbacks

Topic C:
Natural hazards and high impact events

Topic D:
Sea level dynamics, coastal morphology and erosion

Topic E:
Regional variability of water and energy exchanges

Topic F:
Multiple drivers of regional Earth system changes

Topic G:
Regional climate system modeling

Keynotes

and Special Presentations

Baltic Earth Research: Challenges in the international context

Ulrich Bathmann[1]

[1] Leibniz Institute for Baltic Sea Research Warnemünde, Germany, Leibniz-IOW (ulrich.bathmann@io-warnemuende.de)

1. International Context in the Baltic

International research has a sound tradition in the Baltic. The international Baltic Year 1969/70, the experiments BOSEX 77, PEX-86 and SKAGEX-90/91 (1,2) are examples of joint scientific activities across strong political boundaries. Similarly, the congresses of the Baltic Oceanographers, (CBO), the Baltic marine biologists (BMB) and the Baltic geoscientists (BSG) emerged and now form the three pillars of the regular meetings of the Baltic Sea Science Congress (BSSC) since 1996 serving as a discussion forum by bridging disciplinary and political borders. On the scientific-political level, and especially since the HELCOM agreements in 1974 and 1992 (3) the Baltic nations agreed on political actions and implemented the Baltic Sea Action Plan 2007 (4) towards the vision of a healthy Baltic Sea environment till 2021. This was included in the European Marine Strategy Framework Directive 2008. Thus, sciences in Baltic from early on strongly communicated to politics.

Baltic research also linked to global science programs also. BALTEX (the Baltic Sea Experiment) was a Regional Hydroclimate Project (RHP) within the Global Energy and Water Exchanges Project (GEWEX) of the World Climate Research Program (WCRP) since 1993. BALTEX converted to Baltic Earth and extended its scientific scope beyond physical disciplines. Other international programs like IODP, BIODIVERSITAS and Census of Marine Life, had components in the Baltic Sea. Also, citizen science activities like the Ocean Sampling Day were quite successful.

2. Recent global (and national) science programs

The Intergovernmental Panel on Climate Change (5) founded 1988 has recently published its 5th report, stating that "Human influence on the climate system is clear, and recent anthropogenic emissions of green-house gases are the highest in history. … Effective adaptation and mitigation responses will depend on policies and measures across multiple scales: international, regional, national and sub-national." The follow-up COP 21 Paris Climate Summit clearly addressed the 1.5°C goal to ensure a tolerable climate development on Earth, similar to what we now experience (6). IPCC started the 6th report assessment cycle in 2016 to be finalized in 2022. Unfortunately, these findings and agreements are now emotionally questioned leaving aside scientific evidence. Nonetheless the community of world nations has adapted the Sustainable Development Goals (SDG´s) with the specific mentioning "Our Ocean, Our Future: Call for Action" by the UN General Assembly on 6 July 2017 resulting in the 2030 Agenda for Sustainable Development. In concert, the international activity "Future Earth" emerged in 2012 (7). Future Earth is a 10-year international research program which aims to build knowledge about the environmental and human aspects of Global change, and to find solutions for sustainable development (8). It aims to increase the impact of scientific research on sustainable development. It operates with >20 national and regional sub-groups.

In Europe, the EU HELCOM Ministerial Declaration 2018 agreed upon a continuation with a 2030 Agenda (9). As we speak, the EU is setting up its Framework Program 9 (FP9) by defining very precise missions. We might expect future EU calls for proposals to achieve such missions.

Also, nationally science and politics accompany such international developments. The German government as one example has published its MARE:N program (10) including and coordinating activities of four ministries. German marine and climate science is well prepared to react on such new challenges, as we operate two national coordination activities, the German Climate Consortium (DKK) and the Consortium German Marine Research (KDM, (11)) involving 19 scientific institutions (universities, Helmholtz, Leibnitz, Max Planck, federal research units, museums). As we speak, the new German Alliance of Marine Research emerges, combining beyond institutions and with additional financial support the largest marine activities in Germany. All these national activities rely on international cooperation.

3. Challenges for Baltic Earth Research

Baltic Earth research furthermost needs to be at the international forefront of science. In addition, it will be judged upon in the international context, but also faces the challenge to approach regional and national authorities, thus, it need to cover applied aspects on top of basic science. A logic strategy would be to applying the system approach, i.e. bridging disciplinary views by transdisciplinary work on the identified scientific challenges. One example is to present regional climate models nested in global circulation models and link these to the IPCC frame (12). Such an exercise could include biological processes as well as feedback mechanisms to human activities. Naturally, the consideration of reactions and interactions of the ocean (i.e. Baltic Sea system) to activities in the "Hinterland" e.g. in agriculture, urbanization, tourism, industrialization and pollution would be very valuable. Data accessibility, data management, secure and open data repositories, and user-customized science products should also be included. Such approaches are not entirely new, but not available at the moment in the needed complexity.

Another challenge is to relate the relevance of "Baltic" research questions to problems occurring world-wide (eutrophication, Mega-Cities, marine pollution, changes in biodiversity, industrialization).

The outreach activities of Baltic Earth will further need to include the information transfer to political levels like the Baltic Parliamentarians, e.g. with scientific sessions during their regular political meetings. In this line of thinking, scientists will need to more jointly work with international, national and regional authorities (UNESCO, IOC, BSH). Especially the next generation of scientist should be exposed to all these aspects, to provide the option for placing their specific scientific interest in a broader context.

Last but not least it would be wise to expose taxpayers i.e. the civil society much more intense to the world of science. Providing Baltic museums with current research information, promoting new media information and stimulate citizen science projects where appropriate would be easy tasks to fulfill. Why not adapting the BBC “Blue Planet” series to the Baltic, e.g. as “The Baltic Sea Heritage: 12.000 years of history guiding Europe´s future”?

Now we face the task to teach the next generation scientists in an open-minded, scientific excellent way so they become experts in their fields. For the next scientific generation, it should be going without saying that they will be perfectly able to communicate to other disciplines and outside science, and carry on a true international thinking.

References

Kullenberg, G. (1978) Some experiences from participation in BOSEX 77 and FLEX 76 . ICES C.M. /C:24, 16 pp.

Schulz, S., Matthäus, W. (1986) "PEX-86" in der Gotlandsee. Spectrum, H. 11, 5-7

HELCOM (1992) Convention On The Protection Of The Marine Environment Of The Baltic Sea Area, (Helsinki Convention) 44 pp.

HELCOM Baltic Sea Action Plan. HELCOM Ministerial Meeting Krakow, Poland, 15 November 2007, 101 pp.

IPCC (2014) Climate Change 2014: Synthesis Report. Contribution of Working Groups I, II and III to the Fifth Assessment Report of the Intergovernmental Panel on Climate Change [Core Writing Team, R.K. Pachauri and L.A. Meyer (eds.)]. IPCC, Geneva, Switzerland, 151 pp.

http://climateparis.org/

SDG (2012) UN Sustainable Development Goals https://sustainabledevelopment.un.org

Future Earth (2012) http://www.futureearth.org/about

HELCOM (2018) Declaration of the Ministers of the Environment of the Baltic Coastal Countries and the EU Environment Commissioner, Brussels 6 March 2018. Baltic Marine Environment Protection Commission. 10 pp. http://www.helcom.fi/Documents/HELCOM%20at%20work/HELCOM%20Brussels%20Ministerial%20Declaration.pdf

MARE:N (2016) Küsten-, Meeres- und Polarforschung für Nachhaltigkeit. Bundesministerium für Bildung und Forschung (BMBF) Referat System Erde. Publikationsversand der Bundesregierung Postfach 48 10 09, D-18132 Rostock. 42 pp.

KDM http://www.deutsche-meeresforschung.de/en/index

Meier, H. E. M., B. Müller-Karulis, H. C. Andersson, C. Dieterich, K. Eilola, B. G. Gustafsson, A. Höglund, R. Hordoir, I. Kuznetsov, T. Neumann, Z. Ranjbar, O. P. Savchuk and S. Schimanke (2012) Impact of climate change on ecological quality indicators and biogeochemical fluxes in the Baltic Sea: a multi-model ensemble study. Ambio 41: 558-573, doi:10.1007/s13280-012-0320-3

International science collaboration for ocean climate

Anne Christine Brusendorff, General Secretary, International Council for the Exploration of the Sea (ICES)

The International Council for the Exploration of the Sea (ICES) is an intergovernmental[1] marine science organization headquartered in Copenhagen, Denmark. ICES coordinates and promotes research on oceanography, the marine environment and ecosystems, and living marine resources in the North Atlantic and adjacent sea areas, including the Baltic Sea.

ICES is a global scientific community that is relevant, responsive, and credible concerning marine ecosystems and their relation to humanity. Every year more than 1500 experts contribute to fulfilling the organization's mission to advance the capacity to give advice on human activities affecting, and affected by, marine ecosystems. Science is the foundation on which successful environmental and integrated marine policies are built to achieve societally agreed objectives. ICES coordinates and promotes research of the sea, particularly in relation to living resources and marine ecosystems. We are working at the science-policy interface, to provide the best available science to management. The science is carried out in a way which is transparent and auditable, covering areas from the regional to the global.

Climate change is already leading to fundamental changes in the productivity, variety, and distribution of marine life with consequences for marine ecosystems and people who depend on them. The ICES work programme on ocean climate engages global experts in a variety of initiatives. Together we are working to better understand and advise on the whole range of climate impacts on marine systems, from physical processes to consequences for fishing and marine industries.

[1] ICES has 20 member countries: Belgium, Canada, Denmark, Estonia, Finland, France, Germany, Iceland, Ireland, Latvia, Lithuania, the Netherlands, Norway, Poland, Portugal, Russian Federation, Spain, Sweden, United Kingdom, and the United States of America.

Update on GEWEX in its 30th anniversary

Joan Cuxart

GEWEX Hydroclimate Panel (GHP) co-chair (joan.cuart@uib.cat)

Last January in Washington DC was held the 30th Scientific Steering Group meeting of GEWEX (Global Energy and Water cycle EXchanges project). GEWEX aims to increase the understanding of the Earth's water cycle and energy fluxes at the surface and in the atmosphere. It is composed by a network of scientists that gather data and perform research on subjects related to this main objective, including to predict changes in the world's climate. GEWEX is one of the four core projects of the World Climate Research Program (WCRP).

WCRP has the following main challenges: i) melting ice and global consequences; ii) clouds, circulation and climate sensitivity; iii) carbon feedbacks in the climate system; iv) near-term climate prediction; v) regional sea-level changes and coastal impacts; vi) weather and climate extremes and vii) food baskets of the world. GEWEX leads the two last of the list. It proceeds by coordinating science activities to facilitate research into the global water cycle and interactions between the land and the atmosphere. The other core projects are related to Climate and Cryosphere (CLIC): Climate and Oceans (CLIVAR) and stratosphere-troposphere exchanges (SPARC). Furthermore, there is a special project on coordinated regional climate downscalling experiment (CORDEX). There are a number of Working Groups addressing some specific initiatives, such as WGNE (on numerical modelling), CMIP (on climate modelling intercomparison), or the subseasonal to seasonal prediction (S2S), among others.

GEWEX mission is to measure and predict global and regional energy and water variations, trends, and extremes, such as heat waves, floods, and droughts. It is in its third phase (2013-2022), taking advantage of mature modelling and observing systems. Its methodology is to facilitate research into the global water cycle and interactions between the land and the atmosphere, identifying gaps in knowledge and trying to fill them through new studies, reviews of datasets, gathering of experts or other opportunities. GEWEX has defined four main scientific questions: i) understanding the precipitation variability; ii) changing water availability; iii) extreme events like drought and floods and iv) processes in the water and energy cycles. It proceeds through seven imperatives that establish a detailed framework for its activities: development of data sets; analysis of spatial and temporal variations, process understanding, model development, applications (causes and predictability), technology transfer and capacity building.

There are four panels forming the basic structure of GEWEX: GDAP on Data, GLASS on land-atmosphere interactions, GASS on Atmospheric System studies and GHP is the Hydroclimate panel. The former three will be summarily introduced and more detail will be given on GHP, which hosts the Regional Hydroclimate Projects (RHPs), that are large, regionally-focused multidisciplinary projects aiming to improve the understanding and prediction of that region's weather, climate, and hydrology, often also addresing societal impacts. Currently there are three RHP's in Europe (HyMeX, Baltic Earth and PannEx), two in the Americas (CCRN in Canada and AndEX, the latter still prospective), one in Africa (HyVic in the Victoria Lake Basin) and one in Australia (OzeWEX). Each of them addresses different specific scientific questions of interest, all in good accordance to the main general GEWEX scientific questions.

GHP also hosts Crosscut activities (CCs), which are focused activities that address specific science questions. Through them, GHP i) addresses the GEWEX Science Questions; ii) evaluates and applies the knowledge developed in RHPs; iii) keeps completed RHPs involved; iv) generates interactions between RHPs; v) provides a tool for collaboration with other GEWEX Panels and WCRP activities. Currently the active CCs include the study of subdaily precipitation, the mountain hydrology and the cold-shoulder precipitation near 0ºC. The prospective ones, being currently defined, will address mountain precipitation, water management in models, water security in the third pole and evapotranspiration determination.

At the time of writing this abstract, the main goals of WCRP are being revised by a Panel. If the conclusions are available by the time of the meeting, they will be summarized to the audience.

Natural hazards and socio-technical vulnerabilities in the Baltic Sea region

Giuliano Di Baldassarre[1,2]

[1] Department of Earth Sciences, Uppsala University, Uppsala, Sweden (giuliano.dibaldassarre@geo.uu.se)
[2] Centre of Natural Hazards and Disaster Science, CNDS, Sweden

Social and economic losses caused by natural hazards – such as droughts, earthquakes, floods and storms – are increasing in many regions of the world (Fig.1), despite scientific progress and community efforts to enhance disaster risk reduction (DRR).

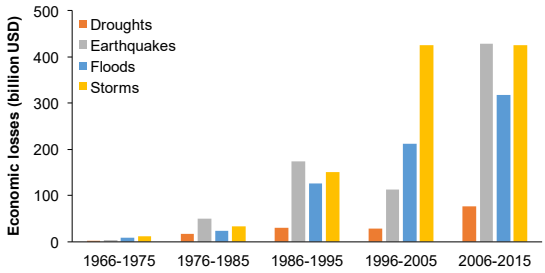

Figure 1. Global trends of economic losses (billion USD) over the past decades. Data from EM-DAT: The Emergency Events Database - Université catholique de Louvain (UCL) - CRED, D. Guha-Sapir, www.emdat.be, Brussels, Belgium.

The UN International Strategy for Disaster Reduction (ISDR) currently spearheads international cooperation on DRR, and it aims to anticipate and plan for reducing economic losses and fatalities caused by natural hazards based on knowledge about the underlying drivers of risk. Yet, climate change, globalization, urbanization, social isolation, and increased interconnectedness between natural, social, and technological systems challenge our ability to plan appropriate risk reduction measures (Kreibich et al., 2017).

Here I critically discuss two main paradigms that have dominated the assessment and management of disaster risks: the hazard-based paradigm and the vulnerability-based paradigm. I then argue that there is a need to integrate both of them to enhance evidence-based DRR policy-making. To this end, scientists affiliated to the Centre of Natural Hazards and Disaster Science (CNDS) have proposed a new integrative framework recognising the complexity as well as the spatial and temporal evolution of both socio-technical vulnerabilities and natural hazards.

The framework (Fig. 2) acknowledges careful treatment of individual cases as tightly coupled socio-natural systems and it emphasizes the role of reciprocal feedback mechanisms between socio-technical vulnerabilities and natural hazards.

Figure 2. Analytical framework focusing on the dynamics produced by the (local) interplay of natural hazards and vulnerabilities under (global) environmental change and socio-economic trends (Di Baldassarre et al., 2018).

An application to a flood risk example in the Baltic Sea region is shown to demonstrate the potentials (and limitations) of the proposed framework.

References

Di Baldassarre, G., et al. (2018). An Integrative Research Framework to Unravel the Interplay of Natural Hazards and Vulnerabilities, *Earth's Future*, 6.

Kreibich, H. et al (2017), Adaptation to flood risk: Results of international paired flood event studies, *Earth's Future*, 5.

Regional and Global Earth System Modelling Activities in MERGE

Paul A. Miller[1,2], on behalf of MERGE

[1] Dept. Physical Geography & Ecosystem Science, Lund University, Lund, Sweden (paul.miller@nateko.lu.se)
[2] MERGE, Centre for Environmental and Climate Research, Lund University, Lund, Sweden

1. What is MERGE?

MERGE stands for ModElling the Regional and Global Earth System, a strategic research area hosted by the Faculty of Science at Lund University. MERGE (www.merge.lu.se) is a collaboration between Lund University, University of Gothenburg, Rossby Centre/SMHI, Linnaeus University, Chalmers University of Technology and the Royal Institute of Technology.

Reliable modelling of the Regional and Global Earth system is of utmost importance for society. Even though climate science is sufficiently robust to justify action on climate change mitigation and adaptation, the need to narrow down uncertainties that are central to assessing climate change and its impacts persists. Such uncertainties pertain to climate sensitivity, Earth System feedbacks and interactions and to incomplete understanding of key climate forcings and the interplay of physical and biological climate/Earth System components. This can be tackled with research that in turn supports mitigation and adaptation efforts on global, regional and local arenas.

Our **main aim** is to further develop and evaluate key global and regional Earth System models, focusing on the terrestrial biosphere as a critical climate-system component. This will lead to improved local, regional and global climate/Earth System models including biophysical and biogeochemical climate/vegetation interactions.

2. The MERGE Research Areas

MERGE research is organized into four interlinked Research Areas (RA), each contributing to this aim.

RA1 (Development, modelling and evaluation of climate-vegetation processes in Earth System Models) aims to develop and implement approaches and model components for regional climate system models (RCMs) and global Earth system models (ESMs).

RA2 (Earth System Model evaluation and development with paleoclimate data) aims to use empirical data on past climate and land cover to evaluate and develop ESMs and regional, coupled vegetation-climate models. Data and modelling communities collaborate on data-model comparison using paleoclimate data and model output.

RA3 (Terrestrial carbon cycle and aerosol–cloud–climate interaction) aims to formulate and validate a model framework linking vegetation, aerosols, clouds and their climate feedbacks. It uses a combination of laboratory studies, field studies and modelling. Process parameterizations are then tested in the EMEP chemical transport model and evaluated against field observations, then to be included in climate models. A particular focus is the representation of the C and N cycles, emissions of biogenic volatile organic compounds (BVOCs) and N-based trace gases from ecosystems, the subsequent atmospheric oxidation of BVOCs and their secondary organic aerosol (SOA) formation potential, with consequences for clouds, global radiation and precipitation.

RA4 (Advanced statistics for model evaluation, simulation set-up and analysis) aims to improve the analysis and evaluation of RCMs and ESMs by means of systematic methods to combine data of different types and measurement platforms, and over different time and space scales.

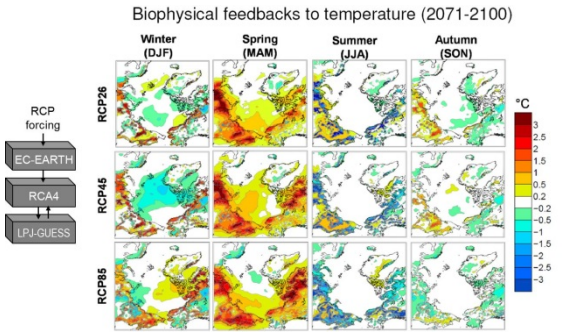

Figure 1. Additional temperature change, (2071-2100) – (1961-1990), as simulated by RCA-GUESS (Zhang et al., *in revision*) due to vegetation feedbacks in the Arctic CORDEX domain, for all four seasons, and for three RCPs.

3. Regional Earth System Modelling Activities

MERGE research uses a wide array of modelling tools and methods. For regional Earth System modelling, one such tool is the RCA-GUESS RCM (Smith et al. 2011), which is best described as a regional ESM, or RESM. RCA-GUESS is the first published RESM and also the result of a long-standing collaboration between SMHI and Lund University. In RCA-GUESS, the static vegetation in the RCA RCM (Samuelsson et al. 2011) is replaced and updated with the vegetation as simulated by the LPJ-GUESS dynamic global vegetation model (Smith et al. 2014) in response to RCA's dynamically generated climate fields. RCA-GUESS has been used to study vegetation dynamics and biophysical feedbacks to climate change in Europe (Wramneby et al. 2010), the Arctic (Zhang et al. 2014), Africa (Wu et al. 2016) and South America (Wu et al. 2017).

As an example of MERGE regional Earth System modelling, Figure 1 shows the additional temperature change as simulated by RCA-GUESS (Zhang et al., *in revision*) due to vegetation feedbacks in the Arctic CORDEX domain, for all four seasons, and for three RCPs. The time period is (2071-2100) – (1961-1990). We find strong seasonal and local

differences that can be explained by the response of the vegetation to climate change.

4. Global Earth System Modelling Activities

MERGE global Earth System Modelling activities focus on the further development of the EC-Earth ESM (www.ec-earth.org), built by a European EC-Earth consortium with 26 partners. The model will be used in various configurations in CMIP6 (Eyring et al. 2016) to answer research questions posed by the endorsed MIPs, such as ScenarioMIP, LUMIP, C4MIP, PMIP etc.

One such configuration is EC-Earth3-Veg (Weiss et al. 2014), which is an Earth System configuration that now has interactive vegetation as a result of coupling to LPJ-GUESS carried out in MERGE. It will be used in CMIP6 ScenarioMIP and LUMIP. Another configuration, EC-Earth3-CC, is a fully coupled ESM with a closed carbon cycle, with dynamic vegetation and terrestrial carbon (and nitrogen) cycling coming from LPJ-GUESS, and ocean biogeochemistry and carbon cycling from the PISCES model. Atmospheric transport of CO2 is handled by TM5. EC-Earth3-CC will be used in CMIP6 C4MIP simulations to examine questions relating to coupled climate-carbon feedbacks.

References

Eyring, V., et al. (2016) *Geosci. Model Dev.*, 9, 1937-1958
Samuelsson, P., et al. (2011) Tellus, 63A, 4–23.
Smith, B., et al. (2011) *Tellus* 63A: 87-106.
Smith, B., et al. (2014) *Biogeosciences* 11: 2027-2054.
Weiss, M., Miller, P.A., et al. (2014) *J. Climate*, **27**, 8563–8577.
Wramneby, A., Smith, B. & Samuelsson, P. (2010) *J. Geo. Research* 115, D21119.
Wu, M., et al. (2016) *Earth Sys. Dyn.* 7: 627-647.
Wu, M., et al. (2017) *Env. Res. Lett.* 12 054016.
Zhang, W., et al. (2014) *Biogeosciences* 11: 5503-5519.

The development of climate science of the Baltic Sea region

Anders Omstedt[1]

[1] Department of Marine Sciences, University of Gothenburg, Sweden

1. Introduction

Oxford University Press has taken the initiative to generate new Encyclopedias, the Oxford Research Encyclopedias (OREs). The initiative offer long-form overview articles written, peer-reviewed, and edited by leading scholars. One of the science area addressed is Climate Science generating now many interesting overview papers and Baltic Earth contributes by a number of papers related to climate change in the Baltic Sea region. The following presentation is part of one such an overview paper (Omstedt, 2017). Here we follow the development of climate science of the Baltic Sea from when observations began in the 18th century to the early 21st century.

2. Short on the development

The question of why the water level is sinking around the Baltic Sea coasts could not be answered until the ideas of postglacial uplift and the thermal history of the earth were better understood in the 19th century and periodic behavior in climate related time series attracted scientific interest. Fishing successes and failures have led to investigations and speculations of fishery and climate. Scientists later introduced the concept of regime shifts when interpreting their data, attributing these to various causes. The increasing amount of anoxic deep water in the Baltic Sea and eutrophication have prompted debate about what is natural and what is anthropogenic, and the scientific outcome of these debates now forms the basis of international management efforts to reduce nutrient leakage from land. The observed increase in atmospheric CO_2 and its effects on global warming have focused the climate debate on trends and generated a series of international and regional assessments and research programs that have greatly improved our understanding of climate and environmental changes, bolstering the efforts of earth system science, in which both climate and environmental factors are analyzed together.

3. Ideas debated

The development of climate sciences cannot be understood without also considering urgent environmental questions. Going back to the 18th century I have focused on some of the major scientific discussions such as:

- Are the water sinking or due to land uplift?
- What can we learn from indirect or direct observations?
- Are the marine resources unlimited?
- Why is fishing success changing?
- What can observations of winter condition teach us?
- Why do climate change?
- Is anoxic water natural or anthropogenic?
- How will increasing CO_2 in the atmosphere influence climate?
- How will increasing CO_2 in the atmosphere influence the Baltic Sea?

4. Summary and some conclusions

Dramatic climate changes have occurred in the Baltic Sea region at many different time scales and with large influence for the humans living in the region. The knowledge of climate has been hampered by the temporal and spatial limitations of observations and by an incomplete understanding of the driving mechanisms, leaving room for speculation as to both the reasons for changes and the role of climate. Past centuries have witnessed major achievements, namely, the development and organization of regular observations; monitoring programs; international assessments addressing fishery, pollution loads and climate change; and atmospheric and hydrologic modeling as well as Baltic Sea modeling. The scientific literature is full of crucial knowledge but also misleading errors that are communicated to society.

Freely available observations, data products, and models as well as regular assessments are fundamental to science but it must also be realized that science is not just a quest to discern the truth; science is also a social process in which researchers are strongly influenced by currently discussed ideas and available research programs.

Why the water level was sinking around the Baltic Sea could not be determined until the idea of postglacial uplift and the thermal history of the Earth were better understood in the 19th century and periodic behavior in climate related time series attracted more scientific interest.

Fishing successes and failures led to investigations of fishery and climate and to the realization that fishing itself has strongly negative effects on the marine environment. Scientists later introduced the concept of regime shifts when interpreting abrupt changes in fish stock data.

Several datasets from the region reveal large temporal variations in which 90% and more of the variance in the time series are at time scales of less than a typical climate time scale. These time series illustrate a stochastic behavior and the importance of taking a long-term perspective when interpreting climate dynamics.

The large scale atmospheric circulation plays a major role in the Baltic Sea climate but a single number characterizing, such as e.g. the winter North Atlantic Oscillation (NAO) index, will not help as the correlation with Baltic Sea properties is not stable and change considerably over time and therefore does not necessary hold in changing climate conditions.

The increasing amount of anoxic deep water in the Baltic Sea and anthropogenic eutrophication has prompted debates about what is natural and what is anthropogenic. The scientific outcome of these debates forms the basis of international management efforts to reduce nutrient leakage from land. However, climate warming may reduce the surface water uptake of oxygen from the atmosphere, and phosphorous-leaking anoxic sediments may counteract management efforts to reduce nutrient fluxes from land.

Observed increases in atmospheric CO_2 levels and their effects on global warming have focused the climate debate on trends and generated a series of international and regional assessments and research programs. These have considerably improved our understanding of climate and environmental changes, giving more impetus to earth system science in which both climate and environmental factors are analyzed together.

The Baltic Sea is facing serious climate and environmental threats, and strong international management plans are needed based on the best available knowledge. Several aspects of regional climate and environmental changes and how they interact are, however, unknown and merit future research.

References

Omstedt, A. (2017). The Development of Climate Science of the Baltic Sea Region. In *Oxford Research Encyclopedia of Climate Science.* Oxford University Press. doi:10.1093/acrefore/9780190228620.013.654.

Baltic Sea Operational Oceanographic System (BOOS) – a stimulator to Baltic earth system research

Jun She[1], Pia Andersson[2], Tarmo Kõuts[3], Darecki Mirawslov[4], Jan Hinrich Reißmann[5] and Laura Tuomi[6]

[1] Danish Meteorological Institute, Denmark (js@dmi.dk)
[2] Swedish Meteorological and Hydrological Institute, Sweden
[3] Marine Systems Institute, Tallinn Technological University, Estonia
[4] Institute of Oceanology of the Polish Academy of Sciences, Poland
[5] Federal Maritime and Hydrographic Agency, Germany
[6] Finnish Meteorological Institute, Finland

1. Abstract

The BOOS (Baltic Sea Operational Oceanographic System, http://www.boos.org) is an organization with 22 met-ocean agencies and institutes around the Baltic Sea. It is in the frontier of generating, using and validating marine data, products and models. New technological and knowledge gaps on monitoring, modelling and forecasting of the Baltic Sea have been constantly identified, not only for physical oceanography (ocean hydrodynamics, ice, waves) but also for biogeochemical state of the Sea. Four research priorities have been identified for European operational oceanography: sustained ocean observing, modelling and forecasting technology, coastal operational oceanography and operational ecology. The presentation will introduce state-of-the-art of BOOS monitoring and modelling capabilities and recent BOOS research in related to interesting Baltic Earth topics, e.g., salinity and sea level dynamics, inter-basin and inter-sub-basin exchanges, (sub)mesoscale variability and seamless modelling. Potential win-win cooperation and interaction between BOOS and Baltic Earth community will also be discussed.

2. Introduction

Seamless modelling and forecasting for the earth system has been proposed by World Meteorological Organization (WMO, 2015) as the main future direction of WMO prediction capacity development. EuroGOOS also sets seamless ocean system modelling and forecasting as one of its four future research priorities (She et al. 2016) in which ocean (both physical and biogeochemical) states are regarded as sub-systems of the whole earth system. The knowledge and state-of-the-art modelling/forecasting technologies on ocean-ice-wave-ecosystem and coupling processes with atmosphere and fresh water systems are the basis for developing this seamless capacity. BOOS aims at developing this seamless capacity and providing a corresponding seamless marine service. The main activities in BOOS include three components: observing, modelling/ forecasting and service. With sustained observing, the ocean state is identified and new phenomena and related knowledge are discovered. A large part of the new knowledge on the ocean system is transferred to the operational hindcast and forecast platforms (models) to optimize existing models; the observations are assimilated into the operational models to optimize the initial state and model parameters which are further used to make forecast and reanalysis modelling. The products generated will be used in marine service for blue growth, ecosystem-based management and climate change adaptation and mitigation. In this paper, the state-of-the-art of BOOS R&D activities will be reviewed and potential interactions with Baltic Earth Community are discussed.

3. Sustained operational observing in BOOS

Sustained ocean observing is essential to provide timely ocean-ecosystem state for improving and validating the operational models. A near real-time (NRT) monitoring and data exchange system is maintained by BOOS members, providing high temporal resolution data of sea level, temperature/salinity (T/S), currents, waves, dissolved oxygen and chl-a (Tab. 1). This forms a basis for Baltic Sea In-Situ Thematic Assembling Centre (BAL INS-TAC) in Copernicus Marine Environment Monitoring Service (CMEMS) and EMODnet (European Marine Observation Data Network) Physics.

Table 1. Monitoring capacities from BOOS partners

Instruments	Variables	Number of stations in 7d/10y	Delivery time
Tidal gauges	Water level	148/169	1-60min.
	SST	24/27	
Moorings	Waves	12/21	<1hour
	SST	26/49	
	T/S	8/19	
	Currents	7/17	
	Chl-a	3/3	
	DO	3/3	
Ferrybox	SST	15/30	NRT
	SSS	4/19	
	Surf-DO	3/17	
	Surf-Chl-a	3/17	
	SSC	11/11	
Drifter	SST	0/5	NRT
Argo	T/S	0/10	NRT
Profiler	T/S	0/1	NRT
R/V BOOS	T/S	109	NRT
R/V HELCOM*	T/S	834/797	>1yr
	Chl-a	755	
	DO	792	
	Secchi Dep.	702	
	PH	409	
	N/P/Si	501-549	
	Phytoplankton	257	
	Zooplankton	141	
	Primary prod.	27	

*for HELCOM, 2013 number is used.

New cost-effective monitoring technologies have been used, e.g., ferrybox, gliders and shallow water profilers. In

addition, some BOOS partners (e.g., AU, IOW, IOPAN, MSI, SMHI and SYKE) are also main players in providing offline, regular basin wide environmental monitoring, coordinated by HELCOM. It is expected that the operational and environmental monitoring components will be further integrated in future EOOS (Sustained European Ocean Observing System).

4. Operational seamless model development in BOOS

Seamless modelling can be developed in spatial, temporal and parametric scales. Current operational model systems in the Baltic Sea include both basin-scale systems and local systems for national sea waters, fjords and lakes (Tab. 2). This builds up a spatial seamless modelling platform. The existing coupled ocean-ice-biogeochemical models and on-going coupling efforts with waves will ensure full seamless operational ocean model system in the coming 3 years, largely benefited from CMEMS BAL MFC (Baltic Sea Monitoring and Forecasting Centre, Tuomi et al. 2017). For temporal seamless modelling, the calibrated operational ocean-ice-wave-biogeochemical models have been used for long-term hindcast, reanalysis and scenario simulations (Liu et al, 2017). The model system has been further coupled with regional climate models for climate scenario projections (Tian et al., 2016).

Table 2. Baltic Sea basin/local ocean forecasting systems

Product. Unit	Basin system		Local system		
	Model	Reso	Model	Reso	Area
BAL MFC	HBM	1nm			
BSH (GE)	HBM	1nm	HBM	0.5nm	TW*
DMI (DK)	HBM	3nm	HBM	450m	Limf.*
			HBM	0.5nm	TW*
FCOO (DK)	GETM	1nm	GETM	0.5nm	TW*
FMI (FI)	OAAS	3nm	HELMI (ice)	1nm	N.Bal. Sea
	HBM	3nm			
MSI (EE)			HBM	0.5km	GoF-GoR*
SMHI (SE)	NEMO-Nordic	1nm	NEMO	360m	Lake Vänern
			NEMO	60m	Brof.*
UL (LV)			HBM	100m	Latvia lakes

*TW: transition waters; Limf.: Limfjoden; GOF: Gulf of Finland; GoR: Gulf of Riga; Brof.: Brofjoden

In order to keep high efficiency and quality, the extensive seamless modelling framework needs flexible grid, efficient high performance computing and handling of model input/output (I/O). HBM system has gone through code modernization in the past decade, with dynamic two-way nesting, synchronized I/O and efficient hybrid parallel computing for both multi-core and many-core architectures. NEMO also developed two-way nesting facility (using Agrifs) and synchronized I/O.

Although the seamless ocean system modelling framework has been established, regular validation of the forecasts and reanalysis constantly reveal areas for further improvements. They are addressed by on-going BOOS modelling activities, e.g., multi-model ensemble prediction, improved modelling on inter-basin and inter-sub-basin exchange, coast-estuary continuum, meso- and submeso-scale eddies, basin scale sea level and sea ice. Capacities for precisely predicting currents, upwelling, extreme sea level and waves in icing waters, skin temperature, algae bloom and oxygen depletion are yet to be improved. Recent progresses in the above areas will be introduced in the presentation.

5. Grand challenges and opportunities in developing integrated marine service

Through integrating sustained model platforms and observations, historical ocean-ecosystem state can be reconstructed, present state can be analyzed, and future state can be predicted and projected according to scenarios. The data and products are regularly provided through the integrated, seamless service. One of the main challenges is how to improve the quality and efficiency of the system. New knowledge generation is the key. Product and service validations have constantly raised new R&D issues. Through knowledge innovation, new generations of operational monitoring and modelling capabilities are developed.

However, for next generation operational service system, there exist grand challenges. The capacities are needed on reconstructing, forecasting and projection the states of inter-sub-basin transport, mesoscale and sub-mesoscale variability, coast-estuary continuum, sediment transport, algae bloom, oxygen depletion and marine litter. To tackle these grand challenges, integrated and targeted research experiment programs are needed (She et al. 2016). BOOS invites Baltic Earth Community for responsive and collaborative research on Coastal Operational Oceanography and Operational Ecology. Well-designed research programs should cover not only dedicated field experiment and new knowledge generation but also knowledge transfer into seamless operational model system and product service. Even if significant funding is not available, collaboration mechanism between BOOS and Baltic Earth can still be established and enhanced. Through accessing and using BOOS modelling platforms and observations and sharing BOOS research challenges, Baltic Earth community may extend her research responsiveness, scope and capacity; through transferring relevant Baltic Earth research achievements into BOOS operational systems, the upgrade of the BOOS seamless service system can be speeded up.

References

Liu, Y., Meier, H. E. M., and Eilola, K. (2017): Nutrient transports in the Baltic Sea – results from a 30-year physical–biogeochemical reanalysis, *Biogeosciences*, 14, pp2113-2131

She J., Allen I., Buch E., Crise A., Johannessen J.A., Le Traon P.-Y., Lips U., Nolan G., Pinardi N., Reißmann J.H., Siddorn J., Stanev E. and Wehde H.(2016): Developing European operational oceanography for Blue Growth, climate change adaptation and mitigation, and ecosystem-based management. *Ocean Sci.* **12**(4), pp. 953-976

Tian T., Su T., Boberg F., Yang S. and Schmith T., 2016. Estimating uncertainty caused by ocean heat transport to the North Sea: experiments downscaling EC-Earth. *Climate Dynamics* 46 (1-2), pp99-110

Tuomi L., She J., Lorkowski I., Axell L., Lagemaa P., Schwichtenberg F. and Huess V. (2017): Overview of CMEMS BAL MFC Service and Developments. Proceedings of the 8th EuroGOOS Conference, accepted.

World Meteorological Organisation (WMO), 2015. Seamless prediction of the Earth system: from minutes to months. https://public.wmo.int/en/resources/library/seamless-prediction-of-earth-system-from-minutes-months

Baltic Earth, Outreach and Communication

Hans von Storch

Helmholtz-Zentrum Geesthacht, Institute of Coastal Research, Geesthacht Germany (hvonstorch@web.de)

Outreach is the collection of efforts of a scientific project to embed its work in the social landscape of social, political and economic interests. This landscape is mostly „external“ to the project. These interests feedback on the project itself and may help to sharpen the focus and increase the societal/scientific significance of the project.

Outreach serves a number of purposes, and takes different forms, and addresses different groups, in particular other scientific projects, funding agencies, managerial and political decision bodies, or the general public

In all cases, it is needed to have an understanding of the knowledge system adopted by the addressee, its interests and motives. These “alternative” knowledge systems in most cases satisfy certain cultural preferences, interests and social inertia. Fundamental problems in “outreach” are: competition of knowledge claims; “truth” is a powerful but invalid concept; a successful communication recognizes that the “others” (those to whom we want to reach out) cannot be simply taught, but that a dialogue must be built with specific decision makers and stakeholders.

Topic A

Salinity dynamics in the Baltic Sea

Analysis of factors influencing the salinity of Baltic inflows and how these may change with sea level rise.

Lars Arneborg

Department of Research and Development, Swedish Meteorological and Hydrological Institute, Gothenburg, Sweden (lars.arneborg@smhi.se)

Recent model studies suggest that saline inflows to the Baltic Sea increase with rising sea levels (Hordoir et al. 2015) and that this has deteriorating effects on the oxygen conditions in the Baltic deepwater (Meier et al. 2017). Arneborg (2016) discusses processes in the Danish straits that influence the salinity of inflows and the sensitivity to sea level change, and the ability of existing 3D models to describe these. For example, internal hydraulic controls have been observed in the Sound and in the Belts (e.g. Nielsen 2001, Nielsen et al. 2017), and these may influence the relative amounts of bottom and surface layer Kattegat waters that flow over the sills and through the constrictions. Hydraulic controls are sensitive to the geometry of the straits and to the magnitude of barotropic volume fluxes, which in turn are sensitive to sea level change. Entrainment into an inflowing bottom current, and the duration of inflows of a certain magnitude are also factors that may change with rising sea levels.

Here we present analyses of high-resolution salinity and current observations over the Darss and Drogden sills and discuss these in terms of various processes that may govern the inflow of saline water.

References

Arneborg L (2016) Comment on “Influence of sea level rise on the dynamics of salt inflows in the Baltic Sea” by R. Hordoir, L. Axell, U. Löptien, H. Dietze, and I. Kuznetsov. J Geophys Res Oceans, Vol 121, pp. 2035–2204.

Hordoir R, Axell L, Löptien U, Dietze H, Kuznetsov I (2015) Influence of sea level rise on the dynamics of salt inflows in the Baltic Sea. J Geophys Res Oceans, Vol 120, pp. 6653–6668.

Meier, H. E. M., Höglund, A., Eilola, K., & Almroth-Rosell, E. (2017). Impact of accelerated future global mean sea level rise on hypoxia in the Baltic Sea. Climate Dynamics, Vol. 49, No. 1-2, pp. 163-172.

Nielsen, M. H. (2001), Evidence for internal hydraulic control in the northern Øresund, J. Geophys. Res., Vol. 106, No. C7, pp. 14,055–14,068.

Nielsen, M. H., Vang, T., & Lund-Hansen, L. C. (2017). Internal hydraulic control in the Little Belt, Denmark–observations of flow configurations and water mass formation. Ocean Science, Vol. 13, No. 6, 1061.

The impact of the Atlantic Multidecadal Oscillation on the salinity variability of the Baltic Sea

Florian Börgel[1], Claudia Frauen[1] , Semjon Schimanke[2] and H. E. Markus Meier[1,2]

[1] Leibniz Institute for Baltic Sea Research, IOW, Warnemuende, Germany (florian.boergel@io-warnemuende.de)
[2] Swedish Meteorological and Hydrological Institute, Norrköping, Sweden

1. Baltic Sea

The salinity of the Baltic Sea is mainly driven by freshwater input and by saltwater inflows from the North Sea. The freshwater input into the Baltic Sea comes either as river runoff or as positive net precipitation (precipitation - evaporation) over the sea surface. The river runoff is influenced by precipitation over the drainage basin. The discharge of the Baltic Sea drainage basin is exposed to low-frequency variations due to changes in precipitation and evaporation (Meier and Kauker, 2003b). Hence, the mean salinity in the Baltic Sea is affected by dry and wet periods that occur due to low-frequency changes in precipitation and evaporation patterns. In contrast, saltwater inflows are characterized by exceptional periods of strong easterly winds and following westerly winds on time scales of about 40 days. This suggests that the Baltic Sea and its ecosystem are strongly influenced by external atmospheric forcing.

2. Atlantic Multidecadal Oscillation

Schimanke and Meier (2016) analyzed the decadal to centennial variability of the Baltic Sea. A wavelet analysis of the mean salinity of the Baltic Sea showed significant power in the 60-120 year periodicity band, which we link to the Atlantic multidecadal oscillation (AMO), i.e. variations in northward heat transport in the ocean. The Atlantic multidecadal oscillation (AMO) is defined as a multidecadal climate variability (60-90 years) of sea surface temperature (SST) in the North Atlantic with alternating warm and cool phases (Knight et al., 2006)(see Figure 1). It has been shown that regional multidecadal variability in the European region can be linked to the AMO, e.g extreme precipitation (Casanueva et al., 2014) and European summer climate (Enfield et al., 2001). In addition, there are several studies that focus on the physical mechanism behind warm AMO+ phase and cold AMO- affecting Europe (Peings and Magnusdottir, 2014; Zampieri et al., 2017).

Even though several regional climate conditions have been related to the AMO, the origin of the AMO remains still unclear and its unique periodicity needs to be proven (Ruprich-Robert et al., 2017). Some studies even use the term Atlantic multidecadal variability (AMV), since this does not imply that the AMV is only created by internal climate processes (Wang et al., 2017).

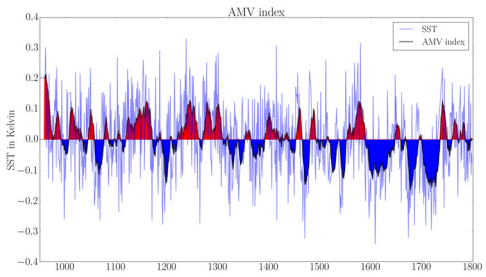

Figure 1. AMO/AMV index for the time 950-1800. Red (blue) areas indicate AMO+ (AMO-) phases.

3. AMO in General Circulation Models

General circulation models have shown that the AMO signal is closely related to the Atlantic Meridional Overturning Circulation (AMOC) which appears to drive the AMO. This multi-decadal variability can emerge in the absence of any external forcing but is also likely to be influenced by external forcing (Sutton and Dong, 2012). Zhang and Wang (2013) analyzed 27 coupled general circulation models (GCMs) and found a large inter-model spread in amplitudes and frequencies with respect to the AMO. The spatial structure of the AMO also varies from model to model. This leads to the conclusion that most models can reproduce an AMO like variability, but we cannot yet expect them to reproduce comparable atmospheric patterns in every detail. Still GCMs are necessary since observations of the AMO are limited to a period of roughly 150 years. With a defined frequency in the range of 60-90 years, the results of a spectral analysis of the AMO must be considered with caution.

In our study we used the Rossby Centre Ocean model (RCO) to simulate the period from 950 – 1800 (Schimanke and Meier, 2016). RCO is a primitive equation circulation model with a horizontal resolution of 2 nm and 83 vertical layers. With a thickness of 3m per vertical layer this results in a maximum depth of ~ 250m. RCO is forced by the Rossby Centre Atmosphere Model (RCA3) with a horizontal resolution of 0.44° covering nearly the whole area of Europe. RCA3 provides 10-m wind, 2-m air temperature 2-m specific humidity, precipitation, total cloudiness and sea level pressure fields. RCA3 itself is driven by ECHO-G at the lateral boundaries.

4. AMO and its influence on the Baltic Sea

The goal of this study is to find a coherence of the mean salinity of the Baltic Sea and the mean sea surface temperature in the North Atlantic which we define as AMO.

A wavelet coherence analysis revealed a significant coherence between the AMO and the mean salinity of the Baltic Sea for the periodicity of 60-120 years. The phase relationship is also in good agreement with a lagged response of the mean salinity. Since the salinity of the Baltic Sea is mainly driven by river runoff, we analyzed the coherence between AMO and precipitation over the Baltic Sea drainage basin. Again, the wavelet coherence revealed significant coherence between AMO and precipitation in the period of 60-120 years with both signals in phase.

This relationship is also shown in Figure 2. The correlation of the AMO index and precipitation over the Baltic Sea indicates a positive correlation. AMO+ phases appear to cause wetter conditions in our simulation, followed by a decrease of the mean salinity of the Baltic Sea.

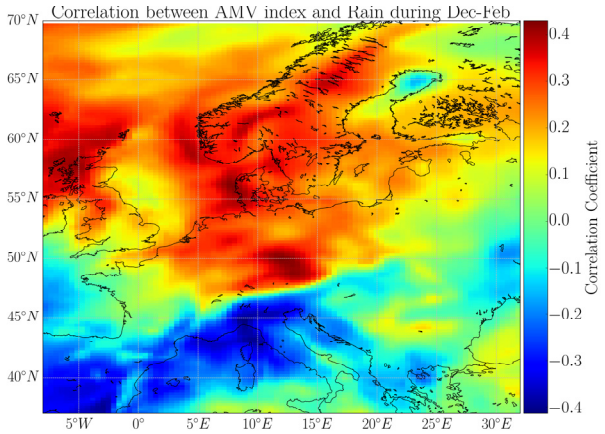

Figure 2. Correlation of precipitation (10yr running mean) during wintertime (DJF) and AMO index for the period 950-1800.

The spatial response to different AMO phases is complex. Therefore, we analyzed season composites. Our study reveals that in winter the state of the AMO can make up to 7% of the mean yearly precipitation. In addition, Figure 1 shows the tendency of an increased number of warm AMO+ phases during the Medieval Climate Anomaly (MCA) compared to more AMO- phases during the Little Ice Age (LIA). In our simulation, these phases can be linked to dry and wet conditions over the Baltic Sea. This allows us to compare the mean salinity of the Baltic Sea during the MCA and the LIA and its relation to the AMO.

In the future we will analyze in detail how the AMO signal impacts the mean salinity of the Baltic Sea and discuss in detail the influence of wind and sea level pressure patterns over the Baltic Sea area.

References

Casanueva, A., Rodríguez-Puebla, C., Frías, M. D., and González-Reviriego, N. (2014). Variability of extreme precipitation over europe and its relationships with teleconnection patterns. Hydrology and Earth System Sciences, 18(2):709–725.

Enfield, D. B., Mestas-Nuñez, A. M., and Trimble, P. J. (2001). The atlantic multidecadal oscillation and its relation to rainfall and river flows in the continental u.s. Geophysical Research Letters, 28(10):2077–2080.

Knight, J. R., Folland, C. K., and Scaife, A. A. (2006). Climate impacts of the atlantic multidecadal oscillation. Geophysical Research Letters, 33(17):n/a–n/a. L17706.

Landrum, L., Otto-Bliesner, B. L., Wahl, E. R., Conley, A., Lawrence, P. J., Rosenbloom, N., and Teng, H. (2013). Last millennium climate and its variability in ccsm4. Journal of Climate, 26(4):1085–1111.

Peings, Y. and Magnusdottir, G. (2014). Forcing of the wintertime atmospheric circulation by the multidecadal fluctuations of the north atlantic ocean. Environmental Research Letters, 9(3):034018.

Ruprich-Robert, Y., Msadek, R., Castruccio, F., Yeager, S., Delworth, T., and Danabaoglu, G. (2017). Assessing the climate impacts of the observed atlantic multidecadal variability using the gfdl cm2.1 and ncar cesm1 global coupled models. Journal of Climate, 30(8):2785–2810.

Schimanke, S. and Meier, H. E. M. (2016). Decadal-to-centennial variability of salinity in the Baltic Sea. Journal of Climate, 29(20):7173–7188.

Sutton, R. T. and Dong, B. (2012). Atlantic Ocean influence on a shift in European climate in the 1990s. Nature Geoscience, 5:788–792.

Trenberth, K. E. and Shea, D. J. (2006). Atlantic hurricanes and natural variability in 2005. Geophysical Research Letters, 33(12):n/a–n/a. L12704.

Zampieri, M., Toreti, A., Schindler, A., Scoccimarro, E., and Gualdi, S. (2017). Atlantic multi-decadal oscillation influence on weather regimes over europe and the mediterranean in spring and summer. Global and Planetary Change, 151:92 – 100. Climate Variability and Change in the Mediterranean Region.13

Zhang, L. and Wang, C. (2013). Multidecadal North Atlantic sea surface temperature and Atlantic meridional overturning circulation variability in CMIP5 historical simulations. 118:5772–5791.

Water exhange through the Danish Straits with global mean sea level rise

Sandra-Esther Brunnabend[1], Ulf Gräwe[1], Xaver Lange[1],and H. E. Markus Meier[1]

[1] Leibniz Institute for Baltic Sea Research Warnemuende, Rostock, Germany (Sandra.Brunnabend@io-warnemuende.de)

1. Introduction

The semi-enclosed Baltic Sea, which is connected to North Sea via the Danish Straits, experience regular salt inflow events with Major Baltic Inflows (MBI) occurring about every one to ten years. These salt inflow events have impacts on the oxygen concentration and the hypoxic areas in the Baltic Sea.

The strength and duration of salt inflow events may change in a warming climate and the corresponding global mean sea level (GMSL) change. Meier et al. (2017) showed that a one meter GMSL rise could cause an increase in frequency and magnitude in inflow events, salinity and phosphate concentration that would lead to increased hypoxic zones. In addition, Arneborg (2016) argued that with GMSL rise the increase in relative salt transport is higher than the increase in the cross section and largest changes are expected in the Oeresund.

Therefore, the regional General Estuarine Transport Model (GETM) is used to simulate the change in the characteristics of the water exchange through the Danish Straits, during inflow events, and with a GMSL rise of one meter.

2. General Estuarine Transport Model

The regional model GETM (Burchard et al., 2004) applies the Boussinesq and boundary layer approximation to solve the primitive equations. The two model setups used in this study comprise the western Baltic Sea with a horizontal resolution of 200m and 600m, respectively (Gräwe et al., 2015). Both setups use 40 vertical adaptive coordinates with the adaption based on stratification (Gräwe et al., 2015).

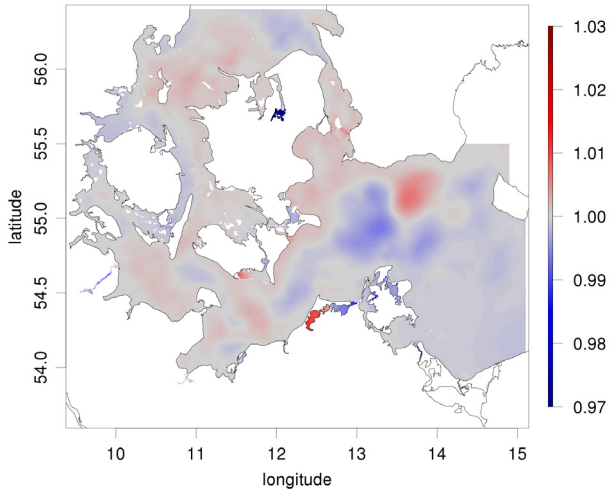

Figure 1. Difference in mean sea surface height in meter of the reference simulation and the simulation including one meter GMSL rise at the boundaries of simulation of year 1993

The reference simulations are forced with present day atmospheric forcing and sea level (coastDat2: Geyer, 2014; freshwater runoff: (LUNG-MV, LLUR-SH), for Oder river by HELCOM; boundary data: Gräwe et al., 2015). The 200m GETM setup applies nudging of sea surface height (SSH) observations at the boundaries to increase the correlation of SSH at the model boundaries compared to observation and to improve the general accumulated transport of ocean water through the Danish Straits. The simulations are performed for the years 1992 and 1993 for the 200m GETM setup and from 2012 to 2017 for the 600m GETM setup. Beside the reference simulations, additional simulations have been perform using the same setups, only the SSH at the boundaries of the model domain is increased by one meter.

3. Model evaluation

The SSH at the Station Viken (Northern Oeresund) and Klagshamn (Southern Oeresund) agree well with observations derived from tide gauge records (Figure 2). The correlation amounts to 0.97 and the short term variability is well represented in the modeled time series at the station Klagshamn. At the station Viken the correlation between model and observations is still high, which is due to the applied nudging. But the amplitude of the variability is still reduced in the model results compared to the observations, although improved with the applied nudging.

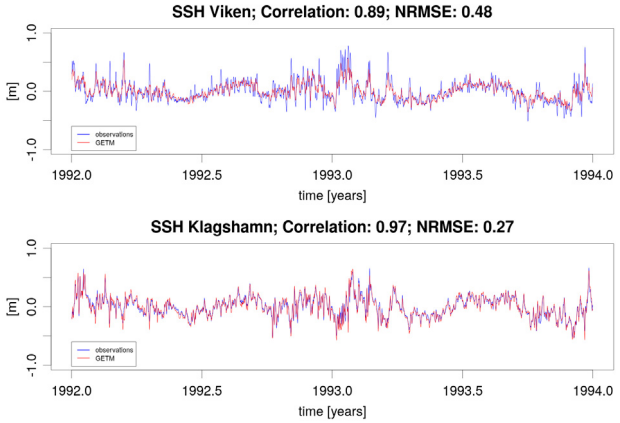

Figure 2. Comparison of sea surface height anomalies modeled with GETM using the 200m setup and time series derived from tide gauges in Viken and Klagshamn

The Volume transport through the Oeresund is computed from observed and modeled water height anomalies at the tide gauge locations Viken (Northern Oeresund) and Klagshamn (Southern Oeresund). The transports are computed after the studies of Hakansson (2003) and Meier et al. (2003). Comparing volume transport derived from model results and observations, both time series agree well, only the amplitude of the variability of the modeled volume transport is reduced. This is caused by the lower amplitude in modeled SSH at station Viken, as mentioned before.

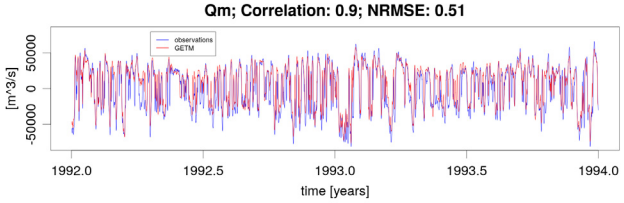

Figure 3. Volume transport (Qm) through Oeresund computed from SSH time series SSH at Viken and Klagshamn using the 200m GETM setup and observation from tide gauge records, after Hakansson (2003), and Meier et al. (2003); temporal mean of Qm is removed

4. Analysis

We will present an analysis of water exchange during small inflow events, MBIs and the outflow of brackish water. In addition, the change in water exchange between the Baltic Sea and North Sea due to projected GMSL of the RCP8.5 scenario is analyzed using both model setups. A detailed process study of water exchange study during MBI events will be presented. Here, the MBI will be analyzed under simulated present day conditions, and also the differences to the simulation including the GMSL rise of one meter will be evaluated.

For example, the reference simulation of the 200m GETM setup shows an accumulated volume transports through the Danish Straits of 1249 km^3 (Great Belt: 782 km^3; Little Belt: 53 km^3; Oeresund: 414 km^3) in 1992 and 1993. The negative volume transport of 102 km^3 through the Drodgen Sill in January 1993 corresponds to an MBI occurring during this time period (Figure 4).

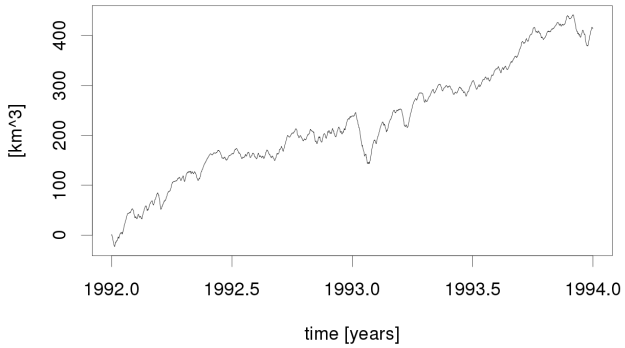

Figure 4. Accumulated volume transport through the Drodgen Sill, Oeresund derived from the reference simulation using the 200m GETM setup

The differences of the simulation (200m GETM setup) including the GMSL of one meter and the reference simulation shows an increase in the relative salt transport through the Danish Straits increased in total by 8.5% and the relative increase in volume transport by 8.2% at the critical transects at Darss Sill and Drodgen Sill. This does not support the hypotheses of Arneborg (2016) as the higher increase in salt transport is quite small compared to the increase in the volume transport. However these results account only for a time period when one inflow event occurred and natural variability is high. Therefore, the 600m GETM setup is used to simulate water exchange through the Danish Straits for a longer time period (2012-2017), indicating that during other inflow events the relative change in salt transport is higher than the change volume transport. Therefore, a detailed analysis of the processes during different inflow events will be presented.

References

Arneborg, L., (2016), Comment on ‘‘Influence of sea level rise on the dynamics of salt inflows in the Baltic Sea’’ by R. Hordoir, L. Axell, U. Löptien, H. Dietze, and I. Kuznetsov, J. Geophys. Res. Oceans, 121, doi:10.1002/2015JC011451.

Burchard, H., Bolding, K., and Villarreal, M. R., (2004), Three-dimensional modelling of estuarine turbidity maxima in a tidal estuary, Ocean Dynamics 54 (2), 250–265, doi:10.1007/s10236-003-0073-4.

Geyer, B., (2014), High-resolution atmospheric reconstruction for Europe 1948-2012: coastDat2, Earth Syst. Sci. Data, 6, 147–164, doi: 10.5194/essd-6-147-2014.

U. Gräwe, P. Holtermann, K. Klingbeil, H. Burchard, Advantages of vertically adaptive coordinates in numerical models of stratified shelf seas, Ocean Modelling 92, 56-68 (2015). doi: 10.1016/j.ocemod.2015.05.008.

Håkansson, B. G., (2003), On water and salt exchange in a frictionally dominated strait: Connecting the Baltic with the North Sea, Cont. Shelf Res., in press, (2003).

H.E.M. Meier, R. Döscher, B. Broman, and J. Piechura, (2004), The major Baltic inflow in January 2003 and preconditioning by smaller inflows in summer/autumn 2002: a model study. Oceanologia, 46, 557-579.

H.E.M. Meier, R. Döscher, and T. Faxén, (2003), A multiprocessor coupled ice-ocean model for the Baltic Sea: Application to salt inflow. J. Geophys. Res., 108(C8), 3273, doi:10.1029/2000JC000521.

H.E.M. Meier, Höglund, A., Eilola, K. and E. Almroth-Rosell, Impact of accelerated future global mean sea level rise on hypoxia in the Baltic Sea, Climate Dynamics, Volume 49, Issue 1–2, pp 163–172, (2017), doi:10.1007/s00382-016-3333-y.

Acknowledgments

The model development, simulations and validation were performed with resources provided by the North-German Supercomputing Alliance (HLRN).

Using model-based sub-regional EOF patterns to reconstruct temperature and salinity fields from observations

Jüri Elken[1], Mihhail Zujev[1]

[1] Department of Marine Systems, Tallinn University of Technology, Estonia (juri.elken@ttu.ee)

1. Introduction

Many oceanographic applications, like map reconstruction, total amount and gradient estimation and data assimilation, emphasize the need to fill in the spatial, time-varying gaps of observations. Developments of observation techniques such as ferryboxes, automatic profiling stations, floats and gliders, as well as remote sensing, provide interesting new high-resolution data sets that were impossible just a few decades ago. Still, the data coverage is fragmentary and special analysis methods are needed for obtaining consistent gridded oceanographic data. Reanalysis is a powerful, but costly method for production of gridded fields. Widely used optimal interpolation works well in the densely sampled regions. However, methods for using irregular data, like the data from marine monitoring, are not perfect. Quite often we see in the results "bull eyes" around the observation points or other unrealistic features.

For the reconstruction of gridded fields, we can use full knowledge of global (in the sub-region) correlation fields, obtained via dense data set like model data. Global variability patterns can be determined by the EOF/PCA method as a limited number of dominating modes. Observational data sets that contain gaps, can still be used to estimate the time-dependent amplitudes of dominating "full" EOF modes (spatial eigenvectors). By this method, we can reconstruct global gap-free patterns of observational data. Within the forecasting process, the model data can be corrected in the analysis step in relation to mismatch in the seasonal and shorter period large-scale responses. Remaining shorter scale processes (as deviations from the large-scale patterns) that have local correlation scales, can be further assimilated using optimal interpolation or its extended methods.

2. Method

We use the sequence of modelled $M \times 1$ state vectors $\mathbf{x}'(n)$ (deviations at time $n = 1\mathrm{K}\ N$ from temporal mean) that are decomposed by space-dependent empirical orthogonal mode vectors $\mathbf{f}_m$ and time-dependent amplitudes $a_m(n)$ as $\mathbf{x}'(n) = \sum_{m=1}^{M} a_m(n)\mathbf{f}_m$. The modes are calculated as eigenvectors of $M \times M$ covariance matrix $\mathbf{D} = \left\{ \frac{1}{N} \sum_{n=1}^{N} x_i'(n) x_j'(n) \right\}$. Observations $\mathbf{y}$ as $K \times 1$ vector are taken from different (fewer) locations $K < M$ than $\mathbf{x}$. Extracting the values of mode vectors at observation points $\mathbf{g}_m = \mathbf{T}\mathbf{f}_m$, where $\mathbf{T}$ is the $K \times M$ spatial mask, the products $\mathbf{g}_i \mathbf{g}_j^{\mathrm{T}}$ are only approximately orthogonal. Therefore, the standard EOF procedure to find the amplitudes cannot be used. Instead, we find the "observational" amplitudes b_i by least-square minimization of analysis errors over the first L (most energetic) modes compared to the observation vector: $E = \left(\mathbf{y}' - \sum_{i}^{L} b_i \mathbf{g}_i \right)^2 \rightarrow$ min. This results in the system of linear equations regarding $L \times 1$ amplitude vector $\mathbf{b} = \{b_i\}$: $\mathbf{C}\mathbf{b} = \mathbf{h}$, where $\mathbf{C} = \{\mathbf{g}_i \mathbf{g}_j^{\mathrm{T}}\}$ is $L \times L$ and $\mathbf{h} = \{\mathbf{y}\,\mathbf{g}_i\}$ is $L \times 1$. The reconstructed field is then found from the "original" model-based EOF patterns $\mathbf{x}_b'(n) = \sum_{i=1}^{L} b_i(n)\mathbf{f}_i$.

Maximum number of modes $L_{\max}$ included in the particular reconstruction is limited by (1) configuration of observation points in relation to high/low regions in the mode patterns, and by (2) comparing the calculated amplitudes b_i with the range of temporal variability of $a_m(n)$: the condition is $|b_L| < s[a_L(n)]$, where $s[\ ]$ is specific adopted statistical limit. Regarding the criterion (1), unfavorable clustering of observation points in the positive or negative areas of the pattern of the specific mode can be identified, if the average of $\mathbf{g}_m$ components is significantly larger (in absolute value) than the average of $\mathbf{f}_m$ components; this mode and higher modes have to be omitted.

3. Example from the northeastern Baltic

We have used the surface data (SST and SSS) from sub-regional Estonian implementation of the HBM model (Lagemaa, 2012) in the period 2010-2015. High-resolution (grid step 0.5 nautical miles) daily extracts were spatially averaged over bins of 5 nautical miles, resulting in 744 wet points over 2191 days.

In the resulting EOF patterns, first spatially uniform SST mode is governed by seasonal heat cycle and covers 97.6% of total variance. Second mode (Fig. 1a) encounters differential heating and cooling in shallow coastal and deeper offshore area (1.3% of variance). Obviously, this mode has also dominating seasonal character, but the phase is shifted in relation to the first mode: positive amplitudes appear during the spring warming and negative ones during the autumn cooling. The amplitudes of third and fourth mode (presenting transverse and longitudinal gradients, respectively) are related to the wind forcing over the region.

First SSS mode (not shown) is also of the same sign like SST, but it covers only 34.0% of variance and its spatial variations are larger. It has highest values near the eastern freshwater sources and in the western saline water area. Second mode (Fig. 1b, 16.0% variance) presents the transverse gradients in the basins and third mode (11.4%) the longitudinal gradients.

Tests were made with the monitoring data available from the HELCOM/ICES database. Superposition of three

first modes was considered acceptable for both SST and SSS (Fig. 2) by the "representativeness" criteria.

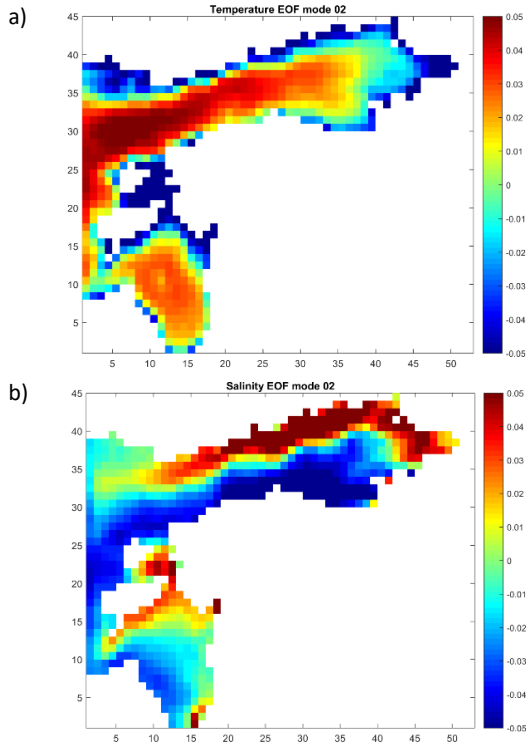

Figure 1. Second EOF modes for SST (a) and SSS (b).

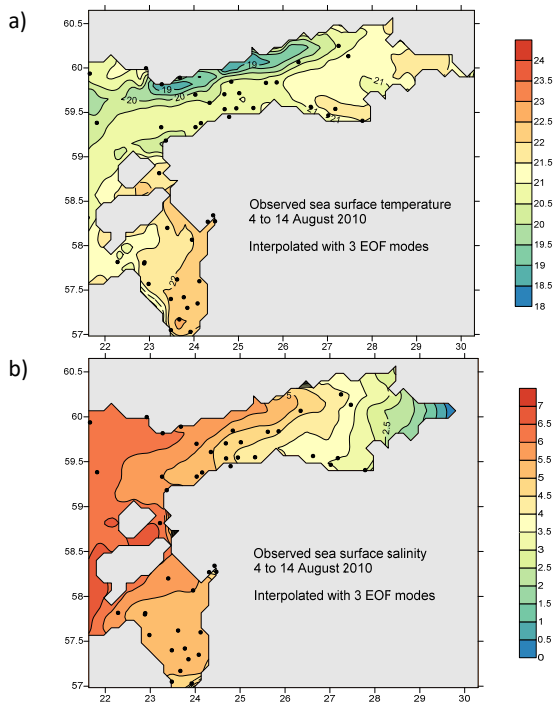

Figure 2. Maps of SST (a) and SSS (b) reconstructed from the HELCOM/ICES data from 4 to 14 August 2010, using the superposition of three first EOF modes. Dots represent observation points.

4. Discussion and outlook

It is often considered that one of the weakest points of EOF method is sensitivity of the results on the definition of the area. The modes, calculated over the whole area of the multi-basin sea like the Baltic and Mediterranean, tend to have variance distributed over a large number of modes, which makes practical implementation of the method difficult.

We have demonstrated high convergence of modes in the sub-regional implementation: three first modes cover 99% of variance for SST and 61.4% for SSS. Such sub-regions have been identified by geographic criteria already centuries ago. Regarding physical and ecosystem dynamics, the sub-regions have similar (nearly uniform) atmospheric forcing and distinct sources of freshwater and saline water, both acting upon specific basin geometries, which determine spreading of low- and high-saline waters, differential heating and cooling, upwelling-downwelling patterns and other processes of large-scale effect. First tests have shown that such sub-regions may have slightly overlapping boundaries; then individual sub-regional patterns can be "clued" together by spatial filtering. In this process, it is helpful that the amplitudes of modes are well correlated in time: in one-month time lag, both the first SST and SSS modes have correlation above 0.7, while "wind-dependent" third and fourth SST modes are not correlated.

This study came up from the data assimilation problem (Zujev and Elken, 2018), where forecasts by free model run exhibited large scale errors, mainly of seasonal character which are well correlated over large distances. This error has to be removed prior using the assimilation algorithms on the local scales.

For the coming conference, the above data reconstruction method will be further implemented to bigger number of Baltic Sea sub-regions, based on the model data from Copernicus programme reanalysis of the Baltic Sea state during 1989-2015. The method will be tested for joint inclusion of shipborne monitoring, ferrybox, coastal station, buoy and remote sensing data.

It is also challenging to find further relations of the EOF amplitudes and spatial patterns to atmospheric and terrestrial forcing factors and to the exchange processes between the sub-basins.

References

Lagemaa, P. (2012) Operational forecasting in Estonian marine waters, TUT Press, B128, 130 pp.

Zujev, M., Elken, J. (2018), Testing marine data assimilation in the northeastern Baltic using satellite SST products from Copernicus Marine Environment Monitoring Service, Proceedings of the Estonian Academy of Sciences (in press).

Atmospheric Forcing of Major Baltic Inflows in a 750 Years Simulation

Claudia Frauen[1], Florian Börgel[1] and H.E. Markus Meier[1]

[1] Leibniz Institute for Baltic Sea Research Warnemünde, Rostock, Germany (claudia.frauen@io-warnemuende.de)

1. Introduction

The Baltic Sea is a semi-enclosed shallow sea in northern Europe with a complex marine ecosystem. The salinity of the Baltic Sea is determined by river runoff, net precipitation and saltwater inflows from the North Sea. Of special importance are so-called Major Baltic Inflows (MBIs), through which large amounts of salty and oxygen-rich water are transported into the deeper parts of the central Baltic. They occur on average once every year, but there have also been longer periods without any MBIs.

The occurrence of MBIs depends strongly on the short-term local atmospheric conditions, which are driven by the large-scale atmospheric circulation (Matthäus and Schinke, 1994), but also in the months preceding the main inflow season differences can be found in the atmospheric circulation patterns between seasons with and without MBIs (Schinke and Matthäus, 1998). These early studies were based on relatively short observational records. To understand in depth the role of local and large-scale atmospheric forcing both in the months preceding the main inflow season and in the weeks before and during an event longer time series are needed, which only exist from climate model simulations.

2. Model and Data

To study the role of atmospheric forcing for the occurrence of MBIs an 850 years long transient climate simulation under pre-industrial conditions, which has been performed by Schimanke et al. (2016) with the regional ocean model RCO (Meier et al. 2003), has been analyzed. To force the model data from a paleo simulation performed with the global coupled model ECHO-G (Legutke and Voss, 1999) has been downscaled with the regional atmospheric model RCA (Samuelsson et al., 2011). The first 100 years of the simulation have been discarded as spin-up.

3. Detection of MBIs

The criterion for the occurrence of an MBI in the observational dataset is a period of at least 5 days with the bottom salinity at the station Darss Sill larger than 17 g/kg (Matthäus and Franck, 1992). A corresponding criterion for model data would mean that the volume of water with a salinity larger than 17 g/kg in the Arkona basin must be larger than 50km^3 (Meier and Kauker, 2003). Since the model data is only two-daily, it is required that this criterion is met for three consecutive timesteps. As an example a 50 years time slice is shown in Figure 1, where years with and without MBIs are indicated. It can be seen that the model also simulates longer periods without MBIs, like here e.g. 7 years, as happened also during the recent observational period.

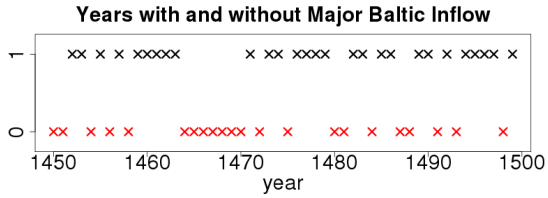

Figure 1. Exemplary 50 years time slice with black crosses indicating years with MBI and red crosses indicating years without MBIs.

4. Role of Atmospheric Forcing

The atmosphere plays an important role for the occurrence of MBIs both in the months preceding the main inflow season and in the weeks before and during individual events.

To study the role of the large-scale atmospheric circulation in the months before the main inflow season composites of monthly means of different atmospheric variables, like e.g. sea level pressure (SLP), have been calculated for years with and without MBIs. As an example Figure 2a shows the average SLP over the whole simulation period for the month of October, which is before the main inflow season in winter. On average there is lower pressure over Scandinavia and higher pressure to the south. During years with an MBI this pressure gradient is reduced (Fig. 2b), which would correspond to less westerly winds.

On the shorter time scale the local atmospheric conditions are of greater importance and composites have been calculated to show e.g. the role of the local wind on a daily time scale for the 30 days preceding all MBIs and the 20 days after the beginning of an event.

References

Legutke, S. and R. Voss (1999) The Hamburg atmosphere-ocean coupled circulation model ECHO-G, DKRZ-Report, German Climate Computer Centre (DKRZ), Hamburg, Germany

Matthäus, W. and H. Franck (1992) Characteristics of major Baltic inflows—a statistical analysis. Continental Shelf Research, 12(12), 1375-1400.

Matthäus, W. and H. Schinke (1994) Mean atmospheric circulation patterns associated with major Baltic inflows. Deutsche Hydrografische Zeitschrift, 46(4), 321-339

Meier, H. E. and F. Kauker (2003) Modeling decadal variability of the Baltic Sea: 2. Role of freshwater inflow and large-scale atmospheric circulation for salinity. Journal of Geophysical Research: Oceans, 108(C11)

Meier, H. E. M., R. Döscher, and T. Faxen (2003) A multiprocessor coupled ice-ocean model for the Baltic Sea: application to salt inflow, J. Geophys. Res., 108, 3273

Samuelsson, P., C. G. Jones, U. Willen, A. Ullerstig, S. Gollvik, U. Hansson, C. Jansson, E. Kjellström, G. Nikulin, and K. Weyser (2011) The Rossby Centre regional climate model RCA3: model description and performance, Tellus A, 63, 4–23

Schinke, H. and W. Matthäus (1998) On the causes of major Baltic inflows—an analysis of long time series. Continental Shelf Research, 18(1), 67-97.

Schimanke, S. and H. M. Meier (2016) Decadal-to-Centennial Variability of Salinity in the Baltic Sea, Journal of Climate, 29(20), 7173-7188

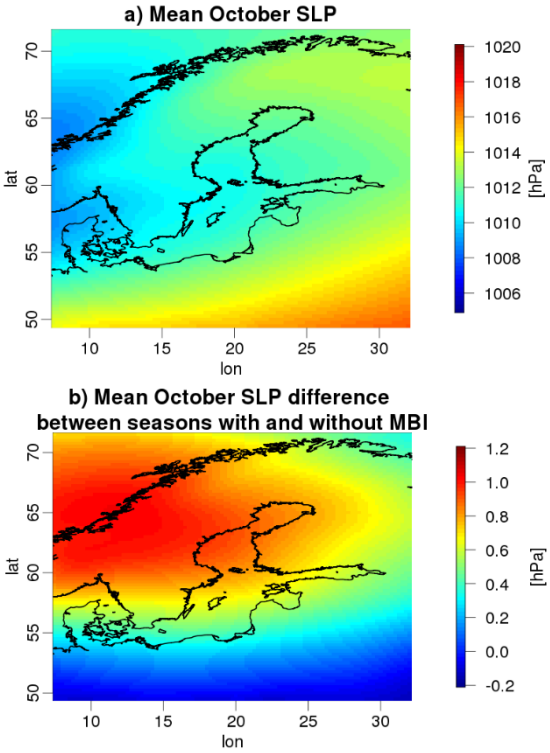

Figure 2. a) 750 years mean sea level pressure for the month of October and b) Difference in October mean sea level pressure for years (July-June) with and without MBIs. Unit [hPa].

Haline convection due to sea ice brine rejection in the Northern Baltic Sea

Céline Gießе[1], H. E. Markus Meier[1,2]

[1] Leibniz Institute for Baltic Sea Research Warnemünde, Germany (celine.giesse@io-warnemuende.de)

[2] Swedish Meteorological and Hydrological Institute, Norrköping, Sweden

1. Abstract

The aim of this study is to investigate the role of haline convection due to sea ice brine rejection in the water mass formation and circulation of the Baltic Sea. The main research questions are to what extent and under which conditions brine release in the Northern Baltic Sea (Gulf of Bothnia and Gulf of Finland) leads to deep water formation, and whether there is an inflow of this water into the Baltic proper.

Simulations of the Baltic Sea circulation with and without the effect of brine rejection are conducted using the General Estuarine Transport Model (GETM, Burchard and Bolding, 2002) and compared to each other. The brine release is simulated via an "artificial salt source", i.e. negative freshwater fluxes are prescribed as a surface boundary condition. The pathways of the different water masses are tracked using passive tracers.

In a second step, the simulation is repeated with a subgrid-scale brine rejection parametrization, based on ideas of Duffy and Caldeira (1997) and Nguyen et al. (2009), implemented into the GETM model. With the parameterization, rejected salt is directly transported down to greater depths and it is expected to yield much more realistic results due to a reduction of excessive grid-scale vertical mixing.

With the brine rejection parameterization running, it is further planned to perform a sensitivity study in order to investigate the importance of haline convection in different climate states. Therefore, experiments with varying strengths and patterns of freshwater fluxes, being representative for (a) an average winter in the present climate state, (b) a severe winter in the present climate state and (c) an average winter during the Little Ice Age, are conducted and evaluated.

2. Introduction

The process of brine release associated with the formation of sea ice is a major source of deep water formation in the polar regions and an important driver of the global thermohaline circulation. When sea water freezes, salt accumulates into so-called brine droplets, which are gradually rejected back into the ocean. The increase of near-surface water salinity leads to buoyancy fluxes destabilizing the water column and resulting in (possibly deep) haline convection. The major part of sea ice formation and with that brine rejection occurs in openings of the sea ice which can be either induced by ice motion (leads) or by persistent winds or upwelling of warm water (polynyas). The rejected salt is sinking down as plumes with a typical horizontal extent of several hundred meters (Nguyen et al., 2009).

While in the Arctic and Antarctic ocean the process has been studied extensively, not much attention has been drawn to haline convection in temperate seas as the Baltic Sea. The latter freezes regularly each winter with largely varying ice extents ranging from 50.000 – 420.000 km^2 (Seinä and Palosuo, 1996) and typical ice thicknesses of 65-80 cm in the Bothnian Bay (Alenius et al., 2003).

In 1993, Marmefelt and Omstedt presented a study concluding from rough estimations based on measured salinity profiles and typical ice thicknesses that deep haline convection is not likely to occur frequently in the entire water mass of the Gulf of Bothnia. As localized effects like the formation of salt plumes in leads are neglected in these estimations, it seems worthwhile to re-investigate this process for the Baltic Sea using a sophisticated, high-resolution circulation model.

3. Method

The simulations presented in this study are conducted with the General Estuarine Transport Model (GETM) with a Baltic Sea setup of 1 nm resolution. The GETM model uses vertically adaptive coordinates, which is favorable for the addressed problem because numerical mixing is substantially reduced as shown by Gräwe et al. (2015).

The GETM model is coupled to a simple, thermodynamic sea ice model which does not include fluxes between the water and sea ice. Instead, the brine release is simulated by prescribing negative freshwater fluxes as a surface boundary condition, which effectively leads to an increase of sea surface salinity. The strengths, temporal and spatial patterns of the input fluxes are chosen based on output data of simulations from Neumann et al. (2017) conducted with the Modular Ocean Model (MOM version 5.1, Griffies et al., 2004) using a 3-nm-resolution Baltic Sea setup. The MOM model includes a dynamic-thermodynamic ice model yielding realistic ice data for the Baltic Sea.

In order to track the pathways of the different water masses, six passive tracers are introduced into the model. Each is marking the surface water of a different area, namely the shallow (up to 30 m) and deep water areas of the Bothnian Bay, Bothnian Sea and Gulf of Finland as shown in Fig. 2.

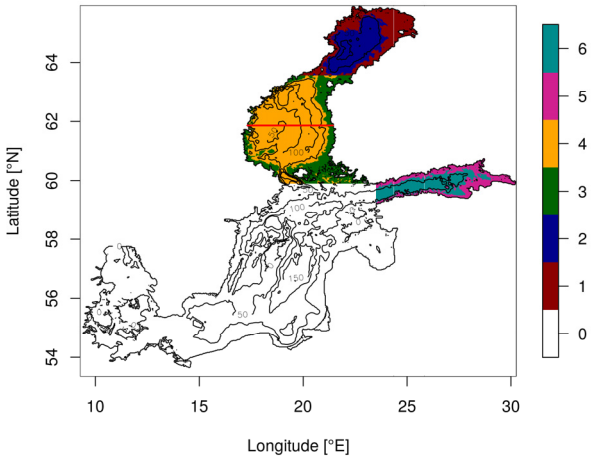

Figure 2. Model domain and mask of the six different passive tracers used to track the pathways of the water masses. The red line marks a transect used for evaluation.

4. Preliminary results

By tracking the water masses with passive tracers, it can be seen that a mean cyclonic circulation takes place in each sub-basin and how the water from the different sub-basins is entering the Baltic proper (not shown here). The comparison of

the simulation with brine rejection to the control simulation without brine rejection shows significant differences in the tracer distribution during the winter/brine rejection season, which are reduced afterwards on a timescale of a few months. In both simulations, there is a sinking down of the surface water marked by tracers, but in the “brine rejection”-simulation the tracer penetrates down to greater depths due to the additional negative freshwater fluxes leading to a higher surface buoyancy forcing. This can be seen for instance in Fig. 3, showing the concentration of tracer 4 in the Bothnian Sea cross-section for both simulations as well as the difference of both concentrations.

Nonetheless, the results also show that even with brine rejection included there is no real deep water formation happening. Despite the quite high horizontal resolution of one nautical mile, the model resolution is still to coarse to depict the process of brine rejection correctly with the associated formation of convective subgrid-size plumes. Instead the rejected salt is spread across the entire surface grid cell leading to large-scale convection, i.e. the instable water masses are mixed down until a stable configuration is reached. This emphasizes the need for a subgrid-scale brine rejection parameterization, distributing the rejected salt down more realistically.

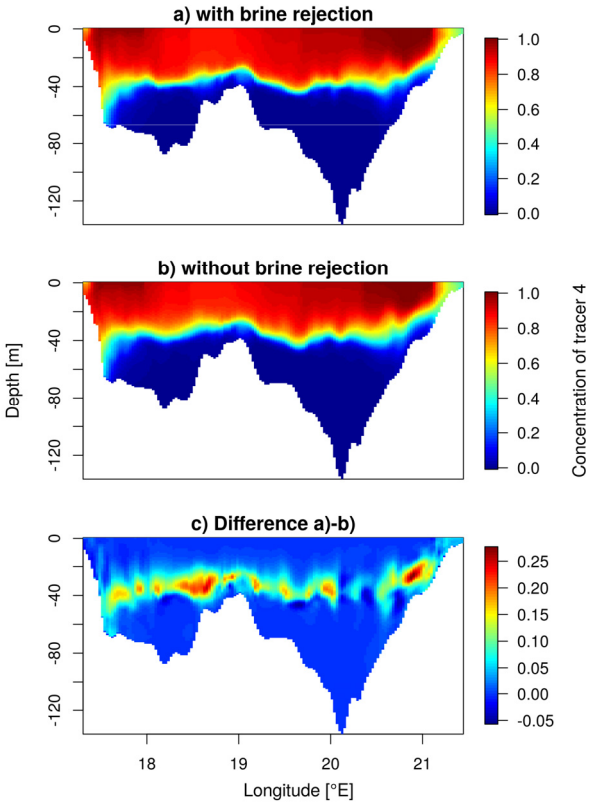

Figure 3. a) Mean concentration of tracer 4 (originating at sea surface of Bothnian Sea deep waters) in January 1987 in a zonal transect across the Bothnian Sea (see Fig. 2) for the simulation with brine rejection. b) Same as a) for simulation without brine rejection. c) Differences of tracer concentrations a) and b), i.e. with and without brine rejection.

References

Burchard, H., K. Bolding (2002), GETM: A General Estuarine Transport Model; Scientific Documentation, Tech. Rep. EUR 20253 EN, Eur. Comm

Duffy, P. B., K. Caldeira (1997), Sensitivity of simulated salinity in a three-dimensional ocean model to upper ocean transport of salt from sea-ice formation, Geophysical Research Letters, 24(11), 1323-132

Nguyen, A. T., D. Menemenlis, R. Kwok (2009), Improved modeling of the Arctic halocline with a subgrid-scale brine rejection parameterization, Journal of Geophysical Research: Oceans, 114(C11)

Seinä, A., E. Palosuo (1996), The classification of the maximum annual extent of ice cover in the Baltic Sea 1720–1995, Meri, 27, 79-91

Alenius, P., A. Seinä, J. Launiainen, S. Launiainen (2003), Sea ice and related data sets from the Baltic Sea AICSEX: Metadata report

Marmefelt, E., A. Omstedt (1993), Deep water properties in the Gulf of Bothnia, Continental Shelf Research, 13(2-3), 169-187

Gräwe, U., P. Holtermann, K. Klingbeil, H. Burchard (2015), Advantages of vertically adaptive coordinates in numerical models of stratified shelf seas, Ocean Modelling, 92, 56-68

Neumann, T., H. Radtke, T. Seifert (2017), On the Importance of Major Baltic Inflows for oxygenation of the central Baltic Sea, Journal of Geophysical Research: Oceans, 122(2), 1090-1101

Griffies, S. M., M. J. Harrison, R. C. Pacanowski, A. Rosati (2004), A technical guide to mom4 gfdl ocean group technical report no. 5,

Hydrophysical conditions in the southern part of the Baltic Sea in summer and autumn seasons of 2016-2017

Maria Golenko, Paka V., Kondrashov A., Korzh A., Zhurbas V.

Shirshov Institute of Oceanology, Russian Academy of Sciences, Moscow, Russia (m.golenko@yahoo.com)

In August-September 2016, June-July, and October 2017, the 32nd , 34th, and 36th cruises of the r/v "Academic Strakhov" took place. Detailed survey of the water structure in the southern and central parts of the Baltic Sea had been carried out. Special attention was paid to the bottom layer, in which the inflow waters spread. To get quality data each cast should reach the bottom. Therefore, the measurement procedure was changed: instead of the scanning from the moving ship (U-tow CTD), measurements at densely spaced drift stations were made with guaranteed bottom reaching for each sounding.

A number of repeated transects from the Arkona to Gdansk Basins and to the entrance into the Gotland Basin were made. An elevation of the halocline in the Bornholm Basin above the crest of the Slupsk Sill was estimated owing its special role for the saline water penetration into the Slupsk Channel. Particular attention was paid to the Slupsk Sill, where an overflow is formed under favorable conditions. In summer 2016, the overflow was absent. In 2017, signs of the overflow were discovered, and for its description, special surveys were performed using the microstructure profiler. Longitudinal and transverse sections relative to the crest of the sill were made, which allowed to determine boundaries of the overflow current and to estimate the entrainment velocity. The work was supported by the state assignment No. 0149-2018-0012.

Decadal variations in barotropic inflow characteristics and their relationship with Baltic Sea salinity variability

Katharina Höflich[1] and Andreas Lehmann[1]

[1] GEOMAR Helmholtz Centre for Ocean Research Kiel, Germany (khoeflich@geomar.de)

1. Motivation

The semi-enclosed Baltic Sea is a permanently stratified system, and has only restricted water exchange with the world ocean. Saltwater inflows that replace existing deepwater occur only sporadically, and depths below the permanent halocline are recurrently subject to both oxygen and salinity declines. During the past century several prolonged periods of stagnation happened, with harmful consequences for the habitats of higher trophic marine life. Variations in Baltic Sea deepwater conditions can in general be regarded as record of variations in the water exchange between North Sea and Baltic Sea (Matthäus, 1995) and comprehension of the latter therefore forms an important base in understanding system-wide variability in physics and biogechemistry.

2. Related Work

A strong driver of salinity variability in the central Baltic Sea is the occurrence of major saltwater inflows. These can be understood as subset to barotropic inflows which happen in response to a specific sequence of atmospheric circulation patterns (Lehmann and Post, 2015) and clustering of deep cyclones in space and time (Lehmann et al., 2017). The atmospheric viewpoint from these studies was recently extended by investigating the impact of hydrography and total freshwater supply on the occurrence of highly saline barotropic inflows. A mechanistic explanation was proposed that included both the salinity in the Danish Straits, and the evolution of the atmospheric forcing during the inflow period. The latter projects onto the magnitude and rapidness of inflow events as deduced from the sea-level at Landsort, where higher salinities of the inflowing water were found to be related to larger total sea-level changes and a greater rapidness of the inflow process.

3. Goals

The aim of this study is to establish the potential relationship between observed Baltic Sea salinity variations during the last century and decadal variations in barotropic inflow characteristics in terms of magnitude and rapidness of the inflow process. The question if the mechanistic framework developed during previous work can be used to understand the occurrence of stagnation periods is investigated. To this end, the analysis of large barotropic inflows is applied and extended.

4. Methods

Variations in barotropic inflow characteristics are studied based on the observed sea-level at Landsort provided by the Swedish Meteorological and Hydrological Institute (http://opendata-download-ocobs.smhi.se/explore/) covering the 131-year period since November 1886. The sea-level series is low-pass filtered using a Butterworth filter with cutoff period 44.1 days and barotropic inflows are identified according to local extrema. The analysis of barotropic inflow characeristics is supplemented by simulated sea-levels, currents and hydrographic fields provided by the three-dimensional hydrodynamic Baltic Sea Ice Ocean Model (e.g. Lehmann et al., 2014 and references therein). The setup aims at realistic representation of Baltic Sea variability and is currently forced by ERA-Interim reanalysis data (Dee et al., 2011). The total simulation period covers the 38 years between 1979 and 2017.

5. Preliminary Results

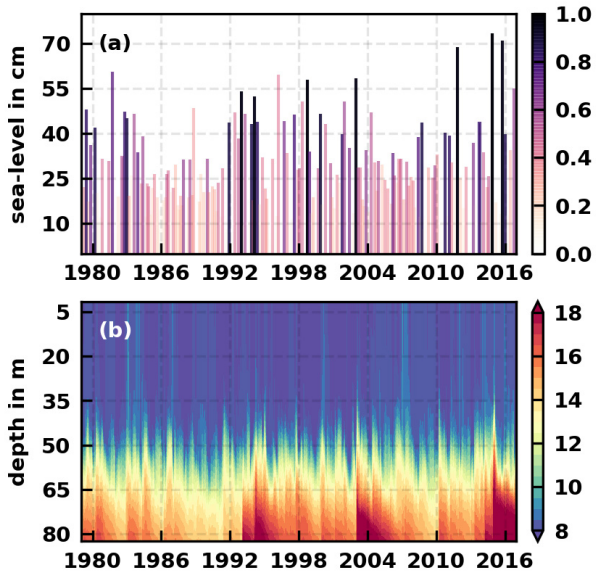

Figure (1a) Barotropic inflow activity during the 38-year period 1979 to 2017 based on the observed and low-pass filtered sea-level at Landsort. The y-axis shows the total Landsort sea-level change in cm, the colorization ranks the single inflows after their strength. Figure (1b) Salinity in the Bornholm Basin as simulated by the Baltic Sea Ice Ocean Model for the same period. Units are in PSU.

A non-dimensional index developed to summarize the differences in magnitude and rapidness of barotropic inflows is shown in Figure 1a. It has been calculated based on percentiles of score and is confined to values between zero and one. During the simulation period several extreme inflow events (as indicated by the darker color) can be observed, some of which coincide with observed strong major saltwater inflows (see e.g. Jan/1993, Jan/2003, and Dec/2014). The corresponding simulated Bornholm Basin salinity is shown in Figure 1b. Visible is the sporadic increase in bottom layer salinity associated with the inflow of saltwater through the Danish Straits. Stagnation periods are associated with a freshening of the bottom layer, where during the simulation period a pronounced decrease is found e.g. during the 1990s. In the literature, this stagnation period is described as the most severe during the last century. Associated is a drop in average barotropic inflow strength, which indicates a significant contribution of atmospheric forcing in causing absence of saltwater inflows.

6. Outlook

In this study, the causal relationship between Baltic Sea salinity variations and barotropic inflow activity will be investigated due to analysing output from an ocean model. Based on this observed Baltic Sea salinity variations will be discussed with respect to decadal variations in barotropic inflow characteristics

as deduced from the observed sea-level at Landsort. Potential large-scale impacts upon the development of regional weather patterns causal to the occurrence of barotropic inflows are discussed based upon the available literature.

References

Dee, D. P., and others (2011) The ERA-Interim reanalysis: configuration and performance of the data assimilation system, Quarterly Journal of the Royal Meteorological Society, 137, pp. 553-597

Johansson, J. (2017) Total and Regional Runoff to the Baltic Sea, Baltic Sea Environment Fact Sheets, provided at http://www.helcom.fi/baltic-sea-trends/environment-fact-sheets/hydrography/total-and-regional-runoff-to-the-baltic-sea/

Lehmann, A., Höflich, K., Post, P., Myrberg, K. (2017) Pathways of deep cyclones associated with large volume changes and major Baltic inflows, Journal of Marine Systems, Volume 167, pp. 11-18

Lehmann, A., Post, P. (2015) Variability of atmospheric circulation patterns associated with large volume changes of the Baltic Sea, Advances in Science and Research, 12, pp. 219-225

Lehmann, A., Hinrichsen, H.-H., Getzlaff, K., Myrberg, K. (2014) Quantifying the heterogeneity of hypoxic and anoxic areas in the Baltic Sea by a simplified coupled hydrodynamic-oxygen consumption model approach, Journal of Marine Systems, 134, pp. 20-28

Matthäus, W. (1995) Natural variability and human impacts reflected in long-term changes in the Baltic deep water conditions — A brief review, Deutsche Hydrografische Zeitschrift, 47(1), pp. 47-65

Long-term changes in stratification in the Baltic Sea

Taavi Liblik[1], Urmas Lips[1]

[1] Department of Marine Systems, Tallinn University of Technology, Tallinn, Estonia (Taavi.liblik@ttu.ee)

1. Introduction and results

The ecosystem of the Baltic Sea has been described as very vulnerable to the changes in temperature and salinity. Moreover, consequences of eutrophication, such as toxic algae blooms or hypoxia are linked to the hydrography.

Due to small volume of the Baltic Sea, the dynamics here is largely controlled by the prevailing air masses and therefore changes in atmospheric conditions impact the Baltic Sea quite rapidly. The rise of air temperature in the Baltic region and corresponding rise of water temperature in recent decades have been detected and reported by numerous studies. Most of the studies are based on the satellite-derived sea surface temperature or (near) coastal time-series. Long-term trends and variability of temperature and salinity in the subsurface layers are largely unknown.

The aim of the present study was to investigate the decadal variability of temperature, salinity and stratification during last 30 years. Available data from ship-based and autonomous devices were compiled. The data set under investigation includes data from ship-based CTD, thermosalinographs (ferryboxes) and moored/fixed instruments. Eight time-series areas were selected for analysis (Fig. 1).

The warming observed by satellites can be confirmed by temperature trend in the surface layer in most of the selected areas by a magnitude of 0.4-0.5 °C decade^{-1}. This statistically significant trend can be observed in the upper 10-20 m layer and is strongest in most of the basins in autumn. Similar temperature trend can be detected in the deep layer in several basins. No significant temperature trend can be found in the cold intermediate layer.

Surface salinity trend in most of the basins is negative while salinity in the deeper layers has been increased in recent decades. Salinity changes in the deep layers have rather pulsating nature: it is strongly related to the so-called Major Inflows (1993, 2003 and 2014-2016).

As a consequence of freshening and warming in the upper layer, the density gradient through the seasonal thermocline has increased. Density of the deep layer and pycnocline strength between cold intermediate layer and deep layer has increased in most of the basins. An exception is the Gulf of Bothnia, where the permanent halocline is absent and density has decreased in the whole water column. In conclusion, stratification has become stronger in most of the Baltic Sea during last 30 years.

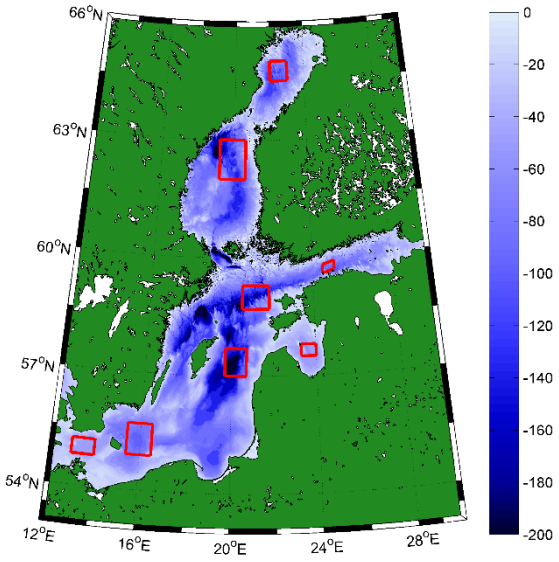

Figure 1. Bathymetry of the Baltic Sea and eight time-series areas.

The Słupsk Sill overflow – mixing hot spot of eastward spreading saline water

Volker Mohrholz[1] and Toralf Heene[1]

[1] Leibniz-Institute for Baltic Sea Research Warnemünde, Germany (volker.mohrholz@io-warnemuende.de)

1. Overturn circulation and mixing

On longer time scales the brackish character of the Baltic is maintained by its mean estuarine overturn circulation. Their main components are the inflow of saline water from the North Sea, lateral spreading of saline water towards the central Baltic, upwelling and diapycnal mixing of saline water into the upper layer, fresh water surplus and surface outflow of less saline water through the Danish Straits. Some parts of the overturn circulation are well investigated (Meier et al., 2006; Reissmann et al., 2008), but there are also significant gaps in our present knowledge. An important, but not fully understood process is the entrainment of ambient low saline water into the saline bottom water along its pathway to the central Baltic. Neumann et al. (2017) have demonstrated the crucial role of entrainment for oxygen supply to the deep basins.

The topography of the Baltic is characterized by the cascade like alignment of basins and sills. In the basins entrainment occurs mainly at the halocline due to shear instability and diapycnal mixing and at locations where the halocline hits the sloping sea floor. The sill overflows between the basins are occasionally another hot spot for the transformation of spreading saline water. This study is focused on the mixing processes at the Słupsk Sill during an active overflow of saline water, follow-up a minor barotropic inflow from end of February 2017.

2. The Słupsk Sill

The Słupsk Sill with 55m depth separates the Bornholm Basin, maximum depth of 95m, from the Słupsk Furrow in the east (Figure 1). The sill depth determines the usual halocline depth in the Bornholm basin of 55 to 60m and the volume of the permanent saline bottom water pool.

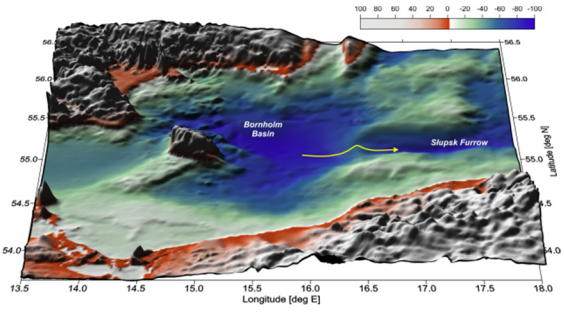

Figure 1. Map of study area in the western Baltic. The yellow line indicates the Słupsk Sill overflow and the location of MSS transect.

The overflow of the Sill can be triggered by an uplift of the halocline due to upwelling, internal Kelvin waves or an inflow of dense water from the Arkona Basin. There exist a number of observations and model studies of the Słupsk Sill overflow, which highlight its pulse like behavior and submesoscale structure (eg. Piechura and Beszczyńska-Möller, 2004; Zhurbas et al., 2012). However, direct observations of turbulence and mixing in an active overflow at the sill are rare.

3. Observations

In the second half of February 2017 a minor barotropic inflow event transported approximately 77km^3 saline water (ca. 1.2Gt salt) into the western Baltic. After reaching the Bornholm Basin the inflow waters lift the halocline in the basin from 55m to 48m depth. This forced for a limited time a steady overflow of the Słupsk Sill.

During the cruise EMB150 of the RV Elisabeth Mann-Borgese in March 2017 a high resolution hydrographic transect was performed at the Słupsk Sill. A new measurement strategy was applied, using a free falling microstructure profiler (MSS) with an attached high resolution current profiler (Aquadopp). This provided spatially consistent, contemporary observations of shear microstructure, density stratification and local vertical current shear. Combining these parameters the local gradient Richardson number was estimated.

The transect covers the eastern part of the Bornholm Basin, the Słupsk Sill and the entrance of the Słupsk Furrow on 24./25. March 2017. The transect consists of 291 single MSS/Aquadopp profiles with spatial resolution of 0.5m vertically, and 250m horizontally.

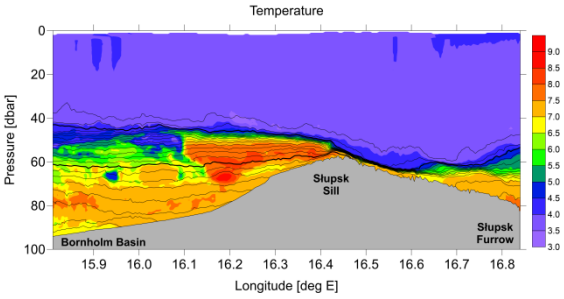

Figure 2. Temperature (contour) and salinity (isolines) distribution along a transect from the Bornholm basin across the Slupsk Sill into the Slupsk Furrow. Data were gathered with a microstructure profiler (MSS) on 24./25. March 2017.

The density stratification in the Bornholm Basin was controlled by a strong vertical salinity gradient (Figure 2). The salinity increases from 9g/kg near the halocline to 18.8 g/kg at the bottom. The temperature distribution indicates the complex water mass structure in the Bornholm Basin due to several subsequent inflow events from late summer 2017 to February 2018. Thus, the temperature can be used as a water mass tracer. The saline overflow of the Słupsk Sill was feed by a warm water body of 8°C originating from a minor inflow in autumn. Since the halocline in the Bornholm basin was 7 to 8m above the sill depth the overflow was gravity forced. After passing the sill crest the flow was accelerated, and the saline bottom layer was compressed to a thin layer of only 3 to 4m thickness. The overflow water entered the dense water body of the

Słupsk Furrow at a depth of 64m. Here it was sandwiched and mixed with the saline deep water of the Słupsk Furrow.

4. Internal hydraulic jump

The saline overflow observed at the Słupsk Sill in March 2017 was hydraulically controlled. It is characterized by three subsequent dynamical stages.

Upstream of the sills crest the saline water is accelerated by the horizontal baroclinic pressure gradient across the sill. The increasing eastward velocity enhances the vertical current shear at the top and the bottom of the overflowing saline water body. The increased shear leads to TKE production near the halocline and the bottom, depicted by increasing TKE dissipation (Figure 3). Till the sill crest the flow remains subcritical with Froude number below 1.

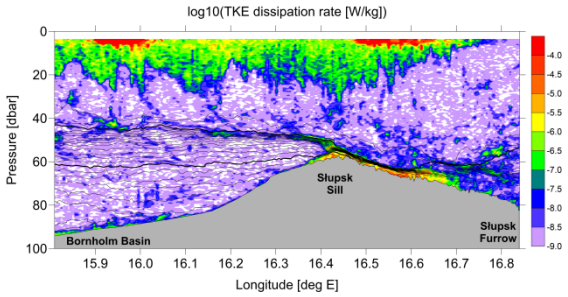

Figure 3. Dissipation rate of turbulent kinetic energy (contour) and salinity (isolines) distribution along a transect from the Bornholm basin across the Slupsk Sill into the Slupsk Furrow. Data were gathered with a microstructure profiler (MSS) on 24./25. March 2017.

Above the crest the overflow becomes super critical (Froude number > 1). This is accompanied with a steep jump of the interface between saline water and the upper layer, and an enhanced salinity gradient at the top of the inflowing saline layer. The TKE dissipation rates in the supercritical flow are large and increased by about one order of magnitude from $5*10^{-6}$ W/kg near the sill crest to $5*10^{-5}$ W/kg near the halocline of the Słupsk Furrow. The gradient Richardson number is well below 0.25 at the top and the bottom of the saline layer. This indicates the development of shear instabilities and the entrainment of upper layer water into the saline overflow.

The super critical flow hits the halocline in the Słupsk Furrow at about 65m depth and forms an internal hydraulic jump. Here the flow becomes subcritical again. In the wake of the super critical flow the TKE dissipation remains at a high level. The strong halocline of the super critical flow regime fans out vertically.

Towards east the salinity stratification weakens and the TKE dissipation is decreasing. However, it remains at about 10^{-8} W/kg which is significantly higher than in the deep water range of the Bornholm Basin.

From the sill crest to the end of the super critical flow the mean salinity in the saline overflow decreased from 15g/kg to 14g/kg. The volume of the inflowing saline water body increased by about 18%, assuming that entrainment was fed by the overlaying water with 8.5 g/kg salinity. A further reduction of bottom water salinity to about 13.5g/kg was observed in the hydraulic jump. The rough estimate for the total entrainment into the saline overflow at the sill is a volume surplus of approximately 30%.

5. Conclusions

Mixing and entrainment of ambient water into inflowing saline water occurs mainly at distinct hot spots along the pathway to the central Baltic Basins. The overflow at Słupsk Sill is one of these mixing hotspots. The observed TKE dissipation rates at the Sill exceed the TKE dissipation in the adjacent Bornholm Basin and Słupsk Furrow by two orders of magnitude. Mixing in the Bornholm Basin was weak, except at some locations at the halocline where a Ri < 0.25 indicate the development of shear instabilities and enhanced dissipation rates.

The observed overflow at the Słupsk Sill was hydraulically controlled. This may be the typical situation after an inflow event when the halocline depth in the Bornholm Basin is shallower than the sill depth.

The energy for mixing and entrainment is provided by the transformation of potential energy into kinetic energy of overflowing saline water, and finally into TKE. This is in contrast to mixing processes in the Basin where diapycnal mixing increases the potential energy.

The overflow at the Słupsk Sill consists of a super critical flow followed by an internal hydraulic jump. Mixing and entrainment at the super critical part can be attributed to generation of shear instabilities between the inflowing saline water and the overlaying water. At their interface the estimated gradient Richardson number is well below 0.25. Further mixing and entrainment occurred in the hydraulic jump due to dynamically forced overturns and shear stress.

The total entrainment of ambient water into the inflowing saline water at the Słupsk Sill was estimated with about 30% of the inflow volume.

References

Meier, H.E.M., Feistel, R., Piechura, J., Arneborg, L., Burchard, H., Fiekas, V., Golenko, N., Kuzmina, N., Mohrholz, V., Nohr, Ch., Paka, V.T., Sellschopp, J., Stips, A., Zhurbas, V., (2006) Ventilation of the Baltic Sea deep water: A brief review of present knowledge from observations and models. Oceanologia, 48 (S), pp. 133–164.

Neumann, T., Radtke, H., Seifert, T., (2017) On the importance of Major Baltic Inflows for oxygenation of the central Baltic Sea. Journal of Geophysical Research: Oceans, 122(2), pp. 1090-1101.

Piechura, J., Beszczynska-Möller, A., (2003) Inflow waters in the deep regions of the southern Baltic Sea - transport and transformations. Oceanologia, 45(4), pp. 593-621

Reissmann, J.H., Burchard, H., Feistel, R., Hagen, E., Lass, H.U., Mohrholz, V., Nausch, G., Umlauf, L., Wieczorek, G., (2009) Vertical mixing in the Baltic Sea and consequences for eutrophication – A review. Progress in Oceanography, 82, pp. 47-80, doi:10.1016/j.pocean.2007.10.004

Zhurbas, V., Elken, J., Paka, V., Piechura, J., Väli, G., Chubarenko, I., Golenko, N., Shchuka, S., (2012). Structure of unsteady overflow in the Słupsk Furrow of the Baltic Sea. Journal of Geophysical Research, Oceans 117(C4), pp. 1-17

The study has been carried out in frame of the long term observation program of the Leibniz-Institute for Baltic Sea Research. We greatly acknowledge the technical assistance of Sebastian Beier and the support by the captain and crew of RV Elisabeth Mann Borgese.

Major Baltic Inflow statistics - revisited

Volker Mohrholz[1]

[1] Leibniz-Institute for Baltic Sea Research Warnemünde, Germany (volker.mohrholz@io-warnemuende.de)

1. Major Baltic Inflows

Major Baltic inflow events (MBI) transport large amounts of saline water into the Baltic. They are the solely source for deep water ventilation in the central Baltic basins, and control to a large extent the environmental conditions below the halocline. The available time series of MBI frequency and intensity depict strong decrease of MBI frequency after the 1980ies, followed by long lasting stagnation periods in the central Baltic basins.

However, the expected decrease in mean salinity of the Baltic was not observed. This was explained by a compensation effect of increased frequency of baroclinic saline inflows. Also the frequency of large volume changes of the Baltic has not changed (Lehmann and Post, 2015), and recent model studies predict a slight increase of MBI frequency with warming climate. Additionally, the lack of minor MBI since the early 1980ies pointed to a bias in the MBI time series.

2. A revised time series

Triggered by the exceptional MBI in December 2014 (Mohrholz et al., 2015) the MBI time series was revisited. Using long term data series of sea level, river discharge, and salinity from the Belt and Sound a continuous time series of barotropic inflows was constructed for the period from 1890 till present (DS5). A comparison with the MBI time series FM96 of Fischer and Matthäus (1996) revealed significant differences in the period since the 1980ies (Figure 1). The reasons for the deviations between both time series are mainly the lack of appropriate data between 1976 and 1991, and the change in observation methods afterwards, which caused a bias in the inflow statistics.

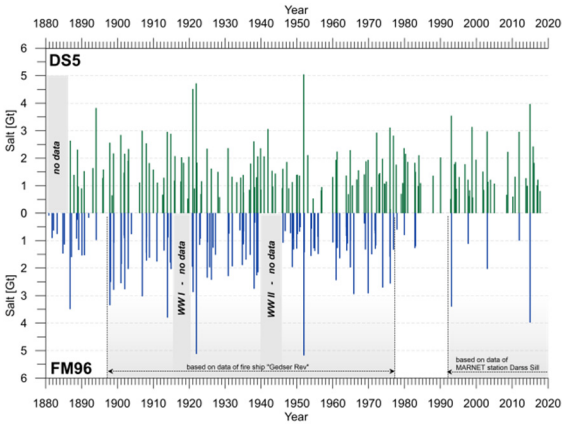

Figure 1. Comparison of the MBI time series DS5 (top) and FM96 (bottom). Grey areas indicate periods with no data. At the bottom the availability of time series observation at Gedser Rev and Darss Sill is depicted.

The frequency distribution of MBI in the revised time series depicts no statistically significant difference for three subsequent forty year periods (Figure 2). The inflow class distribution follows the expected exponential distribution.

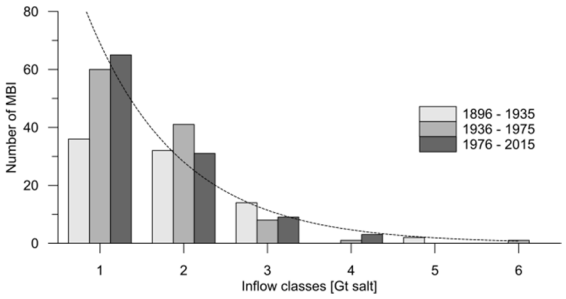

Figure 2. Total frequency of inflow classes in the time series DS0 for the three subsequent 40-year periods 1896-1935, 1936-1975 and 1976-2015.

3. Results

In contrast to earlier investigations the revised MBI time series depicts no significant long term trend in MBI frequency and intensity, contradicting the hypothesis that climate change caused a decreasing MBI frequency.

However there exists a decadal variability of MBI. Three periods with reduced MBI frequency were identified. The revised MBI time series was verified with observations of dissolved oxygen and salinity in the bottom layer of the Bornholm basin.

Until today climate change has no obvious impact on the MBI related oxygen supply to the central Baltic Sea. The increased eutrophication during the last century is most probably the main driver for temporal and spatial spreading of suboxic and anoxic conditions in the deep layer of the Baltic Sea.

References

Fischer, H., Matthäus, W., (1996) The importance of the Drogden Sill in the Sound for major Baltic inflows. J. Mar. Sys. 9, pp. 137-157

Lehmann, A., Post, P., (2015) Variability of atmospheric circulation patterns associated with large volume changes of the Baltic Sea. Advances in Science and Research 12, pp. 219-225.

Mohrholz, V., Naumann, M., Nausch, G., Krüger, S., Gräwe, U., (2015) Fresh oxygen for the Baltic Sea—An exceptional saline inflow after a decade of stagnation. J. Mar. Sys. 148, pp. 152–166

The study has been carried out in frame of the long term observation program of the Leibniz-Institute for Baltic Sea Research.

Benthic foraminifera distribution in the South-Eastern Baltic Sea in relation to the North Sea Water Inflow

Ekaterina Ponomarenko[1], Evgeniya Dorokhova[2] and Viktor Krechik[2]

[1] Immanuel Kant Baltic Federal University, Kaliningrad, Russia (ponomarenko.katharina@gmail.com)
[2] Shirshov Institute of Oceanology, Russian Academy of Sciences, Moscow, Russia

1. Introduction

The aim of the present study is to describe the distribution of benthic foraminifera in the South-Eastern Baltic Sea in relation to hydrology, grain size and organic content of the bottom sediment. This information will be further used as a modern analogue for palaeoecological interpretation of fossil assemblages. The Baltic Sea is a brackish water semi-enclosed water body, with a stratified water column and restricted exchange of deep waters. The hydrological regime of bottom water mass is strongly influenced by irregular inflows of high-saline oxygen-rich North Sea water through the narrow Danish straits (Hermelin, 1987).

2. Methods

A total of 24 surface sediment samples were collected in the Russian sector of the South-Eastern Baltic Sea (Gdansk basin and slope of the Gotland basin) with OCEAN sediment grab in the spring (May - April) and winter (October - December) of 2016. The top centimeter of sediments was sieved over >63 μm. For benthic foraminiferal analysis wet counting method was applied to avoid agglutinated tests breakage (Brodniewicz, 1965, Binczewska, 2017). Concentration of benthic foraminifera was counted as number of individuals per gram of dry sediment. Water salinity and temperature were measured by Sea&Sun CTD 90M. In addition, the organic carbon content in sediments was estimated by coulometric method and sediment grain size composition was determined with laser diffractive particle size analyzer SALD-2300.

3. Results and discussion

The unusually high bottom water salinity and temperature values (13 – 14.5 psu and 7.5 – 8.5 °C) indicating the advection of the North Sea waters were recorded in the deeper parts of the Gdansk Basin at the time of sediment collection. The species diversity of the benthic foraminifera in the studied region is very low. Agglutinated species are the most abundant in the assemblages. They are dominated by small sized individuals which belong to *Psammosphaera*, *aff. Thuramminoides, Saccammina* and *Reophax* genera. The decrease in the size of benthic foraminifera in the Baltic Sea was also noted in the studies of Brodniewicz (1965), Hermelin (1983) and Binczewska (2017), as the reaction to a reduced salinity. Calcareous species are dominated by *Cribroelphidium* and are present only at the stations showing the highest salinity values (>14 psu). As was already shown in Binczewska (2017), species of this genus are characterized as opportunistic, occurring under conditions of increased productivity and reduced salinity. The distribution of the benthic foraminiferal concentrations in the sediments has similar spatial pattern for both seasons. Benthic foraminifera diversity demonstrates a good correlation with salinity of the bottom waters (R=0.74). High foraminifera concentrations as well as increase in faunal diversity correspond to the deeper parts of the study region where saline North Sea water flowing via Stolpe Furrow is accumulated. Maximum concentration of foraminifera was determined in the sediments of the Gdansk-Gotland Sill where halocline reaches the bottom. However, the sharp dominance of very small (up to 100 microns) single-chamber *aff. Thuramminoides* individuals indicates that only some species can adapt to the variable conditions associated with the halocline. There is no clear correlation between distribution of concentration and diversity of foraminifera and organic carbon content in the sediments. Though, *Saccammina* species are mainly associated with organic rich sediments (R=0.95). None of the foraminiferal distribution parameters correlate markedly with the sediment grain size composition. Higher faunal diversity has a weak tendency (R=-0.2) to more fine sediments. However, finer grains accumulate in deeper parts of the basin where high salinity values were measured. So, it is more probable that in this case salinity is the factor controlling species diversity distribution.

Thus, the main factor determining the benthic foraminiferal distribution in the southeastern part of the Baltic Sea is the characteristics of bottom water salinity. This supports the future application of information on benthic foraminiferal distribution in sediment cores for the reconstruction of saline water inflows into the Gdansk Basin.

References

Binczewska A., Moros M., Polovodova-Asteman I., Sławinska J., Bak M (2017) Changes in the inflow of saline water into the Bornholm Basin (SW Baltic Sea) during the past 7100 years – evidence from benthic foraminifera record, Boreas, doi.org/10.1111/bor.12267. ISSN 0300-9483

Brodniewicz I. (1965) Recent and some Holocene Foraminifera of the southern Baltic Sea, Acta Palaeontologica Polonica, № 10(2), pp. 131-260

Hermelin J.O.R. (1987) Distribution of Holocene benthic foraminifera in the Baltic Sea, The Journal of Foraminiferal Research, № 17(1), pp. 62-73

Salinity dynamics and inter-sub-basin transport in the Baltic Sea

Jun She[1] and Jens Murawski[1]

[1] Danish Meteorological Institute, Denmark (js@dmi.dk)

1. Introduction

In the Baltic Sea, large scale salinity dynamics is mainly reflected by Baltic-North Sea water exchange and inter-sub-basin exchange, which is governed by many factors e.g. atmospheric forcing, river runoff, seasonal stratification and channelized bathymetry etc. Historically, main research has focused on the Major Baltic Inflow, especially in the western Baltic Sea. The intermediate inflow events and inter-sub-basin water exchange has been less addressed, partly due to lack of observations.

Modelling has been used as an alternative tool to study the water transport and related inflow events. However, due to channelized features, numerical mixing has been a major obstacle for realistic inflow modelling. Existing models such as HBM (HIROMB-BOOS Model, Berg and Poulsen, 2012), GETM (General Estuary Transport Model, Burchard et al. 2009) and NEMO-Nordic (Hordoir et al. 2015) have shown their capacity in simulating major inflow events, still, major limits exist. A realistic modelling should show accurate simulation on salinity, currents and sea level in entire basin for the inflow period, including both preface and post-inflow phases. The post-inflow phase covers the entire period of westward and northward transport of the inflow waters, which can last for more than six months. Hofmeister et al. 2011 demonstrated that GETM model with an adaptive vertical grid and 1 nm (nautical mile) resolution is able to reconstruct the inflow feature at Gotland Deep for the Major Baltic Inflow (MBI) in 2003. However the bottom salinity was a bit too high. A comprehensive validation for this inflow event was not available. A NEMO-Nordic 1 nm setup is able to keep reasonable and stable bottom salinity at Gotland Deep (Pemberton et al. 2017). However, this model has biased sea level in transition waters and southwest Baltic coast. HBM, a two-way nested operational model (1 or 3 nm resolution for the Baltic Sea and 0.5 nm for the transition waters) is good at reconstructing sea level in the entire Baltic Sea basin and modelling the inflow through the Danish Straits (Golbeck et al. 2017). However, the inflow is diluted when it passes Stople channel mainly due to numerical mixing. This caused a problem in HBM to keep sufficiently high bottom salinity in deep Baltic Sea.

In this study, inter-basin and inter-sub-basin water exchange during the most recent four MBI events in 2011, 2014, 2015 and 2016 are investigated by using results from multiple hydrodynamic models. The impact of model resolution is studied by using HBM with a 0.5 nm horizontal resolution and 122 vertical layers covering the entire Baltic Sea.

2. Inter-basin-sub-basin exchange

Daily mean net transport through multiple sections in Baltic Sea has been calculated in near real-time from BOOS members BSH, DMI and FCOO since 2009. The outputs are derived from operational forecast products based on DMI-HBM, BSHcmod and FCOO GETM. Both

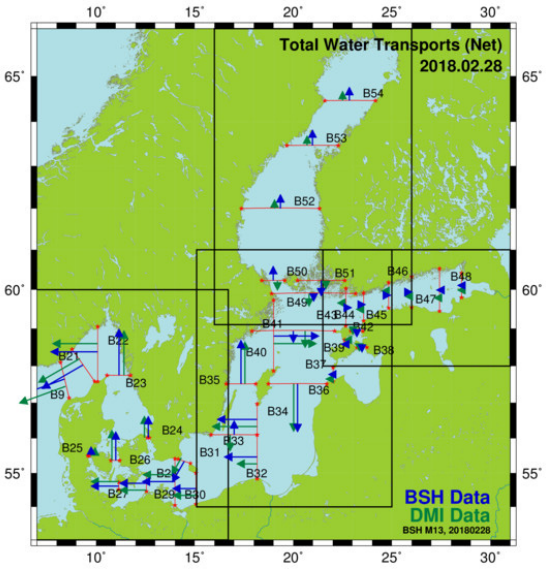

Figure 1. Total water transport in selected Baltic Sea sections based on BSH and DMI operational models (map source: http://www.boos.org)

DMI-HBM and BSHcmod have horizontal resolution in 3 nm for the Baltic Sea and 0.5 nm in the transition waters while FCOO GETM has horizontal resolution in 1 nm for the Baltic Sea and transition waters. The sections are shown in Fig. 1.

During November 2014 to Febuary 2016, three MBI events are identified in transition warters (Fig. 2 transect 26) in December 2014, November 2015 and January 2016. There are also intermediate inflow events in January 2015 and August/ September 2015. In the western Baltic Sea (Fig. 2 transect 30 and transect 31), MBI signals look differently in their south and northern passages. In south of Bornholm, major inflow signals still exist but intermediate inflow are found in January 2015 and June/July 2015. In the north of Bornholm, the signals are less clear than that in the south, also the BSHcmod and DMI-HBM show different features. DMI-HBM gives more inflow with significant signals in December 2014, January 2015, June 2015 and August/september 2015. Although no sustained period of inflow shown in October 2015 – Febuary 2016 crossing transect 31, the inflow is in general larger than outflow. However, BSHcmod gives much less inflow crossing this transect. When reach central Baltic Sea (Fig. 2 transect 36), the signals of three MBIs are clear and intermediate inflow are found in July and September 2015, respectively.

The features of the inter-sub-basin water exchange between North Baltic Proper and Gulg of Finland, Bothnian Sea are also studied by using transports through transects 43 and 50. The inflow signals differ significantly from the MBI signals identified in western Baltic Sea (figures not shown here).

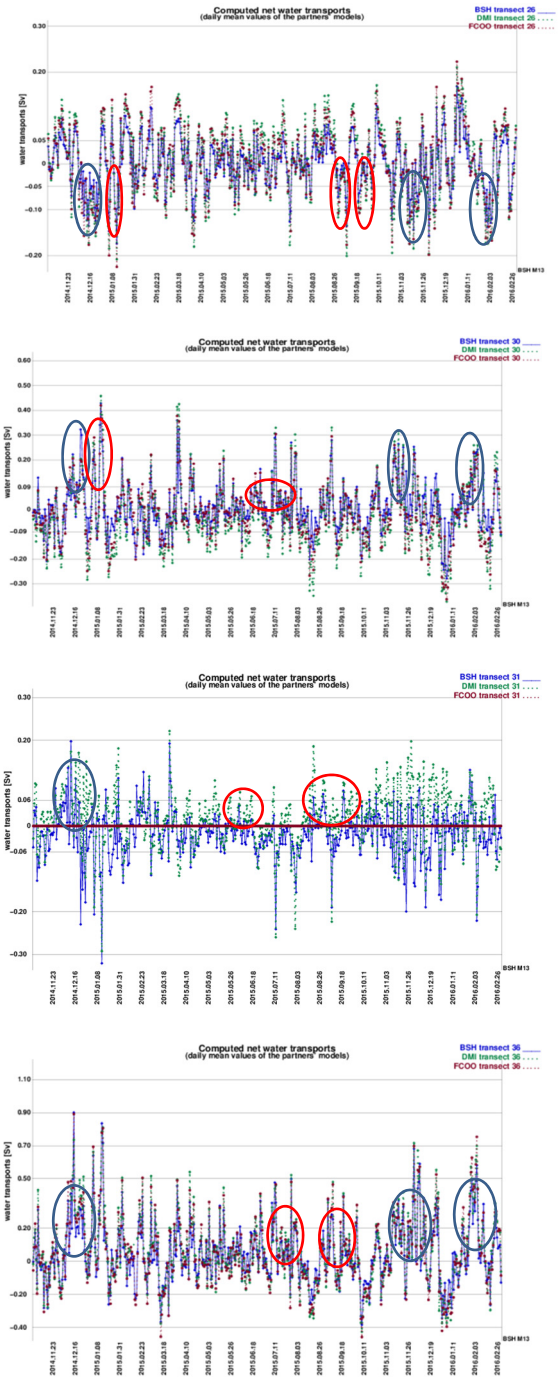

Figure 2. Vertically integrated net water transport crossing transects 26 (Great Belt), 30 (South of Bornholm), 31 (North of Bornholm) and 36 (Baltic Proper), derived from operational forecasting products from BSHcmod, DMI-HBM and FCOO-GETM. Be noted that FCOO-GETM data for transect 31 is not valid. (map source: http://www.boos.org)

3. Impact of resolution on MBI simulation

In order to improve HBM's abilities in simulating eater exchange in deep Baltic Sea, a 0.5 nm horizontal resolution set-up for the Baltic Sea and the Transition Zone to the North Sea. The setup requires less than 7 minutes time per day when 480 cores are employed in Cray XT30. A model simulation is made for the period 1 October 2014 – 31 Dec. 2015 which covers the 2014/15 Major Baltic Sea Inflow (MBI) event. The high salinity water flows into the Baltic Sea since 3 December 2014. The intra-basin transport of saline bottom water lasts for several months and reaches Baltic Proper (Neumann et al., 2017). The high resolution results are analysed and compared with results from a preliminary version which has a horizontal resolution of 1 nm. Figure 3b shows that the 1 nm resolution HBM generates little impacts on bottom salinity in the central Baltic Sea. However, the high resolution run (Fig. 3a) gives significant salinity increase in Baltic Proper, Gulf of Finland, Gulf of Riga and Bothnian Bay. The bottom salinity in the two model runs differ significantly in most of the Baltic Sea (Fig. 3c).

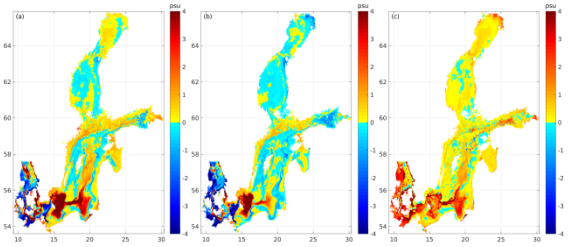

Figure 3. Impact of model resolution on the Baltic inflow – (a) bottom salinity difference between 15 November 2014 and 15May 2015 in HBM with 0.5 nm resolution, showing the impact of MBI on the salinity; (b) the same as in (a) but for HBM with 1 nm resolution and (c) bottom salinity difference in 15 May 2015 between the 0.5 nm resolution HBM and 1 nm resolution HBM.

References

Berg, P., and Poulsen, J. W. (2012). Implementation details for HBM. DMI Technical Report No. 12-11. Copenhagen, 149 pp. (Available at: www.dmi.dk/fileadmin/ Rapporter/TR/tr12-11.pdf).

Burchard, H., Janssen, F., Bolding, K., Umlauf, L., Rennau, H., 2009. Model simulations of dense bottom currents in the Western Baltic Sea. Cont. Shelf Res. 29, 205{220.

Golbeck I., Izotova J., Jandt S., Janssen F., Lagemaa P., Brüning T., Huess V., Hartman A. 2017. Quality Information Document (QUID) Baltic Sea Physical Analysis and Forecasting Product BALTICSEA_ANALYSIS_FORECAST_PHY_003_006: issue 4.0 http://marine.copernicus.eu/documents/QUID/CMEMS-BAL-QUID-003-006.pdf

Hofmeister R, Beckers J-M, Burchard H(2011) Realisticmodelling of the exceptional inflows into the central Baltic Sea in 2003 using terrainfollowing coordinates. Ocean Model 39:233–247. doi:10.1016/j.ocemod.2011.04.007

Hordoir R., Axell L., Löptien U., Dietze H. & Kuznetsov I. 2015. Influence of sea level rise on the dynamics of salt inflows in the Baltic Xea. *Journal of Geophysical Research: Oceans* 120: 6653–6668

Neumann, T., H. Radtke, and T. Seifert, 2017. On the importance of Major Baltic Inflows for oxygenation of the central Baltic Sea, J. Geophys. Res. Oceans, 122, 1090–1101, doi:10.1002/2016JC012525.

Pemberton, P., U. Löptien, R. Hordoir, A. Höglund, S. Schimanke, L. Axell, J. Haapala (2017), Sea-ice evaluation of NEMO-Nordic 1.0: a NEMO–LIM3.6-based ocean–sea-ice model setup for the North Sea and Baltic Sea *In Geoscientific Model Development*, volume 10, 2017.

Topic B

Land-sea-atmosphere biogeochemical feedbacks

The Impact of Water Constituents on Radiative Heat Transfer in the Open Ocean and Shelf Seas

Bronwyn Cahill[1], Juergen Fischer [1], Ulf Graewe[2], Hans Burchard [2], John Wilkin[3], John Warner[4], Neil Ganju[4]

[1] Institute for Space Science, Free University Berlin, Carl-Heinrich-Becker-Weg 6-10, 12165 Berlin, Germany (bronwyn.cahill@fu-berlin.de)

[2] Leibniz Institute for Baltic Sea Research Warnemuende, Physical Oceanography and Instrumentation, Seestrasse 15, 18119 Rostock, Germany

3 Marine and Coastal Sciences, Rutgers University, 71 Dudley Road, New Brunswick, NJ 08901, USA

[4] U.S. Geological Survey, Coastal and Marine Geology Program, 384 Woods Hole Road, Woods Hole, MA 02543, USA

1. Introduction

Radiant energy fluxes impact biological production in the ocean and are modulated as a result of biological production. This has fundamental consequences for upper ocean physics, surface nutrient supply, net primary and export production and the exchange of soluble gases across the air-sea interface into the marine atmospheric boundary layer. The contribution of optically active water constituents to heating rates in the upper ocean is intrinsically linked to net primary and export production, through the direct effect of temperature on metabolic rates of marine plankton. This plays an important role in controlling the flow of carbon and energy through pelagic systems (Wohlers et al., 2009; Taucher and Oschlies, 2011), in particular, the partitioning between particulate and dissolved organic carbon, the transfer of primary produced organic matter to higher trophic levels, the efficiency of the biological carbon pump and the exchange of CO_2 across the air-sea interface.

Heterogeneity of water constituents in shelf seas and coastal waters is increased by the presence of inorganic suspended particulate matter and coloured dissolved organic matter (CDOM). Sources of CDOM and changes to its composition through non-conservative processes are tightly coupled to the underwater light field. These will vary with environmental conditions and phytoplankton community structure. Moreover, heterogeneity in phytoplankton pigments and other water constituents will have implications for sub-mesoscale vertical mixing and advective fluxes, and thus water temperature, density and the supply of nutrients to the surface. Understanding what the consequences are for energy fluxes in the upper ocean and across the air-sea interface, and the accumulative effect on the upper ocean heat budget in shelf seas and coastal waters is of particular importance for our capacity to adequately model regional ocean climate.

2. Approach

We are using a coupled ocean-atmosphere circulation model (Figure 1) incorporating a bio-optical module with multiple phytoplankton groups in tandem with an atmosphere-ocean radiative transfer model to explore the contribution of optically active water constituents (including phytoplankton, CDOM and inorganic suspended sediments) to energy fluxes in the upper ocean and across the air-sea interface. Specifically, we are investigating:

- How heterogeneity in optically active water constituents in shelf seas affects the characteristics of sub-mesoscale vertical turbulent mixing and advective fluxes, through feedbacks with upper ocean heating rates and water density?
- What are the consequences for the supply of surface nutrients and the transport and transformation of phytoplankton biomass?
- What is the seasonal modulation of the flux of thermal energy across the ocean atmosphere interface as a result of heating rates induced by optically active water constituents?

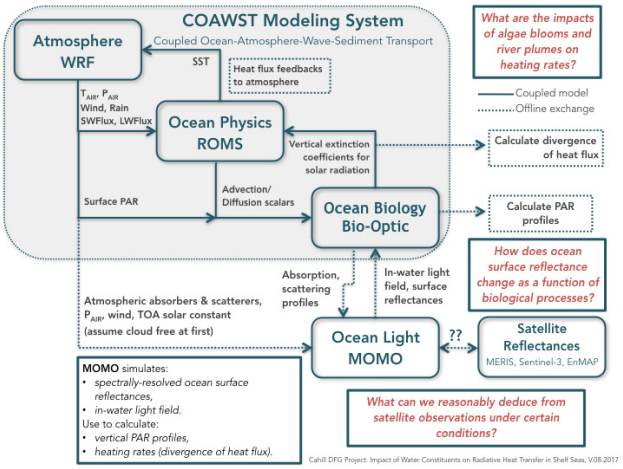

- To what extent is variability in CDOM attenuation reflected by environmental conditions and phytoplankton community structure?

Figure 1. Overview of modelling system(s), interaction between components and data streams.

The coupled ocean-atmosphere-bio-optical circulation model is being applied to selected shelf sea regions characterized by different freshwater and nutrient regimes, and complex bio-optical and hydrodynamic processes (Figure 2). The bio-optical module, which explicitly follows the spectrally-resolved vertical light stream, accounts for optically active water constituents' contribution to the divergence of the heat flux within the full hydrodynamic solution. This means that heating rates due to the highly variable concentrations of optically active water constituents can be estimated and their impact on ocean biophysical processes evaluated.

We will evaluate these modelled heating rates against more rigourous co-located heating rate calculations performed using the atmosphere-ocean radiative transfer model, MOMO. The coupled 3D model solution will thus be optimized for regional applications. This will lead to improved net surface solar radiation forcing fields, an accurate underwater vertical description of the light field and a resolution of the radiative flux divergence between physics and biology in the ocean. In so doing, we expect to make a major contribution toward overcoming some of the obstacles inherent in studying optically complex shelf and coastal waters. The outcome will be a rigorous assessment of the impact of optically active water constituents on upper ocean heat budgets and will establish a framework for regional two-way coupled ocean-atmosphere investigations with important consequences for weather forecasting and climate change.

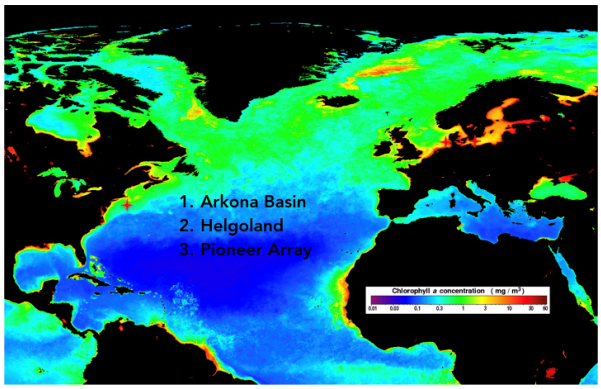

Figure 2. Ocean colour image of annual average chlorophyll concentration in 2007 (source: NASA GFSC) indicating location of three sites: (a) coastal waters of the western Baltic Sea, (b) the central German Bight and (c) Central Mooring of the Pioneer Array in Northwest Atlantic.

3. Acknowledgements

This project is funded by the German Research Foundation (DFG Grant No. CA 1347/2-1), 2018 – 2021.

References

Wohlers, J., A. Engel, E. Zöllner, P. Breithaupt, K. Jürgens, H.-G. Hopper, U. Sommer and U. Riebesell, 2009. Changes in biogenic carbon flow in response to sea surface warming. P. Natl. Acad. Sci. USA, 106, 7067-7072.

Taucher, J. and A. Oschlies, 2011. Can we predict the direction of marine primary production change under global warming? Geophysical Research Letters, 38, L02603, doi: 10.1029/2010gl045934.

Nutrient retention along the Swedish coastline

Moa Edman[1], Kari Eilola[1], Elin Almroth-Rosell[1], H.E. Markus Meier[1,2], Iréne Wåhlström[1], Lars Arneborg[1]

[1] Swedish Meteorological and Hydrological Institute, Norrköping, Sweden (moa.edman@smhi.se)
[2] Department of Physical Oceanography and Instrumentation, Leibniz Institute for Baltic Sea Research Warnemünde, Rostock, Germany

1. Introduction

Most of the Swedish coast boarders the brackish, semi-enclosed Baltic Sea, while the Swedish west coast is connected to the Kattegat and Skagerrak system that acts as a transitional zone between the North Sea and the Baltic seas. All inputs from land first enter the coastal zone and depending on the nutrient transports and transformations in this zone, not all reach the open ocean domain. The coastal zone filters some of the land nutrient input and thus the nutrient transports that exit the coastal zone are often much smaller than the riverine nutrient loads that enter the coastal zone. The coastal filter is thus important for open sea eutrophication.

The filter capacity was calculated from a 30-year model simulation of the Swedish coastal zone and the averaged model skill was evaluated to be good or acceptable. The Swedish Coastal zone Model (SCM) is a multi-basin, 1D-model based on the equation solver PROgram for Boundary layers in the Environment (PROBE; Svensson, 1998), coupled to the Swedish Coastal and Ocean Biogeochemical model (SCOBI; Eilola et al., 2009; Marmefelt et al., 1999). The set-up used here includes 653 coupled basins covering the entire Swedish coast. The basins follow the water bodies defined by the water framework directive and mainly follow natural topographic constraints.

2. Results

The nutrient filter capacity of the entire Swedish coast is estimated to be approx. 50-70%, and thus less than half of the input from land can be assumed to be exported from the coastal zone to the open sea. However, the differences between the water districts are large. The lowest filtering of land nitrogen occurs along the coast of the Bothnia Gulf, while the lowest phosphorous filtering is calculated for the Swedish west and south (Skåne) coast. Water district three that includes the Stockholm archipelago, and the south coast in water district 4, all retain more than 100% of the land and air load they receive. These areas thus have a net import of nutrients from the open Baltic Sea and retain open Baltic Sea nutrients. Hence they filter not only the land load, but also the Baltic Sea water.

In addition to the entire Swedish coast, the retention at selected key sites representing different coastal types was also estimated. The variability of both the filter and retention efficiency was found to be large, and larger within the types than between the average values of the types. The modelled long term nutrient retention was instead found to be to a large extent dependent on the physical characteristics of a waterbody, such as area, mean depth and the residence time of water.

The nutrient removal is most efficient close to land, where the area specific retention efficiency is the highest. On interannual timescales temporal changes in the coastal nutrient pool can have a large influence on perceived nutrient retention.

3. Acknowledgement

The research presented in this study is part of the Baltic Earth programme (Earth System Science for the Baltic Sea region, see http://www.baltex-research.eu/balticearth) and is part of the BONUS COCOA (Nutrient COcktails in COAstal zones of the Baltic Sea) project which has received funding from BONUS, the joint Baltic Sea research and development programme (Art 185), funded jointly from the European Union´s Seventh Programme for research, technological development and demonstration and from the Swedish Research Council for Environment, Agricultural Sciences and Spatial Planning (FORMAS), grant no. 2013-2056. Additional financing has been received from the Swedish Agency for Marine and Water Management grant 1:12 Environmental management of marine and inland waters, tasks performed in accordance with regulation (204:660) regarding water quality considerations.

References

Eilola, K.,Meier, M. H. E., Almroth, E., (2009). On the dynamics of oxygen, phosphorus and cyanobacteria in the Baltic Sea; A model study. Journal of Marine Systems 75, 163-184.

Marmefelt, E., Arheimer, B., Langner, J., (1999). An integrated biochemical model system for the Baltic Sea. Hydrobiologia 393, 45-56.

Svensson, U., (1998). PROBE An instruction manual, Report Oceanography. SMHI.

High resolution nutrient data to unravel the post-nitrate bloom elemental cycling in the central Baltic Sea

Anja Eggert, Bernd Schneider, Jens D. Müller, Norbert Wasmund, Monika Nausch, Günther Nausch and Gregor Rehder

Leibniz Institute for Baltic Sea Research Warnemünde, Germany (anja.eggert@io-warnemuende.de)

1. Motivation

Since 2003, high resolution measurements of the surface water CO_2 partial pressure, pCO_2, are performed in the central Baltic Sea using a fully automated system on the cargo ship FINNMAID (Finnlines). The data have been successfully used to study the surface water biogeochemistry and in particular to quantify net community production in spring and mid-summer (Schneider et al., 2009; 2014).

A major finding of the pCO_2 data refers to the period after termination of the nitrate bloom in spring. At this time, nitrate is virtually zero down to a depth of ~40 m, but a considerable fraction of the winter phosphate is still present in the surface water. During this post-nitrate bloom period, pCO_2 in the surface mixed layer continues to decline despite the absence of dissolved inorganic nitrogen, DIN. This observation had stimulated a vivid discussion within the Baltic Sea biogeochemical community. Raised explanations of the observed pCO_2 signal include "cold" nitrogen fixation by unusual diazotrophs (Schneider et al. 2009), the impact of a mixotrophic ciliate *Mesodinium rubrum*, which shows marked vertical migration and exploits DIN pools below the halocline (Lips & Lips, 2017) or variable, non-Redfieldish nutrient stoichiometry of phytoplankton (Kreus et al. 2014).

All in all, currently there exists no consolidated knowledge on the biogeochemical processes controlling the observed pCO_2 signal after termination of the nitrate bloom. Our objective for this study was to unravel the elemental cycling in the central Baltic Sea during the post-nitrate phase of the spring bloom by using high resolution inorganic nutrient, particulate elementary composition, and pCO_2 data collected during spring 2015 on the cargo ship FINNMAID.

2. Sampling strategy

Between 12 April and 15 May 2015, we sampled surface water on the cargo ship FINNMAID and obtained a quasi-daily data set of dissolved organic and inorganic as well as particulate organic nitrogen and phosphorus compounds at seven stations in the Eastern Gotland Basin. Chlorophyll-*a*, silicate, and phytoplankton samples were also taken. These data were complemented by the high resolution data of the surface water pCO_2 recorded throughout the year.

3. A less pronounced post-nitrate bloom 2015

The decrease in Chlorophyll-*a* concentration in combination with the exhaustion of DIN marks the termination of the nitrate bloom in spring 2015 on 21-April. A considerable fraction of the winter phosphate (>0.3 µmol l^{-1}) was still present in the surface water at that time.

Surface water total CO_2, C_T, decreased over the last nine days of the nitrate bloom, between 12 and 21-April 2015, by 34 µmol kg^{-1} from 1642 to 1608 µmol kg^{-1}, and then continued to decrease by another 34 µmol kg^{-1} until 28-April (Fig. 1). At the same time, phosphate concentration decreased only moderately from 0.37 to 0.27 µmol l^{-1}. Accordingly, the post-nitrate bloom in 2015 lasted only six days from 22 until 28-April and was less pronounced than in previous years.

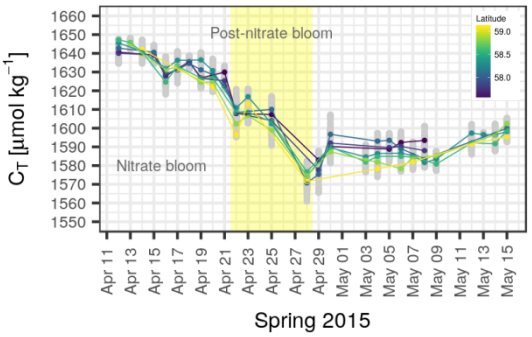

Figure 1. Surface water total CO_2 concentrations, C_T, derived from pCO_2 measurements on the cargo ship FINNMAID (for method, see Schneider & Müller 2017). Grey dots are single measurements, coloured dots are station means, with purple beeing the southernmost and yellow the most northern station. A decreasing signal reflects net carbon uptake.

4. No significant nitrogen source in 2015

Eggert & Schneider (2015) applied a mass balance for total nitrogen, TN, and calculated a significant nitrogen source of unknown origin, ΔTN^{us}, in the surface mixed layer in May in the Baltic Proper. It is argued that this nitrogen source is closely linked to organic matter production. The long-term mean (1995-2016) of ΔTN^{us} in the Eastern Gotland Basin is 2.7 mmol m^{-3} (Fig. 2). The same calculation with the data of this study yields ΔTN^{us} of only 0.4 mmol m^{-3} for the post-nitrate bloom 2015. However, ΔTN^{us} shows a strong interannual variability and the period 1995-2016 includes a few other years with low (2002, 2006) or even negative values (2009).

5. Nutrient composition of particulate organic matter

Raised explanations for the observed total CO_2 signal during the post-nitrate bloom relate to non-Redfieldish particulate organic matter. In particular, two processes could play a part: (1) excess N-uptake of phytoplankton during the nitrate bloom supporting net community production in the time thereafter and (2) continued carbon fixation during the post-nitrate bloom. Notably large diatoms can take up nitrate in excess of nutritional requirements and store it in large internal vacuoles. But also the production of carbon-rich transparent exopolymer particles by phytoplankton is regarded a significant mechanism for the selective export of carbon from the surface water (Passow 2002).

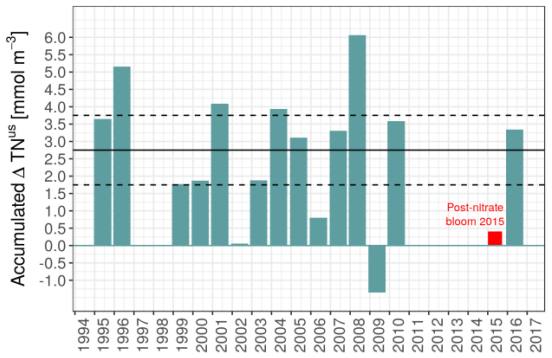

Figure 2. Green bars: Accumulated ΔTN^{us} in the surface water (0–15 m) at the Eastern Gotland Basin station BY15 for May 1995-2016 (reference month=April). Calculations based on monthly monitoring data of the Swedish National Monitoring Program (SMHI). No data were available for 1997, 1998, 2011 to 2015. Horizontal lines show the long-term mean of 2.7 mmol m^{-3} and its 95% confidence interval. Red bar: ΔTN^{us} calculated for the six days post-nitrate bloom 2015. Figure extended from Eggert & Schneider (2015).

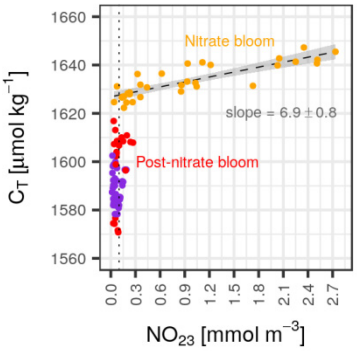

Figure 3. Temporal changes of dissolved nutrient species, C_T versus NO_{23}, as an estimate of nutrient composition of produced organic matter. Data points between 12-Apr 2015 and 21-Apr 2015 are colored orange and represent the nitrate bloom, data points of the post-nitrate bloom are red and the days thereafter violet.

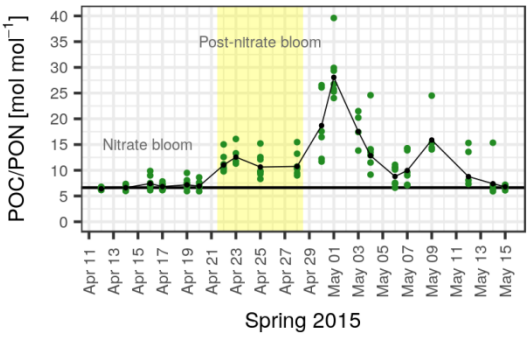

Figure 4. The molar C/N ratio of surface water particulate organic matter. The horizontal line denotes the Redfield C/N ratio of 106/16 = 6.625.

Our data strongly suggest that there is no preferential N-uptake during the nitrate bloom, which could sustain further production after DIN depletion. 'Large' diatom species had a low abundance in spring 2015, supporting long-term observations of Wasmund & Siegel (2008). Furthermore, the build-up of organic matter during the nitrate bloom occurred very close to the Redfield C/N ratio of 106/16. This is noticeable in the temporal changes of the dissolved nutrient concentrations C_T *versus* nitrate (Fig. 3) and in the measured POC/PON ratios (Fig. 4). In contrast, our data show a sudden increase in POC/PON after termination of the nitrate bloom, indicating the production of carbon-rich organic matter in that period (Fig. 4).

6. Conclusions

The post-nitrate bloom 2015 was less pronounced than in most years, the drawdown of excess phosphate was only moderately, and the calculated nitrogen source during the six days period was very low. High resolution data of dissolved organic and inorganic nutrients and elemental composition of particulate organic matter do not support preferential N-uptake prior to DIN depletion. Instead, the production of carbon-rich organic matter after termination of the nitrate bloom could, at least for the year 2015, partly explain the observed pCO_2 decrease during the post-nitrate bloom.

7. Acknowledgments

This work is embedded in the BONUS INTEGRAL project that receives funding from BONUS (Art 185), funded jointly by the EU, the German Federal Ministry of Education and Research, the Swedish Research Council Formas, the Academy of Finland, the Polish National Centre for Research and Development, and the Estonian Research Council. The pCO2 instrumentation on VOS FINNMAID is part of the European ICOS RI and its implementation was supported by the German Federal Ministry of Education and Research though grants 01LK1101F and 01LK1224D. We are indebted to Finnlines for supporting our instrumentation throughout the years and generously hosting a scientist onboard during the period of our campaign from April to May 2015.

References

Eggert A., Schneider B. (2015) A nitrogen source in spring in the surface mixed-layer of the Baltic Sea: Evidence from total nitrogen and total phosphorus data. Journal of Marine Systems, 148, pp. 39–47.

Lips I., Lips U. (2017) The importance of *Mesodinium rubrum* at post-spring bloom nutrient and phytoplankton dynamics in the vertically stratified Baltic Sea. Frontiers in Marine Science, 4(DEC). http://doi.org/10.3389/fmars.2017.00407.

Passow, U. (2002) Transparent exopolymer particles (TEP) in aquatic environments. Progress in Oceanography, 55, pp. 287-333.

Schneider B., Kaitala S., Raateoja M., Sadkowiak B. (2009) A nitrogen fixation estimate for the Baltic Sea based on continuous pCO_2 measurements on a cargo ship and total nitrogen data. Continental Shelf Research, 29, pp. 1535–1540.

Schneider B., Gustafsson E., Sadkowiak B. (2014) Control of the mid-summer net community production and nitrogen fixation in the central Baltic Sea: An approach based on pCO_2 measurements on a cargo ship. Journal of Marine Systems, 136, pp. 1–9.

Schneider B., Müller J.D. (2018) Biogeochemical transformations in the Baltic Sea: Observations through carbon dioxide glasses. Springer.

Wasmund N., Siegel H. (2008) Phytoplankton. In R. Feistel, G. Nausch, N. Wasmund (Eds.), State and Evolution of the Baltic Sea, 1952 – 2005 (pp. 441–481). Hoboken: John Wiley & Sons.

Spatial and seasonal phosphorus changes in the water column of an estuary of the southern Baltic Sea

Lisa Felgentreu[1], Günther Nausch[1], Franziska Bitschofky [2], Monika Nausch[2] and Detlef Schulz-Bull[1]

[1] Leibniz-Institute of Baltic Sea Research, department of marine chemistry, Rostock, Germany (lisa.felgentreu@io-warnemuende.de)
[2] Leibniz-Institute of Baltic Sea Research, department of marine biology, Rostock, Germany

1. Introduction

Phosphorus (P) is one of the most critical elements forcing eutrophication. The P-input into the Baltic Sea increased during the second half of the 20th century, which led to a shift in its trophic status (Gustafsson et al. 2012). Despite numerous efforts to reduce nutrient inputs, the coastal waters of the southern Baltic Sea are still subject to a high level of eutrophication (Nausch et al. 2011). Within the PhosWaM project (Phosphorus from the source to the sea) our studies focus on the Warnow estuary as a transition between the agrarian catchment and the Baltic Sea. We assume that introduced P underlies intensive transformation.

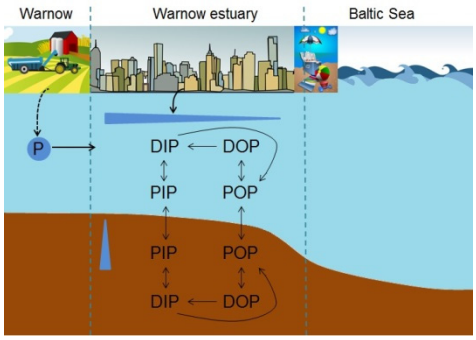

Figure 1: Schematic P cycling in the water column and sediment of the Warnow estuary. DIP = dissolved inorganic P, PIP = particulate inorganic P, DOP = dissolved organic P, POP = particulate organic P.

The estimated P cycling in the water column and the sediment is shown schematically in Fig. 1. The P from the river Warnow, originating mainly from diffuse sources, enters the estuary when it reaches the city of Rostock. During its passage through the estuary the different forms of P are cycling in the water column and the sediment. It is also possible that P is punctually introduced to the estuary, e.g. by the sewage plant of the city. We suppose that the P concentration decreases in the water column towards the Baltic Sea and increases in the sediment with the depth.

P appears in different functional fractions as it can be in solution or attached to particles. Otherwise, it can also be bound to organic or inorganic material. If it is in solution it can be the dissolved inorganic P (DIP), which gets ingested by organisms and changed into particulate organic P (POP). When The P is released by the organism it is again in solution, dissolved organic P (DOP). The DOP can be transformed into DIP by mineralization. DIP and PIP can be transformed into each other and back by adsorption and desorption.

Particulate P sinks to the bottom while dissolved P reaches the sediment by diffusion. In the sediment degradation of organic matter occurs. Sedimental P can enter the water column again by resuspension and diffusion.

It is important to differentiate between the different P fractions, because for example the dissolved organic P is counted to the most popular P sources during the productive season for the growth of algae and bacteria (Nausch & Nausch 2006). Thus, the potential of eutrophication based on the various P components has not been considered in the catchment area until now. Summarizing, the elucidation of the P fluxes, especially the processes concerning the transport to the coast and exchange with the coastal waters is important to bring to a unified outline.

Paragraphs are indented but not separated by an empty line. Margins need to be 2.5cm from each side of the sheet. One blank line should be typed before each new section.

2. Sampling and Method

Since September 2016 water samples were taken monthly along the estuary. Here, we measured in addition to the P fractions also chlorophyll a and the content of seston to characterise the organic matter.

P is detected spectrometrically by the molybdenum blue colorimetric method (Murphy & Riley 1962). Here, the reaction of P in a filtered water sample with molybdenum blue does not only detect DIP. The reagent can gather also labile organic P in the solution (Jarvie et al. 2002). As consequence, we rename the traditional P species (Tab. 1).

Table 1: List of the traditional and new nomenclature of the different P fractions.

traditional nomenclature	new nomenclature
dissolved inorganic P (DIP)	dissolved reactive P (DRP)
particulate inorganic P (PIP)	particulate reactive P (PRP)
dissolved organic P (DOP)	dissolved non-reactive P (DNP)
particulate organic P (POP)	particulate non-reactive P (PNP)

For detection of these P fractions we follow an analysis scheme (Fig. 2). The unfiltered water sample is measured immediately with the molybdenum blue colorimetric method. As result we get the total reactive P (TRP). A subsample is frozen for a later digestion with an oxidant (potassium peroxydisulphate) in a lab-microwave. After this digestion we get the total P (TP). The same procedure takes place with the filtrate after the filtration of the samples. Here we measure DRP and after the digestion in the microwave total dissolved P (DP). By building differences we can calculate total particulate P (PP), PRP, PNP and DNP.

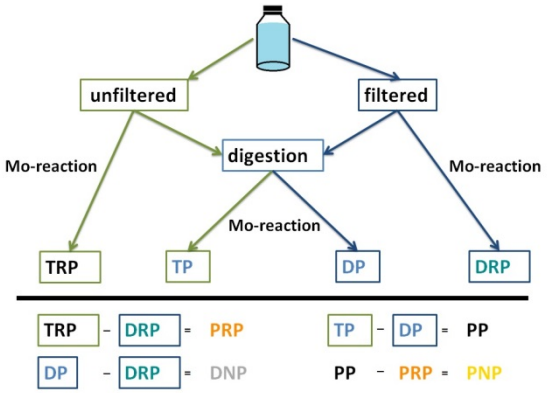

Figure 2: Analysis scheme for detection of P fractions. TP = total P, DP = total dissolved P, PP = total particulate P, TRP = total reactive P, DRP = dissolved reactive P, PRP = particulate reactive P, DNP = dissolved non-reactive P, PNP = particulate non-reactive P.

3. Results and Discussion

The Warnow estuary is a typical partially mixed estuary. The salinity in the surface water is lower than in the near bottom water. Also there is a lower salinity in general near the river (0 - 6 g kg^{-1} at the surface and 0 - 11 g kg^{-1} near the bottom). In contrast, the salinity close to the sea is higher (8 - 18 g kg^{-1} at the surface and 8 - 20 g kg^{-1} near the bottom). So, the water of both the Baltic Sea and the river Warnow influence the estuary.

The TP concentration varied between 0.34 µM (10.53 µg l^{-1}) to 6.12 µM (189.54 µg l^{-1}) near the river and 0.19 µM (5.88 µg l^{-1}) to 1.14 µM (35.31 µg l^{-1}) at the mouth. Thus, the TP concentration decreased towards the Baltic Sea. Additional, there is also a variation of the different P fractions. In winter the dissolved P, especially the DRP, is dominating. With spring, when the productive season begins, the portion of the P fractions is shifted. In summer the particulate P, mainly PNP, dominates.

4. Outlook

According to the different P fractions, bioavailability experiments are planned. With these results we hope to give more detailed information about the potential of eutrophication of the various P species.

References

Gustafsson, B. G., F. Schenk, T. Blenckner, K. Eilola, H. E. M. Meier, B. Müller-Karulis, T. Neumann, T. Ruoho-Airola, O. P. Savchuk and E. Zorita (2012): Reconstructing the Development of Baltic Sea Eutrophication 1850-2006. Ambio 41(6): 534-548.

Jarvie, H. P., P. J. A. Withers and C. Neal (2002): Review of robust measurement of phosphorus in river water: sampling, storage, fractionation and sensitivity. Hydrology and Earth System Sciences 6(1): 113-131.

Murphy, J. and J. P. Riley (1962): A modified single solution method for the determination of phosphate in natural waters. Analytica Chimica Acta 27(Supplement C): 31-36.

Nausch, G., A. Bachor, T. Petenati, J. Voß and M. Von Weber (2011): Nährstoffe in den deutschen Küstengewässern der Ostsee und angrenzenden Gebieten. Meeresumwelt Aktuell Nord- und Ostsee. 2011: 16.

Nausch, M. and G. Nausch (2006): Bioavailability of dissolved organic phosphorus in the Baltic Sea. Marine Ecology Progress Series 321: 9-17.

Air-sea Methane fluxes in the Baltic Sea using eddy covariance

Lucía Gutiérrez-Loza[1], Anna Rutgersson[1], Marcus B. Wallin[1] and Erik Sahlée[1]

[1] Department of Earth Sciences, Uppsala University, Sweden (lucia.gutierrez_loza@geo.uu.se)

1. Introduction

Methane (CH_4) is the most abundant hydrocarbon in the atmosphere, where it plays an important role on tropospheric and stratospheric chemistry (Reeburgh, 2007). Further, CH_4 is an important greenhouse gas with a 28 times higher warming potential than CO_2 over a 100 years horizon. The increasing concentration of greenhouse gases in the atmosphere, including CH_4, and their effect on global climate is well recognized (IPCC, 2013). Thus, the need of constraining the carbon and methane budgets at regional and global scales urges for a more detailed knowledge of the processes within the carbon cycle (both natural and anthropogenic components), including the gas flux across the air-sea interface.

To our knowledge, no study has directly investigated the turbulent air-sea CH_4 flux (F_{CH4}) using micrometeorological methods in a marine environment. Hence, the aim of this study is to evaluate the viability and quality of micrometeorological measurements in order to account for the CH_4 contributions to the regional budget. Furthermore, to contribute to a better understanding of the interaction processes involved in the air-sea gas exchange.

2. Data and measurements

The Östergarnsholm measurement site is located at 57°27'N, 18°59'E (see Fig. 1) on a small and flat island in the Baltic Sea about 4 km from the east coast of the bigger island of Gotland. The station at Östergarnsholm has a 30-m land-based meteorological tower located on the southern tip of the island. The tower is equipped at various levels with high-frequency (20 Hz) sensors used for the estimation of CO_2 and momentum turbulent fluxes, as well as with slow response instrumentation for mean profile measurements of meteorological variables. Several studies have been published describing the oceanic and atmospheric characteristics of the Östergarnsholm site (Högström et al., 2008; Sahlée et al., 2008) and assessing the air-sea interaction processes in the region (Smedman et al., 1999; Rutgersson et al., 2008; Rutgersson et al., 2011).

In addition to the Campbell CSAT3 sonic anemometers and the LICOR LI-7500 gas analyzers placed at two levels (9 and 25 m) used for air-sea CO_2 turbulent flux estimations, a CH_4 LI-7700 gas analyzer was installed in the tower (at 9 m) in September 2017. The recent installation of the high-frequency CH_4 sensor allows us to estimate F_{CH4} in the coastal station. Here we present the results of a 2-months sample period where atmospheric concentrations of CH_4 and F_{CH4} were analyzed.

3. Air-sea CH_4 flux

The air-sea gas flux on the tower is estimated using the eddy covariance method (see Baldocchi et al., 1988). This method has been widely used for the estimation of turbulent fluxes of momentum, energy, and mass in terrestrial, coastal, and oceanic environments.

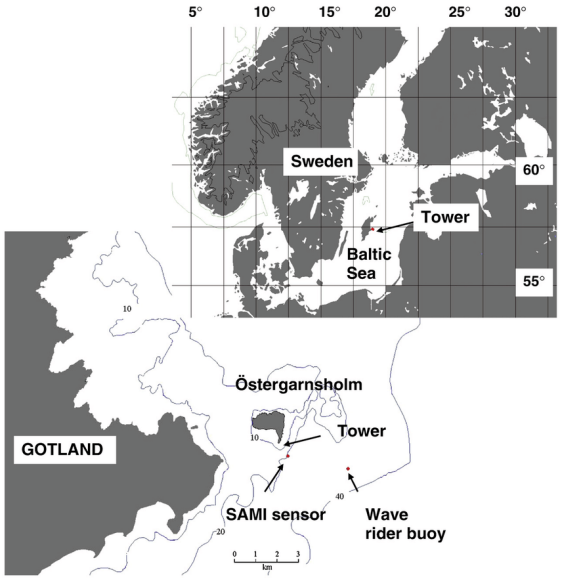

Figure 1. Map of the Baltic Sea and the Östergarnsholm station including locations of the measurement tower and the two measuring buoys (a SAMI sensor and a wave rider buoy) (from Rutgersson et al., 2008).

The eddy covariance technique allows direct estimations of the magnitude and direction of the flux of a certain constituent (in this case CH_4) based on the covariance of the high-frequency fluctuations of vertical wind speed and the gas concentration. The turbulent fluctuations are obtained through a Reynolds decomposition from the simultaneously measured signals.

Although the eddy covariance technique is a straightforward method for flux estimations, strict quality control criteria are required. The so-called Webb correction (Webb et al., 1989) was applied to account for the density fluctuations that cause the non-negligible mean vertical velocity during flux calculations. In addition, a manual inspection of the normalized cospectra was carried out; further discussion about the co-spectra selection is presented in section 4.

Two months of CH_4 turbulent data were analyzed to evaluate the quality and viability of the measurements in a marine station. The results presented here are preliminary and based on them further analysis of F_{CH4} is being conducted.

4. Results and discussion

In order to select the high-quality data for the flux estimations, a manual inspection of the normalized cospectra was carried out. The cospectra were obtained from the 20-Hz measurements of the vertical wind speed and the molar concentration of the gas, and calculated for every 30 min. An example of an accepted cospectrum is shown in Fig. 2. Only data showing the appropriate shape

of the cospectrum (Norman et al., 2012) was used for the flux calculations.

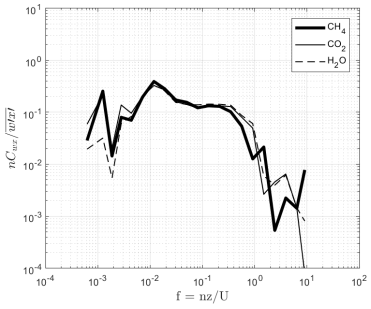

Figure 2. Example of an accepted normalized cospectrum of CH_4, CO_2 and water vapor plotted on a log-log scale. The corresponding mean RSSI values were 98% and 63% for the LI-7500 and the LI-7700 instruments, respectively, during a 30-min period on September 29, 2017.

The quality of the measurements recorded with a gas analyzer can be associated with the RSSI (Relative Signal Strength Indicator) given by the instrument. However, it has been shown (Nilsson et al., 2018) that the RSSI might not be enough to determine the high quality of the data from CO_2 gas analyzers. Furthermore, Nilsson et al. (2018) found systematic differences between RSSI values reported from different instruments making it difficult to set a threshold to select good-quality data based on this criterion; instead, they suggested to use the variance of RSSI (σ^2_{RSSI}).

Similar results were found in this study based on the cospectral inspection and the respective RSSI values from the CH_4 LI-7700 gas analyzer. The results suggest that a more detailed quality control processing must be made in order to systematically select the good-quality data for F_{CH4} calculations.

Molar densities of CH_4 and the calculated fluxes from the selected 30-min periods are shown in Fig. 3. The negative values of F_{CH4} found in this study are in disagreement with other studies that report positive mean fluxes in the Baltic Sea (e.g. Bange et al., 1994). However, there are no studies presenting direct estimations from eddy covariance; thus, these measurements still need to be validated. In order to account for the liability and quality of the measurements, a systematic quality control criteria needs to be established and longer measurement periods must be evaluated. In addition, measurements of CH_4 concentrations in the water, as well as other chemical parameter, obtained from manual samplings conducted within the footprint area at Östergarnsholm site will be used in the analysis.

5. Conclusions

Continuous and direct measurements of the CH_4 air-sea fluxes are being recorded at the Östergarnsholm site. Such measurements are essential for evaluating the magnitude and temporal variability of the sink/source function of CH_4 for coastal seas. Furthermore, they could provide valuable information for the understanding of the interaction processes controlling the air-sea gas exchange.

The results presented here are preliminary and based on them further analysis must be conducted. A systematic and strict quality control criteria needs to be established for further analysis of the data.

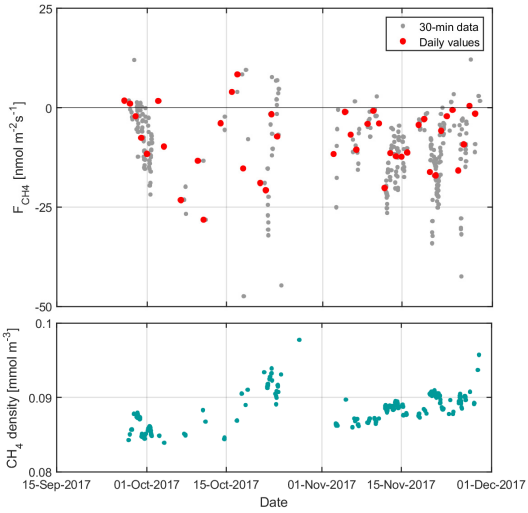

Figure 3. Half-hour averages of air-sea CH_4 flux (F_{CH4}) with daily averages (upper panel), CH_4 molar density (central panel) and, wind speed (lower panel) at Östergarnsholm site from September 27 to November 30 2017.

References

Baldocchi, D.D., B.B. Hincks, T.P Meyers (1988) Measuring biosphere-atmosphere exchanges of biologically related gases with micrometeorological methods. Ecology, 69, 5, pp. 1331-1340

Bange, H.W., U.H: Bartell, S. Rapsomanikis, M.O Andreae (1994) Methane in the Baltic and North Seas and a reassessment of the marine emissions of methane. Global Biogeochem Cycles, 8, 4, pp.465-480

Högström, U., E. Sahlée, W.M. Drennan, K.K. Kahma, A.S. Smedman, C. Johansson, H. Pettersson, A. Rutgersson, L. Tuomi, F. Zhang, M. Johansson (2008) Momentum fluxes and wind gradients in the marine boundary layer – a multi-platform study. Boreal Environ Res, 13, pp. 475-502

IPCC (2013) Climate change 2013: The physical science basis. Contribution of Working Group I to the Fifth Assessment Report of the Intergovernmental Panel on Climate Change. Cambridge University Press, 1535 pp.

Nilsson, E., H. Bergström, A. Rutgersson, E. Podgrajsek, M. Wallin, G. Bergström, E. Dellwik, S. Landwehr, B. Ward (2018) Evaluating humidity and sea salt disturbances on CO_2 flux measurements. J Atmos Ocean Tech, *in review*.

Norman, M., A. Rutgersson, L.L. Sørensen, E. Sahlée (2012) Methods for estimating air-sea fluxes of CO2 using high-frequency measurements. Bound-Lay Meterol, 144, 3, pp.379-400

Reeburgh W.S. (2007) Oceanic methane biogeochemistry, Chem Rev, 107, 2, pp. 486-513

Rutgersson A., M. Norman, B. Schneider, H. Pettersson, E. Sahlée (2008) The annual cycle of carbon dioxide and parameters influencing the air-sea carbon exchange in the Baltic Proper, J Marine Syst, 74, 2008, pp. 381-394

Rutgersson A., A.S. Smedman, E. Sahlée (2011) Oceanic convective mixing and the impact on air-sea gas transfer velocity. Geophys Res Lett, 38, L02602

Sahlée E., A. S. Smedman, A. Rutgersson, U. Högström (2008) Spectra of CO_2 and water vapor in the marine atmospheric surface layer. Bound-Lay Meteorol, 126, 2, pp. 279-295

Smedman A.S., U. Högström, H. Bergström, A. Rutgersson, K.K. Kahma, H. Pettersson (1999) A case study of air-sea interaction during swell conditions. J Geophys Res, 104, C11, pp. 25,833-25,851

Webb E.K., G.I. Pearman, R. Leuning (1980) Correction of flux measurements for density effects due to heat and water vapor transfer. Q J Roy Meteor Soc, 106, 447, pp. 85-10

The structure of the CO_2 system in the mouths of the continental rivers: Odra, Vistula, Leba and Slupia.

Karoline Hammer[1], Karol Kuliński[2] , Beata Szymczycha[2], Katarzyna Koziorowska[2], Marcin Stokowski[2] and Bernd Schneider[1]

[1] Leibniz Institute for Baltic Sea Research Warnemünde, Rostock, Germany (karoline.hammer@io-warnemuende.de)
[2] Institute of Oceanology of the Polish Academy of Sciences, Sopot, Poland

1. Introduction

Under oceanic conditions the structure of the marine CO_2 system is well understood. However, in coastal waters and estuaries it is much more complex due to the local anomalies in seawater composition and the influence of the non-CO_2 substances that have acid-base properties. In the Baltic Sea most of CO_2 system studies focus in the open sea though it is well known that river discharge influence significantly the composition of seawater. Generally, the Scandinavian rivers are poor in A_T, while those draining the limestone-rich continental part can be considered as an important source of A_T (Beldowski et al., 2010). However it is highly unknown how much the structure of the CO_2 system differs between the individual rivers and how it changes along with the mixing between river and the open sea. This was the motivation for our study, in which we focused on the characterization of the CO_2 system in the mixing zones of 4 Polish rivers: Odra, Vistula, Slupia, and Leba.

2. Methods

During the two RV Oceania cruises in May 2014 and 2015 surface water samples for A_T, C_T, pH, DOC, PIC, nutrients and total boron were collected in the salinity gradients of four Polish rivers. Two of them: Odra and Vistula drain huge area and belong to the largest rivers flowing to the Baltic Sea, while the two others (Slupia, Leba) are relatively short and small rivers flowing entering the Baltic at the Polish mid-coast.

All the samples were measured onshore within 2 months after sampling. Alkalinity was measured by open-cell titration method, while C_T was measured coulometrically on the SOMMA-system. The pH was measured on total scale by a spectrophotometric method (Carter et al., 2013). Furthermore, we used the method described by Kuliński et al. (2014) to calculate organic alkalinity. In short, we calculated on CO2SYS A_T from C_T and pH and subtracted it from the measured A_T. Since the CO2SYS contains only inorganic components of the acid-base system the calculated A_T refers to inorganic substances. On the other hand when measuring A_T both inorganic and organic substances are titrated. Thus the calculated ΔA_T can be considered as the organic alkalinity.

3. Results and Discussions

We put all the A_T results on the A_T vs. S diagram published by Beldowski et al. (2010) (Fig. 1). The data lie down along the A_T vs. S dependency detected for the Gulf of Riga. However, all the investigated rivers differ in terms of A_T. This gives not one single line but instead an area, which additionally broadens with a salinity decrease. The highest A_T (3490 µmol/kg) was found in the Vistula river. At the same time the A_T vs. S dependency for Vistula has the steepest slope. The lowest A_T (1925 µmol/kg) and also the lowest slope was identified for the Slupia river.

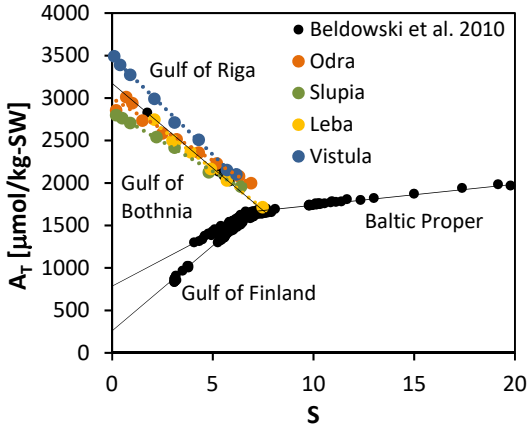

Figure 1. The A_T vs. S relationships reported for the open Baltic Sea (Beldowski et al., 2010) supplemented with experimental data from the mouths of four Polish rivers.

A_T measured was always higher from that calculated from C_T and pH. The ΔA_T oscillated between approx. 25 µmol/kg found in the open Baltic Sea waters (S~7) and 264 µmol/kg noticed in Leba river (Fig. 2). The ΔA_T constitutes a significant share within A_T. The maximum one of 11% was found in Leba. Taking into account high DOC concentrations, especially in rivers (600-700 µmol/L), this high ΔA_T can be attributed to the influence of organic substances. The increase of ΔA_T with decreasing hydrogen ion concentration (or increasing pH) (Fig. 2) is plausible and fits to the acid-base properties of organic matter described previously by Kuliński et al. (2014) and Ulfsbo et al. (2015). However, taking into account the hypothetical structure of dissolved organic matter and reported share of acidic functional groups in DOC (12-17% of DOC) (Kuliński et al., 2014; Ulfsbo et al., 2015; Hammer et al., 2017) the organic alkalinity does not explain fully the ΔA_T. We put the hypothesis, that some ΔA_T was due to the particles. We identified both particulate carbonates and particulate organic matter in the samples. Although the methodology does not require filtration of A_T samples, we noticed that for samples containing lot of particles it is hard to avoid their influence even when treating samples gently.

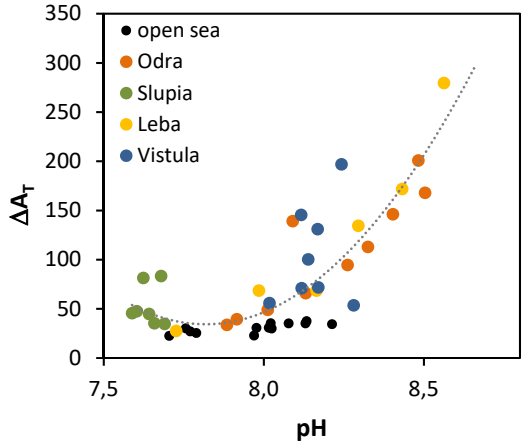

Figure 2. pH dependence of $\Delta A_T = A_T$(measured) - A_T(calculated from C_T and pH) in the mixing zones for the continental rivers: Odra, Vistula, Leba and Slupia.

4. Conclusions

It was found that rivers entering the Baltic Sea along the Polish coast are important sources of A_T. This high A_T is due to the high supply the river waters with ionic carbonates and bicarbonates – a result of draining the limestone-rich catchment. However, the non-CO_2 constituents having acid-base properties play the role. The significant contribution is from dissolved organic matter, that is present in the mixing zones in high concentrations. It was also found that particles, both suspended carbonates and particulate organic matter, can disturb the measurements of the CO_2 system.

References

Beldowski, J., Löffler, A., Schneider, B., and Joensuu, L. (2010) Distribution and biogeochemical control of total CO2 and total alkalinity in the Baltic Sea, Journal of Marine Systems, 81, 252-259

Carter, B., Radich, J., Doyle, H., and Dickson, A. (2013) An automated system for spectrophotometric seawater pH measurements, Limnol. Oceanogr.: Methods, 11, 16-27.

Hammer, K., Schneider, B., Kuliński, K., and Schulz-Bull, D. E. (2017) Acid-base properties of Baltic Sea dissolved organic matter, Journal of Marine Systems, 173, 114-121

Kuliński, K., Schneider, B., Hammer, K., Machulik, U., and Schulz-Bull, D. (2014) The influence of dissolved organic matter on the acid–base system of the Baltic Sea, Journal of Marine Systems, 132, 106-115

Ulfsbo, A., Kuliński, K., Anderson, L. G., and Turner, D. R. (2015) Modelling organic alkalinity in the Baltic Sea using a Humic-Pitzer approach, Marine Chemistry, 168, 18-26

Measuring turbulent sea-air CO_2 fluxes with a closed-path gas analyzer

Martti Honkanen[1], Juha-Pekka Tuovinen[2], Tuomas Laurila[2], Timo Mäkelä[2], Juha Hatakka[2], Sami Kielosto[1,3] and Lauri Laakso[1,4]

[1] Meteorological and Marine Research Programme, Finnish Meteorological Institute, Helsinki, Finland (martti.honkanen@fmi.fi)
[2] Climate Research Programme, Finnish Meteorological Institute, Helsinki, Finland
[3] Marine Ecology Research Laboratory, Finnish Environment Institute, Helsinki, Finland
[4] School of Physical and Chemical Sciences, North-West University, Potchefstroom Campus, South Africa

1. Introduction

Direct measurements of carbon dioxide (CO_2) exchange between the atmosphere and the sea surface are used in quantifying the global carbon cycle and developing parametrizations of gas transfer velocity used in global carbon models. The sea-air CO_2 flux measurements are often carried out with the eddy covariance (EC) method using infrared gas analyzers (IRGAs), which have been found to be prone to water vapor interference, especially in marine environment (Blomquist et al., 2014), where CO_2 fluxes are small.

In this presentation, which is based on Honkanen et al. (2018), we analyze sea-air CO_2 fluxes measured on a shore of an island. We compare measurements made with two identical closed-path IRGA-based systems, one of which is equipped with a Nafion drier, to eliminate water vapor interference, and a virtual impactor, to protect the instrument from possible exposure to liquid water. The quality of these land-based flux measurements is addressed by analyzing the fulfillment of theoretical assumptions of the EC method.

2. Materials and methods

Sea-air fluxes of CO_2 were measured on the island of Utö in the Archipelago Sea in the Baltic Sea in 1 July — 1 November 2017. The EC tower was 9 m tall and only the western wind directions (180—340°) representing open sea were considered. Two closed-path IRGAs (LI-7000, LI-COR) were used for measuring CO_2 molar fractions at 10 Hz, which were corrected for the dilution effect due to water vapor. Wind velocity components and air temperature were measured using an acoustic anemometer (uSonic-3, METEK) placed directly above the sample air inlets (11.5 m a.s.l). The calculated half-hourly fluxes were experimentally corrected for high frequency attenuation.

Additionally, CO_2 partial pressure (pCO_2) at 5 m depth was measured using an equilibration chamber and an IRGA (SuperCO_2, Sunburst Sensors) connected to a flow-through pumping system. The atmospheric pCO_2 at 57 m height was observed in the atmospheric ICOS station (Kilkki et al., 2015).

3. Results

The pCO_2 difference between the sea and the atmosphere shifted from negative (-92 µatm on average in July) to positive (164 µatm in October) as a result of diminished primary production and enhanced vertical mixing in the water column. The direction of the sea-air CO_2 flux followed the evolution of pCO_2 difference: the monthly mean flux was -0.23 µmol m^{-2} s^{-1} in July and 0.30 µmol m^{-2} s^{-1} in October.

The homogeneity of the flux footprint area was analyzed in terms of surface roughness length, which was found to be independent of wind direction and mainly lower than 1 mm. The cospectra between vertical wind speed and CO_2 agreed with the universal model cospectrum (Horst, 1997) and showed a moderate high frequency attenuation. Turbulence was well-developed, as integral turbulence characteristics were found to be unique functions of stability parameter and friction velocity.

The non-stationarity of the CO_2 fluxes was examined by calculating the relative non-stationarity, *RN*, as a difference between the 30 min flux and the mean of the corresponding 5 min fluxes (Foken and Wichura, 1996). It was found that non-stationarity conditions (*RN* > 0.3) generated unphysical sea-air CO_2 fluxes. During July, negative fluxes were expected due to the negative pCO_2 difference. If the non-stationary cases were not discarded, 25% of the sea-air fluxes of CO_2 were positive; this was reduced to 4% when non-stationary fluxes were discarded. This, however, resulted in a high rejection rate of 63 %. The non-stationarity of the CO_2 fluxes was linked to the change in atmospheric CO_2 concentration during the averaging period. A change larger than 2 ppm was associated with the rejection rate of 95 % due to non-stationarity.

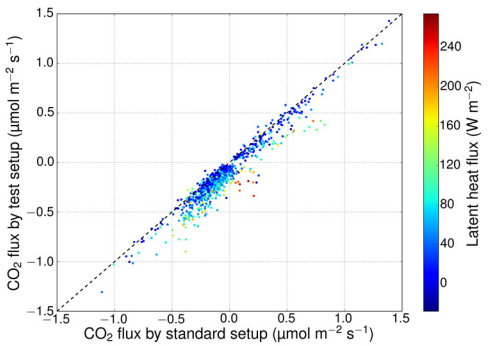

Figure 1. The sea-air CO_2 flux measured with the standard setup vs. the test setup (incl. the drier and the virtual impactor). The concurrent latent heat flux is depicted by the color of the dot and the dashed line indicates the 1:1 relationship.

Two setups showed similar sea-air fluxes of CO_2 (R^2 = 0.96). The undried measurement, however, tended to show slightly more positive fluxes (Fig. 1). The difference between the measurements increased with increasing latent heat flux. During low latent heat fluxes, R^2 was 0.99 and the average difference between the measurements was negligible. During high latent heat fluxes (~100 W m^{-2}), however, the average difference between the measurements was 0.15 µmol m^{-2} s^{-1}, which is comparable to the typical monthly mean sea-air CO_2 flux.

References

Blomquist, B. W., B. J. Huebert, C. W. Fairall, L. Bariteau, J. B. Edson, J. E. Hare and W. R. McGillis (2014) Advances in air-sea CO_2 flux measurements by eddy correlation, Bound.-Layer Meteorol., 152, 3, pp. 245-276

Foken, T. and B. Wichura (1996) Tools for quality assessment of surface-based flux measurements, Agric. For. Meteorol., 78, 1-2, pp. 83-105

Honkanen, M., Tuovinen, J.-P., Laurila, T., Hatakka, J., Kielosto, S., and Laakso, L. (2018) Measuring turbulent CO_2 fluxes with a closed-path gas analyzer in marine environment, Submitted to Atmos. Meas. Tech.

Horst, T. W. (1997) A simple formula for attenuation of eddy covariance measured with a first-order response scalar sensors, Bound.-Layer Meteorol., 82, 2, pp. 219-233

Kilkki, J., T. Aalto, J. Hatakka, H. Portin and T. Laurila (2015) Atmospheric CO_2 observations at Finnish urban and rural sites, Boreal Env. Res., 20, 2, pp. 227-242

Understanding the ecocline at shallow coasts of the Baltic Sea

Gerald Jurasinski[1], Maren Voss[2] , Manon Janssen[3], Bernd Lennartz[3], and the Baltic TRANSCOAST team

[1] Landscape Ecology, University of Rostock, Rostock, Germany
[2] Leibniz Institute for Baltic Sea Research Warnemuende (IOW), Biological Oceanography, Rostock, Germany
[3] Soil physics, University of Rostock, Rostock, Germany

1. Background

Coastal zones connect terrestrial and marine ecosystems, forming a unique environment, which is increasingly under anthropogenic pressure (Bollman et al. 2010). Rising sea levels, sinking coasts and changing precipitation patterns modify hydrodynamic gradients and possibly increase sea-land exchange in tidal and non-tidal systems alike (ibid.). Flood protection is one important aspect of changing coastlines while in some locations coastal protection like dykes are removed making the coastal interface further permeable (Hahn et al. 2015). In the future the exchange processes between shallow coasts and low-lying lands will very likely get considerably more intense and at places might change completely. Unfortunately, we are lacking a thorough understanding of the ecosystem functioning of such coastal zones and the reciprocal influences between terrestrial and marine ecosystems.

Here, we report on results of the Research Training Group Baltic TRANSCOAST. In Baltic TRANSCOAST we are using the nature reserve 'Heiligensee und Hütelmoor' ('Hutelmoor' in the following), a low-lying fen peat site on the southern Baltic Sea coast, including the offshore shallow sea area as a model ecosystem to quantify hydro-physical, biogeochemical, and biological processes across the whole land-sea gradient. Coastal fen peats are abundant in some regions along the Baltic Sea coast and its estuaries (Lampe & Janke 2004), but most of them are drained and converted to polders. However, many of these areas might be flooded again—at least occasionally—under future sea level rise. Therefore, our study site is an interesting model ecosystem that allows us to investigate possible future conditions already now.

2. The Baltic TRANSCOAST approach

The research in Baltic TRANSCOAST is conducted by 13 PhD students and 14 principal investigators with support from several associated research groups in Europe as well as visiting scientists. The overall aim of Baltic TRANSCOAST is to enhance our knowledge of the shallow coast ecocline (Fig.1). How is the marine coastal zone influenced by terrestrial processes? How is the terrestrial coastal zone influenced by marine processes? These questions lead our research within the three research fields covering hydro-physical, (bio)geochemical and biological processes. Regarding the hydro-physics we assess how the peatland's water balance, the current dynamics and hydraulic properties of the marine sediments, and the subsoil influence sea water intrusions into the peatland and/or submarine groundwater discharge into the Baltic Sea. With respect to (bio)geochemical processes we address how the related transformation processes both in the marine and the terrestrial part of the coast are influenced by water and matter inputs from the respective other coastal domain. Finally, regarding the biological processes, we are interested in revealing how the primary production and the composition of micro- and macro-phytobenthos in the shallow Baltic Sea influence matter transformation processes.

The integrative approach of Baltic TRANSCOAST allows us to get to grips with questions that are otherwise hard to tackle. For instance, we address how the pore water constituents drive microbial processes and the deposition of nutrients and how they are impacted by sediment resuspension and translocation. We investigate how the hydrology of the peat layers interferes with the generation of trace gases and investigate the role of the nearby Warnow river and its plume and how this changes under the impact of wind direction and wind strength. Further, as a common basis for all topics addressed in Baltic TRANSCOAST we established the geology of the study area and learned that regional variability may play a major role in shaping the processes under study.

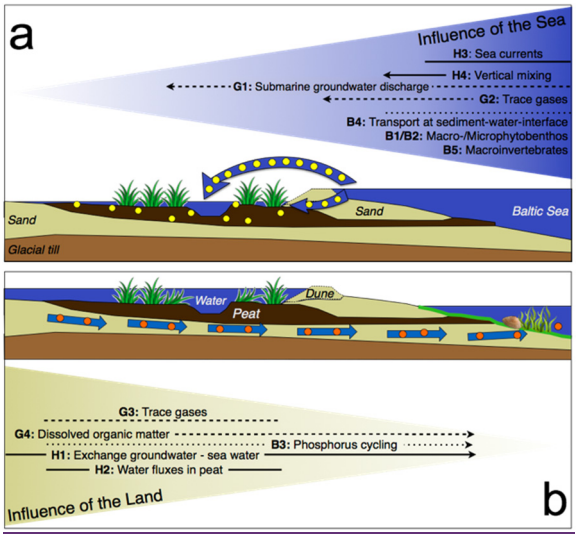

Figure 1. Baltic TRANSCOAST scheme showing prevailing water and substance exchange pathways across the coast line at two different possible states: a) During storm surge events brackish seawater flows into the coastal peatland (above and below surface; b) When ground and surface water levels are high during winter, submarine groundwater discharge may export nutrients and DOM to the shallow sea. Arrows show BT research topics.

3. Study site

The 'Hutelmoor' is located on the southern Baltic Sea coast in north-eastern Germany, near the city of Rostock and the estuary of the river Warnow. A local depression formed by a early-holocene glacial stream (Kolp 1957) was the basis for the development of a coastal paludification fen, which developed when the rising sea level of the Baltic Sea caused rising groundwater levels on the landside. The Hutelmoor covers 540 hectares and features 1 to 3 m thick layers of sedge and reed peat. Due to its low elevation (-0.1 to +0.7 m HN), the site was influenced by intermittent

flooding events resulting in occasional thin sand layers within the peat. In the surroundings of the lake Heiligensee, organic and mineral gyttjas are found at the basis of the peat. Underneath, 3 to 10 m thick basin sands form an aquifer, which is underlain by glacial till. The peatland is surrounded by forest on mineral soils. Originally, the area discharged directly into the Baltic Sea via a small brook cutting through the dunes. The climate is temperate in the transition zone between maritime and continental with an average annual temperature of 9.1°C and an average annual precipitation of 645 mm (data derived from grid product of the German Weather Service, reference climate period: 1981–2010).

Today, the plant community is dominated by emergent macrophytes like Common reed (*Phragmites australis* (Cav.) Trin.) and Cattail (*Typha angustifolia* L.). Especially later in the vegetation period submerse aquatic species like *Ceratophyllum demersum* L. dominate the relatively abundant areas of open shallow water. The typical brackish water emergent macrophyte Sea clubrush (*Bolboschoenus maritimus* L.) was almost completely displaced, whereas another brackish water species, the Softstem bulrush (*Schoenoplectus tabernaemontani* (C.C.Gmel.) Palla, was able to increase its cover considerably in the last decade (Koch et al. 2017). Dryer areas at the boundaries to the forest are mainly colonised by the Lesser pond sedge (*Carex acutiformis* Ehrh.) and Common rush (*Juncus effusus* L.).

The geomorphology seawards the Hutelmoor is formed by abrasive processes driven by westerly winds that are dominant along the East German Baltic Sea coast and have shifted the coastline landwards. Most of the coastal area between 0 and 10 m depth is covered by coarse-grained sediments with gravel and stones dominating at some sites. A few tens of meters away from the shoreline an underwater barrier has developed. This seems typical for the southern German Baltic coastline where no fine-grained sediments can be found (Leipe et al. 2010). Roughly 10 km west from the study area, the Warnow river enters the Baltic Sea with relatively low outflow and a mean discharge of 1450km³ y^{-1}.

4. Selected results

Our hydro-geological surveys suggest that at the Hütelmoor the coastline receded considerably in the last centuries exposing former land-based geological strata (i.e, peat) to the sea. This submerged peat now extending to the sea forms a unique habitat for micro- and macro-phytobenthos alike. Landwards, rewetting measures introduced in late 2009 along with increases in winter precipitation seem to induce submarine groundwater discharge (SGD) into the shallow coastal waters. Distinct patterns in electric conductivity as well as the patterns of Radon variability in the near shore seawater confirm that the shallow coastal waters in front of the Hütelmoor are a mixing zone with freshwater. However, in the future also more frequent flooding, and, thus, salt water intrusion, seems to be likely since an analysis of sea level flood thresholds over the past 60 years shows that the number of hours per year exceeding 0,5m, 0,75m and 1,0m levels above a.s.l., respectively has increased.

The impact of nutrient laden freshwater on biogeochemical reactions including greenhouse gas emissions and the biota in the shallow sea water is poorly understood. However, high loadings of nutrients and complex organic molecules originating from the degraded peat indicate that micro- and macro-phytobenthos are affected with the impacts propagating to the higher trophic levels such as benthic communities.

The terrestrial part of the study site is subject to periodic brackish water intrusions caused by flooding altering the hydro-physical and geochemical properties of the prevailing peat soils. The relatively stable salinity distribution in the main part of the peatland reveals the legacy of past flooding events, while dynamic below ground changes in salinity closer to the shoreline document more dynamic salt water intrusions on much smaller temporal and spatial scales.

The observed shifts in salinity do not severely alter the hydraulic properties of organic soils despite a rearrangement of organic matter complexes as detectable from the leaching patterns of dissolved organic molecules. It is generally assumed that salinity influences greenhouse gas emissions, mainly by inhibiting methane production since sulfate reducers out-compete methanogens (e.g., Bartlett & Harriss 1993). However, repeated porewater analyses and peat corings revealed a distinct depth separation of biogeochemical and, thus, microbiological activity zones driven by episodic flooding which allows for high methane production (Koebsch et al. 2015) in the peatland despite high sulfate concentrations.

5. Conclusions

Our results show that sea land interactions of shallow coasts at low-lying land are far reaching, occurring on either side of the interface, and may only be properly described when long-term temporal patterns and different spatial scales are considered. Therefore, in future research we will explicitly address temporal variability and the scale dependence of the exchange and transformation processes. Further investigations should include numerical model analyses and should expand to other low-lying coastal segments of the Baltic Sea and comparable systems.

References

Bartlett KB, Harriss RC (1993) Review and assessment of methane emissions from wetlands. Chemosphere 26:261–320

Bollmann M et al. (2010) World ocean review: living with the oceans. Maribus, Kiel

Hahn J, Glatzel S, Köhler S, Jurasinski G (2015) Greenhouse gas exchange in a coastal fen in the first year after flooding – a systems shift. PLOSone 10:e0140657

Koch M, Koebsch F, Hahn J, Jurasinski G (2017) From meadow to shallow lake: Monitoring secondary succession in a coastal fen after rewetting by flooding based on aerial imagery and plot data. Mires & Peat 19(11):1–17

Koebsch F, Jurasinski G, Koch M, Hofmann J, Glatzel S (2015) Controls for multi-scale temporal variation in ecosystem methane exchange during the growing season of a permanently inundated fen. AFM 204:94–105

Kolp O (1957) Die nordöstliche Heide Mecklenburgs. VEB Deutscher Verlag der Wissenschaften, Berlin

Kotwicki L, Grzelak K, Czub M, Dellwig O, Gentz T, Szymczycha B, Böttcher ME (2014) Submarine groundwater discharge to the Baltic coastal zone: Impacts on the meiofaunal community. Journal of Marine Systems 129:118–126

Leipe T, Tauber F, Vallius H, Virtasalo J, Uścinowicz S, Kowalski N, Hille S, Lindgren S, Myllyvirta T (2010) Particulate organic carbon (POC) in surface sediments of the Baltic Sea. Geo-Marine Letters

Hydrochemical characterization of SGD in the Bay of Puck, Southern Baltic Sea.

Żaneta Kłostowska[1,2], Beata Szymczycha[1], Karol Kuliński[1], Monika Lengier[1] and Leszek Łęczyński[2]

[1] Institute of Oceanology, Polish Academy of Sciences, Powstańców Warszawy 55, 81-712 Sopot, Poland (klost@iopan.pl)
[2] Institute of Oceanography, University of Gdańsk, Al. Marszałka Piłsudskiego 46, 81-378 Gdynia, Poland

1. Introduction

Submarine groundwater discharge (SGD) has been recognized as a significant source of water and chemical substances such as trace metals, nutrients, organic and inorganic carbon to the coastal zone (Burnett et al. 2006; Moore 2010). In some regions SGD has been responsible for a deterioration of the coastal environment affecting the local economy and management of the area (Valiela et al., 2002). Particularly sensitive to the SGD are enclosed or semi-enclosed reservoirs of a limited water exchange with the open sea (Cyberski, 1993). The Bay of Puck, southern Baltic Sea, due to its morphological and hydrological features, is a good example of a basin partially separated from the open sea waters (Nowacki, 1993). Moreover, the bay itself is divided into two parts by the Rybitwa Shallow (the average depths: 21m in the outer and 3m in the inner part, that additionally impedes highly the water renewal in the inner part) (Urbanski et al., 2007). The Bay of Puck borders with the continental land in the west and the thin Hel Peninsula in the north and north-east. Both, the continental part and the peninsula differ in terms of land use and management. The first studies on the SGD in the Baltic Sea region were also performed at the Hel Peninsula (Sadurski, 1987). They were related to the seawater intrusion due to the intense exploitation of aquifers. As a consequence several groundwater wells were closed along the Hel Peninsula. Later a reverse phenomenon has started to be observed and scientists became interested in the identification and quantification of the groundwater seepage to the marine environment (Piekarek-Jankowska et al., 1994). The anomalies in the chloride distribution due to the groundwater discharge were identified in the pore waters of the Bay of Puck sediments (Bolałek, 1992). Recently, the fluxes of different chemical substances via SGD to the Bay of Puck have been estimated based on the experimental studies performed at the Hel Peninsula, off Hel (Szymczycha et al., 2012; Szymczycha et al., 2014; Szymczycha et al., 2016). Interestingly the loads of P, Mn and DIC via SGD to the Bay of Puck reported by the authors are comparable to the loads supplied by the local rivers entering the basin. This suggests that the SGD can also be an important source of other chemical constituents and thus has a potential to shape the functioning of the unique ecosystem of the Bay of Puck. Those estimations and conclusions were based on the assumption that the composition of the groundwater coming from the side of the Hel Peninsula and the continental part are similar. Our present research hypothesis assumes that the different aquifers exploitation, land use and management, diversified geological structure and differences in land-sea interactions along the Hel Peninsula and at the continental part differentiate the chemical composition of SGD coming from both these sides. The main aim of this study was to identify the provenance of the groundwater discharged to the bay and processes influencing its composition. This was done based on the chemical composition of SGD.

2. Methods

The research was carried out in years 2016-2017. Three active areas of SGD off Hel Peninsula (Hel, Jurata, Chałupy), and three off continental part of the bay (Puck, Swarzewo and Osłonino) were identified based on salinity and chloride measurements (Fig. 1). Water samples were collected along the salinity transition zone: groundwater from piezometers located in the coastal zone, groundwater and seepage water from the subterranean estuary (groundwater – seawater mixing zone) and seawater. The major ions (Ca^{2+}, Mg^{2+}, Na^{+}, K^{+}, Cl^{-}, SO_4^{2-}, HCO_3^{-}) content was analyzed in 198 samples. The measurements of Ca^{2+}, Mg^{2+}, Na^{+}, K^{+} were conducted by means of AAS (SHIMADZU 6800). Concentrations of HCO_3^{-} and Cl^{-} were determined by potentiometric titration using ion-selective electrodes (ISE) Cerko Lab System Potentiometry. SO_4^{2-} was quantified by the precipitation method. Separation of individual types of water was made based on Cl^{-} content (Bolałek, 1992). The seepage samples with chloride ions content smaller than 1 $gCl^{-}\cdot dm^{-3}$ were idetified as groundwater samples.

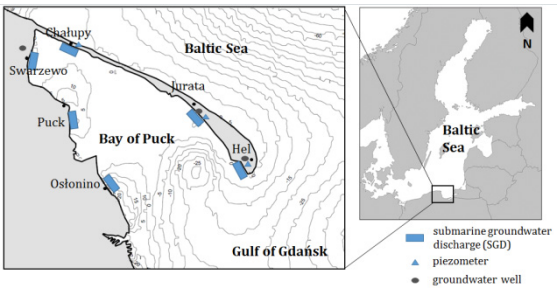

Figure 1. Map of the Bay of Puck showing the active areas of submarine groundwater discharge (SGD), locations of piezometers and groundwater well, along the Hel Peninsula (Hel, Jurata, Chałupy), and in the continental part of the bay (Puck, Swarzewo and Osłonino).

3. Results

The major ions ratios in all groundwater samples fluctuated in the range: from 0.11 to 0.94 for Ca^{2+}/Cl^{-}, from 0.08 to 1.23 for Mg^{2+}/Cl^{-}, from 2.23 to 93.50 for Na^{+}/Cl^{-}, from 0.03 to 0.66 for K^{+}/Cl^{-}, from 0.01 to 0.32 for SO_4^{2-}/Cl^{-}, from 0.07 to 0.39 for HCO_3^{-}/Cl^{-}, from 0.57 to 3.42 for Mg^{2+}/Ca^{2+}, while for seawater samples were in the range from 0.01 to 0.02 for Ca^{2+}/Cl, from 0.01 to 0.06 for Mg^{2+}/Cl^{-}, from 0.58 to 0.75 for Na^{+}/Cl^{-}, from 0.01 to 0.02 for K^{+}/Cl^{-}, from 2.98 to 4.79 for Mg^{2+}/Ca^{2+}. The ionic ratios in water samples from piezometers ranged from 0.04 to 1.97 for Ca^{2+}/Cl^{-}, from 0.01 to 0.32 for Mg^{2+}/Cl^{-}, from 1.11 to 88.68

for Na^+/Cl^-, from 0.01 to 0.44 for K^+/Cl^-, from 0.01 to 0.06 for SO_4^{2-}/Cl^-, from 0.01 to 1.16 for HCO_3^-/Cl^- and from 0.20 to 2.20 for Mg^{2+}/Ca^{2+}. Water samples collected in the groundwater wells were characterized by the range: from 0.45 to 5.67 for Ca^{2+}/Cl^-, from 0.09 to 0.62 for Mg^{2+}/Cl^-, from 0.78 to 0.85 for Na^+/Cl^-, from 0.08 to 0.34 for K^+/Cl^-, from 0.03 to 4.49 for SO_4^{2-}/Cl^-, from 2.90 to 20.23 for HCO_3^-/Cl^- and from 0.18 to 0.35 for Mg^{2+}/Ca^{2+}. The maximum ratios in groundwater samples collected in the subterranean estuary were observed in Chałupy region and equal to 0.79 for Ca^{2+}/Cl^-, 1.23 for Mg^{2+}/Cl^-, 25.17 for Na^+/Cl^- and 0.66 for K^+/Cl^-, respectively. Comparable results were detected also in Swarzewo. In case of water samples coming from piezometers, the maximum ratios were observed in Hel and equal to 0.72 for Ca^{2+}/Cl^-, 0.27 for Mg^{2+}/Cl^-, 34.87 for Na^+/Cl^-, 0.08 for K^+/Cl^-, 0.06 for SO_4^{2-}/Cl^-, 0.46 for HCO_3^-/Cl^-, while the lowest ratios were recorded in Jurata and equal to 0.04, 0.01, 0.01, 0.0048 and 0.01, respectively. The ratios for groundwater samples collected in wells were highest in Swarzewo and equal to 5.67 for Ca^{2+}/Cl^-, 0.62 for Mg^{2+}/Cl^-, 0.85 for Na^+/Cl^-, 0.34 for K^+/Cl^-, 4.49 for SO_4^{2-}/Cl^-, 20.24 for HCO_3^-/Cl^-, except Mg^{2+}/Ca^{2+} (0.35) that was identified in the Jurata.

4. Discussion and conclusions

The preliminary results indicate that SGD composition in Chałupy and Swarzewo are comparable. This suggests that groundwater discharged from both these sites located in the Inner Bay of Puck can have similar source. This hypothesis will be further verified by the analysis of the oxygen stable isotopes. For Hel and Jurata the ionic composition of the groundwater samples is mainly influenced by the land-sea interactions. Thus the increase of seawater level and atmospheric conditions such as storms will result in higher seawater intrusion (Sadurski, 1987). The vertical cross-section of groundwater composition located in Hel (Fig. 2) is conditioned by the processes associated with the movement of sea water masses. This is observed at both sites of the peninsula. Osłonino and Swarzewo characterized with totally different ratios in comparison to other areas which can be explained by possible different source of groundwater relating to different land use and management. The preliminary results do not fully verify our hypothesis and therefore further studies are necessary in other to understand the groundwater provenance and factors influencing SGD in the Bay of Puck. The results show that there is no clear separation between continental part and peninsula in terms of groundwater composition. Further studies are necessary to understand the groundwater provenance and factors influencing SGD in the Bay of Puck.

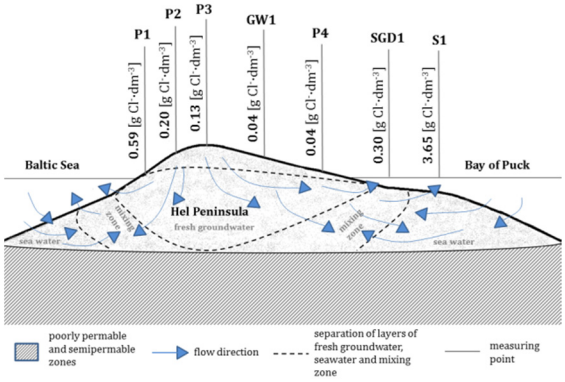

Figure 2. Schematic distribution of chloride concentration [$gCl^-{\cdot}dm^{-3}$] at submarine groundwater discharge (SGD), piezometers (P), groundwater well (GW) and sea water (S) in the Hel Peninsula, off Hel.

5. References

Bolałek J. (1990) Ionic macrocomponets of the interstitial waters of Puck Bay, Oceanologia, 33, 131-159.

Burnett W.C., Aggarwal P.K., Aureli A., Bokuniewicz H.J., Cable J.E., Charette M.A., Kontar E., Krupa S., Kulkarni K.M., Loveless A., Moore W.S., Oberdorfer J.A., Oliveira J., Ozyurt N., Povinec P., Privitera A.M.G., Rajar R., Ramessur R.T., Scholten J., Stieglitz T., Taniguchi M., Turner J.V. (2006) Quantifying submarine groundwater discharge in the coastal zone via multiple methods. Science of the Total Environment, 367, 498-543.

Cyberski J. (1993) Hydrologia zlewiska i morfometria zatoki, (ed) Korzeniewski K., Zatoka Pucka, Gdańsk, Instytut Oceanografii Uniwersytetu Gdańskiego, 40.

Moore W.S. (2010) The Effect of Submarine Groundwater Discharge on the Ocean, Annual Review of Marine Science, 2, 59-88.

Nowacki J. (1993) Thermics, salinity and density of water, [in:] Puck Bay, Korzeniewski K. (ed.), Fundacja Rozwoju Uniwersytetu Gdańskiego, Gdańsk, 79–111.

Piekarek-Jankowska H., Matciak M., Nowacki J. (1994) Salinity variations as an effect of groundwater seepage through the seabed (Puck Bay. Poland), Oceanologia, 36, 33-46.

Sadurski A. (1987) Warunki hydrogeologiczne i hydrochemiczne Mierzei Helskiej, Geological Quarterly, 31, 767-782.

Szymczycha B., Vogler S., Pempkowiak J. (2012) Nutrient fluxes via submarine groundwater discharge to the Bay of Puck, Southern Baltic, Sci. Total Environ., 438, 86-93.

Szymczycha B., Maciejewska A., Winogradow A., Pempkowiak J. (2014) Could submarine groundwater discharge be a significant carbon source to the southern Baltic Sea? In Oceanologia, 56, 327–347.

Szymczycha B., Kroeger K. D., Pempkowiak J. (2016) Significance of groundwater discharge along the coast of Poland as a source of dissolved metals to the southern Baltic Sea, Marine Pollution Bulletin, 109, 151-162.

Urbański J., Grusza G., Chlebus N. (2007) Fizyczna typologia dna Zatoki Gdańskiej. Gdynia: Pracownia Geoinformacji Zakładu Oceanografii Fizycznej, Instytut Oceanografii UG. 8

Valiela I., Bowen J.L., Kroeger K. D. (2002) Assesment of models for estimation of land-derived nitrogen loads to shallow estuaries, Applied Geochemistry, 17, 935-953.

The acid-base system of the Baltic Sea

Karol Kuliński[1,*], Marcin Stokowski[1], Beata Szymczycha[1], Karoline Hammer[2], Katarzyna Koziorowska[1], Aleksandra Winogradow[1], Monika Lengier[1], Żaneta Kłostowska[1], Bernd Schneider[2],

[1] Institute of Oceanology, Polish Academy of Sciences, Sopot, Poland
[2] Leibniz Institute for Baltic Sea Research, Warnemünde, Germany
* corresponding author, e-mail: kroll@iopan.gda.pl

1. Introduction

The marine acid-base system is relatively well understood for oceanic waters. It is controlled to large degree by the CO_2 system. All four measurable variables (pCO_2, pH, C_T, A_T) are interacting and control the pH by a set of equilibrium constants and mass balance equations. In general the interrelationships between these four parameters facilitate the calculation of any two variables, when the two others are known, e.g. through measurements, and when the dissociation constants of the involved acid-base reactions are known for the respective temperature and salinity. This fact is used in biogeochemical models aiming at simulation of marine CO_2 system.

The structure and functioning of the acid-base system is less obvious for the coastal and shelf seas due to the number of regionally specific anomalies. In this context the Baltic Sea can be considered as a very complex ecosystem, in which on one hand the low buffer capacity makes the seawater vulnerable to acidification, and on the other hand the sea is exposed to various anthropogenic influences which have the potential to change the acid-base system and thus also seawater pH and all pH-related processes. In this study we collect and integrate existing knowledge on the acid-base system in the Baltic Sea.

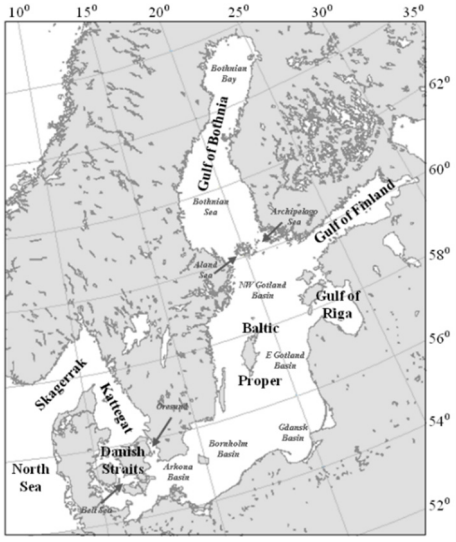

Figure 1. Map of the Baltic Sea showing its division into natural basins and sub-basins.

2. Dissociation constants in brackish water

Globally, the validity of most of the constants was confined to salinities that are encountered in ocean water. However, with regard to research in the Baltic Sea where large areas, e.g. in the Gulf of Bothnia, have surface water salinities less than 5, the situation was unsatisfactory. It took until 2006 when Millero et al. (2006) published dissociation constants that covered the salinity range from 0 to 50 and that were consistent with the constants for fresh water. An update of these constants was performed in 2010 (Millero, 2010) and since then this set of dissociation constants is state of the art for CO_2 research in brackish waters. The salinity and the temperature dependency of K_1 and K_2 are presented in Fig. 2a and 2b, respectively.

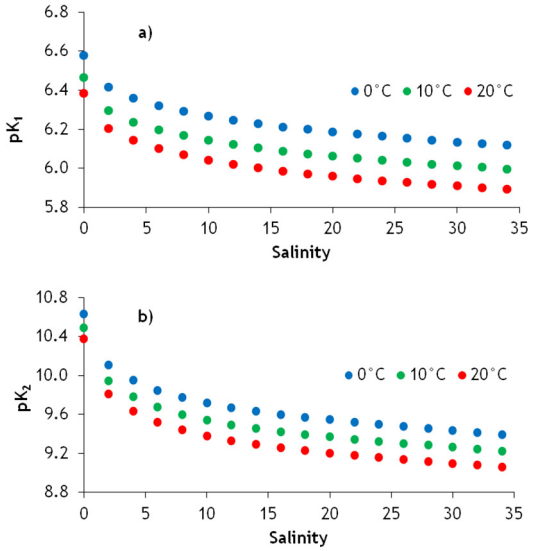

Figure 2. Dissociation constants (a) pK_1 and (b) pK_2 as a function of salinity calculated according to Millero (2010) for three different temperatures: 0, 10 and 20 °C.

3. Anomalies of the Baltic Sea acid-base system

With our study we have proposed that the Baltic Sea acid-base system cannot be explained by dissolved CO_2 and a minor contribution of boric acid. Whereas acid-base components other than CO_2 and borate may be ignored in ocean waters, this is not the case in the Baltic Sea and, presumably, other marginal and semi-enclosed seas, which in a similar way are strongly impacted by high biomass production and natural and anthropogenic processes in connected catchment areas as well. The complexity of the Baltic Sea acid-base system is displayed in the formulation of the A_T, which is the central variable for the characterization of the acid-base properties of seawater. The peculiarities of the Baltic Sea alkalinity system are either caused by specific internal processes related to intense production/mineralization of organic matter, or to the immediate effect of riverine input of acidic substances. This riverine input refers mostly to dissolved organic matter which may strongly affect the composition of the alkalinity in the Baltic Sea surface water (Kuliński et al., 2014), but also to boric acid (borate) which

in ocean water is linked to salinity by a constant ratio, but show distinct deviations from this ratio in the coastal, brackish waters. In this study we clearly identified total boron concentration anomaly in the Baltic Sea. This conclusion was taken based on the re-analysis of 161 total boron (TB) measurements made by Kremling (1970 and 1972) and on our own measurements of 133 samples. Both data sets characterize with high spatial and vertical coverage the Baltic Sea and include the samples of the salinity range from 0.1 to 19.9. This testifies the representativeness of the obtained results and taken conclusions. The freshwater entering the Baltic Sea contains about 13.8 µmol TB kg^{-1}. This finding is against the reports from the open ocean (e.g. Uppström 1974), which indicated that TB vs. S relationship contains no intercept (TB = 0 at S = 0).

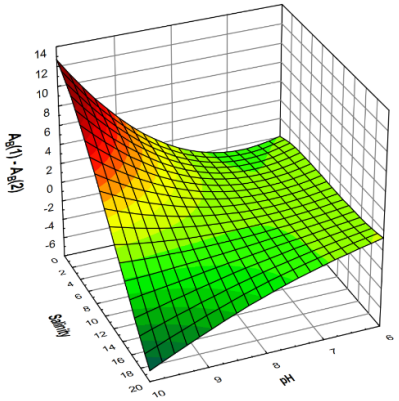

Figure 3. The difference between borate alkalinity calculated from TB vs. S relationship determined in our study ($A_B(1)$) and that reported by Uppström (1974) ($A_B(2)$) presented in µmol kg^{-1} against pH and salinity.

Internal biogeochemical processes such as organic matter production or mineralization also have the potential to affect the acid-base system in the Baltic Sea. Alkalinity changes by organic matter production caused by the removal of H^+ during the uptake of nitrate are of minor importance. This may be different if the production is associated with calcification, which reduces the alkalinity, but the abundance of calcifying plankton in the Baltic Sea is restricted to the high-salinity Kattegat region. Although the effect of organic matter production on alkalinity is minor, it is the major control for the seasonal modulation of the acid-base properties such as pH and pCO_2.

In contrast, organic matter mineralization taking place at anoxic conditions in the Baltic Sea deep basins causes changes in the acid base system which are specific for marine systems with a pelagic redoxcline. Anoxic mineralization of organic matter generates large amounts of alkalinity by the formation of sulphide ions and the release of ammonia. This reduces the increase of the pCO_2 in the deep water and stabilizes the pH at a value close to 7. Although these processes are reversed upon re-oxidation during a deep water renewal event and do not affect the acid-base system of the Baltic Sea as a whole, they do influence the deep water redox chemistry which is partly controlled by the pH. On the other hand the existence of a pelagic redoxcline has another more far-reaching importance. It is the medium for intense denitrification, which increases the alkalinity not only locally, but may affect the alkalinity budget of the entire Baltic Sea proper (Gustafsson et al., 2014).

Our compilation of the major features of the Baltic Sea acid-base system indicates that an exact quantitative treatment of its properties is difficult to achieve. This refers to both the biogeochemical modelling and the interpretation of measured alkalinity in terms of the calculation of individual alkalinity contributions. An example is the calculation of the carbonate alkalinity that is necessary for the full characterization of the CO_2 system based on measurements of alkalinity together with another variable. This requires knowledge of the dissociation constants and the determination of the total concentrations of the individual compounds with acid-base properties. Regarding inorganic alkalinity contributions, it may be realistic to obtain this information. But in view of our limited knowledge concerning the composition of the dissolved organic matter, it is currently impossible to specify and characterize the contributions of individual organic acid-base compounds to the alkalinity. Hence we conclude that this is one of the greatest challenges for more adequate comprehensive physico-chemical characterization of the acid-base system in the Baltic Sea and likely in other coastal seas. Another important bottleneck, especially for the biogeochemical modelling, is also an insufficient knowledge on short and long term development of alkalinity loads from land caused by processes occurring in the catchment. This gains high importance as Müller et al. (2016) identified an increase in the Baltic Sea A_T, that compensates to large degree the ocean acidification effect, especially in the Gulf of Bothnia.

Acknowledgements

The study was completed thanks to the funding provided by the National Science Centre, Poland, grant no. 2015/19/B/ST10/02120. Important contribution to the study was also provided by BONUS and the Polish National Centre for Research and Development – sponsors of the BONUS INTEGRAL (BONUS-BB/INTEGRAL/05/2017)

References

Kuliński, K., Schneider, B., Hammer, K., Machulik, U. and Schulz-Bull, D. (2014) The influence of dissolved organic matter on the acid-base system of the Baltic Sea. J. Marine Syst., 132, 106-115.

Millero, F.J. (2010) Carbonate constants for estuarine waters, Mar. Freshwater Res., 61, 139–142.

Millero, F.J., Graham, T.B., Huang, F, Bustos-Serrano, H. and Pierrot, L.D. (2006) Dissociation constants of carbonic acid in seawater as a function of salinity and temperature, Mar. Chem, 100, 1-2, 80-94.

Kremling, K. (1970) Untersuchungen über die chemische Zusammensetzung des Meerwassers aus der Ostsee II. Frühjahr 1967 – Frühjahr 1968. Kiel Meeresforsch, 26, 1-20.

Kremling, K. (1972) Untersuchungen über die chemische Zusammensetzung des Meerwassers aus der Ostsee III. Frühjahr 1969 – Herbst 1970. Kiel Meeresforsch, 27, 99-118.

Uppström, L.R. (1974) The boron/chlorinity ratio of deep-sea water from the Pacific Ocean, Deep-Sea Res., 21, 161–162.

Gustafsson, E., Wällstedt, T., Humborg, Ch., Mörth, C. M., and Gustafsson, B. G. (2014) External total alkalinity loads versus internal generation: The influence of nonriverine alkalinity sources in the Baltic Sea, Glob. Biogeochem. Cycles 28, 1358-1370.

Müller, J.D., Schneider, B. and Rehder, G.: Long-term alkalinity trends in the Baltic Sea and their implications for CO_2-induced acidification, Limnol. Oceanogr., 61, 1984-2002, 2016.

Sediments of the Baltic Sea as a source of C, N and P

Monika Lengier[1,*], Beata Szymczycha[1], Karol Kuliński[1], Aleksandra Brodecka-Goluch[2], Żaneta Kłostowska[1,2]

[1]Institute of Oceanology, Polish Academy of Sciences, Powstańców Warszawy 55, 81-712 Sopot, Poland
[2]Institute of Oceanography, University of Gdańsk, Al. Marszałka Piłsudskiego 46, 81-378 Gdynia, Poland
*corresponding author, e-mail: mlengier@iopan.pl

1. Introduction

Burial in the bottom sediments is one of the two vital organic matter sinks in the Baltic Sea (Kuliński and Pempkowiak, 2011).The amount of organic matter being buried only in the deep depositional areas equals 2.64 TgC yr^{-1} (Thomas et al., 2010). As stated by Kuliński and Pempkowiak (2011) sediments should also be regarded as a carbon source since up to 30% of organic matter deposited to the Baltic Sea sediments returns to the water column as dissolved substances. What is more, mineralization and hydrolysis of organic matter that occur in the sediments supply the overlying water not only with carbon, but also with nitrogen and phosphorus. The amount and form of C, N, P released from sediments depend largely on the oxygen availability (Conley et al. 2002).

The data concerning quantitative studies of carbon, nitrogen and phosphorus return fluxes from sediments to the water column in the Baltic Sea are very sparse. As a consequence, these processes are not well parameterized and thus are often missing in the biogeochemical models describing the Baltic Sea marine ecosystem (Thomas et al., 2011). Even though, recent studies have focused on the carbon (Kuliński and Pempkowiak, 2011) and nutrients (Wulff et al., 2011) budgeting, sediments were generally regarded only as a sink without paying a lot of attention to sediments as a source (Thomas et al., 2010). The reason for that is lack of studies including C, N and P release from sediments covering larger area (Wulff et al., 2010; Łukawska- Matuszewska and Burska, 2011; Kuliński and Pempkowiak, 2011). Only Winogradow and Pempkowiak (2014) extended their research on DIC and DOC return fluxes to the Baltic Sea. The first attempt to calculate inorganic phosphorus return fluxes has been recently made by Łukawska-Matuszewska and Burska (2011) but their studies were restricted to the Gulf of Gdańsk.

The aim of this study is to provide the C, N, P return flux data for the Baltic Sea taking into account type of sediments, salinity and oxygen availability. This study has been divided into two parts. Firstly, we determined the concentration of dissolved inorganic carbon (DIC), dissolved organic carbon (DOC) and nutrients (NO_2^-+ NO_3^-, NH_4^+, PO_4^{3-}) in bottom and pore waters within the whole investigated area (Fig. 1). The major interest was put on water-sediment interface but also on the vertical characteristics of the profiles. Based on C, N, P distribution in the sediment, we will continue with second part covering the calculations of diffusive return fluxes.

2. Methods

Water and sediment samples for this study were collected during the research cruise of r/v Oceania in May 2017 at 23 sites located along the north-south axis in the Baltic Sea (Fig.1). Sediment cores were collected by the Gemax gravity corer. Interstitial water from surface-most 5 cm of sediments was extracted by means of Rhizons. At 4 stations located in the Gdańsk Deep, Gdańsk Bay, Gotland Deep and Bothnian Sea (Fig. 1) the sampling of pore waters was additionally continued to the depth of approx. 120 cm. Additionally, for all stations the overlying bottom water was sampled for the same set of measurements. The concentrations of DIC and DOC were analyzed by an automated total organic carbon analyzer TOC-L (Shimadzu). Water samples for nutrients (nitrates plus nitrites, ammonium and phosphates) were analyzed with colorimetric methods described by Strickland and Parsons (1967) and Salley et al. (1986). Other properties of seawater(O_2, pH, ORP) were measured using a multimeter (Hach-Lange, HQ40D).

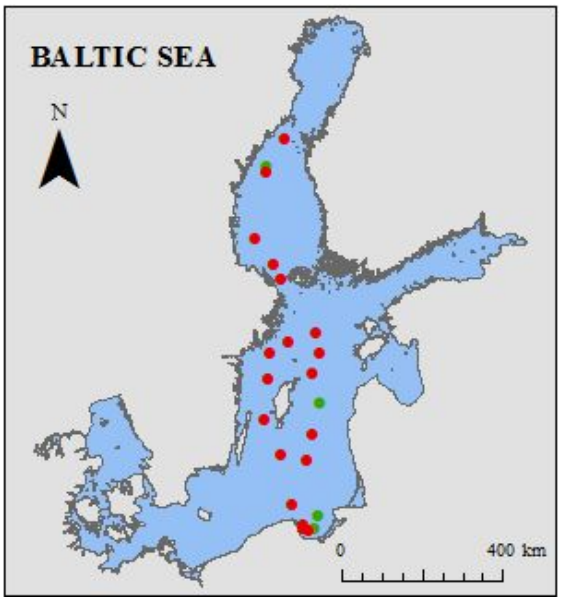

Figure 1. Localization of the sites. Red points refer to sites where interstitial water from surface-most 5 cm of sediments and above-sediments water were collected. Green points refer to sites where long cores have been collected, additionally.

3. Results

At most sites concentrations of DIC and DOC were much higher in the surface sediment layer than in the above-sediment water. This suggests that sediments were a source of both DIC and DOC in these regions. Within the whole investigated area DIC concentrations ranged from 1.4 to 3.2 mmol C·dm^{-3}in bottom waters and from 1.5 to 9.0 mmol C·dm^{-3}in surface-most pore waters. For DOC the ranges were from 0.3 to 0.4 mmol C·dm^{-3} and from 0.3 to 1.2 mmol C·dm^{-3}, respectively. In surface-most pore waters the maximum DIC and DOC values were observed in the Bothnian Sea. On the other hand, the maximum

concentrations of DIC and DOC in bottom waters were found in the Eastern Gotland Basin.

Surprisingly, the highest values of DIC and DOC both in the above-sediment water and the pore water were not observed at stations having the biggest depths. This was clearly seen in the Eastern Gotland Basin and in the Bothnian Sea, where the highest concentrations were found at stations located at the slopes - BY20 and F33, respectively.

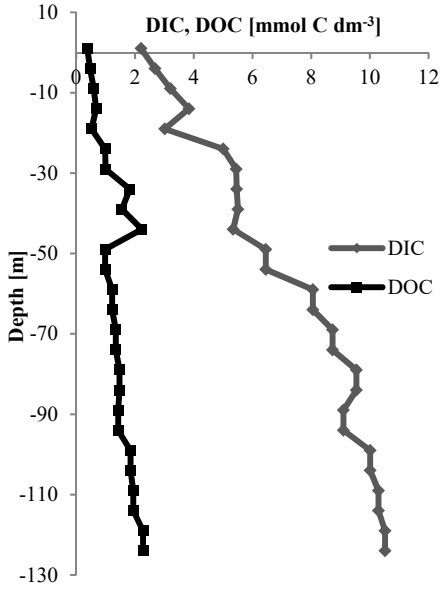

Figure 2. DIC (grey line) and DOC (black line) concentration profiles in the pore water sediments from the Gotland Deep (BY15).

Concentrations of ammonium (NH_4^+) oscillated from 1.5 to 182.5 µmol·dm^{-3} in above sediment water and from 3.0 to 377.9 µmol·dm^{-3} in shallow pore water (0-5 cm). For all stations the concentration of NH_4^+ was higher in pore waters than in the bottom water above sediments suggesting sediments as important source of ammonium.

The concentrations of nitrates and nitrites (NO_2^-+NO_3^-) have also been analyzed, nevertheless, they never exceeded the limit of detection.

Phosphates (PO_4^{3-}) concentrations in above-sediment water oscillated from 0.4 to 37.6 µmol·dm^{-3} and in shallow pore water (0-5 cm) from 1.1 to 125.2 µmol·dm^{-3}. Similar as for NH_4^+, the PO_4^{3-}concentrations were always higher in the pore waters than in the bottom waters indicating PO_4^{3-} release from sediments to the water column.

The water overlying the sediments was oxic at all the investigated sites. The oxygen concentrations within the whole area ranged from 2.9 to 14.3 mg·dm^{-3}, reaching the lowest value in the Western Gotland Basin, where the effects of the deep water renewal are always the smallest due to the specific deep-water circulation in the Baltic Proper.

The pH values within the water-sediment interface in the whole investigated area oscillated from 7.2 to 8.1. The oxidation-reduction potential values ranged from -196.8 to 366.3 mV within the whole investigated sediment-water interface.

4. Conclusion

DIC, DOC, NH_4^+ and PO_4^{3-} concentrations in most cases were the highest in the pore water (0-5 cm), exceeding usually the concentrations observed in the overlying bottom water. This indicates that sediments should be considered as a significant source of C, N and P. Results obtained in this study will lead us in the next step to DIC, DOC, DIN, DIP return fluxes in the different regions of the Baltic Sea. These data will enable us to make a revision of the carbon, nitrogen and phosphorus budgets in the Baltic Sea and may lead to better parameterization of sediments' role in the biogeochemical models.

Acknowledgements

The results were obtained within the framework of the following projects: 2016/21/B/ST10/01213 and 2015/19/B/ST10/02120 sponsored by National Science Center and WaterPUCK financed by the National Centre for Research and Development (NCBR) within BIOSTRATEG program.

References

Conley D. J., Humborg C., Rahm L., Wulff F. (2002) Hypoxia in the Baltic Sea and Basin-Scale Changes in Phosphorus Biogeochemistry, Environmental Science and Technology, 36, 24, 5315-5320.

Kuliński K., Pempkowiak J. (2011) The carbon budget of the Baltic Sea, Biogeosciences, 8, 3219-3230.

Łukawska-Matuszewska K., Burska D. (2011) Phosphate exchange across the sediment-water interface under oxic and hypoxic/anoxic conditions in the southern Baltic Sea, Oceanological and Hydrobiological Studies, 40, 2, 57-71.

Martens C. S., Haddad R. I., Chanton J. P. (1992) Organic matter accumulation, remineralization, and burial in an anoxic coastal sediment. In: Whelan J. K. and Farrington J. W. (eds), Organic matter: Productivity, accumulation and preservation in recent and ancient sediments, Columbia University Press, NY, 82-98.

Salley B. A., Bradshaw J. G., Neilson B. J. (1986) Results of Comparative Studies of Preservation Techniques for Nutrient Analysis on Water Samples, U. S. Environmental Protection Agency, CBP/TRS 6/87.

Strickland J. D. H., Parsons T. R. (1968) A Practical handbook of Seawater Analysis. Ottawa: Fisheries Research Board of Canada, 167.

Thomas H., Pempkowiak J., Wulff F., Nagel K. (2010) The Baltic Sea, in: Carbon and Nutrient Fluxes in Continental Margins, edited by: Liu K.-K., Atkinson L., Quinones R. A., Talaue-McManus L., Springer-Verlag, Berlin, 334-346.

Winogradow A., Pempkowiak J (2014) Organic carbon burial rates in the Baltic Sea sediments, Estuarine, Coastal and Shelf Science, 138, 27-36.

Wulff F., Rahm L., Hallin A-K. et al (2001) A nutrient budget model of the Baltic Sea. In: Wulff F., Rahm L., Larsson P (ed) A system analysis of the Baltic Sea. Springer, Berlin, 354-372.

A Baltic Sea Ecosystem Model with non-Redfield Stoichiometry for Carbon Fixation

Thomas Neumann[1] and Anja Eggert[1]

[1] Leibniz Institute for Baltic Sea Research Warnemünde, Germany (Thomas.Neumann@io-warnemuende.de)

1. Introduction

During the last decades, intensive observations of the carbon system in the Baltic Sea have been performed (e.g. B. Schneider et al., 2014). One of the specific features is the low surface pCO_2 in the central Baltic lasting the whole vegetation period. While the spring-pCO_2 decline and the low pCO_2 in mid-summer could be explained by the vernal and the cyanobacteria blooms, respectively, the reasons for the ongoing low pCO_2 after the vernal bloom remains largely unknown. Several hypotheses have been developed for processes fixing carbon dioxide in the time after the vernal bloom. Here we will test a non-Redfield stoichiometry for carbon fixation and its impact on the annual surface pCO_2 cycle.

2. Non-Redfieldish Carbon Fixation

With the aid of a 3D ecosystem model of the Baltic Sea, we tested the impact of non-Redfieldish carbon fixation on the surface pCO_2 in the central Baltic Sea. Our approach is, that phytoplankton in a nutrient limited environment produces non-Redfieldish organic carbon as long as light fuels primary production. As a result, carbon fixation is ongoing (e.g. after the vernal bloom) even if macro-nutrients (N,P) are exhausted.

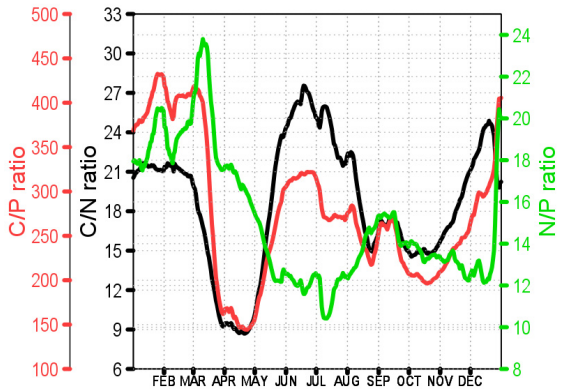

Figure 1. Molar carbon to phosphorus (C/P), carbon to nitrogen (C/N), and nitrogen to phosphorus (N/P) ratios in organic carbon at a station in the central Eastern Gotland Sea (BY15) in 1976.

Figure 1 shows the simulated molar carbon to phosphorus and nitrogen, and the nitrogen to phosphorus ratios at station BY15 in the Eastern Gotland Sea for the year 1976. The carbon to phosphorus/nitrogen ratios are always above the Redfield ratio (106 and 6.625) while the nitrogen to phosphorus ratio shows values above and below the Redfield ratio (16) which could be understand as a buffering of a surplus nitrogen or phosphorus.

3. Impact on surface pCO_2

The continuous carbon fixation prevents a strong pCO_2 increase after the vernal bloom. A comparison of pCO_2 in both models, with Redfieldish and non-Redfieldish carbon fixation, is shown in Figure 2.

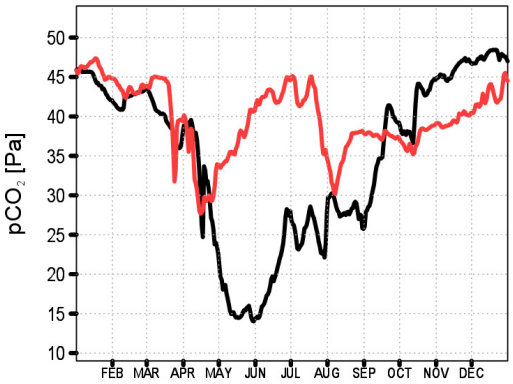

Figure 2. Simulated surface pCO_2 at BY15 in 1976. Redline with redfieldish carbon fixation, black line with non-redfieldish carbon fixation.

Non-Redfieldish carbon fixation may be a process which controls the observed pCO_2 in the central Baltic Sea. However, dedicated field studies are necessary to validate this hypothesis. The BONUS-INTEGRAL project provides an ideal framework to foster these combined filed and model experiments.

References

Bernd Schneider, Wanda Gülzow, Bernd Sadkowiak and Gregor Rehder (2014) Detecting sinks and sources of CO2 and CH4 by ferrybox-based measurements in the Baltic Sea: Three case studies, Journal of Marine Systems, Vol. 140, pp. 13-25

The chemical composition of *Mytilus trossulus* carbonate shells from the southern Baltic Sea: implications for environmental monitoring

Anna Piwoni-Piórewicz[1], Piotr Kukliński[1,2], Stanislav Strekopytov[3], Emma Humphreys-Williams[3], Jens Najorka[3], Anna Iglikowska[1]

[1]Institute of Oceanology, Polish Academy of Sciences, Powstańców Warszawy 55, 81-712 Sopot, Poland (apiwoni@iopan.pl)
[2]Department of Life Sciences, Natural History Museum, Cromwell Road, London SW7 5BD, United Kingdom
[3]Imaging and Analysis Centre, Natural History Museum, Cromwell Road, London SW7 5BD, United Kingdom

1. Introduction

The marine invertebrates such as molluscs, brachiopods, corals, echinoderms, bryozoans or foraminifera are able to precipitate shells and skeletons as composite materials consisting of calcium carbonate ($CaCO_3$) settled on the species-specific organic matrix. In a living system $CaCO_3$ is deposited mainly in the form of two polymorphs, calcite and aragonite, with identical chemical composition but different spatial layout of crystal lattice, thus different properties (e.g. Morse et al., 2007). The important part of biomineralization process is the incorporation of free ions into the crystal lattice as substitutes for the calcium ions (Ca^{2+}) (e.g. Cusack and Freer, 2008). Due to the ionic radius, the Ca^{2+} is mainly replaced by large strontium ions (Sr^{2+}) in aragonite and small magnesium ions (Mg^{2+}) in calcite beside the broad spectrum of chemical elements occurring in the corresponding environment. In the last few decades increasing attention has been paid to the relationship between the elemental composition of shells or skeletons and environmental factors. The complex subject of biomineralization combines mineralogical, geochemical, physiological and environmental investigators searching for patterns in the mechanisms that regulate growth of mineral parts.

It has been repeatedly investigated that shells and skeletons of calcifiers are deposited successively at regular periodicities, preserving records of ambient environmental conditions (e.g. Rodland et al., 2006). The elements incorporated in crystal lattice can thus provide a reliable chronological record of their exposure in the environment. Chemical profile from sequential sampling along the shell or skeleton sections turned out to act a high-resolution records of seawater chemistry, becoming the basis during interpretation of patterns in ocean history (e.g. Gillikin et al., 2006). For such proxies to be accurate and robust, the influence of biological effects including the size of studied organism must be examined and minimized, so that the environmental signal can be efficiently extracted.

The aim of this study is an analysis of the 16 elements important physiologically or in environmental monitoring: Ca, Fe, Mg, Na, Sr, Ba, Mn, Cd, Co, Cu, Ni, Pb, U, V, Y and Zn. Finding the variability of these elements within four size classes of a bimineralic species *Mytilus trossulus* has potential to increase the validity of using this species as a tool for environmental monitoring in the Baltic Sea and other regions within its extent of occurrence.

2. Study area in the context of biomineralization process

Samples were obtained from the Gulf of Gdansk located in the southern region of the Baltic Sea (Fig. 1). This is the unique ecosystem in terms of environmental conditions for biominaralization research. The Gulf is partially sheltered by the Hel Peninsula and Polish coastline. It is a low salinity system under the influence of brackish water from the open southern Baltic Sea and fresh waters from rivers, mainly Vistula, the largest river in Poland (e.g. Uścinowicz, 2011). The hydro-physical parameters of the Gulf are mostly driven by temperate climate of Central Europe and the following seasonal changes. Differences in air temperature and water mixing cause yearly fluctuations in surface water temperature ranges from about 4 to 22°C.

The Gulf of Gdansk is known as a marine area highly exposed to human impacts. This is due to intensive usage of its resources and anthropogenic emissions coming from various coastal sources, river inflows and atmospheric deposition. The important inflow of industrial and municipal pollution to the Gulf is derived from the Vistula River, which transports pollutants from the entire catchment area of 194,000 km^2. The river is a source of the elements in water-soluble form and contained in the sediment. Both water discharge and sediment load into the Gulf are strongly seasonally dependent (e.g. Pruszak et al., 2005). Because of the natural conditions, mainly limited exchange of water, loading substances remain in ecosystem for decades, accumulate in the sediments and in living organisms.

Generally, The low salinity increases free ion activity and this activity rather than total metal concentration determines the biological availability of dissolved metals. During the shell calcification at salinity below 10, the decrease of Ca^{2+} concentration in water promotes influx of ions such as Cd^{2+}, Co^{2+}, Cu^{2+} or Zn^{2+} by reducing competition for the same sites in the crystal lattice. This tendency is enhanced by the fact that the bioavailability of Sr^{2+} and Mg^{2+}, major substituents of Ca^{2+} in biocarbonates, is usually much lower in freshwater than in seawater. Furthermore, lower salinity means lower level of chloride ions (Cl^-) forming complexes with metals, hence, their availability is higher in brackish than in marine environment (e.g. Fritiof et al. 2005, Poulain et al. 2015).

The *M. trossulus* are calcifying organisms needing calcite or aragonite for development. Low salinity compounded by the lower than in oceanic surface alkalinity cause reduced $CaCO_3$ and Ca^{2+} concentrations in the Gulf. Further, seasonal changes of water temperature and chemistry makes that in wintertime seawater in the Gulf of Gdansk might be in equilibrium with respect to calcite and undersaturated with respect to aragonite (e.g. Findlay et al., 2007).

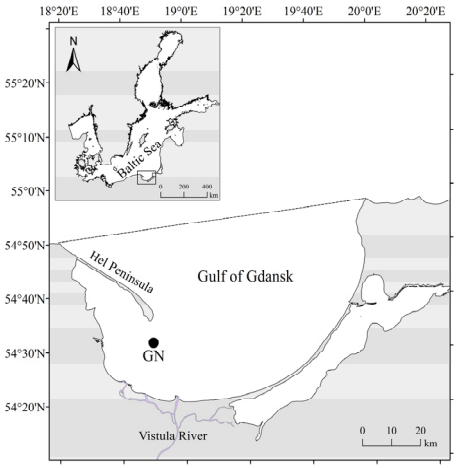

Figure 1. Study area and the site of collection (GN) of *M. trossulus* in the Gulf of Gdansk and its location in the Baltic Sea. The broken line indicates the northern border between the Gulf of Gdansk and the open sea.

3. Materials and methods

Bivalves were collected from 36 m depth in the Gulf of Gdansk in May 2013 at GN station (Fig. 1) using a Van Veen grab sampler from RV *Oceanograf-2*.

Each shell was cleaned, treated by sonication for 30 minutes and air-dried. By measuring along the shell height, individuals were divided into four size classes, reflecting the range in sizes for the southern Baltic Sea population.

From all individuals (N=136) one valve was subjected to mineralogical analysis using XRD-PSD unit to evaluate the calcite and aragonite content. To estimate the chemical composition of *M. trossulus* shells, the second valve from six individuals at each size class was selected for elemental determination using the ICP-AES and ICP-MS analysis.

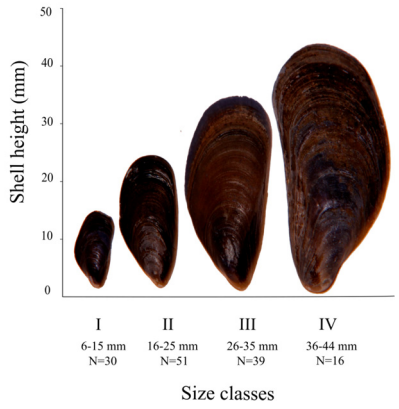

Figure 2. The ranges of each size classes of *M. trossulus* shells from the Gulf of Gdansk. N is a number of analyzed individuals.

4. Results

Obtained results suggest that mineralogy and chemical composition of *M. trossulus* shells change throughout the shell development due to most likely a combination of environmental and biological factors. The content of aragonite increases with increasing shell size, while the bulk concentrations of Na, Cd, Cu, U, V, Zn and Pb were found to decrease with increasing height of the shells.

5. Conclusions

The shells of *M. trossulus* tend to be accumulators of wide spectrum of metals from corresponding environment. This promotes them as good tools in tracking the environmental conditions. However, the concentrations on many metals in shells varied during organism development what if ignored, would bias reliable environmental monitoring and reconstructions. Examples considered in this study suggest that the elemental concentrations in shells are coupled with their mineralogical composition and crystal lattice properties. The vital effects linked with seasonal changes and ontogenetic trends are also the sources of variable fractionation. Consequently, this study indicates that, when using mineralogical and chemical composition of the shells as environmental indicators, the size of the organisms should be taken into account. In order to minimize the bias in mineralogical or chemical composition related to the size of the shell, individuals of the same or very similar dimensions should be selected for the analysis.

References

Cusack, M., & Freer, A., 2008. Biomineralization: elemental and organic influence in carbonate systems. Chemical reviews, 108(11), 4433–4454.

Findlay, H., Tyrrell, T., Bellerby, R., Merico, A., & Skjelvan, I., 2007. Ecosystem modelling of the Norwegian Sea: investigating carbon and nutrients dynamics as a consequence of biological and physical processes. Biogeosciences Discussions, 4, 3229–3265.

Findlay, H., Tyrrell, T., Bellerby, R., Merico, A., & Skjelvan, I., 2007. Ecosystem modelling of the Norwegian Sea: investigating carbon and nutrients dynamics as a consequence of biological and physical processes. Biogeosciences Discussions, 4, 3229–3265.

Fritioff, Å., Kautsky, L., & Greger, M., 2005. Influence of temperature and salinity on heavy metal uptake by submersed plants. Environmental Pollution, 133, 265–274.

Gillikin, D.P., Dehairs, F., Lorrain, A., Steenmans, D., Baeyens, W., & André, L., 2006. Barium uptake into the shells of the common mussel (*Mytilus edulis*) and the potential for estuarine paleo-chemistry reconstruction. Geochimica et Cosmochimica Acta, 70(2), 395–407.

Morse, J.W., Andersson, A.J., & MacKenzie, F., 2006. Initial responses of carbonate-rich shelf sediments to rising atmospheric pCO_2 and 'ocean acidification': role of high Mg-calcite. Geochimica et Cosmochimica Acta, 70, 5814–5830.

Poulain, C., Gillikin, D.P., Thébault, J., Munaron, J.M., Bohn, M., & Robert, R., et al., 2015. An evaluation of Mg/Ca, Sr/Ca, and Ba/Ca ratios as environmental proxies in aragonite bivalve shells, Chemical Geology, 396, 42–50.

Pruszak, Z., van Ninh, P., Szmytkiewicz, M., Hung, N.M., Ostrowski, R., 2005. Hydrology and morphology of two river mouth regions (temperate Vistula Delta and subtropical Red River Delta). Oceanologia 47(3), 365–385.

Rodland D.L., Schöne B.R., Helama S., Nielsen J.K. & Baier S., 2006. A clockwork mollusc: ultradian rhythyms in bivalve activity revealed by digital photography. Journal of Experimental Marine Biology and Ecology, 334, 316–323.

Uścinowicz, Sz. (Ed.), 2011. Geochemia osadów powierzchniowych Morza Bałtyckiego. Warszawa: Państwowy Instytut Geologiczny.

BONUS INTEGRAL: Improved Biogeochemical Monitoring and Greenhouse Gas Flux assessment for the Baltic Sea through high resolution trace gas data acquisition

Gregor Rehder[1], Anna Rutgersson[2] , Lauri Laakso[3], Karol Kuliński[4], Urmas Lips[5], Hermann W. Bange[6], Kristin Andreasson[7], Jamie Shutler[8], and the BONUS INTEGRAL science party[9]

[1]Leibniz-Institute for Baltic Sea Research Warnemünde, Germany (IOW), gregor.rehder@io-warnemuende.de
[2]University of Uppsala, Sweden (UU)
[3]Finnish Meteorological Institute, Finnland (FMI)
[4]Institute of Oceanology of the Polish Academy of Sciences, Poland (IOPAN)
[5]Tallinn University of Technology, Department of Marine Systems, Estonia (TTU)
[6]GEOMAR Helmholtz Centre for Ocean Research Kiel, Germany (GEOMAR)
[7]Swedish Meteorological and Hydrological Institute, Sweden (SMHI)
[8]University of Exeter, Centre for Geography, Environment and Society, United Kingdom (UNEXE)
[9]https://www.io-warnemuende.de/integral-partner.html

1. Introduction

BONUS INTEGRAL (Integrated carboN and TracE Gas monitoRing for the bALtic sea) is an integrated project funded within the BONUS Blue Baltic Call. It comprises eight partners from five nations and runs from July 2017 to June 2020. BONUS INTEGRAL seeks to demonstrate and exploit the potential added value of the marine stations of ICOS and similar instrumentation for the ecosystem state assessment of the Baltic Sea as an important contribution to a state-of-the-art HELCOM monitoring. This presentation will give an overview of the scientific approach of the project, some of the intended goals, and exemplary early results of the project. It will also introduce some more topical contributions of BONUS INTEGRAL at the 2nd Baltic Earth conference.

2. Approach

Twelve European nations are national partners of the Integrated Carbon Observation System (ICOS, https://www.icos-ri.eu), the pan-European research infrastructure (RI) to provide high-precision data on Greenhouse Gas (GHG) fluxes and budgets. Four of the pan-Baltic countries (Finland, Sweden, Germany, Denmark) are already partners in the ICOS RI with partly or fully established infrastructure, other countries like Poland and Estonia are currently in the process of developing their strategy towards ICOS. The overall aim of ICOS with its large investments is to provide European-wide CO_2 and – to a lesser extent – non-CO_2 (i.e. methane and nitrous oxide) greenhouse gas concentration and flux data.

BONUS INTEGRAL seeks to demonstrate and exploit the potential added value of the marine stations of ICOS and similar instrumentation for the ecosystem state monitoring of the Baltic Sea as an important contribution to an improved HELCOM monitoring. In direct response to the requirements of the European Marine Strategy Framework Directive, BONUS INTEGRAL will provide new approaches for the monitoring of marine eutrophication and acidification, and explore the integrated greenhouse gas flux as a potential new indicator for the good environmental status of the Baltic Sea.

3. The Observational Network

To fulfil its tasks, BONUS INTEGRAL will collect and integrate carbon system, GHG and auxiliary data within a network of observational lines on voluntary observing ships (VOS, commercial ships hosting scientific instrumentation) and fixed permanent stations, comprising the ICOS ocean stations Östergarnsholm, Utö, the ICOS VOS line Finnmaid, and the time series station Boknis Eck. Other lines will be amended with respective instrumentation, and a completely new line will be set up between Gdynia and Baltijsk, allowing the investigation of carbon transformations near the mouth of the River Vistula. This work will be complemented by additional trace gas and carbon system sampling by joining standard HELCOM monitoring cruises.

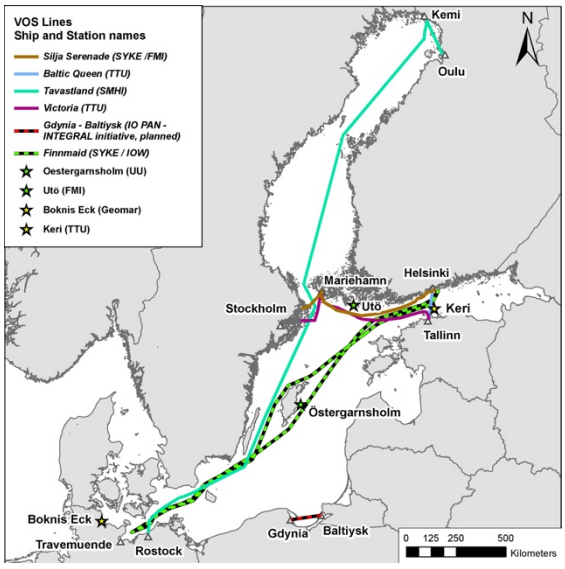

Figure 1. VOS and station network used within BONUS INTEGRAL for the assessment of biogeochemical functioning and GHG fluxes in the Baltic Sea.

Two research vessel based field campaigns in winter and summer are planned to scrutinize the representativeness of the BONUS INTEGRAL network and develop smart extrapolation schemes.

4. Major Objectives

Scientifically, two major objectives are addressed within BONUS INTEGRAL:

- Provide best experimentally based surface concentration charts of seasonal carbon dioxide and methane/nitrous oxide concentrations over the Baltic Sea, and explore and implement tools to derive flux estimates

Work towards this goal comprises integration of ancient and new surface pCO_2, methane and nitrous oxide data, development of suitable extrapolation tools using advanced state-of-the-art remote sensing approaches in combination to in situ field data, development of a new, turbulence based air-sea exchange parameterization for the Baltic Sea, and integration of this parameterization into the Flux Engine software toolbox (Shutler et al., 2016).

- Development of a high resolution coupled physical-biogeochemical model towards full expression of the carbon system using BONUS INTEGRAL observations.

The overarching approach for this task is to scrutinize our existing knowledge of the carbon cycling in the Baltic Sea based on existing and new data retrieved within the project and to use this knowledge to upgrade the parameterizations of an existing coupled physical-biogeochemical model. Due to its nature, the carbon system provides the most powerful tool to trace acidification, but also to link eutrophication driven-net productivity to deep-basin oxygen demand and thus, deoxygenation trends. The improved model will then be used for hindcast simulations of carbon fluxes, and to derive model based optimization of monitoring efforts within the Baltic Sea.

5. A Glimpse on Scientific Results

a.) Surface methane measurements have been introduced in 2010 on VOS Finnmaid, which operates between Lübeck and Helsinki with approximately four transects a week (Gülzow et al., 2011 & 2013). The long term data set provides insight into the surface concentration pattern over some of the major Baltic Sea Basins. Findings include episodic high concentrations in the western basins due to storm-driven interaction with the methane-rich sediments, upwelling-induced high concentrations in summer in sub areas of the central basins, and highest dynamic and oversaturation in the Gulf of Finnland due to mixing of methane-enriched oxygen-poor subsurface waters (Fig. 2).

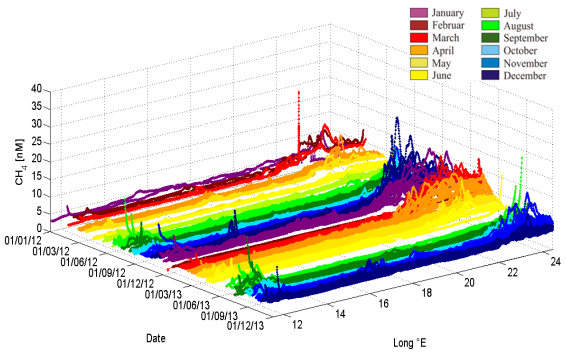

Figure 2. Methane surface concentrations from January 2012 to December 2013 between Lübeck and Helsinki. For exact location of transects, see Figure 1 (VOS Finnmaid).

b.) Measurements of the surface partial pressure of CO_2 (pCO_2) can be used to infer the surface content of total inorganic carbon (C_T). The changes in C_T over time over the productive period can be used for a precise estimate of net primary production (Schneider and Müller, 2017). Net primary production is a measure for the carbon exported from the productive zone, and thus tightly linked to oxygen demand at depth.

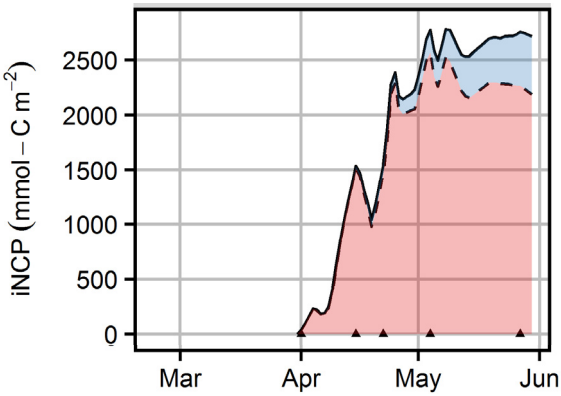

Figure 3. Net depth-integrated accumulated primary (carbon) production over the course or the spring bloom in the Eastern Gotland Sea for 2009 (from Schneider and Müller, 2017). Red area represents measured loss in CT, blue a "correction term" to account for uptake of CO_2 from the atmosphere.

6. Acknowledgments

BONUS INTEGRAL receives funding from BONUS (Art 185), funded jointly by the EU, the German Federal Ministry of Education and Research, the Swedish Research Council Formas, the Academy of Finland, the Polish National Centre for Research and Development, and the Estonian Research Council. The instrumentation on VOS Finnmaid is part of the European ICOS RI and its implementation was supported by the German Federal Ministry of Education and Research though grants 01 LK 1101F and 01LK1224D. We are indebted to *Finnlines* for hosting our instrumentation throughout the years.

Further information about BONUS INTEGRAL can be found at https://www.io-warnemuende.de/integral-home.html.

References

Gülzow, W., Rehder, G., Schneider v. Deimling, J., Seifert, T. and Tóth, Z., (2013). One year of continuous measurements constraining methane emissions from the Baltic Sea to the atmosphere using a ship of opportunity. Biogeosciences, 10: 81-99.

Gülzow, W., Rehder, G., Schneider, B., Schneider v. Deimling, J. and Sadkowiak, B., (2011). A new method for continuous measurement of methane and carbon dioxide in surface waters using off-axis integrated cavity output spectroscopy (ICOS): An example from the Baltic Sea. Limnol. & Oceanogr. Methods, 9: 176-184.

Schneider, B. and Müller, J.D., (2018). Biogeochemical Transformations in the Baltic Sea - Observations Through Carbon Dioxide Glasses. Springer Oceanography. Springer, ISBN 978-3-319-61699-5.

Shutler, J.D., Land, P.E., Piolle J.-F., Woolf, D.K., Goddijn-Murphy, L., Paul, F., Girard-Ardhuin, F., Chapron, B. and Donlon, C.J. (2016). FluxEngine: a Flexible Processing System for Calculating Atmosphere–Ocean Carbon Dioxide Gas Fluxes and Climatologies. Journal of Atmospheric and Oceanic Technology, 33(4), 741-756.

Using land-based sites for air-sea interaction studies

Anna Rutgersson[1], H. Pettersson[2], E. Nilsson[1], H. Bergström[1], M. B. Wallin[1], E. D. Nilsson[1], E. Sahlée[1], L. Wu[1], E. M. Mårtensson[1]

[1] Department of Earth Sciences, Uppsala University, Sweden (anna.rutgersson@met.uu.se)
[2]FMI, Finnish Meteorological Institute
[3]Department of Environmental Science and Analytical Chemistry, Stockholm University, Stockholm, Sweden

1. Introduction

In-situ measurements representing the marine atmosphere are mainly taken at ships, buoys or stationary moorings, or on land-based towers. These different systems are complementary and have different advantages and disadvantages. By using fixed towers it is possible to avoid motion correction and it is also possible to design the site and the set-up so that flow distortion is minimized. For practical reasons, land-based towers are easier to access and run. One needs, however, to be very careful to make sure the measurements actually represents the sea area one wishes to describe, and it is very important to make a careful analysis of the site and the data before applying them to air-sea interaction studies.

As the coastal zone is very productive and heterogeneous it is likely a hot-spot in the global carbon cycle. Increased understanding of the processes in coastal regions and the impact on the gas-exchange is needed. Different coastal regions are different, but most likely also have similarities. One step to understand data from the coastal zone is to categorise stations and data based on the degree of land influence.

Data is defined according to the following categories:

1) CAT1: Marine data representing open sea
2) CAT2: Disturbed wave field resulting in physical properties different from open sea conditions and likely also heterogeneity of water properties in the foot-print region of the flux tower.
3) CAT3: Mixed land/sea footprint of the tower, very heterogeneous conditions and a very active carbon production/consumption.

2. Data and measurements

The Östergarnsholm measurement site is located at 57°27'N, 18°59'E (see Fig. 1) on a small and flat island in the Baltic Sea about 4 km from the east coast of the bigger island of Gotland. The station at Östergarnsholm has a 30-m land-based meteorological tower located on the southern tip of the island. The tower is equipped at various levels with high-frequency (20 Hz) sensors used for the estimation of CO_2 and momentum turbulent fluxes, as well as with slow response instrumentation for mean profile measurements of meteorological variables. Several studies have been published describing the oceanic and atmospheric characteristics of the Östergarnsholm site and assessing the air-sea interaction processes in the region.

In addition to the Campbell CSAT3 sonic anemometers and the LICOR LI-7500 gas analyzers placed at two levels (9 and 25 m) used for air-sea CO_2 turbulent flux estimations, a CH_4 LI-7700 gas analyzer was installed in the tower (at 9 m) in September 2017.

3. Characterising a site

There are a number of factors to consider when examining a micrometeorological site and characterization of the data. Some factors are common for both land and sea stations, some more specific for marine stations. Here some of the most relevant factors are discussed. As turbulence levels are lower and fluxes generally smaller for marine sites (with the exception of sea spray), data is more sensitive to disturbances. We here apply the different factors to the Östergarnsholm site, partly referring to previous studies, having investigated various aspects. Main aspects discussed are: down-wind disturbances, flow distortion, foot-print area, wave field, biogeochemical homogeneity and hydrographical features, Categorisation of the wind direction intervals. Also quality control of data and flux calculation methodologies needs to be considered.

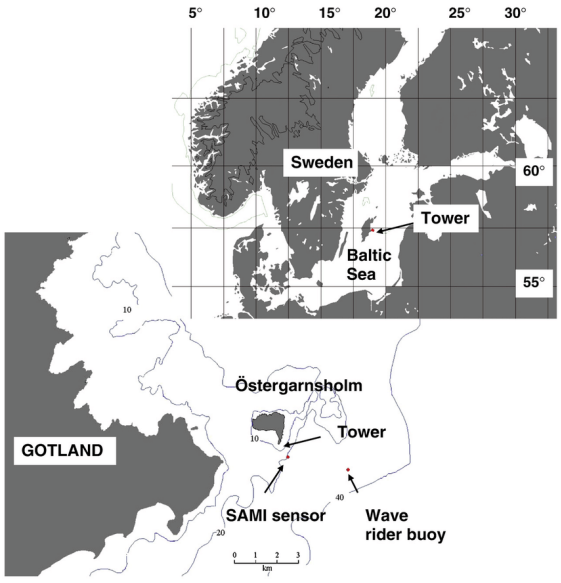

Figure 1. Map of the Baltic Sea and the Östergarnsholm station including locations of the measurement tower and the two measuring buoys (a SAMI sensor and a wave rider buoy) (from Rutgersson et al., 2008).

4. Results and discussion

In Figure 2 C_D and C_{DN} averaged over wind-speed intervals are shown representing data for the different categories defined in Table 1. In Figure 2a the black curve (representing open sea conditions; CAT1) are shown with

one standard deviations representing the scatter of the data. The scatter for the coastal sea (CAT2; blue) and mixed land-sea (CAT3; red) is significantly larger compared to open sea data due to the larger variability of data in these sectors (variability of CAT2 and CAT3 not shown). In Figure 2b the neutral drag coefficient is shown and for comparison the drag coefficient calculated from wind speed using the Charnock relation. The open sea drag coefficient (or roughness length) is well known to also depend on the wave conditions, wave age and/or wave steepness, and this variation is reflected in the scatter of the data.

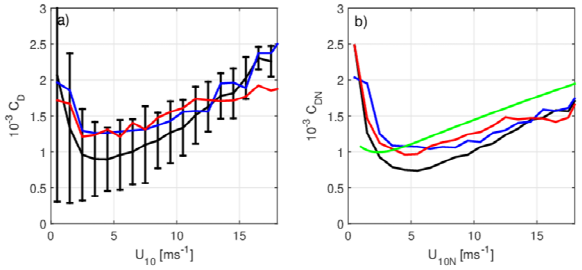

Figure 2. Drag coefficient averaged over wind-speed intervals (a) and corresponding neutral drag coefficient (b). Black lines represent open sea sector (CAT1), blue lines coastal sector (CAT2) and red lines mixed land-sea sector (CAT3). Error bars in (a) show one standard deviation of the variability of CAT1, for clarity of the figure variability is not shown for the other sectors, being larger than for CAT1. Green line in (b) is the drag coefficient calculated using Charnock equation.

The open sea drag coefficient estimated at Östergarnsholm is lower on the average compared to using the Charnock equation, this is in agreement with previous studies e.g. Carlsson et al (2009) showing a reduction of the neutral drag coefficient during swell dominated conditions in the Baltic Sea.

There is a clear seasonal variation in the direction of the CO_2 flux (Figure 3). For the open sea sector, uptake is dominating during spring, summer and fall. During winter outgassing is dominating for CAT1 data, and relatively large magnitudes of the fluxes (large fluxes due to the higher winds during winter season). The seasonal cycle of CAT1 data agrees qualitatively with results from other studies of air-sea CO_2 flux for open Baltic Sea conditions (e.g Norman et al., 2013). The open sea sector has in general the highest frequency of small magnitude fluxes, probably due to the smallest air-sea CO_2 gradients. The data for the coastal sector (CAT2) shows outgassing as a seasonal mean for all seasons (during spring uptake and outgassing balances out on the average) and largest during fall. This has, most likely two explanations; the coastal sector is influenced by runoff, with water of high carbon content leading to an oversaturation of pCO_2 and an upward directed flux.

5. Conclusions

There is a great potential in using land-based micrometeorological stations, both for monitoring of ocean and coastal conditions and for understanding of air-sea interaction processes. For land-based sites some land impact is unavoidable, but for high quality flux-data it is important to classify and clearly quantify the land impact. We here suggest all measuring sites to distinguish defined categories for the data, this framework is suggested to be further developed and to be used for categorizing data and sites to clearly define the properties of data and make intercomparisons between different sites and conditions easier. We suggest to distinguish characterization of physical parameters (momentum, heat and aerosol fluxes) and biogeochemical fluxes separately. Suggested categories for ice free seas are:

When using the suggested categorization for data taken at the well-studied Östergarnsholm site in the Baltic Sea we find (not very surprisingly) a larger variability in surface drag, heat and CO_2 fluxes for mixed land-sea and coastal data compared to open sea conditions, this is due to the greater heterogeneity of surface water and atmospheric conditions. The drag coefficient is largest (at least for winds below 10 m/s) for the mixed land-sea data and smallest for open sea conditions, the larger drag for the coastal sector can probably be explained by more strongly forced and generally steeper waves. Seasonal cycle of CO_2 flux is different for the different category data where open sea data show uptake during spring and summer. Coastal and mixed land-sea data show outgassing during all seasons probably due to larger impact of runoff of high DOC concentrations in the water. It should be noted that upwelling signals are seen during several seasons.

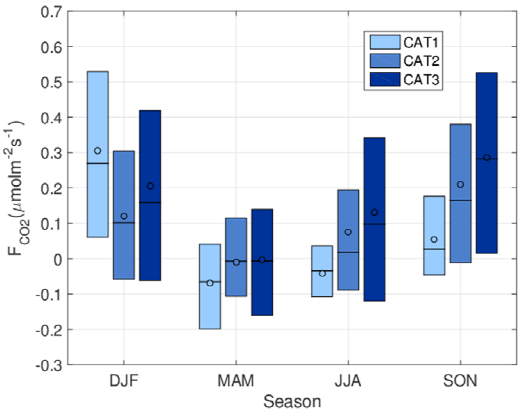

Figure 3. Seasonally averaged flux of carbon dioxide for the different category data. Note here the difference in wind direction ranges for physical and biogeochemical parameters for the different categories. The boxes are defined based on the first and third quartile of the distribution and thus show the interquartile range corresponding to 50% of the data, the circles are the mean and thin vertical lines the median.

References

Carlsson, B., Rutgersson A., and Smedman, A. 2009. Impact of swell on simulations using a regional atmospheric climate model, *Tellus A*, **61** (4), 527-538.

Norman, M., Parampil, S., Rutgersson, A. and Sahlée, E. 2013. Influence of coastal upwelling on the air-sea gas exchange of CO2 in a Baltic Sea Basin, *TellusB*, **65**

Rutgersson A., A.S. Smedman, E. Sahlée (2011) Oceanic convective mixing and the impact on air-sea gas transfer velocity. Geophys Res Lett, 38, L02602

Organic matter mineralization in Baltic Sea deep waters: Rates and stoichiometry

Bernd Schneider

Leibniz Institute for Baltic Sea Research, Warnemünde, Germany (bernd.schneider @io-warnemuende.de)

1. Introduction

The kinetics and the stoichiometry of organic matter (OM) mineralization control the cycling of biogeochemically relevant elements. Understanding of the fundamental processes are an indispensible requisite for realistic numerical simulations of the Baltic Sea biogeochemistry including its alterations in a changing environment. The deep water of the eastern Gotland Basin offers unique conditions for studying the mineralization processes because it is regularly subjected to long lasting stagnation and can thus be considered as a natural laboratory. By the use of total CO_2 measurements in combination with nutrient and oxygen/hydrogen sulfide measurements, we are aiming at the determination of (1) mean mineralization rates including the demand for oxidants and (2) the related release of phosphate.

2. The data base

Vertical profiles of total CO_2 concentrations (C_T) were measured since 2003 in the eastern Gotland Sea (station BY15) during monitoring cruises of the IOW (Leibniz Institute for Baltic Sea Research) which took place five times per year and provided nutrient and O_2/H_2S data for our study. Mean concentrations were calculated for three boxes below 150 m: 150m – 175m, 175m – 200m and 200m – 235m. Using T-S diagrams, two periods were identified which could be considered as almost ideally stagnant: MAY 2004 – JUL 2006 and JUL 2007 – FEB 2014. Although lateral water exchange was excluded for these periods, vertical mixing must be taken into account in order to calculate mineralization rates in the individual boxes. Therefore, mixing coefficients were calculated on the basis of the temporal changes of the salinity in the three considered boxes.

3. Mineralization rates and redox chemistry

The temporal development of the accumulated C_T release, $Q(C_T)$, within the individual boxes for the stagnation period JUL 2007 – FEB 2014 showed a linear increase with time (Fig. 1). The slopes of the regression lines correspond to mineralization rates expressed as µmol-C_T/dm^3 per day. Relating these rates to the sediment surface below 150 m, yielded a mean mineralization rate of 1.9 mol/m^2 yr^1. A similar rate was obtained for the period MAY 2004 – JUL 2006 (Schneider et al., 2010) whereas Gustafsson and Stigebrandt (2007) report a mean rate of only 1.3 mol m^{-2} yr^{-1} on the basis of O_2 and H_2S data during the stagnation periods that occurred between 1965 and 2007.

To estimate the demand for oxidants during OM mineralization, the loss of O_2 and NO_3, and the generation of H_2S in the different boxes were calculated and converted to oxygen equivalents, $Q(O_2,equ.)$. Distinct linear relationships between $Q(C_T)$ and $Q(O_2,equ.)$ were obtained with a mean slope of 1.18 (an example is given in Fig. 2). This conflicts with the standard Redfield stoichiometry for the mineralization (production) of OM that suggests a relationship of 1:1. Our enhanced factor indicates that OM does not consist solely of carbohydrates, but holds also additional C-H bonds which increase the consumption of O_2 or other oxidants (Anderson, 1995).

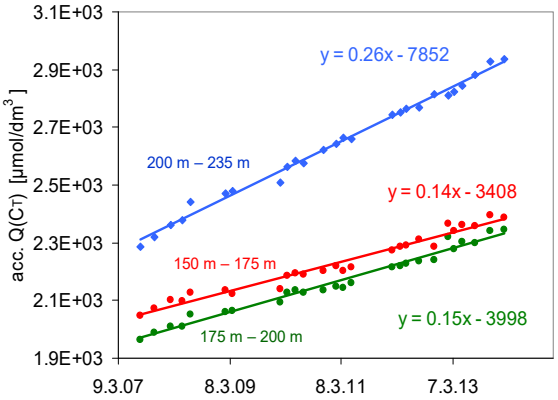

Figure 1. The accumulated release of total CO_2, $Q(C_T)$, in different water layers (boxes) as a function of time. The slopes corresponds to the mineralization rates in (µmol/dm^3)/d.

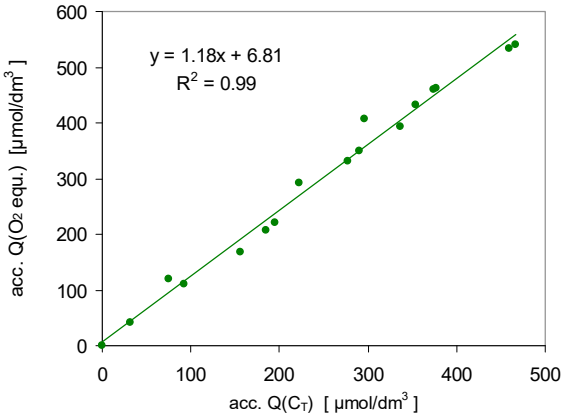

Figure 2. Relationship between the accumulated oxidant demand, $Q(O_2,equ.)$ and the accumulated release of total CO_2, $Q(C_T)$ for the water layer between 200m and 235m during the stagnation period JUL 2007 – FEB 2014.

4. Release of phosphate

The release of PO_4 from OM during the mineralization process is superimposed by the formation/dissolution of PO_4-FeO(OH) aggregates. The interplay between insoluble and dissolved PO_4 could be tracked because the first considered stagnation period was characterized by the transition from oxic to anoxic conditions after a major inflow of oxygen-rich water which had caused the precipitation of insoluble PO_4-FeO(OH). In the course of the subsequent O_2 depletion and H_2S formation, Fe^{3+} is reduced to soluble Fe^{2+}

and PO_4 is again dissolved. This process is reflected in a relationship between $Q(C_T)$ and the PO_4 release, $Q(PO_4)$, that is much lower than the C/P ratio of OM (Fig. 3, red dots). However, at the onset of the following and permanent anoxic stagnation period, the deposits of insoluble PO_4-FeO(OH) are exhausted and C_T and PO_4 are released at a ratio that corresponds to the Redfield C/P ratio of OM (Fig. 3, blue dots).

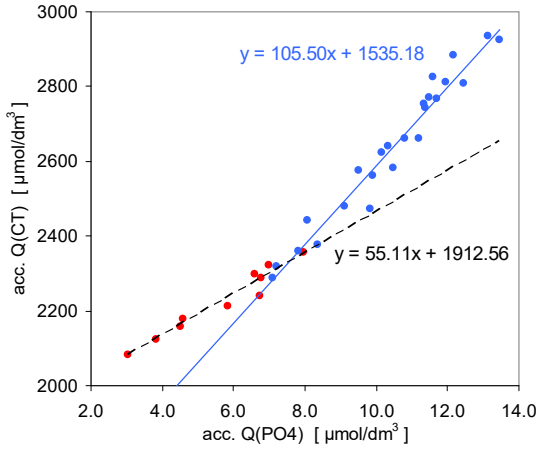

Figure 3. Accumulated total CO_2 release, $Q(C_T)$, versus accumulated PO_4 release, $Q(PO_4)$, during the transition from oxic to anoxic conditions (red) and during permanent anoxic conditions (blue).

5. Conclusions

- estimation of mineralization or any other process rates in stagnant deep waters must include transport by vertical mixing;
- annual OM mineralization rates in the Gotland Basin are relatively stable (about 2.0 mol $m^{-2}yr^{-1}$) and show only low decadal variability;
- the oxygen demand for OM mineralization exceeds the Redfield stoichiometry by 10% - 20%;
- enhanced release of phosphorus occurs during the transition from oxic to anoxic conditions and is a temporary phenomenon. During long lasting anoxic conditions the sediments release PO_4 approximately according to the C/P ratio of OM;

References

Anderson, L.A. (1995) On the hydrogen and oxygen content of marine organic matter. Deep Sea Res., 42, 1675 – 1680.

Gustafsson, B.G., Stigebrandt, A. (2007) Dynamics of nutrients and oygen/hydrogen sulphide in the Baltic Sea deep water. J.Geophys.Res., 112, G02023.doi:10.1029/2006JG000304.

Schneider, B., Nausch, G., Pohl, C. (2010) Mineralization of organic matter and nitrogen transformations in the Gotland Sea deep water. Mar.Chem., 119, 153 – 161.

Transformations of the carbonate system in the Odra estuary

Marcin Stokowski[1], Bernd Schneider[2], Gregor Rehder[2], Jens D. Müller[2] and Karol Kuliński[1]

[1] Institute of Oceanology, Polish Academy of Sciences, Sopot, Poland (stokowski@iopan.pl)
[2] Leibniz Institute for Baltic Sea Research, Warnemünde, Germany

Globally estuaries are very important regions for the carbon cycle as they form a transition zone between land, open ocean and the atmosphere. In the Baltic Sea the studies on the carbon cycle and especially on the CO_2 system are mostly focused in the open waters, while estuaries are poorly investigated in this respect.

The aim of our study was to characterize the CO_2 system and its transformations along the salinity gradient in the estuary of the Odra River - one of the biggest rivers entering the Baltic Sea. Water discharged by the Odra first enters the relatively large (ca. 680 km^2) and shallow (mean depth ca. 3.8 m) Szczecin Lagoon, which is further connected to the Pomeranian Bay via narrow channels of three rivers: Dziwna, Peene and Świna.

During the two RV Oceania cruises in May and November 2016 all four measurable parameters describing the CO_2 system (A_T, C_T, pCO_2, pH) were obtained together with O_2, salinity (S) and temperature (T). The results of the measurements are shown in the Fig. 1. Four characteristic sections were identified along the estuary (Fig. 1): freshwater in the Odra river (S < 0.5), low saline water in the Szczecin Lagoon (S = 1-3), steep salinity gradients in the mixing zone (Świna river) (S = 2-6) and the Baltic Sea water in the Pomeranian Bay (S = 6-7). Along the salinity gradients large A_T and C_T changes were observed in the estuary. A_T varied between 2940 and 1770 µmol·kg^{-1}, while C_T ranged between 2971 and 1676 µmol·kg^{-1} - values found in the Odra river and the Pomeranian Bay, respectively. The Odra river water was oversaturated with CO_2 irrespective of the season (pCO_2 of 1119-1351 µatm) - most likely as consequence of intensive mineralization of terrigenous organic matter. In the Szczecin Lagoon, pCO_2 dropped significantly down to 336 µatm in November and as low as 63 µatm in May. The latter was accompanied by O_2 saturation of 135 %. The inverse correlation between the O_2 distribution and pCO_2 suggests that the CO_2 system in the estuary is controlled mostly by the biological activity (extremely high production in May and predominance of mineralization processes in November).

The very high primary production in the Szczecin Lagoon in May caused extremely low pCO_2 which led to increase of carbonates (thus oversaturation of $CaCO_3$) resulting in the precipitation of calcium carbonate. As a consequence the C_T and A_T were much lower in May than in November. Additionally the C_T in May was lowered due to the organic matter production. The detailed analysis of the data allowed to quantify the influence of both these effects (Fig. 2). Precipitation of $CaCO_3$ lowered C_T by approx. 400 µmol·kg^{-1}, while the combined effect of primary production and gas exchange was responsible for C_T decrease by approx. 600 µmol·kg^{-1}.

The performed studies significantly improve our knowledge on the structure and transformations of the CO_2 system in the Odra estuary. They also indicate the importance of processes occurring in the estuaries for shaping the marine CO_2 system.

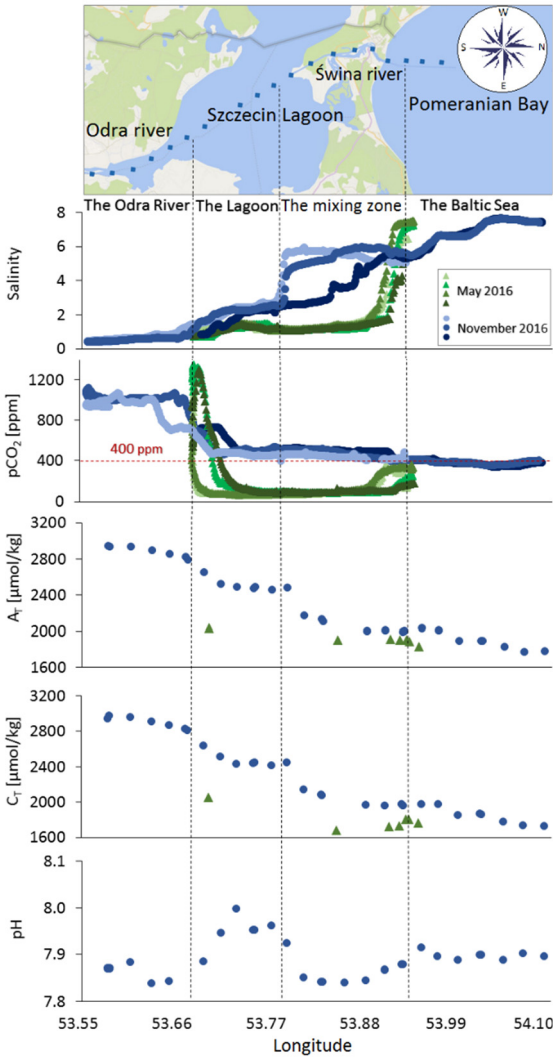

Fig. 1. Four measurable carbonate system parameters and salinity along the Odra river estuary in May (green) and November (blue) 2016

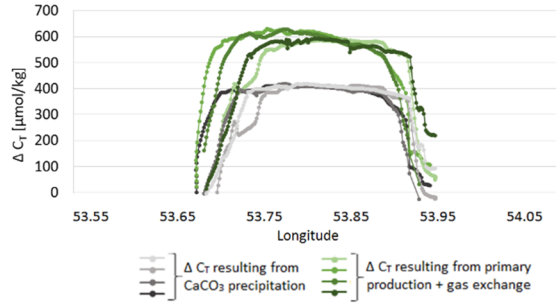

Fig. 2. C_T change (ΔC_T) resulting from $CaCO_3$ precipitation and primary production together with gas exchange in May 2016

Deep submarine groundwater discharge indicated by pore water chloride anomalies in the Gulf of Gdańsk, southern Baltic Sea.

Beata Szymczycha [1,*], Żaneta Kłostowska[1,2], Karol Kuliński[1], Aleksandra Winogradow[1], Jaromir Jakacki [1], Zygmunt Klusek [1], Miłosz Grabowski [1], Aleksandra Brodecka-Goluch[2], Bożena Graca[2], Marcin Stokowski[1], Katarzyna Koziorowska[1], Daniel Rak [1]

[1] Institute of Oceanology, Polish Academy of Sciences, Powstańców Warszawy 55, 81-712 Sopot, Poland (beat.sz@iopan.gda.pl)

[2] Institute of Oceanography, University of Gdańsk, Al. Marszałka Piłsudskiego 46, 81-378 Gdynia, Poland

1. Introduction

Submarine groundwater discharge (SGD) is a significant pathway for material transport to the coastal zone (Burnett et al., 2006). For some elements and isotopes SGD has been thought to be the principal source (Lin et al., 2010). Therefore, the interest in coastal groundwater flow systems has increased rapidly during the last decades. Most of the studies have been focused on shallow (<20m), narrow zone (<5km) along the coastline (Lin et al., 2010). Interestingly, some deep seafloor studies (Wilson, 2005; Lin et al., 2010) indicated that SGD can occur a long distance from the shoreline (~25km). In the Baltic Sea SGD has been mainly investigated in the southern part primarily at coastal zones demonstrating that groundwater seepage is comparable to rivers in case of selected chemical substances (Piekarek-Jankowska, 1994; Shlüter et al., 2004; Szymczycha et al., 2012, 2014, 2016). In this study we identified deep SGD located at acoustically turbid sediments in the Gulf of Gdańsk (~70 km from the shore). Given the significance of benthic nutrients dynamics and sediment biogeochemical processes implications for Baltic Sea environment, such as eutrophication, hypoxic and anoxic events, we aim to characterize the potential role of deep SGD in the Baltic Sea cycles of elements.

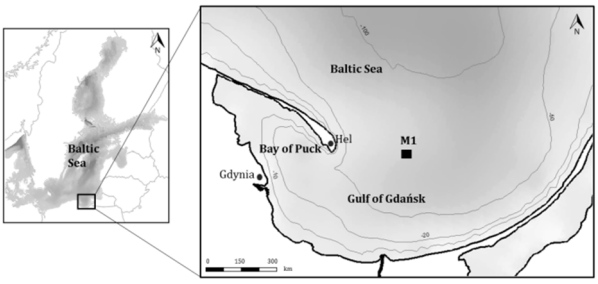

Figure 1. Location of the study area (M1).

2. Materials and methods

The study area is located in the Gulf of Gdańsk, southern Baltic Sea (Fig.1). Sea water, pore water and sediments samples were collected on board the R/V Oceania during three cruises in May 2015, January 2017 and May 2017. Seawater salinity and temperature was retrieved from CTD files while sediment cores were collected by the Gemax gravity corer. Additionally acoustic observations of the sediments were made in order to detect gas distribution. In collected sediment samples water content, calcium (Ca), total organic (TOC) and inorganic carbon (IC) were analyze while in collected pore water samples nutrients (PO_4^{3-}, NO_3^-+NO_2^-, NH_4^+), dissolved organic carbon (DOC), dissolved inorganic carbon (DIC), metals (Na, K, Mg, Ca, Al, Mn, Fe, Ni, Cr, Cu, Cd, Co, Pb) and alkalinity were analyzed. Parameters such as ORP, pH and salinity were measured *in situ*. The SGD rate was calculated via modelling chloride pore water concentrations modified after Shlüter et al. (2004).

3. Results and discussion

Seawater salinity, temperature and density were typical of the seasons when the samples were taken. The pore water depth profiles for both salinity and chloride significantly decreased with depth during every sampling campaign indicating freshwater source. The exemplary profiles are presented at Figure 2. The pore water concentrations of the main cations such as Na, Ca, Mg, K showed similar trend to chloride. Generally, pore water profiles for Cl, Na, Ca, Mg and, K, unaffected by freshwater, are constant or increase linearly with depths (Carman and Rahm, 1997, Shlüter et al., 2004). The curvature profiles are characteristic for areas affected by fluid flow, in this case SGD (Shlüter et al., 2004).

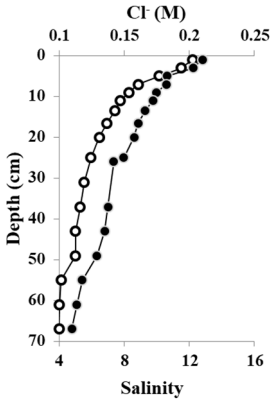

Figure 2. Examples of pore water depth profiles for chloride (hollow symbols) and salinity (solid symbols) in the study area.

The general pore water trend of DIC, DOC, trace elements, PO_4^{3-}, NH_4^+, TDS and alkalinity are comparable to those observed in deep sea anaerobic sediments. Interestingly, in the deepest layers of pore water increased concentrations of Mn, Fe, Al, PO_4^{3-}, NH_4^+, DIC, DOC and alkalinity were observed most probably due to groundwater seepage.

The calculated SGD rates ranged from 0.3 to 0.7 (L m^{-2} d^{-1}). Comparable results were observed in the coastal area of the Eckernförde Bay, western Baltic Sea, where beside groundwater seepage increased methane production and consequently methane release from sediments were detected (Shlüter et al., 2004). In our study area the sediments acoustic disturbance has been previously correlated with methane presence (Brodecka et al., 2013) while in the neighboring Bay of Puck, inner part of the Gulf of Gdańsk SGD occurrence was accompanied by methane and increased P, Si and DOC fluxes (Donis et al., 2017).

4. Conclusions

The main impacts of the anoxic deep SGD are increased efflux of chemical substances such as PO_4^{3-}, NH_4^+, DIC, DOC, trace elements (Mn, Fe, Al) and possibly methane. Therefore, SGD significantly changes their distribution both within the sediments and at the water-sediment interface.

5. Acknowledgments

The study reports results obtained within the framework of the following projects: UMO-2016/21/B/ST10/01213 sponsored by National Science Center and WaterPUCK financed by the National Centre for Research and Development (NCBR) within BIOSTRATEG program.

References

Burnett W.C., Aggarwal P.K., Aureli A., Bokuniewicz H.J., Cable J.E., Charette M.A., Kontar E., Krupa S., Kulkarni K.M., Loveless A., Moore W.S., Oberdorfer J.A., Oliveira J., Ozyurt N., Povinec P., Privitera A.M.G., Rajar R., Ramessur R.T., Scholten J., Stieglitz T., Taniguchi M., Turner J.V. (2006) Quantifying submarine groundwater discharge in the coastal zone via multiple methods. Science of the Total Environment, 367, 498-543.

Carman R., Rahm L. (1997) Early diagenesis sediments in and chemical characteristics of interstitial water and the deep deposition bottoms of the Baltic proper. J. Sea Res. 37, 25-47.

Donis D., Janssen F., Wenz F., Dellwig O, Escher P., Spitzy A., M.E. Böttcher (2017). Biogeochemical impact of submarine ground water discharge on coastal surface sands of the southern Baltic Sea. Estuar Coast Shelf S 189, 131- 142.

Lin T-I, Wang C-H, You C-F, Huang K-F, Chen Y-G (2010) Deep submarine groundwater discgage indicated by tracers of oxygen, strontium isotopes an barium content in the Pingtung coastal zone southern Taiwan Mar Cem 122, 51-58.

Piekarek-Jankowska H., Matciak M., Nowacki J. (1994) Salinity variations as an effect of groundwater seepage through the seabed (Puck Bay. Poland), Oceanologia, 36, 33-46.

Schlüter M., Sauter E.J., Andersen C.A., Dahlgaard H., Dando P.R., 2004. Spatial distribution and budget for submarine groundwater discharge in Eckernförde Bay (Western Baltic Sea). Limnol. Oceanogr. 49, 157–167.

Szymczycha B., Vogler S., Pempkowiak J. (2012) Nutrient fluxes via submarine groundwater discharge to the Bay of Puck, Southern Baltic, Sci. Total Environ., 438, 86-93.

Szymczycha B., Maciejewska A., Winogradow A., Pempkowiak J. (2014) Could submarine groundwater discharge be a significant carbon source to the southern Baltic Sea? In Oceanologia, 56, 327–347.

Szymczycha B., Kroeger K. D., Pempkowiak J. (2016) Significance of groundwater discharge along the coast of Poland as a source of dissolved metals to the southern Baltic Sea, Marine Pollution Bulletin, 109, 151-162.

Wilson A.M. (2005) Fresh and saline groundwater discharge to the ocean : A regional perspective. Water Resour Res 41, WO2016.

Eddies' impact on biological processes – A case study in the Western Baltic Sea for the algal blooming season 2010

Rahel Vortmeyer-Kley[1,2], Maximilian Berthold[3], Ulf Gräwe[1] and Ulrike Feudel[2]

[1] Leibniz Institute for Baltic Sea Research, Warnemünde, Germany (rahel.vortmeyer@io-warnemuende.de)
[2] Institute for Chemistry and Biology of the Marine Environment, University of Oldenburg, Germany
[3] University of Rostock, Institute for Biological Sciences, Applied Ecology and Phycology, Biological Station Zingst, Germany

1. Introduction

Flow structures like eddies or fronts have a strong impact on biological processes in the ocean. They distribute nutrients, transport plankton or provide a fluid dynamical niche for specific species (d'Ovidio et al. (2010)).
As shown in numerical modeling studies eddies can act as incubators for algal blooms (Sandulescu et al. (2007), Bastine and Feudel (2010)).
This case study focuses on the impact of eddies on plankton growth in the Western Baltic Sea for the algal blooming season March to October 2010.

2. Material and methods

The case study is based on data from a coupled hydrodynamical-biogeochemical model of the Western Baltic Sea (ERGOM (Ecological Regional Ocean Model) www.ergom.net) with 1h temporal and 600m spatial resolution. The data set contained velocity fields, different plankton groups, different nutrients as well as temperature and salinity fields. All fields were averaged over the upper 10 m to investigate surface layer processes.
The eddy detection and tracking tool is based on the idea of Lagrangian coherent structures that separate regions of different dynamical behavior and make use of the concept of the Lagrangian descriptors to detect them (Mancho et al. (2013), Vortmeyer-Kley et al. (2016)).
We investigated the dynamics of plankton and nutrient concentrations inside the eddy during its lifetime.
Only eddies that live longer than 100h were selected for the case study, to take the match of fluid dynamical and biological time scales into account. Furthermore, the selected eddies travel longer than 8km to investigate their transport properties of plankton and nutrients. An example of a selected eddy's track can be found in Figure 1.

3. Results

We found eddies acting as transporter of enclosed plankton communities and nutrient compositions from the coastal regions into the open Arkona or Bornholm Basin in this study. In this sense, plankton is supported in areas that were *a priori* not connected to external (rivers or land run-off) and internal (upwelling regions) nutrient supplies, but actually were after the decay of an eddy.
During their lifetime eddies may acted as fluid dynamical niche providing optimal temperature and/or nutrient compositions for enhanced growth of specific species or species groups inside the eddy. In this way some species inside the eddy can have a competitive advantage.

4. Outlook

The gained knowledge of the case study provides a first step towards a better understanding of eddy mediated transport of nutrients and plankton and eddies' impact on plankton growth in the Baltic Sea.
Further research dealing with a three-dimensional eddy detection and tracking could provide an estimate of the transported water volume and the amount of carried nutrients and plankton biomass from the coastal regions into the open sea.

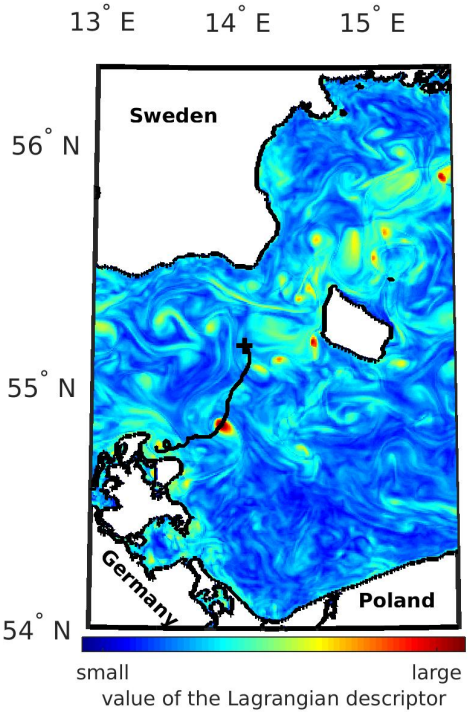

Figure 1. Vorticity based Lagrangian descriptor and a selected eddy at 9. April 2010 20:00. The black line indicates the whole track of the eddy. The position where the eddy decays is marked with a cross.

References

Bastine D. and U. Feudel (2010). Inhomogeneous dominance patterns of competing phytoplankton groups in the wake of an island. Nonlinear Processes in Geophysics, 17, 715–731.

d'Ovidio F., S. De Monte, S. Alvain, Y. Dandonneau, and M. Lévy (2010). Fluid dynamical niches of phytoplankton types. Proceedings of the National Academy of Sciences, 107(43), 18366–18370.

Mancho A., S. Wiggins, J. Curbelo, and C. Mendoza (2013). Lagrangian Descriptors: A method of revealing phase space structures of general time dependent dynamical systems. Communications in Nonlinear Science, 18, 3530–3557.

Sandulescu M., C. López, E. Hernández-García, and U. Feudel (2007). Plankton blooms in vortices: the role of biological and hydrodynamic timescales. Nonlinear Processes in Geophysics, 14, 443–454.

Vortmeyer-Kley R., U. Gräwe, and U. Feudel (2016). Detecting and tracking eddies in oceanic flow fields: a Lagrangian descriptor based on the modulus of vorticity. Nonlinear Processes in Geophysics, 23(4), 159–173.

Variation of organic carbon cycling modulated by benthic animals in the Baltic Sea in the past six decades

Wenyan Zhang[1], Ute Daewel[1], Kai Wirtz[1], and Corinna Schrum[1]

[1] Institute of Coastal Research, Helmholtz Zentrum Geesthacht

Field data collected from the Baltic Sea indicate a prominent seasonal variation in the vertical distribution of total organic carbon (TOC) and macrobenthic biomass in sediments. The importance of benthic animals in the benthic-pelagic coupling and early diagenesis of organic carbon has long been recognized but has not been quantified. We here present a mechanistic model to quantify, for the first time, the dynamic interaction between sedimentary TOC and benthic fauna. The major model principles include that (i) the vertical distribution of macrobenthic biomass is a trade-off between nutritional benefit (quantity and quality of TOC) and the costs of burial (respiration) and mortality, and (ii) the vertical transport of TOC is in turn modulated by macrobenthos through bioturbation. A novelty of our model is that bioturbation is resolved dynamically depending on variation of local food resources and macrobenthic biomass. This allows capturing of the benthic response to both depositional and erosional conditions and improving estimates of the material exchange flux at the sediment-water interface. The TOC-benthos model is coupled to 3D hydrodynamic-ecological simulations (ECOSMO) to reconstruct the benthic response to organic matter sedimentation from 1960 to 2015. Model results are compared with an extensive published field dataset. An satisfactory model performance reveals that the fate of OC in the Baltic Sea sediments can be explained as a combined response to pelagic conditions (oxygen level, shear stress and primary production) and the synergy between bioturbation, vertical location of high quality TOC and corresponding positioning of benthos.

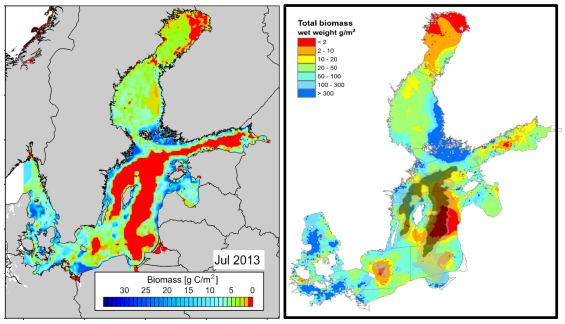

Figure 1. Left: modeled distribution of macrobenthic biomass in July 2013; Right: Interpolated macrobenthic biomass based on available field data from Gogina et al. (2016)

Model results indicate that macrobenthos annually ingest 1.5-2 × 10^8 ton OC and in addition diffuse 1.7-2.3 × 10^8 ton OC into subsurface sediments, accounting for 11-15% of the budget of TOC in the upper-most 30 cm sediments in the Baltic Sea. Although the seafloor in shallow water (<50m) stores only 40% of the total TOC budget, it receives about 66% of the deposited fresh organic matter (produced by primary production) that fosters about 75% of benthic animals in the entire Baltic Sea. The fraction of TOC reworked by benthos in shallow-water sediments ranges between 22-28% annually, being twice of that in deeper water. Increased eutrophication and hypoxia from 1995 to 2010 in the Baltic Sea result in a net reduction of benthic fauna by about 0.4 million tons (Carbon) compared to the result in 1994. This net reduction is comparable to the natural seasonal fluctuation caused by variation of food input.

Figure 2. Left: temporal variation of hypoxic area, budget of fresh organic matter in surface sediments and macrobenthic biomass in the Baltic Sea; Right: corresponding results in shallow water sediments.

References

Daewel, U., and C. Schrum. (2013) Simulating long-term dynamics of the coupled North Sea and Baltic Sea ecosystem with ECOSMO II: model description and validation. *JMS* 119: 30-49.

Gogina, M., Nygard, H., Blomqvist, M., Daunys, D., Josefson, A. B., Kotta, J., Maximov, A., Warzocha, J., Yermakov, V., Graewe, U., and Zettler, M .L. (2016) The Baltic Sea scale inventory of benthic faunal communities. ICES Journal of Marine Science 73(4): 1196-1213.

Zhang, W., and K. Wirtz. (2017). Mutual dependence between sedimentary organic carbon and macrobenthos resolved by mechanistic modelling. *JGR-Biogeosci.* 122: 2509–2526

Topic C
Natural hazards
and high impact events

Reliability of HIPOCAS wind wave hindcast data for the southern Baltic Sea.

Witold Cieślikiewicz[1] and Aleksandra Cupiał[1]

[1] Institute of Oceanography, University of Gdańsk, Poland (witold.cieslikiewicz@ug.edu.pl)

1. Introduction

With possible changes in wind patterns and growing interests in the development of wind farms and other forms of renewable energy on the Baltic Sea, statistical characteristic of prevailing wave conditions at chosen sites and changes in energy distribution, are essential. Even more so, since the wave fields of the Baltic Sea are characterized by great spatiotemporal variability as indicated by Soomere and Räämet (2011). Difference in wave conditions as well as in trends in different sites is expected (Wei et al.,2016).

With some regions exhibiting 10–15 yearlong cycle in changes in wave heights (Soomere and Räämet, 2014), and the fact that changes in dominant wind direction may result in change in local sediment transport, via shift in dominant wave direction (Kelpšaitė et al., 2011) it is crucial to recognize changes corresponding to analyzed area. In this work, the main focus was on the southern part of the Baltic Proper. Lower number of measuring devices deployed in this area through the time that wave measurements have been carried out in the Baltic results in the fact, that this area is more thoroughly researched by modelling and visual observations (Soomere and Räämet, 2011). It also means that the results of the modelling should be even more rigorously verified.

During the HIPOCAS project, from which the data is used in this study, the WAM model was validated with good results. It was also confirmed during number of other research (e.g. Soomere and Räämet, 2011; Paplińska, 1999) that this model is adequate for modeling wave field in the Baltic Sea, providing that the wind fields are homogeneous in time. There is a question, however, whether it is equally good for prediction of extreme values, especially since there are reported cases of underestimating extreme values using this model (Soomere and Räämet, 2011). This information is crucial for many engineering applications, for example development of wave converting technology (Wei et al., 2016) or wind farms. To verify model's capacity in this area the data must be put through rigorous reliability tests.

The main purpose of this work was to calculate series of statistics describing wave climate of the southern Baltic Proper using modelled data spanning almost half century. A verification of goodness of fit between modelled wave fields and measured wave data from the COPERNICUS vast database is performed through detailed analysis of the wave statistics at carefully selected sites in the Polish Economic zone, including areas of proposed wind farms.

2. Methods

The modelled data, used in this study, is the result of an EU-funded project HIPOCAS (Cieślikiewicz et al., 2005), which generated long-term statistical information about, among others, wind waves over the Baltic Sea for years 1958–2001. Input meteorological data, e.g., wind velocity fields came from dataset produced by hindcast with the REMO model (Jacob and Podzun, 1997; von Storch et al., 2000 and Feser et al., 2001) Wave data have been produced with wave model WAM in a rectangular grid in spherical rotated coordinates with the resolution 5'×5' and 1-hour time step. The output wave data were validated against observed records presenting a good agreement by Cieślikiewicz and Paplińska-Swerpel, (2008). In this study, resulting gridded long-term statistical data has been interpolated over the entire sea area of interest, with a specially prepared procedure. Using this method, several contour plots and maps presenting the spatial distributions of various wave climate probabilistic characteristics have been created.

The long-term stochastic properties of wind wave field over the southern Baltic Sea, are being analyzed based on modelled data spanning years 1958–2001. Those properties cover not only basic statistics of significant wave height H_S, including its maximum value and 95th and 99th percentiles, as well as the mean and peak periods, T_z and T_p, respectively, and mean direction of wave propagation θ_0, associated with extreme H_S. In addition, the analysis of spatiotemporal distribution of significant steepness is performed. We also examine whether it remains, with changing wind patterns, in an interval between 1/16 and 1/20 that is typical for stormy waves (Tucker and Pitt, 2001).

For the reliability tests, the significant wave height and the maximum wave height at the selected site for different return periods are compared. The similar comparison is performed for the wave period, mean wave direction and some other integral wave parameters. For further analysis, new approach of using mixed-model distributions, proposed by Wei et al. (2016) is tested.

Within this reliability study of HIPOCAS wind wave parameters database, not only the basic statistics are compared against observed data, but also the underlying probability distributions of basic wave parameters are verified in the same manner. In this work we pay a special attention to extreme value statistics.

3. Conclusions

In this study, resulting gridded long-term statistical data has been interpolated over the entire analysed area, with a specially prepared procedure. Using this method, a number of contour plots and maps presenting the spatial distributions of various wave climate probabilistic characteristics and long-term analysis have been created. In the context of potential applications in the field of oceanography, and coastal and offshore engineering, they show promising results. An exemplary contour plot of the significant wave field H_S during peak of the selected storm, modelled with WAM within the HIPOCAS project, is presented in Fig. 1.

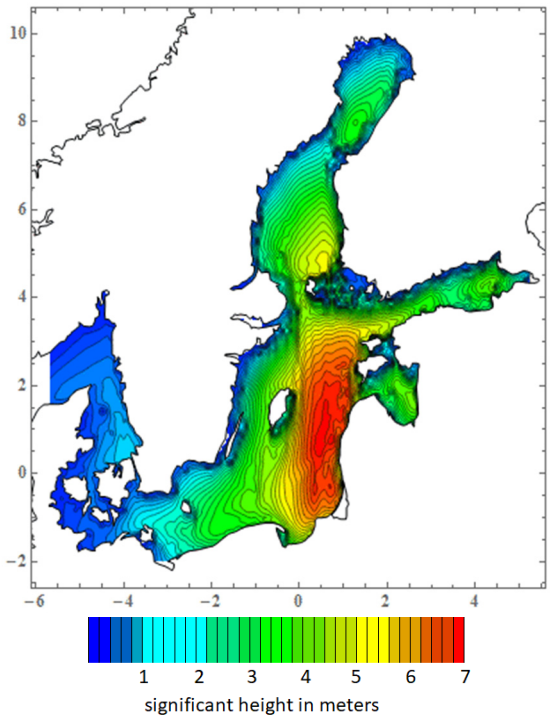

Figure 1. Distribution of significant wave height H_S modelled over the Baltic Sea modelled during HIPOCAS project (Nov 1st ,2001 at 21:00).

For example, the mean values for H_S, are in agreement with the literature. They fall in range of, for the most part 0.8–1.2 m for the analysed region.

The HPOCAS database of hindcast wind wave parameters provides many possibilities to examine the long-term variability of the storm climate over the southern Baltic Sea. The value of such continuous wind wave data, spanning such a long period, with 1-hour time resolution, and extending over such a relatively wide sea area, with five nautical mile spatial resolution, cannot be overestimated. The principal question we ask in this work is how reliable this data set is in the context of maritime engineering applications. The presented study assesses the weaknesses and strengths of the HIPOCAS wind wave hindcast data. The detailed results of the performed reliability analysis will be presented at the time of the conference.

This study has been conducted using E.U. Copernicus Marine Service Information. Calculations were carried out at the Academic Computer Centre (TASK) in Gdańsk.

References

Cieślikiewicz, W., Paplińska-Swerpel, B. (2008) A 44-year hindcast of wind wave fields over Baltic Sea, *Coastal Engineering*, **55**, pp. 894–905

Cieślikiewicz, W., Paplińska-Swerpel, B., Guedes Soares, C. (2005) Multi-decadal wind wave modelling over the Baltic Sea, *Proc. 29th Intern. Conf. Coastal Engng*, ICEE 2004, Lisbon, pp. 778–790

Feser, F., Weisse, R., von Storch, H. (2001) Multi-decadal atmospheric modelling for Europe yields multi-purpose data, *EoS*, Vol. 82, No. 28, July 10

Jacob, D., Podzun, R. (1997) Sensitivity studies with the regional climate model REMO, *Meteorol. Atmos. Phys.*, **63**, pp. 119–129

Kelpšaitė, L., Dailidienė, I., Soomere, T. (2011) Changes in wave dynamics at the south-eastern coast of the Baltic Proper during 1993–2008, *Boreal Env. Research*, **16** (suppl. A), pp. 220–232

Paplińska B., (1999) Wave analysis at Lubiatowo and in the Pomeranian Bay based on measurements from 1997/1998 – comparison with modelled data (WAM4 model), *Oceanologia*, **41** (2), pp. 241–254

Soomere T., Räämet A. (2011) Spatial patterns of the wave climate in the Baltic Proper and the Gulf of Finland, *Oceanologia*, **53**, 1-TI, pp. 335–371

Soomere T., Räämet A. (2014) Decadal changes in the Baltic Sea wave heights, *J. Mar. Syst*., **105**, pp. 96 – 105

Tucker, M.J., Pitt., E.G. (2001) *Waves in Ocean Engineering*, Elsevier Ocean Engineering Series, Vol. 5, Elsevier, 521 pp

Von Storch, H., Langenberg, H. and Feser, F. (2000) A spectral nudging technique for dynamical downscaling purposes. *Mon. Weather Rev*., **128**, pp. 3664–3673

Wei, L., Isberg, J., Waters, R., Engström, J., Svensson, O., Leijon, M. (2016) Statistical analysis of wave climate data using mixed distributions and extreme wave prediction, *Energies*, **9**, pp. 1–17

Reproduction of 10m-wind and sea level pressure fields during extreme storms with regional and global atmospheric reanalyses in the North Sea and the Baltic

Natacha Fery[1], Birger Tinz[1], Anette Ganske[2] and Lydia Gates[1]

[1] Deutscher Wetterdienst (National German Meteorological Service, DWD), Marine Climate Monitoring Division, Hamburg, Germany (natacha.fery@dwd.de)
[2] Bundesamt für Seeschifffahrt und Hydrographie, Hamburg, Germany

1. Purpose

In the context of global climate change, interest in the study of very severe storms and their impacts on the coasts of the North Sea and the Baltic has increased over the last decades.

In this work, we investigate whether global and regional atmospheric reanalyses can be used to compensate the lack of historical meteorological observations during storms with high impact on the coasts. An extensive validation of the different reanalyses with observations is realized. An assessment of the limits of application of global reanalyses for the reproduction of storms is as well provided. Emphasis is given to the analysis of the 10m-wind and the sea level pressure fields above both, the North Sea and the Baltic.

2. Methods

Global reanalyses provide continuous gridded information of the atmospheric state over the full globe while regional reanalyses are developed for smaller areas. In this study, the outputs of the global reanalyses 20CRv2vc (NOAA, Compo et al., 2011), ERA-40 (ECMWF, Uppala et al., 2005) and ERA-Interim (ECMWF, Dee et al., 2011) were extracted for the North and Baltic Seas region. The regional reanalysis is the COSMO-REA6 reanalysis (DWD, University of Bonn, Bollmeyer et al, 2015).

The reanalyses are validated against independent 10m-wind and sea level pressure observations at the three offshore research platforms (FINO) and at the station Helgoland (German Naval Observatory 1883-1991, DWD Climate Data Centre 1987-present) (see locations in Fig. 1). The selected case studies were the severe storms of 1906, 1962, 1973, 2006, 2007 and 2013.

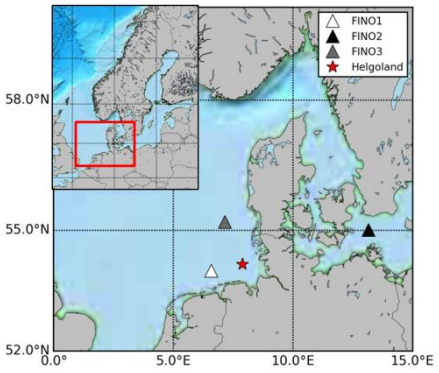

Figure 1. Locations of the stations in the North Sea and the Baltic considered for the study.

Additional work consisted in comparing the spatial patterns of the 10m-horizontal wind and the sea surface pressure during the storm events.

3. Results

The global reanalyses used in this study were able to reproduce the storms that have a duration larger than their 6 h time resolution. They failed in reproducing the fast moving and strongest storms. Both types of events were, however, well captured by the regional reanalysis. It highlights the importance of spatial and temporal resolutions for the modelling of local events such as storms. In addition, it was found that the distribution of the wind speed and the wind direction during the considered storms were similar on both scales, global and regional (Fig. 2).

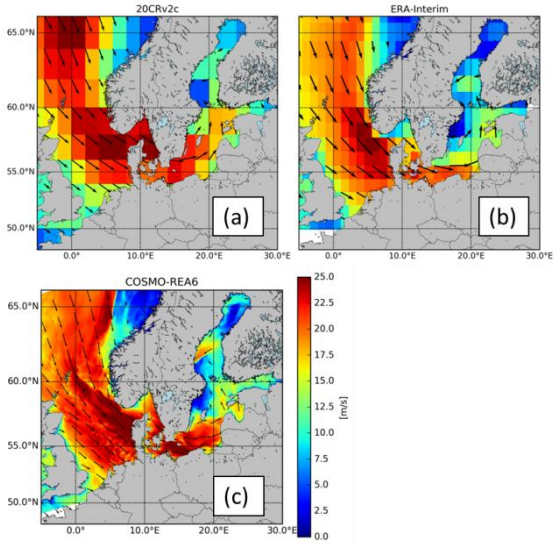

Figure 2. Wind speed and direction during the storm Xaver on 06.12.2013 00:00UTC, a) global reanalysis 20CRv2c; b) global reanalysis ERA-Interim and c) regional reanalysis COSMO-REA6.

4. Conclusions

Reanalyses are a useful tool to reconstruct the past atmospheric variability and historical storms. While observations are sparse in space and in time, the gridded information provided by the reanalyses present the advantage of being continuous in space and in time.

Global reanalyses can be used for the study of long lasting historical storms. Regional reanalyses are better suited for the analysis of short and strong storms that do not normally induce a storm tide at the coasts.

References

Bollmeyer et al. (2015) Towards a high-resolution regional reanalysis for the European CORDEX domain, Q J ROY METEOR SOC, 141, pp. 1-15

CDC, DWD Climate Data Center ftp://ftp-cdc.dwd.de/pub/CDC/

Compo, G. P. et al. (2011) The Twentieth Century Reanalysis Project, Q J ROY METEOR SOC, 137, pp. 1-28

Dee, D. P. et al. (2011) The ERA-Interim reanalysis: configuration and performance of the data assimilation system, Q J ROY METEOR SOC, 137, pp. 553-597

Uppala, S. M. et al. (2005) The ERA-40 re-analysis, Q J ROY METEOR SOC, 131, 612, pp. 2961-3012

Variability of wind storms during cold season in Northern Europe over the past 70 years

Indre Gecaite[1]

[1] Institute of Geosciences, Vilnius University, Vilnius, Lithuania (gecaite.indre@gmail.com)

1. Introduction

The changing climate brings new uncertainties and induces local studies to answer an important questions, related to public safety and impact on natural environment. Obviously, changes in climate extremes are one of the most important aspects and also are of great concern. Wind speed, if it reaches a certain threshold, causes considerable damage and economic loss. As the climate warms, new conditions in certain regions may occur. One of the factors is the strengthening of the mid-latitude jet stream in the upper troposphere and lower stratosphere and it's shift poleward along with storm tracks (Wang et al., 2011; Ihara and Kushner, 2009; Ulbrech et al., 2009). This could cause an increase in storminess and thus wind speeds along the high latitudes of the northern hemisphere. Positive trend in the storminess is one of the factors influencing wind speed changes over time. Increasing storminess and cyclonic activity in Europe (especially in northern and central parts) was found by many authors, for instance (Molter et al., 2016; Mizuta et al, 2011; Wang et al., 2011). As a result, there should be noticeable increase in wind-induced damage in the future.

2. Data and methods

This research deals with atmospheric circulation weather types (CWt), related to the appearance of gale days. For the daily classification CWt and number of gale days an objective scheme is used that was initially proposed by Lamb (1972) and later described by Jenkinson and Collison (1977) and Jones et al. (1993). This scheme is based on the original manual Lamb weather types, where 16 SLP points for determination of CWt is employed. The scheme could be expanded up to 32 SLP points as described by Bartoszek (2017) and this approach was applied in current research.
The main goal of this research is the determination of annual variability of the number of gale days and related CWt during cold season in Northern Europe in the period of 1948–2017. In the process 27 circulation types for three central points are obtained as a final result. Daily mean SLP data over the area covering 40–70°N and 5–40°E is used. Gridded SLP data fields (2.5° x 2.5° longitude–latitude) are received from the NCEP/NCAR Reanalysis dataset (access https://www.esrl.noaa.gov/psd/data/gridded/data.ncep.reanalysis.html). The specific computational procedures are adopted to the three central points: P55 (55°N and 25°E), P60 (60°N and 25°E) and P65 (65°N and 25°E). The computational scheme for every central point includes 32 points with daily SLP data. A gale index (Donat et al., 2010) is defined considering strength of directional flow (F) and vorticity (V). Different thresholds for gale days, when G>30 and severe gale days, when G>40 are used.

3. Analysis of gale days and circulation weather types

For the different points of the investigated area the number of gale days per cold season (October-March) differs and increases with latitude: P55=10.4, P60=16.9, P65=25,8 days (G>30) and P55=0.5, P60=1.8, P65=4.7 days (G>40). Two periods with high intensity in wind storms are detected: 1971–1976 and 1989–2000. The lowest wind storm activity was recorded in the period of 1955-1964.
An increased number of gale days is found in all analyzed points. The higher the latitude, the more changes are obtained. For P65 the increase in gale days equals 5 days per 70 years, P60 – 2,8 days and P55 – 1,5 days. However, all changes are insignificant and p-values are greater than 0.05.

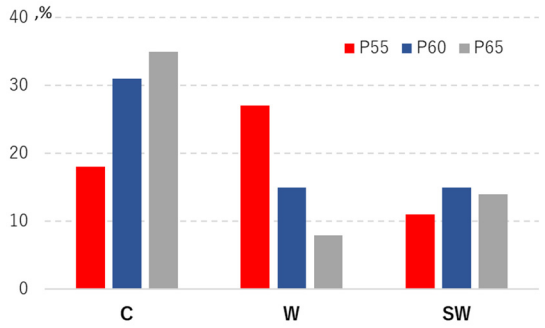

Figure 1. Occurrence (%) of the most common circulation weather types during gale days (G>30) in different points of investigated area during 1948–2017

More than 50% of gale days (G>30) occur with cyclonic circulation and westerly, south westerly flow (Fig. 1). 9–6% occur during WA, NW, S, WC and SWC circulation types (not shown). Other CWt are rare during wind storms over the investigated area and apparently are irrelevant for the occurrence of gale days. More intense (G>40) gale days are mostly related to cyclonic circulation (more than 55% of all events in P60 and P65 and 36% of all events in P55).

Table 1. Changes (days per year) of the most common circulation weather types during gale days (G>30) in different points of investigated area during 1948–2017

	C	W	SW	WA	S
P55	-0.067	**0.142**	**0.092**	**0.067**	**-0.079**
P60	-0.010	**0.089**	0.065	**-0.032**	-0.058
P65	**0.070**	-0.038	0.013	-0.002	-0.037

Detected changes could be related to the changes in occurrence of particular CWt. The statistically significant changes found over the analyzed period (1 table) are marked in bold. The increase in cyclonic circulation in P65, increase in western flow and decrease in western anticyclonic flow in P60 and increase in western, south

western and western antyciclonic flow with a decrease in southern flow in P55 is found.

Several wind storms in the investigated area were observed in all three points in one day. 312 such gale events were found and analyzed. In most cases a cyclonic circulation in P65 and P60, and western flow in P55 was recorded. Also the combination of cyclonic circulation in P65, westerly flow in P60 and westerly anticyclonic flow in P55 is often found.

The changes partly reveal characteristics of cyclones, travelling from the North Atlantic to the north east with the anticyclonic circulation to the south of 55 °N. It was found by Donat et al. (2010) that significant positive changes in storm activity are related to changes in atmospheric circulation in North Atlantic region, in particular to a positive North Atlantic oscillation (NAO) phase. At the same time, an increasing NAO index and increasing storminess have a connection with increased GHG forcing (Pinto et al., 2007). Identification of any links between wind storms and atmospheric circulation could help to better prepare for future storm consequences.

Acknowledgements

This work was co-funded from the EU Structural Funds through project Nr.09.3.3-LMT-K-712-02-0141.

References

Bartoszek K. (2017) The main characteristics of atmospheric circulation over East-Central Europe from 1871 to 2010, Meteorol Atmos Phys Vol. 129, pp. 113–129.

Ihara C., Kushner Y. (2009) Change of mean mid-latitude westerlies in the 21st century climate simulations, Geophys Res Lett, Vol. 36, pp. L13701.

Jenkinson A. F., Collison F. P. (1977) An initial climatology of gales over the North Sea, Technical report, Synoptic Climatology Branch Memorandum, N. 62. Meteorological Office, Brecknell, pp.18.

Jones P.D., Hulme M., Briffa K.R. (1993) A comparison of Lamb circulation types with an objective classification scheme, International Journal of Climatology, Vol.13, pp. 655–663.

Lamb H.H. (1972) British Isles Weather Types and a Register of Daily Sequence of Circulation Patterns, 1861–1971, Geo-physical Memoir 116, HMSO, London (UK), pp. 85.

Mizuta R., Matsueda M., Endo H., Yukimoto S. (2011) Future Change in Extratropical Cyclones Associated with Change in the Upper Troposphere, Journal of Climate, Vol.24, pp. 6456-6470.

Molter T., Schindler D., Albrecht A.T., Kohnle U. (2016) Review on the Projections of Future Storminess over the North Atlantic European Region, Atmosphere, Vol.7, No.60, pp.1-40.

Pinto J.G., Ulbrich U., Leckebusch G.C., Spangehl T., Reyers M., Zacharias S. (2007) Changes in storm track and cyclone activity in three SRES ensemble experiments with the ECHAM5/MPI-OM1 GCM, Climate Dynamics Vol. 29, pp. 195–210.

Ulbrich U., Leckebusch G.C., Pinto JG (2009) Extra-tropical cyclones in the present and future climate: a review, Theor Appl Climatol, Vol. 96, pp. 117–131.

Wang X.L.L., Wan H., Zwiers F.W., Swail V.R., Compo G.P., Allan R.J.,Vose R.S., Jourdain S., Yin X. (2011) Trends and low-frequency variability of storminess over western Europe 1878–2007, Clim Dyn, Vol. 37, pp. 2355–2371.

Baltic storm surge event Axel along the German Baltic Sea coast in a climate perspective

Nikolaus Groll[1], Ralf Weisse[1] and Lidia Gaslikova[1]

[1] Institute for Coastal Research, Helmholtz-Zentrum Geesthacht, 21502 Geesthacht, Germany (nikolaus.groll@hzg.de)

1. Introduction

Associated with the extratropical storm Axel, a storm surge along the southwestern Baltic Sea taken place in January 2017. This event caused severe inundation, coastal erosion and damaged coastal infrastructure along the coast. Such extreme marine events occur every 10 to 20 years in this region and are often compared to the dramatic storm and surge event of 1872. Even if such a severe event never occurred again, we put the water level of the recent event into relation to extreme events over the last 60 years using a hydrodynamic hindcast simulation for the Baltic Sea region.

2. Data

The hydrodynamic model TRIM-NP was used in a four way nesting approached for the southwestern Baltic Sea area with a resolution of the finest grid of about 1.6 km x 1.6 km. The hydrodynamic model was forced by a regional atmospheric hindcast with the COSMO-CLM model. To test if the model can simulate reasonable results it was compared with observational data along the German coastline.

3. Method

The water level during a storm surge is normally triggered by the atmospheric pressure via the inverse barometric effect and the direct wind stress. For the Baltic Sea two other effects can contribute to the water level: the level of filling of the Baltic Sea, which is caused by inflow of water masses via the Skagerrak and seiches stimulated by prevailing winds. The simulated water level was decomposed taken into account these effects for extreme events in the simulation period and then the recent event was then compared with the simulated climatology.

4. Results

Whereas for most locations along the German coastline, the atmospheric components (sea level pressure and wind stress) contribute an average amount and seiches contribute almost nothing to the local water level, the level of filling showed relatively high values compared to the climatology.

Integrated coastal hazard risk reduction and management – a closer look at the dynamical damage cost methodology used in the COHERENT project

Kirsten Halsnæs[1], Morten Andreas Dahl Larsen[1], Nils Drønen[2], Freja Bach Kristensen[3], Carlo Sørensen[4] and Bo Brahtz Christensen[2].

[1] Technical University of Denmark, Kgs Lyngby, Denmark (khal@dtu.dk)
[2] DHI, Hørsholm, Denmark
[3] Smith Innovation, Kbh Ø, Denmark
[4] The Danish Coastal Directorate. Lemvig, Denmark

1. Introduction

The COHERENT project, funded by Innovation Fund Denmark, was instigated on Nov. 1 and addresses risks in the coastal zone of both natural and anthropogenic origin and the interplay between them. The project is highly multidisciplinary spanning natural, social and economic sciences as well as time scales from the immediate hazard response to longer term adaptation and management and with a high degree of cross-work package dependencies and coordination. This enables a 'COHERENT' approach in line with the session topic of 'smart livable cities.

The key aim for COHERENT is to create demand driven knowledge co-creation regarding coastal hazard risk reduction and management by research, governments, business sector and the civil society.

2. COHERENT multidisciplinary components

The project is made of multiple work packages which coordinate efforts and together form the multidisciplinary basis for the COHERENT approach: 1) Physical pressures on the coastal system: – hazards and impacts, 2) Hydrology-land use interactions in the coastal zone, 3) Hazard management, response capacities and human dimensions, 4) Dynamic damage curves reflecting coping options and human capacities and 5) Risk reduction options, intelligent planning, warning systems and business.

3. Dynamical damage costs

COHERENT is developing and testing a new methodological approach for dynamic damage cost curves; see Figure 1 for an illustration. The starting point for damage cost assessments is the establishment of a flooding vulnerability state (square 1) and, given this, a flood event (red oval 1) results in specific damage costs. Society can then decide to invest in risk-reduction measures (green oval 1), and the coastal area will accordingly move into a new vulnerability state (square 2). If another flooding event happens (red oval), new damage costs will emerge that are expected to be reduced compared with the damage before the implementation of risk-reduction measures,

The dynamic damage cost curve approach combines quantitative assessment and modelling with social-science studies of risk perception, institutional, legal and social coping capacities, and the engagement of government agencies, hazard management organizations and civil society in the development of an integrated coastal risk

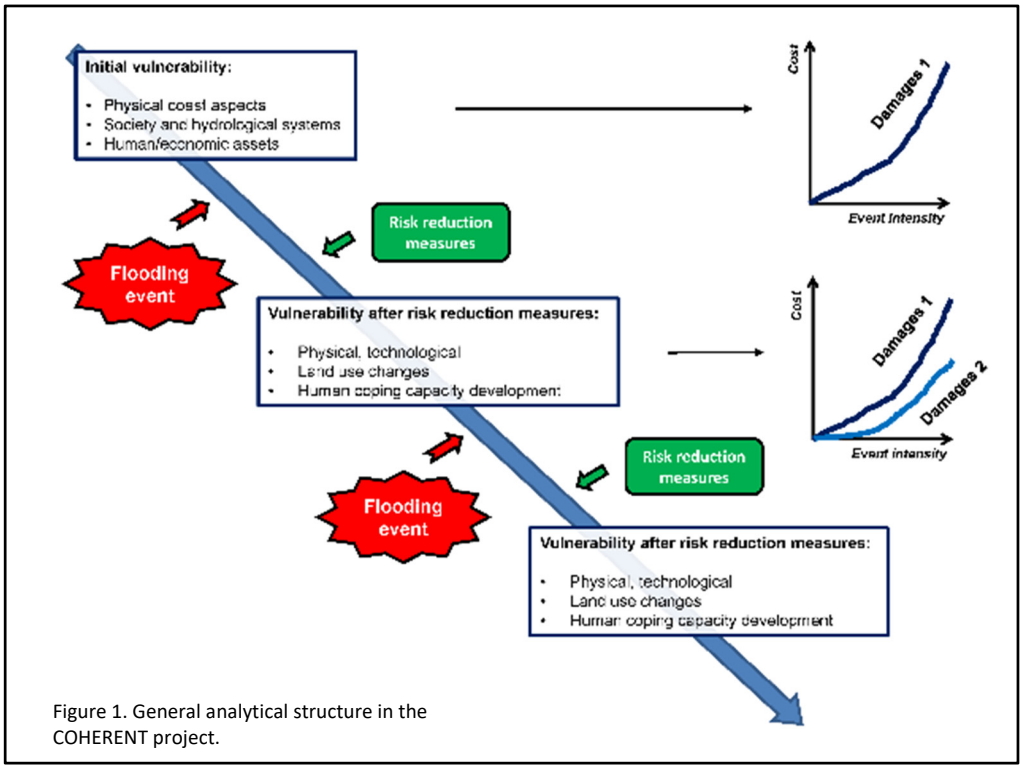

Figure 1. General analytical structure in the COHERENT project.

management strategy. Risks and uncertainties will be addressed in a probabilistic manner by assessing the tail of event probabilities in an integrated way involving the areas of science/policy, natural/social science and the short and long -terms.

4. Case studies

The project includes case studies across all work packages (Figure 2): 1) Skive, including adjacent land (Limfjorden), with a focus on interactions between flooding from the fjord/sea, the Karup stream, and urban development, 2) Aabenraa (Western Baltic Sea/Belt location), with a focus on storm surge risks, coping strategies and hazard management, 3) Ringkøbing (North Sea/fjord location), with a focus on protecting the fjord with an eroding barrier currently maintained by sand nourishment and 4) Emden (Germany/North Sea/high tide/harbour location), based on the results of an ongoing EU project, we focus on the human dimensions of coping strategy development and hazard management.

5. Output

The COHERENT output includes: 1) A new adaptation/decision software toolkit, 2) Coupled methods within 'most severe' storm-surge events, hydrology and costs, 3) Warning system, hazards and management and 4) Behavioral experiments and studies linking research, governance and risk.

Figure 2. COHERENT case study sites.

6. Partners

The project includes partners from universities (DTU), GTS institutes (DHI), national research and data supply (DMI), national authorities (The Coastal Directorate and Styrelsen for Dataforsyning og Effektivisering), private SMEs (Smith Innovation, Environment Solutions and Stormflodssikring), three municipalitites which for the basis for the case studies (Aabenraa, Skive and Ringkøbing-Skjern) and an international research partners (Helmholtz-Zentrum Geesthacht, Germany).

Extreme sea levels on the German Baltic Sea coast

Jürgen Holfort, Bärbel Weidig, Ines Perlet and Sandra Schwehmann

Bundesamt für Seeschifffahrt und Hydrographie, Rostock, Germany (juergen.holfort@bsh.de)

1. Introduction

Long-term sea level observations along the German Baltic Sea coast reveal that extreme water level variations appear regularly, and depending on their strength, they may cause economic and ecological damages. In order to study which regions are particularly endangered by storm surges and low sea levels we analyzed sea level data for the German Baltic Sea coast for a period between 1950 and today. For various stations, we show the variability of storm surge and low sea level frequency and give an estimate about the recurrence probability, which was found to vary regionally between 5 and more than 50 years and does generally not show a significant trend, i.e. it seems that storm surge and low sea level frequency has not increased significantly over the last 60 years. However, older data records exist and may reveal other results. Therefore we started to digitize and analyze paper gauges that date back to 1900 or some years earlier.

2. Data

The period for which data is available is different for the various tide gauge stations. Hourly data is available for many stations starting around 1956 until today. From these data the maximum/minimum within 3 day periods were extracted for the calculation of the recurrence periods of high/low sea level events. For longer recurrence times, also a list of yearly maximum sea levels at some stations was used, some dating back for more than 100 years. For direct comparisons hourly data for shorter time periods dating back to 1894 were available from the station Warnemünde, which were digitized from scanned papers gauges.

3. Variability and trends

Just counting the number of storm surges (defined as events with a water level above 600cm above gauge zero or about 100cm above normal water) a temporal variability is apparent, with many stations showing a maximum in the decade 1981-1990. Calculating the height for several recurrence periods using a sliding temporal window (10, 20, 30 and 40 years) the maximum values occur around 1987 at Flensburg. But the maximum can also be in 1992 or another year around 1990, depending on station, recurrence period and used distribution.

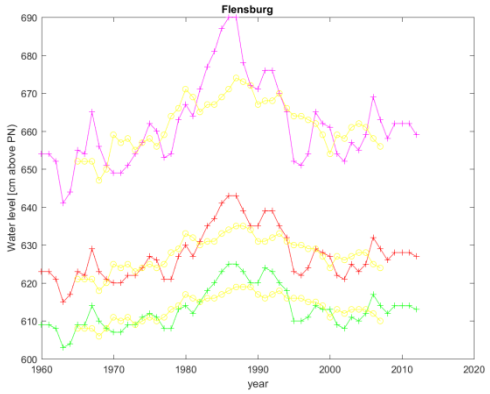

Figure 1. Water level for recurrence periods of 1 (green) ,2 (red) and 10 (magenta) years for the station Flensburg calculated using a 10 year sliding window and using the generalized extreme value distribution.. The yellow curves show the same, just with a 20 year sliding window.

At some stations the temporal linear trend in the heights of a fixed recurrence period is almost equal to the observed trend in the mean sea level (e.G. station Flensburg using a generalized extreme value distribution an 10 or 20 years sliding window). This is the expected behavior in the simple case if storm surges and sea level rise are independent, so both just add linearly. But in other cases also another behaviors can be found (e.G. Kiel-Holtenau with almost no trend in recurrence height).

4. Further work

At the conference we hope to give information about more stations and about statistical significance of the found trends. We will also present some first results looking at the duration of storm surges and low level events.

Changes in drought indices in Estonia during the period of the contemporary climate warming

Jaak Jaagus[1] and Anto Aasa[1]

[1] Department of Geography, University of Tartu, Tartu, Estonia (jaak.jaagus@ut.ee)

1. Introduction

The Baltic Sea region is located in the humid zone where precipitation is generally higher than potential evapotranspiration. Sometimes, high rainfall events cause flooding of large areas in Estonia. Drainage of agricultural lands has been historically a big challenge for farmers. At the same time, interannual variability of precipitation is very high. A lack of rainfall in the growing season has sometimes caused severe droughts leading to the crop failure. Therefore, studies on drought climatology are of a great importance.

Global warming during the last decades has been faster than the global mean (BACC, 2015). Annual mean air temperature has increased by more than 2°C in Estonia during 1951-2015 while the higher increase was observed in spring and winter, and the lower increase has been typical for summer and autumn (Jaagus et al., 2017). Trends in precipitation are not so clear. A considerable increase in precipitation has taken place during the cold season and also in June. GCM outputs for the future climate indicate a continuing warming and a moderate increase in precipitation while some GCMs project even a decrease during the summer season (Jaagus and Mändla, 2014).

It is not clear how the frequency and severity of droughts have been changed in the past and how it will change in the conditions of climate warming on the high latitudes. Droughts in the eastern Baltic region were studied in the relation NDVI and SPI (Rimkus et al., 2017). The objective of this study is to analyze long-term changes in drought indices in Estonia. We assume that trends, which have been observed during last decades, i.e. during the period contemporary climate warming, will be continued in future.

2. Data and methods

There are a big number of characteristics of drought conditions. Palmer Drought Severity Index has been the most popular. Here we used two other indices Standardized Precipitation Index (SPI) and Standardized Precipitation–Evapotranspiration Index (SPEI). They have been widely used in climatology during the last decade. SPI needs only monthly precipitation data while SPEI uses also mean wind speed, relative humidity, solar radiation, sea-level pressure, and monthly mean daily maximum and minimum temperatures. Data from nine stations (Vilsandi, Ristna, Pärnu, Kuusiku, Tallinn, Võru, Tartu, Jõgeva and Tiirikoja) from different parts of Estonia in 1951-2015 were used for the calculation of the drought indices Figure 1).

Calculations of monthly SPI and SPEI values were made using the special program in R environment. SPEI was found using three methods for the calculation of potential evapotranspiration: Penman-Monteith, Hargraves and Thorntwaite methods. Seasonal and annual values were calculated by averaging monthly values. Trend analysis of the time series was realized using the linear regression, the Student's t-test, the Mann-Kendall test for trends and the Sen's method for calculating the slope.

Figure 1. Location map of the stations in Estonia.

3. Results

During the cold period (November – March) increasing of SPI and SPEI has been detected in all stations but the trends are statistically significant not at all stations. Stronger changes were detected in the eastern Estonia while weaker trends were typical in western Estonia near to the Baltic Sea (Figure 2). The highest trend values during the cold period were obtained for SPEI using the method by Penman-Monteith for calculation of potential evapotranspiration.

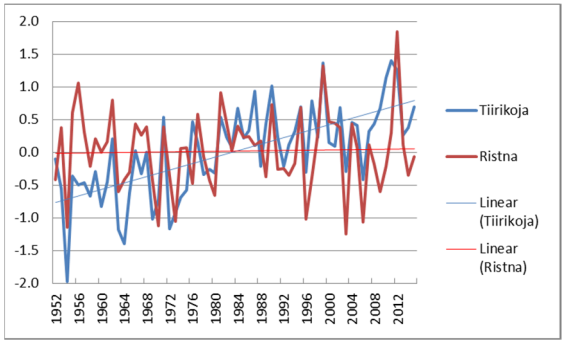

Figure 2. Time series of SPEI in winter (December – February) in Tiirikoja and Ristna stations calculated using the Penman-Monteith method, and their linear trendlines.

During the warm season (April – October) statistically significant increasing trends in time series of SPI and SPEI revealed only in June that correspond to the similar trend in June precipitation (Jaagus et al., 2017). These changes in June were stronger in the coastal stations and in case of SPEI by Penman-Monteith (Figure 3). Weak positive changes were detected in October.

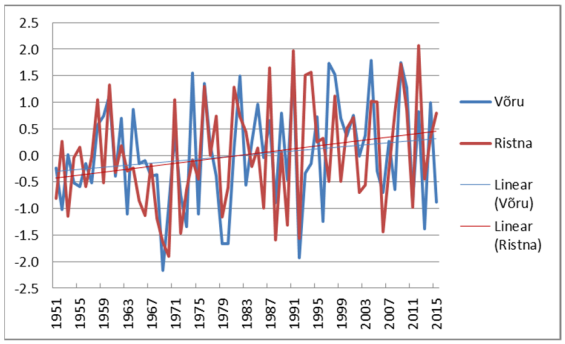

Figure 3. Time series of SPI in June in Võru and Ristna stations and their linear trendlines.

During the warm season decreasing tendencies, i.e. drying was found in April in eastern Estonia (Figure 4), and in some stations also in July and September. Statistically significant trends were detected in case of SPEI Hargraves and Thorntwaite but not in SPEI Penman-Monteith and SPI. No trends were detected in May and August

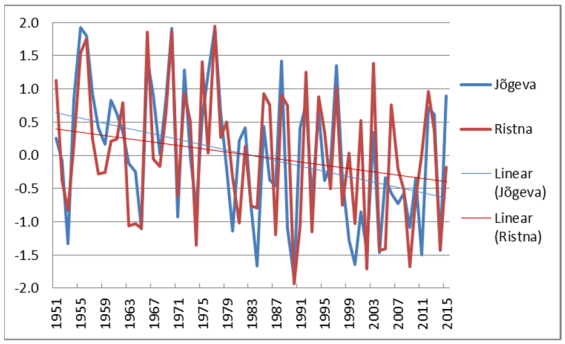

Figure 4. Time series of SPEI Thorntwaite in April in Jõgeva and Ristna stations and their linear trendlines.

In general, time series of annual mean drought indices have increasing trends. They have been caused by strong trends during the cold season. In climatic conditions of Estonia winter drought has no sense. The increasing trends in SPI and SPEI in winter reflect climate warming. It means that the frequency of cold anticyclonic weather conditions has decreased and the frequency of mild cyclonic weather with a lot of precipitation has increased.

An increasing tendency in spring was observed in case of SPI but not in SPEI. In summer, a positive trend in SPI and SPEI (Penman-Monteith) was detected in two stations (Tiirikoja and Pärnu) but no trends in summer SPEI Hargrave and Thorntwaite. A weak increase in SPI and SPEI was also revealed in autumn, which was significant in Tartu, Pärnu and Tiirikoja in case of SPEI Penman-Monteith.

4. Conclusions

The study on time series of the drought indices did not reveal very clear changes in Estonia. It means that moisture conditions have not changed in the contemporary global climate warming. The warming has influenced on the increase of SPI and SPEI during the cold period from November to March.

Precipitation is the main factor determining moisture conditions in Estonia. Trends in precipitation are reflected in trends of the drought indices. This is clearly expressed in June where precipitation amount has increased significantly in 1951–2015. During the other months of the warm season there were no such clear trends. A weak drying tendency revealed in April, July and September. But changes in trend values between stations vary quite a lot. It is result of a very high spatio-temporal variability of summer precipitation.

References

BACC Author Team (2015): Second assessment of climate change for the Baltic Sea basin. Springer, Cham Heidelberg New York Dordrecht London, 501 pp.

Jaagus, J. and Mändla, K. (2014): Climate change scenarios for Estonia based on climate models from the IPCC Fourth Assessment Report. Estonian Journal of Earth Sciences 63, 166-180.

Jaagus, J., Sepp, M., Tamm, T., Järvet, A., and Mõisja, K. (2017) Trends and regime shifts in climatic conditions and river runoff in Estonia during 1951–2015. Earth Systems Dynamics 8, 963-976.

Rimkus, E., Stonevicius, E., Kilpys, J., Maciulytė, V., and Valiukas, D. (2017) Drought identification in the Eastern Baltic region using NDVI. Earth Systems Dynamics 8, 627-637.

Spatial variability of extreme precipitation in Estonia

Jüri Kamenik[1], Piia Post[2], Jaak Jaagus[3], Ain Kull[4], Ants Kaasik[5], Svetlana Aņiskeviča[6]

[1] Institute of Ecology and Earth Sciences, University of Tartu, Vanemuise 46, Tartu, Estonia (kamenikmeister@gmail.com) [2] Institute of Physics, University of Tartu, Ostwaldi 1, Tartu, Estonia

[3] Department of Geography, Institute of Ecology and Earth Sciences, University of Tartu, Vanemuise 46, Tartu, Estonia

[4] Department of Geography, Institute of Ecology and Earth Sciences, University of Tartu, Vanemuise 46,Tartu, Estonia

[5] Institute of Ecology and Earth Sciences, University of Tartu, Vanemuise 46, Tartu, Estonia

[6] Climate and Methodological Division, Latvian Environment, Geology and Meteorology Centre, Maskavas street 165, Riga, Latvia

1. Introduction

Precipitation is an extremely variable climatic parameter in space and time. It has a direct effect on many kinds of human activity. Precipitation influences on water management, agriculture, water transport and also on the humans' everyday life. Therefore, precipitation extremes – extensive periods with little or without any precipitation leading to droughts, and extremely high precipitation amounts causing floods – are related to the severest damages to human activity in nearly all regions of the world. The global climate warming is one of the reasons why the analysis of extreme precipitation events and their long-term trends has become an important topic in climatological studies.

An increase in the frequency and magnitude of extreme precipitation events has been observed in many regions worldwide. It was likely that since 1951 there have been statistically significant increases in the number of heavy precipitation events in more regions than there have been statistically significant decreases. But strong regional and sub-regional variations revealed in the trends (Groisman et al. 2005, Alexander et al. 2006, IPCC 2013, Donat et al. 2016). The number of heavy precipitation events increased even in the regions with a decrease in annual precipitation. These changes are considered to be related to general climate warming (Groisman et al. 1999, Allen and Ingram 2002).

Changes in extreme precipitation have been significant in the Baltic Sea region. Using daily data at five stations in Poland a positive trend was found in the number of wet spells and days with precipitation while a negative trend was detected in mean precipitation during the second half of the 20th century (Wibig 2009). The analyses based on much larger amount of observational data (48 stations in 1951–2006) using five indices of precipitation extremes demonstrated diverse results for Poland (Lupikasza 2010). Decreasing trends in extreme precipitation indices dominated in summer mostly in southern Poland while increasing trends revealed in spring and autumn in its northern regions.

Jaagus et et. (2009) analysed the mean precipitation pattern in the Baltic countries (Estonia, Latvia, Lithuania) and the influence of local landscape factors on it, to derive a regionalization and relationships between precipitation and characteristics of the large-scale atmospheric circulation.

The Baltic Sea proved to be the main factor determining precipitation pattern in the study region. The presence of different precipitation zones parallel to the coastline is typical for the windward lowland region, whereas the belt of maximum precipitation is located at 10–60 km from the coast. Surface elevation is the second important factor causing higher precipitation on uplands (Jaagus et et. 2009).

Data and methods

The study is based on daily precipitation data measured at 81 stations in Estonia during the period 1958–1987. Data are provided by the Estonian Weather Service. 30-year period time frame was selected because it was with the maximum number of stations with continuous precipitation observations in Estonia. The stations were included into the analysis using the criteria of 3% allowed missing data (gaps) as a maximum. Data from four Latvian meteorological stations were provided by the Latvian Environment, Geology and Meteorology Centre. All the measurements have been carried out manually using the Tretyakov precipitation gauges (Groisman et al 1991).

The warm half-year is defined as the period from May to October, and the cold half-year from November to April.

Precipitation amounts should be described as the gamma distribution, and its special case is the exponential distribution (Stoyan et al. 1995, Haight 1967, Kilpeläinen et al. 2008).

Because of the studying highly unusual values of precipitation amounts, it is suitable to use the extreme value theory (Coles 2001). GEV distribution is a three-parameter distribution. Distribution of this random variable can be approximated by the GEV distribution with its respective cumulative distribution function

$$F(x;\mu,\sigma,\xi)=\exp\{-[1+\xi((x-\mu)/\sigma)]^{(-1/\xi)}\} \quad (1)$$

where μ, σ and ξ, denote location, scale and shape parameters, respectively, ξ≠0, σ and 1 + ξ (x-μ)/σ must be greater than zero; the shape and location parameter can be any real numerical value.

L-moment method was used for fitting the distribution to the data. L-moment method is often more appropriate (it gives the nearest results to the “actual parameters” of the ξ, μ and σ) in case of shorter samples (Kharin and Zwiers, 2000).

In the study, the R statistical environment and its package extRemes (version >= 2.0) was used (Gilleland, 2015). In the R, a return period is model-based and it is derived from GEV via quantiles: return period is 1/p, where the return level is expected to be exceeded on average once every 1/p years, it means, return level is exceeded by the annual maximum in any particular year with probability p (Coles, 2001).

To estimate return levels and periods fitting of the distribution function for given daily precipitation amounts and vice versa was performed, then 2-, 5-, 10-, 20-, 50-, 100-year return levels were computed for each station.

The sampling uncertainty of the estimates is determined by the parametric bootstrap procedure. In this procedure 5000 samples of size 30-year are generated

from the fitted GEV distribution. A return value is estimated from each generated sample by fitting and inverting a GEV distribution as derived above (Kharin and Zwiers, 2000).

Return level values were mapped using point kriging for spatial interpolation using the Surfer software.

2. Results

Mapping of warm half-year results for 2–, 5–, 10–, 20– and 50–year return levels results confirm that the respective field of values is very complicated where the sensitivity test showed how much the estimated return level depends on the choice of the period, or on the number of rare events in observed period.

2– and 5–year return levels between different stations are similar, being a 22–38 mm/d (Fig. 1). However, the 2– and 5–year return levels are higher in the higher areas: 30–50 mm/d (supporting Latvian stations), but also moderate distance of coastal areas: 30–40 mm/d, and smaller in the islands and coastal regions (20–30 mm/d). Similar pattern for overall precipitation has been shown also in Jaagus et al. (2009) work.

It can be observed that maximum values over South-eastern Estonia shifts more eastward if compared 10- and 50-year return levels but are still much higher compared to values of other parts of Estonia: over 100 mm/d and averagely 50–70 mm/d, respectively.

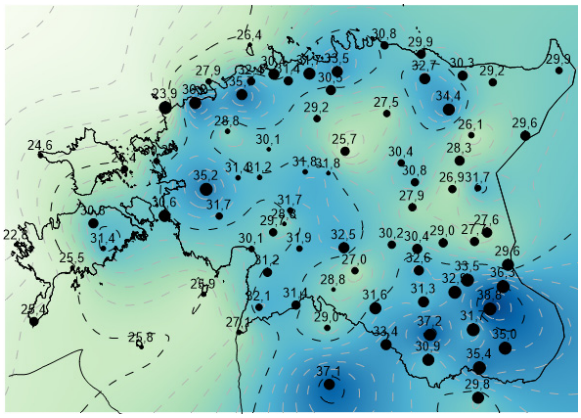

Figure 1. 2-year warm half-year return levels of precipitation in mm/d. The point size indicates the amplitude of the confidence intervals classified by decile; the upper and lower return level of confidence intervals are shown numerically in each station; the colour scale indicates the return levels (mm/d).

In case of 10– and even more 20– and 50–years return levels the belt of maximum values from moderate distance of coastal areas becomes less evident and values are ranging from 45–60 mm/d (10–years) up to 90 mm/d (50–years) between them.

The situation becomes considerably more complicated in the case of 50–return levels: smallest values are 40–50 mm/d and highest more than 100 mm/d. Even larger territorial differences were observed at the 100–return levels period: they differ between stations more than twice: 50 mm/d (Gulf of Riga and some inland places) up to 110 mm/d (south-eastern tip of Estonia).

In case of cold half-year (November to April) return level it is evident the values are substantially lower: 10–20 mm/d for 2–years and 19–44 mm/d for 50–years return levels. In case of 2–years return levels it is observable maximum values mainly over South-western Estonia (bordering by Gulf of Riga), up to 21 mm/d in Saaremaa, and lesser evident western island bordering by Baltic Sea. Lowest values are in North-eastern Estonia: 12 mm/d.

In case of 50-year return levels it is clearly two areas with maximum values: coastal areas of Gulf of Finland with values over 30 mm/d in some places, and Southern Estonia together with Saaremaa supporting also Latvian stations with values up to 44 m/d. The lowest values are Eastern Estonia bordering by Lake Peipus: 19 mm/d in some places.

3. Discussion

The primary reason for being 2- and 5-year return levels estimated values are higher in the uplands, but smaller in the islands and coastal regions is a different type of surface: the land warms up faster and stronger than water. As a result, there is a higher amount of convective precipitation, which is characterized by higher intensity.

But the pattern of higher return levels of moderate distance of coastal areas need special attention and explanation: it is possible to explain this pattern by the mechanism of the breeze front. This pattern is probably influenced by some other mechanisms also, e.g.: late summer the sea is warmed up, so convection can start already over the sea, then during the daytime, surface heating can cause intensification of precipitation and this is more possible late August and September. Another explanation can provide for areas of moderate distance from Gulf of Finland: this is mean south-westerly airflow possibly behind of observed pattern. It means when cumulus cloud form near Gulf of Riga, then they pushed by south-westerly airflow toward the Gulf of Finland, especially toward North-eastern Estonia. During the movement, the cumulus clouds can grow into cumulonimbus if air mass is unstable enough, and then there is higher probability of extreme precipitation near Gulf of Finland.

The smaller variation of lower return levels are because the randomness is not so high – events with a daily precipitation amount between 20 and 30 mm occur at a higher frequency and the determining factor is probably the circulation which drives also heavy stratiform precipitation – they form due to cyclone and frontal activity.

To sum up explanation of found patterns: 2-, 5- or even 10-years lower return levels show simpler and more clear patterns over Estonia than higher return levels and this difference is caused by different mechanism, which controls respectively very rare and less rare precipitation events: events with a daily precipitation amounts until 20–30 mm are associated with special circulation types which drives also heavy stratiform precipitation – they form due to cyclone and frontal activity and therefore occur at a higher frequency and spatial pattern is more clear, but very rare events are controlled very likely convection which is itself spatially very variable phenomena, thus the respective pattern is much more complex.

References

Alexander L, Zhang X, Peterson T, Caesar J, Gleason B, Klein Tank A, Haylock M, Collins D, Trewin B, Rahimzadeh F, Tagipour A, Ambenje P, Rupa Kumar K, Revadekar J, Griffiths G. 2006. Global observed changes in daily climate extremes of temperature and precipitation. Journal of Geophysical Research 111: D05109. DOI: 10.1029/2005JD006290

Allen MR and Ingram WJ 2002. Constraints on future changes in climate and the hydrologic cycle. Nature 419: 224–232.

Coles, S., 2001. An introduction to statistical modelling pf extreme values. Springer-Verlag London.

Donat MG, Alexander LV, Herold N, Dittus AJ 2016. Temperature and precipitation extremes in century-long gridded observations, reanalyses, and atmospheric model simulations. Journal of Geophysical Research, Atmospheres, 121, 11174–11189.

Gilleland, E., 2015. Package 'extRemes'. Eos, 92(2), 13–14

Groisman, P. Y., Koknaeva, V.V., Belokrylova, T.A., Karl, T.R, 1991. Overcoming biases of precipitation measurement: a history of the USSR experience. Bulletin of the American Meteorological Society 72, 1725–1733.

Haight, F. A.,1967. Handbook of the Poisson Distribution. New York: John Wiley & Sons.

IPCC, 2013. Climate Change 2013: The Physical Science Basis. Contribution of Workin Group I to the Fifth Assessment Report of the Intergovernmental Panel on Climate Change [Stocker, T.F., D. Qin, G.-K. Plattner, M. Tignor, S.K. Allen, J. Boschung, A. Nauels, Y. Xia, V. Bex and P.M. Midgley (eds.)]. Cambridge University Press: Cambridge, United Kingdom and New York, NY, USA.

Jaagus, J.; Briede, A.; Rimkus, E.; Remm, K.(2009). Precipitation pattern in the Baltic countries under the influence of large-scale atmospheric circulation and local landscape factors. International Journal of Climatology, Published online in Wiley InterScience. J. Climatol. 30: 705–720.

Kilpeläinen, T., Tuomenvirta H., Jylhä, K., 2008. Climatological characteristics of summer precipitation in Helsinki during the period 1951–2000. Boreal Env. Res. 13, 67–80.

Lupikasza, E. 2010. Spatial and temporal variability of extreme precipitation in Poland in the period 1951–2006. Int J Climatol 30, 991–1007.

Stoyan, D., Kendall, W. S., Mecke, J., 1995. Stochastic geometry and its applications, volume 2. Wiley

Wibig, J. 2009. The variability of daily precipitation totals in Poland (1951–2000). Geographia Polonica 82:21–32.

Strong currents in a cross section of two narrow straits in the Finnish Archipelago Sea

Hedi Kanarik[1], Laura Tuomi[1], Elina Miettunen[2], Riikka Hietala[1] and Pekka Alenius[1]

[1] Finnish Meteorological Institute, Helsinki, Finland (hedi.kanarik@fmi.fi)

[2] Finnish Environment Institute, Marine Research Centre, Helsinki, Finland

1. Introduction

The Finnish Archipelago Sea in the northern part of the Baltic Sea is a complex and highly trafficked sea area. The area consist of over 2000 different sized islands with narrow straits in between them. Strong currents can occur in the narrow channels of this area occasionally causing problems for navigation. The Lövskär area, where two major fairways cross (Fig. 1), has been identified as an area, where currents have an impact for navigation and the knowledge of the conditions is important (Söderholm, 2013).

Our aim is to study these strong currents and how they are formed in the Lövskär area using in situ measurements and a 3D hydrodynamic model.

2. Data and methods

We used current measurements available for June 18—Nov 13 2013 made with a Teledyne RD Instruments' Workhorse Sentinel (300 kHz) ADCP. The measurements were 20 min averages from 5 to 38 meters depths at 1 m intervals. Additionally we used wind measurements from coastal weather stations Utö and Isokari and sea level measurements from Turku and Föglö tide gauges.

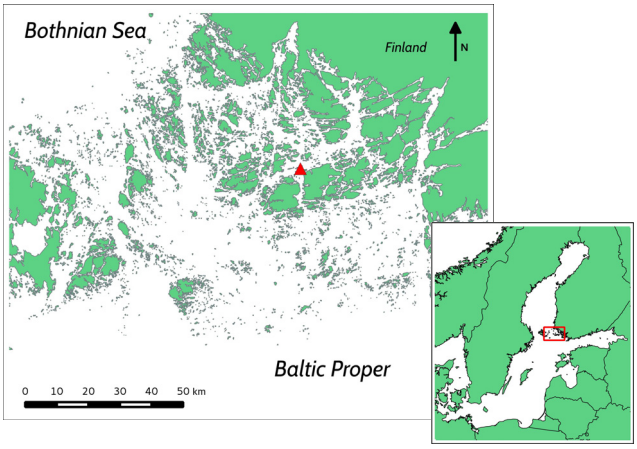

Figure 1. The Finnish Archipelago Sea is located in southwest Finland dividing the northern Baltic Proper from the Bothnian Sea together with the Åland Sea. The studied site (Lövskär area), in cross section of the two narrow straits, is marked with a red triangle.

As the measured time series of currents was relatively short, we utilized data from 3D hydrodynamic model COHERENS in evaluation of occurrence and seasonality of the strong current events. The model grid covers the Archipelago Sea with a high resolution of c. 460 m and it is nested inside a coarse resolution (3.7 km) Baltic Sea grid. Tuomi et al. (2018) showed that the model was able to simulate well the temperature and salinity in the area and the seasonal variation in those parameters.

3. Preliminary results

Measurements showed that the currents were strongly stratified during the time when there was a strong seasonal thermocline. The flow directions were often from opposite directions in the upper and lower layer. Over the whole water column the velocity was 74 % of the time less than 10 cm/s. During the ADCP deployment there were five cases of very sudden strong currents, with velocities of over 40 cm/s.

Currents had two major directions, northeast and southwest, following the bathymetry of the area. The strongest current speed measured was almost 50 cm/s and the current direction during the strong current events was mainly towards the north-northeast. These cases were linked with occasional southeasterly winds that are able to push water from the Baltic Proper directly along the southern part of the strait into the inner Archipelago Sea. These strong currents occurred normally some hours after southeasterly wind, of over 10 m/s, had been measured in Utö station and started to decrease as wind in Utö station turns southwesterly.

References

Söderholm, P (2013) Kysely merellisistä olosuhdetieto-tarpeista. Publications of the Centre for Maritime Studies, University of Turku (in Finnish) http://www.doria.fi/handle/10024/941

Tuomi, L., Miettunen, E., Alenius, P., & Myrberg, K. (2018). Evaluating hydrography, circulation and transport in a coastal archipelago using a high-resolution 3D hydrodynamic model. *Journal of Marine Systems*, *180*, 24-36.

Causes, frequency and strength of severe high water events in the Odra River mouth area (the southern Baltic Sea)

Halina Kowalewska-Kalkowska[1]

[1] Institute of Marine and Coastal Sciences, University of Szczecin, Poland (halina.kowalewska@usz.edu.pl)

1. Headline

The system of downstream reaches of the Odra River and the Szczecin Lagoon is an estuarine water body in the southern Baltic Sea strongly affected by sea level changes (Buchholz, 1990). The flood threat is posed by storm surges, snow-melt and rainfall events as well as ice jamming. The study analyses causes, frequency and strength of severe high water events in the Odra River mouth on the basis of water level data from 1993-2017.

2. Storm surges

Storm surges at the coast of the Pomeranian Bay are associated with low-pressure systems travelling over the Baltic Sea. They result in the intrusion of the Bay's brackish waters into the Szczecin Lagoon, which raise the water level there and in the lower Odra channels (Kowalewska-Kalkowska and Wiśniewski, 2009). Since the 1990s, the number of storm surges has differed greatly from year to year; the highest was in 2007. Although most of the surges were recorded from November to February, some exceptions were detected in other moths, like the extensive storm surge which appeared on the turn of August and September 1995. During the period discussed, the most severe storm surge at the coast of the Pomeranian Bay was detected in November 1995, whereas in the system of downstream reaches of the Odra River and the Szczecin Lagoon the heaviest storm event was induced in October 2009. The surge extent in the Odra mouth depended not only on the distance from the sea, but also on the magnitude of the river discharge (Kowalewska-Kalkowska, 2016).

3. The Odra high water events

The Odra is one of the biggest rivers in the Baltic Sea Catchment Basin. The Odra opens first into the Szczecin Lagoon; then it drains into the Pomeranian Bay. In its downstream reaches, it shows the features of a lowland river with a very low slope of water surface. The effect of the instantaneous Odra discharge on water levels in the Odra mouth area is of less importance because it affects only the mean water level. During the year, the increased Odra discharge was recorded mainly from January to May, indicating the prevalence of snow-melt floods in this section of the river. Although snow-melt mediated Odra floods were predominant in the Lower Odra, the two highest floods in summer 1997 and late spring 2010 resulted from an increased river discharge due to heavy rains in the upper Odra basin.

4. Extreme high water events in the Odra mouth

In 1993-2017 the long-lasting very high extensive high water events in the system of downstream reaches of the Odra River and the Szczecin Lagoon resulted from the superposition of a few factors. First of all they were recorded when a few surges, one by one, took place at the Pomeranian Bay coasts. Such events were usually observed under the condition of the increased water volume in the Baltic Sea (e.g., winters 2007, 2012). Severe high water events were also noted when storm surges limited the outflow of the Odra River during snow-melt (e.g., spring 2002) or rainfall events (e.g., spring 2010).

The increased flood threat for low-lying coastal areas was posed while the increased Odra outflow was slowed down by ice jams and storm surges. The temporal and spatial water level variations during such events in the area were visualized especially during the winter 2010/2011 (Fig. 1).

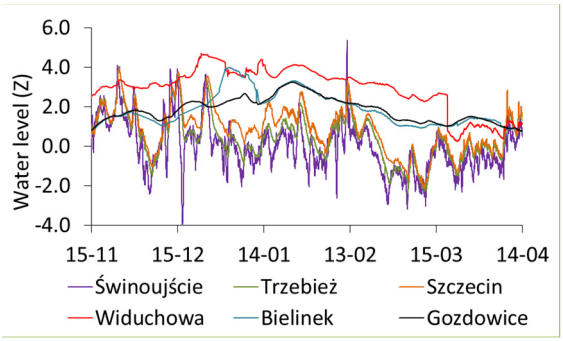

Figure 1. Water level changes in the Odra River mouth area in winter 2010/2011 (water level readings were converted to standardized values – Z).

5. Conclusions

The analysis of water level readings collected at gauges located in the Odra River mouth area in 1993-2017 revealed that extreme high water events in the system of downstream reaches of the Odra River and the Szczecin Lagoon were caused by combined effects. Under such conditions, many days' maintenance of high water levels within the whole system posed a flood threat for low-lying areas around the Szczecin Lagoon, the Dąbie Lake and areas adjacent to the lower Odra channels.

References

Buchholz W. (ed.) (1990) Materiały do monografii dolnej Odry, Warunki hydrologiczno-hydrodynamiczne, Prace IBW PAN, 22, Gdańsk [In Polish].

Kowalewska-Kalkowska H. (2016) Multivariate methods of data analysis in assessment of sea impact on the water level in the downstream Odra River system and the Szczecin Lagoon, In: Chaberek-Karwacka G., Malinowska M. (ed.), Geography in the Face of Modern World Challenges, Wyd. Libron, Kraków, pp. 131-147.

Kowalewska-Kalkowska H., Wiśniewski B. (2009) Storm surges in the Odra mouth area during the 1997–2006 decade, Boreal Env. Res., 14, pp. 183–192.

Storm surge modelling in the Baltic Sea using the high resolution PM3D model

Halina Kowalewska-Kalkowska[1], Marek Kowalewski[2,3]

[1] Institute of Marine and Coastal Sciences, University of Szczecin, Poland (halina.kowalewska@usz.edu.pl)
[2] Institute of Oceanography, University of Gdańsk, Gdynia, Poland
[3] Institute of Oceanology of Polish Academy of Sciences, Sopot, Poland

1. Introduction

A reliable prediction of water level is essential for the emergency centers and services responsible for the storm-flood protection of the Baltic coastline. The paper discusses the application of the parallel version of three-dimensional hydrodynamic model of the Baltic Sea (PM3D), developed at the Institute of Oceanography, University of Gdańsk in Poland to storm surge modelling in the region of the Baltic Sea.

2. The model study

The three-dimensional hydrodynamic model of the Baltic Sea (M3D) has provided operational forecasts since the end of the 1990s. The tool, based on the Princeton Ocean Model (Blumberg and Mellor, 1987), was adapted to the Baltic conditions by Kowalewski (1997). In 2015, within the framework of SatBałtyk System, the operational, parallel version (PM3D) of the model was run. In the PM3D two grids with different spatial resolution were used: 1 NM (c. 1.8 km) for the Baltic Sea and the Skagerrak, and 0.5 NM (c. 0.9 km) for the southern part of the Baltic (Fig. 1). Parallel calculations used in the model enabled to reduce the computation time for 1 day simulations in two domains, 1 NM and 0.5 NM, to 64 minutes (Kowalewski and Kowalewska-Kalkowska, 2017). The PM3D assimilates the sea surface temperature data retrieved from the AVHRR and MODIS radiometers. Meteorological data were supplied by the Unified Model run by Interdisciplinary Centre for Mathematical and Computational Modelling, University of Warsaw.

The better description of the intricate coastline and bottom topography of the Baltic Sea improved the prognostic reliability of the PM3D. The coefficients of correlation between the numerical simulations and hourly sea level readings collected at 9 Baltic gauges in 2010-2015 exceeded 0.90 (Kowalewski and Kowalewska-Kalkowska, 2017). The evaluation of the model quality during the storm surges showed a good representation of events characterized by rapid water level fluctuations. The highest rate of predictions matching the observed readings within the range of ±0.15 m was found for the stations located along the southern Baltic coast.

Temporal variability of sea level changes along the Baltic Sea coast, as approximated by the PM3D, may be visualized for a case involving a storm surge that occurred in February 2011. The storm event was induced by the passage of a deep low pressure system called Olaf over the Baltic Sea. During the surge, the PM3D mimicked sea level fluctuations with a high accuracy, properly predicting the timing and extent of extreme values, with errors usually not exceeding 0.15 m (Fig. 2).

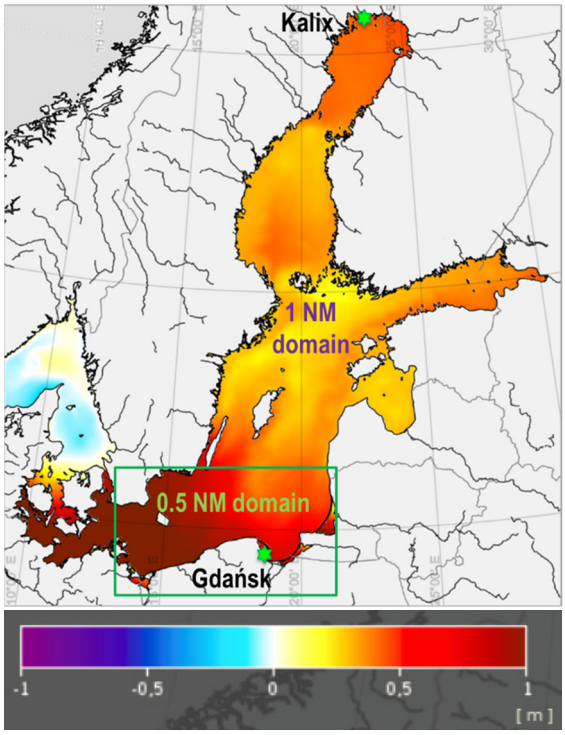

Figure 1. Sea level on 12 February 2011, 0:00 hrs., as simulated by the PM3D (http://satbaltyk.iopan.gda.pl)

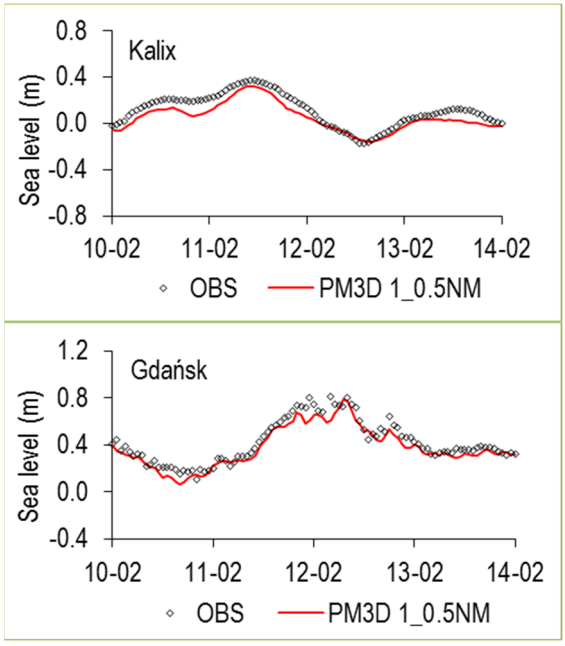

Figure 2. Simulations produced by the PM3D and sea level readings at the Kalix and Gdańsk stations during the February 2011 storm surge.

3. Conclusions

A high-resolution parallel version of 3D hydrodynamic model of the Baltic Sea (PM3D) was applied in analyses of extreme storm surges in the region of the Baltic Sea. Testing the applicability of the PM3D during storm surges that occurred in 2010-2015, showed a good fit between the observed and computed data. The model satisfactorily predicted the timing and level of extreme values; it also generated relatively good simulations of rapid water level variations. The best fit between the numerical calculations and readings from the sea level gauges was obtained for the southern Baltic Sea, modelled with the 0.5 NM grid resolution. A slightly worse agreement was shown for the other parts of the Baltic Sea, modelled with 1 NM spatial spacing.

Parallel calculations used in the PM3D enabled to reduce significantly the time necessary for computing the simulations and apply the high-resolution grid to the operational version of the model, available within the SatBałtyk System (http://satbaltyk.iopan.gda.pl). The website provides a quick online access to the daily-updated 72-h predictions of hydrodynamic conditions generated by the PM3D, with 1 NM grid resolution for the Baltic Sea and 0.5 NM resolution for its southern part.

References

Blumberg A. F., Mellor G. L. (1987) A description of a three-dimensional coastal ocean circulation model, In: Heaps N. S. (ed.), Three-dimensional coastal ocean models, Am. Geoph. Union, pp. 1–16.

Kowalewski M. (1997) A three-dimensional hydrodynamic model of the Gulf of Gdańsk, Oceanol. Stud., 26 (4), pp. 77–98.

Kowalewski M., Kowalewska-Kalkowska H. (2017) Sensitivity of the Baltic Sea level prediction to spatial model resolution, Journal of Marine Systems, 173, pp. 101–113, doi:10.1016/j.jmarsys.2017.05.001.

Supercomputer-aided analysis of wave impact on coastal infrastructure

Andrey Kozelkov[1,2] , Rashit Shagaliev[1], Sergey Dmitriev[2], Andrey Kurkin[2], E Pelinovskiy[2]

[1] Federal State Unitary Enterprise «Russian Federal Nuclear Center – All-Russian Research Institute of Experimental Physics» (FSUE «RFNC-VNIIEF»), Sarov, Nizhny Novgorod region (askozelkov@mail.ru)
[2] Federal State Budgetary Educational Institution of Higher Education «Nizhny Novgorod State Technical University n.a. R.E. Alekseev»

This work has been funded by grants of the President of the Russian Federation for state support of research projects by young doctors of science (MD-4874.2018.9) and leading schools of thought of the Russian Federation (NSh-2685.2018.5), and supported financially by the Russian Foundation for Basic Research (RFFI Project 16-01-00267).

1. Introduction

Development of a technology to assess the wave impact on coastal infrastructure is a highly relevant problem, which can be solved to the full extent by three-dimensional numerical simulations. As present, the most promising approach to free-surface dynamics simulations involves three-dimensional Navier-Stokes equations, Ubbink (1997). Their use removes constraints on the infrastructure configuration to be simulated, and intensity and shape of running-up waves.

However, the use of the Navier-Stokes equations for free-surface simulations requires an efficient numerical method and is highly demanding computationally. The paper deals with the development, verification and application of a numerical simulation technology within the Navier-Stokes framework to model the wave impact on coastal infrastructure using supercomputing capabilities.

2. Mathematical model and numerical experiments

To simulate the wave impact on the coastal infrastructure, the Navier-Stokes equations are used in combination with the Volume of Fluid method, Ubbink O. (1997). The numerical algorithm involved is based on a fully implicit method, Kozelkov et al. (2016), Kozelkov et al. (2017a). The system of linear equations is solved by the Algebraic Multi-Grid (AMG) method, Kozelkov et al. (2016).

Verification of the technology presented in the paper is performed on a number of problems supported by experimental evidence. The paper reports the results of technology verification for the cases of a collapsing liquid column with or without obstacle and pool sloshing, Ubbink (1997). The results show that the proposed numerical simulation technology can be used to assess the wave impact on coastal infrastructure. One should note, however, that as compared to the classical wave impact prediction methods, Weiss (2007), this technology requires using supercomputers, Kozelkov et al. (2016), but it for sure produces a more accurate simulation result.

To demonstrate that this technology can be used for the assessment of the wave impact on coastal infrastructure we present simulation results for waves flowing over a single obstacle (fig.1) and multiple obstacles (fig.2).

We show that our technology makes it possible to calculate a detailed shape of wave perturbations acting both on single and multiple obstacles. One can not only assess how the process develops qualitatively, but also obtain quantitative characteristics of wave impact, such as transient load distribution across obstacles and wave impact area.

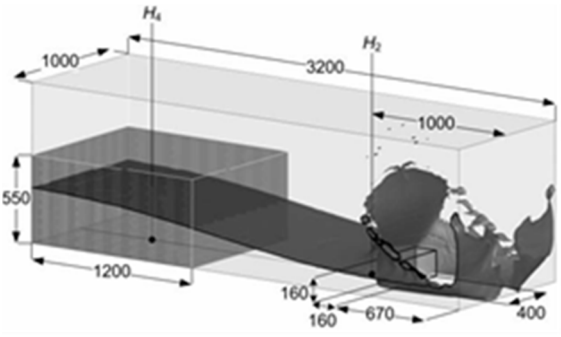

Figure 1. Free surface in the simulation of a wave flowing over a single obstacle.

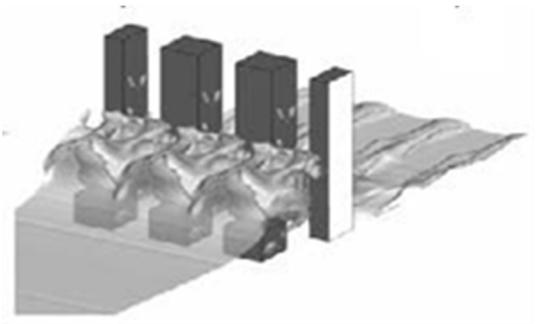

Figure 1. Free surface in the simulation of a wave flowing over multiple obstacles.

The technology has been implemented in the Russian software package LOGOS intended for multi-physics simulations of convective heat-and-mass transfer, aerodynamics and hydrodynamics on parallel computers, Kozelkov et al. (2016), Kozelkov et al. (2015). LOGOS is successfully used for various hydrodynamic simulations, including modeling of tsunamis, Kozelkov et al. (2017a, 2017b).

References

Kozelkov A. S. et al. (2015) Zonal RANS–LES Approach Based on an Algebraic Reynolds Stress Model, Fluid Dynamics, vol. 50, №5, pp. 621–628.

Kozelkov A. S. et al. (2016) Investigation of supercomputer capabilities for the scalable numerical simulation of computational fluid dynamics problems in industrial applications, vol. 56, № 8, pp. 1506-1516.

Kozelkov A.S. et al. (2017a) Three-dimensional numerical simulation of tsunami waves based on the Navier-Stokes

equations, Science of Tsunami Hazards, Journal of Tsunami Society International, vol. 36, №4, pp.183-196.

Kozelkov A.S. et al. (2017b) Numerical modeling of the 2013 meteorite entry in Lake Chebarkul, Russia, Nat. Hazards Earth Syst. Sci., vol. 17, pp. 671-683.

Ubbink O. (1997) Numerical prediction of two fluid systems with sharp interfaces, PhD, Department of Mechanical Engineering Imperial College of Science, Technology & Medicine.

Weiss R. et al. (2006) Numerical modelling of generation, propagation and run-up of tsunamis caused by oceanic impacts: model strategy and technical solutions, Geophys. J. Int., vol. 167, pp. 77-88.

Non-stationary modeling of extremes in water levels along the Baltic Sea coast

Nadia Kudryavtseva[1], Katri Pindsoo[1] and Tarmo Soomere[1,2]

[1] Department of Cybernetics at Tallinn University of Technology, Akadeemia tee 21, 12618 Tallinn, Estonia (nadia@ioc.ee)
[2] Estonian Academy of Sciences, Tallinn, Estonia

1. Introduction

Most of the scenarios for future climate changes (e.g., Torresan et al., 2012) predict a gradual rise in the frequency and severity of intense storms. The storm impact often causes a constant increase in heights of extreme water levels in many coastal areas. Proper quantification of extreme water levels and their return periods is crucial to establish appropriate mitigation and adaptation strategies for potential coastal erosion, flooding, and associated problems, such as agricultural soil contamination and changes in habitat for fish and plants in countries with extensive low-lying nearshore areas.

The classic approach to extreme water levels and their return periods relies on the analysis of stationary extreme value distributions. However, the current climate change is not a linear process, and in the changing climate and presence of climate variability, the classical stationary approach can significantly underestimate the 50-yr and 100-yr return periods (e.g., Mudersbach and Jensen, 2010), which can lead to significant damage of coastal constructions if not taken into account. In this abstract, we describe an attempt to systematically detect long-term changes (first of all trends) in the location and scale parameters of the standard Generalized Extreme Value (GEV) distribution along the Baltic Sea coast with block maxima approach. For the first time, non-stationary extreme value analyses (e.g., Vanem, 2015) of water levels have been consistently applied in the Baltic Sea region. We also discuss the spatial properties of the found linear trends in the location and scale parameters in the water levels and try to quantify the relation of these trends to changes in the climatic indices.

2. Methods

The analysis relies on simulated sea surface heights obtained from the high-resolution NEMO-Nordic (BaltiX, joined Northern Sea – Baltic Sea model area) model (Hordoir et al., 2013) provided by the Swedish Meteorological and Hydrological Institute. The water level data are from 1979 to 2012 and have a temporal resolution of one hour. The model covers the Baltic Sea with the spatial resolution of ~3.7 km (2 nm) and is extensively validated. The sea surface heights were extracted for 3042 grid cells along the Baltic Sea coastline. An algorithm (implemented in R version 3.4.1) was developed to choose suitable model cells to select grid points along the sandy beaches and rocky coasts.

For each grid cell, the data were extracted (Figure 1a), then annual maxima and annual mean were calculated (Figure 1b). The yearly mean exhibits variability with time in most of the grid cells, reflecting the well-known gradual increase in the average sea level in this water body (Hünicke et al., 2015). However, a mathematically correct application of non-stationary extreme value methods requires the time series to be stationary (in a statistical sense, so that the mean of the time series does not change with time). Also, the focus of the study is on changes and linear trends in the extreme water levels and do not consider the variations in the mean sea level. Therefore, the annual means were subtracted from the yearly maxima values (Figure 1c). In this study, a block maxima approach is used based on maxima for each calendar year, which should follow asymptotically follow the GEV model

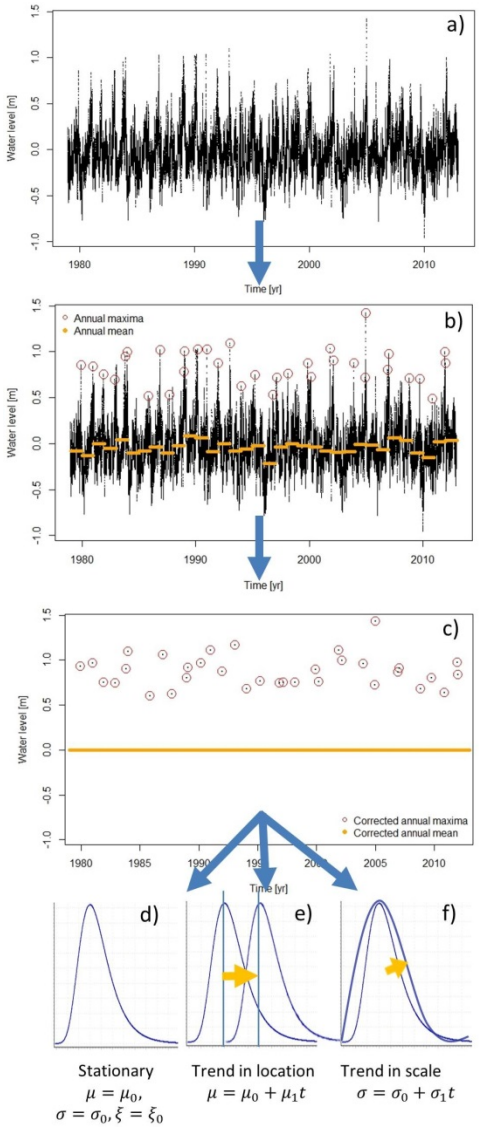

Figure 1. Illustration of the method applied to the water level time series. a) the time series is extracted from the model; b) non-stationarity of the time series is removed subtracting the annual mean from the data; then c) a series of yearly maxima created and d) stationary and (e,f) non-stationary GEV distributions with linear trends in location parameter (e) and scale parameter (f) are fitted to the data.

$$F_{st}(x;\mu,\sigma,\xi) = \exp\left\{-\left[1+\xi\left(\frac{x-\mu}{\sigma}\right)\right]^{-\frac{1}{\xi}}\right\}$$

with a fixed location parameter $\mu \in \mathbb{R}$, scale parameter $\sigma \in \mathbb{R}$, and shape parameter $\xi \in \mathbb{R}$. In a non-stationary case (Figure 1e,f), it is assumed that the location and scale parameters are changing linearly with time:

$\mu = \mu_0 + \mu_1 t,\ \sigma = \sigma_0 + \sigma_1 t$

To test whether the hypothesis of linearly changing with time location or scale parameters is correct, a likelihood ratio test is applied.

3. Results

In Figure 2, for the first time, we show 30-yr return values calculated for the stationary case along the whole Baltic Sea coast. The estimated 30-yr return values qualitatively agree with the previous studies. The highest 30-year return values are in the Gulf of Finland, gradually changing from ~1 m at the entrance to the Gulf of Finland and reaching ~1.7 m close to Saint-Petersburg, Russia, at the eastern bayhead of the gulf. The Gulf of Riga also shows higher return values of 1.2 m compared to the rest of the Baltic Sea.

The analysis showed a significant linear trend (at a 90% significance level) in the location parameter of the relevant GEV in the southern parts of the Baltic Sea along the Pomeranian Bay in Germany and the island of Bornholm (Figure 3). The difference between stationary and non-stationary 30-yr return values reaches 0.15 m, which indicates that the difference can be up to 0.5 m for the 100-yr period, strongly suggesting a very large discrepancy.

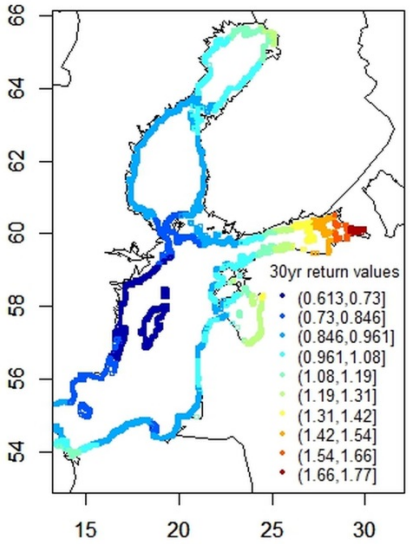

Figure 2. 30-year return values in meters along the Baltic Sea coast

The results show high spatial variations in the presence of linear trends in the location parameter of GEV, suggesting that in case of the Baltic Sea, the changes in the extreme value behavior can have a characteristic spatial scale as small as ~ 100 km. A significant linear trend was found in the location parameter along the Pomeranian Bay, meaning that the GEV distribution is shifting as a whole in this region. In that case, the most severe extremes are getting higher, as well as "medium-range" and "low-range" extremes.

The scale parameter also showed significant linear trends, mainly in the Gulf of Riga (90% s.l.) with the difference between two approaches reaching 0.4 m for 30-yr return values. The linear trend in the scale parameter signifies a different type of processes compared to the linear trends in the location parameter. In case of the location parameter, the linear trends mean that all extremes are getting more intense. However, in case of a linear trend in the scale parameter, the highest extremes are almost the same, but a substantial change is observed in "medium-range" extremes (see Figure 1f).

4. Conclusions

In this study we introduced a non-stationary approach to the extreme value modelling of sea surface height in regional applications (Baltic Sea) and it was shown that it is essential to use the non-stationary extreme value modelling in the presence of climate variability for calculating the return values for engineering applications, whereas using a stationary equivalent will lead to erroneous estimates of the return values (up to 0.15 m difference due to linear trends in the location parameter and up to 0.4 m difference due to linear trends in the scale parameter). We also showed that a very significant linear change in the location parameter is observed along the Pomeranian bay, indicating a strong increase in the most intense extremes, as well as "medium-range" and "low-range" extremes. The Gulf of Riga showed a strong increase in the "medium-range" extreme events.

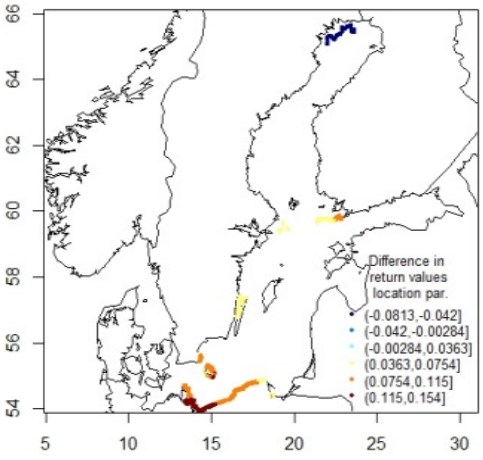

Figure 3. Difference between stationary 30-year return values and non-stationary (assuming linear trend in the location parameter) 30-year return values in meters along the Baltic Sea coast.

Acknowledgements: The research is supported by the Estonian Ministry of Education and Research (Grant IUT33-3) and the ERA-NET+RUS EXOSYSTEM grant ETAG16014.

References

Hordoir R., et al. (2013) Freshwater outflow of the Baltic Sea and transport in the Norwegian current: A statistical correlation analysis based on a numerical experiment, Continental Shelf Research, 64, 1–9.

Hünicke B., et al. (2015) Recent change – sea level and wind waves, in: The BACC II Author Team, Second Assessment of Climate Change for the Baltic Sea Basin. Springer, 155–185.

Mudersbach C., Jensen J. (2010) Nonstationary extreme value analysis of annual maximum water levels for designing coastal structures on the German North Sea coastline, Journal of Flood Risk Management, 3(1), 52–62.

Torresan S., Critto A., Rizzi J., Marcomini A. (2012) Assessment of coastal vulnerability to climate change hazards at the regional scale: the case study of the North Adriatic Sea, Natural Hazards and Earth System Science, 12 (7), 2347–2368.

Vanem E. (2015) Non-stationary extreme value models to account for trends and shifts in the extreme wave climate due to climate change, Applied Ocean Research, 52, 201–211.

Three-dimensional LOGOS simulations of a Chelyabinsk-like meteorite drop into the Baltic Sea

Vadim Kurulin[1] , Andrey Kozelkov[1,2], Rashit Shagaliev[1], Elena Tyatushkina[1,2], Andrey Kurkin[2]

[1] Federal State Unitary Enterprise «Russian Federal Nuclear Center – All-Russian Research Institute of Experimental Physics» (FSUE «RFNC-VNIIEF»), Sarov, Nizhny Novgorod region (kurulin@mail.ru)
[2] Federal State Budgetary Educational Institution of Higher Education «Nizhny Novgorod State Technical University n.a. R.E. Alekseev»

This work has been funded by grants of the President of the Russian Federation for state support of research projects by young doctors of science (MD-4874.2018.9) and leading schools of thought of the Russian Federation (NSh-2685.2018.5), and supported financially by the Russian Foundation for Basic Research (RFFI Project 16-01-00267).

1. Introduction

In 2013, as a result of deceleration in Earth's atmosphere, a meteorite exploded and broke down to fragments not far from the Russian city of Chelyabinsk. This meteorite drop was accompanied by a series of air bursts with shock waves propagating over the territory of the Chelyabinsk region. Small fragments of the meteorite fell onto the territory of the region. It is the largest celestial body to hit Earth after the 1908 Tunguska meteorite. Popova et al. (2013), De Groot-Hedlin (2014), and Kozelkov et al. (2017c) give the following estimated characteristics of the meteorite: diameter - 16-19 m, velocity - 150-300 m/s, entry angle - 20°.

The paper discusses simulations of a similar meteorite drop into the Baltic Sea. The simulations were done based on three-dimensional Navier-Stokes equations. The report describes the physical and mathematical model and the numerical simulation technology used to simulate such events. Numerical simulations are presented for a number of cases with variation of meteorite velocity and diameter.

2. Mathematical model and numerical experiments

The most complete system of equations that allows incorporating specific modeling features of waves caused by a meteorite drop is the Navier-Stokes system, Ubbink (1997). It enables end-to-end modeling of all stages of the process: entry of a solid object into water, evolution of the wave pattern, and wave run-up on a beach. The technology also naturally accounts for the bottom topography of any water area configuration.

Applicability of this approach is currently limited because it requires using large-size three-dimensional discrete models and is highly demanding to the stability of high-velocity body/water impact and large-distance small-amplitude wave propagation simulations. However, advanced computational technologies currently used in engineering studies of high-tech products, Kozelkov et al. (2016), make it possible to bring simulations as applied to the problem of tsunami to a qualitatively new level.

To simulate a meteorite drop into the Baltic Sea followed by propagation and run-up of waves, this work combines the Navier-Stokes equations with the Volume of Fluid (VOF) method, Ubbink (1997). The numerical algorithm that we use is based on a modification of the method SIMPLE, Kozelkov et al. (2002), with a fully implicit integration scheme, Kozelkov et al. (2018). Motion of a solid body is modeled using the overlapping-grids method, Wang (2000).

The technology has been implemented in the Russian software package LOGOS intended for multi-physics simulations of convective heat-and-mass transfer, aerodynamics and hydrodynamics on parallel computers, Kozelkov et al. (2016). LOGOS is successfully used for various hydrodynamic simulations, including modeling of tsunamis, Kozelkov et al. (2017a, 2017b).

The paper reports the results of simulations of a meteorite drop into the Baltic Sea for various meteorite parameters. Estimates and amplitude characteristics of tsunami waves are presented for various scenarios of their run-up on different beach areas as a result of a meteorite drop in both northern and southern parts of the Baltic Sea. The diameter of a meteorite, the drop of which into the Baltic Sea can be potentially hazardous, is estimated.

References

De Groot-Hedlin C., Hedlin M.A.H. (2014) Infrasound detection of the Chelyabinsk meteorite the US Array, Earth and Planetary Science Letters, Vol 402, pp. 337-345

Ferziger J.H. et al. (2002) Computational Method for Fluid Dynamics, Springer-Verlag, New York, 2002, 423 p.

Kozelkov A. S. et al. (2016) Investigation of supercomputer capabilities for the scalable numerical simulation of computational fluid dynamics problems in industrial applications, vol. 56, № 8, pp. 1506-1516.

Kozelkov A.S. et al. (2017a) Three dimensional numerical simulation of tsunami waves based on the Navier-Stokes equations, Science of Tsunami Hazards, Journal of Tsunami Society International, vol. 36, №4, pp.183-196.

Kozelkov A.S. et al. (2017b) Numerical modeling of the 2013 meteorite entry in Lake Chebarkul, Russia, Nat. Hazards Earth Syst. Sci., vol. 17, pp. 671-683.

Kozelkov A.S., Kurkin A.A., Pelinovsky E.N., Kurulin V.V., Tyatyushkina E.S., Numerical modeling of the 2013 meteorite entry in Lake Chebarkul, Russia // Nat. Hazards Earth Syst. Sci., 2017c, v. 17, p. 671-683.

Kozelkov A. S. et al. (2018) An implicit algorithm of solving Navier–Stokes equations to simulate flows in anisotropic porous media, Computers and Fluids, vol. 160, pp. 164-174.

Popova O.P. et al. (2013) Chelyabinsk Airburst, Damage Assessment, Meteorite Recovery, and Characterization, Science, Vol 342, pp. 1069¬1073

Ubbink O. (1997) Numerical prediction of two fluid systems with sharp interfaces, PhD, Department of Mechanical Engineering Imperial College of Science, Technology & Medicine

Wang, Z.J. et al. (2000) A Fully Automated Chimera Methodology for Multiple Moving Body Problems // International Journal for Numerical Methods in Fluids, vol. 33, № 7, pp. 919-938.

The Connection of Storms and Significant Wave Heights in the Baltic Sea with Indices of Large-scale Atmospheric Circulation (NAO, AO, SCAND)

Alisa Medvedeva[1], Stanislav Myslenkov[1,2] and Viktor Arkhipkin[2]

[1] P.P. Shirshov Institute of Oceanology, Russian Academy of Sciences, Moscow, Russian Federation (alisa.bannikova@gmail.com)

[2]Lomonosov Moscow State University, Moscow, Russian Federation

1. Introduction

Wind waves are important component of climate system and study of their interannual variability helps to understand current climate changes and to assess wave impact in the future. The wave conditions in the Baltic Sea were investigated in several studies in Kriezi (2008); Medvedeva et al. (2015); Sommere (2008); Zaitseva-Pärnaste (2009). Regional trends are influenced by large-scale interannual climate oscillations like the North Atlantic Oscillation (NAO) and Pacific Decadal Oscillation. There are limited number of studies devoted to storm number, their interannual variability and their connection with global atmosphere circulation in the Baltic Sea, so these subject still remains challenging.

2. Data and Methods

In order to estimate decadal and interannual changes of the wind wave fields the SWAN, short from Simulating WAves Nearshore, Booij et al. (1999) numerical wave model was used. This model is a third-generation spectral wind wave model developed by Delft University of Technology. It is widely applied for reconstruction of wave fields and such parameters as significant wave heights (H_s), periods, lengths, swell heights and energy transport with different spatial and time resolutions by solving the energy balance equation in spectral dimensions. These parameters in this paper were reconstructed for the period from 1979 to 2015.

We used 10-m wind from Climate Forecast System Reanalysis from the National Centers for Environmental Prediction (NCEP/CFSR) with a spatial resolution 0.3°×0.3° and a time step 1 hour (Saha et. al. 2014) for the period from 1979 to 2010 and its extension NCEP/CFSv2 with a spatial resolution ~ 0.205×0.204 and a time step of 1 hour. The accuracy of the obtained wave parameters is high and it has been estimated by using measurements of the wave parameters (Medvedeva et al. 2016).

Calculations have been performed using rectangular grid with a spatial resolution 0.05°×0.05°. The grid was created on the basis of the General Bathymetric Chart of the Oceans (GEBCO).

All situations when H_s exceeded the chosen threshold (from 2 to 5 meters) were considered as a storm. The number of storm situations with different *Hs* was calculated for every year from 1979 to 2015. For example if H_s in one grid node is higher than 4 meters then it was considered as the start of a storm with criteria $H_s \geq 4$ m. An event is considered to be finished when the H_s in all nodes became less than the chosen threshold.

3. Storm number and trends

For the Baltic Sea in 37 years the number of storms with $Hs \geq 2$ m amounts to 2559, approximately 70 per year, with criteria 3 m – 1285, 4 m – 1107, 5 m – 649. These results indicate that about a half of all storm situations has a significant wave height of more than three meters.

Typical periods of intensification and relaxation of wind waves are 10–12 years for the Baltic Sea, Soomere et al. (2008). According to obtained storm number, there is a 10-year period of intensification / weakening of the storm activity. For various parts of the Baltic Sea, there is a discrepancy between the trends of the ten-year increase or decrease. Notably, that the rapid changes of intensification or weakening of wave activity can happen during one decade, Soomere et al. (2008); Kriezi and Broman (2008).

There is no significant tendency in storm number in the Baltic Sea with $Hs \geq 2$ m. However, for criteria $Hs \geq 4$ m we found statistically significant negative trend. For 37 years (1979–2015) the maximum computed significant wave height amounts to 8.5 m, wave length – 130 m, wave period – 10 s.

For comparison, Medvedeva et al. (2015) showed a similar trend, but the simulations were based upon other reanalysis data NCEP/NCAR. They had a longer time coverage from 1948 to 2010 but less accuracy of the modeled results, and errors are twice as high. As for the connection between the global atmosphere circulation and the number of storms the maximum $R = 0.49$ was identified for AO and storms with $Hs \geq 3$ m. To compare with previous version of the reanalysis (NCAR) the coefficient *R* with AO amounts to 0.46. With SCAND, the correlation is negative as for H_s (from -0.59 to -0.32).

4. Connections of storm number with large-scale atmosphere indices

In order to study the connection with the global atmosphere circulation, 3 indices North-Atlantic Oscillation (NAO), Arctic Oscillation (AO), Scandinavian Index (SCAND) have been considered (http://www.cpc.ncep.noaa.gov/ 2017, Barnston and Livezey 1987). The correlation coefficient *(R)* was calculated between these indices and storm number.

For the Baltic Sea $R = 0.49$ for the total amount of the storms with $Hs \geq 3$ m and indices was obtained only with the AO and for events with $Hs \geq 4$ m $R = 0.45$; and $R \leq -0.5$ – with SCAND. With NAO the connection is not obvious. As for SCAND pattern it is worth noting that *R* is negative about -0.59 for $Hs \geq 2$ m and -0.52 for $Hs \geq 4$ m and -0.47 with $Hs \geq 3$ m. It means that the increase in storm number over the Baltic Sea corresponds to negative phase of

Scandinavian pattern associated with negative height anomalies in this region.

5. The connections with indices estimated for 5 different areas of the Baltic

The entire Baltic Sea was divided into 5 areas in which trends of max H_s and storm number were estimated: I – the Southeastern Baltic (in rectangular from Slupsk to Liepaja), II – the Gulf of Bothnia (including the Bothnian Bay and the Bothnian Sea), III – the Gulf of Finland, IV – the Gulf of Riga, V – the Baltic Proper. As maximum H_s we considered maximum value registered in this area for selected period (for example maximum value of H_s in one node in the Gulf of Finland in January 1990).

The field variability connected to the NAO is most pronounced in the cold season. If we take into account only the period from December to March (with $R \geq 0.5$), the connection of max H_s is more significant with AO, slightly less significant with NAO and negative (-0.4; -0.5) with SCAND (Table 1).

Table 1. Correlation coefficient between max H_s and indices of atmospheric circulation for different parts of the Baltic Sea.

Month	1	2	3	12	Area
NAO	0.47	0.29	**0.57**	0.59	Southeastern Baltic
	0.18	0.53	0.55	0.43	Gulf of Bothnia
	0.36	**0.54**	0.55	**0.70**	Gulf of Finland
	0.44	0.49	0.49	0.65	Gulf of Riga
	0.52	0.38	**0.57**	0.60	Baltic Proper
AO	**0.64**	0.54	0.51	0.44	Southeastern Baltic
	0.17	0.49	0.47	0.49	Gulf of Bothnia
	0.57	0.55	**0.58**	0.56	Gulf of Finland
	0.50	**0.57**	0.55	0.50	Gulf of Riga
	0.56	0.55	0.50	**0.58**	Baltic Proper
SCAND	**-0.67**	**-0.65**	-0.40	-0.37	Southeastern Baltic
	-0.19	-0.45	-0.21	-0.31	Gulf of Bothnia
	-0.41	-0.57	-0.31	-0.28	Gulf of Finland
	-0.42	-0.46	-0.39	-0.27	Gulf of Riga
	-0.60	-0.58	-0.35	-0.35	Baltic Proper

We observe a positive high correlation coefficient of ≥ 0.5 with the NAO index for five months: January, February, March and April, and for the Baltic Proper also for November. The highest value of R = 0.7 was observed for December in the Gulf of Finland. Every increase of the H_s in the Gulf of Finland corresponds to the positive phase of the NAO and AO indices. Negative NAO phase in most cases coincides with the *Hs* decrease and positive NAO phase with H_s increase. The AO index $R \geq 0.5$ was identified for the winter period (plus April), the maximum value equal 0.64 for the Southeastern part of the Baltic Sea for January.

All coefficients R with the SCAND are negative. Notably, for January, February, April and September with $R \leq -0.5$, i.e. the H_s increases with the negative phase of the index. The highest values of R -0.67, -0.65 are found in the Southeastern part of the Baltic Sea.

Thus, with such complex configuration of the Baltic Sea, the NAO and AO indices have the most influence on the Gulf of Finland and secondly on the Baltic Proper. The lowest R coefficients were observed for the Gulf of Bothnia. It is worth noting, that in the last decade from 2005 to 2015 the storm number with $Hs \geq 2$, 3, 4 m increases in the entrance of the gulf. In addition, it propagates deeper to the east, so it reflects the displacement of the trajectories of cyclones, which have moved 5° to the north. It changes the length of the wave fetch and promotes wave penetration into the Gulf of Finland.

As for separate parts of the sea, the highest R is noted in the Baltic Proper with AO for $Hs \geq 3$ m and R = 0.62. For storm events with $Hs \geq 4$ m the situation is the same: the correlation for the Baltic Proper is stronger.

6. Conclusions

The numerical model simulations of storm activity in the Baltic Sea were analyzed. From 1979 to 2015 the number of storms with different *Hs* threshold were calculated. In the Baltic the small-scale increase of the number of storms was found in 1992−1994 years. It corresponds to the high positive NAO and AO and significant negative SCAND values. On average, the connection with global atmosphere circulation is stronger ($R \geq 0.5$) for the Baltic Sea. The connection with SCAND index is clearer than with NAO and AO. Notably, that for stronger storms with $Hs \geq 4$ m for the Baltic Sea significant negative linear trend was revealed.

This research was performed in the framework of the state assignment of FASO Russia (theme No. 0149-2018-0015), supported in part by RSF (project No.14-50-00095).

References

Booij, N., Ris, R. and Holthuijsen, L. (1999). A Third-Generation Wave Model for Coastal Regions. 1. Model Description and Validation. *Journal of geophysical research: Oceans,* 104(C4), pp.7649-7666.

Kriezi, E., and Broman, B. (2008, May). Past and future wave climate in the Baltic Sea produced by the SWAN model with forcing from the regional climate model RCA of the Rossby Centre. In *US/EU-Baltic International Symposium, 2008 IEEE/OES* , pp. 1-7.

Medvedeva, A., Arkhipkin, V., Myslenkov, S. and Zilitinkevich, S. (2015). Volnovoj klimat Baltijskogo morya na osnove rezul'tatov, poluchennyh s pomoshch'yu spektral'noj modeli SWAN [Wave climate of the Baltic Sea following the results of the SWAN spectral model application]. *Moscow University Bulletin. Series 5. Geography* (1), pp.12-22 (in Russian with English summary).

Medvedeva, A., Myslenkov, S., Medvedev, I., Arkhipkin, V., Krechik, V. and Dobrolyubov, S. (2016). Modelirovanie vetrovogo volneniya v Baltijskom more na pryamougol'noj i nestrukturnoj setkah na osnove reanaliza NCEP/CFSR [Numerical Modeling of the Wind Waves in the Baltic Sea using the Rectangular and Unstructured Grids and the Reanalysis NCEP/CFSR], *Proceedings of the Hydrometeorological Research Center of the Russian Federation* (362), pp. 37-54 (in Russian with English summary).

Saha, S. et al. (2014). The NCEP Climate Forecast System Version 2. *J. Climate*. 27, pp.2185-2208. DOI: 10.1175/JCLI-D-12-00823.1.

Soomere, T., Behrens, A., Tuomi, L. and Nielsen, J. (2008). Wave conditions in the Baltic Proper and in the Gulf of Finland during windstorm Gudrun. *Natural Hazards & Earth System Sci*., 8(1), pp.37-46.

Zaitseva-Pärnaste, I., Suursaar, Ü., Kullas, T. et al. (2009). Seasonal and long-term variations of wave conditions in the northern Baltic Sea. *J. Coast. Res*. SI(56) pp.277-281.

A comparison of observed extreme water levels at the North- and Baltic Sea with extremes derived from a regionally coupled ocean-atmospheric climate model (MPI-OM) and their impact on dewatering potential at Kiel-Canal

Jens Möller[1] and Birger Tinz[2]

[1] Federal Maritime and Hydrographic Agency (BSH), Hamburg, Germany (jens.moeller@bsh.de)
[2] The German Meteorological Service, Hamburg, Germany

1. Introduction

As a consequence of climate change atmospheric and oceanographic extremes and their potential impacts on coastal regions are of growing concern for governmental authorities responsible for the transportation infrastructure. Highest risks for shipping as well as for rail and road traffic originate from combined effects of extremes of storm surges and heavy rainfall which sometimes lead to insufficient dewatering of inland waterways. The German Ministry of Transport and digital Infrastructure therefore has tasked its Network of Experts to investigate the possible evolutions of extreme threats for low lands and especially for Kiel Canal, which is an important shortcut for shipping between the North and Baltic Seas. In this study we present results of a comparison of an Extreme Value Analysis (EVA, see as an example Fig. 1) carried out on gauge observations and values derived from a coupled Regional Ocean-Atmosphere Climate Model (MPI-OM). We also demonstrate the change of common appearance of high water levels with high precipitation events in the future with the model.

2. Extreme water levels

High water levels at the coasts of the North and Baltic Seas are one of the most important hazards which increase the risk of flooding of the low-lying land and prevent such areas from an adequate dewatering. In this study changes in the intensity (magnitude of the extremes) and duration of extreme water levels (above a selected threshold) are investigated for several gauge stations with data partly reaching back to 1843. Different methods are used for the extreme value statistics, (1) a stationary general Pareto distribution (GPD) model as well as (2) an instationary statistical model for better reproduction of the impact of climate change (see Coles, 2002). Most gauge stations show an increase of the mean water level of about 1-2 mm/year, with a stronger increase of the highest water levels and a decrease (or lower increase) of the lowest water levels. The duration of possible dewatering times for the Kiel-Canal as well as the dewatering potential at Kiel-Canal (see. Fig. 2) were analysed.

3. The ocean-atmospheric climate Model (MPI-OM)

The results for the historical gauge station observations are compared to the statistics of modelled water levels from the coupled atmosphere-ocean climate model MPI- OM for the time interval from 1951 to 2000. We demonstrate that for high as well as for low water levels the observations and MPI-OM results are in adequate agreement. Also we investigated the change in common appearances of water levels too high to dewatering with high precipitation events. While the future change in these common appearances are small (+5%) for only one event (able to blocking the dewatering), these changes are much larger for consecutively events, blocking dewatering up to 72 hours.

Additionally, our study demonstrated, that the future increasing of the common appearances of extreme water levels with high precipitation events is mainly caused by the sea level rise.

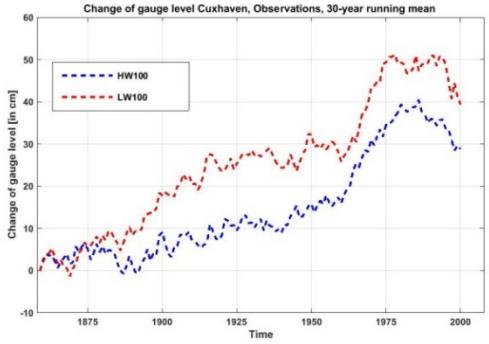

Figure 1. The change of the expected centennial gauge levels for High (dashed blue) and Low water (dashed red), calculated with Gumbel distribution, for observed gauge data of about 30 years. For better comparability, all data are set to zero for the time period 1843 to 1872. Data displayed as running mean about 30 years (exemplary, the value at time 2000 means the running mean from 1985 to 2014).

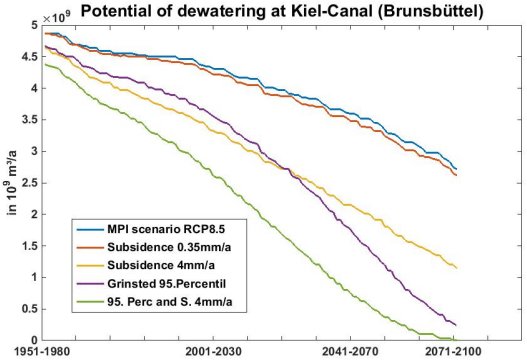

Figure 2. Shown is the dewatering potential (the maximum possible dewatering) at Kiel-Canal for different scenarios. Blue line estimated with the sea level rise (SLR), calculated from MPI-OM under scenario RCP8.5, red and yellow line the same as blue with additionally land subsidence of 0.35mm/year (red) respectively 4mm/year (yellow). Purple line displays the high end scenario from Grinsted (174 cm SLR towards the end of 21th century) and green line the same as purple, but with additionally land subsidence of 4mm/year.

References

Coles, S. (2011), An Introduction to Statistical Modeling of Extreme Values, Springer Series in Statistic.

Temporal development of residence times and the power impact to the German Baltic coastline induced by storm surge events

Justus Patzke[1], Jessica Kelln [2], Doerte Salecker [1], Peter Froehle [1]

[1] Institute of River and Coastal Engineering, Hamburg University of Technology, Germany (Justus.Patzke@tuhh.de)
[2] Research Institute for Water and Environment, University of Siegen, Germany

1. Introduction

Within the research project AMSeL Baltic Sea a database was generated including water level time series from 185 stations along the Baltic sea coasts for time spans from 2016 down to 1774 (Kelln et al. 2017). For historical time series before 1900 the temporal resolution varies (depending on the station) between monthly and yearly values. For younger time series high resolution data, e.g. hourly values, have been acquired where available. Within this paper the focus lies in the analysis of hourly datasets from six different stations along the German Baltic coastline: Flensburg, Kiel-Holtenau, Travemuende, Warnemuende, Wismar and Sassnitz.

The impact of storm surges is often determined by the absolute or relative height of peak water level. Beside the maximum water level another issue which is causing damage to flood protection systems is the retention time of storm event water levels. While the peak water level mostly lasts only for short timespans, lower water levels introducing the storm events have a much longer residence time. Hence the resulting power impact to the coast and flood protection measures might be higher within moderate storm surge levels. This paper aims to give an overview of the past and current status of the residence times and their resulting power impact to the coast.

2. Data & Methods

The chosen time series mentioned above cover an overlapping time span from 1957 to 2016. A plausibility validation procedure has been developed within the research project AMSeL Baltic Sea to find statistical significant deviations in high frequency water level data. This method has been applied to all of the used time series. Inaccuracies have been excluded from this analysis by replacing them by error values. Additionally all years have been excluded from the analysis when there was missing data for more than 25 % of the annual time span. All water level measurements have been reduced to the German height system NHN. The stations have been analyzed to determine residence times based on water level height steps of ΔH = 0.25 cm. Because hourly values do not estimate precise enough durations of the residence of water levels different calculation methods have been tested. A comparison has been made between the calculated residence times of minutely, hourly, cubic-and as well linear interpolated hourly data from station Travemuende within the years 2015 and 2016 to determine the best fit for further analyses of historical data where only hourly values are available.

Further on a study has been carried out to evaluate annual residence times for the whole time span with spline interpolated data to a minutely resolution. For every year the residence times within the classes between the minimum and the maximum values are given and by regression the linear trends of residence times for each class are computed and tested for significance.

The developed matlab code for these analysis is adoptable for the whole database requiring hourly time series as input format and additionally the chosen class width, a selection whether MSL reduction by a 19yr-moving mean should be taken into account and a selection of the interpolation method (none, linear or cubic spline). Reducing the time series with a moving mean consequently shortens the covered time span by the chosen window length.

Residence times of high water levels are a major factor for destruction consequences during storm events. To estimate potential damages to the coast and corresponding protection measures, the power impact induced by waves has been estimated using an approach given by Führböter (1982) and adopted by Meinke (1998). According to linear wave-theory (Airy-Laplace) the sum of potential and kinetic power of a travelling wave (E) underlies the formula (1).

(1) $E = \frac{1}{8}\rho * g * H^2 * L$

Where $\boldsymbol{\rho}$ is density of the water [t/m³], g is gravity [m/s²], H is wave height [m] and L corresponds to the wave-length [m]. Assuming this to be true until the wave's breakpoint and no reflection of waves occurs, the power output N during a wave period can be described by dividing wave-length (L) with the wave-period (T).

L/T can be written also as wave velocity c which according to Seifert (1973) leads to H proportional to depth d. Finally, with applying $g = 9{,}81\frac{m}{s^2}$ and $\rho = 1{,}028\ \frac{t}{m^3}$ (seawater) the maximum power output of a wave at depth (d) on a width of 1m equals formula (2) (Führböter (1982)).

(2) $N\ [\frac{kW}{m}] = 3{,}914 * d^{2{,}5}$

Additional assumptions made are a salinity of 15 % and a water temperature at 5 °C (Meinke 1998). Class dependent power impact is then resulting from the product of the power output of each wave and the residence time within each class.

3. Results

The results of comparing input data of different resolutions to compute residence times indicate that spline-functions can reduce the averaged relative error (residence $\text{time}_{\text{spline minutes}}$ / residence $\text{time}_{\text{raw minutes}}$) compared to hourly input data by 10 %. Hence a cubic spline interpolation has been used for analyzing residence times in historical time series.

Within this abstract the results of Travemuende station are shown exemplary. Figure 1 summarizes the calculated residence times in positive classes with given lower boundaries from 0.75 m NHN up to 2.00 m NHN.

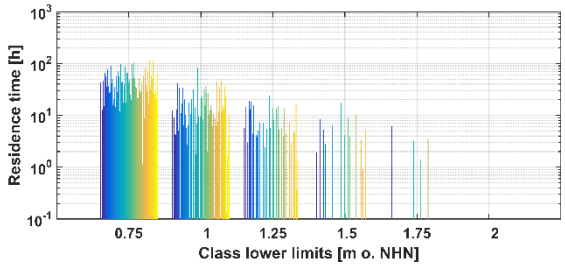

Figure 1: Residence times sorted by classes within the timespan of the series for station Travemuende (1950-2016)

For every year a bar is fitted into the class. After examining significance in the classes by applying the Mann-Kendall trend test it can be stated that no trend above a significance level of $\alpha = 5$ % could be observed. Anyway, it is shown that the total residence times within the classes decrease almost linearly within a logarithmic scale by increasing class boundaries. Consequently the occurrence of events with residence times decreases with increased class boundaries as well.

Figure 2 states the calculated power impact to the coast with given mean wave heights according to the assumptions made in chapter 2.

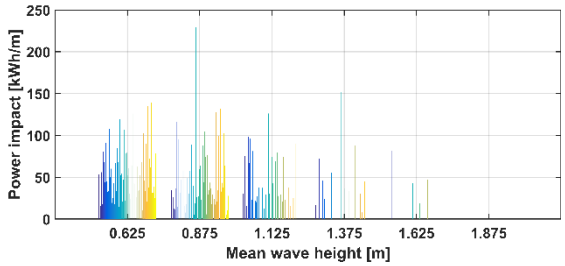

Figure 2: Power impact by storm surges within the timespan of the series for station Travemuende (1949-2016)

The power impact is computed for every year of the given time span (1950-2016) within each class. It can be seen that induced damages on the coast by long lasting moderate storm surges can be way higher than from very rare extreme events of a short duration.

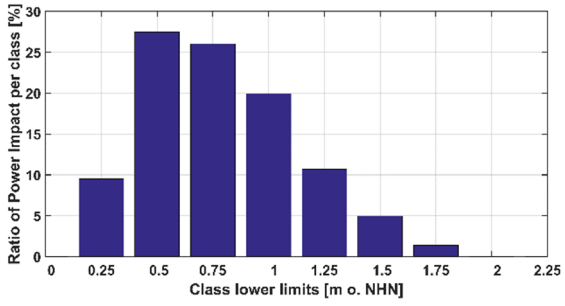

Figure 3: Ratio if power impact per class [%] for station Travemuende, 1950-2016

In total the input from classes in lower water levels induce more absolute impact and a more often occurring impact than higher water levels. Calculated trends within the residence-time-classes shown here indicate no significant trends applying the Mann-Kendall-Test.

Summarizing, more than 50 % of the total impact of water levels above 0. 5 m NHN is induced by classes lower 1 m NHN (27% and 26%) while only 6 % is induced by heavy storm surges above 1.5 m NHN, see Figure 3. This behavior is similar for the other analyzed stations.

4. Conclusions & Outlook

Due to onward trends of a changing climate leading to a mean sea level rise the results of this investigation should be noticed for future coastal protection planning. Especially in the range of moderate storm surges it was found that the power impact tends to increase. Nevertheless we evaluated no significant trends indicating an increase in the power impact for positive water level classes above 0.5 m NHN. While the method of using cubic equations to interpolate hourly data was proven to be accurate by Jensen et al. (2010) for water level time series from stations at the North Sea coast, we could successfully assign this method to datasets from the Baltic Sea.

The calculated residence times show the influence of sea level rise, which leads to longer residence times in positive classes close to mean sea level (<0.5 m NHN). Moderate storm surges with water levels between 0.75 and 1.5 m NHN could be assigned to have the most impact on the coast. Assuming the climate change to hold on and following the findings of Sztobryn et al. (2005) that storm surges almost occur twice as often in the end of the 20th century compared to the middle period an increase in residence times above the actual 0,5 m NHN water level can be expected. Further analysis is going to focus on differences between the stations along the whole Baltic Sea regarding residence times and power impact.

Acknowledgements

The authors would like to thank the BMBF for funding the research project AMSeL Baltic Sea. As well we're grateful for provided data by the German federal institutions BSH Rostock, WSA Lübeck and WSA Stralsund.

References

Führböter, Alfred (1982): Über Verweilzeiten und Wellenenergien bei Sturmfluten. In: Rudolf Schwab (Hg.): Jahrbuch der Hafenbautechnischen Gesellschaft, Bd. 38. Berlin: Springer-Verlag (38), S. 269–282.

Jensen, Jürgen; Dr.-Ing. Thorsten Frank; Dipl.-Ing. Thomas Wahl; Dipl.-Ing. Sönke Dangendorf (2010): Analyse von hochaufgelösten Tidewasserständen und Ermittlung des MSL an der deutschen Nordseeküste. AMSeL_KFKI_Bericht Abschlussbericht. Projektbericht. Universität Siegen, Siegen. Forschungsinstitut Wasser und Umwelt.

Kelln, Jessica; Dangendorf, Sönkte; Calafat, Francisco; Patzke, Justus; Jensen, Jürgen (2017): A novel tide gauge dataset for the Balitc sea - Part 1: Spatial features and temporal variability of the seasonal sea level cycle. Hg. v. European Geoscience Union. Wien.

Meinke, Insa (1998): Das Sturmflutgeschehen in der südwestlichen Ostsee - dargestellt am Beispiel des Pegels Warnemünde. Diplomarbeit. Philipps Universität, Marburg. Fachbereich Geographie.

Seifert, Winfried (1973): Über den Seegang in Flachwassergebieten. Sonderdruck der Institutsmitteilungen der TU Braunschweig. Braunschweig: TU Braunschweig.

Sztobryn, Marzenna; Stigge, Hans-Joachim; Wielbińska, Danuta; Weidig, Bärbel; Stanisławczyk, Ida; Kańska, Alicja et al. (2005): Storm Surges in the Southern Baltic Sea (Western and Central Parts). Hamburg Rostock: BSH (Berichte des Bundesamtes für Seeschifffahrt und Hydrographie, 39). In: BSH Berichte.

Wave hindcast statistics in the Gulf of Bothnia

Jani Särkkä[1], Laura Tuomi[1], Riikka Marjamaa[1], Robinson Hordoir[2] and Kari Eilola[2]

[1] Finnish Meteorological Institute, Helsinki, Finland (Jani.Sarkka@fmi.fi)

[2] Swedish Meteorological and Hydrological Institute, Norrköping, Sweden

1. Introduction

Wave models are efficient tools in simulating past and future wave conditions. The quality of the Baltic Sea wave models has been shown to be good in open sea areas and even near coastal areas and archipelagos, if measures are taken to account for unresolved islands at the used resolution. Earlier studies have also shown that in the open sea areas, the quality of the wind forcing is the main factor in the accuracy of the wave model results.

The operational wave forecasts in the Baltic Sea utilize wind forcing from high-resolution numerical weather prediction systems. Many of the present wave hindcasts and reanalyses are based on using wind fields collected from operational forecasting systems. They have been shown to give an accurate description of the Baltic Sea wave conditions, but the heterogeneous quality of the wind fields (due to the changes in the forecast system), and the temporal extent of the hindcasts (numerical weather prediction systems with good quality and resolution are available only starting from c. 2000 onwards) have been discussed as limitations of these hindcasts.

2. Methods

For a long time, the resolution and quality of the atmospheric reanalyses has limited their use in the Baltic Sea. Nowadays, there are downscaled reanalysis products, such as the RCA4-ERA-Interim produced by SMHI, that give us possibility to do wave hindcasts using wind forcing with adequate horizontal temporal resolution. Furthermore, the seasonal ice conditions, that are important for the wave reanalysis, can be calculated with an ice-ocean model using the same atmospheric forcing, thus providing a compatible forcing dataset.

Within the SmartSea project (http://smartsea.fmi.fi/), we perform wave hindcast simulation 1979-2013 for Baltic Sea in 1 nmi resolution using WAM model. We use wind forcing from downscaled RCA4-ERA-Interim and ice concentrations from SMHI's Nemo-Nordic model of Baltic and North Seas. Wave buoy data is used to evaluate the quality of the model results. The wave hindcast is used to assess the extreme wave conditions in the Gulf of Bothnia and to calculate the statistics of significant wave heights. In the future, we plan to do scenario simulations to estimate the future wave conditions in the Gulf

Distribution of droughts and dry winds in the Black Sea Steppe province under current climate conditions

Inna Semenova[1], Mariya Slizhe[1]

[1] Odessa State Environmental University, Odessa, Ukraine (innas.od@gmail.com)

1. Introduction

The territory of Ukraine almost every year is exposed the droughts of different intensity and duration. Meteorological and seasonal (or agroclimatic) droughts are widespread.

The Ukrainian steppe encompasses most of western segment of the Eurasian steppe that is known as the Black Sea (or Pontic) steppe province. This territory belongs to driest areas of Ukraine.

Drought is a normal, recurring feature of climate. It occurs in high and low rainfall areas in virtually all climatic regimes. Generally, a natural drought is defined as a deviation of hydro-meteorological parameters (e.g., precipitation, soil moisture, river flow, groundwater level etc.) from the climatic condition. A shortage of weather-related water supply is usually caused by a deviation of precipitation, soil moisture and river discharge that constitute meteorological, agricultural and hydrological droughts, respectively. Socio-economic drought is defined as a lack of weather-related water supply to meet the normal water demands for human activities. In some cases, drought may be accompanied by dry and hot winds that cause additional damage.

There is still no universally method to describe all drought related processes due to complexity of drought phenomena. The main approach to drought assessment is using of different drought indices such as hydro-meteorological non-standardized drought indices (e.g. HTC, PDSI) and more flexible and all-applicable standardized indices (e.g. SPI, SPEI) as well as the satellite-based indices (VCI, WCI) (Handbook (2016)).

The aim of study is to define the features of repeatability the droughts and dry winds in changing climate conditions in southern areas of Ukraine, which belong to the Black Sea steppe province.

2. Methods and materials

This study evaluates a spatial structure of droughts and their dynamics during April-August of 1995-2015. An assessment based on the Standardized Precipitation-Evapotranspiration Index (SPEI), which time series were obtained from the Global 0.5° gridded SPEI database (http://spei.csic.es/database.html). The SPEI was introduced by Vicente-Serrano et al. (2010) and it based on monthly precipitation data and potential evapotranspiration data, which depends on air temperature. A temperature is especially important in the warm season and under the global warming process, when evapotranspiration increases.

The SPEI may be defined for various time intervals. Short time intervals (from one to few months) shows short- and medium-range conditions of moistening and provides seasonal assessment of precipitation, therefore these scales are widely used for detecting meteorological and agroclimatic droughts.

A drought event for selected time scale is defined as a period, in which the SPEI is continuously negative. Drought intensity is defined for values of the SPEI with the following categories: values from 0 to -0.99 correspond to mild drought; from -1.00 to -1.49 correspond to moderate drought; from -1.50 to -1.99 correspond to severe drought; values less than -2.00 characterize an extreme drought.

In our study six months period was applied for detections of growing period drought (from April to August).

According to criteria of the national meteoservice in Ukraine, dry wind is fix, if at least in one term of observation, values of the meteorological parameters simultaneously amounts: air temperature 25°C and higher, wind speed at 10 m height is 5 m/s and more, and relative air humidity is 30% or lower (Climate of Ukraine (2003)).

An assessment of the spatiotemporal distribution of dry winds was done using the data of station observations for air temperature, humidity and wind at the 5 meteorological stations of Ukraine, located in the coastal zone of the Black and Azov Seas, from April to August of 1995-2015.

3. Results and discussion

The climate in the Northern Black Sea region has undergone significant changes over relatively short periods at the end of the 20th century - beginning of the 21st century (Semenova (2015)). At the end of the 20th century the winter temperatures were close to climate conditions. But in the first decade of the 21st century positive temperature anomalies (+0.2, +0.4^{o}C) were observed. The end of the 20th century showed little negative anomalies of summer temperatures. At the first decade of the 21st century are observed strong positive temperature anomalies (up to +1.5^{o}C). It is means that winters and especially summers became warmer.

Summer precipitation in the Black Sea Steppe province was close to climatic rates at the end of the 20th century. But at the first decade of the 21st century there was a strong disadvantage of precipitations, especially in Western Steppe. So, the current climate characterizes by hot and dry summer conditions, which often lead to drought.

During 1995-2015 the drought episodes in the Black Sea Steppe province were observed more than one half of period. The mild drought occurred 11 times, moderate drought was observed in 3 years, and severe drought appeared once. Extreme drought covered the steppe zone in growing season 2007 (Fig. 1). The linear trend of the SPEI values shows that drought prevailed in the Ukrainian Steppe every year after 2007, which correspond to observed negative anomalies of

precipitation and positive anomalies of temperature at this period.

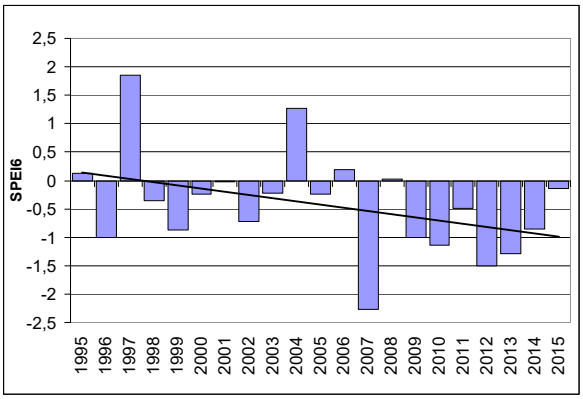

Figure 1. Time series of the SPEI at 6 months time scale (April-August) during 1995-2015 (with linear trend).

An analysis of dry winds' frequency shown that an increase of the number of days with dry winds was observed in 1996, 2000-2003, 2007, 2012-2013 (Fig. 2). As seen, in these years the largest negative values of the index SPEI were noted. In these years, as shown by Cherenkova et al. (2015), over the East European Plain during vegetation period an anticyclonic pressure field was dominated accompanied by blocking processes, which led to the formation of extensive droughts.

In 1997 and 2004, at all stations were observed a lowest number of days with dry wind, at the same time the index SPEI were reaching the highest positive values.

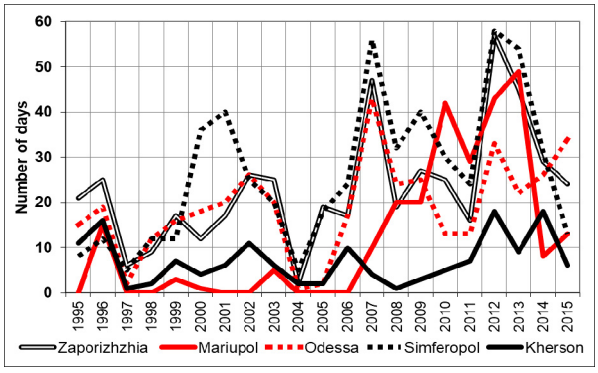

Figure 2. Dynamics of the total number of days with dry wind during April-August of 1995-2015 at the stations located in the Black Sea Steppe province.

Analysis of the repeatability of dry winds by months showed that sum of days increase from April to August (Fig. 3), when the dry winds appear most frequently (excluding Kherson, where maximum is observes in July). Total sum of days with dry wind for investigated period in August varies from 107 days in Mariupol to 215 days in Simferopol .

In some cases meteorological parameters during the dry wind phenomenon can reach to extreme values. Thus, the maximum air temperature of 40.0° C was fixed on 8 and 10 August, 2010 in Zaporizhzhia and on 23 July 2007 in Odessa. The maximum wind speed 15 m/s was observed on 29 August 2011 in Simferopol. The air relative humidity during the dry wind in Odessa in five cases fell to 4 %.

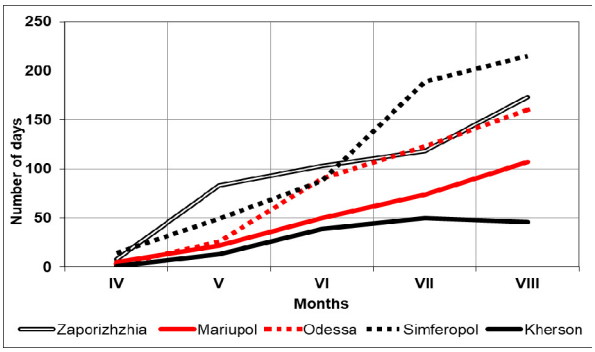

Figure 3. The total sum of days with dry wind by months of growing season of 1995-2015 at the stations located in the Black Sea Steppe province.

4. Conclusions

The obtained in study results clearly demonstrates that current climate conditions in southern steppe part of Ukraine characterized by strong increasing of arid phenomena, such as the droughts and dry winds.

Frequency of drought in growing season especially increased after 2007, when the extreme drought was fixed over the Black Sea Steppe province. The interannual dynamics of repeatability of dry winds demonstrates opposite tendency according to the SPEI values.

As the territory of Ukraine is one of major agricultural area in Eastern Europe, the spring-summer droughts and dry winds can considerably worsen a productivity of grain crops or completely damaged their. Therefore the increasing of aridity of current climate require the timely estimates of risks of developing the seasonal droughts, which can be done with considering the obtained trends of arid phenomena.

References

Cherenkova E.A., Semenova I.G., Kononova N.K., Titkova T.B. (2015) Droughts and dynamics of synoptic processes in the south of the East European Plain at the beginning of the twenty first century, Arid Ecosystems, 5(2), pp. 45-56.

Climate of Ukraine (2003) Lipinskiy V.M., Djachuk V.A., Babichenko V.M. eds., Raevskyy Publishing House, Kyiv, 343 p.

Handbook of Drought Indicators and Indices (2016) M. Svoboda and B.A. Fuchs, eds. Integrated Drought Management Programme (IDMP), Integrated Drought Management Tools and Guidelines Series 2. Geneva, 45 p.

Semenova I.G. (2015) Climate conditions and droughts in the Black Sea Steppe province under the modern period and the near future, XIX INQUA Congress: Quaternary Perspectives on Climate Change, Natural Hazards and Civilization. 26 July - 2 August 2015, Nagoya, Japan (http://inqua2015.jp).

Vicente-Serrano S.M., Santiago Beguería, Juan I. López-Moreno (2010) A Multi-scalar drought index sensitive to global warming: The Standardized Precipitation Evapotranspiration Index – SPEI, Journal of Climate, 23, pp. 1696-1718.

On Cyclones Causing Storm Surges in Pärnu and Narva-Jõesuu

Mait Sepp[1], Piia Post[2] and Ülo Suursaar[3]

[1] Department of Geography, University of Tartu, Tartu, Estonia (mait.sepp@ut.ee)
[2] Institute of Physics, University of Tartu, Tartu, Estonia
[3] Estonian Marine Institute, University of Tartu, Tallinn, Estonia

1. Introduction

In connection to climate change, floods that may cause material damages as well as loss of human life have become an important risk in coastal areas. For floods with catastrophic consequences to occur, several unfavorable circumstances have to coincide. For example, in order for a very large flood to take place in Pärnu, synoptic events that give rise to high water level in the Gulf of Riga and a storm that pushes the water into Pärnu Bay are required (Post, Kõuts, 2014; Suursaar et al. 2018). In the present study, we analyse synoptic situations that have caused a storm surge in Pärnu and Narva-Jõesuu in the period of 1951-2012. The purpose is to understand what are the similarities in the trajectories, life cycle indicators, and weather pattern characteristics of cyclones that caused storm surges.

2. Data and Methods

We analyse 34 cases whose storm surge reached at least 100 cm in height in Pärnu and 29 cases in Narva-Jõesuu that surpassed the 85 cm threshold. Here, the storm surge is defined as local, storm-generated sea level rise, i.e. sea level height on the moment of the surge minus background sea level in the sub-basin that precedes the storm event.
These cases are compared with data from cyclone trajectory database (Tilinina et al. 2013) and COST733 Action weather pattern data (Philipp et al. 2014). Only the lows moved through a 1000 km radius circle whose center was in the center of Estonia (58°45´N and 25°30´) were considered. In case of Narva-Jõesuu storm surges, a cyclone corresponding to these criteria was not found in three cases, which were consequently left out of analysis.

3. Results

Out of the 34 Pärnu cyclones, 24 were formed outside of the 1000 km radius circle (max 7522 km); out of the 26 Narva-Jõesuu cyclones, 18 were born further than 1000 km. The rest were mainly formed near the Swedish coast of the Baltic Sea.
In most cases of the Pärnu storm surges, the cyclone's center is located in a rather limited area over southern Finland, i.e. approximately 350 km from the center of Estonia. It may be said that in comparison to the cyclone's center's location 6 h earlier, the cyclone is moving away by the time the storm surge takes place (previous point's median is 320 km from the center of Estonia).
The centers of cyclones causing storm surges in Narva-Jõesuu have a bit more northward trajectories in comparison to Pärnu ones, and they are located about 580 km north-west from the center of Estonia during the storm surge. The Narva-Jõesuu cyclones are also characterized by the cyclone's center's moving away. The cyclone's center is about 130 km closer to the center of Estonia 6 h before the surge.
Circulation type analysis shows that there is only one weather pattern that causes storm surges in Pärnu. This pattern involves a relatively strong low staying over the Gulf of Finland and southern Finland. There are more evident patterns in Narva-Jõesuu, but most cases are covered by the pattern that involves a low's center over Lake Ladoga or southern Karelia.
The results show that in Pärnu, storm surges are caused by cyclones whose center moves along a rather narrow trajectory and is describable with one weather pattern. Narva-Jõesuu storm surges have a bit more diverse reasons of occurrence, but are in most cases connected to dominant northern winds in the western edge of a passing cyclone.

References

Philipp, A., Beck, C., Huth, R., Jacobeit, J. (2014) Development and comparison of circulation type classifications using the COST 733 dataset and software, Int. J. of Clim. Vol. 36, pp. 2673–2691

Post, P. and Kõuts, T., (2014) Characteristics of cyclones causing extreme sea levels in the northern Baltic Sea. Oceanologia, Vol. 56, pp. 241−258.

Suursaar, Ü., Sepp, M. Post, P., Mäll, M. (2018). An Inventory of Historic Storms and Cyclone Tracks That Have Caused Met-Ocean and Coastal Risks in the Eastern Baltic Sea. Journal of Coastal Research, Special Issue 85, 10.2112/SI85-004.1 [in print].

Tilinina N., Gulev S.K., Rudeva I. & Koltermann P. 2013. Comparing Cyclone Life Cycle Characteristics and Their Interannual Variability in Different Reanalyses. J. Climate 26: 6419–6438.

ERA5: High temporal and spatial resolution reanalyses as a tool to investigate high impact events and other natural hazards in the Baltic Earth region

Martin Stendel

Danish Meteorological Institute, Dept. for Arctic and Climate, Copenhagen, Denmark (mas@dmi.dk)

1. Introduction

Analyses of high impact events and other natural hazards often lack continuity in available data (for example over land compared to over sea) and/or adequate spatial and temporal resolution. This is obviously generally the case in data-sparse regions (e.g. most of the Southern Hemisphere, deserts, the Arctic), but can also be challenging in regions of the world which generally are considered data-rich, like the Baltic.

The challenge of data continuity, including changes in instrumentation, observation times and the like have been addressed already three decades ago by Bengtsson and Shukla (1988) who proposed that atmospheric observations routinely made by the national weather services, but prone to data inhomogeneities, should be "reanalyzed" over a period long enough to be useful for climate studies by using a fixed dynamical system for assimilation of the observations. Several such reanalyses were conducted successfully since the mid-1990s.

However, the spatial and temporal resolution of those reanalyses has remained a challenge if limited-area short-timescale events like the storms of 3 December 1999 or 5 December 2013 (named "Bodil" in Denmark) are to be analyzed. As an example, the spatial resolution of the widely used ERA-Interim reanalysis (Dee et al., 2011) is 71 km, while the temporal resolution is 6 hours.

2. ERA5

Recently, a new generation reanalysis, ERA5, has been made available to the general public. It has been produced using ECMWF's Integrated Forecast System (IFS) using Copernicus Climate Change Service (CCCS) information. ERA5 has a much higher temporal resolution than its predecessors (1 hour), and the spatial resolution is as high as 31 km. It is available for the period 2010 to near present (two or three months behind the actual date), but will be extended back to 1950. ERA5 opens new possibilities for the analysis of small scale (both temporal and spatial) events. It is freely available to the public.

As an example, Figure 1 shows an analysis of potential causes for flooding in the watersheds of Ribe, Randers and Vejle in Jutland and Odense on Fyn, conducted for the Danish Coastal Authority (Kystdirektoratet, Madsen et al., in review).

Examples of the potential and limitations of ERA5 data as an augmentation to conventional point observations will be discussed.

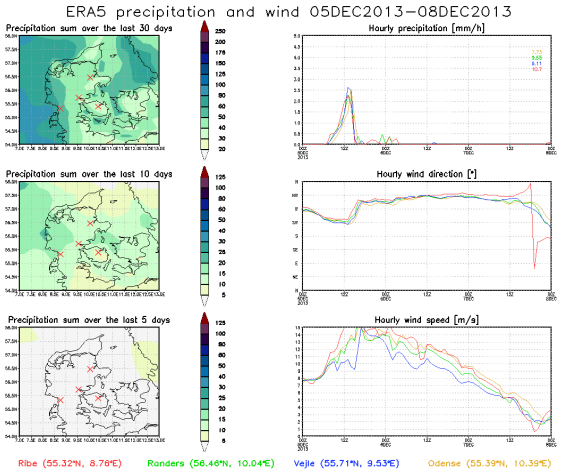

Figure 1. An example for the spatial and temporal resolution of ERA5, storm "Bodil" in early December 2013, which brought catastrophic flooding in Roskilde Fjord and along the north coast of Sealand in Denmark. Left column: precipitation sums for the previous 30 (top), 10 (middle) and 5 days (bottom). Often, floods in winter are not only due to wind storms, but also to a predisposition because the ground is already saturated with water due to previous rainfall. It is obvious that this was not the case for "Bodil". Right column: hourly values of precipitation (mm/hour, top), wind direction (degrees, middle) and wind speed (bottom, m/s) for the four Danish stations Ribe (red), Randers (green), Vejle (blue) and Odense (orange). Among other details, it can be seen that the maximum wind increase associated with the postfrontal trough behind the cold front of "Bodil" was observed three hours earlier in Ribe in the west than in Randers and Odense further east and much earlier than in Vejle, which is due to local effects in the rather steep Vejle Fjord area.

References

Bengtsson, L. and Shukla, J., 1988: Integration of space and in situ observations to study global climate change. Bull. Amer. Meteor. Soc. 69, 1130-1143.

Dee, D. P., Uppala, S. M., Simmons, A. J., Berrisford, P., Poli, P., Kobayashi, S., Andrae, U., Balmaseda, M. A., Balsamo, G., Bauer, P., Bechtold, P., Beljaars, A. C. M., van de Berg, L., Bidlot, J., Bormann, N., Delsol, C., Dragani, R., Fuentes, M., Geer, A. J., Haimberger, L., Healy, S. B., Hersbach, H., Hólm, E. V., Isaksen, L., Kållberg, P., Köhler, M., Matricardi, M., McNally, A. P., Monge-Sanz, B. M., Morcrette, J.-J., Park, B.-K., Peubey, C., de Rosnay, P., Tavolato, C., Thépaut, J.-N. and Vitart, F., 2011: The ERA-Interim reanalysis: configuration and performance of the data assimilation system. Q.J.R. Meteorol. Soc., 137: 553–597. doi: 10.1002/qj.828.

Madsen, K. S., Nielsen, F., Stendel, M. and Thejll, P., 2018: Analyse af meteorologiske og oceanografiske forhold ved oversvømmelseshændelser i udvalgte danske byer (Analysis of meteorological and oceanographic conditions connected with flooding events in selected Danish cities): Odense, Randers, Ribe, Vejle. DMI Report for the Danish Coastal Authority (in review).

The regional features of cyclonic activity and frequency of weather extremes over the territory of Belarus

Katsiaryna Sumak[1], Inna Semenova[2]

[1] Center of Hydrometeorology and Control of Radioactive Contamination and Environmental Monitoring, Minsk, Belarus (katyasbelarus@gmail.com)
[2] Odessa State Environmental University, Ukraine

Weather extreme events are registered over the territory of Belarus every year. They are originated under the influence of various natural factors or their combinations, and have a damaging effect on people, agriculture, economic objects and the environment. In last years the economic losses of the country are increased due to more frequent cases of their manifestation. As a result of the destructive squalls the lodging of grain crops was observed over the territory of agricultural enterprises, the trees were killed in forestry and the power lines were becoming unusable in the communal services. The establishment of patterns of formation and spatio-temporal changes of weather extremes becomes particularly relevant and has practical significance.

As known, the most of weather extremes, causing serious material damage, arise in the area of cyclonic circulation. Intencity of cyclonic activity in the center of Europe depends on dynamics of main baric centers in atmosphere of the North Atlantic (described by NAO) and location of main tropospheric flows. Therefore, the current climate changes might influence to trajectories and intensity of cyclones and consequently for the emergence of weather extremes. The Republic of Belarus is located in the center of East Europe, therefore most of cyclones in this part of the continent are passing over its territory.

The objective of the study is analysis of trajectories and frequency of cyclones, which were moving by the territory of Belarus during the period of 1995-2015 and connected with them weather extremes.

The research was conducted in two phases: at the first phase by dint of methods of synoptic analyses a cyclone database was created for the period of 1995-2015 and then at the second stage it has been identified the relation between weather extremes and the trajectories of cyclones.

During the studied period 329 cyclones moved over the territory of Belarus. So, about 15-16 cyclones per year affected the weather conditions. 22% were of western and northwestern types of cyclones separately, 56% constituted southern cyclones. The maximum number of all types of cyclones (21-23 cases per year) observed in 1998, 2004, 2008 and 2009. Minimum of cyclone activity (about 10 cases) was in 2015.

The most of western cyclones, which moved over the territory of Belarus formed between 50N and 60N over regions of the Northwest Atlantic, the British Isles, the North Sea and south of the Baltic Sea. The southern cyclones came to the territory of Belarus from all the Mediterranean regions, the Balkan Peninsula, the Black Sea and from Ukraine. The northwestern cyclones generally formed over the Norwegian Sea and moved through Scandinavia to the territory of Belarus, where the significant part of them turned toward northeast.

Mean pressure in the center of cyclones over the territory of Belarus constituted 992 hPa for the western and northwestern types and 997 hPa for the southern cyclones.

The cyclones accompanied by weather extremes constituted 23% of the total number of cyclones, the southern cyclones amounted 66 cases, the western cyclones – 10 and north-western cyclones didn't cause the weather extremes.

The maximum of southern cyclones, which caused weather extremes was observed in 1996-1998, 2008, 2009 and 2013 – 5-7 cases, minimum number – in 2001, 2003, 2011 and 2015 – 2 cases/per year. The western Atlantic cyclones which caused weather extremes were observed in 1998 and 2004 - 2 cases, in other years – 1 case/per year.

The highest frequency of southern cyclones, which caused weather extremes, was observed in warm season (from May to August), an average about 10-11 cases and was associated with the severe convection (showers, thunderstorms, squalls, tornadoes and large hail).

The main part of weather extremes (149 cases) in southern cyclones constituted very intensive showers during the studied period. Heavy snowfalls and squalls were 38 and 47 cases respectively. Minimum cases of weather extremes constituted a large hail and strong sticking of wet snow – 11 and 4 cases respectively. An average 4 cases of weather extremes was observed in one cyclone. Trend lines were demonstrated a positive dynamics of frequency of heavy snowfalls during the study period and the amount of squalls and severe winds was decreased from year to year.

The most frequency of intensive showers in southern cyclones was typical for the July and August (72 and 46 cases respectively). Minimum of them fell out in September, October and May. Severe intensive snowfalls often were observed in March – 22 cases, in last months of the cold period were noted from 1 to 7 cases of intensive snowfalls. Squalls were observed mainly in warm period, maximum was in June and July (15 and 14 cases respectively) and minimum frequency was typical in April and October.

The most part of southern cyclones accompanied of weather extremes events was formed over the Western Mediterranean, the Gulf of Genoa and Hungarian and Danube lowlands. Minimum cyclones were shifted from the Aegean Sea and Crete.

Half of cases of western cyclones, which caused weather extremes, were observed in July and August. In winter months and transitional seasons of the year the cyclones of western origin didn't cause the weather extremes events.

The western cyclones mainly caused squalls, very intensive snowfalls and showers. The highest frequency of

very intensive showers was observed in summer months as a result of deep convection on atmospheric fronts. An average 2 cases of weather extremes were noted in each western cyclone.

The cyclones of western origin, which caused weather extremes events over Belarus during the study period, were formed mainly Atlantic Ocean.

Thus, the main part of weather extremes events, which were observed over the territory of Belarus during the period of 1995-2015, related to the cyclonic activity. The most of them associated with cyclones of southern origin in all seasons of the year.

Rogue Waves in the southern North Sea

Ina Teutsch[1]

[1] Helmholtz-Zentrum Geesthacht, Institute for Coastal Research, Germany (ina.teutsch@hzg.de)

1. Introduction

Rogue waves are extreme events characterised by a wave height of more than twice the significant wave height of the underlying wave field and/or with exceedingly high crests compared to the surrounding waves (Haver 2000). They may develop tremendous forces and thus imply a high risk on ships and offshore structures.

2. Study Area and Data

A radar measurement data set from platforms, some of which has been published before, together with new buoy measurement data from the southern North Sea, are examined with regard to the occurrence of rogue waves. The good spatial coverage of the southern North Sea together with the extended period for which high-resolution wave measurements are available provides an opportunity to improve detection of rogue waves and to study their statistics.

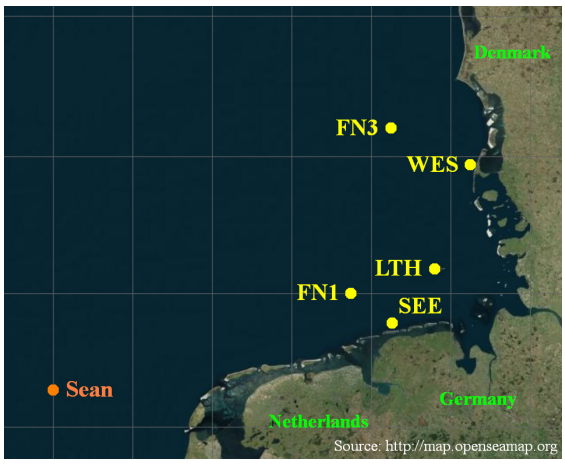

Figure 1. Distribution of measurement stations in the southern North Sea. Yellow: wave buoys. Orange: radar station.

3. Analysis

Temporal and spatial distributions of rogue wave occurrence are investigated and compared at the different stations. An example is shown in Figure 2.

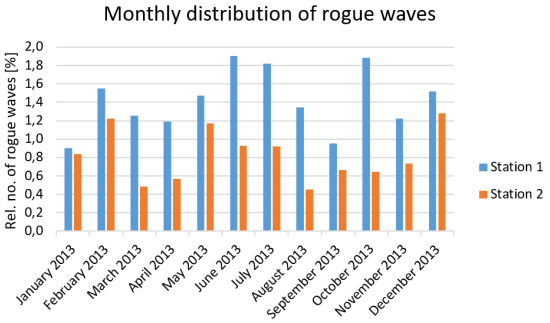

Figure 2. Comparison of rogue wave occurrences at two stations throughout the year 2013.

A possible link between rogue wave occurrence and the characteristics of the underlying wave field is investigated. The results are compared to the statistical analysis of North Sea data performed by Stansell (2004).
In addition, the frequency of rogue wave occurrence is compared to theoretical models like the Rayleigh distribution, as done by Forristall (1978).

4. Outlook

In a next step, it is intended to investigate a relation between prevailing weather conditions and the probability of rogue wave occurrence.

Acknowledgements

The buoy data were kindly provided by the Federal Maritime and Hydrographic Agency in Germany (BSH) and the Lower Saxony Water Management, Coastal Defence and Nature Conservation Agency (NLWKN). The author is grateful to G. Feld and Shell for providing the radar data.

References

Forristall, G.Z. (1978) On the statistical distribution of wave heights in a storm, J. Geophys. Res., 83., pp. 2353-2358

Haver, S. (2000) Evidences of the Existence of Freak Waves, Proc. Rogue Waves, Ifremer, pp. 129-140

Stansell, P. (2004), Distributions of freak wave heights measured in the North Sea, Applied Ocean Research, vol. 26, pp. 35-48

Seasonal and long-term dynamics of snow cover regime in Estonia

Birgit Viru, Jaak Jaagus

Department of Geography, Institute of Ecology and Earth Sciences, University of Tartu, Tartu, Estonia
(birgitviru@gmail.com)

1. Introduction

According to the IPCC report the global average temperature has increased by 0.85˚C since 1880. According to different climate change scenarios it is predicted to rise up to 2–5°C for the end of this century (IPCC, 2013). Climate warming will inevitably induce a decrease of seasonal snow cover in higher latitudes.

Snow has an important role in the climate system, because the most important properties of snow – large albedo, low thermal conductivity and the ability to change from one state to another – cause energy transformations between the ground and the atmosphere. Due to the high albedo and irradiance, the snow cover cools significantly the overlying air layer. Cool weather conditions, in turn, promote additional snow accumulation after snowfall. But when the snow has started to melt and the albedo to decrease, then it accelerates the melting of snow.

The aim of this study is

1. to analyze spatial and temporal variability of the start and end dates and duration of the permanent snow cover in Estonia;
2. to analyze spatial, temporal and seasonal variability of median and maximum snow depth;
3. to study the dynamics of the seasonal snow cover;
4. to determine the presence of long-term changes of these parameters during the period 1951–2016.

2. Data and methods

Daily data of snow depth in 17 meteorological stations and 5 posts at different locations in Estonia in 66 winter seasons 1950/51–2015/2016 (months from October to April) were used (Figure 1). In addition 3 stations and 21 posts were used in shorter period 1956–2010. Data were derived from Estonian Weather Service. By using the daily data, snow cover statistics were calculated.

There were some gaps in these data, which were filled by using nearest neighbour interpolation (for shorter gaps), or left blank.

Snow depth measurements at the meteorological stations are made once a day at 8:00 in the morning by the wintertime. Snow depth in centimeters is measured as an average of records at three snow bars (120 cm), which have been placed like an equilateral triangle. The distance between the bars is at least 10 meters (Tooming and Kadaja, 2006).

Snow cover day is defined as a day when the snow cover in the area fulfils two requirements: at least half of the observation field is covered by snow, and the minimum snow depth is 1 cm. In case when at least half of the observation field covered by snow, but with depth less than 1 cm, the snow depth is considered to be 0 cm.

Snow cover data were non-normally distributed, therefore, median was used to describe the characteristics of snow cover instead of arithmetic average and quartile range instead of standard variation to describe variability. Statistics were found only for these dates when snow cover was observed at least 50% of winters. In this study, the Mann-Kendall (MK) test has been used to analyse trends in snow cover parameters.

Figure 1. Location of the meteorological stations and posts in Estonia used in the study.

3. Results

The start, end and duration of the permanent snow cover vary widely in the territory of Estonia. On the average, the start date of the permanent snow cover was 23 December, the end date was 26 March, and the duration resulted in 84 days, i.e. nearly three months. During the short period 1956–2010 these dates were 19 December, 27 March and 89 days, respectively.

The permanent snow cover forms the earliest in the Pandivere Upland, in north-eastern Estonia and in the south-eastern uplands (Haanja, Otepää) (Figure 2). Due to the warming effect of the sea, the permanent snow cover forms the latest on the West-Estonian islands and on the western coast of the mainland. Permanent snow cover was formed at the earliest on Haanja Upland in Mauri (on the average on the 25 November). On the islands of western Estonia it happens about two months later (in Vilsandi on 24 January). Permanent snow cover disappeared at the earliest in West-Estonia in Vilsandi (8 March) and the latest on Pandivere and Haanja upland (on the average at the beginning of April) (Figure 3). The duration of permanent snow cover is the longest on uplands and shortest on the West-Estonian islands (Figure 4).

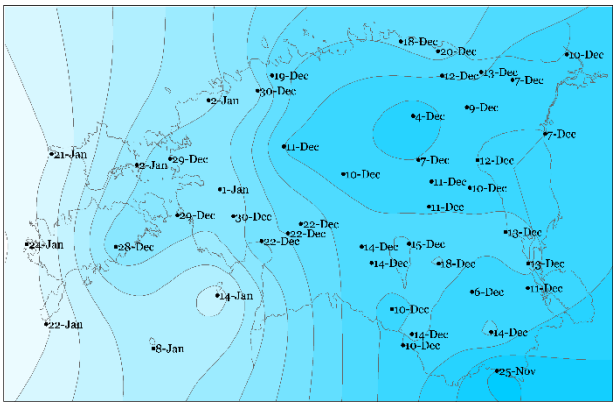

Figure 2. Mean start date of the permanent snow cover in 1956–2010.

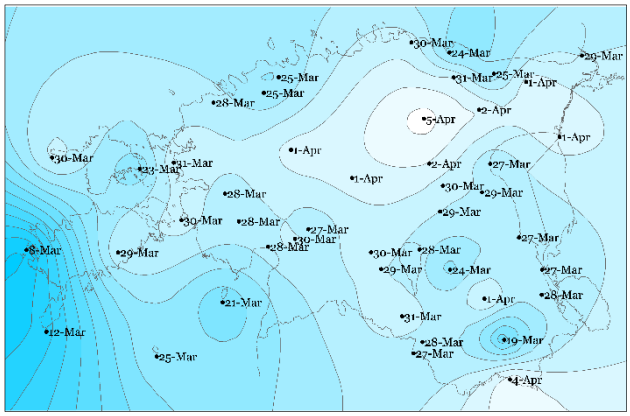

Figure 3. Mean end date of the permanent snow cover in 1956–2010.

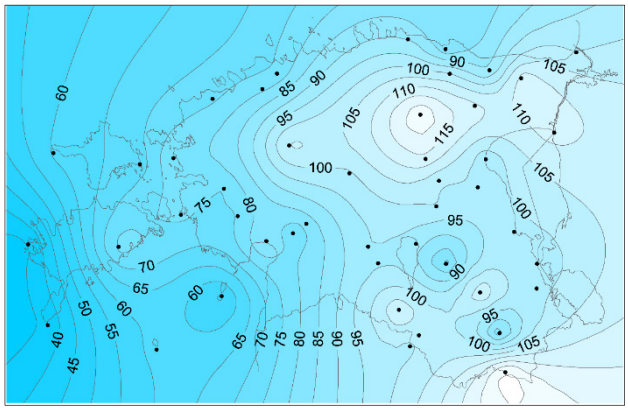

Figure 4. Mean duration of the permanent snow cover in 1956–2010.

The interannual variability of the permanent snow cover characteristics was the largest on the West-Estonian islands and the smallest in North-Eastern and South-Eastern Estonia.

The beginning of the permanent snow cover has statistically significantly changed to the later time during the period 1951–2016 in Piigaste (1.25 days per decade) and during the shorter period in Kunda and Vasknarva (6.1 and 3.85 days per decade). The end date of the permanent snow cover has shifted earlier at the most of stations. The highest change took place in Oandu – by 7 days per decade. The duration of the permanent snow cover has statistically significantly shortened at most of stations while the most remarkable change was obtained in Koodu – by 12 days per decade, i.e. more than two months throughout the whole period.

The maximum snow depth has been the deepest on Haanja upland in Mauri – more than 40 centimetres in the average (Figure 5). At many stations there were decreasing trends in annual maximum snow depth. The largest statistically significant change had occurred in Väike-Maarja (-31 cm throughout the entire study period 1956–2010) and Piigaste (Figure 6).

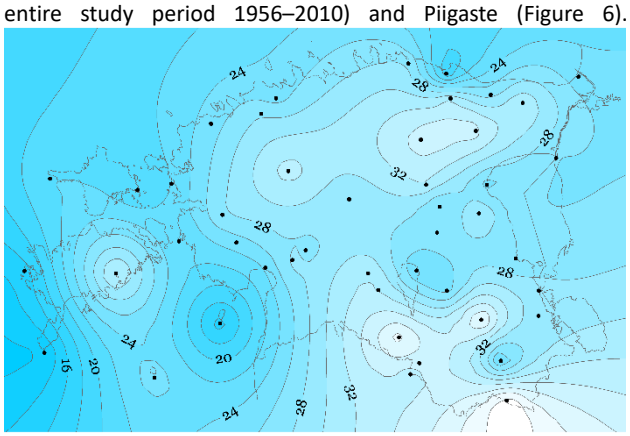

Figure 5. Median of annual maximum snow depth in 1956–2010.

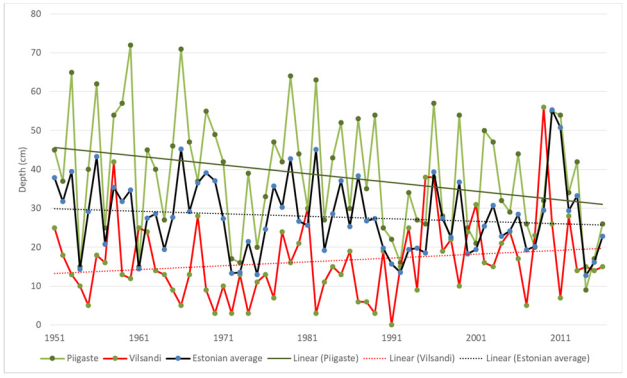

Figure 6. Annual maximum snow depth in 1951–2016 (solid line – trend is significant, dashed line – no significant trend).

Snow depth starts to increase after the permanent snow cover is formed in December and reaches its maximum in late February/early March, when the average snow depth in inland is more than 15 cm, and on Pandivere, Haanja and Otepää uplands more than 20 centimetres (Figure 7).

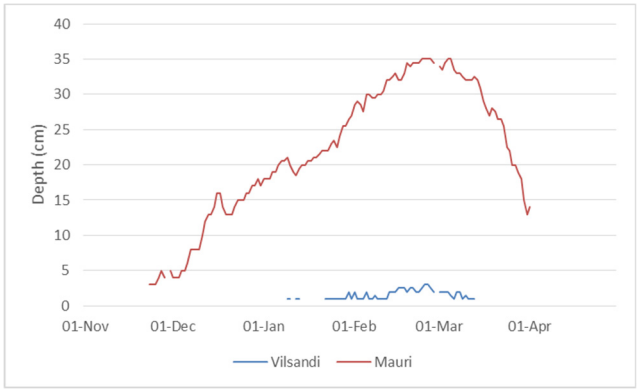

Figure 7. Median of snow depth in Vilsandi and Mauri in 1951–2016.

Seasonal snow depth interquartile range was the largest at the end of February and in the beginning of March. There was a negative trend of snow depth from January to the end of March. Trend was not statistically significant at all months. The decrease in snow depth was the largest at the end of February and in March, when there were statistically significant trends at many stations.

4. Conclusions

Global warming is affected the snow cover in Estonia. Duration of permanent snow cover is shortened, especially due to earlier melting period. Also there is a decreasing trend in maximum and average snow depth in most stations.

References

IPCC, 2013: Summary for Policymakers. In: Climate Change 2013: The Physical Science Basis. Contribution of Working Group I to the Fifth Assessment Report of the Intergovernmental Panel on Climate Change [Stocker, T.F., D. Qin, G.-K. Plattner, M. Tignor, S.K.

Allen, J. Boschung, A. Nauels, Y. Xia, V. Bex ja P.M. Midgley eds.)]. Cambridge University Press, Cambridge, United Kingdom ja New York, NY, USA.IPCC.

Tooming, H.and Kadaja, J. (2006). Eesti lumikatte teatmik = Handbook of Estonian snow cover. (A. Kallis, Toim.) Tallinn-Saku: Eesti Meteoroloogia ja Hüdroloogia Instituut, Eesti Maaviljeluse Instituut.

Extreme rainfall analysis and estimation of intensity-duration-frequency curves using dual polarization weather radar data of Estonia and Italy

Tanel Voormansik[1,2], Roberto Cremonini[3], Dmitri Moisseev[4] and Piia Post[2]

[1] Estonian Weather Service, Estonian Environment Agency, Tallinn, Estonia
[2] Institute of Physics, University of Tartu, Estonia (tanel.voormansik@ut.ee)
[3] Regional Agency for Environmental Protection of Piemonte, Department of Forecasting Systems, Torino, Italy
[4] Department of Physics, University of Helsinki, Finland

1. Introduction

Rain gauge data has often been used to estimate the rainfall intensity for a given return period. However, the main issue of using rain gauges for this purpose is their low spatial and temporal resolution. Here the radar data has obvious advantage with its higher spatial and temporal resolution.

Studies on this topic up to this date have used horizontal reflectivity (Zh) based rainfall estimates (Marra and Morin 2015, Marra et al. 2017, Overeem et al. 2009), but they come with a great caveat – while proven reliable on low rainfall rates they are subject to major errors in extreme rainfall and convective cases. Especially shorter wavelength radars that belong to X-band and C-band are shown to underestimate precipitation intensity due to attenuation (Delrieu et al. 2000) and overestimate due to hail (Ryzhkov et al. 2013).

This study attempts to circumvent these shortcomings by using specific differential phase (KDP) data from dual polarization radars which is immune to attenuation and hail contamination issues (Ryzhkov et al. 2005).

The aim of this study is to derive and analyse intensity duration frequency (IDF) curves from polarimetric weather radar data using KDP based quantitative precipitation estimation (QPE). Furthermore, these parameters were also calculated from legacy Zh based radar rainfall and rain gauge data and they were included in the comparative analysis. Data from Italy and Estonia were used to study the performance of the method in different climate conditions and radar hardware setups.

2. Data

Data from warm period of the year was used as the heaviest precipitation events take place at this time. Limiting the dataset to this period also helps to ensure that radar reflectivities are only from liquid precipitation which is required for reliable rainfall intensity estimation. For Estonia the warm period was defined as months from April to October and for Italy from March to November.

Single radar site data was used both from Estonia and Italy. From Italy radar data from Bric della Croce dual-polarization Doppler C-band radar located in Turin, northern Italy were used. It was available with 5 minute temporal resolution and from years 2012-2016. From Estonia radar data from Estonian Weather Service operated Sürgavere dual-polarization Doppler C-band radar located in central Estonia in Viljandi county were used. It was available with 15 minute temporal resolution and from years 2010-2016.

Rain gauge data was used for the reference IDF curves calculation. From Italy 1 minute tipping bucket rainfall data was available from 1988-2016 for the area. From Estonia 10 minute gauge data was available from 2011-2016. From the period 2003-2010 rain gauge data was available with 1 hour resolution.

3. Methods

The first step to derive radar IDF curves was QPE calculation. For this purpose the lowest level Plan Position Indicator (PPI) scans were used. To eliminate the possibility of using radar data that originates from the freezing level and above a maximum radius limit was set for the radar data. From KDP the rainfall rate (R) was calculated by using the following equation:

$$R = 21.0K_{dp}^{0.720}.$$

For comparison Zh based IDF curves were also calculated. The corresponding rainfall rate was derived by using the following Z-R relationship:

$$Z = 300R^{1.5}.$$

Based on the QPE estimations annual maxima for each radar data bin inside the radius limit were derived for 15, 30, 45 and 60 minutes intensities. To describe the annual radar rainfall maxima a generalized extreme value (GEV) distribution was assumed and it was used to fit the annual maxima series of rainfall intensities of aforementioned periods. In order to get longer data series for extreme value statistic calculations radar rainfall maxima from multiple locations were used in the calculations. Included bin locations were chosen so that they would belong to the area with similar precipitation regime and that they would be located at such distance from each other which would ensure independence of each data point. The corresponding distance was determined from empirical variogram.

In addition to the IDF calculations various extreme rainfall statistics were analysed and a comparison between Estonian and Italian results were made.

References

Delrieu, G., Andrieu, H. and Creutin, J.D. (2000). Quantification of path-integrated attenuation for X-and C-band weather radar systems operating in Mediterranean heavy rainfall. Journal of Applied Meteorology, 39(6), pp.840-850.

Marra, F. and Morin, E. (2015). Use of radar QPE for the derivation of Intensity–Duration–Frequency curves in a range of climatic regimes. Journal of Hydrology, 531, pp.427-440.

Marra, F., Morin, E., Peleg, N., Mei, Y. and Anagnostou, E.N. (2017). Intensity–duration–frequency curves from remote sensing rainfall estimates: comparing satellite and weather radar over the eastern Mediterranean. Hydrology and Earth System Sciences, 21(5), p.2389.

Overeem, A., Buishand, T.A. and Holleman, I. (2009). Extreme rainfall analysis and estimation of depth-duration-frequency curves using weather radar. Water resources research, 45(10).

Ryzhkov, A.V., Schuur, T.J., Burgess, D.W., Heinselman, P.L., Giangrande, S.E. and Zrnic, D.S. (2005). The Joint Polarization Experiment: Polarimetric rainfall measurements and

hydrometeor classification. Bulletin of the American Meteorological Society, 86(6), pp.809-824.

Ryzhkov, A.V., Kumjian, M.R., Ganson, S.M. and Zhang, P. (2013). Polarimetric radar characteristics of melting hail. Part II: Practical implications. Journal of Applied Meteorology and Climatology, 52(12), pp.2871-2886.

The atmospheric circulation as a driver of dry spell in Poland

Joanna Wibig[1]

[1] Department of Meteorology and Climatology, University of Lodz, Lodz, Poland (zameteo@uni.lodz.pl)

1. Introduction

Droughts are periods with precipitation amiunts considerably lowe than long-term average for analysed region. Atmospheric drought can last from a few week to several years. They usually are acompanied by the presence of high pressure systems, when high temperature causes the drop of relative humidity (Dai, 2011). Contemporary warming manifesting itself in Poland by the rise of average temperature reaching almost 1˚C has increased the risk of water deficit. More dynamic water cycle can manifests by stronger showers, but also longer dry periods.

The aim of this paper is to distinguish the atmospheric circulation types favoring the emergence of dry spells in Poland

2. Data

Daily precipitation totals from 24 meteorological stations in Poland were used for distinguishing dry spells.Their location isshown on Fig. 1. To describe atmospheric circulation the daily values of SLP and daily values of geopotential heights of 500 hPa level from NCEP/NCAR reanalysis 1 (Kalnay et al., 1996) were applied. The SLP data cover the area between the meridians 60˚W and 60˚E and the parallels 30˚ and 70˚N with the resolution 2.5 x 2.5 degree. Geopotential data were taken from two parallels: 40˚ and 60˚N from the area between the meridians 90˚W and 90˚E. All data cover the period 1951-2015.

.

Figure 1. Location of station with precipitation data.

3. Methods

Selection of dry spells: for each station the days in at least 10 day long spells of dry days (precipitation <1 mm/day) were picked out. From this set the days which were dry on at least 13 stations at the same time (more than 50% of all analysed stations) were selected and divided into four seasons (Winter: DJF, Spring: MAM, Summer: JJA and Autumn: SON).

Based on daily patterns of SLP on selected days, the Ward's k-mean method (Ward, 1963) was applied to distinguish atmospheric circlulation patterns. In thisstudy, selected days were the clustered objects. The clustering was based on raw daily SLP data. Then the maps of SLP and itsanomalies from seasonal averages were created for each cluster.

The blocking index (BI) was also calculated for selected days in each season separately according to Lejenäs and Økland (1983) formula:

$$BI(\lambda) = Z_{40N}(\lambda) - Z_{60N}(\lambda),$$

where λ is a longitude, ZiN(λ) is a value of geopotential height of 500 hPa at longitude λ and latitude i. To find a relation between blocking events and dry spells the anomalies of BI in selected days in comparison with seasonal averages were calculated.

4. Results

According to presented method three atmospheric circulation types were distinguished in Winter and Summer and five in Spring and Autumn. Because of limited size of abstract only results for summer are presented here.

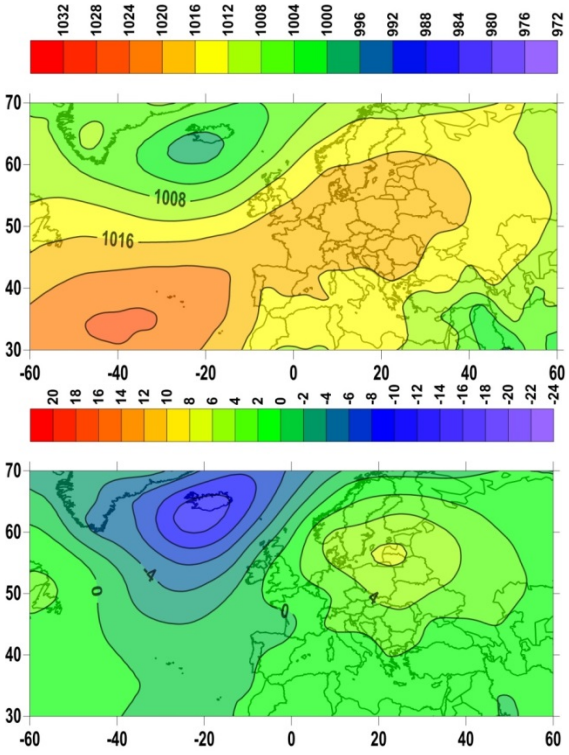

Figure 2. The average SLP pattern (upper graph) and SLP anomalies field (lower graph) for type one in Summer

The first Summer type involves 90 days. Dry days occur when the high pressure system with a ridge of high pressure stretching to the north-east and encompasing almost all Europe (Fig. 2). The strong negative anomaly od SLP is close to Iceland indicating that Islandic Low is

especially deep, but stretching to the north-east. Poland is in the area of pressure slightly higher than normal with calm weather.

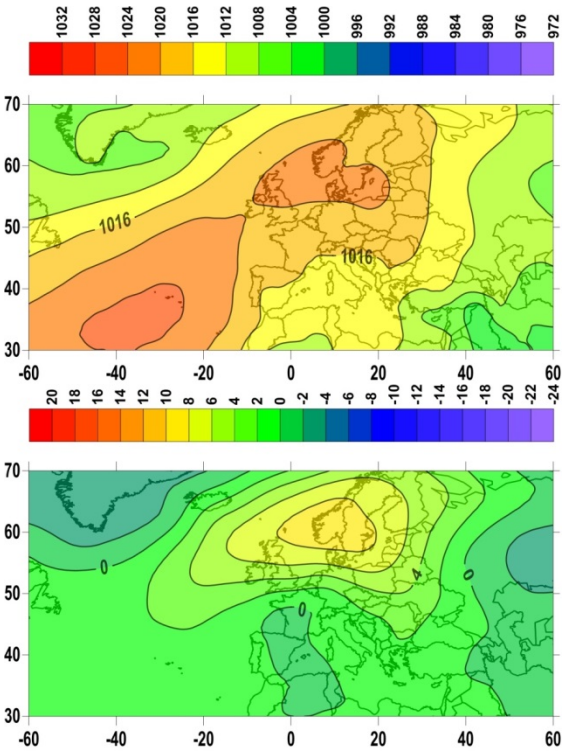

Figure 3. As on Fig. 2 but for the second type in Summer.

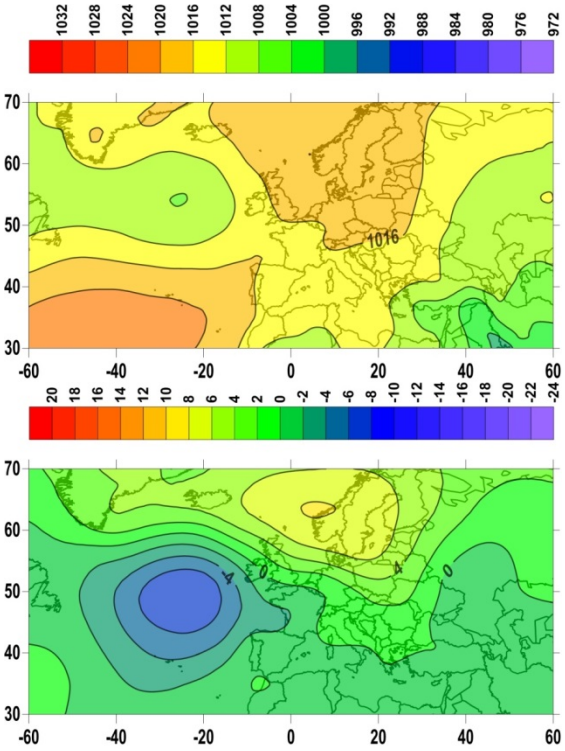

Figure 4. As on Fig. 2 but for the third type in Summer.

The second Summer type involves 96 days. As in type 1 dry days occur when the high pressure system with a ridge of high pressure stretching to the north-east and encompasing all Europe without its eastern part (Fig. 3). But this time the low over Iceland almost disappears and the highest pressure along the ridge is over Scandinavia. The negative anomaly od SLP is over Greenland and in the eastern Europe. Positive anomalies concentrate over southern Scandinavia. Poland is in the area of pressure slightly higher than normal with calm weather.

The third Summer type involves 69 days. As in type 1 and 2 dry days occur when the high pressure system with a ridge of high pressure stretching to the north-east and encompasing almost all Europe (Fig. 4). But this time the low over Iceland almost disappears and the highest pressure along the ridge is over Scandinavia. Almost all analysed area is covered by positive pressure anomalies, anly in eastern Mediterranean region the pressure is slightly below normal.

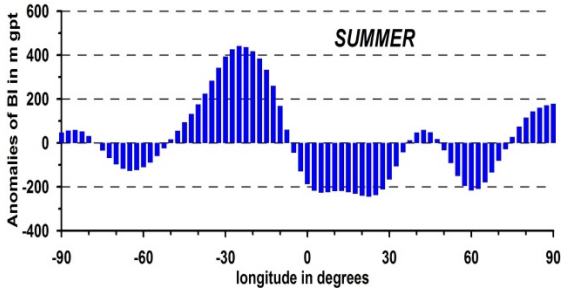

Figure 5. Anomalies of BI in dry days in Summer in the function of longitude.

Anomalies of BI indicate that dry daysin Summer occur when the strong blocking exists in middle latitudes over the Northern Atlantic (Fig. 5).

5. Summary

Dry days in Poland are accompanied by higher bthan average pressure over Poland. In summer dry spells occur when the High over azores is well developed with a ridge of high pressure stretching to the north-east. At 500 hPa level blocking is enhanced over eastern part of Atnantic in middle latitudes.

6. Acknowledgements

The work is supported by grant 2012/05/B/ST10/00945 founded by Polish National Science Centre. Author thanks the IMWM for kindly providing the Polish data as well as NCAR/UCAR for provision of Reanalysis1 data.

References

Dai A., (2011) Drought under global warming: areview. Wiley Interdisciplinary Reviews: Climate Change, 2, pp. 45-65.

Kalnay E, et al. (1996) The NCEP/NCAR 40-Year Reanalysis Project, Bull. Am.Meteorol. Soc., 77, pp. 437-471.

Lejenäs H, Økland H (1983) Characterictics of Northern Hemisphere blocking as determined from a long time series of observational data, Tellus, 35A, pp. 350-362.

Ward JH (1963) Hierarchical grouping to optimize an objective function, J. Amer. Statist. Assoc., 58, pp. 236-244.

Topic D

Sea level dynamics, coastal morphology and erosion

Interannual coastal processes in Estonia, Peraküla beach monitored by laser scanning technology

Maris Eelsalu[1], Katri Pindsoo[1], Tarmo Soomere[1,2] and Kalev Julge[3]

[1] Wave Engineering Laboratory, Department of Cybernetics, School of Science, Tallinn University of Technology, Akadeemia tee 21, 12618 Tallinn, Estonia
[2] Estonian Academy of Sciences, Kohtu 6, Tallinn, 10130, Estonia
[3] Chair of Geodesy, School of Engineering, Tallinn University of Technology, Ehitajate tee 5, 19086 Tallinn, Estonia

1. Introduction

The evolution of sandy beaches in the Baltic Sea is mostly driven by the highly intermittent wave regime that is interspersed with aperiodic variations in the water level and seasonal ice-cover. The conditions that define the beach evolution vary remarkably along the coasts, mostly depending on the exposure to the predominant wind directions.

The small sandy beaches on the southern coast of the Gulf of Finland mostly overlie the ancient dunes. They are usually geometrically sheltered from most of the approaching directions of severe wave storms and thus typified as "almost equilibrium beaches" (Soomere and Healy, 2011). Owing to the extensive variability in the strong wind directions in the Baltic Sea high waves sometimes reach the shores of semi-sheltered bays from unusual directions. In these cases, the usual slow evolution of beaches may be overridden by drastic changes in the beach morphology (Tõnisson et al., 2013).

In this paper we explore the course of sediment transport along an about 1000 m long section of a sandy beach at Peraküla with an average width of about 13 m in 2008–2017 (Fig. 1). This beach stretches over more than 10 km on the southern coast of Gulf of Finland in the north-western Estonia (Fig. 2). The overall intensity of coastal processes in this region is moderate because the shore is largely sheltered against the majority of wave storms. The study area is partially open to northern directions from where high waves are relatively infrequent. It occasionally hosts up to 1 m high waves, but mostly these do not cause any visible damage to the subaerial beach, and usually no erosion scarp is developed.

Figure 1. Peraküla beach in 2010 (left panel; photo by T. Soomere) and in Detsember 2017 (right panel; photo by K. Pindsoo).

2. Methods

The sand volume of the dry beach and regions that host either accumulation or erosion are evaluated using a scanning laser that yields a high-resolution three-dimensional surface of the measured object. The repeated use of this technique by alternatively employing the terrestrial (TLS) and airborne (ALS) laser scanning makes it possible to remove the bias between the subsequent ALS measurements and to reduce all measurements to a fixed reference surface and thus allows to identify the absolute height of the subaerial beach at each measurement instant (Eelsalu et al. 2015). This approach allows to adequately identify spatio-temporal changes on the dry beach but is not able to describe changes to the underwater the beach profile. Ideally, it should be complemented with beach profile measurements down to the closure depth. In practice, a rough estimate of underwater changes can be done by applying the theory of Equilibrium Beach Profile and the inverse Bruun's Rule.

The ALS data was gathered in March-May 2008 and 2012 by Estonian Land Board with Leica ADS40 ALS50-II LIDAR scanner with the average point density of 0.45 points/m^2. The TLS data was gathered in May 2015 and in December 2017 with pulse-based Leica ScanStation C10 that provides an average spatial resolution of ~2,500 points/m^2. The two data sets were linked using the parking lot next to the beach as a horizontal reference surface and scanned during the TLS survey in 2015. See for detailed information in Julge et al. (2014). During the survey in 2017 the water level was +0.23 m above the long term mean. Thus, the surveyed area was narrower than in the previous ALS and TLS surveys.

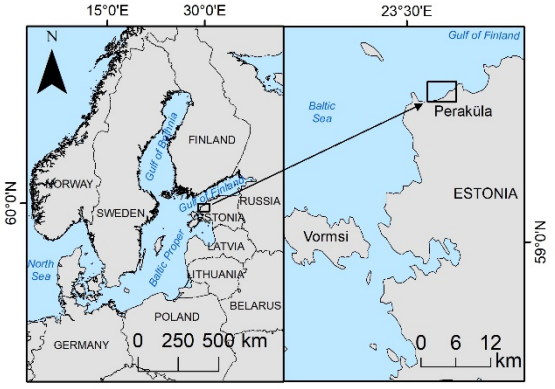

Figure 2. Location scheme of Peraküla beach at the southern coast of the Gulf of Finland.

3. Interannual variability of the dry beach

During the years 2008–2012 about half of the study area experienced erosion and another half accumulation. The eroding (north-eastern) area lost about 1,820 m^3 of sand whereas the south-western segment gained about 1,805 m^3. Therefore, the sand volume of the entire study area was in an almost perfect equilibrium. The study area experienced several wave storms during this time interval that drove the sediment flow from the north-east side of the beach to the south-west.

During the next three years 2012–2015 the study area gained almost 3,000 m^3 of sediments. The excess sand was distributed rather evenly. Most of the beach sections became by 0.2–0.5 m higher. Only the central part of the beach experienced erosion by about 110 m^3 and a reduction of the beach height by about 0.1 m.

During the subsequent years 2015–2017 the beach gained about 1860 m^3. The accumulation rate was comparable to that in 2012–2015. The process, however, had quite different spatial pattern. Namely, some segments experienced remarkable erosion with the total ratio of 1,125 m^3.

It is likely that the biggest erosion occurred in November 2017 due to a combination of an elevated water level (+0.2 m compared to the long-term mean) and a wave storm from an unusual direction. The local newspapers reported that a remarkable amount of sediment was removed from the (fore)dunes far from the usual waterline (Fig. 1 right panel). At some locations the height of the erosion scarp at the dune toe was up to 2 m.

Figure 3. The net erosion (red) and accumulation (blue) in Peraküla beach in 2008–2017.

As opposite to the years 2008–2012, in 2015–2017 the sediment flow was from south-west to north-east. There was no major damage to the beach during this time interval. The coastal segments in the south-western part of the beach that gained sand until 2015 simply restored the shape and height they had in 2008.

The predominant process in the entire study area in 2008–2017 was accumulation (Fig. 3). The net gain of sand was about 3,570 m^3, that is, about 3.6 m^3 on average per each meter of the shoreline or about 360 m^3 of sand per year in the entire area. The biggest accumulation occurred in the central part of the study area (Fig. 3). Erosion was observed in the few locations in the eastern and western segments of the beach. The total amount of lost sand was about 600 m^3.

The established pattern indicates that the sand in the beach has been in active motion. It is natural that severe waves combined with elevated water levels lead to the erosion from the upper part of the beach. Our analysis strongly suggests that this material is not lost from the beach. It is likely that storms approaching from different directions just move the material back and forth along the beach and the net loss of sand is minor even during the severest events. Even then it is likely that the material is used to widen the equilibrium beach profile. The main difference from the classic "cut and fill" process on open ocean beaches, therefore, is that material mostly moves along the shoreline in the study area. Similarly to the "cut and fill" process, during calmer weather conditions the material is brought back to the central segment of the subaerial beach. In general, the beach is healthy: within the time interval covered in this study more material was added to the dry beach than eroded from there.

The described patterns suggest that the damages caused by a mild storm in November 2017 will recover soon. Nevertheless, the beach is still vulnerable with respect to the combination of high water level and high waves. In some occasion remarkable damage may occur.

4. Conclusions

The combination of airborne and terrestrial laser scanning offers high-quality temporal and spatial data that gives a reliable insight to the internal structure of beach processes. It highlights local alongshore and cross-shore changes and erosion or accumulation in some parts of the beach.

The results indicate that coastal processes are actively distributing sand in the alongshore direction in the study area. The process is non-stationary: during some years the subaerial beach gains sand while in other years sediments are carried away. The same pattern applies for the whole beach as well as for the smaller scale of single beach profiles.

Differently from the public perception, the beach in Peraküla is generally healthy and the predominant process is accumulation. This course is at times stopped by strong wave storms from unusual directions. Even though they may create some features typical to beach degradation, their impact apparently is short-term, the sand is carried along the shore to a certain distance but does not exist the system and the beach rapidly regains its status. The loss of small amounts of sand during certain events is a natural feature of beaches in this area. Nevertheless, the proper understanding of the mechanism and time-scales of the whole system requires long-term observing monitoring of the beach.

5. Acknowledgements

The research is supported by the Estonian Ministry of Education and Research (Grant IUT33-3) and the Estonian Research Infrastructures Roadmap object „Infotechnological Mobility Observatory (IMO)", funded by European Regional Development Fund.

References

Eelsalu M, Soomere T, Julge K (2015). Quantification of changes in the beach volume by the application of an inverse of the Bruun Rule and laser scanning technology, Proceedings of the Estonian Academy of Sciences, 64 (3), 240–248.

Julge K, Eelsalu M, Grünthal E, Talvik S, Ellmann A, Soomere T, Tõnisson H (2014). Combining airborne and terrestrial laser scanning to monitor coastal processes, 2014 IEEE/OES Baltic International Symposium, May 26.–29, 2014, Tallinn, Estonia. IEEE, 10 pp.

Soomere T, Healy T (2011) On the dynamics of "almost equilibrium" beaches in semi-sheltered bays along the southern coast of the Gulf of Finland. In The Baltic Sea Basin (Harff J, Björck S, Hoth P., eds). Springer, Heidelberg, 255–279.

Tõnisson H, Suursaar Ü, Rivis R, Kont A, Orviku K (2013). Observation and analysis of coastal changes in the West Estonian Archipelago caused by storm Ulli (Emil) in January 2012, Journal of Coastal Research, Special Issue 65, 832–837.

Seasonal variability of diurnal seiches in Gulf of Riga

Vilnis Frishfelds[1], Juris Sennikovs[1], Uldis Bethers[1]

[1] Faculty of Physics and Mathematics, University of Latvia, Riga, Latvia (frishfelds@latnet.lv)

1. Water level oscillations in Gulf of Riga

Observations show that Gulf of Riga has distinct diurnal oscillations which usually have certain daily pattern with amplitude 5-10 cm in relatively calm days. On the other hand typical tidal amplitudes in Gulf Riga does not exceed 2 cm. That rises a question whether seasonal variability of phase and amplitude plays an important role in these water level oscillations.

Otsmann et al. (1999) noted that model of Helmholtz oscillator can be applied to Gulf of Riga. Inserting the properties of the Irbe strait the estimation yields that Gulf of Riga has a single resonance frequency close to 24 hours.

In order to do it more accurately, we simulated the oscillations with HBM ocean circulation program, where the water level of western boundary has forced oscillations with given period. The results showed that Gulf of Riga likes to oscillate with respect to Baltic proper as single body with frequency of about 25-27 hours, see Figure 1. Because, there is strong dissipation of energy, there must be periodic forcing that maintains these oscillations which can be tides or effect of solar radiation.

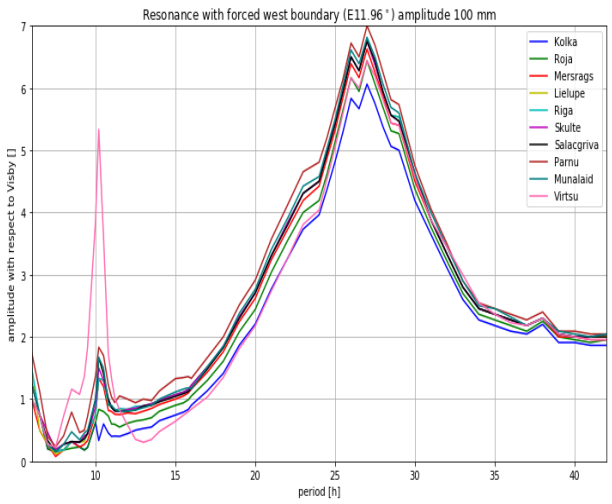

Figure 1. Relative amplitude of water level oscillations in Gulf of Riga with respect to Baltic proper vs. period.

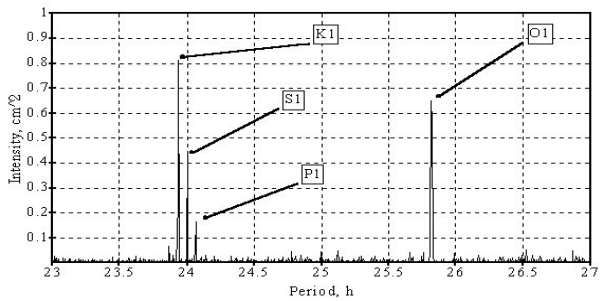

Figure 2. Diurnal spectrum of observed water level in Daugavgriva station in years 1960-1999.

2. Spectrum of observed water level oscillations

Long term water level spectrum in Gulf of Riga is well established, see Figure 2 (Keruss & Sennikovs (1999)). As it should be, the diurnal tides dominates. The main tidal components are K_1, S_1, P_1 and O_1 with amplitudes of around 1 cm. Main semi-diurnal component M_2 has several times lower amplitude.

3. Gravitational tides

Tides are produced by gravitational action of the Moon and the Sun. Diurnal tides produced by varying declination are the strongest in mid-latitudes. The Moon produces K_1 and O_1 tides while the Sun K_1 and P_1 tides. So, K_1 is the strongest diurnal component as it combines the Moon and the Sun.

In order to estimate the gravitational components in stations of Gulf of Riga, numerical simulations with HBM ocean circulation software are performed, where the tidal potential is included, but all other kinds of forcing are excluded. The water is assumed homogeneous with no stratification. The spectrum produced in this way has almost absent S_1 component, whereas the amplitude of K_1 component is increased in comparison with observations. This suggests that S_1 is not related with gravitational forcing, but with daily cycle caused by solar radiation.

The tidal effects may interfere with atmospheric forcing. Also the role of stratification may be important. Therefore, the tidal contribution is accounted also in the real case wit atmospheric forcing, temperature and salinity distribution. The difference between simulations with and without tidal potential gives the effect of gravitational tides in real case. The results for years 2014-2018 showed that atmospheric influence slightly minimizes gravitational tides. There is also effect of stratification as summer tides are slightly stronger than winter, see Müller 2012. Interestingly, there exist also S_1 tidal component in this case, but it is still weaker than in observations.

4. S_1 tidal component

S_1 tidal component should be studied more in detail as it is not related with gravitational tides, see Ray & Egbert 2004. If it has and influence of solar radiation then there should be strong seasonal variability of S_1 (see Rabinovich et al. 2015), i.e., it should be stronger in June and weaker in December. However, the analysis of observations show that S_1 is stronger in April-May and weakest in late autumn. Thus effect of solar radiation alone cannot describe S_1 tidal component.

5. Sea breeze effect

Solar radiation directly cannot cause significant daily change of water level as water has too high heat capacity to have distinct heating of water during the day. Thus, the typical S_1 amplitudes within the oceans rarely exceed 1 cm which are primarily caused by effect of atmospheric pressure. However, inland locations have distinct temperature variations during the day. This creates strong temperature gradient at coastal locations which leads to sea and land breeze.

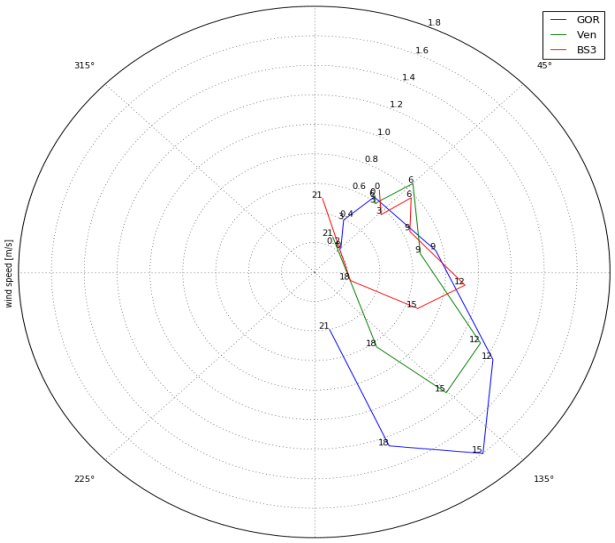

Figure 3. Hodogram of 10 m daily wind (time in UTC) in May at various locations: GOR – Gulf of Riga, Ven – at Irbe strait close to Ventspils, BS3 – between Gotland and Irbe strait.

As there are no stations within the Gulf of Riga, atmospheric reanalysis product ERA-Interim is applied to analyze the wind data in years 1979-2018. The spectrum of 10m wind shows that there is distinct S_1 component in Gulf of Riga along with higher modes S_2 and S_3. There also K_1 and P_1 components in wind spectra which suggest strong seasonal cycle of S_1 component.

The daily wind rotates clockwise in Gulf of Riga as it is placed in northern hemisphere, see Figure 3. The strongest zonal wind occurs at 12 UTC. Because there is about 6 hour time lag between Baltic proper and Gulf of Riga, then the maximum water level is reached at 18 UTC for summer months when solar radiation is the strongest.

There is also slight oscillation of mean sea level pressure difference between Baltic proper and Gulf of Riga, but it is less than 100 Pa in summer. Thus, the pressure difference is not the reason of daily water level oscillation in Gulf of Riga, but it just the effect of sea and land breeze.

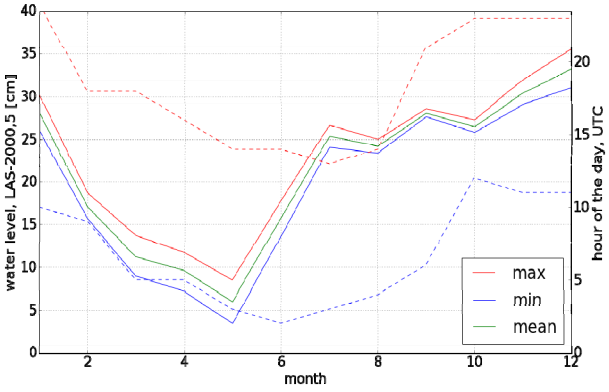

Figure 4. Dashed lines - daily hourss (UTC) of maximal and minimal water level in Skulte station at various months . Red and blue solid lines – water level at these times.

6. Interference between tides and see breeze

If sea breeze effect is dominant then water level should have a peak in late afternoon at about 18 UTC. Data for the station Skulte shows that it is the case for spring and summer, see Figures 4-5. However, there is also distinct daily pattern in December when breeze effect is absent. Then tidal forcing is dominant when the Sun is close to antipodal location at midnight, see Figure 6. S_1 component is stronger in spring than in autumn because see breeze is nearly in phase with gravitational tides. Whereas see breeze and tides are nearly in anti-phase in August-October and they cancel each other.

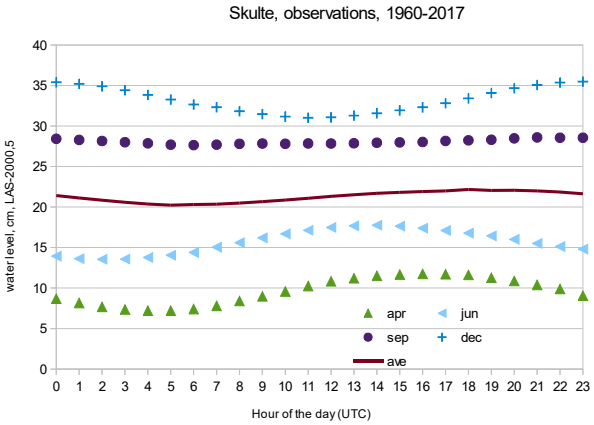

Figure 5. Daily variations of observed water level at various moths in Skulte station.

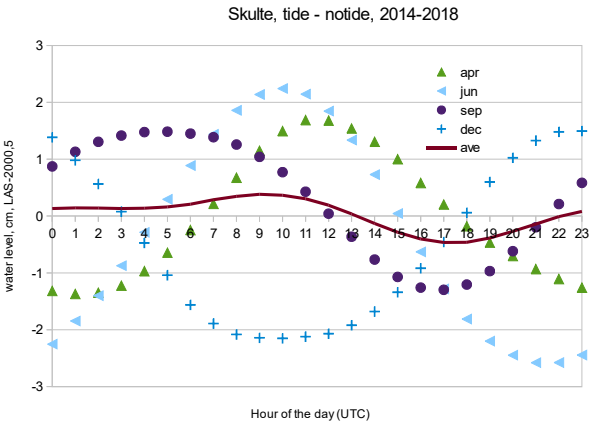

Figure 6. Daily variations of water level caused by gravitational tides in Skulte station.

References

Otsmann M., U. Suursaar, T. Kulla (1999) Modelling currents along the western coast of Estonia as superposition of Helmholtz oscillators. Transactions on the Built Environment, Vol. 40

Keruss M., J. Seņņikovs (1999) Determination of tides in Gulf of Riga and Baltic Sea. Proc. International Scientific Colloqium 'Modelling of Material Processing', Riga

Müller M. (2012) The influence of changing stratification conditions on barotropic tidal transport and its implications for seasonal and secular changes of tides, Continental Shelf Research, Vol. 47, pp. 107–118

Ray R.D., G.D. Egbert (2004) The Global S_1 Tide. Journal of Physical Oceanography, Vol. 34, pp. 1922-1935

Rabinovich A., I. Medvedev (2015) Radiational Tides at the Southeastern Coast of the Baltic Sea, Oceanology, Vol. 55, No. 33pp.3333xxx333319319–326 319–326 319–326

Modeling patchiness on the sea surface caused by the interplay of winds and currents in the Gulf of Finland

Andrea Giudici[1], Jaan Kalda[1] and Tarmo Soomere[1,2]

[1] Department of Cybernetics, School of Science, Tallinn University of Technology, Tallinn, Estonia (andrea@cens.ioc.ee)
[2] Estonian Academy of Sciences, Tallinn, Estonia.

1. Introduction

Marine ecosystems in the World Ocean generally show high heterogeneity of physical, biological and chemical quantities. Clusters (or "patches" as defined in, e.g., Kononen et al., 1992; Levin, 1994; Grünbaum, 2012) of substance in the ocean are among the most frequent observed phenomena in oceanography and may be caused by a multitude of different dynamic mechanisms (e.g., Giudici and Soomere, 2014).

Several phenomena, often stemming from the interplay of different drivers (e.g., Vucelja et al., 2007), may significantly augment the mechanisms of patch formation, and therefore the clustering rate of, e.g., floating litter.

In real-world conditions, floating patches are occasionally built of particles that can interact with each other (e.g., oil slicks or plastic debris). Their motion is affected by different ocean drivers such as currents, waves and wind (Kalda, 2007). Moreover, the behaviour of a parcel or an existing patch may depend on its size. The resulting relative motions of patches eventually lead initially separated clusters to collide.

We make an attempt to model the behaviour of initially separated patches, carried by currents and winds, and allowed to collide with each other. It is usually thought that advection by converging currents leads to the development of patches of different size. Wave or wind drag alone is normally not able to significantly contribute to the patch formation or growth (e.g., Vucelja et al., 2007). However, as the wind drag may depend on the size of a patch (e.g., via its extension over the sea surface or different surface roughness), the resulting variability in the drift speed may enhance the overall clustering rate.

To investigate the joint effect of the current-driven advection of patches and the potential difference in the wind drag for patches of different size, we built a novel numerical model that is able to simulate clustering of pollution patches floating on the sea surface.

The model was fed with data from the Gulf of Finland where areas of rapid clustering often occur (Giudici and Soomere, 2014). We focus on the increase rate of the size of the patches, specifically in terms of the final distribution of the size of patches developed from an initially uniform field of patches impacted by size-dependent wind-drag.

2. Methods and data

We make use of the 1987 subset of surface velocity data extracted from the long-term simulations of circulation in the Gulf of Finland (Figure 1) performed with the OAAS hydrodynamic model (Andrejev and Sokolov, 1989) forced with adjusted geostrophic wind fields. The spatial resolution of the model and the wind forcing data is 1 nautical mile and about 15 nautical miles, respectively.

At the beginning of each simulation, one circular patch (of a varying initial radius of 50–300 m) is placed at a random position of each wet grid cell. It is assumed that the patch is always floating on the sea surface. The model simulates the relocation of the patches under the combined effect of winds and currents and resolves their reciprocal collisions

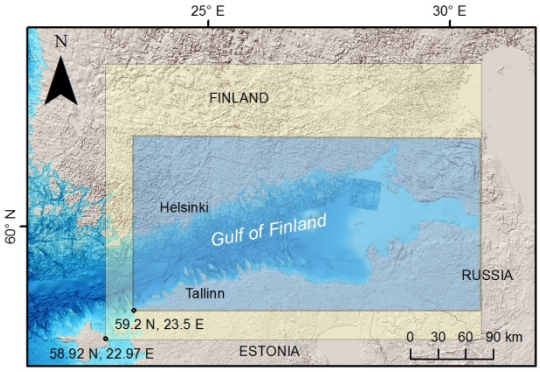

Figure 1. Study area in the eastern Baltic Sea. The light blue and yellow rectangles shows the coverage of data sets of currents and winds, respectively.

We use a maximally simple method (an Euler-type Runge-Kutta first-order method) for the tracking the patches. The model evaluates at each time step their coordinates, radius, and vertical cross-sectional area. The radius and cross-sectional area only changed via collisions of the patches. When the distance between the patches was smaller than the sum of their radii, the patches were merged into one, with the location of the larger one and the surface area as the sum of the areas of the two patches.

3. Properties of patchiness

We ran the model across a number of simulations spanning over four calendar months. For each simulation, the set of floating patches was tracked for three days using a time step of three hours. In different simulations we varied the initial patch size and wind properties.

The resulting distributions of the frequency of occurrence of patches of different size in all cases roughly follow a stretched-exponential power law $f(x) = A\exp(-\alpha x^B)$ (Figure 2). The values A and B depend on the initial set-up and particular forcing but the overall shape of the limiting distribution apparently is universal.

In order to quantify the impact of wind speed (equivalently, the contribution of differential drift speed on the collisions of patches) on the distribution of the frequency of occurrence of patches of different size, we varied the wind drag coefficient by up to ±50%. This variation led to drastic changes in the parameters of the distributions of the frequency of occurrence of patches of

different size. The qualitative shape of this distribution remained basically invariant with respect to the described variation but the time during which the limiting distribution was formed varied markedly.

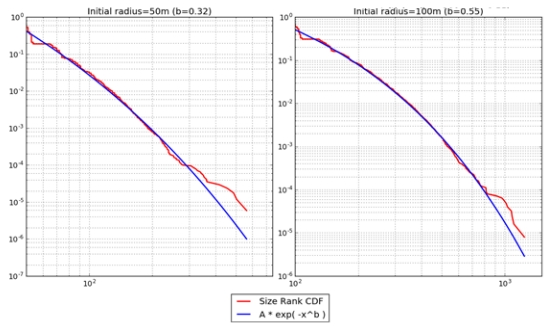

Figure 2. The cumulative distribution function of the probability of occurrence of patches of different size for the initial patch size of 50 m and 100 m.

One the one hand, when the wind drag is reduced by a factor of 2, the final maximal patch size is much larger compared to the case when the wind drag is neglected but also much smaller compared to the case with the reference level of wind drag.

On the other hand, the impact of wind drag on enhancing the collisions seems to reach a sort of saturation when the drag strength is increased by a factor of 1.5. It is still likely that this saturation level is not a universal feature because the properties of collisions and the parameters of the final distribution depend on the initial density and mutual positioning of seeded patches, the size of the basin, and the duration of evolution.

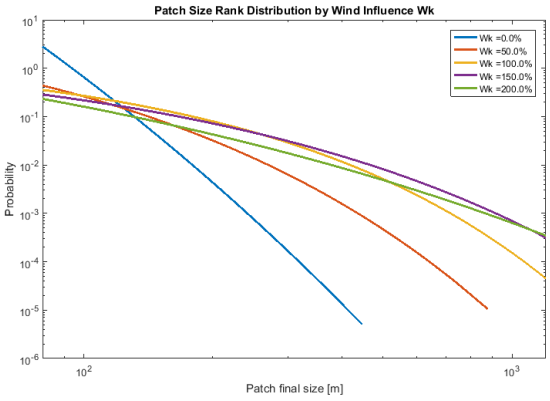

Figure 3. The cumulative distribution function of the probability of occurrence of different final patch sizes for different levels of wind-induced drift coefficient.

4. Discussion

Even though adequate representation of the drift of single parcels or patches is only possible for a limited time (Vandebulcke et al., 2009), many statistical properties of the dynamics of single parcels and pollution patches are adequately represented by a number of simulations in spite of major uncertainties in single trajectories (e.g., Viikmäe et al., 2013).

In this light it is likely that the presented statistical information reflects certain basic features of the potentially colliding patches on the sea surface. First of all, the differential impact of wind drag on patches with different properties may substantially increase the collision rate of current-advected patches even in the areas that often host converging currents and explosive patch formation regions. This kind of interaction of wind drag and current-driven advection may be the one of the driving forces behind the formation of large patches of litter on the sea surface.

Interestingly, the qualitative shape of the resulting distribution of the frequency of occurrence of patches of different size seems to be universal. All such distributions follow a stretched exponential law. The parameters of this distribution and the time it takes for this distribution to build up depend on certain patch properties. An increase in the strength of wind drag results in a faster formation of large patches as well as in an increase in the average final size of the simulated patches.

5. Acknowledgements

This work was done with the support of the Estonian Ministry of Education and Research (Grant IUT33-3), the ERA-NET+RUS EXOSYSTEM (grant ETAG16014), the ERA-NET FLAG-ERA project FuturICT2.0 (grant ETAG17089) and the Estonian Research Infrastructures Roadmap object „Infotechnological Mobility Observatory (IMO)“, funded by European Regional Development Fund. Thanks to O. Andrejev and A. Sokolov for providing the model data.

References

Andrejev, O. and Sokolov, A. (1989). Numerical modelling of the water dynamics and passive pollutant transport in the Neva inlet. Meteorology and Hydrology, 12, pp. 75–85 (in Russian).

Giudici, A. and Soomere, T. (2014). Finite-time compressibility as an agent of frequent spontaneous patch formation in the surface layer: A case study for the Gulf of Finland, the Baltic Sea. Marine Pollution Bulletin, 89, pp. 239–249.

Grünbaum, D. (2012). The logic of ecological patchiness. Interface Focus, 2(2), pp. 150–155.

Kalda, J. (2007). Sticky particles in compressible flows: Aggregation and Richardson's Law. Physical Review Letters, 98, Art. No. 064501.

Kononen, K. and Nõmmann, S. (1992). Spatio-temporal dynamics of the cyanobacterial blooms in the Gulf of Finland, Baltic Sea. In: Carpenter, E.J.; Capone, D.G., and Rueter, J.G. (eds.), Marine Pelagic Cyanobacteria: Trichodesmium and other Diazotrophs. NATO ASI Series, vol. 362. Springer, Dordrecht, pp. 95–113.

Levin, S.A. and Whitfield, M. (1994). Patchiness in marine and terrestrial systems: from individuals to populations. Philosophical Transactions of the Royal Society of London B: Biological Sciences, 343(1303), pp. 99–103.

Vandenbulcke, L., Beckers, J.-M., Lenartz, F., Barth, A., Poulain, P.-M., Aidonidis, M., Meyrat, J., Ardhuin, F., Tonani, M., Fratianni, C., Torrisi, L., Pallela, D., Chiggiato, J., Tudor, M., Book, J.W., Martin, P., Peggion, G., and Rixen, M. (2009). Super-ensemble techniques: Application to surface drift prediction. Progress in Oceanography, 82, pp. 149–167.

Viikmäe, B., Torsvik, T., and Soomere, T. (2013). Impact of horizontal eddy-diffusivity on Lagrangian statistics for coastal pollution from a major marine fairway. Ocean Dynamics, 63(5), pp. 589–597.

Vucelja, M., Falkovich, G., and Fouxon, I. (2007). Clustering of matter in waves and currents. Physical Review E, 75(6), Art. No. 065301 Part 2.

Distinctive features of surface circulation in the southeastern part of the Baltic Sea by subsatellite oceanographic experiments held in 2014-2017.

Evgeny V. Krayushkin, Olga Yu. Lavrova and Ksenia R. Nazirova

Space Research Institute RAS, Moscow, Russia (box_evk@mail.ru)

1. Introduction

During the period 2014-2017 in summer months Space Research Institute held oceanographic experiments in the southeastern part of the Baltic Sea along the coastline of Kaliningrad Region of Russia. The main aim of the work was to provide comprehensive in situ oceanographic data to describe spatial and temporal features of the surface circulation patterns determined by remote sensing data.

2. Data

The work is primarily based on remote sensing data being a first step to determine circulation patterns on the sea surface. Figure 1 shows a color composite image by Landsat-8 OLI on July 07, 2014 showing an array of dynamic processes clearly seen by satellite data (Lavrova et al., 2016).

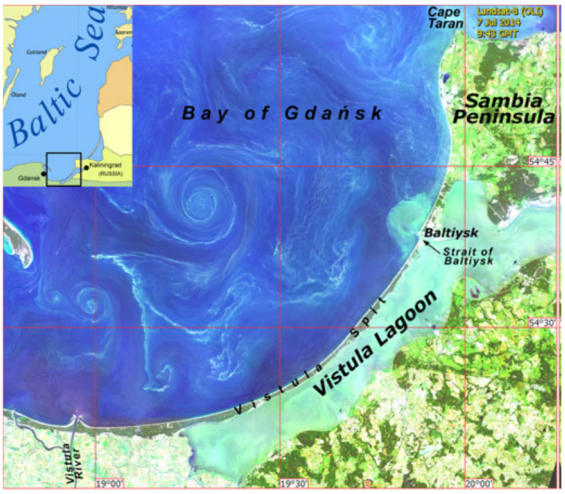

Figure 1. Landsat-8 OLI color composite image with an array of different processes determined on the sea surface.

During the work we could analysis different types of remote sensing data including color composite images from Terra/Aqua MODIS, Landsat-7,8; MSI Sentinel 1,2 and radar images from Radarsat-2.

Oceanographic experiments included different methods to determine ocean currents: more than 20 ship mounted ADCP (Acoustic Doppler Current Profiler) transects were done in the coastal zone of the Baltic sea to the depths up to 80 m. 9 lagrangian drifters with GPS positioning kit and GSM telemetry channel were launched offshore Kaliningrad region simultaneously with ADCP survey. Thermohaline structure was determined with the use of modern CTD instrument with additional turbidity and CHL-a fluorescence sensors. Meteorological conditions during experiments were determined with the use of a ship mounted meteorological station.

3. Results

The influence of wind and hydrodynamic processes on the spreading of turbid waters from the Vistula Lagoon into the Baltic Sea was studied. We found out that in certain wind conditions, the lagoon waters can propagate long distances from the Baltiysk Strait mouth both northeast. We managed to track from ocean color data the spreading of the lagoon water over the Bay of Gdansk for over two weeks in late July—early August 2014 in almost cloudfree weather conditions. Because optical properties of the lagoon water were quite distinct from those of the open sea due to intense cyanobacteria blooming, the outflow stream was very well visualized even in satellite Terra/Aqua MODIS images of 250 m pixel size. Along with satellite observations, in-situ measurements were conducted aimed at verifying satellite data as well as deducing the three-dimensional structure of the stream.

In 2014, we managed to detect and describe a complex dynamic vortex structure near Cape Taran (figure 2). An eddy propagated to the depth of 20 m and had a linear scale of ~ 25 km. This vortex structure was identified using Radarsat-2 images and optical data, obtained by OLI Landsat-8, ETM+ Landsat-7, Modis Terra/Aqua and confirmed by ADCP data (Lavrova et al., 2016).

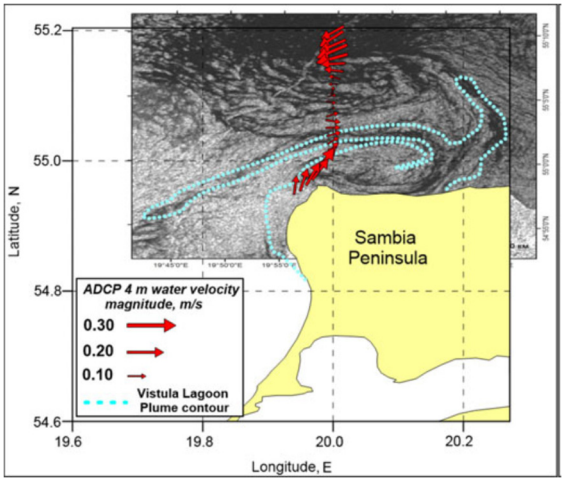

Figure 2. Vortex dipole formed in the coastal zone at the Cape Taran.

Set of lagrangian drifters launched in the study area showed the variability of surface circulation from year to year and could determine main physical processes influenced the nature of this variability. Drifter trajectories got in 2016 showed that circulation during the oceanographic experiment was primarily formed by winds. During the campaign drifter travelled long distance and its trajectory was complicated with inertial oscillations, sharp turns.

In 2015 drifters launched in the same area travelled within a very localized region during a week. As it was shown the drift was influenced by a vortex dipole structure formed offshore and clearly determined on Landsat and MSI remote sensing data (Golenko et al., 2017).

Acknowledges

The scientific project was supported by grant of Russian Science Foundation № 14-17-00555.

References

Lavrova Olga; Krayushkin Evgeny; Golenko Maria; Golenko Nikolay (2016) Effect of Wind and Hydrographic Conditions on the Transport of Vistula Lagoon Waters Into the Baltic Sea: Results of a Combined Experiment, IEEE Journal of Selected Topics in Applied Earth Observations and Remote Sensing, Vol. 9, Issue 9, DOI 10.1109/JSTARS.2016.2580602

M.N. Golenko, E.V. Krayushkin, O.Yu. Lavrova (2017) Investigation of coastal surface currents in the South-East Baltic based on concurrent drifter and satellite observations and numerical modeling, Sovremennye problemy distantsionnogo zondirovaniya Zemli iz kosmosa, Vol. 14, No. 7, pp. 280-296 (in Russian, abstract in English).

Modeling of internal waves in the Baltic Sea

Andrey Kurkin[1], Oxana Kurkina[1], Efim Pelinovsky[1], Ekaterina Rouvinskaya[1]

[1]Nizhny Novgorod State Technical University n.a. R.E. Alekseev, Nizhny Novgorod, Russia (aakurkin@gmail.com)

1. Introduction

The main mechanism for the generation of internal waves in the ocean is the interaction of the barotropic tide with the uneven relief of the bottom. The Baltic Sea is a shallow shelf sea with predominant depths from 40 to 100 m and is practically non-tidal (Alenius et al. (1998)). However, even in such seas there are mechanisms for generating intense internal waves. So, for example, they can be generated during the course of active dynamic processes associated with the emergence and relaxation of coastal upwelling and downwelling, vortices of various scales, surge phenomena, oscillations of hydrological fronts, and so on. In Mityagina et al. (2010), Lavrova et al. (2010), satellite observations of surface manifestations of internal waves in seas without tides are summarized. Packages of internal waves in the Baltic Sea are clearly visible on satellite photographs on the Space Research Institute website (http://iki.rssi.ru/asp/iw_images/index.html#baltic).

The active use of wind power plants, oil platforms and pipelines running along the seabed in the Baltic Sea forces us to take a fresh look at the problems of redistribution of sediments and the dynamics of erosion near subsea parts of hydraulic structures. Influence of internal waves in the greater part determines this dynamics, which can lead to the formation of unstable states of hydraulic structures and, as a consequence, to an increase in the risk of anthropogenic disasters in the coastal zone. Therefore, the development of methods for modeling and analyzing of internal wave regimes and their corresponding velocity and pressure fields for developing recommendations for assessing safety and improving hydraulic structures becomes particularly relevant.

In the present paper we give a review of observations of the internal wave manifestations in the Baltic Sea and simulate the transformations of internal solitary waves along some vertical sections in the Baltic Sea.

2. Observations of internal waves in the Baltic Sea

Since the stratification of the Baltic Sea is stable, internal waves must be a common feature there, even though the number of studies into such waves is relatively small (Leppäranta and Myrberg (2009)). Several kinds of internal waves can exist in this water body because of the variety of forcing factors and the complexity of its bathymetry. The relevant field data are limited. In the existing studies the generation of internal waves in the Baltic Sea is mainly explained by the strong winds (Axell (2002)) and the radiation of barotropic intertial waves passing stratified water on a sloping bottom and generating baroclinic inertial waves, and they, in turn, cascade energy into small-scale internal waves (Feistel et al. (2008), Van der Lee and Umlauf (2011)).

Tidal oscillations of the Baltic Sea level are extremely small: from 4 cm (Klaipeda) up to 10 cm in some sections of the Gulf of Finland (Alenius et al. (1998)). The associated current speed, however, cannot be neglected. It reaches about 10 cm/s in the middle of the Gulf of Finland (Lilover (2012)) but still remains much below the level of motions driven by internal waves.

Generation of internal waves in microtidal seas is possible due to several other dynamic processes such as the development and relaxation of coastal upwelling, vortices of different scales, surge phenomena, oscillations of hydrological fronts, etc. Several studies are devoted to in situ observations and numerical modelling of the generation and propagation of short-period internal waves in microtidal and nontidal seas, based on experimental data obtained by contact probes (Ivanov et al. (1987), Vlasenko et al. (1998), Ivanov and Lisichenok (2002)).

In Lavrova et al. (2010) one can find 11 events of surface manifestations of internal waves in the Baltic Proper and in the Gulf of Bothnia and 12 events detected in the Danish Straits in 2009–2010. Internal waves in the Danish Straits are generated by tides. The number of waves in the trains usually was not more than 10, maximal wavelength did not exceed 1 km, and the length of the leading wave front was less than 25 km. In July 2010 surface manifestations of internal waves were periodically detected in the southern part of the Gulf of Bothnia and to the north and north-west of Gotland.

In situ measurements in the Baltic Sea show fluctuations in current velocities and motions of isotherms on different timescales (Leppäranta and Myrberg (2009)). Periods of 1–30 min have been observed in the Kiel Bight, while periods of 5–6 h have been reported from the Gulf of Finland, the Arcona Basin and the Darss Sill area. The largest changes are usually found at the pycnocline. When there is both a thermocline and a halocline, two internal wave structures can be observed in the resulting three-layer medium.

Cyclones providing winds of 10−15 m/s in the Baltic Sea cause the generation of internal waves with amplitudes of 11–15 m. The associated current velocities in the upper layer are about 11–15 cm/s and in the lower layer about 5–8 cm/s (Chernysheva (1987)). The characteristics of internal waves and internal seiches measured in the Baltic Sea are given in Kol'chitskii et al. (1996), Golenko and Mel'nikov (2007). In particular, internal waves with periods of 0.1–1 h, observed in the central part of the Gotland Deep formed internal wave trains with duration of several hours and current amplitudes of about 3 cm/s. Internal waves in the inertial frequency range can induce currents reaching 20 cm/s.

All available data on internal waves in the Baltic Sea were collected, systematized and structured. The resulting database includes: graphical display of information, the possibility of replenishing data and searching by various parameters, export of bibliographic data. The database is integrated into an electronic atlas (http://lmnad.nntu.ru/ru/projects/igwatlas_online/).

3. Solitary internal wave evolution in the Baltic Sea

It is feasible to derive examples of possible internal solitary wave transformations in the Baltic Sea from the existing databases. The hydrological data for the sections to set up the model are taken from the GDEM V.3.0 database for July. We used classic weakly nonlinear model for inhomogeneous medium, described in details, for example, in Kurkina et al. (2017). The sections are choosen so as to show changes of signs for nolinear coefficients (passage through critical points). As the Baltic Sea is an almost nontidal sea and does not host major jet-like currents with substantial horizontal or vertical shear (Leppäranta and Myrberg (2009)), the direction of internal wave propagation depends almost entirely on the source of their generation listed in Sections 1, 2 and on refractive properties of bathymetry. Therefore a large variety of paths of internal wave propagation in the Baltic Sea may exist, and we are not limited in the choice of sections for the modelling. Furthermore, each transformation of an internal solitary wave can be inverted to demonstrate the possibility of a reverse metamorphosis: focusing of a wave train into an internal solitary wave.

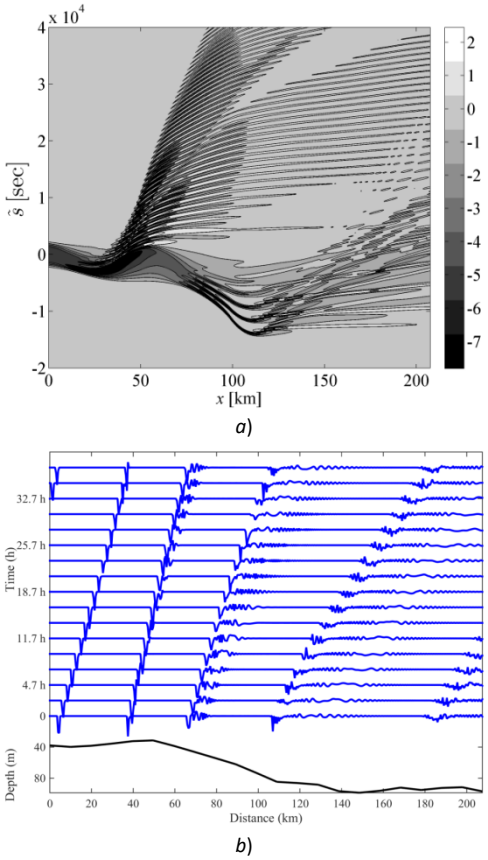

Figure 1. *a* - Contour plot in the space-time domain of a internal solitary wave; *b* - Transformation of an internal solitary wave (the vertical shift between successive curves is 5 m)

The numerical results of simulations for internal wave propagation are shown in Figs. 1. The complex behaviour of internal waves can be observed there, including adiabatic adjustment, wave amplification, transformation of a wide solitary wave into a sequence of narrow ones, change of their polarity, appearance of multiple breather-like disturbances and radiation of oscillatory dispersive tails of small amplitude. All of these nonstationary and nonlinear effects developed due to the inhomogeneity of the environment lead to the formation of complex field of internal wave-induced currents, which can be easily reconstructed and further used as an input for models of the near-bottom boundary layer, as well as for advective-diffusive models of pollution dynamics.

The numerical modeling within this study was carried out in the framework of the grant of Russian Science Foundation (project No. 16-17-00041).

References

Alenius P., Myrberg K., Nekrasov A. (1998) The physical oceanography of the Gulf of Finland: a review, Boreal Env. Res., Vol. 3, pp. 97-125.

Mityagina M.I., Lavrova O.Yu. (2010) Satellite observations of surface manifestations of internal waves in non-tidal seas, Modern problems of remote sensing of the Earth from space, Vol. 7, No. 1, pp. 260-272.

Lavrova O.Yu., Karimova S.S., Mityagina M.I., Bocharova T.Yu. (2010) On-line satellite monitoring of the aquatories of the Black, Baltic and Caspian Seas in 2009 – 2010, Modern Problems of Remote Sensing of the Earth from Space, Vol. 7, No. 1, pp. 168-185.

Leppäranta M., Myrberg K. (2009) Physical oceanography of the Baltic Sea. Praxis, Berlin, Heidelberg, New York: Springer.

Axell L. (2002) Wind-driven internal waves and Langmuir circulation in a numerical ocean of the Baltic Sea, J. Geophysical Research, Vol. 107(C1), pp. 3204-3218.

Feistel R., Nausch G., Wasmund N. (Eds.) (2008) State and evolution of the Baltic Sea, 1952-2005: a detailed 50-year survey of meteorology and climate, physics, chemistry, biology, and marine environment, John Wiley & Sons, Inc..

Van der Lee E.M., Umlauf L. (2011) Internal wave mixing in the Baltic Sea: near- inertial waves in the absence of tide, J. Geophysical Research, Vol. 116, pp. C10016-1-16.

Lilover M.-J. (2012) Tidal currents as estimated from ADCP measurements in „practically non-tidal" Baltic Sea, In: Proceedings of the IEEE/OES Baltic 2012 International Symposium "Ocean: Past, Present and Future. Climate Change Research, Ocean Observation & Advanced Technologies for Regional Sustainability," May 8–11, Klaipėda, Lithuania, IEEE; pp. 4.

Ivanov V.A., Lisichenok A.D., Nemirovsky M.S. (1987) Excitation of short-period internal waves by wind pulsations, Izvestiya - Atmospheric and Ocean Physics, Vol. 23, No. 2, pp. 179-185.

Vlasenko V.I., Ivanov V.A., Krasin I.G., Lisichenok A.D. (1998) The generation of intensive short-period internal waves in the frontal zone of a coastal upwelling, Phys. Oceanogr., Vol. 9, Iss. 3, pp. 155-168.

Ivanov V.A., Lisichenok A.D. (2002) Internal waves in the shelf zone and near the shelf edge in the Black Sea, Phys. Oceanogr., Vol. 6, pp. 353-360.

Chernysheva E.S. (1987) On the modeling of long internal waves, In: Davidan, I.N. et al. (eds.), Problems of the Studies and Mathematical Modeling of the Baltic Sea Ecosystem. Modeling of the Ecosystem Components Issue No. 3, Leningrad, Gidrometeoizdat, pp. 50-54.

Kol'chitskii N.N., Monin A.S., Paka V.T. (1996) On internal seiches in the deep Baltic Sea, Doklady Akademii Nauk, Vol. 346, No. 2, pp. 249-255.

Golenko N.N., Mel'nikov V.A. (2007) Estimation of spatio-temporal parameters of the internal wave field in the Southwest Baltic Sea using data by towed probe. Scientific reports of the Russian Geographic Union (Kaliningrad branch), Russian State Univ., Kaliningrad, Vol. 5, pp. C1–C4.

Kurkina O., Rouvinskaya E.,Talipova T.,Soomere T. (2017) Propagation regimes and populations of internal waves in the Mediterranean Sea basin, Estuarine, Coastal and Shelf Science, Vol. 185, pp. 44-54.

Observations, modeling and analysis of internal gravity waves in Sea of Okhotsk

Oxana Kurkina[1], Andrey Kurkin[1], Ekaterina Rouvinskaya[1] and Ayrat Giniyatullin[1]

[1]Nizhny Novgorod State Technical University n.a. R.E. Alekseev, Nizhny Novgorod, Russia (Oksana.Kurkina@mail.ru)

1. Introduction

Internal waves play a special role in the functioning of ecosystems of seas and oceans. They enhance mixing of water masses, induce the processes of resuspension and transport of bottom sediments (Bourgault et al. (2014)), and also influence the distribution of nutrients, and, consequently, the biological productivity of the seas (Pan et al. (2012)). The propagation and breaking of internal waves often contributes to the formation of strong currents, which pose a serious danger to underwater parts of hydraulic structures (see, for example, Osborne (2010)). The presence of internal waves changes the local density field and, consequently, transforms the modes of propagation of acoustic waves through water masses (Warn-Varnas et al. (2009), Rutenko (2010)).

The main mechanism for the generation of internal waves - the interaction of a barotropic tidal wave with an uneven bottom - is most clearly manifested in the shelf zone of marginal seas, contributing to the formation of intense soliton-like formations. This is evidenced by the data of numerous satellite observations of such wave structures, including those in the investigated Far Eastern region (Jackson (2004)). The processes of active generation of internal waves in the Sea of Okhotsk are also confirmed by field observations. On the basis of experimental data, it was shown in Refs. Nagovitsyn and Pelinovsky (1988), Nagovitsyn et al. (1991), that the generated solitary internal waves can have amplitudes from 5 to 15 m and a length on the order of 200-400 m.

Accordingly, it is difficult to overestimate the role of internal waves in the hydrophysical, biological, ecological, morphological and geophysical processes in the Sea of Okhotsk. But despite the active economic activity in this region, which is connected with the development of hydrocarbon fields and with the fishing of seafood, internal waves here are still insufficiently studied.

2. Hydrodynamic models for describing internal waves

At present, the solution of most problems in fluid mechanics reduces to the direct numerical integration of the systems of Navier-Stokes or Euler equations using special software. There is a fairly large number of software complexes implementing this procedure, however, their use for specific tasks is not trivial: it is necessary to adapt these software products to the tasks of a particular study.

To simulate the nonhydrostatic dynamics of water masses, including processes of generation and transformation of internal waves, we use the software complex IGW Research (Tyugin et al. (2012)) to numerically integrate the fully nonlinear two-dimensional (vertical plane) system of hydrodynamic equations for non-viscous incompressible stratified fluid in the Boussinesq approximation, taking into account the generating effect of the barotropic tide and rotation of the Earth.

Another class of models describing evolution of internal waves is based on the application of the weakly nonlinear evolution equations of the KdV (Korteweg-de Vries) family. For a horizontally inhomogeneous medium, the Gardner equation with variable coefficients has already became classical for this type of studies (see, for example, Holloway et al. (1997), Grimshaw et al. (2010), O'Driscoll and Levine (2017)). Equations of this class contain parameters determined by the properties of the medium (sea water density field), analysis of these parameters allows one to determine the influence of individual factors on the formation of specific regimes of nonlinear wave motions.

3. Mapping of kinematic and nonlinear parameters of internal waves of the first and second modes for the Sea of Okhotsk

For the development of maps of kinematic and nonlinear characteristics of internal wave fields within the framework of weakly nonlinear models (playing the same role as the bathymetric maps for surface waves) data were used from the international climaticological atlas GDEM (Generalized Digital Environment Model) v. 3.0, which are monthly averaged data on temperature and salinity for 77 levels in depth and with a horizontal resolution of 1/2º for the ocean and 1/6º for most marginal seas.

Vertical structure (linear baroclinic mode) of internal wave field and depending on it coefficients of the Gardner equation for the particular nonlinear wave mode are determined by the solution of the eigenvalue and boundary value problems and can be easily calculated numerically on a basis of known vertical density profiles. We have constructed maps of kinematic and nonlinear parameters of internal waves of the first and second modes for the Sea of Okhotsk.

The alternation of the regions of positive and negative values of the quadratic and cubic nonlinearity coefficients on these maps indicates a wide variety of wave regimes for internal waves of both modes. It is also worth noting that, closer to the coastal zone in the Sea of Okhotsk, the coefficient of cubic nonlinearity of the second mode has predominantly negative values, and this fact theoretically excludes the possibility of generation of second-mode breathers in these regions.

4. Transformation of the baroclinic tidal wave along the transect in the Sea of Okhotsk

To simulate the transformation of a baroclinic tidal wave along a vertical section of 150 km in the Sea of Okhotsk (Fig. 1, incut), we used a model based on the Gardner equation with variable coefficients (for the lowest mode). A detailed description of the model can be found, for example, in Kurkina et al. (2017). The hydrological data for the calculations are taken from the GDEM V 3.0

atlases for July and January. Throughout the chosen path the coefficient of cubic nonlinearity in July is positive, and the quadratic nonlinearity coefficient is negative, so the existence of solitary waves of both positive and negative polarity is possible. On the contrary, for the conditions of January, the emergence of solitary waves of only negative polarity is possible. However, in both cases, for both summer and winter hydrological conditions, the disintegration of the tidal sinusoid leads to the formation of solibores with negative solitons at the front.

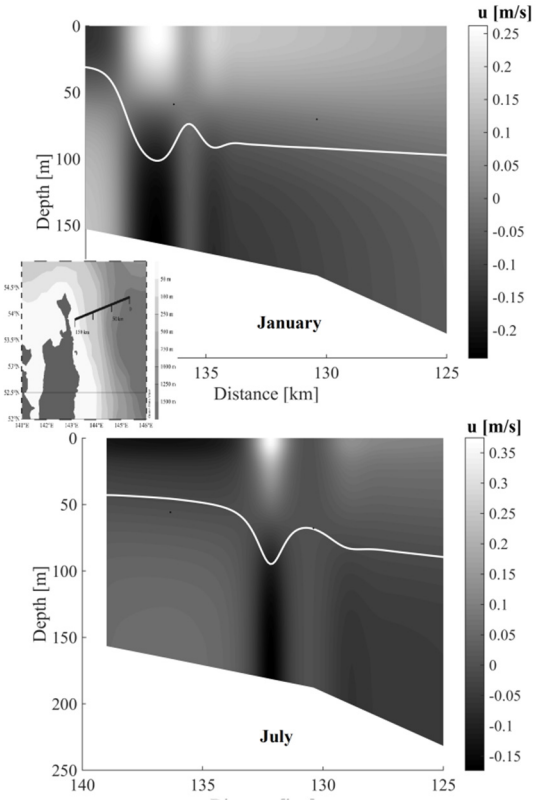

Figure 1. The horizontal velocity of neutral particles during the propagation of internal waves along the transect on the north-east shelf of the Sakhalin Island; white lines indicate maximal isopycnal displacements (upper panel – for January hydrological conditions, lower panel – for those in July). Geographic location of the transect is shown in the incut.

In the process of transformation of the wavefield, a complex flow induced by internal waves is formed (Fig.1), which can be used, for example, to calculate loads on underwater parts of hydraulic structures. To estimate the dynamic loads acting on the vertical cylindrical supports on the on-shore boundary of the transect, Morison's formula was used. In the considered case, the bending moment in the middle of the tidal cycle reaches values of the order of $2 \cdot 10^6$ N·m.

This study was initiated in the framework of the state task programme in the sphere of scientific activity of the Ministry of Education and Science of Russian Federation (projects No.5.4568.2017/6.7 and No. 5.1246.2017/4.6) and with the financial support of the grants of the President of the Russian Federation for state support of leading scientific schools of the Russian Federation (NSH-2685.2018.5) and young candidates of sciences of the Russian Federation (МК-1124.2018.5).

References

Bourgault D., Morsilli M., Richards C., Neumeier U., Kelle D.E. (2014) Sediment resuspension and nepheloid layers induced by long internal solitary waves shoaling orthogonally on uniform slopes, Continental Shelf Research, Vol. 72, pp. 21-33.

Pan X., Wong G.T. F., Shiah F.-K., Ho T.-Y. (2012) Enhancement of biological productivity by internal waves: observations in the summertime in the northern South China Sea, Journal of Oceanography, Vol. 68, pp. 427-437.

Osborne A.R. (2010) Nonlinear Ocean Waves and the Inverse Scattering Transform. Elsevier, San Diego, 944 p.

Warn-Varnas A., Chin-Bing S.A., King D.B., Hawkins J., Lamb K. (2009) Effects on acoustics caused by ocean solitons, Part A. Oceanography, Nonlinear Analysis, Vol. 71, pp. e1807-e1817.

Rutenko A.N. (2010) The influence of internal waves on losses during sound propagation on a shelf, Acoustical Physics, Vol. 56, pp. 703-713.

Jackson C.R. (2004) An Atlas of Internal Solitary-like Waves and Their Properties. Prepared for Office of Naval Research, Code 322 PO. Global Ocean Associates, 560 p.

Nagovitsyn A.P., Pelinovsky E.N. (1988) Observations of solitons of internal waves in the coastal zone of the Sea of Okhotsk, Meteorology and Hydrology, No. 4, pp. 124-126.

Nagovitsyn A.P., Pelinovsky E.N., Stepanyants Yu.A. (1991) Observation and analysis of solitary internal waves in the coastal zone of the Sea of Okhotsk, Soviet Journal of Physical Oceanography, No. 2, pp. 65-70.

Tyugin D., Kurkin A., Pelinovsky E., Kurkina O. (2012) Increase of productivity of the program complex for modeling of internal gravity waves IGW Research with the help of Intel® Parallel Studio XE 2013, Fundamentalnaya i prikladnaya gidrofizika, Vol. 5, No. 3, pp. 89-95.

Holloway P., Pelinovsky E., Talipova T., Barnes B. (1997) A nonlinear model of internal tide transformation on the Australian North West shelf, J. Physical Oceanography, Vol. 27, pp. 871-896.

Grimshaw R., Talipova T., Pelinovsky E., Kurkina O. (2010) Internal solitary waves: propagation, deformation and disintegration, Nonlin. Processes Geophys., Vol. 17, pp. 633-649.

O'Driscoll K., Levine M. (2017) Simulations and observation of nonlinear internal waves on the continental shelf: Korteweg–de Vries and extended Korteweg–de Vries solutions, Ocean Sci., Vol. 13, pp. 749-763.

Kurkina O., Rouvinskaya E., Talipova T., Soomere T. (2017) Propagation regimes and populations of internal waves in the Mediterranean Sea basin, Estuarine, Coastal and Shelf Science, Vol. 185, pp.44-54.

Sea level change: mapping municipality needs for climate information

Kristine S. Madsen[1], Jens Murawsky[1], Jun She[1] and Peter L. Langen[1]

[1] Danish Meteorological Institute, Copenhagen, Denmark (kma@dmi.dk)

1. Introduction

Climate change will affect the coastline of the Baltic Sea through changes in sea level, storm surges and waves. In Denmark, a large part of the responsibility for climate adaptation lies with the local municipalities. In this study, we have mapped the user needs for coastal climate change information of five municipalities in the Køge Bay region – the south coast of Copenhagen – in the south western Baltic Sea (Figure 1). The mapping is a part of a C3S use case.

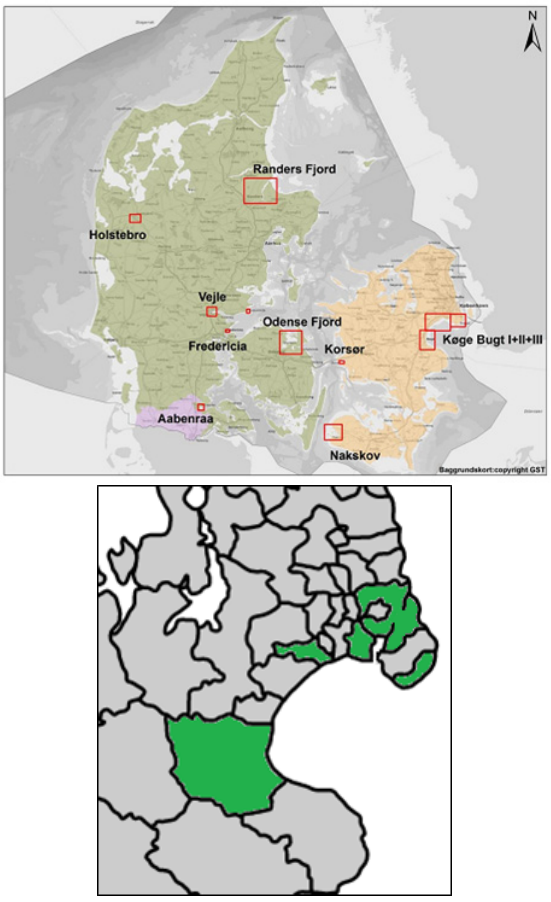

Figure 1. Top: map of the 10 flood prone areas of Denmark selected for the EU flood directive (Danish Coastal Authority, 2015). Bottom: zoom to Køge Bay, in green the five municipalities of Copenhagen, Dragør, Hvidovre, Ishøj and Køge.

2. Findings

The five municipalities include the central Copenhagen Municipality representing the Copenhagen historical, governmental and cultural capital centre and dense urban population, and suburban municipalities which also encompass rural areas and areas of natural and recreational interest.

The municipalities have access to extensive information on the population and infrastructure, as well as detailed geographical information.

The main interest is in very high quality storm surge warnings and projections of possible present day and future extreme sea level and wave heights for the detailed coastline, based on modelling of past storm surges and future changes, taking observations and historical records into account. There is a big wish for more detailed information than presently available (CRES 2014, Olesen et al., 2014), and for authoritative scenarios, which will help the collaboration between municipalities.

There were additional requests for indicators on runoff and groundwater, and especially their interaction with sea level changes and storm surges. However, this is outside the scope of the present study.

The municipalities generally relate to present day situations when discussing future climate change, and thus it will clearly make communication of climate change information, e.g. a future storm surge height indicator, easier if it can be presented in the same terms as used for present day storm surge warnings and statistics.

With regards to data formats, all municipalities are advanced users of GIS software and would like to integrate the climate information into their present systems, where many other layers of information is available.

The municipalities are generally aware of the need for uncertainty information, and are ready to handle uncertainties in the form of standard deviations, percentiles or upper- and lower bounds. The knowledge of ensembles is limited.

3. Targeted climate indicators

The next step will be to create targeted climate indicators, based on a downscaling of European scale storm surge and wave simulations to local scale. Based on the user interviews, the following indicators are planned for the region:

Mean Sea level change indicator: mean sea level change of selected reference periods, with and without local land rise.

Storm Surge indicator: Storm surge height, duration and frequency changes.

Gate index: Number of flood barriers closures per year and amount of time barriers are closed during an event.

Sea State (Waves) indicator: Changes in wave period, height and duration in a future climate, both for average conditions and high-sea level events, that is, the wave setup during storm surges.

Ocean current indicator: Strength and direction of average currents during normal and stormy conditions.

4. Outlook – The Danish Climate Atlas

This use case is designed to investigate needs and develop use of climate change information in the coastal region, based on European-wide data of the Copernicus Climate Change Service.

The work will further feed in to and support the newly financed Danish Climate Atlas, which will focus on developing authoritative climate change information for the Danish municipalities, among other things specifically on storm surges.

Acknowledgements

The work is performed as a part of the C3S_422_Lot2_Deltares contract on coastal climate change, for the Copernicus Climate Change Service. The Danish Climate Atlas is funded through the Danish law of finance.

References

Danish Coastal Authority (Kystdirektoratet), Danish Nature Agency (Naturstyrelsen) (2015) Risikostyringsplan for Vanddistrikt Sjælland (Risk management plan for water district Sjælland), Danish Coastal Authority, Lemvig, Denmark, ISBN no. 978-87-92124-01-2

Martin Olesen, Kristine S. Madsen, Carsten A. Ludwigsen, Fredrik Boberg, Tina Christensen, John Cappelen, Ole Bøssing Christensen, Katrine K. Andersen & Jens H. Christensen (2014) Fremtidige klimaforandringer i Danmark (Future Climate Change in Denmark), DKC report 14-06, Danish Meteorological Institute, Denmark, ISBN no. 978-87-7478-652-8

CRES (2014) Analyse af IPCC delrapport 2 – Effekter, klimatilpasning og sårbarhed (Analysis of IPCC report 2 – effects, climate adaptation and vulnerability), Danish Nature Agency (Naturstyrelsen), Copenhagen, Denmark, ISBN no. 978-87-7091-633-2

Validation of altimetry-derived regional sea level trends based on reconstruction of Baltic Sea 2D sea level of the last century

Kristine S. Madsen[1], Jacob L. Høyer [1], Jun She[1], Per Knudsen[2], Ülo Suursaar[3]

[1] Danish Meteorological Institute, Copenhagen, Denmark (kma@dmi.dk)
[2]DTU Space, Denmark
[3]University of Tartu, Estonia

1. Abstract

The satellite altimetry data record is now long enough to compute regional sea level trends, but can these products really be used in regions close to the coast?
The ESA Sea Level CCI product is developed based on open ocean altimetry data, and constitutes high quality monthly sea level variability and trend analysis for the open ocean. However, it is commonly used in the coastal zone and e.g. provided by MyOcean (now Copernicus Marine Service) to the European Environmental Agency for use in their Global and European sea level rise indicator for northern Europe (http://www.eea.europa.eu/data-and-maps/indicators/sea-level-rise-2/assessment). Here we assess the quality of the Sea Level CCI in the coastal zone of the Baltic Sea.
We validate the sea level variability using a 2D sea level field based on statistical modelling of monthly tide gauge observations and model reanalysis as reference. The sea level product was constructed for the EMODnet Baltic Sea Check Point. The statistical model is based on least squares regression and uses monthly mean tide gauge observations retrieved from PSMSL and model reanalysis from the Copernicus Marine Service, taking land rise information into account.
The reconstruction provides monthly mean sea level of the Baltic Sea in 10 km resolution during 1900-2014, and can reconstruct the variability of the Baltic Sea with an average correlation of 96% and RMS error of 3.8 cm to 56 independent tide gauges.
The validation against this independent source of sea level information allows assessing the quality of the CCI product approaching the coast, and can therefore be used to determine how close to the coast the Sea Level CCI can be considered reliable. The CCI sea level anomalies match reconstructed sea level variability of the southern open parts of the Baltic Proper with correlation above 90% and RMS difference below 6 cm. However, the coastal zone, areas with small islands or sea ice, and areas of high natural variability needs special treatment, and the increased uncertainty of these areas is not reflected in the trend error field provided in the present version if the Sea Level CCI.

On the water level measurements in the Gulf of Riga during 1961–2016

Rain Männikus[1], Tarmo Soomere[1,2] and Nadezhda Kudryavtseva[1]

[1] Wave Engineering Laboratory, Department of Cybernetics, School of Science, Tallinn University of Technology, Tallinn, Estonia (rain.mannikus@gmail.com)
[2] Estonian Academy of Sciences, Kohtu 6, Tallinn, 10130, Estonia

1. Introduction

The core input to all major coastal management and engineering projects such as construction of breakwaters, shore protections, channels and harbours is the statistics of water levels (Kamphuis, 2010). The relevant means, quantiles, extremes, distributions and trends can be evaluated from long-term water level measurements.

The largest contributions to water level extremes are usually provided by tides, storm surges (low atmospheric pressure and wind-driven surge), wave-induced set-up and site specific effects. Generally, it is assumed that contributions from different impacts to the total water level are basically independent. In this case it is possible to single out the signal of each mechanism and analyse it separately.

The situation is particularly complicated in locations that host substantial aperiodic variations in sea level at daily to monthly (subtidal) scales (Buschman et al., 2009). In the Baltic Sea such components have a typical time scale of a few weeks. Namely, sequences of storm cyclones travelling over the Danish straits often cause major changes to the water volume of the entire sea (Post and Kõuts, 2014). The local impact of storm surge is added to the elevated water levels. The resulting extremes may be further amplified by local effects (e.g. wave set-up) and basin geometry (e.g. when a relatively large water sub-basin has water levels higher than in the rest of the sea).

While most of the listed components are well studied for the Baltic Sea, the possible contribution to extreme water levels from the specific reaction of its sub-basins has not received proper attention. Similarly to the increase in the water volume of the entire sea, a temporary increase in the volume of its subbasins may lead to devastating coastal floodings. In particular, the Gulf of Riga or Curonian Lagoon may experience such events of excess water volume.

In this work we focus on the Gulf of Riga, a relatively large semi-enclosed water body connected to the Baltic Sea via comparatively narrow and shallow straits (Figure 1). The size of this gulf is about 130 × 140 km (Otsmann et al., 2001). It has a surface area of 17 913 km², a volume of 406 km³ and an average depth of about 23 m.

The main connection of the Gulf of Riga with the Baltic Sea proper is Irbe Strait that has a width of 27 km, a sill depth of about 21 m and a cross-sectional area of 0.37 km². The second outlet functions via Väinameri (Moonsund). These two sub-basins are connected by Suur Strait. The narrowest part of this strait is 4–5 km wide and the sill depth is about 5 m (Suursaar et al., 2002).

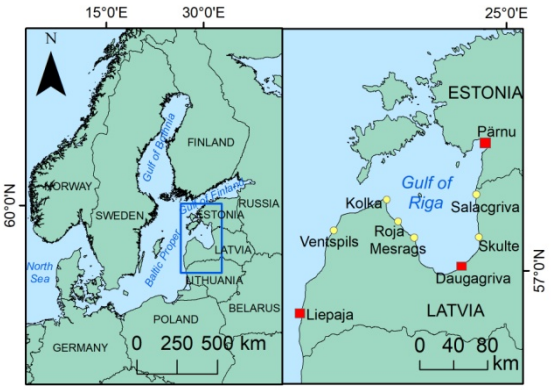

Figure 1. Water level measurement sites in the Gulf of Riga and on the open coast of Latvia. Red rectangles show locations with the highest quality and coverage of observations that are analyzed in this paper. Yellow circles depict stations where measurements were less frequent.

2. Data

We use observed hourly water level data from Latvian Environment, Geology and Meteorology Centre from 01.01.1961 till 31.12.2016 (Table 1). There are gaps and missing values since some stations recorded water levels 2 to 4 times a day. Based on data completeness, we focus on data from Liepaja, Daugavgriva and Pärnu. The uncertainties of recordings are estimated using the fact that the spectral density of water level time series in the Baltic Sea is flat (indicating random white noise properties) on timescales of ~<3 hrs (Medvedev et al., 2013). Using a running average with the window length of 3 hrs, we extracted the non-random signal and estimated measurement errors from the residuals. The Daugavgriva station showed uncertainty of individual measurements of ~0.7 cm, Liepaja ~1.2 cm, and Pärnu ~1.6 cm.

To evaluate the correlations of recordings in different stations, we first excluded the gaps. Not unexpectedly, the readings in all stations had a strong spatial correlation. The lowest values of this correlation showed sites in the ends

Tabel 1. Co-ordinates of measurement stations, water level parameters (Baltic Height System BK77) and data completeness

Location	Measurements since	Co-ordinates	Mean measured level (cm)	Max measured level (cm)	Min measured level (cm)	Hourly data completeness for 01.01.1961–31.12.2016
Daugavgriva	01.01.1875	57°3'22"N, 24°1'40"E	9.2	224	–107	99.98%
Kolka	01.01.1884	57°45'19"N, 24°21'10"E	1.3	161	–113	32.94%
Liepaja	28.07.1931	56°29'7"N, 21°1'32"E	1.9	174	–86	99.68%
Pärnu	(1893) 01.11.1949	58°23'12"N, 24°29'33"E	5.0	275	–121	99.54%
Salacgriva	01.01.1921	57°44'14"N, 22°35'33"E	5.7	215	–116	26.64%
Ventspils	01.01.1873	57°23'43"N, 21°32'3"E	0.9	141	–76	63.95%

of Gulf of Riga. For example, for Liepaja and Daugavgriva/Pärnu R = 0.845/0.890.

Some recordings seem erroneous. The highest value in Liepaja was recorded on 18.10.1967 at 2 am. The water level rose within 2 hrs from 60 cm to 174 cm, remained constant for 5 hrs and dropped in 1 hr to 100 cm. This course can be explained by the location of the measurement site in a narrow canal between a coastal lake and the sea. A measurement failure is also not excluded. As this constant value persisted for a relatively long time and water levels were high in Pärnu and Daugavgriva too, the values are not excluded from the analysis.

3. Methods and results

To identify the components of water level, we used a running average technique. The weekly-scale average reflects well the fluctuations in the entire Baltic Sea water volume (Figure 2). By subtracting this average from the total water level, we got a residual that can be interpreted as a proxy for the local wind-driven surge (Soomere et al., 2015). While the distributions of the total water level and its weekly-scale average were approximately Gaussian, the distribution of the residual was clearly different (Figure 2).

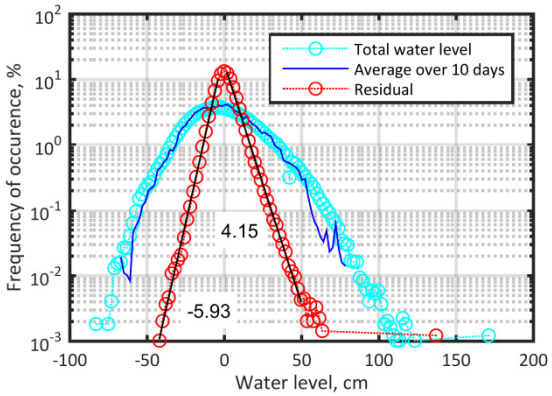

Figure 2. The frequency of occurrence of hourly measured water levels in Liepaja in 1961–2016 for the averaging interval of 240 hrs (10 days). Numbers at black lines indicate the scale parameter.

It is natural that the shape of the distribution of the residual and the number of outliers in the residual depend on the averaging interval. We searched the most suitable averaging interval by tracking the leading coefficient of a quadratic polynomial which fitted the positive or negative branch of the distribution of the residual in log-lin coordinates (Figure 2). If this coefficient vanishes, the distribution of the residual reduces to the exponential distribution (that, among other things, describes time intervals between events in a Poisson process).

The desirable averaging interval was somewhat longer than for the open shores of Estonia (8.25 days). In Liepaja, this length was 10 days while in Daugavgriva (Figure 3) and Pärnu it was 9.5 and 9 days, respectively. For these averaging intervals the distribution of the residual matches an exponential distribution well. This match makes it possible to quantify the probability of high or low local storm surges using the slope λ of the relevant linear interpolation. As in Soomere et al. (2015) we use the associated scale parameter $-1/\lambda$. Note that this quantification ignores the presence of outliers and is thus applicable only to a limited range of upper quantiles of the residual.

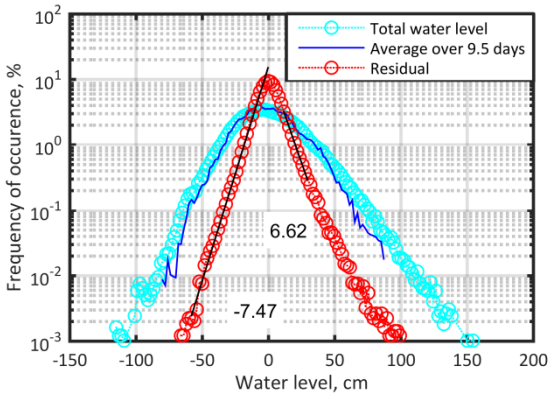

Figure 3. Frequency of occurrence of hourly measured water levels in Daugavgriva in 1961–2016 for the averaging interval of 228 hrs (9.5 days). Numbers at black lines indicate the scale parameter.

4. Discussion

The scale parameters for the positive branch of the residual in Liepaja and Daugavgriva match well the modelled results. In Pärnu, the modelled scale parameter is smaller than the one extracted from observations. The difference probably stems from the mismatch of the measurement site (in the river mouth) and the location of the grid point in the model in the mouth of Pärnu Bay. The scale parameters for the negative branch are larger than the typical values along the open coast of Estonia. This means that very low water levels are much less probable on the Latvian coast than on the Estonian shore.

Figure 3 suggests that in several occasions the water level in the Gulf of Riga was substantially higher or lower than in the Baltic Sea and that this difference lasted for a relatively long time. This feature may reflect the possibility of systematic increase in the water volume in this gulf. A relatively long relaxation time of this phenomenon apparently reflects a small cross-section of Irbe Strait and Suur Strait.

5. Acknowledgements

The research was supported by the Estonian Ministry of Education and Research (Grant IUT33-3).

References

Buschman, F.A., Hoitink, A.J.D., van der Vegt, M., Hoekstra, P. (2009) Subtidal water level variation controlled by river flow and tides. Water Resour. Res. 45, W10420.

Kamphuis, J.W. (2010) *Introduction to Coastal Engineering and Management.*World Scientific.

Medvedev, I.P., Rabinovich, A.B., Kulikov, E.A. (2013) Tidal oscillations in the Baltic Sea. Oceanology, 53(5), 596-609.

Otsmann, M., Suursaar, Ü., Kullas, T. (2001) The oscillatory nature of the flows in the system of straits and small semienclosed basins of the Baltic Sea. Continental Shelf Research 21, pp. 1577–1603.

Post, P., Kõuts, T. (2014) Characteristics of cyclones causing extreme sea levels in the northern Baltic Sea. Oceanologia 56, pp. 241–258.

Soomere, T., Eelsalu, M., Kurkin, A., Rybin, A. (2015) Separation of the Baltic Sea water level into daily and multi-weekly components. Continental Shelf Research 103, pp. 23–32.

Suursaar, Ü., Kullas, T. Otsmann, M. (2002) A model study of the sea level variations in the Gulf of Riga and the Väinameri Sea Continental Shelf Research 22, pp. 2001–2019.

Spatial and temporal features of synoptic and mesoscale Baltic sea level variability

Igor P. Medvedev [1,2], Medvedeva A.Yu.[1]

[1] P.P. Shirshov Institute of Oceanology, Russian Academy of Sciences, Moscow, Russia (patamates@gmail.com)
[2] Fedorov Institute of Applied Geophysics, Moscow, Russia

1. Introduction

In the present study, the spatial and temporal features of synoptic and mesoscale Baltic Sea level variability were studied based on long-term hourly data. Synoptic (2-30 days) and mesoscale (from 2 hours to 2 days) sea level variations are formed directly within the Baltic Sea. The greatest energy contribution to the synoptic sea level variability is caused by the storm surges, the generation of which is related to the atmospheric processes of the synoptic period. The mesoscale sea level variability in the Baltic Sea is determined primarily by the natural frequencies of the sea and gulfs, where resonant amplification of standing waves occurs (Kulikov and Medvedev, 2013). The dominant period of eigen modes of the Baltic Sea and the Gulf of Finland is 26-29 hours, Kulikov and Medvedev (2013). Long series of observations allowed us to consider the climate variability of the energy of sea level fluctuations in these frequency ranges, to identify trends and periodicity in their variation, and to reveal the relationship with the interannual variability of the North Atlantic Oscillation (NAO).

2. Data

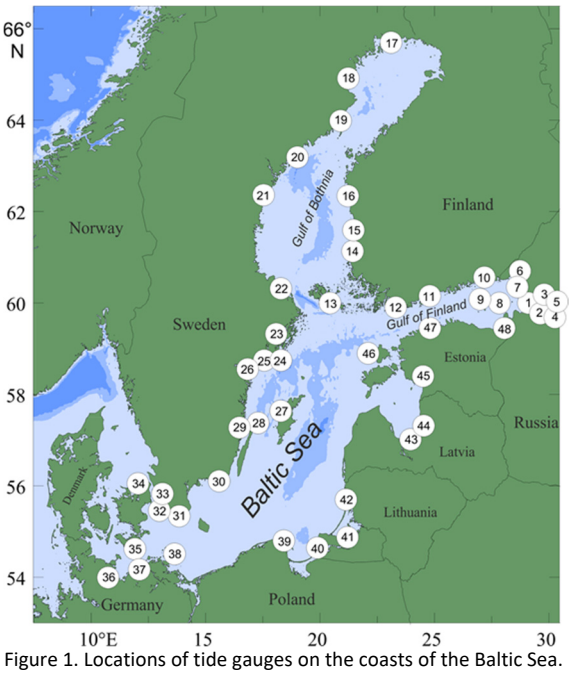

Figure 1. Locations of tide gauges on the coasts of the Baltic Sea.

Hourly sea level observations from 48 tide gauges in the Baltic Sea was used in the present study for the analysis of synoptic and mesoscale sea level variability (Fig. 1). Data for all stations have been adjusted to the Coordinated Universal Time (UTC). The observational series were thoroughly checked, all spikes and shifts were eliminated; short gaps (shorter than a day) were interpolated. For the analysis of the spatial features were used the results of the calculations on a three-dimensional barotropic numerical model of ROMS adapted to the conditions of the Baltic Sea (Kulikov et al., 2015). The energy of the sea level oscillations was calculated in the separate frequency ranges by the results of the spectral analysis. This technique used to analyze the quantitative contribution of the separate frequency ranges to the total variance of sea level variability in the Baltic Sea in Medvedev (2015).

3. Spatial features

Spectral analysis revealed a significant difference in the formation of the spectra of the Gulf of Bothnia and the Gulf of Finland. In the Gulf of Bothnia an increase in the sea level spectral energy towards the head of the gulf is observed only in the synoptic frequency range. In the Gulf of Finland such an increase is observed for both synoptic and mesoscale sea level frequency ranges. These differences in the formation of the sea level spectrum are caused by the influence of the eigen modes of these gulfs. The maximum variance of the synoptic sea level variability is observed at the head of the Gulf of Bothnia and in the southwestern part of the Baltic Sea. The minima in the distribution of the variance of synoptic sea level oscillations are located in the central part of the Baltic Sea. The maximum variance of the mesoscale sea level frequency range is observed at the head of the Gulf of Finland and in the southwestern part of the Baltic Sea, which corresponds to the spatial structure of the main eigen mode of the Baltic Sea with a period of 26-29 hours (Wubber and Krauss, 1979). The minimum variance in this frequency range is observed in the central part of the Baltic Sea, where the minimum amplitudes of the main eigen mode are located. The distribution of the variance of mesoscale sea level variability is a reflection of the energy of storm surges in the Baltic Sea.

4. Interannual variability

Long series of tide gauge observations from Ratan, Stockholm, Kungsholmsfort allow to study the interannual variability of the energy of synoptic and mesoscale sea level oscillations. Changes in the variance of synoptic oscillations happen in phase in different parts of the Baltic Sea. The minimum of the variance of the synoptic sea level oscillations was observed in Ratan in the 50−60s of the 20th century, the maximum – at the beginning and the end of the 20th century. The variance of mesoscale sea level oscillations also significantly changes. The minimum of the dispersion of mesoscale sea level oscillations in Kungsholmsfort was identified in the 30s of the 20th century. The considered series of interdecadal variability of synoptic sea level oscillations have weak negative trend. It has the value from -0.01 cm2/year in Ratan to -0.11 cm2/year in Kungsholmsfort. In interdecadal variability of

mesoscale sea level oscillations, there is no trend at these stations.

By relatively long series of observations in the Gulf of Riga (Pärnu) and in the Gulf of Finland (Gorniy Institute), it was possible to study changes in the variance of the synoptic and mesoscale sea level oscillations from 1977 to 2010. Variance of both ranges, synoptic and mesoscale, varies significantly. In interannual variability of the synoptic sea level oscillations in Gorniy Institute there is no significant trend (0.22 cm2/year), as for station Pärnu a significant negative trend with value -1.16 cm2/year is observed. In variability of mesoscale sea level oscillations at these stations a negative trend is observed, from -0.36 cm2/year in Pärnu to -0.84 cm2/year in the Gorniy Institute.

5. Atmospheric influence

Sea level oscillations of the Baltic Sea in different frequency ranges are mainly determined by atmospheric processes. One of the main factors affecting the formation of sea level fluctuations is wind stress. Long-term changes in wind stress over the Baltic Sea are closely related to large-scale atmospheric circulation over the North Atlantic. The state of the atmosphere is well represented by the North Atlantic Oscillation (NAO) Index. The variance in NAO phases (from negative to positive and back) cause the redistribution of atmospheric masses between the Arctic and the subtropical Atlantic regions, changes in the wind field, in heat and moisture transfer, in intensity, quantity and trajectories of cyclones, etc. There was no significant correlation between interannual variations of the variance of the synoptic sea level variability in the Baltic Sea and changes in the NAO index. The change in the variance of mesoscale sea level variability in the Baltic Sea, on the contrary, repeats the character of the interannual variability of the NAO index. An explicit link was found for the water areas where strong storm surges have been observed – for Pärnu Bay and for the head of the Neva Bay (Gorniy Institute). In Fig. 2 the periods of the positive NAO phase correspond to the interannual maxima of the variance of the mesoscale sea level oscillations in the Gulf of Finland and in the Gulf of Riga. The negative phase, respectively, corresponds to the minima. The correlation coefficient between NAO and interannual variability of the mesoscale sea level oscillations is 0.52 for Gorniy Institute and 0.45 for Pärnu for the period 1984–1989. There were synchronous changes of NAO index and dispersion of mesoscale sea level oscillations at Gorniy Institute, the correlation coefficient is close to 0.93 (Fig. 2a). When NAO is in positive phase, the zonal circulation type intensifies and the trajectories of the storm cyclones shifts northward by 200–400 km in comparison with their mean position. Also, an increase of the NAO index is accompanied by the rise of the number of deep cyclones over the Baltic Sea, which are the main cause of storm surges in the Gulf of Finland. As a result, the dispersion of mesoscale sea level oscillations increases.

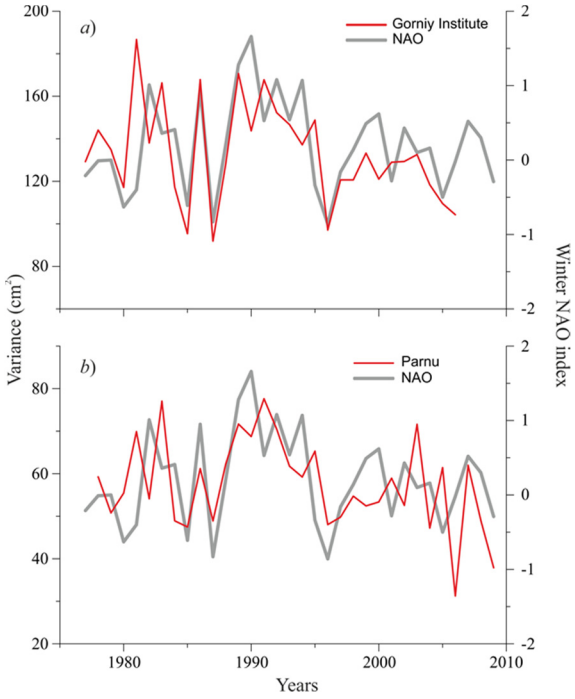

Figure 2. Interannual variability of the variance of mesoscale sea level variability of the Baltic Sea at the stations Gorniy Institute (a) and Pärnu (b). Gray curves show the interannual variations of the winter NAO index.

Acknowledgments

This research was performed in the framework of the state assignment of FASO Russia (theme No. 0149-2018-0015), supported in part by RSF (project No.14-50-00095) and RFBR (project No. 16-35-60071).

References

Kulikov E.A., Fain I.V., Medvedev I.P. (2015) Numerical modeling of anemobaric fluctuations of the Baltic Sea level, Russ. Meteorol. Hydrol, Vol. 40, No. 2, pp. 100–108.

Kulikov E.A., Medvedev I.P. (2013) Variability of the Baltic Sea level and floods in the Gulf of Finland, Oceanology, Vol. 53, No. 2, pp. 145–151.

Medvedev I.P. (2015) Formation of the Baltic Sea level spectrum, Doklady Earth Sciences, Vol. 463, No. 1, pp. 760-764.

Wubber C., Krauss W. (1979) The two-dimensional seiches of the Baltic Sea, Oceanologia Acta, 1979, Vol. 2, No. 4, pp. 435–446.

Building natural morphologies for effective beach nourishment

Kevin Parnell[1]

[1] Department of Cybernetics, Tallinn University of Technology, Estonia (k.e.parnell@gmail.com)

1. Introduction

Beach nourishment is a common response to coastal erosion, building the beach profile to repair past erosion and increase beach resilience to future high-energy events.

Traditionally, beach nourishment aims to place as much sand as possible on the beach as the project budget allows, within the constraints of permits that must be obtained based on the natural dynamics (physical and biological) and the social and economic situation of the coastal section or compartment being nourished. Placement of sand in the upper parts of the profile is generally favored in part because it appears to provide a rapid solution to the erosion problem and in places where there is political pressure to solve a problem, a result is immediately evident.

Large beach nourishment projects are normally undertaken by contractors specialist in dredging, some having extensive experience in beach nourishment projects. It is most frequently the case that sand is placed sequentially from one end of a project area to the other, to fulfil the objective of placing the required volume as quickly and as cost-effectively as possible. Such an approach, however, may result in unexpected outcomes, leading to beach morphologies that are inconsistent with beach processes and community expectations.

Using an example from Australia, the dredging and placement work being undertaken by a contractor based in Denmark, a case is made for the consideration of the natural beach morphology in the placement of sand, and for using placed sand to build desired morphologies to achieve both short-term and long-term coastal erosion resilience.

2. Beach nourishment in the Baltic

Beach nourishment has a long history in Europe with many documented projects (Hansen et al 2002). Recent studies in the Baltic Sea have emphasized the effect of beach nourishment on morphology (Baden and Hansen 2017; Pupienus et al. 2014; Valalitis et al. 2014) but the relationship between morphology and nourishment methodology is rarely considered.

.

3. An alternative framework for beach nourishment

Commonly sand is placed in a way that will build a required 'characteristic' healthy or overfilled beach profile (Dean 1991). This can be achieved by placing sand on the upper beach from the land or by pumping sand onshore from dredgers for redistribution. Sand placed from the sea, by release from a hopper (bottom dumping) or by pumping directly from the dredge (rainbowing) is generally less targeted than sand redistributed after being placed on the upper beach and is therefore not able to achieve high-tolerances for upper beach shape. However, sand placed in the nearshore will move under natural processes to build natural morphologies. Sand placed in shallower water will move under a wide range of energy conditions, whereas sand placed in deeper water, but still within the active profile, will only move under high energy conditions, thereby 'drip-feeding' sand placed during the nourishment project into the beach system over time. Sand placed in locations that form morphologies typical of the beach being nourished as it would be in an accreted state is more likely to achieve a long term positive outcome.

4. The Gold Coast, Australia, nourishment project

From June to October 2017, 3 million cubic meters of sand was dredged from water depths 18-25m and placed in the nearshore (-2m to -12m LAT) along much of the northern Gold Coast, Queensland, Australia (Figure 1). The contractor, Rohde Nielsen A/S (a Danish company) was directed using a weekly placement schedule to nourishment boxes, in varying depths of water (Figure 2), placing sand by bottom-dumping in deeper water and rainbowing (Figure 3) in shallow water.

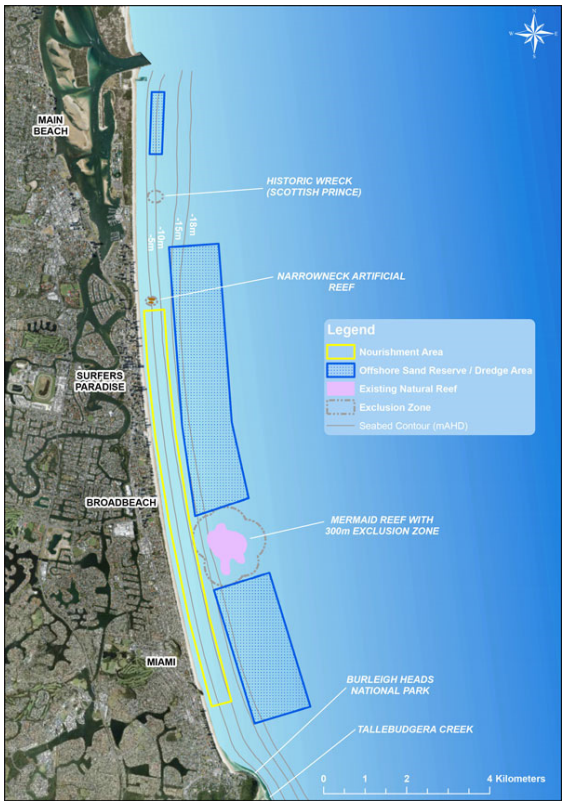

Figure 1. Beach nourishment project, northern Gold Coast, 2017. (Source: Gold Coast City Council)

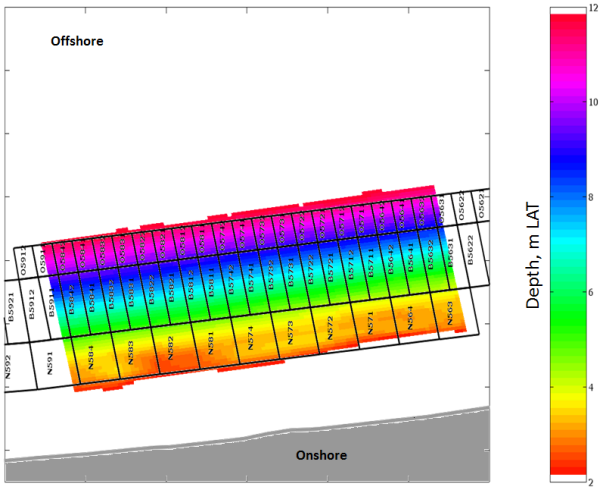

Figure 2. Placement boxes drawn overlying beach topography. Boxes in shallower water were typically filled by 'rainbowing' and offshore boxes by bottom dumping (Source: Colleter 2017)

Figure 3. The dredge 'Balder R' rainbowing sand into the nearshore. (Source: Gold Coast City Council)

Placement was undertaken with multiple sweeps along the placement area, with frequent hydrographic survey, beach-based survey and lidar survey between placements to achieve the desired morphology (Figure 4). An iterative process was undertaken to develop the placement schedule provided to the contractor on a weekly basis, determined to a large degree by the movement of the already-placed sand as evidenced from the surveys.

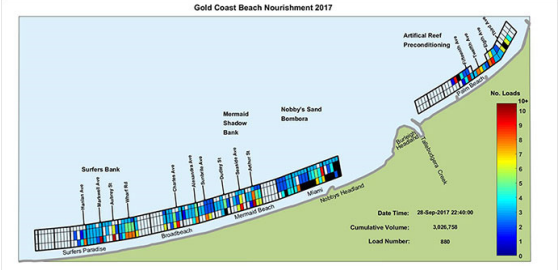

Figure 4. The final placement measured by the number of loads per placement box. Red colors indicate a large number of loads per box. Note that some locations received no sand. (Source: Gold Coast City Council)

While the long-term effectiveness of the nourishment project is still to be determined, the beach has performed well during high-energy storm events in January and February 2018. Importantly in the Gold Coast case, the nourishment project achieved a high degree of community support, due in large part to the maintenance of natural morphologies important to significant stakeholder groups (particularly surfers).

5. Discussion and summary

While all beach nourishment projects are different and subject to a range of influences and pressures, long term performance and community response are important considerations. The Gold Coast nourishment project has provided lessons with respect to building natural morphologies to promote both short-term and long-term benefits. Although traditional placement methodologies might be appropriate for a particular nourishment project, consideration should be given to more refined placement patterns and schedules.

References

Baden E and Hansen JA (2017) Beach restoration and erosion protection on the inner Danish coasts – a case study, Coastal Dynamics 2017, Paper No. 237.

Colleter G (2017) framework for nearshore nourishment and opportunity assessment of sand patterns placement, Coasts and Ports 2017 Conference – Cairns, June 2017.

Dean RG (1991) Equilibrium beach profiles: Characteristics and applications, Journal of Coastal Research, 7(1), pp. 53-84

Hansen H, Brampton B, Capobianco M, Dette HH, Hamm L, Laustrup C, Lechuga A, Spanhoff R (2002) Beach nourishment projects, practices and objectives – a European overview, Coastal Engineering, 47, pp. 81-111.

Pupienus D, Jarmalavicius D, Zilinskas G, Fedorovic J (2014) Beach nourishment experiment in Palanga, Lithuania, Journal of Coastal Research, 70, pp. 490-495.

Valalitis E, Kelpsaite L, Bagdanaviciute I and Gulbinskas S (2014) Short term shoreline changes after beach replenishment at the SE Baltic Sea, Baltic International Symposium (BALTIC) 2014, DOI: 10.1109/BALTIC.2014.6887890.

Modelling the Development of Large-Scale Mud Deposits in the Baltic Sea Basins driven by energetic events

Lucas Porz[1], Wenyan Zhang[1] and Corinna Schrum[1]

[1] Institute of Coastal Research, Helmholtz Zentrum Geesthacht

The Baltic Sea basins are largely covered by Holocene mud with the thickness of a few meters. These mud deposits are major sinks of organic carbon, nutrients and contaminants. They are thus of vital importance in the regional carbon cycle and ecosystem functioning

The distribution of mud is governed by a combined effect of hydrodynamics and source-to-sink transport pathways. A general understanding of fine-grained sediment transport in the Baltic Sea has been derived from previous modeling investigations (e.g. Kuhrts et al., 2004), however, the heterogeneity in the morphogenesis and morphological development of the large-scale mud depocenters among different basins are not yet fully understood.

Modern contouritic mud deposits in the Baltic Sea indicate that strong bottom currents generated during semi-periodic major Baltic Inflows (MBI) play a significant role in the transport and redistribution of fine-grained sediment along their path across the basins (Sivkov et al., 2002). Other energetic events such as storms are also important in transporting, redistributing and reworking fine-grained sediments (Zhang et al., 2016). The aim of this study is to model the impact of energetic events, especially MBI, on the morphodynamics of the mud depocenters in the Baltic Sea by linking sediment distribution patterns with their hydrodynamic sources. The Arkona and Bornholm basins in the south-western Baltic Sea are selected as test areas due to their diverse bathymetry, large volumes of Holocene mud deposits and excellent coverage of available field data.

Following a budget estimation of sediment fluxes in the study area (Fig. 1), we propose two distinct source-to-sink transport pathways: stepwise accumulation from local erosion of soft glacial till cliffs along the coastline and muddy seabed in shallow water, and rapid redistribution and deposition of sediment brought by MBI from remote source (i.e. North Sea) and from erosion long its path through the straights. Riverine sediment input is an order of magnitude smaller. Sediment erosion, transport and deposition across the study area in response to energetic events (storms and MBI) are simulated using an unstructured-grid, finite-element coastal ocean model (Zhang et al., 2016). The results are compared with observational oceanographic data and seismic profiles, with the goal to link the long-term (~6000 a) sedimentary record with short-term accumulation patterns.

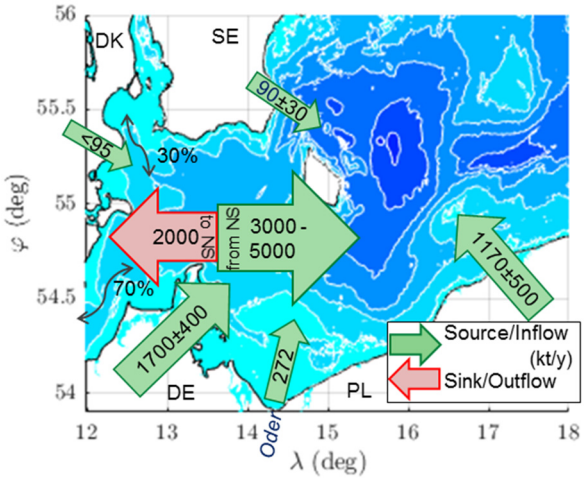

Figure 1. Sediment fluxes in the SW-Baltic Sea. The sum of total erosion and inflow is 5300-9300 kt/y. A sedimentation rate of 3300-7300 kt/y (dry bulk) in the basins located in the area closes the budget.

References

Kuhrts, C., Fennel, W., Seifert, T. (2004) Model studies of transport of sedimentary material in the western Baltic, Journal of Marine Systems, 52, 1–4, pp. 167-190

Sivkov, V., Gorbatskiy, V., Kuleshov, A., Zhurov, Y. (2002) Muddy contourites in the Baltic Sea: an example of a shallow-water contourite system, Geological Society, London, Memoirs, 22, pp. 121-136

Zhang, W., Cui, Y., Santos, A.I., Hanebuth, T.J.J. (2016) Storm-driven bottom sediment transport on a high-energy narrow shelf (NW Iberia) and development of mud depocenters, J. Geophys. Res. Oceans, 121, pp. 5751–5772

Zhang, Y., Ye, F., Stanev, E.V., Grashorn, S. (2016) Seamless cross-scale modeling with SCHISM, Ocean Modelling, 102, pp. 64-81

Scattering and backscattering properties of Estonian coastal waters

Mirjam Randla[1], Martin Ligi[1], Tiit Kutser[2], Ave Ansper[1] and Krista Alikas[1]

[1] Tartu Observatory, University of Tartu, Tõravere, Estonia (mirjam.randla@ut.ee)
[2] Estonian Marine Institute, University of Tartu, Estonia

1. Introduction

Living organisms need sunlight to survive. It is important for the oxygen producing process, photosynthesis. At least 50 % of the oxygen is produced by phytoplankton living in water systems (oceans, seas, lakes) (WHOI, 2015). Ecosystem types in deep-sea, coastal areas and river mouths depend on how much and how deep light can penetrate. Light penetration and interactions in the water are affected by the optically active substances like TSM (Total Suspended Matter), CDOM (Colored Dissolved Organic Matter) and chlorophyll-a contained in the phytoplankton. Chlorophyll-a absorbs light at specific wavelengths, CDOM absorbs light mostly at shorter wavelengths and TSM has the strongest effect on scattering. These capabilities combined are called Inherent Optical Properties (IOPs) of the water. IOPs provide info on the nature and provenance of constituents in water. The signal received by measuring instruments depends much on the concentration, nature and size of the particles. The number of instruments available for in situ IOP measurements has been limited until recent years. The few conducted in situ measurements are often also spatially sparse, which makes it difficult to create time series with only in situ data. Therefore, this data should be combined with new generation of earth observation satellites like Sentinel-2 and Landsat-8 that have sufficient spatial and temporal resolution. Satellites measure remote sensing reflectance spectra. The signal depends directly on the amount and type of the optically active substances present in the water. The measured reflectance spectra give information about the concentration of these substances, water transparency, etc. Satellite measurements alone are not applicable, they have to be calibrated, validated and compared with in situ data. There are several studies that use the band ratio algorithms to retrieve water constituents from reflectance measurements. These algorithms often rely on parameters or ratios of IOPs that are assumed to be constants (Binding et al., 2010). This is often done like this due to the absence of in situ IOP measurements. As is also shown in this study, then these parameters vary on spatial and seasonal scale. These algorithms have provided satisfying results in open sea areas but not in the coastal areas, like bays and river mouths, where optically active substances have different sources and are not directly linked to each other (Darecki et al., 2004). It is the case for the Baltic Sea in general, especially due to high concentrations of CDOM that absorbs most of the light at the visible part of the spectrum (Paavel et al., 2011). This induces need to develop new algorithms that take it account.

In this study we focused on TSM (Total Suspended Matter), its scattering and backscattering properties. We compared parameters of IOPs that are usually taken as constants in three Estonian bays.

2. Study area

Region of interest in the current study is Estonian west coast and its three bays, Haapsalu, Matsalu and Pärnu (Figure 1). Estonian coastal area is shallow, thus one of the particulate matter (organic and inorganic) resuspension driver is the wind that induces waves. Another driver is river discharge and it influences all three bays. Rivers bring into the bay high amount of organic suspended matter and CDOM related to the alteration and leaching of peatlands and agricultural lands (Paavel et al., 2011). Mineral suspended particles from the river beds are also transported into the bays.

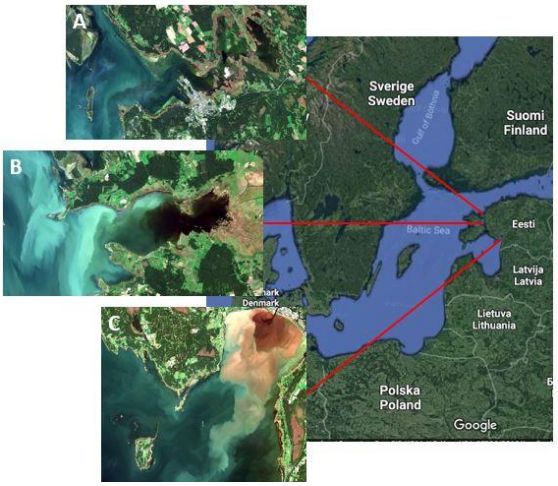

Figure 1: Location of Haapsalu Bay (A), Matsalu Bay (B) and Pärnu Bay (C), L1 image of Sentinel-2 A from 28.08.2016.

Matsalu Bay is a national park and reserve for protection of more than 250 species of birds (KKA, 2016). Human activities are limited in this area. It is also very shallow (average depth is 1.5 m) with plants like reeds and rushes expanding westward 100 m each year (Wikipedia, 2018). Kasari River discharges large quantities of nutrient-rich sediments into the bay.

Haapsalu Bay is influenced by human activities such as tourism. In 2015 it was valued as the bay with the poorest water quality in Estonia (EEA, 2015). Because of the very shallow (around 3 m) and sectioned area, pollution coming from the city of Haapsalu will remain in the sediments. It is the most important peloid (therapeutically used mud) depository in Estonia.

Pärnu bay is the biggest and most human impacted of the three. The Pärnu River, the biggest in Estonia, discharges mineral and organic particulate and dissolved matter into the bay. Although the bay is also shallow (mean depth is around 7m), it is also influenced by intense shipping and fishing activities. Long sandy beaches around the bay means that the region is a popular tourist destination.

3. Methodology

In situ data was collected from 22 stations located in Matsalu, Haapsalu and Pärnu Bay from 2012 to 2017. IOPs were measured with a set of instruments that include AC-S that measures spectral absorption and attenuation; two scatterometers, ECO-BB3 and ECO-VSF, each measuring scattering in water at different angles and in total at 6 wavelengths; a Seabird CTD for salinity, temperature and depth measurements. All IOP data were merged with DH4 data-logger and corrected according to the user manuals. In situ above water reflectance spectra were measured with two TriOS RAMSES setup: an irradiance sensor looking directly upwards and a radiance sensor looking directly downwards (Kutser, et al., 2013).

During the study algorithms based on scattering, backscattering, absorption and different reflectance band ratios found from the literature were tested on our in situ dataset. The results were compared measured reflectance spectra. We were focusing especially on the parameters that are used as constants. For example, we calculated the total backscattering to particulate backscattering ratios, and TSM specific scattering. We were looking if these parameters vary depending on geographical and temporal scale on Estonian coast. This data was compared with measurements from Swedish coastal waters, Gotland during a campaign in 2013.

4. Results and discussion

Figure 2 represents reflectance spectra collected from Matsalu, Haapsalu and Pärnu Bay from 2012 to 2017. The variability is almost in the order of magnitude.

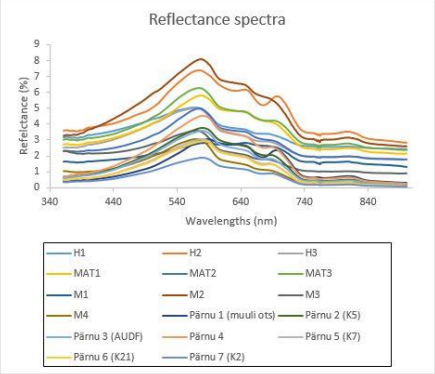

Figure 2: Reflectance spectra of all data from 2012 to 2017 measured by 2 TriOS RAMSES setup.

Table 1 shows that bb/b ratios are wavelength dependent. In one bay the values change from year to year and from season to season. The greatest values are recorded in Haapsalu in late autumn. Gotland results surprisingly stay close to Haapsalu results. Bb/b ratios are dependent on particles sizes (Ronghua Ma et al., 2009). The bigger the ratio value is, the smaller the particles are.

	Wavelengths (nm)	412	470	532	595	660	715
21.07.2012	Matsalu	1.48	2.01	1.82	2.84	1.56	4.89
25.07.2013	Matsalu	2.26	2.25	2.14	2.77	2.17	4.21
24.07.2013	Haapsalu	1.94	1.82	1.75	2.25	1.76	3.47
26.07.2013	Haapsalu	1.43	1.35	1.31	1.69	1.35	2.62
31.05.2016	Haapsalu	1.57	2.13	2.27	3.50	2.15	5.00
14.09.2016	Haapsalu	1.57	2.13	2.27	3.50	2.15	5.00
12.10.2016	Haapsalu	2.19	2.18	2.50	10.11	2.50	15.66
7.07.2017	Pärnu	0.81	1.39	1.63	2.46	1.60	3.62
04.09.2013	Gotland	1.71	1.31	1.37	1.67	1.33	1.58

Table 1: Median bb/b (in percentage) values of each campaign. Comparison with Swedish Gotland campaign.

Table 2 shows the variability (relative to the yearly mean) of TSM specific scattering (according to Binding et al., 2010) in Matsalu Bay. In this case, the differences between the stations during the year 2012 are clearly visible as these ratios vary from 0.4 to 1.7. There is also clear difference in averages of the two years.

Wavelengths (nm)	412	470	532	595	660	715
Matsalu 2012	0.008443	0.01091	0.00891	0.012748	0.005576	0.009476
Matsalu 2013	0.007027	0.006406	0.005612	0.006634	0.004611	0.004712
MAT1 07.2012	1.347	1.287	1.337	1.306	1.448	1.421
MAT2 07.2012	1.705	1.762	1.608	1.647	1.322	1.407
MAT3 07.2012	0.414	0.406	0.444	0.463	0.520	0.506
MAT4 07.2012	0.534	0.003	0.611	0.584	0.710	0.666
MAT1 07.2013	1.110	1.110	1.115	1.107	1.075	1.090
MAT2 07.2013	1.073	1.062	1.295	1.060	1.073	1.081
MAT3 07.2013	0.817	0.828	0.821	0.833	0.852	0.828

*Table 2: b*SPM values in Matsalu Bay stations compared to the yearly averages.*

These results indicate that the parameters that are often taken as constants change in spatial and temporal scale, they affect reflectance spectra measured by in situ instruments, but also the signal measured by satellite sensors. These variabilities have to be taken into account while developing new algorithms for coastal turbid waters.

References

Binding, C.E., Jerome, J.H., Bukata, R.P., & Booty, W.G. (2010). Suspended particulate matter in Lake Erie derived from MODIS aquatic colour imagery. International Journal of Remote Sensing, 31; 19; 5239-5255.

Darecki, M., & Stramski, D. (2004). An evaluation of MODIS and SeaWiFS bio-optical algorithms in the Baltic Sea. Remote Sensing of Environment, 89; 3; 326-350.

Kutser, T., Vahtmäe, E., Paavel, B., & Kauer, T. (2013). Removing glint effects from field radiometry data measured in optically complex coastal and inland waters. Remote Sensing of Environment, 133; 85-89.

Ma, R., Pan, D., Duan, H., & Song, Q. (2009). Absorption and scattering properties of water body in Taihu Lake, China : backscattering. International Journal of Remote Sensing, 30; 9; 2321-2335.

Mobley, C. D. (1994). Light and Water: Radiative Transfer in Natural Waters. Academic Press.

Paavel, B., Arst, H., Metsmaa, L., Toming, K., & Reinart, A. (2011). Optical Investigation of CDOM-rich coastal waters in Pärnu Bay. Estonian Journal of Earth Sciences, 60; 2; 102-112.

WHOI, 2015
https://www.whoi.edu/main/topic/phytoplankton
(consulted on 16.02.2018)

EEA, 2015
https://www.eea.europa.eu/soer-2015/countries/estonia
(consulted on 10.02.2018)

KKA, 2016
https://www.keskkonnaamet.ee/sites/default/public/Matsalu_EN.pdf (consulted on 10.02.2018)

Wikipedia, 2018
https://en.wikipedia.org/wiki/Matsalu_National_Park
(consulted on 10.02.2018)

Radar remote sensing of the meteo-marine parameters in the Baltic Sea

Sander Rikka[1], Rivo Uiboupin[1], Andrey Pleskachevsky[2], Victor Alari[1], Sven Jacobsen[2], Tarmo Kõuts[1]

[1] Department of Marine Systems at Tallinn University of Technology, Akadeemia tee 15a, 12618, Tallinn, Estonia (sander.rikka@ttu.ee)
[2] German Aerospace Center (DLR), Remote Sensing Technology Institute, 28199, Bremen, Germany

1. Introduction

In this work, remote sensing radar data from different sensors, such as X-band Synthetic Aperture Radar (SAR) TerraSAR-X and TanDEM-X (TS-X and TD-X) satellites, marine X-band radar and C-band SAR Sentinel-1A/B, have been used to estimate meteo-marine parameters using empirical methods in the specific condition of the Baltic Sea with archipelago islands and where short steep sea state dominates.

For the semi-enclosed micro-tidal Baltic Sea with the absence of long swell waves and short wave "memory" (Soomere and Räämet 2011), the empirical methods should be used (Pleskachevsky et al. 2016; Rikka et al. 2018a). Since the significant wave height remain mostly between 0–2 m (rarely exceeds 4 m; Tuomi et al. 2011; Björkqvist et al, 2017), the waves are seen as a clutter for radar. Windsea wave crests are short and present a considerable number of small, nonstable, fast and erratically moving targets for a SAR sensor. Such sea state is typically imaged as noise and is hardly recognized as a wave pattern. A strong windsea contribution to the total wave height is therefore equivalent to more substantial uncertainties in SAR imaging.

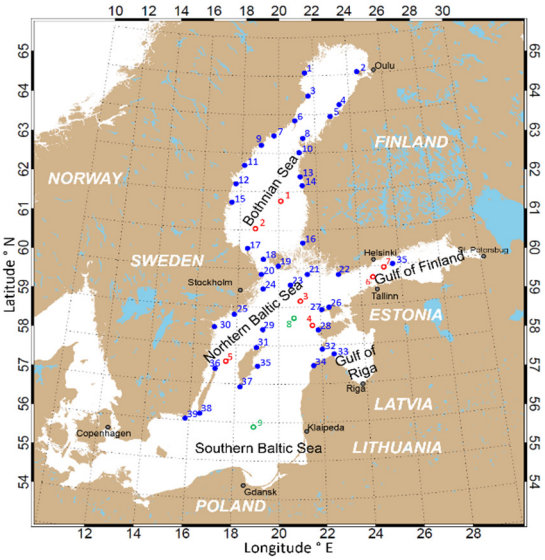

Figure 1. The map of the Baltic Sea and locations of measurement stations used in the study. The location of wave measurements – (red) and coastal wind measurements – (blue) are indicated on the map; green marks extra stations (virtual buoys) used for comparison

2. Data

For the presented study, German X-band SAR data from TS-X and TD-X satellites, European Space Agency (ESA) C-band SAR data from Sentinel-1A/B and X-band coastal Vessel Traffic Service (VTS) radar are used to estimate meteo-marine parameters.

Figure 1 shows an overview of measurement station in Baltic Sea available and used in the current study. For sea state measurements, three types of equipment were available: Acoustic Doppler Current Profiler (ADCP), wave rider buoys and pressure sensors. Wind measurement data from over 30 coastal stations around the Baltic Sea were used for statistical comparison.

3. Methods

The Normalized Radar Cross Section (NRCS) σ_0 is firstly processed from image pixel digital number DN:

$$\sigma_0 = \mathrm{DN}^2 k_s \sin(\theta)$$

where k_s is the calibration factor given in the products metadata and θ is the local incidence angle.

The process of estimating sea state parameters is based on FFT (Fast Fourier Transform) of the subscene. Before the analysis, each pixel value $\sigma_0(x,y)$ of the subscene is normalized resulting in a value $\sigma_n(x,y)$. A FFT window of 1024 × 1024 pixels was used for SAR data and 512 × 512 pixels for marine radar.

Empirical algorithms are used to estimate integrated sea state parameters straight from radar image spectra without transformation into wave spectra. The methods are chosen since traditional functions (image spectrum transfer to wave spectrum) are not able to give accurate results in generally low sea state conditions of the Baltic Sea (Pleskachevsky et al. 2016; Rikka et al. 2018a).

To obtain integrated wave parameters, FFT operation is applied to the radiometrically calibrated subscene. Image power Spectrum $IS(k_x,k_y)$ is calculated by integration over 2D wavenumber domain:

$$E_{\mathrm{IS}} = \int_{k_x^{min}}^{k_x^{max}} \int_{k_y^{min}}^{k_y^{max}} IS(k_x,k_y) dk_x dk_y$$

The resulting function for radar imagery to calculate total significant wave height is expressed as:

$$H_S = a_0 \sqrt{B_0 E_{\mathrm{IS}} tan(\theta)} + \sum_{i=1}^{n} a_i B_i$$

where θ is local incidence angle, a_i are coefficients, and B_i are functions of spectral parameters, wind and GLCM results.

4. Results

The specific sea state conditions in the Baltic Sea and its SAR imaging were investigated, and existing algorithms were enhanced by validation with in situ measurements and wave model results (Rikka et al. 2018). Sea state and wind fields are simultaneously derived from high-resolution satellite radar images acquired by TS-X and TD-X satellites (Figure 2).

Figure 3 represents the average wind speed and significant wave height values from Sentinel-1A/B IW data over the 2015 and 2016 interpolated onto WAM wave model grid (Pleskachevsky et al. 2018; Rikka et al. 2018b). There are clearly higher average wave height values in the open parts of the Baltic Sea (below 1.8 m) and lower values

in the Gulf of Riga (up to 1.0 m in the open part; below 0.8 m in the coastal areas) or the Bothnian Sea (from 0.7 m to 1.2 m) which corresponds to previous studies.

Figure 4 demonstrates the usability of marine radar data for operational and for monitoring purposes. Significant wave height map is calculated for commonly occurring North-West storm lasting between 26.03 and 28.03.2018 (Rikka et al. 2018c)

Table 1 gives an overview of inter-comparison of radar-derived significant wave height and *in situ* measurements for different methods used for different sensors.

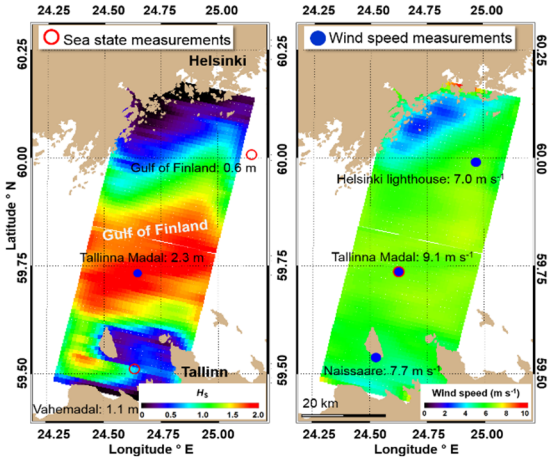

Figure 2. High-resolution meteo-marine parameters processed with the empirical XWAVE_C algorithm from satellite TS-X StripMap scene acquired on 20.022017 at 04:58 UTC

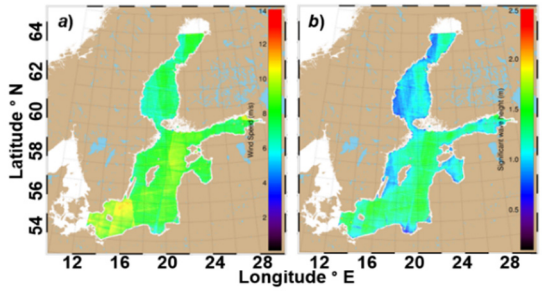

Figure 3. (a) average wind speed and; (b) average significant wave height over 2015 – 2016 calculated from Sentinel-1A/B IW data using empirical algorithm CWAVE_S1-IW.

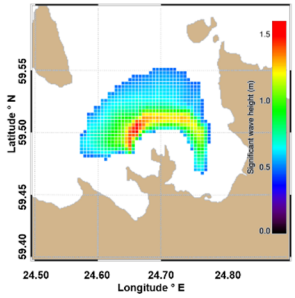

Table 1. Overview of inter-comparison of significant wave height for diferent sensors and *in situ* measurements: correlation coefficient (r) and root mean square error (RMSE).

Sensor/ method	*r*	RMSE
TS-X/TD-X	0.88	0.32 m
Sentinel-1A/B	0.88	0.40 m
Marine radar	0.78	0.23 m

Figure 4. Significant wave height calculated from marine radar for the North-West storm case lasting from 26.03 until 28.03.2017.

5. Summary

The Baltic Sea, in conclusion, is a very complex region for wave height calculations using SAR methods. It is seen from previous studies, that SAR methods work accurately on open ocean region where swell waves are the major contributor to the total wave field (Li, Lehner, and He 2008; Lehner et al. 2013; Pleskachevsky, Rosenthal, and Lehner 2016). In the Baltics, the wave field is mostly influenced by local wind field and is disturbed by numerous shallow areas, islands and rugged coastline, which allow estimating wave height mostly from noise information. The sea state parameters were retrieved from image spectrum using empirical algorithms to estimate integrated sea state parameters directly from SAR image spectra without transformation into wave spectra.

The study demonstrates that the wave retrievals from mentioned sources provide valuable information for operational and/or statistical monitoring of wave conditions in the Baltic Sea. For example, Sentinel-1A/B wave data provide additional value when monitoring coastal region where altimetry data is missing. SAR data is also valuable for model data validation and interpretation in the regions where and during periods when in situ measurements are lacking.

The SAR-derived wave retrievals in general provide more detailed information about spatial variability of the wave field in the coastal zone compared to in situ measurements, altimetry wave products and model forecast. In addition, marine radar data provide sea state information in high spatio-temporal resolution.

6. Acknowledgements

The study was supported by institutional research funding IUT (19-6), by Personal Research Funding PUT1378 of the Estonian Ministry of Education, and Research, by the European Regional Development Fund and through CMEMS Copernicus grant WAVE2NEMO.

References

Björkqvist, J.V., Lukas, I., Alari, V., van Vledder, G.P., Hulst, S., Pettersson, H., Behrens, A. and Männik, A. (2017). Comparing a 41-year model hindcast with decades of wave measurements from the Baltic Sea. arXiv preprint arXiv:1705.00559.

Lehner, S., Pleskachevsky, A., Velotto, D. and Jacobsen, S. (2013). Meteo-Marine Parameters and Their Variability Observed by High Resolution Satellite Radar Images. Oceanography, 26(2), pp.80-91.

Li, X.M., Lehner, S. and He, M.X. (2008). Ocean wave measurements based on satellite synthetic aperture radar (SAR) and numerical wave model (WAM) data–extreme sea state and cross sea analysis. International Journal of Remote Sensing, 29(21), pp.6403-6416.

Pleskachevsky, A.L., Rosenthal, W. and Lehner, S. (2016). Meteo-marine parameters for highly variable environment in coastal regions from satellite radar images. ISPRS Journal of Photogrammetry and Remote Sensing, 119, pp.464-484.

Pleskachevsky, A.L., Jacobsen, S. and Tings, B. (2018). Sea State from Sentinel-1 Synthetic Aperture Radar Imagery for Maritime Situation Awareness. (*submitted*).

Rikka, S., Pleskachevsky, A., Uiboupin, R. and Jacobsen, S. (2018a). Sea state in the Baltic Sea from space-borne high-resolution synthetic aperture radar imagery. International Journal of Remote Sensing, 39(4), pp.1256-1284.

Rikka, S., Pleskachevsky, A., Jacobsen, S., Alari, V. and Uiboupin, R. (2018b). Meteo-marine parameters from Sentinel-1 SAR imagery: towards near real-time services for the Baltic Sea. (*submitted*)

Rikka, S., Uiboupin, R., Kõuts, T., Vahter, K. and Pärt, S. (2018). An Empirical Method for Significant Wave Height from Circularly Polarized X-band Marine Radar Images. (*submitted*)

Soomere, T. and Räämet, A. (2011). Spatial patterns of the wave climate in the Baltic Proper and the Gulf of Finland. Oceanologia, 53, pp.335-371.

Tuomi, L., Kahma, K.K. and Pettersson, H. (2011). Wave hindcast statistics in the seasonally ice-covered Baltic sea. Boreal Environment Research, 16.

Coastal erosion on the Kotlin Island's coastline in the Gulf of Finland, the Baltic Sea: a model study to elaborate mitigation measures

Vladimir A. Ryabchenko[1], Igor O. Leontyev[1], Daria V. Ryabchuk[2,3], Alexander Yu. Sergeev[2], Anton Yu. Dvornikov[1], Stanislav D. Martyanov[1], Vladimir A. Zhamoida[2,3]

[1] Shirshov Institute of Oceanology, Russian Academy of Sciences, Moscow, Russia (vla-ryabchenko@yandex.ru)
[2] A.P. Karpinsky Russian Geological Research Institute (VSEGEI), St. Petersburg, Russia
[3] St. Petersburg State University, Institute of Earth Science, St. Petersburg, Russia

1. Introduction

In recent decades considerable progress has been made in the development of mathematical modeling of the coastal dynamics. Although the possibilities of morphodynamic forecasts are still limited, existing models already provide significant assistance in solving practical problems related, for example, to the assessment of longshore sediment fluxes, changes in the contour of the coastline and also to predictions of storm-induced bed.

The main motivation for the present research was the results of retrospective analysis of the western Kotlin Island's (KI) coastal zone remote sensing data (Fig.1) which revealed the maximal erosion rates of 1.2–1.6 m/year during the last 76 years for the eastern Gulf of Finland (GoF). The established trend can lead to the complete disappearance of sandy beaches of the western KI in the nearest future. In the context of this study the main interest was related to the typical time scale of storm events. The most effective in this case are the so-called process-based models which simulate the local effects of waves and currents on the sand bottom ultimately leading to sediment transport and changes in coastal morphology.

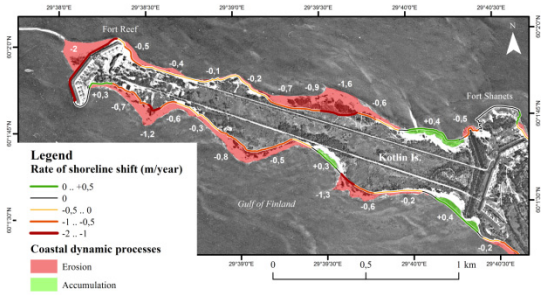

Figure 1. Coastal dynamics of the western KI.

The purpose of this study is to assess the intensity of the coastal erosion of the western part of the KI located in the eastern part of the GoF and to propose a method aimed to maintain the safety of its sand beaches. As a more general result we propose a method for assessing dangerous geological processes in the coastal zone based on actual geological and geophysical information, modeling of the sea circulation, waves and sediment dynamics, and recommendations how to combine them. To this end, the western coastal zone of the KI characterized by the great abrasion intensity was considered.

2. Methods

Circulation model. Calculations of current velocities were performed using the three-dimensional hydrodynamic model of the eastern part of the GoF and the Neva Bay (Ryabchenko et al., 2010). The model is based on the three-dimensional Princeton Ocean Model (POM) (Blumberg and Mellor, 1987). In the current version the model domain covers the eastern GoF including the Neva Bay and the Flood Protection Barrier (FPB). In the horizontal plane a uniform grid with a step of 100 m is used. The number of grid nodes in the x-direction (from west to east) is equal to 600, in the y-direction (from south to north) is equal to 400, the number of uniformly distributed σ-levels is 7. The maximum depth is 34.4 m, the minimum depth is 0.2 m. The FPB has 6 water-gates and 2 ship-gates. The model allows opening and closing these gates during the calculations if necessary.

Wind waves model. Calculation of wave parameters was carried out using the SWAN wind waves model (Booij et al., 1999) on the same computational grid (Martyanov and Ryabchenko, 2016). To generate the boundary conditions at the open boundary we performed SWAN model runs in advance for the entire GoF on a grid of 720×310 nodes.

Morphodynamic model. Modeling of sediment transport is based on the energetics approach [Bagnold, 1963; Bowen, 1980, Leont'yev, 2001].

3. Numerical experiments

In this work the period from the start of the Flood Protection Barrier's (FPB) functioning in August 2011 till the present is being considered. The analysis of data of sea level changes at the stations "Ozerki" and "Kronstadt" has shown that during this period the maximum water levels were observed in 2011. There occurred three storm surges in the Neva Bay in November-December 2011. In this study the strongest flood event occurred on December 26-28 was simulated.

4. Modeled sea level, currents and wind waves

To reproduce the most severe floods in the period under review, which occurred on December 26-28, 2011, a reference model run was performed with the external forcing, including the wind input from HIRLAM (Fig.2).

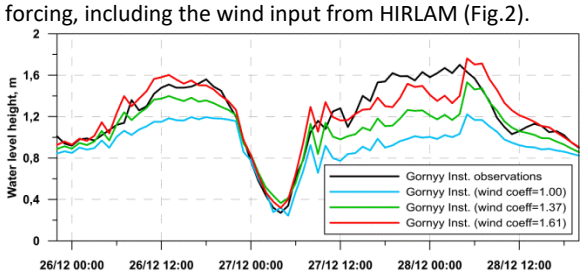

Figure 2. Water level rise at the "Gornyy Institute" station on December 26-28, 2011, based on observations and on model results with different prescribed wind speed: specified by the HIRLAM model only; specified by the HIRLAM model with the wind speed modulus increased by 1.37 and 1.61 times.

The figures 3-4 show examples of the pattern and distribution of the surface current velocity and wind waves in the above-mentioned period.

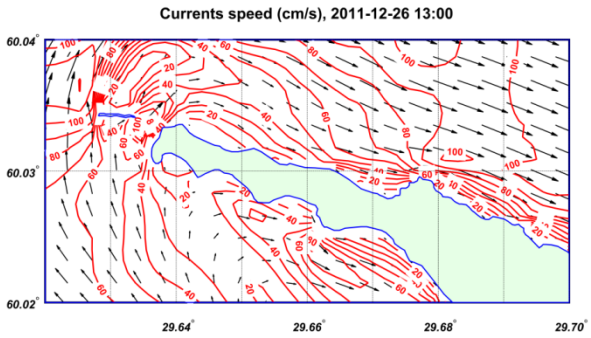

Figure 3. Modeled surface current velocity at the western part of the KI for HIRLAM's wind speed , 26.12.2011, 13:00.

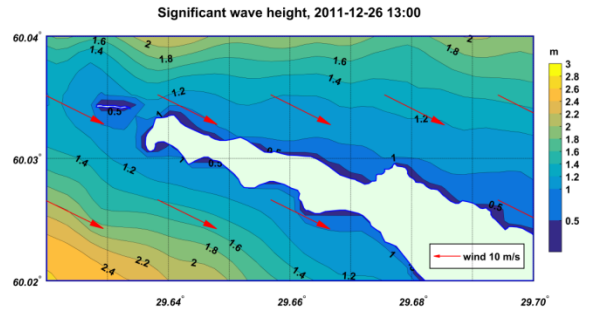

Figure 4. Modeled SWH with HIRLAM wind speed, 26.12.2011, 13:00.

5. Shore dynamics

The longshore sediment transport in the coastal zone is carried out by the joint action of waves and currents. Under conditions of very shallow and gentle coastal slopes in the area the current induced by breaking waves turns out to be comparatively weak (not more 0.3 m/s) and the dominant role is played by the storm currents. The sediment transport modeling during the storm occurred on December 26-28, 2011 is based on computations of storm surge, wind waves and currents for selected coastal profiles.

According to the recommendations of geologists the best way to protect the studied coasts is to create artificial beaches. Their characteristics may be determined by the parameters of an extreme representative storm event. Representative particle size of natural sand in the study area is 0.25 mm. Two options of sediments for artificial beach were considered: a medium sand (0.5 mm) and a gravel (2.0 mm). The results of calculations of the artificial beach profile parameters is shown in Fig. 5.

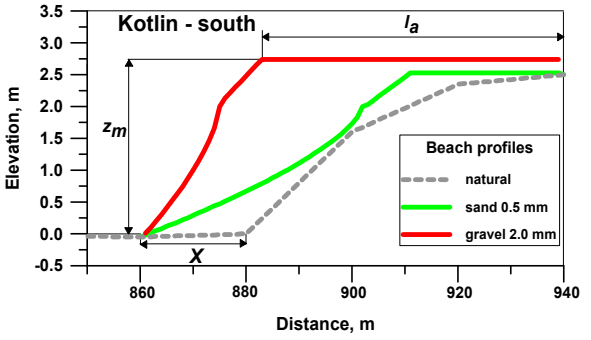

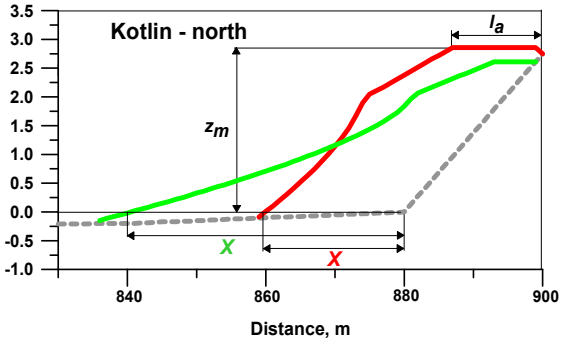

Figure 5. Calculated profiles of the artificial beach for southern and northern Kotlin's coasts.

6. Discussion and conclusions

According to the results of coastal monitoring carried out by VSEGEI since 2000, the frequency of extreme coastal erosion events similar by impact to the storm of 26-28.12.2011 has drastically increased during the last years. In the second half of the 20th century such events took place once in 25 years.

The sediment deficiency is one of the main reasons of the intensive coastal erosion of the western KI along with hydrometeorological and hydrological processes. It is well known that the best method of coast protection in the case of the necessity of sediment deficiency compensation is the beach nourishment. The main problem of the artificial beaches construction is their high cost and requirement of regular compensation of sediment loss caused by the storm impact. The proposed method aimed to maintaining the safety of sand beaches can be applied to other areas of the coast of the Baltic Sea, as well as to other seas.

Acknowledgements

Dvornikov A.Yu., Ryabchenko V.A. and Martyanov S.D. were supported by the grant 16-55-76021 of the Russian Foundation for Basic Research. There results of sections 2-4 were obtained in the framework of the state assignment of FASO Russia (theme No. 0149-2018-0014). Leont'yev I.O. was supported by the grant 15-05-08239 of the Russian Foundation for Basic Research. Sergeev A.Yu. and Ryabchuk D.V. were supported by the Russian Science Foundation (grant 17-77-20041).

References

Bagnold R.A. (1963). Mechanics of marine sedimentation, The Sea. V.3. N. Y.: J. Wiley, P. 507–528.

Blumberg, A.F., Mellor, G.L., (1987) A description of a three-dimensional coastal ocean circulation model, In: Heaps, N. (Ed.), Three-dimensional Coastal Ocean Models. American Geophysical Union, pp. 208.

Booij, N., Ris, R.C., Holthuijsen, L.H. (1999) A third-generation wave model for coastal regions, Part 1.Model description and validation, Journal of Geophysical Research, 104 (C4), 7649-7666.

Leont'yev I.O. (2001) Coastal Dynamics: Waves, Currents, Sediment Transport. M.: GEOS, 272 p.

Martyanov S., Ryabchenko V., (2016) Bottom sediment resuspension in the easternmost Gulf of Finland in the Baltic Sea: A case study based on three–dimensional modeling, Cont. Shelf Res. 117, 126-137. Doi: http://dx.doi.org/10.1016/j.csr.2016.02.011.

Ryabchenko V., Dvornikov A., Haapala J., Myrberg K. (2010) Modelling ice conditions in the easternmost Gulf of Finland in the Baltic Sea, Continental Shelf Research 30: 1458–1471. Doi: 10.1016/j.csr.2010.05.006.

Identification of extreme storm tides with high impact potential for the German North Sea coast

Ralf Weisse[1], Lidia Gaslikova[1] and Iris Grabemann[1]

[1] Helmholtz-Zentrum Geesthacht, Institute of Coastal Research, Geesthacht, Germany (ralf.weisse@hzg.de)

1. Introduction

Planning and design of coastal defenses and protection requires information about the probabilities of very severe storm tides and the possible changes that may occur in the course of anthropogenic climate change. So far this information is mostly provided in the form of high percentiles obtained from frequency distributions or return values. More detailed information and assessment of events that are *highly unlikely* but which are potentially linked with *extreme consequen*ces is so far still unavailable.

We describe the approach taken in the EXTREMENESS project to address these questions and provide some preliminary results.

2. Data and methods

EXTREMENESS first aims at identifying extreme storm tides and related meteorological conditions from a huge number of readily available data sets comprising more than about 1,500 years of data. Data include observations, reanalyzes, and climate change projections.

What actually constitutes an extreme storm tide is developed under participation of a Stakeholder-Science Collaboration Forum established within the project and in which representatives of local and federal authorities, industry and local interest groups are represented. Simple measures such as extreme surge or total water level heights are considered but metrics that are more complicated and narrative scenarios that may represent a threat are also developed.

Factors that may potentially amplify the identified extremes are analyzed using high-resolution atmospheric and tide-surge models. This comprises for example effects of future sea level rise or of the fact that the onset of strong winds is independent of the tide. A systematic assessment will be provided on whether or not the selected storm tides bear potential for amplification; that is, whether or not more severe realizations are possible within physically plausible limits.

As a case study and for the most severe cases an impact assessment for the city of Emden will be made by analyzing consequences of failures in the coastal defense system, which will serve as a basis for development of adaptation options and evaluation criteria.

3. Preliminary results

EXTREMENESS first aims at identifying extreme storm tides and related meteorological conditions from a huge number of available data sets. Figure 1 exemplarily shows the 20 highest storm surges at Borkum, an island at the Lower Saxony coast, that were identified from so far about 500 years of hourly water level data. In addition the same metric as analyzed from observations for two of the so far highest observed surges are shown. Two conclusions can be inferred immediately. First, within the model data analyzed storm surges occur that exceed the height of the events observed so far. Second, highest surges do not necessarily coincide with highest total water levels (Figure 1). While part of this may be explained by tide-surge interaction, it may be assumed that such events bear some potential for amplification, as the timing of the meteorological events is independent from the phase of the astronomical high water. Moreover, contributions from non-local effects such as external surges or monthly and/or longer-term sea level variations associated with state of the atmospheric large-scale circulation need to be considered.

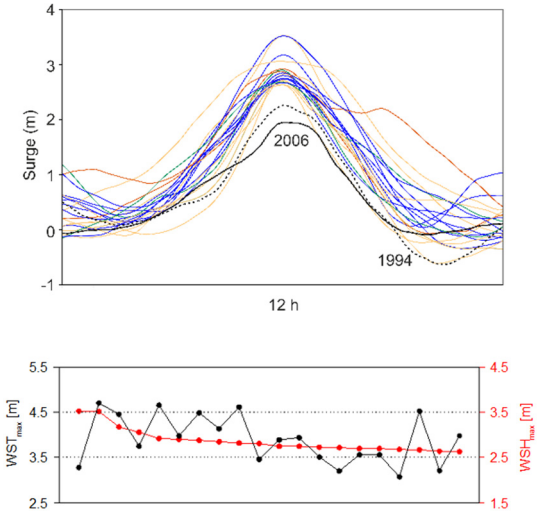

Figure 1. Storm surges heights and corresponding total water levels in Borkum. (Top): Storm surge curves [m] for the 20 highest simulated events identified within the data analyzed so far. Different colors denote different data sets. The curves are centered around their maximum. Also shown are the highest event obtained from observations (1994; black; dotted) and an event in 2006 that caused record water levels in Emden near Borkum (black; solid). (Bottom): Storm surge heights [m] of the 20 largest events (red; red scale right) and corresponding highest total water levels during the events (black; black scale; right).

4. Summary

EXTREMENESS aims at identifying extreme storm tides that are both, highly unlikely but still physically possible and that may be linked with extreme consequences. Preliminary analyzes suggest within the data considered so far unprecedented storm tides exist that may bear potential for amplification. The latter still needs to be investigated in detail. Potential consequences will be assessed based on narrative scenarios developed under participation of local and federal stakeholders.

Geographical diversity in the occurrence of extreme sea levels on the coasts of the Baltic Sea

Tomasz Wolski, Bernard Wiśniewski

[1] Faculty of Geosciences, University of Szczecin, Szczecin, Poland (tomasz.wolski@usz.edu.pl)
[2] Faculty of Navigation, Maritime University of Szczecin, Poland

1. Introduction

At present, the Baltic Sea has a high saturation of rationally located water gauge stations. Thanks to this, phenomena and processes cooperating in raising and lowering the sea level can be characterized adequately. Especially extreme sea levels, that is the highest levels and the lowest recorded in many years, in a given year or at a given storm event, stimulate current processes, marine abrasion and accumulation of sedimentary material on different sections of the coastal zone. High sea levels, usually of a stormy nature, often lead to catastrophic situations, such as loss of shore, beach disappearance, as well as destruction of shore infrastructure. Storm storms flood low-lying areas of the coastal zone, which are usually densely populated and heavily exploited economically. On the other hand, low sea levels cause significant disruptions to shipping by diminishing depths on fairways to ports and at the port's seafront.

The purpose of this research is to show the geographical diversity in the occurrence of extreme water levels on the whole coast of the Baltic Sea on the basis of longterm observations series. Previous work on storm surges and extreme sea levels (apart from some publications on sea level modeling) concerned mostly the coasts of individual Baltic states or included only part of the Baltic coast.

2. Materials and methods

Material research included hourly sea level observation data from 37 gauges stations located along the Baltic Sea coasts from the period 1960-2010 and 12 gauges stations with a shorter observation series. Such period was chosen as the longest possible one that could provide sea level data from national meteorological and hydrological institutes of Baltic countries (Poland, Germany, Denmark Sweden, Finland, Estonia, Lithuania). Hourly sea level data were corrected to the single vertical datum which is NAP in the practical realization of the EVRS system called EVRF 2000. Basic calculations were done using the Coordinate Reference Systems in Europe (CRS EU)

ArcGIS was the basic tool used for a visualisation of the extreme parameters of the Baltic Sea levels in this work. The tool allowed to display a distribution of maximal and minima sea levels and distribution of theoretical water levels. Kriging was the main ArcGIS module that was a basis of spatial analysis.

3. Results

The maps on Fig. 1 (a,b) illustrate the distribution of extreme (maximum and minimum) sea levels drawn on the basis of real, observed water levels at the gauge stations from the period 1960-2010.

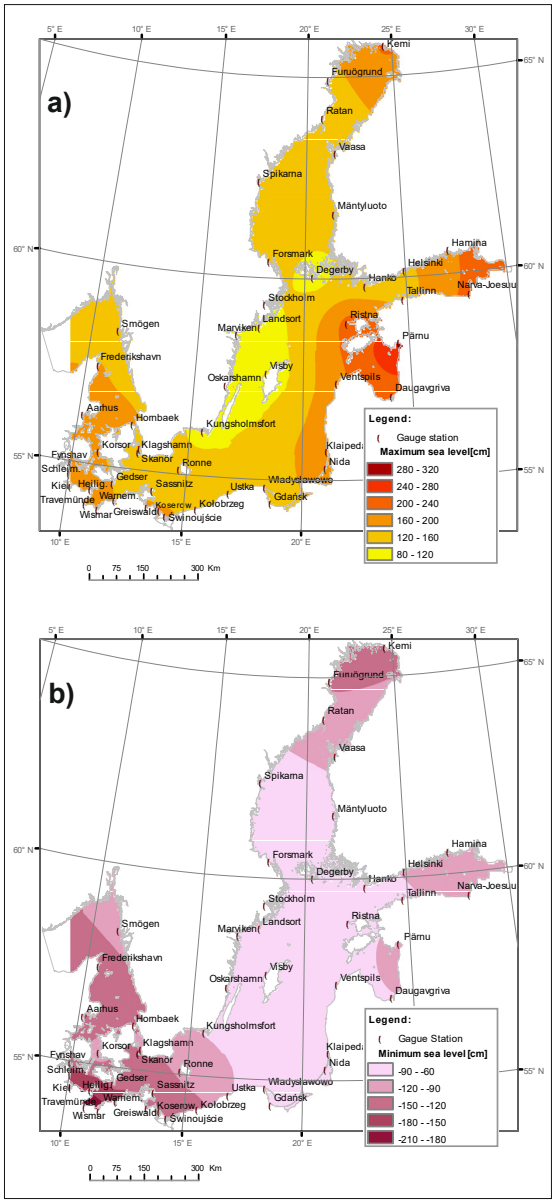

Figure 1. Distribution of maximal (a) and minimal (b) sea levels on the Baltic Sea from the period 1960-2010

The diversity of extreme sea levels results mainly from (Wolski et al. 2014, 2016):

- the various exposures (directions) of the parts of the Baltic Sea coasts (coastline configuration) to the trajectories of passing low-pressure systems;
- the location of the water level gauge stations in relation to the open areas of the Baltic Sea
- the bathymetric and morphological characteristics of the coast in question

From Figure 1 one can observe that the gulf stations situated far away from the open areas of the Baltic Sea, located in areas of relatively shallow depth, have significantly higher extreme water levels (Gulf of Riga with Pärnu Bay, Pärnu: +288 cm, −112 cm; Gulf of Finland, Hamina: +197 cm, −115 cm; Bothnian Bay, Kemi: +201 cm, −124 cm; Bay of Mecklenburg, Wismar: +198 cm, −190 cm) than the stations located directly by the open areas of the Baltic Sea (°Aland Sea, Degerby: +102 cm, −73 cm; Northern Baltic Proper, Landsort: +95 cm, −70 cm; Southern Baltic Proper, Kungsholmsfort: +110 cm, −89 cm).

It was observed (on an example Figure 1) that extreme water levels rise towards the inside of the bay – this is called the bay effect. The Bay of Mecklenburg is that part of the Baltic Sea where the greatest falls in sea level due to storm surges have been recorded (levels lower than −150 cm), which is associated with the relatively small depths and the above-mentioned bay effect

4. Summary - Geographical pattern in the occurrence of the extreme sea levels of the Baltic Sea

From presented the geographical distribution of extreme water levels, and as a result of research carried out in the framework of the project NCN (Wolski 2011–2014) determined a clear regularities on the occurrence of extreme sea levels of the Baltic Sea (so-called the geographical pattern). These patterns also confirmed in the publication Wolski et al. (2016) as well as Wolski (2017) These are the following regularities:

1. Eastern and northeastern coasts of the Baltic Sea, which are exposed to the inflow of western air masses related to a western atmospheric circulation, including the dominant tracks of pressure systems, are especially at risk of extreme hydrological events. In particular, it refers to Gulf of Riga along with Pärnu Bay, Gulf of Finland, and Gulf of Bothnia. These water basins experience the largest amounts of storm surges, the longest duration of high sea levels (≥70 cm) and the highest water levels in general. On the contrary, Swedish coasts of Central and Northern Baltic are the least endangered by extreme sea levels within the Baltic Sea basin. It is explained mostly by their eastern exposition, which constitutes an opposite direction to the inflow of western air masses and to the direction of low pressure systems propagation. In the conditions of western circulation, the filling up of the Baltic Sea increases and the inclination of water surface towards eastern coasts of the Baltic Sea increases as well. This characteristic regularity is in line with the results of works of Averkiev and Klevanny (2010), Suursaar et al. (2003), Johansson et al. (2001), Wolski et al. (2016),
2. South-western coasts of the Baltic Sea: Bay of Mecklenburg and Bay of Kiel are water basins of the most frequent and the deepest falls as well as of the extremely low sea levels (≤–70 cm) Eastern exposition of these bays favours the water outflow from their basins by fast-moving mesoscale low crossing the Baltic Sea from SW to NE. At the same time, Bay of Mecklenburg and Bay of Kiel give way only to big north-eastern gulfs only in terms of frequency of occurrence of high sea levels, maximum heights during high sea level periods and number of storm events, what is a peculiar phenomenon among the basins of the Baltic Sea.
3. Extreme phenomena, related to water dynamics, increase from the open sea waters of the Baltic Sea (Baltic Proper) to the innermost parts of its bays (Gulf of Bothnia, Gulf of Finland, Gulf of Riga, Bay of Mecklenburg and Bay of Kiel). The responsibility for this situation is taken by the so-called bay effect, i.e. the impact of geomorphological and bathymetrical configuration of the coastal zone on water dynamics. This effect cause an increase in extreme sea levels and in time of their occurrence at bay stations of the Baltic Sea from the seaside boundary of the single bay towards its farthest, innermost, cut-into-the-land point (the end of the bay). Narrowing of the bays is the one of the main reasons explaining this phenomenon. The defined volume of water removed or added to a narrowing and shoaling part of the bay will incur more extreme water level compared to its widened seaside part. This interpretation is compliant with results obtained by Sztobryn et al. (2005), Ekman and Mäkinen (1996) and Johansson et al. (2001), who claim that the highest values of sea level oscillations should be expected in the innermost part of these bays.

The occurrence of extreme sea levels is of vital importance not only for the scientific recognition of phenomena, but also for practical use. The conditions and causes of extremes sea levels at the Baltic coasts are of particular interest to designers of harbor infrastructure and marine coastal structures, marine geologists, geomorphologies, and harbor service operators.

References

Averkiev, A.S., Klevanny, K.A. (2010). Case study of the impast of cyclonic trajectories on sea-level extremes in the Gulf of Finland., Continental Shelf Research 30(6): 707-714,

Ekman, M., Mäkinen, J. (1996). Mean sea surface topography in the Baltic Sea and its transition area to the North Sea: A geodetic solution and comparisons with oceanographic models. Journal of Geophysical Research: Oceans (1978–2012) 101(C5)pp. 11993-11999, DOI:_10.1029/96JC00318

Johansson, M, Boman, H, Kahma, K, Launiainen, J. (2001). Trends in sea level variability in the Baltic Sea. Boreal Env Res 6: 159-179,

Suursaar, Ü., Kullas, T., Otsmann, M., Kõuts, T. (2003). Extreme sea level events in the coastal waters of western Estonia._ Journal of Sea Research 49(4): 295-303.

Sztobryn, M., Stigge, H.J., Wielbinska, D., Weidig, B., Stanisławczyk, I. et al. (2005). Storm surges in the Southern Baltic Sea, Warszawa, IMGW

Wolski T. (2011-2014). Extreme sea levels at the Baltic Sea coasts. Scientific project no. 2011/01/B/ST10/06470 funded by the National Science Centre

Wolski, T., Wiśniewski, B., Giza, A. Kowalewska-Kalkowska, H, Boman, H. et al. (2014). Extreme sea levels at selected stations on the Baltic Sea coast. Oceanologia 56(2): 259-290. DOI: 10.5697/oc.56-2.259

Wolski T., Wiśniewski B,. Musielak S., 2016. Baltic Sea datums and their unification as a basis for coastal and seabed studies, Oceanological and Hydrobiological Studies, 2016, 45(2), pp. 239-258, DOI: 10.1515/ohs-2016-0022

Wolski T. 2017. Spatial and temporal characteristics of the extreme sea levels of the Baltic Sea, Wyd. Naukowe Uniwersytetu Szczecińskiego, Rozprawy i Studia, T. 952, Szczecin

Topic E

Regional variability of water and energy exchanges

Impact of «small» climate-forming factors in the formation of the hydrological regime of the basins of the Zapadnaya Dvina and Neman Rivers in Belarus

Maryia Asadchaya, Kvach Alena and Zhuravovich Ludmila[1]

[1] State Institution «Center for of hydrometeorology and control of radioactive contamination and environmental monitoring of The Republic of Belarus» (Belhydromet) (gid2@hmc.by)

1. Introduction

Currently, a number of scientists address the issue of the impact of "small" climate-forming factors (solar and geomagnetic activity, geophysical parameters of the Earth, etc.) on natural processes.

There are several indexes that characterize the solar activity, which is often judged by the size and number of sunspot, flares, bright rings around sunspot etc. The relative Wolfer Number have the longest range.

Solar-terrestrial communications form thermal and water regime of air masses of the Earth, and, consequently, water regime of rivers and reservoirs. The increased or decreased long-term activity of the Sun determines the inflow of solar energy and increases or decreases the amount of precipitation and the stream runoff.

In this paper, the impact of 11-year cycles of solar activity on the hydrological regime of the Zapadnaya Dvina and Neman rivers basin with representative series of observations is estimated.

2. Methods

The study used data of hydrological observations for 3 hydrological stations of the Zapadnaya Dvina River (in the district of Surazh, Vitebsk and Ulla) and 5 hydrological stations in the Neman River basin (Neman River near the Stowbtsy, Belitsa, Masty, Grodno and the Shchara River near Slonim) for the period from 1877 to 2016. One of the objectives of the study is to minimize the impact of anthropogenic factors on the hydrological regime of the studied rivers. The analysis is carried out on the homogeneous series partially restored on the rivers analogs by settlement methods. The average and maximum water levels, minimum winter water levels, minimum water levels of the open channel period are investigated.

Testing the hypothesis of homogeneity of the water level series are made with the use of the ten criteria of Dixon and two criteria Smirnov-Grubbs. Student and Fisher criterions are calculated to check the stationarity of the level series. The Sudent t-test evaluated the stationarity of the time series relative to the mean, and the Fisher – dispersion.

3. Results

The analysis of the level regime values at the investigated hydrological posts for the combined five-year periods together with the relative Wolfer Number made it possible to trace the relationship between the solar activity cycles and the hydrological regime of the rivers of the Zapadnaya Dvina and Neman Rivers basin.

The interrelation of cycles of maximum levels and maximum values of relative Wolfer Number is fixed for all investigated hydrological stations.

Periods of growth of maximum water levels correspond to the maximum values of relative Wolfer Number in the context of 11-year cycles of solar activity. The most robust relationship observed for the periods 1881-1885 (5 years), 1892-1895 gg (4 years), 1905-1909. (5 years), 1915-1919. (5 years), 1926-1929 gg (4 years), 1936-1940 (5 years old), 1946-1949. (4 years), 1956-1960. (5 years), 1967-1970 (4 years), 1978-1982. (5 years), 1988-1992 (5 years) 1999-2002 (4 years) 2011-2014 (4 years).

The periods of minimum levels correspond to the values of reduced solar activity at all the hydrological stations. Periods of lowering the minimum water levels of the open channel correspond to the minimum values of relative Wolfer Number in the context of 11-year cycles of solar activity. The most close relationship observed for the periods: 1887-1891. (5), 1899-1903. (5 years), 1911-1915. (4 years), 1921-1924 (4 years), from 1931 to 1935 (4 years) 1951-1955 (5 years), 1961-1966. (6 years) 1972-1977 (6 years), 1984-1987 (4 years), 1994-1997 (4 years), 2005-2011 (6 years).

The relationship between the average annual levels, as well as the minimum winter levels and the highest values of relative Wolfer Number is differentiated depending on the hydrological stations and the studied cycles of solar activity. One difficulty in an objective assessment is the shorter homogeneous series of observations at average annual levels compared to maximum water levels.

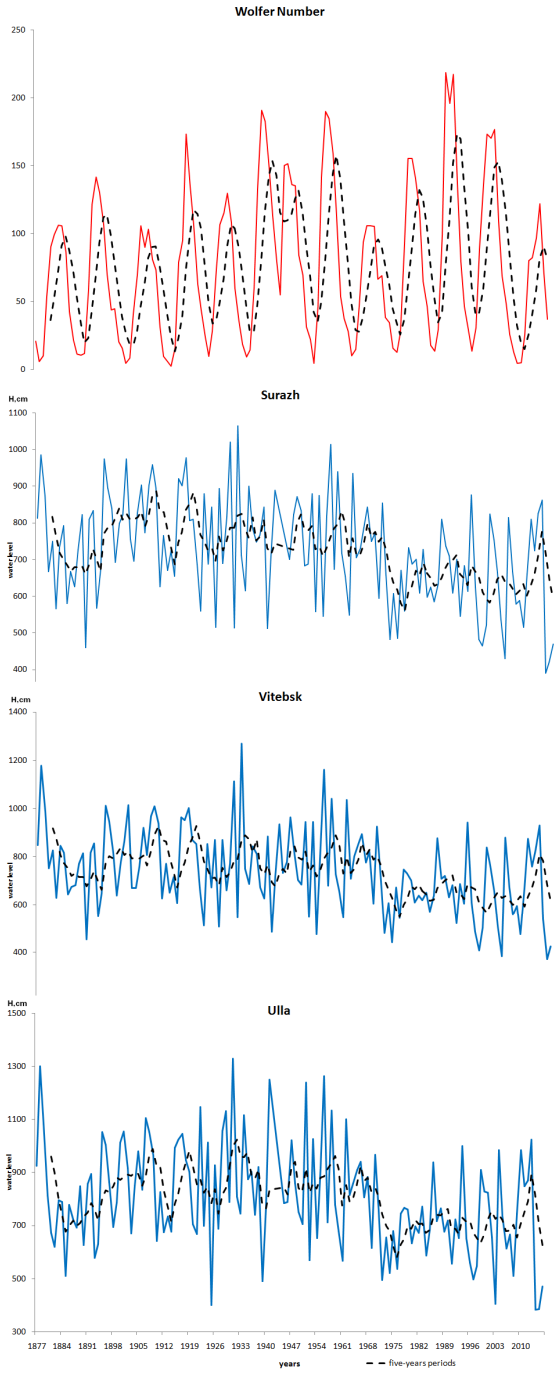

Figure 1. Dynamics of the maximum water levels of the Zapadnaya Dvina River and the relative Wolfer Number for the period from 1877 to 2016

4. Conclusions

As a result of the conducted researches impact of "small" climate-forming factors in formation of hydrological regime of the investigated rivers is noted.

Periods of growth of maximum levels correspond to the values of increased solar activity at all the hydrological stations.

The interrelation of cycles of values of minimum levels of water of the period of the open channel and the smallest quantities of relative Wolfer Number on all investigated hydrological stations is recorded.

The study of cyclic oscillations of hydrological characteristics over long periods of time, taking into account global climatic processes and their relationship with space objects such as the Sun, will allow to develop methods for calculating and predicting extreme hydrological characteristics for a long period of time.

References

State water cadastre. Annual data of a regime and resources of surface water for the period 1877-2016 – Minsk, Belhydromet.

Loginov V.F., Mikucki V.S. Climate change: trends, cycles, pauses Minsk, 2017, pp. 179

A.M. Vladimirov. The Sun-Earth Relationships And Cyclic Fluctuations Of Extreme Water Discharges, Scientific notes, № 29, pp. 7-16

Temporal behavior of atmospheric circulation types in Marmara Region (NW Turkey)

Hakki Baltaci[1]

[1] Turkish State Meteorological Service, Regional Weather Forecast and Early Warning Center, Istanbul, Turkey (baltacihakki@gmail.com)

1. Abstract

This article investigates the temporal variations in the occurrence frequencies and precipitation potentials of the surface atmospheric circulation types (Lamb Weather Types) that influence Marmara Region in NW Turkey, which is the most populated area of the country. These variations are analyzed in terms of their relationship with SSTs and with larger scale circulation, utilizing teleconnection pattern indices. The period of the analysis is 1971-2012. Our results reveal a decreasing frequency of occurrence of the rainfall supplying, vastly dominant northeasterly (NE) type in Marmara Region in all seasons except MAM; counterbalanced by a more frequent southwesterly (SW) type in SON and DJF, and by the easterly (E) type in JJA. This change is caused, at least partly, by trends in the indices of the teleconnection patterns such as the EA/WR, NAO and the AO; which are known to have influence over the entire Eastern Mediterranean. Contrary to its decreasing trend of occurrence, precipitation potential of type NE is increasing in SON and DJF, mainly due to the rising sea surface temperatures of the Black Sea. These changes and their possible continuation in the future imply a decreasing number of wet days during the wettest seasons (i.e. SON and DJF) for the northern and eastern sections of the region including the megacity Istanbul, while precipitation intensities during individual events should increase. Decreasing frequency of the Cyclonic (C) type in MAM and the substitution of NE with E in JJA, imply a drier and warmer future in these seasons; should the trends continue. Finally, less frequent NE occurrence in SON and JJA could partly explain the increasing temperatures in the area during these seasons, too.

2. Introduction

According to the Fifth Assessment Report (AR5) of the Intergovernmental Panel on Climate Change (IPCC, 2014), urbanization will rapidly increase in the countries of East Europe due to continuing growth in economic activities and in population. Parallel to this, it is predicted that fresh water need for agriculture, vegetation and energy production will also increase. As atmospheric precipitation is the main source of fresh water, any significant change in temporal or spatial pattern of rainfall will influence the availability of it. Amount and distribution of precipitation is known to be strongly dependent on the changes in atmospheric circulation. Determining circulation types (CTs hereafter) and establishing their relationship with precipitation is therefore an efficient approach to examine how precipitation varies in response to changing circulation (Huth et al., 2008; Dayan et al., 2012 and references therein). One particular and effective way for the identification of CTs is the Automated Lamb Weather Types (LWT) method (Jenkinson and Collison, 1977; Jones et al., 1993), which classifies daily mean sea level pressure fields according to certain predefined thresholds. LWT methodology proved to be useful for finding linkages between CTs and precipitation (e.g. Linderson, 2001; Brisson et al., 2011); as well as teleconnection patterns (Lorenzo et al., 2008). In this study, temporal variations and trends in the occurrence frequencies of the CTs and how their precipitation potentials change for the Marmara Region (NW Turkey) were investigated for the period 1971-2012.

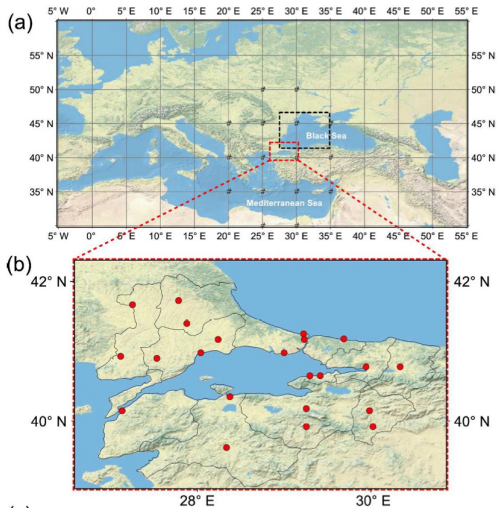

Figure 1. a) Location of the Marmara Region within the Eurasian context (red triangle), along with the section of the Black Sea where the utilized sea surface temperature series are averaged from (black rectangle). The 16 mean sea level pressure (MSLP) grid points used for the determination of the circulation types (Lamb Weather Types) are denoted by the pound sign. b) The Marmara Region and the meteorological stations used in the analysis.

3. First Results

In order to assess the connection of CTs in Marmara Region to the variations in larger scale circulation; it was calculated the correlations between the seasonal occurrence frequencies of each CT and the indices of five teleconnection patterns which are known to influence the Northern Hemisphere climate (Fig. 2). EA/WR is the most influential pattern in the occurrence of CTs during winter exhibiting positive significant (at 99% level) correlations with NE and NW; and negative ones with SW and C. The strongest association of EA/WR is with NE and SW in opposite directions, the negative correlation value with

SW reaching as high as 0.48. The second most influential teleconnection pattern on the CTs of Marmara Region during DJF is the AO, whose relationship with the occurrence of NE, SW and C is in the same fashion with EA/WR; though the correlation values are lower for NE and SW. As the relationship of other teleconnection patterns with CTs become less obvious in other seasons.

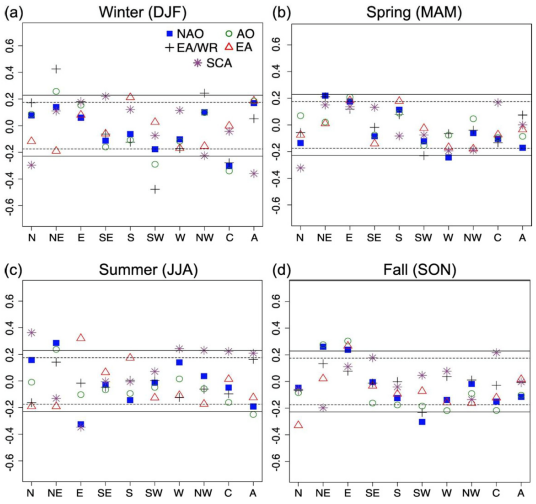

Figure 2. Pearson's correlation coefficients between mean seasonal teleconnection pattern indices and the seasonal number of occurrence days each circulation type for the Marmara Region, for the period 1971-2012. Each panel is for a different season. Statistically significant correlation values at the 99% and %95 levels are the ones which are greater than the absolute values denoted by the solid and dashed lines, respectively.

The increasing intensity of rainfall on NE days during DJF and SON is probably related to the rise in Black Sea SSTs. As Baltacı et al. (2015) thoroughly demonstrated, type NE has the highest potential to cause convective, sea effect precipitation in Marmara Region thanks to the air sea interaction over the Black Sea. This is especially true during SON and DJF when the mean temperature difference between colder air brought by the northeasterly winds and the relatively warmer Black Sea waters reaches its annual maximum. The sensitivity of the precipitation to Black Sea SSTs were demonstrated by Bozkurt and Şen (2011) as well. In accordance with these findings, and reasonably explaining the increase in the precipitation potential of type NE during these seasons, Black Sea SSTs in both SON and DJF have risen significantly through the analysis period (Shaltout and Omstedt, 2014). Fig. 3 shows the rise in both the type NE precipitation and the Black Sea SSTs on type NE days, during DJF.

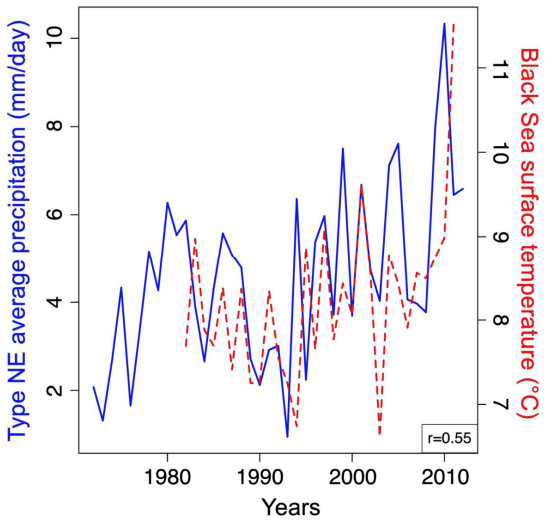

Figure 3. DJF (winter) variations of the regionally averaged precipitation amount associated with the northeasterly (NE) circulation type (solid blue line), along with the Black Sea surface temperatures; with the period 1981-2012. "r" stands for the Pearson's correlation coefficient between the two.

References

Baltacı H, Göktürk OM, Kindap T, Ünal A, Karaca M (2015) Atmospheric circulation types in Marmara Region (NW Turkey) and their influence on precipitation. International Journal of Climatology. 35: 1810-1820.

Bozkurt D, Şen OL (2011) Precipitation in the Anatolian Peninsula: Sensitivity to increased SSTs in the surrounding seas. Climate Dynamics 36: 711-726.

Brisson E, Demuzere M, Kwakernaak B, Van Lipzig NPM (2011) Relations between atmospheric circulation and precipitation in Belgium. Meteorol Atmos Phys 111: 27-39.

Dayan U, Tubi A, Levy I (2012) On the importance of synoptic classification methods with respect to environmental phenomena. International Journal of Climatology 32: 681-694.

Huth R, Beck C, Philipp A, Demuzere M, Ustrnul Z, Cahynova M, Kysely J, Tveito OE (2008) Classifications of atmospheric circulation patterns. Annals of the New York Academy of Sciences 1146: 105–152.

Jenkinson AF, Collison FP (1977) An initial climatology of gales over the North Sea. Synoptic Climatology Branch Memorandum 62, Meteorological Office: Bracknell, UK.

Jones PD, Hulme M, Briffa KR (1993) A comparison of Lamb circulation types with an objective classification scheme. International Journal of Climatology 13: 655–663.

Linderson ML (2001) Objective classification of atmospheric circulation over southern Scandinavia. International Journal of Climatology 21: 155-169.

Lorenzo MN, Taboada JJ, Gimeno L (2008) Links between circulation weather types and teleconnection patterns and their influence on precipitation patterns in Galicia (NW Spain). International Journal of Climatology 28: 1493-1505.

Shaltout M, Omstedt A (2014) Recent sea surface temperature trends and future scenarios for the Mediterranean Sea. Oceanologia 56 (3): 411-443.

The critical role of atmospheric forcing for simulating the dynamics of the Baltic Sea ecosystem

Ute Daewel[1], Corinna Schrum[1,2] and Beate Geyer[1]

[1] Helmholtz Centre Geesthacht, Institute of Coastal Research, Max-Planck-Str. 1, 21502 Geesthacht, Germany
[2] Geophysical Institute, University of Bergen, Allegaten 41, 5007 Bergen, Norway

1. Introduction

Using a fully coupled physical-biological ecosystem model for the coupled North and Baltic Sea system Daewel and Schrum (2013) showed that low frequency long-term changes of primary production depend to a large degree on the wind situation over the area. In the Baltic Sea the wind especially influences surface water nutrient supply through upwelling. Additionally, bottom water nutrient concentrations are controlled by Major Baltic Sea inflow (MBI) events. Due to the restricted exchange capacities and the strong stratification MBIs occur only sporadically under specific weather conditions (Omstedt et al. 2004) leading to a relatively long water residence time in Baltic Sea of about 30 years (Rodhe et al. 2006). Circulation pattern within the transition zone between North and Baltic Seas have been subject to a number of different studies aiming to understand the circumstances that determine MBIs. In Schinke and Matthäus (1998) long time series of oceanographic and atmospheric parameters have been analysed emphasizing that specific atmospheric conditions (e.g. pressure system and wind) are required. Since the time interval between the inflow events can be in the order of several years to decades, the water in the deep basins can be stagnant over long periods and might become anoxic, having thus a major effect on the Baltic Sea biogeochemistry. Hence, modeling the biogeochemistry of the Baltic Sea ecosystem depends strongly on the quality of the utilized atmospheric forcing. Here, we will analyze the response of simulated ecosystem dynamics to the quality and resolution of the atmospheric forcing, by comparatively analyzing model simulation forced by different atmospheric reanalysis/model products.

2. Method and Analysis

The model used is a 3d coupled ecosystem model ECOSMO E2E, which is a novel NPZD-Fish model approach (Daewel and Schrum, 2017a) that allows estimating lower trophic level dynamics, biogeochemical cycling and higher trophic level production potential (Fig. 1). The underlying lower trophic level ecosystem model ECOSMO has previously been shown to reliably simulate Baltic Sea ecosystem dynamics (Daewel & Schrum 2013, 2017b) over long time periods with a NCEP/NCAR reanalysis forcing (Kalnay et al. 1996). However, the model, in the presented setup, was not able to capture all MBIs, observed as changed in oxygen conditions in the Baltic Proper and else, also showed uncertainties in simulating biogeochemistry in the Bothnian Bay.

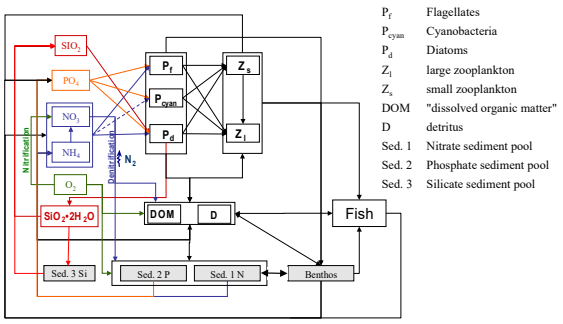

Figure 1. Schematic diagram of biological-geochemical interactions in ECOSMO E2E

The NCEP/NCAR reanalysis product used is available with a resolution of 1.9°, which is relatively coarse concerning the scale that needs to be resolved in the Baltic Sea and especially at the opening to the North Sea and in the Gulf of Bothnia. In Feser et al. (2011) and Winterfeldt et al. (2011) the weaknesses in NCEP re-analysis were discussed. The authors additionally identified critical areas in North Sea and Baltic Sea where downscaling of the atmospheric forcing adds value. These are among others the Kattegat and Belt Sea, the Baltic Sea entrance area in the South and Gulf of Bothnia (in parts) where the NCEP reanalysis is not able to resolve complex orography. Hence, in addition to the course NCEP forcing we will use the coastDat-2 dataset (Geyer 2014) with a resolution of 0.22° so force the ecosystem model. CoastDat-2 is available for 1948 to 2015 and was generated with the regional climate model COSMO-CLM (CCLM) forced by the NCEP/NCAR reanalysis. The third forcing we will apply is coastDat-3, which is a COSMO-CLM simulation forced by the ERA-interim reanalysis (Dee et al. 2011) available from 1979 onwards. We will then analyze the model simulations comparatively focusing specifically on the representations of the MBIs and the consequences for the vertical nutrient distribution in the Baltic Proper as well as the representation of nutrient and system productivity in the Bothnian Bay.

References

Daewel U, Schrum C (2013) Simulating long-term dynamics of the coupled North Sea and Baltic Sea ecosystem with ECOSMO II: Model description and validation. J Mar Syst 119–120:30–49

Daewel U, Schrum C (2017a) Towards End-2-End modelling in a consistent NPZD-F modelling framework: Application to North Sea and Baltic Sea. Prog Oceanogr subm.

Daewel U, Schrum C (2017b) Low frequency variability in North Sea and Baltic Sea identified through simulations with the 3-d coupled physical-biogeochemical model ECOSMO. Earth Syst Dyn Discuss:1–23

Dee DP, Uppala SM, Simmons AJ, Berrisford P, Poli P, Kobayashi S, Andrae U, Balmaseda MA, Balsamo G, Bauer P, Bechtold P, Beljaars ACM, Berg L van de, Bidlot J, Bormann N, Delsol C,

Dragani R, Fuentes M, Geer AJ, Haimberger L, Healy SB, Hersbach H, Hólm E V., Isaksen L, Kållberg P, Köhler M, Matricardi M, Mcnally AP, Monge-Sanz BM, Morcrette JJ, Park BK, Peubey C, Rosnay P de, Tavolato C, Thépaut JN, Vitart F (2011) The ERA-Interim reanalysis: Configuration and performance of the data assimilation system. Q J R Meteorol Soc 137:553–597

Feser F, Rockel B, Storch H von, Winterfeldt J, Zahn M (2011) Regional Climate Models Add Value to Global Model Data: A Review and Selected Examples. Bull Am Meteorol Soc 92:1181–1192

Geyer B (2014) High-resolution atmospheric reconstruction for Europe 1948-2012: CoastDat2. Earth Syst Sci Data 6:147–164

Kalnay E, Kanamitsu M, Kistler R, Collins W, Deaven D, Gandin L, Iredell M, Saha S, White G, Woollen J, Zhu Y, Leetmaa A, Reynolds R, Chelliah M, Ebisuzaki W, Higgins W, Janowiak J, Mo KC, Ropelewski C, Wang J, Jenne R, Joseph D (1996) The NCEP/NCAR 40-year reanalysis project. Bull Am Meteorol Soc 77:437–471

Omstedt A, Elken J, Lehmann A, Piechura J (2004) Knowledge of the Baltic Sea physics gained during the BALTEX and related programmes. Prog Oceanogr 63:1–28

Rodhe J, Tett P, Wulff F (2006) The Baltic and North Seas: A Regional Review of some important Physical-Chemical-Biological Interaction Processes. . In: Robinson AR, Brink K (eds) The Sea, Vol. 14 B. Harvard University Press, p 1033–1075

Winterfeldt J, Geyer B, Weisse R (2011) Using QuikSCAT in the added value assessment of dynamically downscaled wind speed. Int J Climatol 31:1028–1039

Model estimates of climate and streamflow changes in the Western Dvina River basin

Irina Danilovich [1], Zhuravlev S.[2], Kurochkina L.[2], Kvach A.[3]

[1] Institute for Nature Management of the National Academy of Sciences, Minsk, Belarus (irina-danilovich@yandex.ru)
[2] State Hydrological Institute, St. Petersburg, Russian Federation
[3] Belhydromet, Minsk, Belarus

1. Introduction

The considerable changes of streamflow and its intra-annual distribution connected with climate warming during the last decades were noted within the Baltic Sea basin (BACC, 2008, BACC, 2015). The significant climate warming in the eastern part of the Baltic Sea basin (within the territory of Belarus) has begun since abnormally warm weather in 1989 and continues now (Komarovskaya, 2009). The rising of the temperature in the end of 20th century had no effect on the annual amount of precipitation in Belarus. Winter precipitation increased during the warming period. The greatest changes have been observed on the territory of the Western Dvina River basin within the territory of Belarus (Partasenok, 2014).

A number of researches conducted in Belarus convincingly show that climate changes have already led to the essential changes of the hydrological regime of the Western Dvina River. These changes connected with increase of winter and summer low-water water discharges and the reduction of spring flood streamflow. At the same time the gradient of the change of winter flow is higher, than for summer (Gryadunova, 2005).

Despite a significant amount of the publications devoted to the regional issues of changes in hydrological regime the necessity for the detailed researches still remains for the identification of the reasons of these changes and their forecasts for a long-term period. The study presents the results of the model estimations of the expected changes of the regional climate and the Western Dvina (at Vitebsk) streamflow in the 21st century.

2. Materials and methods

A data-set of instrumental observations for runoff on the Western Dvina River near Vitebsk city have been used for trend analysis. The study period is 1945-2015.

Calculations of trends significance and value were carried out according to Sen and Mann-Kendall's tests (Sen, 1968; Mann, 1945)

Modeling of streamflow was carried out applying the model named “Hydrograph”. The model developed at State Hydrological Institute (St. Petersburg) under the leadership of Yu.B. Vinogradov (Vinogradov et al., 2011).

The analysis of future climate changes was provided according to the climate model simulations presented by EURO-CORDEX for the grid entering borders of Belarus. The daily means of air temperature and precipitation with the spatial resolution of 0.44 degrees for the study we used. The study period for future changes covers 2021-2100, the historical period - 1971-2000. The climatic projections have been used according to scenarios RCP4.5 and RCP8.5.

Projections of meteorological and hydrological characteristics are executed on consecutive decades: 2021-2030, 2031-2040, 2041-2050, 2051-2060, 2061-2070, 2071-2080, 2081-2090, 2091-2100.

3. Results and discussion

Assessment of the recent changes

The significant trends of the following hydrological characteristics for Western Dvina-Vitebsk gauge have been established: spring flood peak discharges (-4.6%/10 years) and maximum daily discharges (-4.5%/10 years). The maximum discharges are normally observed during the spring flood. The tendency of insignificant increase have been noted for the values of the spring runoff depth (0.2%/10 years) and flood duration (0.1 days/10 years). The minimum discharges trend during winter low-water period is positive and equal 10%/10 years. The annual discharges trend is about 2%/10 years, however this trend is not statistically significant (at significance value $\alpha = 0.05$). There are no significant changes for the values of the minimum discharges during summer low-water periods.

The analysis of monthly runoff for the period of 1945-2015 showed the existence of a significant positive trend for December (6%/10 years), January (9.9%/10 years), February (9.3%/10 years) and March (8.3%/10 years). Trends are insignificant and negative for monthly discharges in April (-4.3%) and May (-0.6%). There are no significant trends for other months.

Runoff changes in the future

The annual values of air temperature are expected to gradually increase during the period 2021-2100 to 2.4°C under scenario RCP4.5 and to 4.7°C under scenario RCP8.5. Deviations of the seasonal values of air temperature are expected mainly positive and are characterized by gradual growth: during a winter season deviations will increase to 2.8 and 6.0°C (for RCP4.5 and RCP8.5 respectively) by the end of century. During a spring season a deviations are expected up to 2.3 and 4.5° C (for RCP4.5 and RCP8.5). Summer and autumn seasons are characterized by lower values of deviations within 2.0-4.0°C by the end of century, an autumn season is characterized by the smallest values of deviations during the considered period. During a winter season it is expected decrease a numbers of days with near zero temperature, during a summer season – the significant increase of warm days.

According to calculations, the annual sums of precipitation will fluctuate by the end of the study period within 15-30 mm without significant deviations. Distribution of the seasonal deviations of precipitation sums is characterized by the greatest values during the winter and

spring seasons. During the period of 2021-2100 deviations of the winter sums of precipitation will steady increase up to 20-28 mm under scenario RCP4.5. The consecutive decadal increase of the seasonal sums of precipitation expected under scenario RCP 8.5: from 8 mm (2021-2030) to 50 mm by the end of the century. During spring period seasonal deviations are expected at the same level. Their sums will be 15-31 mm for RCP4.5 scenario, the consecutive growth from 14 to 50 mm (2081-2090) is supposed under RCP8.5 scenario.

Precipitation of the warm period according to both scenarios (RCP4.5 and RCP8.5) is predicted with large uncertainty. The further dynamic of the deviations of seasonal precipitation in summer and autumn according to calculations is unclear and it is only possible to assume about variations within the standard of seasonal values.

The expected changes of a streamflow

The criteria of NSE and BIAS have been used for model suitability assessment and the calculations of the expected changes in streamflow regime. The following values of the criteria of NSE and BIAS were received: 0.79 and 9.7% for the period of 1970-2015. Modeling results can be considered as satisfactory according to the criteria offered by Moriasi and coauthors (Moriasi et al., 2015). The high quality of modeling is explained by the uniformity of the conditions of streamflow formation and the dense network of meteorological observations.

Assessments of the expected runoff regime of the Western Dvina River were conducted for the period of 2021-2100 and then compared to the period 1971-2000. It is projected that annual discharges will increase on 8% during 2021-2100 under RCP4.5 scenario and on 12% for the RCP8.5 scenario. There is no accurate trend by decades in annual discharges. Thus, the annual streamflow, as well as in the last decades, presumably will vary within the norm.

Results of the calculations of the expected changes of intra-annual streamflow distribution of the Western Dvina River at Vitebsk are presented in the figure 1. The results show that the current tendency of winter discharges increase and spring flood streamflow reduction will remain in the future.

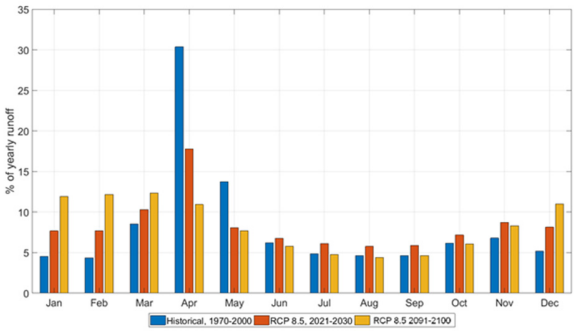

Figure 1. The expected changes of the intra-annual streamflow distribution of the Western Dvina River at Vitebsk for base the period (1971-2000) and for 2021-2030 and 2091-2100 decades under RCP8.5 scenario.

The maximum spring flood discharges are expected to decrease (on average for 21% for RCP4.5 and 24% for RCP8.5). There is no decadal trend for this characteristic as for an average annual streamflow.

The minimum runoff of winter low-water period is expected to increase up to 16% and 20% above norm under RCP4.5 and RCP8.5 respectively. Despite the essential expected decadal changes of meteorological parameters during 2021-2100 the trend is also not revealed.

4. Summary

The comparative analysis of actual and expected changes in the Western Dvina streamflow allowed to conclude that the average runoff over the past decades has varied within normal flow limits without a significant trend. This tendency will continue in the future. Main changes have affected the inter-annual distribution of the streamflow. Currently, there is a steady upward trend in the low flow and downward trend in the spring flow. According to the estimations of the expected changes in streamflow, this tendency will be intensified in the future.

It was found out that possible changes in the maximum water discharges are comparable to their variability ($0.5<SNR<0.9$). The expected changes in the average and minimum runoff are much more less than the intra-model variability.

References

BACC Author Team (2008). Assessment of Climate Change for the Baltic Sea Basin. Springer-Verlag Berlin Heidelberg, p. 474

BACC Author Team (2015). Second Assessment of Climate Change for the Baltic Sea Basin. Springer International Publishing, p. 501

Komarovskaya E.V., Kuleshova I.Yu. (2009) Air temperature, Hydrological monitoring in the Republic of Belarus, p. 260

Partasenok I.S., Groisman P.Ya., Chekan G.S., Melnik V.I. (2014) Winter cyclone frequency and following freshet streamflow formation on the rivers in Belarus, Environmental Research Letters, Vol. 9, No. 9, p. 13

Sen P.K. (1968) Estimates of the regression coefficient based on Kendall's tau, Journal of the American Statistical Association, Vol. 63, No. 324, pp. 1379-1389

Gryadunova O.I. (2005) The minimum runoff on the Western Dvina river, materials of the the II International Ecological Symposium in Polotsk, pp. 98-99

Partasenok I.S., Gayer B. (2015) Studies of possible scenarios of climate change in Belarus on the basis of the ensemble approach, Proceedings of the Hydrometeorological research center of Russian Federation, No. 358, pp. 99-111

Mann H.B. (1945) Nonparametric tests against trend, Econometrica, Vol. 13, No. 3, pp. 245-259

Moriasi D.N., Gitau M.W., Pai N., Daggupati P. (2015) Hydrologic and water quality models: Performance measures and evaluation criteria, Transactions of the ASABE, Vol. 58, No. 6, pp. 1763-1785

Vinogradov Yu.B., Semenova O.M., Vinogradova T.A. (2011) An approach to the scaling problem in hydrological modelling: the deterministic modelling hydrological system, Hydrological processes, Vol. 25, No. 7, pp. 1055-1073

Analysis of bottom and wind friction velocities in inflow and non-inflow periods in the Baltic Sea

Maria Golenko, Zhurbas V.

Shirshov Institute of Oceanology, Russian Academy of Sciences, Moscow, Russia (m.golenko@yahoo.com)

Using a regional circulation model of the Baltic Sea (based on POM) with the horizontal resolution of 0.5 nautical miles time series of bottom friction velocity and bottom salinity were simulated for two 60-days periods, starting from 26.12.2014 and 26.12.2015, and analysed at specific points of interest along the inflow water pathway. Date 26.12.2014 precedes the inflow of saline waters in the Bornholm basin; at that the amount of inflow water in the Arkona Basin is maximum. The second period is non-inflow, and this period was chosen for the comparative analysis with the previous one. In vertical 55 sigma-layers were specified, at that in the deepest area of the Bornholm Basin the thickness of the near bottom sigma-layer was equal to 10 cm.

In the course of the study the spatio-temporal averaging of the squared bottom friction velocity U^{*2}, bottom salinity S, and squared wind friction velocity U^*w^2 was performed for the five regions in the path of the saline water inflow into the Baltic Sea (see fig. 1). For each of the specified 60-day intervals, the simulation was performed in the absence of wind and in real wind according to HIRLAM data. In the absence of wind, the dynamic effect of the gravity current was determined. Calculations with a real wind made it possible to obtain complete estimates of the bottom friction velocity and to compare them with the effect of gravity currents, as well as the wind friction velocity. The bottom friction velocity at chemical warfare dumpsites in the Bornholm and Gotland basins was found to be permanently below the resuspension thresholds for the suspended particulate matter and fine sand, and even the Major inflows could not violate the balance. Some occasional exceedance of the bottom friction velocity relative to the resuspension threshold for the fine biogenic material (fluffy layer and cysts) appeared to be possible. In order to assess the potential threat from the stirring-up of fluffy layer having a thinner, fluffy structure, it is necessary to investigate its ability to accumulate poisonous substances. This new task raises the urgency of the development of methods for the complex study of the bottom layer.

The results of the simulations showed that in the Bornholm Strait bottom friction exceeded the wind friction (fig. 2 (a, b)). The latter circumstance is explained by the narrowness and shallowness of this water channel. It should also be noted that the wind had no significant effect on the character of the salinity variations (fig. 2 (c, d)). This means that the bottom dynamics in this area is determined mainly by the gravity currents that present regardless of the wind effect. The analysed near-bottom dynamic characteristics at the exit from the Slupsk Furrow are similar to the ones in the Bornholm Strait. Apparently, this is due to the similar morphological characteristics of the areas under consideration. The difference is noted only in the salinity field: in the period of inflow the salinity in the Slupsk Furrow is higher than in its absence by 3 psu. This can be explained by the existence of the Slupsk Sill, which blocks the overflow of the most saline near bottom water from the Bornholm Basin to the Slupsk Furrow, while there is no such regulator in front of the Bornholm Strait. In the Slupsk Furrow during the period of the first 30 days, the dynamic effect of the gravity current, formed in the absence of a wind effect, on the bottom area exceeds the dynamic impact of the sea in real wind. In the next 30 days, the dynamic effects of the gravity current and the current formed under the influence of the wind are comparable. It means that the initial volume of salt water in the Arkona Basin is sufficient to maintain a high salinity water flow for 30 days. In the Bornholm Dumpsite area the wind friction velocity U^*w^2, as a rule, exceeds the bottom friction velocity U^{*2}. The absence of a direct dependence of the fluctuations of bottom and wind friction velocities indicates that the wind basically only indirectly affects the bottom dynamics of the investigated regions. Moreover, the positive correlation between U^{*2} and U^*w^2 is more pronounced in the non-inflow period 2015-2016, namely, with weaker gravity currents.

At the chemical warfare dumpsite in the Bornholm basin U^{*2} was found to be permanently below the resuspension thresholds for the suspended particulate matter and fine sand ~ $2*10^{-4}$ м^2/с^2, and even the Major inflows could not violate the balance; only in rare cases U^{*2} reached the resuspension threshold for fluffy material ~ $2.5*10^{-5}$ м^2/с^2.

The work was supported by the state assignment No. 0149-2018-0012 and EU INTERREG Baltic Sea Region Programme 2014-2020, Project DAIMON (Decision Aid for Marine Munition).

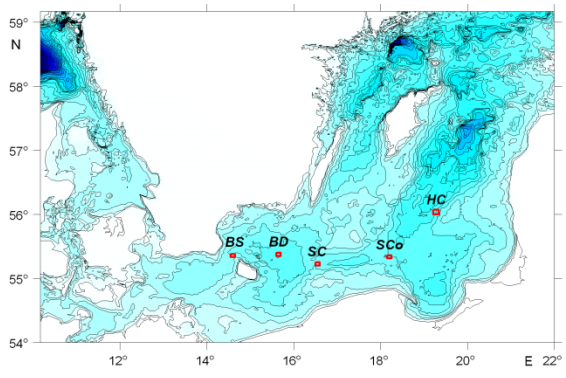

Figure 1. The modeling area with the boundaries of 5 regions - ***BS*** (Bornholm Strait), ***BD*** (Bornholm Dumpsite), ***SS*** (Slupsk Sill), ***SCo*** (Slupsk Channel outlet), ***HC*** (Hoburg Channel), - marked with red rectangles, for which spatial averaging and subsequent analysis of the squared bottom and wind friction velocities (U^{*2} and U^*w^2) were carried out.

(a) 26.12.2014

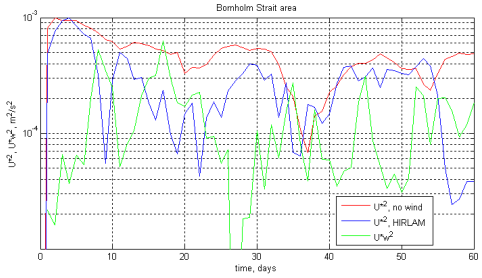

(b) 26.12.2015.

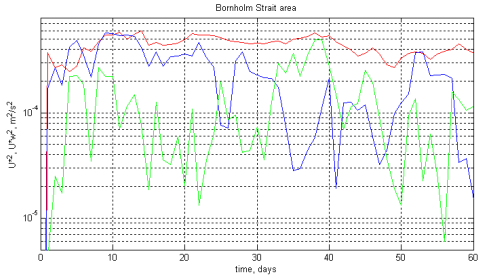

(c) 26.12.2014

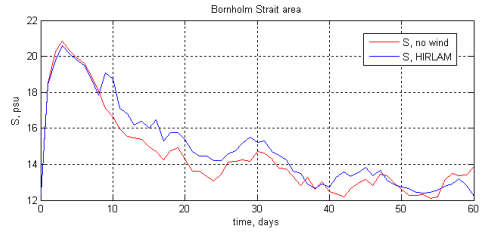

(d) 26.12.2015

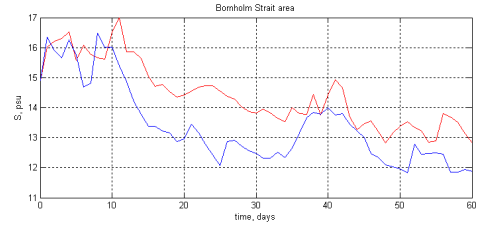

Figure 2. (a, b): Time series of the squared bottom friction velocity U^{*2}, averaged in space, in the absence of wind impact (red line), under the HIRLAM wind (blue line), and squared wind friction velocity $U^{*}w^{2}$ (green line) in the Bornholm Strait (***BS***) area (see fig. 1); (c, d): time series of the near bottom salinity. The simulations were performed with the initial thermohaline stratifications for 26.12.2014 (a, c) and 26.12.2015(b, d).

(a) 26.12.2014

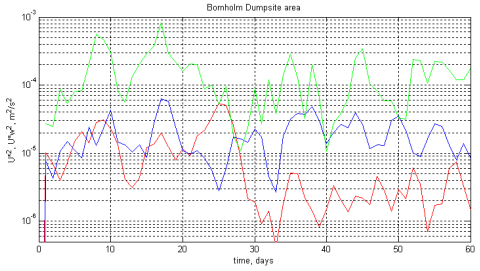

(b) 26.12.2015

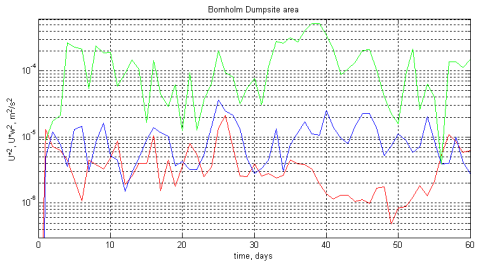

Figure 3. The same as in fig. 2 but for the area ***BD*** (Bornholm Dumpsite).

Changing effect of large scale atmospheric circulation on the regional climate variability of the Baltic Sea over the period 1948-2017

Andreas Lehmann[1], Piia Post[2] and Katharina Höflich[1]

[1] GEOMAR Helmholtz Centre for Ocean Research Kiel, Germany (alehmann@geomar.de)

[2] Institute of Physics University of Tartu, Tartu, Estonia

1. Introduction

A detailed assessment of climate variability of the Baltic Sea area for the period 1958-2008 (Lehmann et al. 2011) revealed that recent changes in the warming trend since the mid-1980s, were associated with changes in the large-scale atmospheric circulation over the North Atlantic. The analysis of winter sea level pressure (SLP) data highlighted considerable changes in intensification and location of storm tracks, in parallel with the eastward shift of the North Atlantic Oscillation (NAO) centres of action. Additionally, a seasonal shift of strong wind events from autumn to winter and early spring exists for the Baltic area. Lehmann et al. (2002) showed that different atmospheric circulation regimes force different circulation patterns in the Baltic Sea. Furthermore, as atmospheric circulation, to a large extent, controls patterns of water circulation and biophysical aspects relevant for biological production, such as the vertical distribution of temperature and salinity, alterations in weather regimes may severely impact the trophic structure and functioning of marine food webs (Hinrichsen et al. 2007). To understand the processes linking changes in the marine environment and climate variability, it is essential to investigate all components of the climate system which of course include also the large scale atmospheric circulation. Here we focus on the link between changes/shifts in the large scale atmospheric conditions and their impact on the regional scale variability over the Baltic Sea area for the period 1948-2017.

2. Changes in contribution of dominant regimes of atmospheric circulation

Following the work of Hurrel & Deser (2009) the clustering algorithm was applied over the North Atlantic domain (80°W-30°E, 20°N-80°N) identifying four winter climate regimes in SLP (Fig. 1). Hurrel & Deser (2009) pointed out that two of the weather regimes correspond to the positive and negative phases of the NAO, while the third and fourth regimes display strong anticyclonic ridges over Scandinavia (the 'Blocking' regime) and off western Europe (the 'Atlantic Ridge' regime). For the period 1949-2008 all four regimes occur with about the same frequency between 23% and 26%. Lehmann et al. (2011) highlighted a change in the contribution of dominant regimes for consecutive 20-year periods using cluster analysis of winter (DJFM) daily SLP data. The total contribution of the 'Blocking' and 'Atlantic Ridge' pattern is between 48-50% and the total contribution of the NAO pattern is between 50-52%. However, the relative contributions of the two NAO pattern are different for consecutive 20-year periods (Fig. 2). For the periods 1949-1968, 1959-1978 and 1969-1988 the NAO$^-$ pattern is prevailing, whereas the most recent periods 1979-1998 and 1989-2008 show an increased contribution of the NAO$^+$ pattern. Lehmann et al (2002) showed that a change of the local atmospheric index (Baltic Sea Index) to positive phases results in inflow conditions accompanied by a substantial increase in mean sea level. Consequently, a change to more frequent and more pronounced winter NAO$^+$ patterns would change the structure of the general circulation in the Baltic Sea.

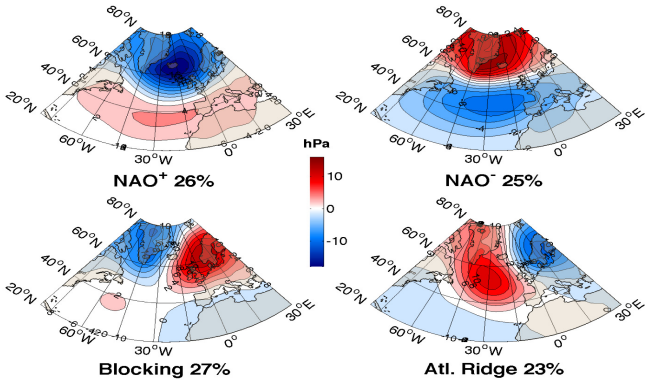

Figure 1. Winter (DJFM) climate regimes in SLP over the North Atlantic domain (80°W-30°E, 20°N-80°N) using daily data over the period 1949-2008. The percentage of each panel expresses the frequency occurrence of a cluster out of all winter days since 1949. Contour interval is 2 hPa.

3. Variability within dominant regimes

Hurrel & Deser (2009) concluded from cluster analysis that there exists a large amount of within-season variance in the atmospheric circulation of the North Atlantic and that most winters are not dominated by any particular regime alone.

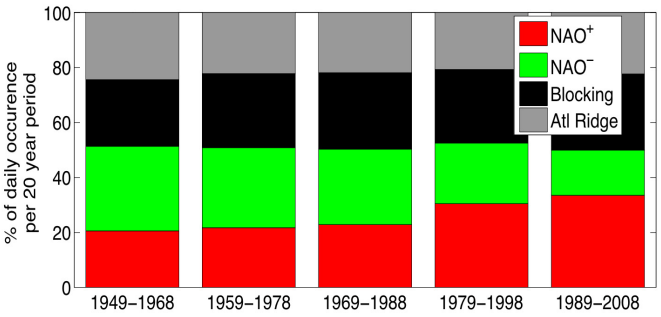

Figure 2. Contribution [%] of occurrence of dominant climate winter regimes NAO$^+$, NAO$^-$, Blocking and Atlantic Ridge, in different 20-years periods, identified by cluster analysis using daily winter (DJFM) SLP anomalies from NCEP/NCAR reanalysis data (1949-2008).

Comparing the time history of occurrence of the four dominant atmospheric circulation regimes with seasonal and monthly resolution confirms these findings (Fig. 3) where the two NAO regimes show larger variability than the 'Blocking' and 'Atlantic Ridge' regime. This within-season variability seems to be

important for the establishment of characteristic regional weather pattern over the Baltic Sea area.

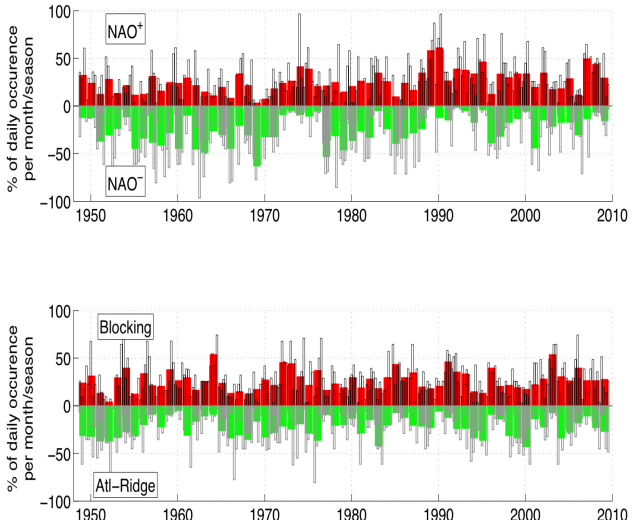

Figure 3. Time history of occurrences of the NAO, Atlantic Ridge and Blocking regimes (cf. Hurrel & Deser 2009) over the period 1949-2009. Vertical bars give the number of daily occurrences per season (filled bars) /per month (contoured bars) during winter (DJFM) for the given regime.

4. Extended analysis 1948-2017

The above described analysis will be extended by new data for the period 1948-2017. We will present an EOF analysis of winter (DJFM) monthly mean SLP anomalies to investigate movements of robust patterns which can be associated with the NAO. Furthermore, from cluster analysis we will get information of prevailing patterns which directly impact regional climate variability of the Baltic area. The analysis will be extended to include also the summer North Atlantic Oscillation (SNAO, Folland et al. 2008), which is the summertime parallel to the winter NAO. It is able to explain the principal variations of summer climate over northern Europe and hence the Baltic Sea area. The large-scale atmospheric variability will be further associated to the regional atmospheric circulation patterns over the Baltic area. We will classify air pressure patterns in order to describe the variability of atmospheric circulation in the Baltic Sea region. For this task we will apply the GWT (Gross Wetter Typen) method that bases on three prototype patterns (Beck et al., 2007).

References

Beck C, Jacobeit J, Jones PD. (2007) Frequency and within-type variations of large scale circulation types and their effects on low-frequency climate variability in Central Europe since 1780. Int. J. Climatol., Vol 27, pp 473-491.

Folland CK, Knight J, Linderholm HW, Fereday D, Ineson S, Hurrel JW (2009) The summer North Atlantic Oscillation: Past, Present, and Future. J Clim, 22, 1082-1103.

Hinrichsen H-H, Lehmann A, Petereit C, Schmidt J (2007) Correlation analysis of Baltic Sea winter water mass formatio and its impact on secondary and tertiry production. Oceanologia, 49, 38-395.

Hurrel JW, Deser C (2009) North Atlantic climate variability; The role of the North Atlantic Oscillation, J. Mar. Sys. 78, 28-41.

Lehmann A, Krauss W, Hinrichsen H-H (2002) Effects of remote and local atmospheric forcing on circulation and upwelling in the Baltic Sea. Tellus A 54299-316.A

Lehmann A, Getzlaff K, Harlass J (2011) Detailed assessment of climate variability in the Baltic Sea area for the period 1958 to 2009. Clim Res 46, 185-1996.

Relationship between satellite measured soil moisture and meteorological parameters

Viktorija Mačiulytė[1]

[1] Institute of Geosciences, Vilnius University, Vilnius, Lithuania (viktorija.maciulyte@gf.stud.vu.lt)

1. Introduction

Soil moisture is one of the decisive factors of the plants state, as it predetermines plant growth and productivity (Valiukas, 2015). Also, soil moisture is an important part of water cycle and plays an important role in global circulation processes (Owe et al., 2001; Wang, Qu, 2009).

Soil moisture measurements are necessary for evaluation of drought, water balance modelling and requires high quality measurements. *In situ* point measurements have quite good accuracy, but poor spatial representation and such measurements are quite expensive. Remote sensing methods, like satellite information, could help to improve spatial resolution of soil moisture measurements (Méndez-Barroso et al., 2009).

2. Data and methods

The goal of this research is to estimate the relationship between satellite soil moisture and meteorological parameters in the eastern part of Baltic Sea region (53–60°N and 20–30°E) covering warm seasons (April–October) of the period from 1979 to 2016.

Remote sensing soil moisture data were derived from ESA Soil Moisture CCI Project soil moisture product which was created from merged active and passive products (water amount m^3/m^3) with 25 km spatial and daily temporal resolution. It was also used minimum, maximum and daily mean air temperature and daily precipitation amount from E-OBS with 25 km spatial resolution.

The relationship between air temperature, precipitation and soil moisture relationship was analyzed using cross correlation with lag up to 10 days for temperature and precipitation sums.

Coefficient *k* was used for the purpose to analyze complex influence of temperature and precipitation:

$$k = \frac{p}{0{,}1 \sum t_d}$$

where p – precipitation sum of period *d*, t_d – daily maximum temperature, *d* – days.

Coefficient k is similar to Hydrothermal Selianinov coefficient (Valiukas, 2015), but it was calculated using daily maximum temperature. In the start or end of season maximum temperature could fall below zero, that why analyzed only positive *k* values. Coefficient *k* was calculated using periods from 1 to 20 days.

3. Results

It was found that the strongest relationship (r=-0.4–-0.5) is between soil moisture and mean and maximum daily temperature. The air temperature impact on soil moisture is the strongest in the central part of the analyzed area, especially in the central and western part of Lithuania (Figure 1). It was found the strongest correlation (r=-0.4–-0.5) between maximum temperature of the 8 previous days and soil moisture in 23 % of analyzed territory (20 % in case of mean daily temperature). Meanwhile, the minimum air temperature almost does not significantly affect the soil moisture throughout the analyzed area in warm period of year.

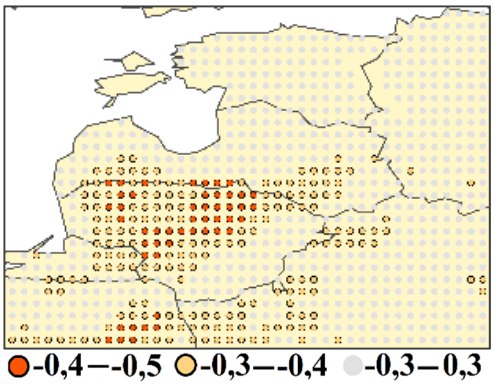

Figure 1. Correlation between maximum air temperature of 8 previous days and soil moisture in April – October.

Other relation was established between soil moisture and precipitation amount. It has been determined that the relationship between of daily precipitation sum and the soil moisture in a same day is weak. However, stronger relationship (r = 0.4–0.5) was found with daily precipitation sum one day prior soil moisture measurement (Figure 2). The strongest connections were found in the north, north-east and south, south-east of analyzed area.

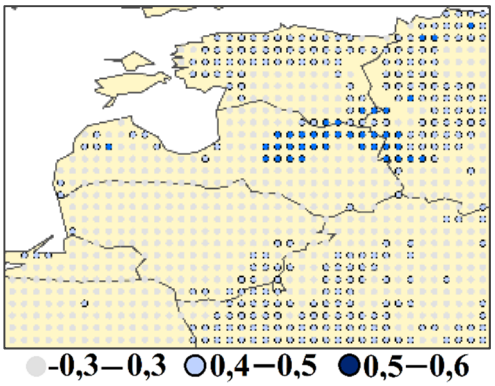

Figure 2. Correlation between soil moisture and precipitation amount in previous day.

Soil moisture is not only a matter of day-to-day precipitation, but also it is a product of a long-term accumulation. Correlation analysis was performed using precipitation sums of the periods from 2 to 10 days. It was found that the strongest relationship is between the precipitation sum of 2–3 days and the soil moisture content one day later. In spatial terms, the correlation is

the strongest in the northern part (r = 0.5), and slightly weaker in the south (r = 0.4).

The effects of precipitation and air temperature on soil moisture are usually complex. The coefficient *k* is used to estimate the complex influence.

The analysis of correlation between coefficient *k* and soil moisture was carried out using a correlation with lag up to 20 days.

The correlation analysis shows different results for different months. In April, the relationship between soil moisture and coefficient *k* of different periods is weak. It means that soil moisture in April is mostly predetermined by conditions of previous winter such as maximum snow water equivalent, frost depth and etc.

In May the soil moisture correlates the best with coefficient *k* calculated using precipitation sum and the maximum air temperature of 7 days, while 5 days is the most important period in June–August. The strongest correlation was found in August. In September the coefficient *k* of 3 days is the most significant while in October this period increases up to 15 days.

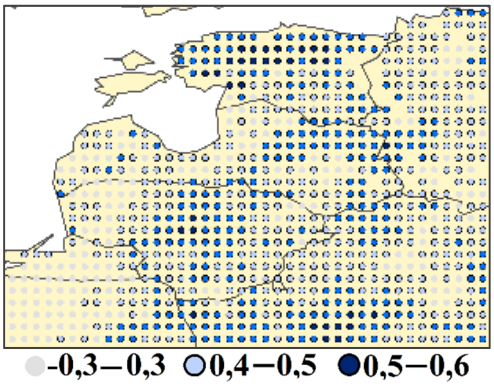

Figure 3. Correlation coefficients between coefficient *k* of 5 days and soil moisture in August.

4. Conclusions

Soil moisture in warm period of year is predetermined by air temperature and precipitation. It has been established that in the central part of the analyzed area, soil moisture is mostly affected by air temperature, while effect of precipitation is not so important. On the other hand, in the northern and southern parts of investigated region soil moisture is more influenced by precipitation. In this area the effect of the air temperature is insignificant.

The combined effect of air temperature and precipitation by last 5 days is most pronounced in June–August. The strongest correlation with soil moisture in June and July was found in the southern part, while in August in most of area. Meanwhile, such effect is weak at the beginning of the warm season, because the conditions of previous winter plays the major role.

References

Méndez-Barroso L. A., Vivoni E. R., Watts C. K., Rodrķguez J. C. (2009) Seasonal and interannual relations between precipitation, surface soil moisture and vegetation dynamics in the North American monsoon region, Journal of Hydrology, 377, 59–70, doi:10.1016/j.jhydrol.2009.08.009

Owe M., de Jeu R., Walker J. (2001) A Methodology for Surface Soil Moisture and Vegetation Optical Depth Retrieval Using the Microwave Polarization Difference Index, IEEE Transactions on Geoscience and Remote Sensing, 39, 8, 1643–1654, doi:10.1109/36.942542

Valiukas D. (2015) Analysis of droughts and dry periods in Lithuania, Doctoral dissertation, Vilnius University

Wang L., Qu J. J. (2009) Satellite remote sensing applications for surface soil moisture monitoring: A review, Earth Sci. China, 3, 2, 237–247, doi:10.1007/s11707-009-0023-7

Evaluating mean circulation and transport in the Archipelago Sea

Elina Miettunen[1], Laura Tuomi[2], Hedi Kanarik[2], Pekka Alenius[2] and Kai Myrberg[1,3]

[1] Finnish Environment Institute (SYKE), Helsinki, Finland (elina.miettunen@ymparisto.fi)
[2] Finnish Meteorological Institute (FMI), Helsinki, Finland
[3] Department of Natural Sciences of Faculty of Marine Technology and Natural Sciences, Klaipeda, Lithuania

We used a 10-year model simulation with a high resolution 3D hydrodynamic model COHERENS to evaluate the mean circulation, transport patterns and year-to-year variability in the Archipelago Sea. This coastal archipelago, located in the northern part of the Baltic Sea, consists of over 40 000 small islands and islets, making it one of the most complex coastal areas. It is also a very vulnerable area, heavily stressed with eutrophication.

The capability of the model to simulate the hydrography of the Archipelago Sea was evaluated by comparing a 3-year simulation with the available observation data (Tuomi et al., 2018). The model was able to simulate well the temperature and salinity fields as well as the seasonal variability in these parameters. However, the modelled vertical density gradients were not as pronounced as seen in the measurement data. Annual mean surface current fields showed a large year-to-year variability but the mean bottom currents were more constant.

The effect of these year-to-year differences in the circulation patterns to the transport of substances in the Archipelago Sea was studied by introducing passive tracers in the model as point sources and through river discharge. The prevailing wind conditions in the area lead to more southward transport through the area, from the Bothnian Sea to the Baltic Proper. However, in certain years, a significant amount of transport could also be northward, from the Baltic Proper towards the Bothnian Sea.

To further evaluate the model's performance, we compare the results from the 10-year simulation with observations including also current measurements at few locations. We present how the model was able to simulate the currents in the narrow channels of the inner archipelago as well as the general features in the outer archipelago.

We also re-evaluate the transport patterns in the Archipelago Sea area based on the longer 10-year simulation, by utilizing a Lagrangian particle modelling software OpenDrift (Dagestad et al., 2017) with the modelled current velocities. Furthermore, we study the water renewal in the archipelago by using age tracers in addition to the passive tracers used in the 3-year simulation. With this, we intend to identify the areas which would be the most vulnerable to eutrophication.

References

Dagestad, K.-F., Röhrs, J., Breivik, Ø., and Ådlandsvik, B. (2017) OpenDrift v1.0: a generic framework for trajectory modeling, Geosci. Model Dev. Discuss., https://doi.org/10.5194/gmd-2017-205 (In review)

Tuomi, L., Miettunen, E., Alenius P., Myrberg, K. (2018) Evaluating hydrography, circulation and transport in a coastal archipelago using a high-resolution 3D hydrodynamic model, Journal of Marine Systems, Vol. 180, pp. 24-36, https://doi.org/10.1016/j.jmarsys.2017.12.006

The maximum runoff of small rivers of the Mountainous Crimea flowing into the Black Sea in modern climatic conditions

Valeriya Ovcharuk[1], Olena Todorova[1] and Ekaterina Myrza[1]

[1] Hydrometeorological Institute, Odessa State Environmental University, Odessa, Ukraine (valeriya.ovcharuk@gmail.com)

1. Introduction

Crimea is located within the 44^0 23 '(Cape Sarich) and 46^0 15' (Perekopsky earth trench) north latitude and 32^0 30 '(Cape Karamrun) and 36^0 40' (Cape lantern) east longitude. Mountain Crimea occupies the southeastern and southern parts of the Crimean peninsula. The mountains stretch along the Black Sea coast at 150-160 km from Sevastopol in the west and in Feodosia in the east. Their maximum width is 50-60 km (Fig.1).

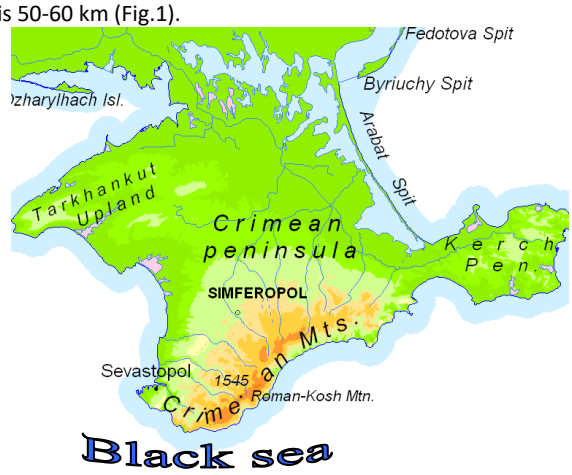

Fig. 1. Location map of Crimea

This study has been examined maximum runoff of the rivers of the Crimean Mountains. This rivers that flow through the western and eastern part of the northern slope Crimean Mountains and on its southern coast. The largest of them - Belbek, Alma, Salgir, Su-Indol and others.

In Crimea, 80-85% of the annual precipitation falls as rain. The characteristic features of the hydrological regime of rivers of the studied area are rain floods. On the catchments areas of the Mountain Crimea, the most frequent maximal daily rainfall is observed, forming floods, within the range of 71-90 mm (27,3%), precipitation is within the range of 31-70 mm (in the sum of the frequency of their occurrence is 40.9%) also typical for the formation of floods of the warm period[1].

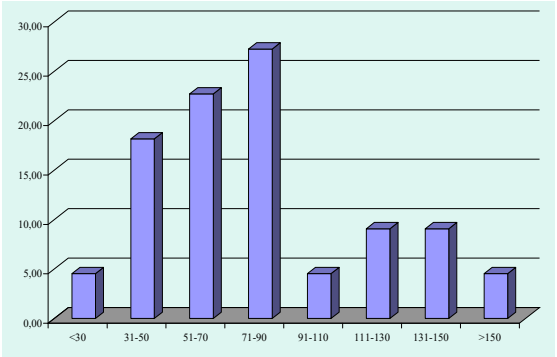

Fig. 2. The distribution of rainfall floods warm period, abscissa - precipitation layer, mm;
the vertical axis - the percentage of the total

One of the factors that significantly influences the water regime of the Crimean rivers is the karst, which causes the redistribution of runoff between the catchment and leads to a violation of zonation in the distribution of surface runoff of the rivers[2,3].

2. Methodology and data

To characterize the maximum runoff of rain floods (the layers of rain floods and maximum discharge of water) on the rivers of the Crimean Mountains were used materials of observations for long-term period (from the beginning of observations to 2010 inclusive) on 54 of streamflow station. The range of watersheds - from 0.32 to 3540 km2, the average height of watershed range from 340 to 980 m, maximum duration of observation - '82 .

The study is devoted rationing characteristics of maximum runoff rain floods of warm period for rivers Mountain Crimea based on a modified reduction structure that was derived directly from the model isochronous channel.

According to the authors [1], the advantage of this structure is its simplicity and a small number of calculation parameters. On the other hand, in contrast to the standard formulas of the reduction form, in the justification of structure (1), the method of isochrons used, which allows more fully to take into account all the runoff factors which in this formula are represented by the constituents of the slope modulus q'_m :

$$q_m = \frac{q'_m}{(A+1)^{n_1}}, \qquad (1)$$

Where A - catchments areas, km2 q'_m – maximal slope modulus that is equal to

$$q'_m = 0.28\frac{n+1}{n}\frac{1}{T_0}Y_{1\%}, \qquad (2)$$

Where $\frac{n+1}{n}$ is a coefficient of time nonuniformity of slope inflow, T_0 - duration of slope influx, hours. $Y_{1\%}$ - runoff depths, mm.

3. Results

In order to justify the calculation parameters, a standard statistical processing of the initial information on the maximum runoff of floods of rivers of the given territory was carried out. As a result, we obtain the average long-term values of maximum water discharges and runoff depths, as well as the corresponding coefficients of variation and asymmetry. Were determined water discharges and runoff depths of rare probability of exceedence (P = 1, 3, 5, and 10%).

Based on the data of statistical processing, as well as on the analysis of conditions for the formation of a flood of warm period, for the considered territory, all parameters in the form of the calculated dependences are determined and summarized.The runoff depths (Y1%), as well as the duration of the slope influx, are summarized as dependencies on the average height of the catchments. The unevenness factor is averaged for the year of the Mountain Crimea at the level of 16.0.

Using formula (2), the calculated maximal slope modulus of 1% for the territory of the Crimean Crimea are summarized and summarized in the form of a map diagram (Fig. 3).

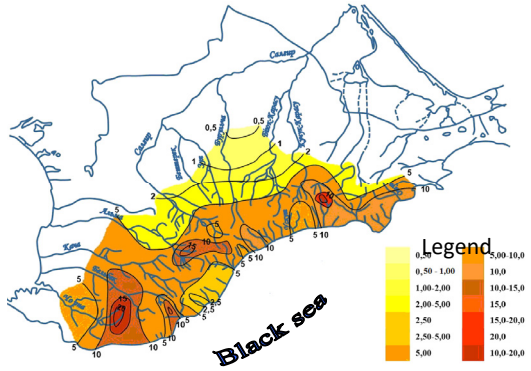

Figure 3. Distribution of maximum slope modulus 1% probability of exceedance in the territory of the Crimean Mountains, $m^3 / (c \cdot km^2)$.

Analyzing the map it can be noted that the calculated boundary modules of the sloping tributary in general increase from north-east to south from 0.5 $m^3 / (c \cdot km^2)$ to 10-15 $m^3 / (c \cdot km^2)$. Local maxima 20 $m^3 / (c \cdot km^2)$ are observed on the rivers Chorna and Raven. Within the catchment areas of these rivers there is an active unloading of karst waters. On the other hand, the minimum values of the maximum modulus of the slope influx (from 0.5 $m^3 / (c \cdot km^2)$ to 2.5 $m^3 / (c \cdot km^2)$ are confined to the karst feeding zone.

In the second variant in the calculated formula introduced factor of underlying surface, which includes the effect of karst and a maximum slope influx module which determined by the altitude.

For the rivers where absence of observational data the coefficient of underlying surface are presented in the form of map (Fig. 4).

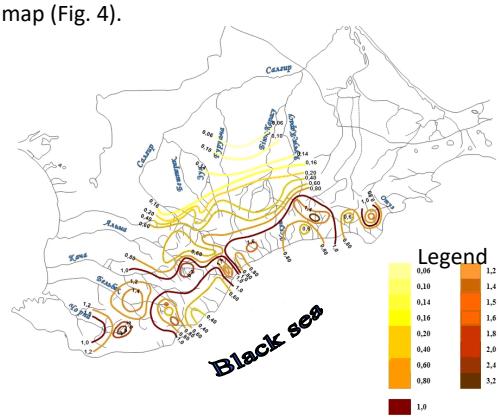

Figure 4. Distribution of the coefficient of the underlying surface for the territory of the Crimean Mountains.

The values obtained vary in the range from 0.06 to 3.20, and in our opinion, reflect the integral effects of karst and features of the underlying surface, which may be related to water management in the catchment; Approximately 1.0 coefficients indicate that there is no influence of the underlying surface on the investigated value.

Comparison of the calculated maximum water discharge (P=1%) shows good convergence as with the original information, and so with the largest maximum water discharge of observation period.

4. Conclusions

• Study of the conditions of the flood formation on the rivers of the Mountain Crimea has confirmed the fact that one of the factors that significantly influences the water regime of the Crimean rivers is karst. The formation of floods is associated with storm rainfall, which covers relatively small areas of the territory, but can lead to catastrophic consequences.

• Analysis of the initial hydrological information on the maximum runoff of the floods, showed that despite global and regional climate change, the number of incidents of catastrophic floods on the rivers of the Mountain Crimea in recent years has not increased.

• Two variants of the calculation model of the formation of the maximum drainage of rain flood in the warm period of year in the Mountains of the Crimea are proposed in the work. In the first variant, the main calculation parameter of the technique is the maximal slope modulus , which is generalized in the form of a map. According to the second, in the calculated formula introduced a coefficient of the underlying surface, taking into account the influence of karst, and the maximum module of the sloping tide is determined taking into account the height of the terrain.

• The average accuracy of the calculation in two variants is ± 21.3%, with the accuracy of the initial information ± 21.6%, which allows to recommend a technique developed for the mountains of the Crimea for practical application

References

Ovcharuk V., Todorova O. Determination of characteristics maximal runoff Mountain Rivers in Crimea. J. Fundam. Appl. Sci. 2016, 8(2). pp. 525-541. DOI: 10.4314/jfas.v8i2.23

Ovcharuk V.A., *Todorova Ye.I.* Research of karst's influence on the characteristics of slope runoff during floods on the rivers of north-western slope of Crimean mountains // Research Bulletin SWorld «Modern scientific research and their practical application», Volume J11302, May 2013, J11302-012

Ovcharuk V., *Todorova E.,* Myrza E. Calculations characteristic of catastrophic floods on the mountain rivers of the Crimean peninsula. Paper 55. 7-th European conference on Severe storms ECSS 2013. 3-7 June 2013, Scandic Marina Congress Center, Helsinki, Finland.

Enhancement of radar rainfall estimates for Estonian territory through optical flow temporal interpolation

Jorma Rahu[1], Tanel Voormansik[1,2] and Piia Post[1]

[1] Institute of Physics, University of Tartu, Tartu, Estonia (jormav@ut.ee)
[2] Estonian Weather Service, Estonian Environment Agency, Tallinn, Estonia

1. Introduction

Accurate and reliable precipitation maps are very important in the fields of hydrology, climatology and meteorology Barge et al. (1979). For Estonia's territory, high spatial and temporal resolution precipitation data is obtained by dual-polarization weather radars. Rainfall products derived from radar data have multiple applications for nowcasting over urban areas, warning systems for airports and agriculture.

Although weather radars have good measurement properties it is still method of remote-sensing and getting reliable data is not straightforward. Various sources of errors are inherent to radar data and also calculations from reflectivity to actual rain rate are done via empirical relations. Therefore, accurate precipitation estimations through radar data requires verification Merker (2017). Quantitative Precipitation Estimation (QPE) concept is introduced, where different measurement methods are compared and analyzed in order to compensate the shortcomings of different methods considering rain gauges, weather radars and satellites Nagata (2011). In case of Estonia, geostationary satellite data has poor spatial resolution due to high latitude and polar-orbit satellites have unsatisfactory temporal resolution. For these considerations rain gauges and radar data are compared.

The purpose of this work is to improve radar data temporal resolution computationally, using optical flow and interpolation of gained velocity fields which should yield more accurate precipitation accumulation estimation compared with available raw data accumulation.

2. Data and method

Estonia's radar network consists of two dual-polarization weather radars with one located near the north coast in Harku and the other in the middle of the country in Sürgavere. Both radars have two different measuring strategies with shorter 125 km range for better Doppler velocities and longer 250 km range for good precipitation measurement near the surface Voormansik (2014).

The problem with radar data can be that with current 15 minutes measurement strategy, precipitation fields can pass gauge locations introducing bias to radar and gauge data as can be seen in Figure 1.

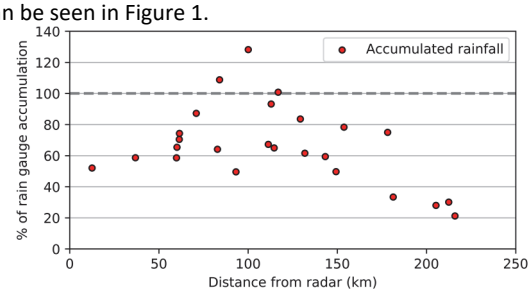

Figure 1. Differences in radar data monthly accumulation compared to gauge measurements, August 2013, using Sürgavere radar data, Estonia, Voormansik (2014)

Therefore, specific interest in this work is at radar data temporal resolution enhancement to make two different datasets more comparable with each other. This problem is addressed with digital signal processing method of optical flow.

Optical flow is a widely used image processing method which extracts apparent motion from 2D image sequence Barron et al (1994). This motion information can be used to infer real 3D movements, detect motion, execute object segmentation and a lot more, but for this work optical flow is used to interpolate more timesteps between two radar image frames. Also, it could be used to extrapolate radar data into near future (nowcasting application) as described by Peura et al. (2004) and Woo et al. (2017). There are plenty of different optical flow methods with very different mathematical approaches including differential methods, region-based matching or frequency-based methods (energy-based or phase-based) where every method depends highly on the specific applicational needs Barron et al. (1994). Choosing optimal method (reasonably good results with reasonable computational difficulty) and implementing it for the weather radar-oriented application is intended with this work. As there is not much to compare the results to, an error estimation is also needed to ensure measure of confidence and accuracy in used method of optical flow.

Difficulties with optical flow lie in the problem setup, as the original method assumes image brightness constancy Horn et al. (1981) and that motion field is small Meinhardt-Llopis et al. (2013), meaning that the shape of the object does not change and movements between frames are tiny. Both of these assumptions are generally violated in real life applications but especially in radar images, as with the 15-minute measurement limitation precipitation fields can move a lot and also change their shape. Different methods exist to overcome these issues. Multi-scale coarse-to-fine schemes for large displacement compensation is very commonly used Meinhardt-Llopis et al. (2013), but also schemes without the need of warping strategy have recently been developed, although they are computationally more demanding Steinbrücker et al. (2009).

3. Preliminary results

Preliminary experiments with the aforementioned method have been conducted. In particular, as described by Proesmans et al. (1994) mixed method of optical flow and correlation-based matching is used, in order to get better flow results at boundaries. A small set of data can be seen in Figure 2. Although the interpolated data still underestimates the gauge data, it still shows better estimations in most cases. At 10:00 and 11.30, the interpolated data shows less precipitation as compared to measured reflectivity values. This can be explained by the

fact that as more timesteps are introduced and the rainfall intensity is uniform (as was the studied case) the mean accumulated rain is decreased. The latter does not explain high measured gauge values which mean further studies are necessary. Studies of convective cases are also needed.

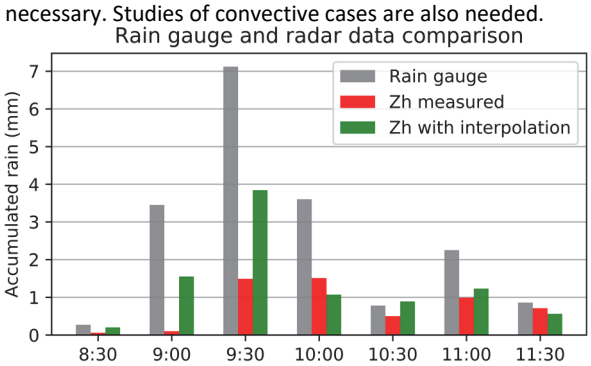

Figure 2. Rain gauge and radar data comparison at Massumõisa station 3rd July 2016, accumulation is done over 30-minute periods

References

Barge B. L., Humphries R. G., Mah S. J., Kuhnke W. K. (1979) Rainfall Measurements by Weather Radar: Applications to Hydrology, Water Resources Research, Vol. 15, No. 6, pp. 1380-1386

Merker C. (2017) Estimating the Uncertainty of Areal Precipitation using Data Assimilation, Dissertation

Nagata, K. (2011) Quantitative precipitation estimation and quantitative precipitation forecasting by the Japan meteorological agency, RSMC Tokyo-Typhoon Center Technical Review., Vol. 13, pp. 37-50

Voormansik T. (2014) Quality Control of Estonian Weather Radar Network, Master Thesis

Barron J. L., Beauchemin S. S., Fleet D. J. (1994) On Optical Flow, 6th Internationaln Conference on Artificial Intelligence and Information-Control Systems of Robots (AIICSR), pp. 3-14

Peura M., Hohti H. (2004) Motion Vectors in Weather Radar Images, Proceedings of the 7th International Winds Workshop, Helsinki, Finland

Woo W.-C., Wong W.-K. (2017) Operational Application of Optical Flow Techniques to Radar-Based Rainfall Nowcasting, Atmosphere, Vol. 8(3), 48

Horn B. K. P., Schunck B. G. (1981) Determining optical flow, Artificial Intelligence, Vol. 17, pp. 185-203

Meinhardt-Llopis E., Sanchez J., Kondermann, D. (2013) Horn-Schunck Optical Flow with a Multi-Scale Strategy, Image Processing On Line, Vol. 3, pp. 151-172

Steinbrücker F., Pock T., Cremers D. (2009) Large Displacement Optical Flow Computation Without Warping, 2009 IEEE 12th International Conference on Computer Vision, Kyoto, Japan

Proesmans M., Van Gool L., Pauwels E., Oosterlinck A. (1994) Determination of optical flow and its discontinuities using non-linear diffusion, Computer Vision — ECCV '94, ECCV 1994, Lecture Notes in Computer Science, Vol. 801, pp. 295-304

Wind and Turbulence Measurements with RPA during the ISOBAR Campaign

Alexander Rautenberg[1], Martin Schön[1] , Kjell zum Berge[1] , Hasan Mashni[1], Patrick Manz[1], Stephan Kral[2], Line Baserud[2], Joachim Reuder[2], Rostislav Kouznetsov[3], Ewan O'Connor[3], Irene Suomi[3], Timo Vihma[3] and Jens Bange[1]

[1] University of Tübingen, Environmental Physics, Tübingen, Germany (alexander.rautenberg@uni-tuebingen.de)

[2] University of Bergen, Geophysical Institute and Bjerknes Centre for Climate Research, Bergen, Norway

[3] Finnish Meteorological Institute, Meteorological Research, Helsinki, Finland

1. Introduction

The remotely-piloted fixed-wing aircraft MASC3 (Multi-purpouse Airborne Sensor Carrier) from the environmental physics working group of the University of Tübingen was used to investigate physical processes in the ABL during the ISOBAR (Innovative Strategies for Observations in the Arctic Atmospheric Boundary Layer) campaign over the frozen Baltic Sea in northern Finland in February 2017 and in February 2018.

2. Multi-purpouse Airborne Sensor Carrier MASC3

MASC3 is equipped with a high resolution thermodynamic sensor package including a five-hole probe and IMU for wind vector measurements (e.g. Van den Kroonenberg et al., 2008 and Wildmann et al., 2014). During the three week long field periods also ground based weather stations, remote sensing systems (Lidar and Sodar) and other fixed-wing (e.g. SUMO by Reuder et al., 2009) and multi-rotor systems for atmospheric profiles of several quantities were applied. Intensive observational periods including nocturnal flights with MASC were performed. Figure 1 shows a picture of MASC3 just before take-off on the frozen Baltic Sea in front of Hailuoto, Finland in February 2018.

Figure 1. Multi-purpous airborne sensor carrier before starting on the frozen Baltic Sea in front of Hailuoto, Finland.

3. Results

Intensive observational periods including nocturnal flights with MASC3 were performed. This talk will focus on results for the wind, turbulence and flux measurements from some flights with MASC. The strategy of the measurements as well as the quality of the data and comparisons will be addressed. The talk will give an overview of the capabilities of MASC3 and it's use for understanding the water and energy cycles in the Earth's atmospheric boundary layer. Furthermore future adoptions and developments of the measurement system and the remotely-piloted aircraft for polar use will be presented.

4. Conclusion

On the basis of the data set of two intensive measurement campaigns on the frozen Baltic Sea the capabilities and potential of MASC3 will be presented. Relatively easy to deploy and with minimal logistical overhead, a precise snapshot of the atmosphere including turbulent atmospheric exchange processes can be sampled.

References

Wildmann, N., and Bange, J.: MASC - A small Remotely Piloted Aircraft (RPA) for Wind Energy Research., Adv. Sci. Res., 11, 55-61, doi:10.5194/asr-11-55-2014, 2014.

Van den Kroonenberg, A., Martin, T., Buschmann, M., Bange, J., and Vörsmann, P.: Measuring the wind vector using the autonomous mini aerial vehicle M2AV, Journal of Atmospheric and Oceanic Technology, 25, 1969–1982, 2008.

Reuder, J., Brisset, P., Jonassen, M., Müller, M., and Mayer, S.: The Small Unmanned Meteorological Observer SUMO: A new tool for atmospheric boundary layer research, Meteorologische Zeitschrift, 18, 141–147, 2009.

On Summer Low Water Periods in Estonian Rivers in the Years 1951-2016.

Mait Sepp[1]

[1] Department of Geography, University of Tartu, Tartu, Estonia (mait.sepp@ut.ee)

1. Introduction

Climate change inevitably causes changes in river runoffs. In Estonia, winters and springs have become drastically warmer over the last decades, which has for example resulted in the shifting of spring high water from April to March (Jaagus et al. 2017). It may be assumed that if the high water period has moved to about a month earlier, the period of minimum discharge in summer has lengthened by a month as well. This, in turn, may cause hydrological and ecological problems. The purpose of the present study is to find out how the length of the summer period of minimum discharge and how the overall amount of discharge through measurement points has changed in the years 1951-2016.

2. Data and Methods

The present study makes use of 24-hour average amounts of discharge from 16 Estonian hydrometrical stations and the Estonian spatial average calculated according to these. The data was received from Estonian Weather Service. For the data to be comparable, discharge amounts were converted into specific runoff (l/s*km^2). To distinguish the summer period of minimum discharge, the STARS method, which is based on the sequential application of the Student's t-test (Rodionov, 2004), was used. In order to decrease the statistical influence of flash floods, the method's input parameters were selected relatively conservative ones– significance level: 0.1; cut-off length: 30; HWP: 1. Changes is parameters characterizing the runoff and period lengths were analyzed with linear trends ($p<0.05$).

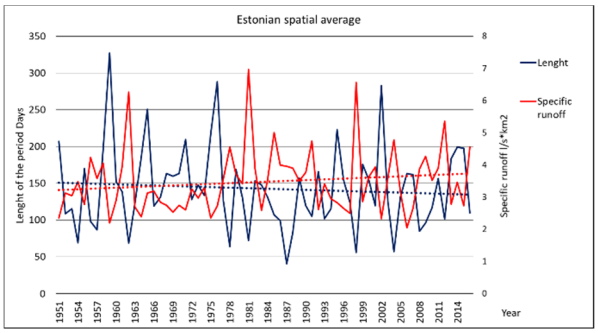

Figure 1. The length of the period of minimum discharge in summer in Estonia and the specific runoff (l/s*km2). Neither of the trend lines is statistically significant.

3. Results

The analysis showed that the input parameters chosen by STARS are not universal for all rivers, particularly for rivers with a smaller catchment areas. In general, there were only a few statistically significant changes in the analyzed indicators. It may be claimed that as a general tendency, the values of the specific runoff have increased and the period of minimum discharge in summer has shortened (Figure 1). This means that the overall amount of water flowing through rivers in Estonia during summer has increased.

References

Jaagus, Jaak; Sepp, Mait; Tamm, Toomas; Järvet, Arvo; Mõisja, Kiira (2017). Trends and regime shifts in climatic conditions and river runoff in Estonia during 1951–2015. Earth System Dynamics, Vol. 8, pp. 963–976

Rodionov, S.N., (2004) A sequential algorithm for testing climate regime shifts. Geophys. Res. Lett., 31.

A descriptive analysis of the linkage between the vertical stratification and current oscillations in the Gulf of Finland

Irina Suhhova[1], Taavi Liblik[1], Madis-Jaak Lilover[1] and Urmas Lips[1]

[1] Tallinn University of Technology, Department of Marine Systems, Akadeemia Rd. 15A, 12618 Tallinn, Estonia (irina.suhhova@ttu.ee)

1. Introduction

Vertical stratification in the gulf is variable and exhibits a clear seasonality. In winter, the water column in deep enough areas has mostly two-layer structure with a well-mixed upper layer extending from the sea surface until the halocline at the depths of 60-80 m (e.g., Alenius et al. 1998). However, considerable haline stratification may appear in the upper layer during calm periods (Liblik et al. 2013), and intensive reversals of estuarine circulation may cause occasional stratification collapse events (Liblik et al. 2013, Elken et al. 2014). As a result, three-, two- and one-layer stratification regime may occur in the gulf in winter. In summer, mostly a three-layer vertical structure exists as the seasonal thermocline develops at the depths of 10 - 30 m (e.g., Alenius et al. 1998, Liblik and Lips 2017).

The vertical structure of currents seems to be linked to the presence and location of the seasonal thermocline (Suhhova et al. 2015) and halocline (Liblik et al. 2013) while, on the other hand, the changes in circulation are reflected in the variability of vertical stratification (Liblik and Lips 2012). Thus, there should exist a strong interplay between the currents and stratification in the gulf.

2. Material and method

A bottom-mounted ADCP (Workhorse Sentinel, Teledyne RDI, 300 kHz) was deployed at five locations (see Fig. 1) for the periods of 29 to 148 days. Current velocity profiles were measured over 2-m depth bin with the sampling interval of 10 minutes and 30 minutes (for ADCP4) as averages of 50 pings. The current velocities were available in the depth range from 62 - 86 m to 8 -10 m, depending on the depth of deployment locations.

CTD profiles acquired using an Ocean Seven 320plus CTD probe (Idronaut S.r.l.) during several cruises were applied as background data on vertical stratification.

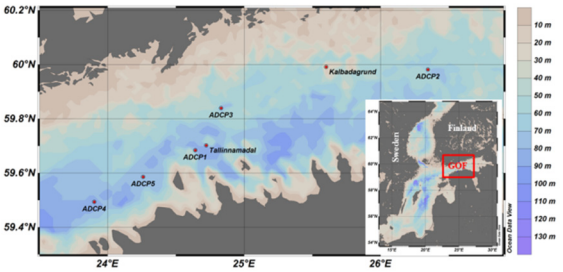

Figure 1. Map of the study area in the Gulf of Finland. Locations of ADCP deployments and wind measurement locations in Kalbådagrund and Tallinnamadal Lighthouse are shown.

Current shear was calculated between the two nearest velocity horizons over the depth range of 2 m using low-pass filtered data.

For spectral structure investigations of current oscillations, rotary spectral analysis technique (e.g., Emery and Thomson 2004) was applied to hourly average current data. Power spectral density (PSD) is usually plotted in coordinates log S(ƒ) versus log(ƒ), where S(ƒ) is the power spectral density and ƒ the frequency. We use another spectral plot in the present paper, namely ƒ S(ƒ) versus log(ƒ) which is a variance-preserving form of spectral presentation. In this presentation, the energy in every frequency interval is proportional to the corresponding area under the spectral line.

3. Results

The analysis of time-series of vertical distributions of currents revealed that one-, two- or three-layer current structure might occur in the Gulf of Finland. The realization of the exact regime depends on the wind forcing and stratification. This layered flow structures emerges as both the local shear maxima in certain layers (see Fig.2) and the differences in the kinetic energy spectra of currents between the vertical layers (see Fig.3). Stratification strength parameter – the Brunt-Väisälä frequency shows that the water column during the two selected winter periods was almost mixed. No clear maxima of period-averaged current shear were detected, so the flow was mostly barotropic. Vertical locations of stronger density stratification in the three other periods – in summers 2010 and 2011 and autumn 2010 roughly match with the current shear maxima.

The energy maxima of current oscillations occurred at a broad semi-diurnal frequency band, broad diurnal frequency band and/or low-frequency seiches band (see Fig.3), as it has also been found earlier in the Gulf of Finland. We showed that the frequency composition differed between the seasons mainly due to the vertical stratification as well as between the layers during a selected period.

The kinetic energy spectra of currents in the periods of strong wind forcing and weak stratification were dominated by current oscillations coinciding with different modes of seiches. During the periods of the two- or three-layer residual flow also inertial oscillations and probably tides contributed remarkably to the kinetic energy of current oscillations. We demonstrated that in summer, the inertial oscillations were dominating from the surface to either the thermocline or the halocline.

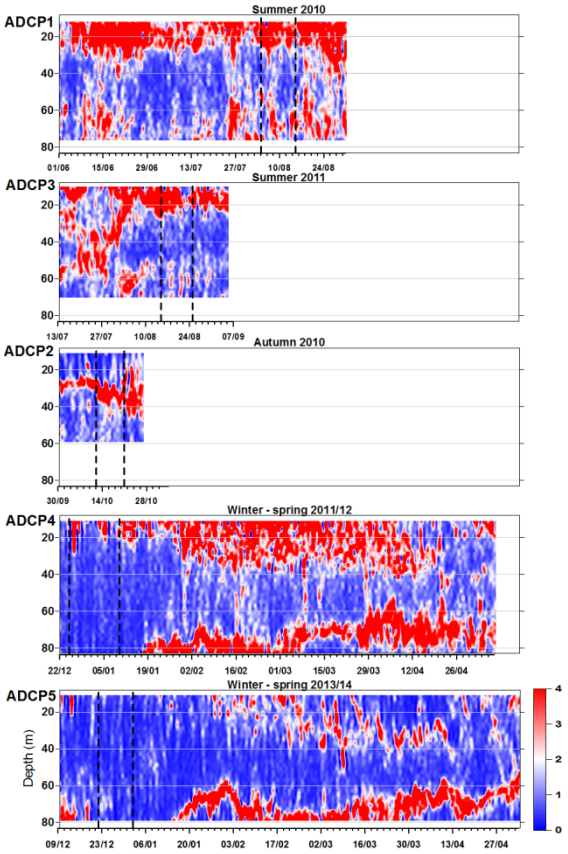

Figure 2. Low–pass filtered time series of a current shear square ($s^{-2} * 10^{-4}$) in (a) summer 2010, (b) summer 2011, (c) autumn 2010, (d) winter-spring 2011/12, and (e) winter-spring 2013/14. Vertical dashed lines indicate the selected periods which were further analyzed.

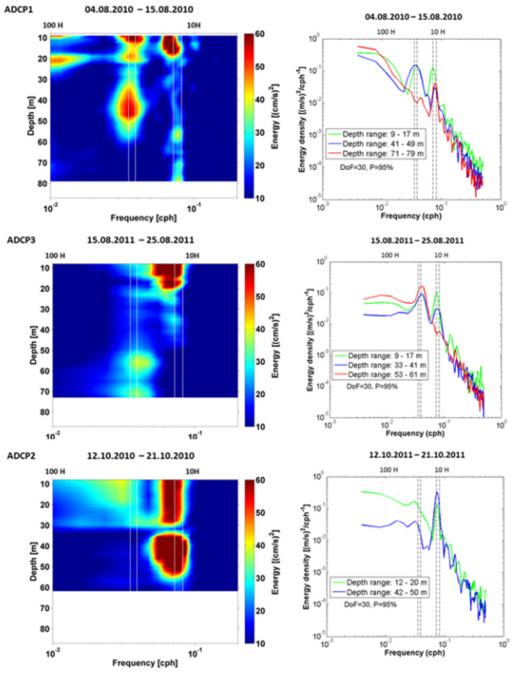

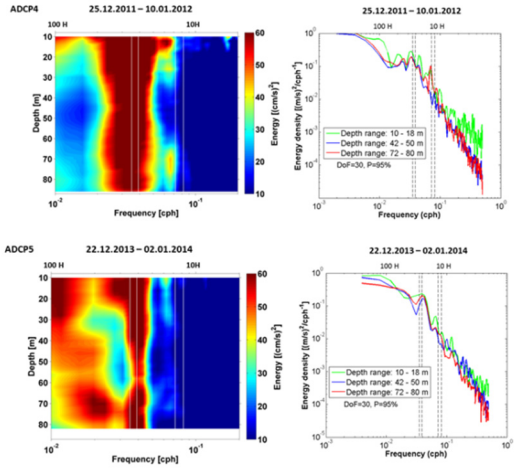

Figure 3. (Left column) Vertical distributions of kinetic energy spectra during selected periods (see Fig. 2) (a, b) three-layer flow, (c) two-layer flow and (d, e) one-layer flow. Vertical white lines indicate the oscillation periods of 28.6 h, 25.6 h, 13.9 h, and 12.42 h. (Right column) Depth averaged kinetic energy density for upper, intermediate and near-bottom layers.

Acknowledgments

The work was supported by institutional research funding (IUT19-6) of the Estonian Ministry of Education and Research. The measurements and analysis were partly funded by the Estonian Ministry of Environment (Nord Stream construction environmental monitoring) and Estonian Science Foundation grants no. 6955, 9023, and 9382.

Participation in the conference was supported by ASTRA "TTÜ arenguprogramm aastateks 2016-2022" DAR16024 (2014-2020.4.01.16-0032).

References

Alenius P., Myrberg K., Nekrasov A. 1998. The physical oceanography of the Gulf of Finland: a review. *Boreal Environ. Res.* 3, 97 -125.

Elken J., Raudsepp U., Laanemets J., Passenko J., Maljutenko I., Pärn O. & Keevallik S. 2014. Increased frequency of wintertime stratification collapse events in the Gulf of Finland since the 1990s. *Journal of Marine Systems*. http://dx.doi.org/10.1016/j.jmarsys.2013.04.015.

Liblik T., Laanemets J., Raudsepp U., Elken J., Suhhova I. 2013. Estuarine circulation reversals and related rapid changes in winter near-bottom oxygen conditions in the Gulf of Finland, Baltic Sea. *Ocean Science*. 9, 917 - 930.

Liblik T. & Lips U. 2017. Variability of pycnoclines in a three-layer, large estuary: the Gulf of Finland. *Boreal Env. Res.* 22, 27 - 47.

Suhhova I., Pavelson J. & Lagemaa P. 2015. Variability of currents over the southern slope of the Gulf of Finland. *Oceanologia*. 57, 132 - 143.

Liblik T. & Lips U. 2012. Variability of synoptic-scale quasi-stationary thermohaline stratification patterns in the Gulf of Finland in summer 2009. *Ocean Science*. 8, 603 - 614.

Emery W.J. & Thomson R.E. 2004. *Data analysis methods in physical oceanography*. Elsvier. London.

Water balance assessment using SWAT for Russian subcatchment of Zapadnaya Dvina River

Pavel Terskii[1], Alexey Kuleshov[2]
[1]Department of land hydrology, Lomonosov Moscow State University, Moscow, Russian Federation (pavel_tersky@mail.ru)
[2]Institute of Hydrology and Meteorology, Dresden University of Technology, Dresden, Germany

1. Introduction

The aim of this study is to create the hydrologic model of Zapadnaya Dvina (Russian part of Daugava) catchment to fill gaps in hydrologic measurements, calculate water balance components and further estimate the amount of dissolved and suspended matter inflow to the of Russian Federation border.

The scope of study is the Russian part of Zapadnaya Dvina river catchment in the outlet of Velizh town (area of catchment is 17,250 km^2). The rivers of Russian part of the Zapadnaya Dvina river catchment are not regulated, not exposed to high human activity impact and poorly studied as well (there are measurements of only five meteorological stations in the catchment neighbor and ongoing measurements of daily discharges of four hydrologic stations).

2. Modeling approach

The chosen model is intended to be freely used and has the mathematic framework with sediment and nutrient load calculation, and with high sensitivity to the catchment condition (relief, soil and land use data). We chose The hydrologic model SWAT v.2012 was chosen (Gassman et. al. 2007). The advantages of the SWAT model are the availability of reliable and helpful documentation, absence of limitations on catchment area, compatibility with GIS software (ArcGIS, QGIS, MapWindow), the open-source module of auto calibration SWAT-CUP (Abbaspour et. Al, 2015), and also the open-access library of publications and scientific community.

The modeling process of different types of fluxes (water, dissolved and suspended matter) is based on calculations of the river discharge and its parametrization. The modeling in SWAT has the following stages: building the catchment model, preparation of the meteorological data and calibration of parameters.

3. Building the catchment model

The catchment model was built with the ArcSWAT 2012 GIS-interface. The following input data was used:
a) Digital elevation models - SRTM v.4 – with spatial resolution of 30 m (http://earthexplorer.usgs.gov), ALOS PALSAR RTC with spatial resolution of 12.5 m (https://www.asf.alaska.edu);
b) World Soil Database HWSD FAO (http://www.fao.org);
c) Raster layers of land cover and land use GLOBCORINE, with spatial resolution of 300 m (http://due.esrin.esa.int) and Global Land Cover, with 30 m spatial resolution (http://www.globallandcover.com).

Monthly time-step model is more rough than daily and is based on SRTM DEM and GLOBCORINE land cover data. The daily-step model is based on ALOS DEM and Global Land Cover and is much more bulky. Preliminary results of daily discharge model allowed to find the best method for determining the "hydrological response units" (the best found distribution is 20/10/20 percent of the threshold values for land cover, soil and slopes areas respectively).

4. Meteorological data analysis

The SWAT model calculates river runoff using daily minimum (TMN) and maximum (TMX) daily air temperatures, precipitations (PCP), relative humidity (HMD), wind speed (WND) and solar radiation downward (SOL).

The meteorological data are the basis of the water balance equations in the hydrological model. During the preparation of the meteorological database we compared two different sources of the daily meteorological data for the period 1981 – 2016: global atmospheric reanalysis ERA-Interim (https://www.ecmwf.int) and observed station data of the GSOD NCDC/NOAA (https://data.nodc.noaa.gov) and ECA&D (www.ecad.eu). The data were analyzed for the plausibility and outliers. The results showed that extremal sums of precipitation (75, 150 and 300 mm per day) from NOAA source are outliers and do not correspond with ECA&D data. Temperatures, precipitation and wind speed were analyzed using the methods of robust statistics.

Considering the relation between the elevation of the meteorological stations above sea level and changes in the distribution of the meteorological variables we established the thresholds for the each month, and the values of daily TMX, TMN, PCP and WND that were out of the threshold ranges were considered as not plausible. Then they were replaced with data from the reliable stations using inverse weighted correlation method (Yang 1992). To compare the results with the reanalysis data the meteorological stations data to the grid with the same size of the highest resolution grid of daily ERA-Interim data were interpolated.

The results showed a good correlation between TMN, TMX of reanalysis and interpolated station data (correlation coefficient (r) and index of agreement (d) are more than 0.99).

From all meteorological data the most unreliable were the daily PCP. The correlation coefficients (r) between the data from nearby stations (Velizh, Belyi, Toropetz, Velikiye Luki and Smolensk) are changing from 0.21 to 0.74. The relation between PCP from stations and reanalysis data is poor (r=0.5-0.6), and Nash-Sutcliff coefficient (NS) is 0.25-0.30. As for the comparison of reanalysis data with interpolated station data, PCP is highly variable in time and space r=0.72, d=0.84. For WND, the reanalysis data overestimates wind speed comparing to the interpolated station data, in spite of the correlation coefficient is quite high (r=0.86),reanalysis

data and interpolated station data do not agreed well (d = 0.74) due to the high difference between average annual range of wind speed (1.38 m/s).

In total, reanalysis overestimates interpolated station data by 33%. One of the possible reasons for this is an underestimation of the surface roughness for the particular region during the reanalysis.

5. Calibration of parameters

The calibration of parameters is based on hydrological observations. The available continuous series of hydrological measurements at the gauging stations Velesa River – Rudnya, Toropa River – Staraya Toropa and Zapadnaya Dvina River – Velizh for 1992-2004 caused the choice of time periods of daily and monthly discharge model: 1989-1992 - warm-up period, 1992-1998 – calibration period, 1999-2004 – verification periods.

The list of the most sensitive modelling parameters depends on the genesis of river flow, the size of the catchment and temporal resolution of the model (daily, monthly or annually), and on the modeling approach – lumped or distributed (for the distributed parameters). The parameters were calibrated on the basis of statistical methods in SWAT CUP.

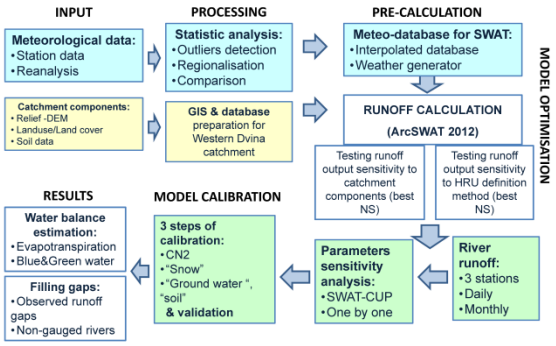

Figure 1. The scheme of SWAT setup, uncertainty analysis, calibration of parameters and water balance calculations for Zapadnaya Dvina catchment.

6. Main results

Two analyzed meteorological databases are in good agreement to each other except of wind speed. Reanalysis dataset for wind speed is overestimated by 33 %. Reanalysis dataset for sunshine duration is not plausible. Reanalysis dataset for surface solar radiation downward can be used in calculations. The use of interpolated station data with solar radiation data from reanalysis is the preferable solution for meteorological input for Zapadnaya Dvina catchment model.

In the Zapadnaya Dvina River catchment the annual distribution of the river flow is genetically non-homogeneous. Due to this fact, the standard approach of the model auto-calibration and the choice of the sensitive parameters based on standard statistics were not successful and lead to the equifinality of the model. Thus, in this study 18 sensitive parameters were chosen manually one by one for monthly and daily runoff. The parameters affecting the snow melt runoff were grouped together and calibrated separately from the others. Results of calibration are good for monthly and satisfactory for daily runoff according to Moriasi (2007) - table 1.

Table 1. Results of model calibration and validation

Objective function	Definition	Monthly model	Daily model
R^2	Square correlation	0.83/0.78*	0.80/0.76*
NS	Nash-Sutcliff coefficient	0.77/0.76*	0.72/0.71*
PBIAS %	percent BIAS	-11.5/-15.5*	-22.4/-24.7*
Model quality		good	good/satisfactory
* - Calibration (1992-1998)/Validation (1999-2004)			

The calibrated model allowed to fill gaps in river discharge observations and calculate water balance components of the catchment (evapotranspiration, surface and lateral flow).

7. Acknowledgements

The authors thank the Volkswagen Foundation for the funding of the project "Management of Transboundary Rivers between Ukraine, Russia and the EU – Identification of Science-Based Goals and Fostering Trilateral Dialogue and Cooperation (ManTra-Rivers)" (Grant No: Az.: 90 426).

References

Abbaspour K.C., Vejdani M., Haghighat S. (2007) SWAT-CUP calibration and uncertainty programs for SWAT. Proc. Intl. Congress on Modelling and Simulation (MODSIM'07). pp. 1603–1609.

Gassman P., Reyes M., Green C., Arnold J. (2007), The Soil and Water Assessment Tool: Historical Development, Applications, and Future Research Directions // Transactions of the ASABE, vol. 50, issue 4, pp. 1211-1250.

Moriasi D.N., Arnold J.G., Van Liew M.W., Bingner R.L., Harmel R.D., Veith T.L. Model evaluation guidelines for systematic quantification of accuracy in watershed simulations. Amer. Soc. Agric. Biol. Eng., 2007, vol. 50, pp. 885-900

Young K. (1992). "Three-way Model for interpolating for monthly precipitation values". American Meteorology Society: pp. 2561-2569.

Assessment of changes in river runoff for small and medium-sized rivers in the Russian part of the Baltic Sea basin under non-stationary climatic conditions

Valery Vuglinsky, Darya Timchenko

Saint Petersburg State University, Saint Petersburg, Russia (darinatimchenko9@mail.ru)

1. Introduction

For the first time, the effect of global warming began to be discussed in the 1960s, but it was officially announced only in the 80th session at the UN meeting.

Global warming is manifested in the warming of the atmosphere and the ocean, the reduction of snow and ice reserves, and rising sea levels. Each subsequent decade is characterized by higher air temperatures than the previous one, and in the northern hemisphere, the last three decades are generally considered to be the warmest for more than a thousand years (IPCC, 2014).

Global warming affects many natural processes, including the hydrological regime of rivers. Changes in the amount of atmospheric precipitation and their annual distribution, duration of snow cover and water supply have a decisive influence on the formation of river runoff, soil moisture and the water resources of the territories.

2. Objectives and data

The main goal of the work is to assess the dynamics of various characteristics of river runoff in the Russian part of the Baltic Sea basin under climate change conditions. To achieve this goal, the geographical conditions of the region were studied, hydrological stations on the rivers of the territory under consideration were selected with long-term series of observations: data were collected on the dynamics of water flow at selected posts, and a corresponding electronic database was created.

3. Methodology

The methodology consists of the analysis in the homogeneity of long-term series of observations, the identification of trend components in time series for the period of the unsteady climate situation (1980-2015), comparison of the mean values of time series for two periods (1952-1979) and (1980-2015) and, finally, the receipt of total quantitative values of changes in river runoff for the period 1980-2015 compared with the previous one. Averaged annual and monthly water flow were used for the calculation.

4. Results

4.1. Homogeneity

It has been established that for river posts homogeneity hypothesis with a probability of 0.95 by the Student's criterion (Samarov, 1998) does not correspond to more than half of the series for the annual water discharge - 11 out of 13. In the calculation of homogeneity for mean monthly discharges, correspondence was observed mainly in the summer months. The largest specific weight of inhomogeneous series (3 of 13) is characteristic for the stations located in the basin of the Luga River.

It was also calculated the significance of trends in the interannual distribution of runoff over three periods: from 1952 to 1979, from 1980 to 2015 and for the entire period from 1952 to 2015.

By using the Student's test an assessment of the significance of trends in river runoff series was made with probability (0.95). The results were obtained for both annual and monthly water flow.

4.2 Assessment of quantitative changes

To obtain summary estimates of the changes in the characteristics of river runoff under consideration during the non-stationary climatic situation, the results of estimations of trend components for the first period and changes in the mean values for the two periods considered were used. It is established that for more than half a stations there is a decrease in the annual river runoff, as well as a decrease in the mean monthly river runoff for a period of the non-stationary climatic situation (1980-2015) in comparison with the previous period. Integrated values of changes in annual river runoff are given in Table 1.

Table 1 Changes in annual river discharges for the period of non-stationary climate

River - station	Annual river runoff (norm)	Changes, m^3/s	
		For the period	Averaged for 10 years
Perevka - Goncharovo	2,61	-0,06	-0,01
Gorokhovka - Tokarevo	8,12	0,92	0,09
Mga - Mountains	6,01	0,99	0,10
Meadows - Meadows	15,64	-2,12	-0,23
Luga - Tolmachevo	43,06	-15,65	-1,63
Luga - Kingisepp	100,29	-2,48	-0,32
Lizard - Dolgovka	4,64	0,36	0,03
Plyussa - Plyussa	9,95	-3,77	-0,39
Plyussa - Brod	40,72	-2,16	-0,24
Sist - Middle Raikovo	6,76	-0,58	-0,06
Kovashi - Lendovshina	4,10	0,72	0,07
Tosna - Tosno	8,67	0,36	0,03
Oredej -Vyritsa	7,93	1,44	0,14

Most significant negative changes in annual river runoff over a non-stationary period were obtained for two rivers – Luga and Plyussa (Table 1).

Comparing the results received for mean monthly water flow, it was concluded that rather significant positive changes took place in winter months and rather significant negative changes - during spring and autumn. Highest changes in mean monthly discharges were discovered for rivers with most negative trends in annual river runoff - Luga – Tolmachevo, Luga – Kingisepp and Plyussa – Plyussa.

An example of interannual distribution of mean monthly changes in river runoff is presented in Figure 1. It reflects positive changes in winter months and negative changes during the rest period.

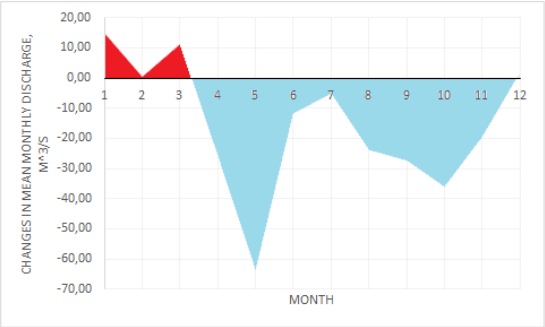

Figure 1. Changes in mean monthly water flow for the period 1980-2015 (Luga – st.Tolmachevo)

References

Climate change 2014: Summary for policymakers, IPCC

Samarov K. L., Mathematical Statistics, 1998

Water resiurces of Russia and Their Use", State Hydrological institute, Saint Petersburg, 2008, 598 p

Cloud and radiation variability and trends for the northern Baltic region as observed and modelled for present day climate and future scenarios

Ulrika Willén

Swedish Meteorological and Hydrological Institute, Norrköping, Sweden (Ulrika.Willen@smhi.se)

1. Abstract

For high latitudes, as the northern Baltic region, the recent observed warming has been faster than the global average warming especially in winter and reductions in winter duration and snow cover have been observed. Wintertime is also the season with the largest inter-annual variability. Climate models predict an amplified Arctic/ high latitude warming compared to the global warming but there is a large spread between the models.

The interaction of wintertime cloudiness with the surface and impact on the Arctic/ high latitude amplification is not well understood even though an increase in clouds in winter is expected to have a warming effect due to their greenhouse effect. We use long term satellite and ground based observations to evaluate the variability of present day climate model simulations and near-future projection simulations performed with the coupled climate model EC-Earth and other CMIP5/6 models.

Topic F

Multiple drivers of regional Earth System changes

The Eckernförde Bay (SW Baltic Sea) through the ages: Time-series measurements at the Boknis Eck time-series station

Hermann W. Bange[1]

[1] Marine Biogeochemistry Res. Div., GEOMAR Helmholtz Centre for Ocean Research Kiel, Kiel, Germany (hbange@geomar.de)

1. Introduction

The Time-Series Station Boknis Eck is located at the north-eastern entrance of the Eckernförde Bay in the SW Baltic Sea (Figure 1). Boknis Eck belongs to the oldest -still operated- oceanic time-series stations worldwide: First regular hydrographic measurements (i.e. salinity) have been made on a daily basis from 1876 to 1893 in the Eckernförde Bay. 'Modern' biological, chemical and physical measurements at Boknis Eck are conducted since 30 April 1957 on a monthly basis. The water depth at Boknis Eck is 28 m. Standards sampling depths are 1, 5, 10, 15, 20 and 25 m.

Salinity, temperature, phosphate and oxygen (O_2) data have been recorded since 1957. Chlorophyll a measurements started in 1960. Additional nutrients (nitrate, nitrite, ammonium and silicate) and Secchi depths are available since 1979 and 1986, respectively. Since riverine and groundwater inputs are negligible, the overall hydrographic setting at Boknis Eck is dominated by the regular inflow of North Sea water through the Kattegat and the Great Belt. Seasonal stratification occurs usually from mid-March until mid-September and causes pronounced hypoxia (O^2 < 10 µmol L^{-1}) which sporadically become anoxic.

The location of Boknis Eck is ideal to study (i) a coastal ecosystem under the influence of pronounced changes of salinity and (ii) biogeochemical processes sensitive to changes of dissolved oxygen.

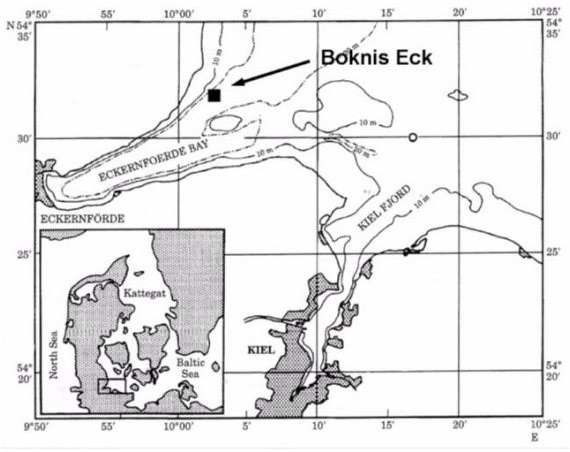

Figure 1. Map of the Eckernförde Bay in the SW Baltic Sea. The sampling site of the Boknis Eck Time-Series Station is indicated by the black square.

2. Long-term trends

Figures 2 and 3 show the time-series of sea surface temperatures (SST) and O_2 concentrations in the bottom layer (25 m) at Boknis Eck (BE) from April 1957 to January 2017.

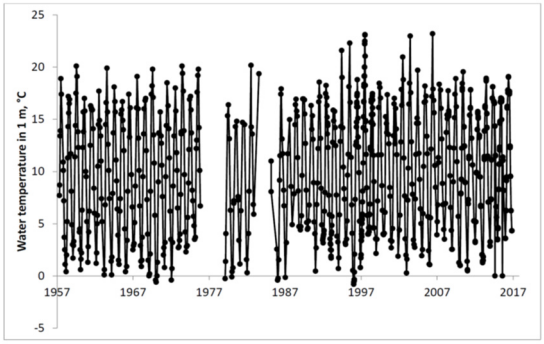

Figure 2. Water temperatures in 1m at Boknis Eck.

SST show a trend to warmer temperatures especially during the last decades which is illustrated by the fact that cold events with winter SST below 0°C have not been recorded during the last 20 years. However, the highest SST (with temperatures >22°C) have been recorded between 1995 and 2006.

Besides the obvious warming of the surface layer there is a trend to decreasing O_2 concentrations in 25m (Figure 3).

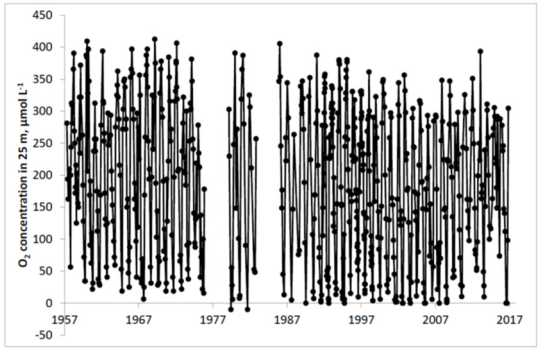

Figure 3. Dissolved O_2 in 25 m water depth at Boknis Eck.

It is obvious that the number of hypoxic/anoxic events (her defined by O_2 <10 µmol L^{-1} has been higher in the last three decades than in the first three decades of measurements (Figure 4).

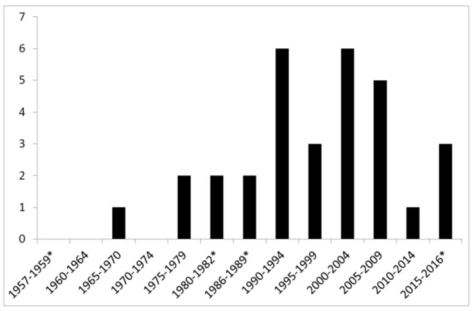

Figure 4: Number of events (i.e. monthly measurements) with O_2 <10 µmol L^{-1} in 25 m grouped for 5 year periods from April 1957 to Dec 2016. Periods marked with * cover less than 5 years of data.

The increasing frequency of hypoxic/anoxic events might in part result from (i) the warming of the surface waters which leads to enhanced stratification during summer and (ii) the shift of strong wind events from autumn to winter and early spring detected for the period 1988-2007 which, in turn, could delay the termination of the stratification period by wind-induced ventilation (Hoppe et al., 2013; Lehmann et al. 2011; Lennartz et al., 2014).

3. Comparison with historical measurements

Salinity has been measured in Eckernförde Bay on a daily basis from 1876 to 1893. (Please note that the exact location of the historical sampling site is unknown but the the maximum sampling depth of 20 m suggests that it was located close to Boknis Eck). Figure 5 shows a comparison of the salinity in 20m for Boknis Eck with the historical salinity data from Eckernförde Bay. Obviously the historical salinity data seem to be lower; however, a methodological bias in the historical data cannot be ruled out entirely (Schwensen, 2016).

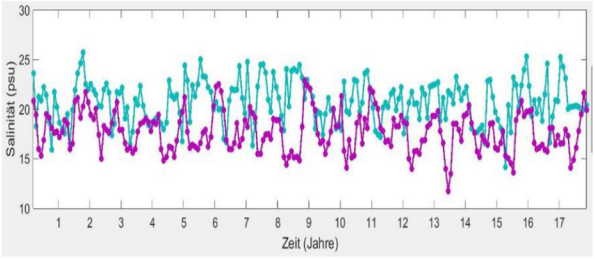

Figure 5: Salinity in 20m depth. The blue line depicts the actual data from Boknis Eck (1998-2015) and the violet line depicts the historical data from Eckernförde Bay (1876-1893) (Schwensen, 2016).

No major North Sea water inflow event could be detected in the historical data from Eckernförde Bay (Schwensen, 2016). Interestingly the historical salinity data show a constant periodicity of one year throughout the entire sampling period which not found for the recent data from Boknis Eck (Figure 6).

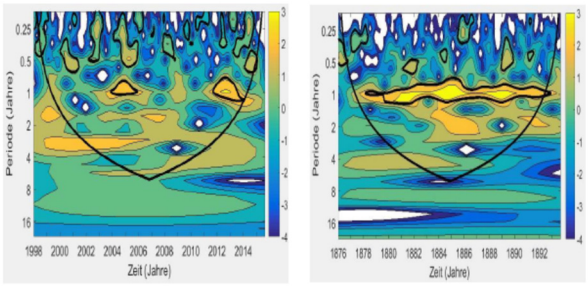

Figure 6: Wavelet power spectra of salinity in 20 m depth at Boknis Eck (left; sampling period 1998-2015) and Eckernförde Bay (right; sampling period 1876-1896) (Schwensen, 2016). The black lines depict 95% significance.

4. Outlook

A cabled underwater observatory for high resolution online measurements (incl. temperature, salinity, ADCP, O_2, CO_2, and CH_4) has been installed in December 2016 at 14.5 m water depth in the vicinity of the monthly time-series site. The complimentary online measurements will help to improve our ability to capture short-term events such as upwelling etc. at the Boknis Eck time-series sampling site.

Further information about Boknis Eck is available under www.bokniseck.de.

References

Hoppe, H.-G., Giesenhagen, H.C., Koppe, R., Hansen, H.-P., Gocke, K. (2013) Impact of change in climate and policy from 1988 to 2007 on environmental and microbial variables at the time series station Boknis Eck, Baltic Sea, Biogeosciences, 10, 4529–4546.

Lehmann, A., Getzlaff, K., Harlaß, J. (2011) Detailed assessment of climate variability in the Baltic Sea area for the period 1958-2009, Clim. Res., 46, 185-196.

Lennartz, S.T., Lehmann, A., Herrford, J., Malien, F., Hansen, H.P., Biester, H., Bange, H.W. (2014) Long-term trends at the Time Series Station Boknis Eck (Baltic Sea), 1957–2013: does climate change counteract the decline in eutrophication?, Biogeosciences, 11, 6323-6339.

Schwensen, S., (2016) Trends in der Ostsee – ein regionaler und historischer Vergleich von Eckernförde und Kiel, MSc thesis, Kiel University, 88 p.

Hydroclimatic dynamics and peatland land cover response over last centuries – A multi-proxy reconstruction from hydro-meteorological data, peat stratigraphy, testate amoebas, tree rings and remotely sense approaches

Ieva Baužienė [1], Johannes Edvardsson[2], Mariusz Lamentowicz [3], Julius Taminskas[1], and Rasa Šimanauskienė[1]

[1] Nature Research Centre, Akademijos str. 2, LT–08412 Vilnius, Lithuania (bauziene@geo.lt)
[2] Lund University, Sölvegatan 12, SE-223 62, Lund, Sweden
[3] Adam Mickiewicz University, Dzięgielowa 27, PL-61-680, Poznan, Poland

1. Introduction

Peatland ecosystems are globally important greenhouse gas sinks contributing to vital carbon sequestration, biodiversity, and fresh-water purification. Over recent decades tree colonization has been observed on many peatlands. The tree colonization is likely due to a combination of climate change and anthropogenic activities, which causes local water-table changes as well as regional land cover transformations (Juszczak et al 2013).

2. Methods

A peat stratigraphic sequence was obtained using a one-meter Wardenaar peat sampler (100 cm^2 in cross-section) Variations in peat composition were identified from studies of washed peat samples under an optical microscope.

The quantitative reconstruction of water-table changes (DWT, cm) based on testate amoebae was conducted with C2 software and Polish calibration data set by Lamentowicz *et al* (2008).

The potential evapotranspiration (PET, mm) could be calculated from the average annual precipitation (P, mm) and temperature data from the Varėna weather station.

In total, 96 peatland trees were sampled for dendrochronological analyses and to age determine the tree colonization.

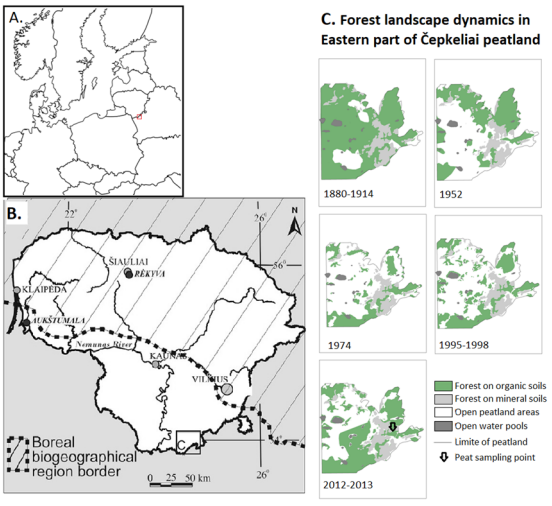

Figure 1. Setting of the Čepkeliai site (A., B. by Stančikaitė *et al* (2017). The development of forest cover in Eastern part of Čepkeliai peatland during the 20th century (on the basis of: topographical map of Russian tsarist empire, M 1: 21 000 and aerial photograph analysis M 1:10 000).

3. Results

Transformation of land cover in Čepkeliai mire was intensive. About 150 years ago Čepkeliai peatland territory was covered by woody vegetation; the oldest map shows a higher percent of woodland in the mire territory in comparison with recent times (Figure 1). An intense clear-cutting took place in 1914s, and is well reflected in the oldest generation of aerial photographs (1952). The ongoing spread of trees (from 1974 till recent times) is most likely related to warmer and drier climatic conditions, and to a minor degree to land-use changes. Water-table fluctuations identified from testate amoebas, chronologically interrelate with local and regional scale hydro-climatic and forest landscape dynamics (Figures 2 and 3). Several tree colonization events could also be detected in the tree-ring data.

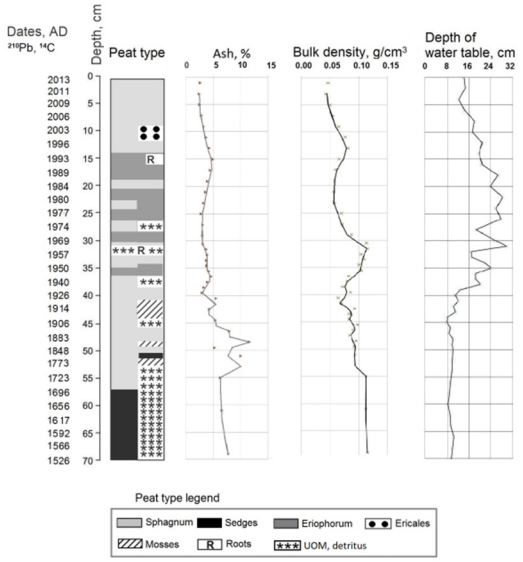

Figure 2. Čepkeliai peat column the peat type, ash content, bulk density and depth of water table (DWT, cm).

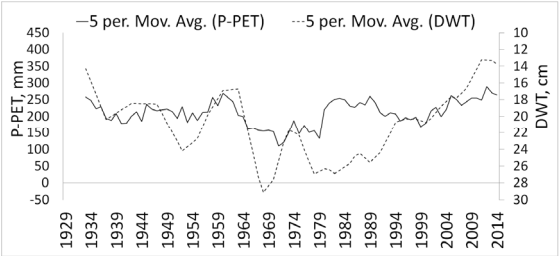

Figure 3. Chronology of DWT (modeled from AT and radioisotopes dating) plotted on P-PET chronology.

4. Synthesis

The multi-proxy results analysis demonstrates the complexity of driving forces and feedbacks influencing peatland ecosystem dynamics. Our investigation show climate change and forest cutting were the equivalent driving forces for changing water level in peatland.

References

Juszczak R., Humphreys E., Acosta M., Michalak-Galczewska M., Kayzer D., Olejnik J. (2013) Ecosystem respiration in a heterogeneous temperate peatland and its sensitivity to peat temperature and water table depth, Plant Soil., 366, pp. 505–520.

Lamentowicz, M., Cedro, A., Gałka, M., Goslar T., Miotk-Szpiganowicz, G., Mitchell, E.A.D., Pawlyta, J. (2008) Last millennium palaeoenvironmental changes from a Baltic bog (Poland) inferred from stable isotopes, pollen, plant macrofossils and testate amoebae. Palaeogeography, Palaeoclimatology, Palaeoecology, 265, pp. 93-106

Sančikaite, M ., Gedminienė, L., Edvardsson, J., Stoffel, M., Corona, C., Gryguc, G., Uogintas, D., Zinkutė, R., Skuratovič, Ž. and Taraškevičius, R. (2017) Holocene vegetation and hydroclimatic dynamics in SE Lithuania–Implications from a multi-proxy study of the Čepkeliai bog. Quaternary International. In press.

Quantifying the land-use climate forcing in the past: a modelling approach focusing on Europe and the Holocene (LandClim II)

Esther Githumbi[1], Anna-Kari Trondman[1], Ralph Fyfe[2], Erik Kjellström[3], Johan Lindström[4], Zhengyao Lu[5], Florence Mazier[6], Anne B. Nielsen[7], Anneli Poska[8, 5], Ben Smith[5], Gustav Strandberg[3], Shinya Sugita[9], Qiong Zhang[10], and Marie-José Gaillard[1]

[1] Department of Biology and Environmental Science, Linnaeus University, Kalmar, Sweden (esther.githumbi@lnu.se)
[2] Plymouth School of Geography, Earth and Environmental Sciences, Plymouth University, Plymouth, UK
[3] Swedish Meteorological and Hydrological Institute, Norrköping, Sweden
[4] Centre for Mathematical Sciences, Lund University, Lund, Sweden
[5] Department of Physical Geography and Ecosystems Analysis, Lund University, Lund, Sweden
[6] GEODE, UMR-CNRS 5602, Université Toulouse Jean Jaurès, Toulouse, France
[7] Department of Geology, Lund University, Lund, Sweden
[8] Institute of Geology, Tallinn University of Technology, Tallinn, Estonia
[9] Institute of Ecology, Tallinn University, Tallinn, Estonia
[10] Bolin Centre for Climate Research, Stockholm University, Stockholm, Sweden

1. Background

There is a need for in-depth knowledge on all climate forcings from anthropogenic land-cover/vegetation changes if land-use policies are to be successful in mitigating climate change. Afforestation/tree plantation is largely promoted today as a way to mitigate climate warming, relying on the assumption that the biogeochemical forcing of an increase in tree cover will override its biogeophysical forcing and imply a carbon sink and a decrease in temperatures. However, many climate modelling studies using global climate models have shown that the biogeophysical forcing may offset or override climate gains from the increased carbon sequestration in forests (e.g. Gaillard et al., 2015). Nonetheless, many of the socio-economic factors and assumptions controlling future land- use policies take indirect biogeochemical processes into consideration while neglecting direct biogeophysical processes.

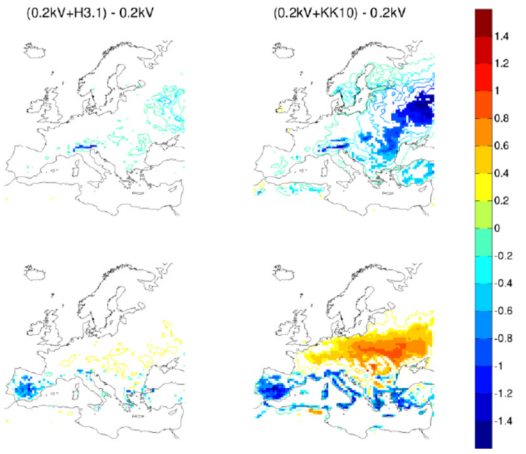

Figure 1. LandClim I, from Strandberg et al. (2014). Upper row: winter temperatures. Bottom row: summer temperatures. Left column: (0.2kV+H3.1) – 0.2kV difference in temperatures caused by deforestation from the HYDE 3.1 (H3.1) scenarios (Klein-Goldewijk et al., 2011) as compared to natural, climate-induced vegetation cover simulated by LPJ-GUESS (Smith et al., 2001) (V). Right column: (0.2kV+KK10) – 0.2kV difference in temperatures caused by deforestation from the KK10 scenarios (Kaplan et al., 2009) as compared to natural, climate-induced vegetation cover simulated by LPJ-GUESS (V). Blue colors represent a negative land-use forcing, red colors a positive forcing.

2. The LandClim I project (2009-2014)

In an earlier project, LandClim I, the effects of anthropogenic land-cover change in Europe between 6k and 0.2 k on biogeophysical forcings were studied using a regional climate model (Strandberg et al., 2014) (Fig. 1). In that project, the first generation of pollen-based REVEALS reconstructions of vegetation cover for the purpose of climate modelling were achieved for several

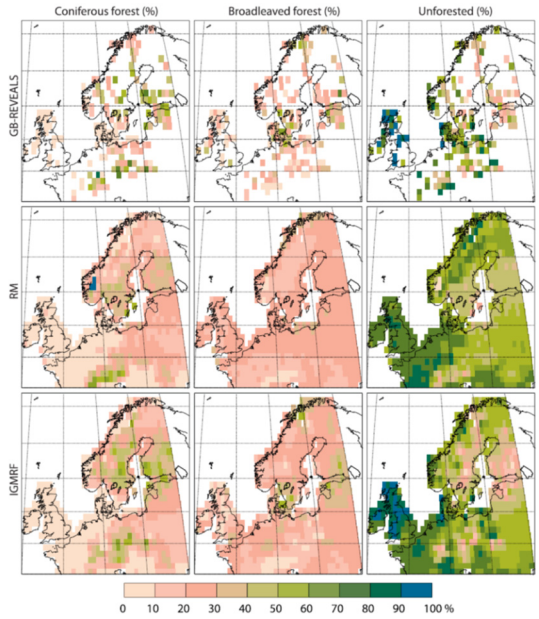

Figure 2. Landclim I, from Pirzamanbein et al. (2014). Upper row: REVEALS-based reconstructions of vegetation cover for the time window 100-350 years BP (1600-1850 CE) using pollen records (Trondman et al., 2015). Second row: spatial statistical modelling using a regression model (RM) and, as co-variate, a combination of climate-induced vegetation cover as simulated by the dynamic vegetation model LPJ-GUESS and the anthropogenic land-cover change scenarios KK10. Bottom row: the same as second row using an Intrinsic Gaussian Markov Random Field (IGMRF).

time windows of the Holocene over most part of Europe (except the Mediterranean area and the easternmost regions) (Trondman et al., 2015; Pirzimanbein et al., 2014) (Fig. 2). REVEALS is a model/algorithm that estimates vegetation cover using pollen records from large lakes or multiple small sites (lakes and bogs) and models of pollen dispersal and deposition (Sugita, 2007). The application of REVEALS requires values of pollen productivity and fall speed of pollen for all plant taxa included in the reconstruction (Trondman et al., 2015). The results of LandClim I showed that land-use affects climate in different ways depending on the geographical location and season.

2. The LandClim II project (2017-2020)

The main purpose of the LandClim II project is to quantify the effects of the biogeophysical forcings induced by human-induced deforestation (i.e. the "land-use" forcing, see IPCC5) on the regional climate of Europe over the last 6000 years using a more sophisticated modelling approach than in LandClim I (Fig. 3) and studying additional time periods of The Holocene. The magnitude and sign, and the seasonal and geographical differences, in the effects will be estimated. To put these forcings into context, we will also quantify the contributions of European deforestation to (global) biogeochemical forcing, i.e. the net land-atmosphere CO2 exchange translated into radiative units, W/m2.

3. This presentation

In this presentation we will i) briefly present the results of the earlier LandClim I project, and ii) explain the research strategy of LandClim II (Fig. 3) and present first results.

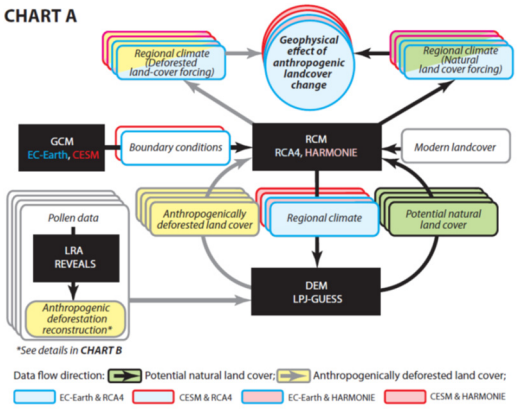

Figure 3. LandClim II modelling approach. Chart A: The regional climate models (RCM) RCA (Samuelsson et al., 2011) (light blue) and HARMONIE (Lindstedt et al., 2015) (pink) are applied to quantify the biogeophysical forcing of anthropogenic deforestation using land-cover descriptions from the dynamic vegetation model (DEM) LPJ-GUESS, both potential, natural (climate-induced) land cover (green) and human-induced deforested land cover (yellow). The boundary conditions used to run the RCMs are from the global climate model (GCM) EC-Earth (Hazelege et al., 2010) (dark blue) and CESM (Hurrell et al., 2013) (red). The combination of two RCMs and two GCMs provide four alternative RCM runs, thus four alternative results. LPJ-GUESS is run with the climate characteristics provided by the four alternative RCM runs. Past deforestation is implemented in LPJ-GUESS through its "land-use" module to produce the anthropogenically deforested land cover (yellow). For details on the reconstruction of past deforestation (Chart B), please contact the authors.

Acknowledgements

LandClim II is a contribution to PAGES LandCover6k (www.pastglobalchanges.org/ini/wg/landcover6k/intro) and to the Strategic Research Area MERGE (www.merge.lu.se/research/past-variations-climate-and-vegetation-ra2). We are grateful for the financial support from the Swedish Research Council (Vetenskapsrådet, VR, grant number 2016-03617) and MERGE.

References

Gaillard M.-J., Kleinen T., Samuelsson, P., Nielsen, AB, Bergh J, Kaplan, J, Poska A, Sandström C, Strandberg G, Trondman AK, and Wramneby A.(2015). Causes of Regional Change—Land Cover. Chapter 25 In The BACC II Author team: *Second Assessment of Climate Change for the Baltic Sea Basin* (BACC II). Springer Open, ISSN 1862-0248 ISSN 1865-505X (electronic), Regional Climate Studies. ISBN 978-3-319-16005-4 ISBN 978-3-319-16006-1 (eBook). DOI 10.1007/978-3-319-16006.

Hazelege, W., Severijns, C., Semmler, T., Stefanescu, S., *et al.* (2010). EC-Earth: a seamless earthsystem prediction approach in action. Bull Amer Meteor Soc 91, 1357-1363.

Hurrell, J. W., Holland, M.M., and Gent, P.R. (2013). The Community Earth System Model: A Framework for Collaborative Research. Bull. Amer. Meteor. Soc. 94, 1339–1360.

Kaplan, J., Krumhardt, K., and Zimmermann, N. (2009).The prehistoric and preindustrial deforestation of Europe, Quaternary Sci. Rev. 28, 3016–3034.

Klein Goldewijk, K., Beusen, A., de Vos, M., and van Drecht, G. (2011). The HYDE 3.1 spatially explicit database of human induced land use change over the past 12,000 years, Global Ecol. Biogeogr. 20, 73–86.

Lindstedt, D., Lind, P., Jones, C. and Kjellström, E. (2015). A new regional climate model operating at the meso-gamma scale; performance over Europe. Tellus A, 67, 24138. DOI: 10.3402/tellusa.v67.24138

Pirzamanbein, B., Lindstrom, J., Poska, A., Sugita, S., Trondman, A., *et al*. (2014). Creating spatially continuous maps of past land cover from point estimates: A new statistical approach applied to pollen data. Ecological Complexity 20, 127-141.

Samuelsson, P., Jones, C. G., Willen, U., Ullerstig, A., Gollvik, S., Hansson, U., Jansson, C., Kjellström, E., Nikulin, G., and Wyser, K. (2011). The Rossby Centre regional climate model RCA3: model description and performance, Tellus A, 63, 4–23.

Smith, B., Prentice, I. C., and Sykes, M. T. (2001). Representation of vegetation dynamics in modelling of terrestrial ecosystems: comparing two contrasting approaches within European climate space. Global Ecol. Biogeogr. 10, 621–637.

Strandberg, G., Kjellström, E., Poska, A., Wagner, S., Gaillard, M.-J., *et al.* (2014). Regional climate model simulations for Europe at 6 and 0.2 k BP: sensitivity to changes in anthropogenic deforestation. Climate of the Past 10, 661-680.

Sugita, S. (2007). Theory of quantitative reconstruction of vegetation I: pollen from large sites REVEALS regional vegetation composition, Holocene 17, 229–24.

Trondman, A., Gaillard, M.-J, Mazier, F., Sugita, S., Fyfe, R., *et al*. (2015). Pollen-based quantitative reconstructions of Holocene regional vegetation cover (plant-functional types and land-cover types) in Europe suitable for climate modelling. Global Change Biology 21, 676-697.

Temperature variability of the Baltic Sea since 1850 in model simulations and observations and attribution to variability in the atmosphere

Madline Kniebusch[1], H.E. Markus Meier[1,2] and Thomas Neumann[1]

[1] Leibniz Institute for Baltic Sea Research Warnemünde, Rostock, Germany (madline.kniebusch@io-warnemuende.de)
[2] Swedish Meteorological and Hydrological Institute, Norrköping, Sweden

1. Introduction

As global mean temperature is increasing due to emission of greenhouse gases, also the Baltic Sea is exposed to changes in surface air temperature (SAT) and sea surface temperature (SST) as well as changes in the atmospheric circulation patterns. Lehmann et al. (2011) showed that the Baltic Sea mean air temperature increased by 0.4 °C per decade during 1970-2008. Belkin (2009) revealed that the Baltic Sea was the fastest warming ecosystem during 1982-2006 considering satellite measured SST. Thus, it is very important to understand, how the Baltic Sea is warming and what the main drivers are.

2. Data

To analyze the temperature variability of the Baltic Sea, model simulations of the Modular Ocean Model coupled with the Ecological Regional Ocean Model (MOM-ERGOM, Neumann, 2000) and the Rossby Centre Ocean circulation model coupled with the Swedish Coastal and Ocean Biogeochemical model (RCO-SCOBI, Meier et al., 1999) have been used. Both models have been forced with the high resolution atmospheric forcing fields from Schenk and Zorita (2012). For the model validation, long term in-situ observations from lightships (http://urn.kb.se/resolve?urn=urn:nbn:se:smhi:diva-2295) and research vessels (IOW database) as well as reconstructed sea surface temperature (SST) time series (Rayner et al., 2003) are used.

3. Findings

The evaluation considering stratification as well as long term temperature changes show good agreement. In addition, the simulated long term temperature changes in the Baltic Sea fit to recent publications. Moreover, both models setups show similar results, although their parameterizations of heat fluxes and ice formation are different. The simulated SST and bottom temperatures have been analyzed considering different sub-basins of the Baltic Sea, seasons and time periods.

Annual mean water temperature changes in the Baltic Sea are always positive. The bottom temperature of the deeper parts of the Bornholm and Gotland Basin showed in the last 150 years highest trends up to 0.15K/decade at Bornholm Deep, while the surface warmed at maximum with 0.07K/decade. Seasonal temperature changes show highest trends in summer SST in the northern basins Bothnian Bay and Bothnian Sea which exceeded the corresponding trends in surface air temperature (SAT). In contrast, there are almost no changes in winter due to ice cover. Additionally, our results confirm, that the Baltic Sea region is warming faster than the global mean considering sea surface as well as surface air temperature.

4. Attribution to atmospheric parameters

A Detection and attribution study revealed that the SST variability of the Baltic Sea has several important drivers. First of all, the air temperature and thus the sensible heat flux in the Baltic Sea catchment area is the dominating factor followed by the latent heat flux, which are both most important at all grid points. Northern areas where the Baltic Sea is covered by ice during winter, the decoupling of the ocean and the atmosphere due to the freezing point is very important, too. In a third order, the wind components are relevant for upwelling areas and the cloudiness as a measure for the radiation budget for open water, while explained variances are much lower.

References

Belkin, I.M. (2009) Rapid warming of large marine ecosystems. Progress in Oceanography, Vol. 81, No.1, pp. 207-213

Lehmann, A., Getzlaff K., Harla, J. (2011) Detailed assessment of climate variability of the Baltic Sea area for the period 1958-2009. Climate Research, Vol. 46, pp. 185-196

Meier, H.E.M., Döscher, R., Coward, A.C., Nycander, J., Döös, K. (1999) RCO - Rossby Centre regional Ocean climate model: model description (version 1.0) and firrst results from the hindcast period 1992/93. SMHI

Neumann, T. (2000) Towards a 3D-ecosystem model of the Baltic Sea. Journal of Marine Systems, Vol. 25, No. 3, pp. 405-419

Rayner, N.A., Parker, D.E., Horton, E.B., Folland, C.K., Alexander, L.V., Rowell, D.P., Kent, E.C., Kaplan, A. (2003) Global analyses of sea surface temperature, sea ice, and night marine air temperature since the late nineteenth century. Journal of Geophysical Research: Atmospheres, Vol. 108, No. D14

Schenk, F., Zorita, E. (2012) Reconstruction of high resolution atmospheric forcing fields for northern europe using analog-upscaling. Climate of the Past: Discussions, Vol. 8, pp. 819-868

Variability of nutrient concentrations in the western Baltic Sea between 1995 and 2017

Joachim Kuss[1], Günther Nausch[1], Michael Naumann[1] and Detlef E. Schulz-Bull[1]

[1] Leibniz Institute for Baltic Sea Research Warnemünde (IOW), Rostock, Germany (joachim.kuss@io-warnemuende.de)

1. Motivation

The temporal trend and the regional peculiarities of the concentrations of major nutrients and their respective ratios are investigated for the period between 1995 and 2017 from Kiel Bight to the Odra Bank. The Western Baltic Sea is a relative dynamic area. Outflow of mainly surface water and inflow of saline mostly cold water along the bottom pass the straits of the Belt Sea. It is a narrow link between the almost oceanic North Sea and the brackish Baltic Proper. The western Baltic Sea is impacted by agricultural and industrial activity of bordering Denmark, Germany, Sweden and Poland, and of course by the adjacent sea areas and the atmosphere. Thus, it is an important and interesting area for a regional analysis of the development of nutrient concentrations in the last two decades.

Beside the dissolved nutrients nitrate, nitrite, ammonia, phosphate, and silicate, we also investigate total nitrogen and total phosphorus as well as the ratios of total nitrogen/total phosphorus and total dissolved nitrogen/phosphate. The aim is to identify regional changes since 1995 that might be explained by either differences in supply pattern or caused by the clearly different behavior in biogeochemical cycling of nitrogen and phosphorus compounds in the atmosphere and seawater. Moreover, differences in applied nutrient load reductions of nitrogen and phosphorus might be reflected during the more than 20 years time span. The data are interpreted with temperature, salinity, and oxygen concentrations determined parallel to the nutrients and by inclusion of data on atmospheric deposition (Fagerli et al., 2016) and river load (HELCOM, 2011, 2015).

2. Methods

All data were obtained during regular monitoring cruises of IOW between 1995 and 2017 during five campaign per year, covering winter by one cruise in January/Februar, spring by two cruises in March and May, respectively, in summer by a cruise usually in July/August, and one cruise in autumn, annually done end of October or November. The chemical analysis of the dissolved nutrients were carried out on-board of filtrated seawater right after sampling using standard spectrophotometric determination by application of an autoanalyzer (Grasshoff et al., 1999). Total phosphorus and total nitrogen were determined after digestion using peroxodisulfate in the home laboratory and subsequently by the same spectrophotometric methods.

3. Results

We here focus on the data obtained from upper 8 m of the water column and the bottom water which was taken from the lower 3 m of the profiles sampled during the campaigns. It is expected that these two water bodies would reflect the most drastic changes on the regional and temporal scales investigated in this study. The data were plotted according to the respective season of sampling, first against time (Figs. 1 & 2) and second, basically following the salinity gradient that is from the Belt Sea area, Kiel Bay, the Mecklenburg Bay, via the Darss sill to the Arkona Sea and to the Odra Bank further south.

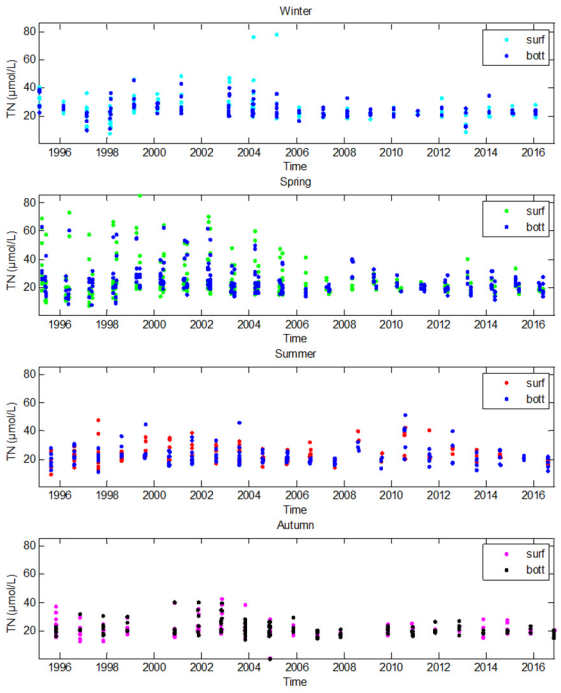

Figure 1. Total nitrogen (TN) concentrations in surface and bottom water according to the different seasons of the western Baltic Sea.

The temporal evolution since 1995 generally appears relative unspectacularly stable, with regard to the efforts that have been undertaken to reduce nutrient supply to the sea. However, looking into details, surface water concentration of total nitrogen (TN) shows clear seasonal differences and appears to have decreased significantly after 2002 (Fig. 1). The concentration of TN scatters around 25 µmol/L in winter, of ~ 40 µmol/L in spring until 2005 and about of ~25 µmol/L thereafter, with higher values in surface waters. In summer and autumn TN was slightly lower at about 20 µmol/L. Also a weak sinuous pattern is recorded during the time period of two decades that shows minima in 1998 and 2007 which is best documented for autumn.

The ratio of TN and total phosphorus (TP) also shows clear seasonal differences and minor changes during the two decades (Fig. 2). TN/TP develops from about 30 mol/mol in winter to a large scatter around ~50 mol/mol in spring. In the second half of the year, TN/TP decreases

to 30 in summer and 20 mol/mol in autumn. Already in spring, it appears that surface water was slightly more enriched in nitrogen compared to the deep water, which is even more pronounced in summer. This could be an indication of additional nitrogen uptake from the atmospheric dinitrogen

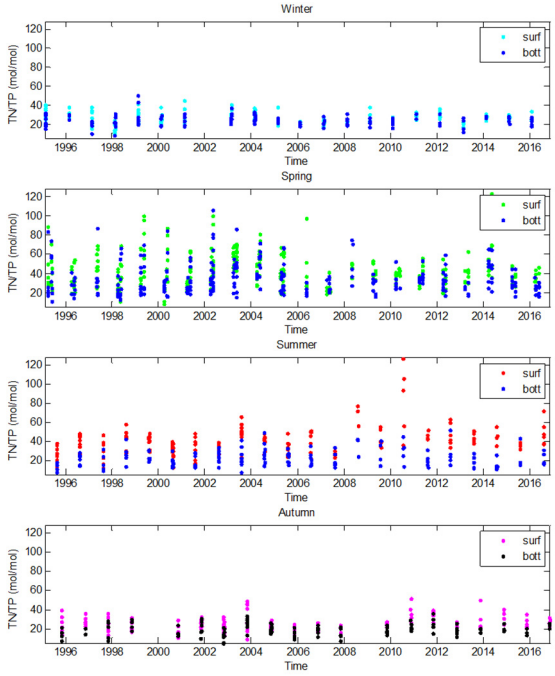

Figure 2. Total nitrogen versus total phosphorus concentration ratio (TN/TP) in surface and bottom water according to the different seasons in the western Baltic Sea.

by diazotrophic cyanobacteria. In the presentation the analysis will be extended to other nutrients and interpreted in terms of temporal and spatial development from 1995-2017 including temperature, salinity and oxygen.

References

Fagerli, H., Tsyro, S., Denby, B.R. et al. (2016) Transboundary particulate matter, photo-oxidants, acidifying and eutrophying components, Joint MSC-W & CCC & CEIP Report, Oslo, Norway, 147.

Grasshoff, K., Kremling, K., and Ehrhardt, M. (1999) Methods of seawater analysis, 3rd edition, Wiley-VCH, Weinheim, Germany, 600 pp.

HELCOM (2011) The Fifth Baltic Sea Pollution Load Compilation (PLC-5), 217.

HELCOM (2015) Updated Fifth Baltic Sea pollution load compilation (PLC-5.5), 143.

Recently accelerated oxygen consumption rates amplify deoxygenation in the Baltic Sea – observations and model results

H. E. Markus Meier[1,2], Germo Väli[3], Michael Naumann[1], Kari Eilola[2] and Claudia Frauen[1]

[1]Department of Physical Oceanography and Instrumentation, Leibniz Institute for Baltic Sea (markus.meier@io-warnemuende.de)

[2]Department of Research and Development, Swedish Meteorological and Hydrological Institute, 60176 Norrköping, Sweden.

[3]Marine Systems Institute, Tallinn University of Technology, 12618 Tallinn, Estonia.

Summary

The Baltic Sea is a semi-enclosed sea with limited water exchange with the North Sea. Due to excessive riverine nutrient loads in the past the Baltic Sea is eutrophied causing deoxygenation of the deep water and extended areas of hypoxia (Figures 1 and 2). Although nutrient loads were reduced after the 1980s, recently observed oxygen consumption rates are still high. Especially, after the saltwater inflow in December 2014 oxygenated bottom water turned rather quickly back to anoxic conditions. In this study, both long-term observations and historical model simulations for the period 1850-2015 have been analyzed to estimate long-term changes in oxygen consumption rates and to find out their causes (Meier et al., 2018). We found that recently observed oxygen consumption rates are unprecedentedly high. One reason for the recent acceleration is that inflowing water after inflow events contained elevated concentrations of organic matter, zooplankton and higher trophic levels causing a relatively larger increase in oxygen consumption in the water column compared to the oxygen consumption in the sediments. Hence, recent saltwater inflows result in less effective ventilation of the Baltic Sea deep water. Although warming of the deep water during the past century is an important driver of deoxygenation, accelerated oxygen consumption rates under contemporary conditions could not be explained by increased water temperatures.

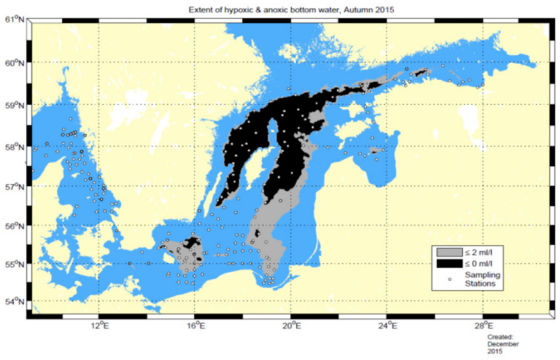

Figure 1: Extent of hypoxic and anoxic bottom water in autumn 2015 (Source: SMHI).

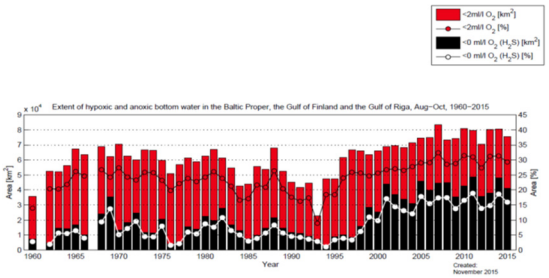

Figure 2: Extent of hypoxic and anoxic bottom water in the Baltic proper, Gulf of Finland and Gulf of Riga in the period August to October during 1960-2015 (Source: SMHI).

References

Meier, H. E. M., G. Väli, M. Naumann, K. Eilola, and C. Frauen, 2018: Recently accelerated oxygen consumption rates amplify deoxygenation in the Baltic Sea. J. Geophys. Res., accepted.

Changes of the frames of agroclimatic areas in the XXI century on the territory of Belarus

Viktar I. Melnik
Institute for Nature Management of the National Academy of Sciences of Belarus, Minsk, Belarus, e-mail: v.melnik 2016@mail.ru

1. Introduction

The most prolonged period of warming in Belarus for the whole time of the instrumental observations of air temperature for the last 130 years was at the end of the XX – XXI century. An average annual air temperature for the warming period (1989-2015) exceeded the climatic norm (1961-1990) to 1,3°C. The analysis of the average annual temperatures for the whole observation (from 1881) on the territory of the Republic of Belarus shows that in most cases (75%) from 20 warmest years, the maximum average annual temperatures were recorded for the warming period from 1989, and average annual temperature 2015 was 8,5°C and was the most highest temperature for the whole period of instrumental observations (Figure 1).

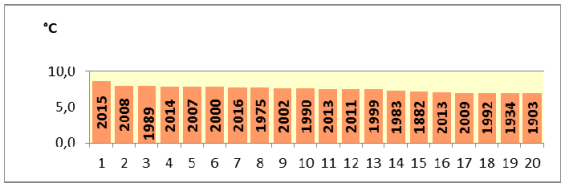

Figure 1 - 20 most warmest years from the ranked raw of observations for the period (1881-2016) on the territory of Belarus

The consequences of climate change, beginning from 1989 (warm winters, the early advent of spring processes, the increase of the duration and heat supply of vegetation period, the increase of draught repetition, heatwaves, high air temperatures, the change of wintering conditions, etc.) are studied enough and have a significant influence on an agricultural sector. That, as an example, there were very significant changes for agriculture in the annual regime of precipitations and in the character of their deposition. Precipitations loss is marked in the warm time of a year, in April, June, July, August, September. A number of precipitation days in warm period decreased (From 175 to 167), at the same time precipitation extreme and their intensity increased. A number of hot days with the maximum air temperature ≥25°C and a number of draughts increased in territory.

An increase in the temperature of the first rays follows by a decrease in temperature up to 0 °C in the upward direction. On average, during the period under review, this transition occurred by 10 to 15 days earlier than mean multiyear values. The duration of snow cover period decreased by 10 to 15 days, and the depth of soil freezing decreased by 6 to 10 centimeters. The dates of the beginning and the end of the transitions of the average daily air temperature and through other characteristic limits have changed, as well as the duration of periods between these dates. So, for a decade, the vegetation period begins earlier, and its duration also increased to 12 days, respectively. Climate changes have a significant impact on the weather-dependent sectors of economy, primarily agriculture and, accordingly, the country's food security. According to experts in the economy of Belarus, agriculture accounts, more than 40% of damage is because of adverse weather and climate conditions. Depending on weather conditions, a gross grain harvest can range from 5.5 to 9.5 million tons.

2. Main research results

Most global climate models indicate the expectation of an increase in future maximum and minimum temperature, an increase in the number of hot days, an increase in the number of the cases of intense precipitation and a decrease in the number of days with low precipitation, a decrease in the number of cold days, a decrease in the amplitude of the diurnal temperature trend for many land regions extratropical latitudes of the Northern Hemisphere. All these conclusions are typical for the territory of Belarus (1-3).

The analysis of the calculations of expected changes in agroclimatic characteristics obtained for the territory of Belarus using data from the ensemble of 31 CMIP5 models in relation to the base period of 1989-2015 for RCP4.5 scenario shows their significant change by the middle of the century, especially with regard to the increase in the duration of the warm period with the sum of air temperatures ≥0 °C. Its duration will increase by 20 days to 2060 year on average by 35 days and will range from 280 to 310 days, and in the extreme south-west in Brest region it will be 365 days (which will lead to the disappearance of climatic winter there). The duration of a growing season (≥5 ° C) and the period of active vegetation (≥ 10 ° C) will also increase, respectively, on average by 18 and 19 days. The sum of temperatures above 10 °C will increase by 2041 - 2060 year on average by 480 °C and will reach 2700 - 2800 °C in the north and 3050-3250 °C in the south of the country. On the sum of temperatures above 10 °C and the duration of the growing season, the new agroclimatic region of Belarus now corresponds to the conditions of the forest-steppe zone, and by 2060 the southern regions of Belarus will meet the conditions of the steppe zone (4) by the indicators highlighted.

The hydrothermal coefficient of Selyaninov-SCC moistening for May-July period will decrease and will amount to 1.0-1.2 percent of the territory, which characterizes arid and slightly arid conditions. On the territory, with the average SCC of 1.0, the probability of arid and very arid conditions will be at least 50%. For sandy and sandy loamy soils that are most vulnerable to droughts, in the southern regions there should be permanent measures to conserve moisture reserves, select drought tolerant crops or carry out measures related to the afforestation of low-productive soils (Table 1).

Table 1 – Change of agroclimatic characteristics, obtained for the territory of Belarus with the use of data from the ensemble of 31 models of CMIP5 in relation to the base period of 1989-2015 for RCP4.5 scenario

Period	Deviation of period duration, days			Sum of air temperatures		SCC change
	≥0°C	≥5°C	≥10°C	≥5°C	≥10°C	
2011-2030	10	7	9	172	186	-0,09-0.1
2021-2040	15	10	12	270	273	-0,1-0,2
2041-2060	35	18	19	466	480	-0,2 - 0,3

The analysis shows that as the result of expected warming according to RCP4.5 scenario, the boundaries of agroclimatic regions will change significantly. There will be even warmer areas with the sum of active temperatures exceeding 2800 °C and even 3000 °C (Figure 2). In spring and summer period, the amount of precipitation will practically not change, but the moisture content in the summer will decrease due to higher air temperatures and plants transpiration. Almost throughout the territory of Belarus, it will be possible to cultivate maize for grain and sunflower. The obtained results show a significant change in agroclimatic characteristics and the need to plan changes in cropping technologies.

The data obtained as the result of the research were used in the development of the main lines of the Strategy for Agriculture Adaptation of the Republic of Belarus to climate change developed in the framework of the international project Clima East in 2017.

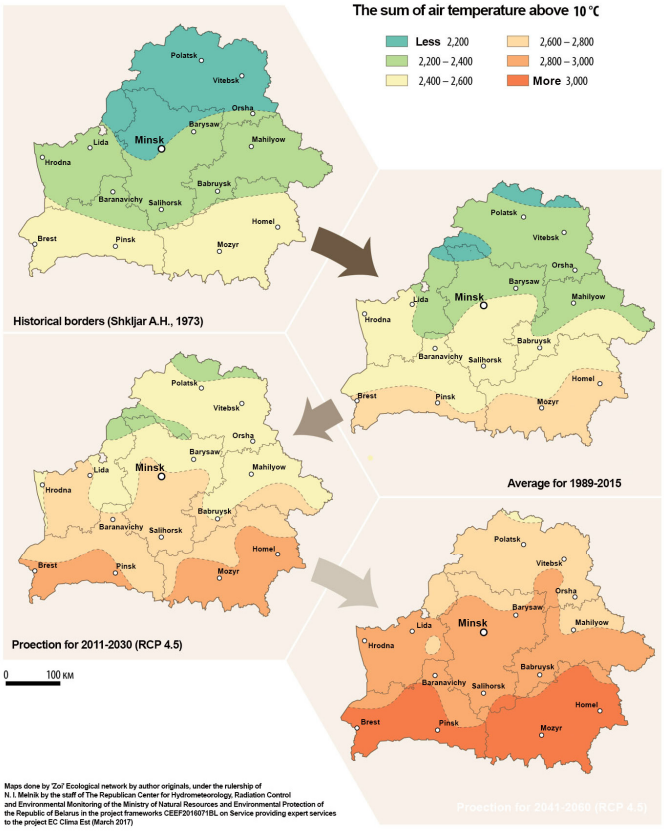

Figure 2 - Historical and expected for RCP4.5 scenario change in the boundaries of agroclimatic areas of Belarus (Melnik and others 2017, Clima East project, 2017)

3. Conclusion

1. New values of the main agroclimatic indicators (sum of air temperatures above 10 °C) and moisture availability (hydrothermal coefficient of Selyaninov-SCC humidification for May-July) for the periods of 2011-2030, 2021-2040, 2041-2060 are obtained for the territory of Belarus, using the data from the ensemble, 31 CMIP5 models for RCP4.5 scenario are relative to the base period of 1989-2015.
2. The climate changes expected in coming decades in the territory of Belarus will continue the trends observed in the last decades (increase in the sum of temperatures, the duration of the vegetation period, the shift of the boundaries of agroclimatic regions to the north and the emergence of new agro-climatic zones, etc.).
3. The obtained research results show the necessity of planning the introduction of changes in the technology of crop cultivation.

4. References

Melnik V.I., Sokolovskaya Y.A., Komarovskaya E.V. 2017, Possible changes of climate and agricultural characteristics in the XXI century on the territory of Belarus and their influence on agriculture, Nature Resources, Vol 2, 118-125.

Partasjonok I.S., Gejer B., Melnik V.I. 2015 Estimation of climate changes in Belarus with the use of estimations on model ensembles EURO-CORDEX, Reports of the hydrometeorological center of Russia, Vol 358, 99-111.

2014 The second estimation report of the Russian Hydrometeorological Center about climate changes and their consequences on the territory of Russian Federation (Technical summary), 94.

Shashko D. I. 1985, Agroclimate resources of the USSR, 249c.

Physical oceanography sets the scene for the Marine Strategy Framework Directive implementation in the Baltic Sea

Kai Myrberg,[1,2], Samuli Korpinen[1] and Laura Uusitalo[1]

[1] Finnish Environment Institute, Marine Research Centre
[2] Department of Natural Sciences of Faculty of Marine Technology and Natural Sciences, University of Klaipeda, Klaipeda, Lithuania

1. Abstract

A challenge of the EU's Marine Strategy Framework Directive (MSFD) is to ensure comparable status assessments for good environmental status (GES) in the European seas. To this end, the role of dynamic oceanographic features affecting the GES must be understood. Natural variability is recognized in the MSFD, but only vague advice is available for scientists and managers to apply this in the marine strategies. We show that physical factors – e.g. stratification, water residence time, irregularity of Major Baltic Inflows, and upwelling, affect each of the 11 descriptors of GES in the Baltic Sea. We recommend that thorough investigations of these effects are carried out in all regional seas; they may lead to insights that promote adaption of environmental monitoring programmes, as well as re-definitions of GES and other elements of the marine strategy.

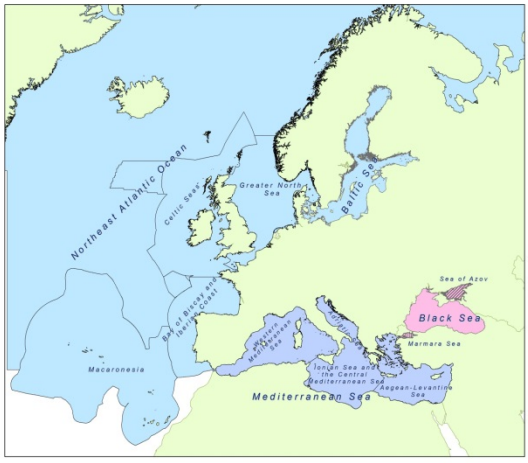

Figure 1. European marine regions and sub-regions as identified for the Marine Strategy Framework Directive. Source: European Environment Agency (https://www.eea.europa.eu/data-and-maps/data/msfd-regions-and-subregions).

Hypoxic to euxinic conditions in the Baltic Sea 1969-2016 – a seasonal to decadal spatial analysis

Michael Naumann[1], Susanne Feistel[1], Günther Nausch[1], Thomas Ruth[2], Jakob Zabel[2], Markus Plangg[2], Martin Hansson[3], Lars Andersson[3], Lena Viktorsson[3], Elzbieta Lysiak-Pastuszak[4], Rainer Feistel[1], Dietwart Nehring[1], Wolfgang Matthäus[1], H.E. Markus Meier[1,3]

[1]Leibniz Institute for Baltic Sea Research Warnemünde, Rostock-Warnemünde, Germany
(michael.naumann@io-warnemuende.de)
[2]Fraunhofer Institute for Computer Graphics Research, Maritime Graphics, Rostock, Germany
[3]Swedish Meteorological and Hydrological Institute, Norrköping and Västra Frölunda, Sweden
[4]Institute of Meteorology and Water Management, Maritime Branch, Gdynia, Poland

Summary

The Baltic Sea is a complex ecosystem characterized by a strongly fluctuating, fragile balance between high freshwater runoff and saline water inflows, a stable stratification and a topography composed of interconnected sub-basins. The sensitivity of the system "Baltic Sea" amplifies climatological fluctuations on the decadal scale. Such changes may be irrelevant in the open ocean but constitute significant indicators in the Baltic Sea. Salt and nutrients in the Baltic Sea remain present there for about 30 years before being flushed to the Atlantic along with the freshwater export. This long residence time attenuates short-time fluctuations in environmental conditions, but highlights systematic, even small long-term anomalies. Thus, a main scientific focus is on the evaluation of inflow events, on the progress of oxygen-consuming processes and on the development of hydrogen sulphide distribution over longer periods of time.

Mapping of hypoxic to euxinic layers in the deep-water from the western to central Baltic Sea visualizes these effects of inflow processes adequately. Based on regular seasonal sampling done by intensive environmental monitoring and long-term data programmes of neighbouring countries since 1969, a most complete dataset was compiled for this study. It shows a spatial analysis of the distribution of oxygen deficiency for the last five decades, which includes more or less the time span of two cycles of water exchange in the Baltic basin. Seasonal to decadal changes are shown for the entire area and separate sub-basins. For example, the mean extent of hypoxic area in the last two decades of around 63.000-64.000 km^2 differs only slightly from the mean value of the seventies with 58.000 km^2 (Fig. 1) and the situation in the Arkona Basin and Bornholm Basin is highly seasonal dynamic with no trend of increasing hypoxia over the time period. More distant from the entrance to the North Atlantic, the eastern Gotland Basin shows like the total areal extent only a slight increase from 19.000 km^2 (1970's) to recent values of 21.000 km^2 and the boundary to oxic conditions was in around 120 m water depth in both stages and differs only slightly in time steered by inflow events (Fig. 2). This shows that a more or less maximum extent of spreading hypoxia was reached early in this timeline and a further increase seems to be restricted under recent conditions. Analysis like this provides a closer look into deep-water oxygen dynamics, their regional differences and changes during the past 47 years. They can support multiple interdisciplinary studies, such as studies on ecosystem modelling, analysis of reproduction rates of vulnerable fish stocks in the highly dynamic western and southern parts or studies concerning trends in regional climate change, as well as studies on human footprints in the sensitive Baltic Sea ecosystem.

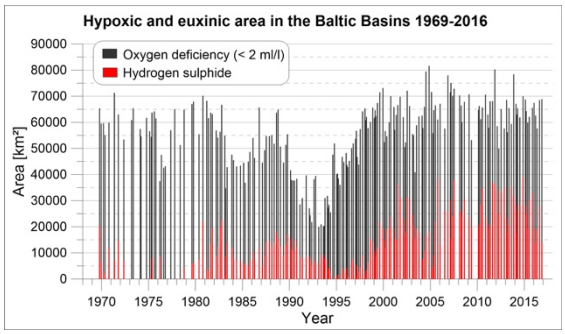

Figure 1. Spatial analysis of hypoxic to euxinic conditions in the Baltic Sea since 1969.

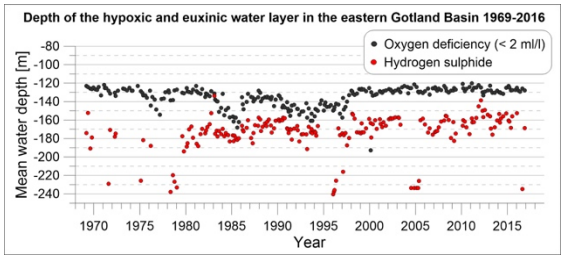

Figure 2: Spatial analysis of hypoxic to euxinic conditions in the eastern Gotland Basin since 1969 – mean value of water depth considering all deep basins

Influence of the Grodno hydroelectric power station on the hydrological regime of the Neman river (Belarus, the Baltic Sea basin)

Ala Pauros[1], Alena Kvach[1] and Ludmila Zhuravovich[1]

[1] State Institution «Center for of hydrometeorology and control of radioactive contamination and environmental monitoring of The Republic of Belarus» (Belhydromet) (gid2@hmc.by)

1. Introduction

The Grodno hydroelectric power station is the largest in the Republic of Belarus. According to the project, its capacity is 17 megawatts. According to the world classification, it is average in capacity (this is the first average hydroelectric power station in Belarus). Construction of hydroelectric power station began in May 2008. It was put into operation in September 2012.

Hydrological monitoring on the Neman River is carried out at 5 hydrological stations in the territory of Belarus. An analysis of changes in the hydrological regime of the Neman River due to the influence of the Grodno hydroelectric power station was carried out in 2 hydrological stations: Neman-Grodno 11.5 km downstream of the existing hydrological power station and Neman-Mosty 66 km upstream of the existing hydroelectric power station by comparing the hydrological characteristics before and after the construction of the hydroelectric power station. In order to exclude the impact of climate change on the hydrological regime of the Neman River, the period from 1989 to 2017 was chosen for analysis.

Figure 1. Grodno hydroelectric power station

2. The water level regim of the Neman River

The construction of the hydroelectric power station affected the regime of the river level. A decrease of 34 cm in the upper annual, 13 cm of the summer-autumn low water at the Neman-Grodno station, and at the same time a slight increase in the upper annual and summer-autumn low water by 2-5 cm at the Neman-Mosty station and a significant increase 28 cm) of the low water levels of the winter period.

3. Runoff

At the stations of the rivers Neman-Grodno and Neman-Mosty, a more even distribution of the river's water content is noted during the year. There is a decrease in runoff in the spring months (spring flood period) and during the summer-autumn low water. In winter there is an increase in runoff. This distribution of the flow is influenced by climate change, rather than the building of a hydroelectric power station (it was assumed at the project of the power plant that it would not affect the water flow regime of the Neman River).

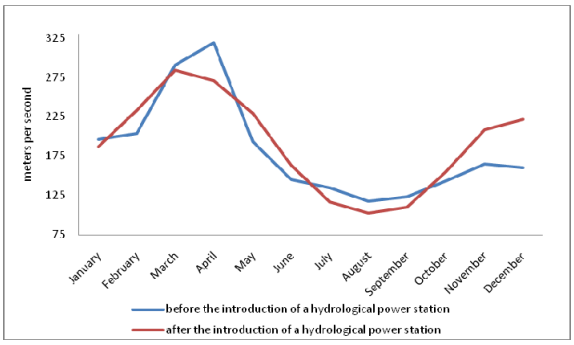

Figure 2. Distribution of runoff by months at the station Neman-Grodno

4. Ice and thermal regime of the Neman River

The construction of hydroelectric power station greatly changes the ice-thermal regime of the river below the dam and the processes of ice formation on it.

As a result of the commissioning of the hydroelectric power station, an increase in the temperature of the water in the autumn-winter period (by 0.1-1.1^{0}C) is observed at the station Neman-Grodno. This contributes to the later formation of stable ice formations on the Neman River. On the Neman-Grodno, the steady ice phenomena in the period after the hydroelectric power station commissioning are formed two weeks later than at the Neman-Mosty station. Before the commissioning of the power station at the Neman-Grodno station, the freez-up was formed in 56% of the years. The average duration of freez-up was 53 days. Since the commissioning of the hydroelectric power station (2012), the freez-up has not formed on this part of the river. At the station Neman-Mosty, the freez-up is formed annually and its average duration for the period before the entry is 63 days and the period after putting the power plant into operation is 66 days.

For 22 days the duration with all the ice phenomena at the station of Neman-Grodno decreased. While the station Neman-Mosty average duration remained about

the same as before the water in operation of the hydroelectric power station.

As a result of commissioning, an increase in the temperature of the water in the autumn-winter period (by 0.1-1.1^{0}C) is observed at the station Neman-Grodno. This contributes to the later formation of ice formations on the Neman River. At the station Neman-Grodno, ice phenomena in the period after the introduction of the hydroelectric power station are formed two weeks later than at the station Neman-Mosty.

5. Conclusions

At present, it is impossible to assess the impact of the hydroelectric power station in full volume, due to the fact that some impacts are not immediately apparent, but after a longer period of time. But already now one can see the influence of hydrological power station on the level, ice and thermal and regime of the Neman River:

- decreased the highest annual and lower levels of the open channel downstream of the current hydroelectric power station;

- the formation of ice phenomena below the current hydrological power station occurs two weeks later than at the post above the hydroelectric power station;

- there is an increase in water temperature in the winter months.

References

1. State water cadastre. Annual data of a regime and resources of surface water for the period 1989-2016 – Minsk, Belhydromet.

Shipping and the environment in the Baltic Sea region - results of the BONUS SHEBA project.

Markus Quante[1], Jana Moldanova[2], Martin Eriksson[3], Erik Fridell[2], Jukka-Pekka Jalkanen[4], Volker Matthias[1], Jenny Tröltzsch[5], Matthias Karl[1], Ilja Maljutenko[6] and the SHEBA team

[1] Helmholtz-Zentrum Geesthacht, Institute of Coastal Research, Germany (markus.quante@hzg.de)
[2] IVL, Svenska miljöinstitutet AB, Gothenburg, Sweden
[3] Chalmers University of Technology, Gothenburg, Sweden
[4] Finnish Meteorological Institute, Helsinki, Finland
[5] Ecologic Institute, Berlin, Germany
[6] Tallinn University of Technology, Estonia

1. Introduction

Since centuries shipping is a major means of trade in the Baltic Sea region. The number of ships employed has increased tremendously and is projected to increase over the next decades. In recent years a considerable fleet of cruise ships has developed and countless leisure boats – sailing and/or motorized – are in use for human recreation.

There are several paths by which ship operations impact the environment. Among them are emissions of exhaust gases and particles to the air, emissions of oil, contaminants of antifouling paint, ballast and scrubber water into the sea, emission of underwater and above water level noise (Andersson et al. 2016). Especially human health effects of atmospheric shipping emissions are present in public perception, and also climatic effects are of relevance (e.g. Sofiev et al. 2018).

The BONUS SHEBA project brought together lead experts from the fields of ship emissions, atmospheric, acoustic and oceanic modelling, atmospheric and marine chemistry, marine ecology and ecotoxicology, environmental economics, social sciences, logistics and environmental law in order to provide an integrated and in-depth analysis of the ecological, economic and social impacts of shipping in the Baltic Sea. Here some highlights of BONUS SHEBA's results generated over the past years are presented.

2. The SHEBA research agenda

SHEBA is assessing the effects of air and water pollution and introduction of energy (including noise) by shipping activities on the marine environment and integrated water management. Combined with the analysis of economical issues, governance structures and policy instruments in the shipping sector suggestions supporting related policies on EU, regional, national and local levels are being developed (Moldanova et al. 2018).

SHEBA has analysed the drivers for shipping, obtained the present and future traffic volumes and developed a set of scenarios, which were then basis for calculations of emissions to water, to air, and of underwater noise using and extending the currently most advanced emission model based on Automatic Identification System (AIS) ship movement data. In a next step, atmospheric, oceanic and noise propagation models in combination with ecotoxicology studies were used to assess spatio-temporal distributions, fates and effects of these stressors in the Baltic Sea region. In addition to modelling activities, a shipborne research campaign was performed in the Kattegat and the Baltic proper to measure various oceanic and atmospheric parameters of special interest. Field experiments were conducted with Baltic Sea fish to learn about hearing abilities and study the behavioural responses of the fish on underwater noise.

Stakeholders have been extensively involved throughout the project during all steps of the refinement of underlying research questions and scenario building. Dedicated stakeholder workshops and quantifying elicitations have been set up for this purpose. Based on the overall gathered knowledge an integrated assessment of policy options to mitigate pressures linked to shipping was accomplished, quantifying as far as possible anticipated changes in ecosystem services compared to an established baseline. The project will end in July 2018.

3. Selected Results

Besides field measurements SHEBA has a strong modelling component. Models are used to quantify the present day spatio-temporal distribution of physical parameters (incl. noise) and chemical species. In order to assess possible future impacts – target year 2040 - and policy options scenario building was central. Future scenarios have been developed for the region within the framework of Shared Socio-Economic Pathways (SSPs) to derive the essential emissions for follow-up modelling studies.

Air pollution

For the assessment of air pollution from shipping, an ensemble of atmospheric chemistry transport models was ran for the year 2012 and for several scenarios for the year 2040, both for the whole Baltic Sea region and for four harbour cities. The model simulations show that today, shipping is the most important source for nitrogen dioxide (NO_2) in the atmosphere over the Baltic Sea. On annual average, NO_2 concentrations are in the order of 10 ppb in busy shipping lanes, a typical value for smaller cities.

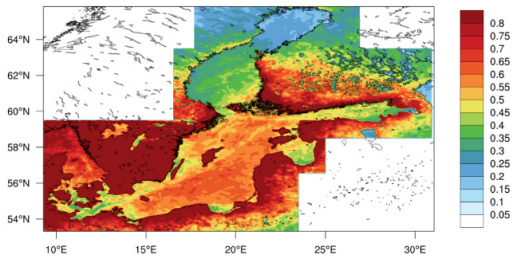

Figure 1. Contribution of ship emissions to atmospheric deposition (wet and dry) of total nitrogen (oxidised, reduced, organic) for the year 2012. Values are given in kg nitrogen per hectare (kgN/ha).

Besides nitrogen oxides, the distribution of sulphur dioxide, black carbon and the formation of particulate matter have been assessed by the modelling studies.

Being an important nutrient, nitrogen emitted by ships is largely deposited onto the sea and the adjacent coastal land areas. Cumulative deposited total nitrogen for the year 2012 is shown in Figure 1, the presented results are from a run with the chemistry transport model CMAQ using a 4 km grid resolution. The strong North-South gradient of deposited nitrogen is clearly visible. The enhanced contribution over coastal land areas is mainly due to dry deposition of particulate nitrate.

Ships visiting ports can be responsible for large parts of the NO_2 concentrations in respective cities (e.g. half of the total in Northern Gothenburg).

Scenarios for 2040 show a significant reduction of the NO_2 concentrations in the Baltic Sea region, including those originating from shipping. The reason is mainly an increase in energy efficiency projected for ships in the next 20 years as well the implementation of a nitrogen emission control area (NECA) in the North and Baltic Seas in 2021.

Water pollution and nutrients

A very high number of different contaminants are released from shipping into the Baltic Sea. Spatio-temporally resolved inventories of pollutants for the entire Baltic Sea have been established based on derived load factors for pollutants from sewage, food waste, bilge water, scrubber water, ballast water, and antifouling paints. As an example, the emission inventory on the load and distribution of copper, a major contaminant of shipping, revealed that more than 99% of about 300 tonnes of copper emitted annually by shipping originates from antifouling paints. Employing a numerical circulation model (GETM with 2 km grid resolution) to calculate transports in the entire Baltic Sea shows that the highest concentrations of copper are not always found around the shipping lanes but are located near the bigger harbours, where ships spend most of their time (Figure 2).

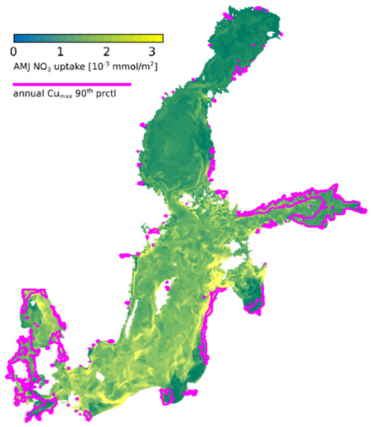

Figure 2. Shipping related nitrate uptake by phytoplankton from April to June (AMJ) in 2012 (colour bar). In addition, pink contour lines enclose areas making up for the 90th percentile of annual maximum copper concentrations in 2012.

Eutrophication is one of the major environmental risks in the Baltic Sea that needs further attention. The effect of additional nutrients from shipping to the marine ecosystem for the year 2012 has been assessed using the biogeochemical model ERGOM (Ecological Regional Ocean Model) coupled to GETM. Figure 2 shows as an example the shipping related nitrate uptake by phytoplankton during the spring bloom period from April to June (AMJ). Again, a strong North-South gradient is obvious reflecting the more intense ship activity in the Southern Baltic Sea.

Underwater noise

Both, natural and man-made activities can generate loud noise, which can disturb marine life. Increase of shipping in the last decades has made the anthropogenic fraction of sounds constantly growing. A profound quantification of sources and effects is pending. For this, a computer model has been developed in SHEBA that is based on estimates of underwater shipping noise (Karasalo et al. 2017). Finally, noise from entire Baltic Sea shipping is modelled by combining ship technical data in conjunction with ship activity data. In Figure 3 an example for the noise energy distribution for a specific frequency band is presented. As it was expected noise energy is concentrated near major shipping lanes, but now estimates of absolute energies are available. These can drive impact models developed using results from in situ fish experiments.

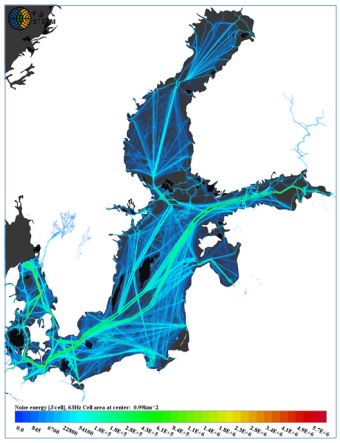

Figure 3. Underwater noise energy from ships, in April 2014, in the 63 Hz band (in J per grid cell, cell size 0.9 km^2, scale from 0 to 5.6 E+6 J)

4. Conclusions

BONUS SHEBA maps all types of pollution originating from ships and provides an integrated and in-depth analysis of the ecological, economic and social impacts of shipping in the Baltic Sea. Unique results and high resolution modelling data sets have been produced. Work on integrated assessments is currently being consolidated. Several journal articles presenting in depth the full range of SHEBA results are in preparation.

References

Andersson, K., Brynolf, S., Lindgren, J.F., Wilewska-Bien, M. (Eds.) (2016) Shipping and the Environment. Springer, 426pp

Karasalo, I., M. Östberg, P. Sigray, J.-P. Jalkanen, L. Johansson, M. Liefvendahl, R. Bensow (2017) Estimates of Source Spectra of Ships from Long Term Recordings in the Baltic Sea. Frontiers in Marine Science, Volume4:164

Moldanova, J. et al. (2018) Framework for the environmental impact assessment of operational shipping. In preparation for Ambio

Sofiev, M., J.J. Winebrake, L. Johansson; E.W. Carr, M. Prank, J. Soares, J. Vira, R. Kouznetsov, J.-P. Jalkanen, and J.J. Corbett (2018) Cleaner fuels for ships provide public health benefits with climate tradeoffs. Nature Communications, volume 9:406

Pinus sylvestris L. inter- and intra-annual growth response to climatic conditions

Egidijus Rimkus[1], Rūtilė Pukienė[2], Adomas Vitas[3] and Justas Kažys[1]

[1] Institute of Geosciences, Vilnius University, Vilnius, Lithuania (egidijus.rimkus@gf.vu.lt)
[2] Institute of Geology and Geography, Nature Research Centre, Vilnius, Lithuania
[3] Environmental Research Centre, Vytautas Magnus University, Kaunas, Lithuania

1. Introduction

The *Pinus sylvestris L.* is widely distributed in boreal and temperate climatic zones and, therefore, predominantly serves as an object to investigate various environmental effects and influences of climatic conditions on different ecosystems (Bogino et al. 2009, Seo et al. 2011).

T. Bitvinkas started dendrochronological investigations in 1961, in Lithuania. The 38-year sequence (1976-2013) of *Scots* pine tree diameter measurements using band dendrometers in Aukštaitija National Park study site make this series unique of its kind.

The main objective of this paper is to assess the impact of temperature and precipitation to inter- and intra-annual *Pinus sylvestis L.* growth fluctuations.

2. Description of study site

The study site is located in the North-East part of Lithuania in the Aukštaitija National Park (Figure 1). The landscape consists of moraines formed by the last glacier. About 70% of the area are covered by forests with dominating pine stands that make 80 % of the forested land. In 1976, a permanent study site with an area of 0.98 ha was established (Vitas, 2011). Geographical coordinates of the site are 55°26' N 26°02'E with elevation around 160 m a.s.l. The soil is podzolic, parent material is sand with gravel and pebble intrusions. Ground water is deeper than 5 m.

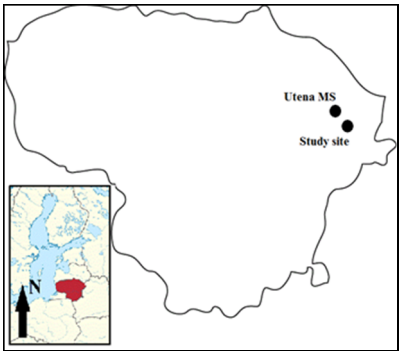

Figure 1. Location of study area and nearby meteorological station.

3. Data and methods

Dendrometrical measurements of tree diameter in Aukštaitija National Park area have been carried out in 1976-2017. Data set includes the warm periods of 36 years (measurements were not carried out in 1987 and 1992). The average start date of measurements is 30 April and the end date – 5 September. Measurements were carried out on a regular basis every three days. We analyzed changes of tree diameter data from 1 May to 31 August.

For measurement of tree seasonal growth manual band dendrometers were installed on 24 pine trees in 1976: 19 mature pine trees and 5 young pine trees (Vitas, 2011). Initial analysis of data quality revealed the 8 cases (<1%), when the individual tree growth dynamics in some years very strongly stood out from others. Such cases were excluded from further analysis. Several cases of failure of dendrometer were also recorded. In such cases the gaps in the data sets were not filled in and the average values of tree growth during warm season were calculated from the trees without gaps in data series.

We used median value calculated from all measured trees as main parameter of annual tree growth in our study because in most cases data distribution is asymmetric. Annual tree growth was calculated by summing up median values of each three-day period. The daily values of tree diameter growth were calculated after interpolation between known measured values.

The Mann-Kendal test was used for evaluation of statistical significance of tree diameter growth tendencies. The changes were considered as statistically significant when the p-value was lower than 0,05.

Meteorological data from the closest to study area Utena meteorological station was used (Figure 1). We analyzed daily and monthly mean, maximum and minimum air temperature as well as daily and monthly precipitation sums. The relationships between tree diameter growth and weather conditions in study area were established.

4. Results

On average, in the study area the tree diameter increased by 0.75 mm annually. This value varies from 0.17 mm in 1979 to 1.16 in 2011 (Fig. 2). The analysis shows a statistically significant ($\alpha<0.05$) positive tree growth trend in May-August during the period from 1976 to 2013. Statistically significant positive changes were recorded in May, June and August. The changes in July are also positive, but statistically insignificant. This corresponds well with the air temperature trends in Utena MS. The air temperature rise was determined during the whole year in Utena. But the most significant changes were recorded in April and July. Temperature increase in April led to earlier start of tree growth while significant temperature rise in July prolonged the period of intensive growth of trees. Increasing precipitation amount on August also favored tree growing conditions.

The largest tree diameter growth was determined in June (35 % of annual increase). Meanwhile in August this value falls to 15 %. Analysis of daily values showed the strongest growth during the period from 14 May to 24 June (maximum - 15 June) (Fig. 3). It was found that during the

period from 14 May until 24 June 58 % of the total annual tree diameter increase was recorded on an average. Keeping in mind the day length influence on a plant photosynthetic activity, we can suggest that strong growth period up to 24 June produces early wood with thin cell walls and wide lumina, while denser late wood start to be formed after summer solstice. However, due to a large variability of the intra-seasonal tree growth dynamics it is very difficult to estimate the precise position of such regime change on an annual scale.

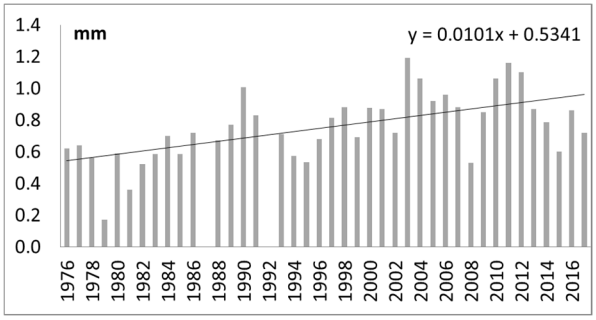

Figure 2. Median of tree diameter growth (mm) in May - August in study area.

We also analyzed the thirty-day periods when the growth of the trees was the most intense. During these thirty-day periods the tree diameter increased between 32% (in 1991) up to 65% (1979 and 1999). The middle dates of these periods mostly fall on 6-10 June. The earliest intense growth (3 May - 2 June) was recorded in 1984, when warmer than normal April and May were followed by abnormally cold summer. The latest period of the most intense growth was recorded in 2005 (16 July – 15 August). This year was marked by a relatively cold spring (especially March) and extremely rainy May. Cool June was followed by a warmer than normal July, and this led to an intensification of tree diameter growth which was further accelerated with the heavy rainfalls in early August.

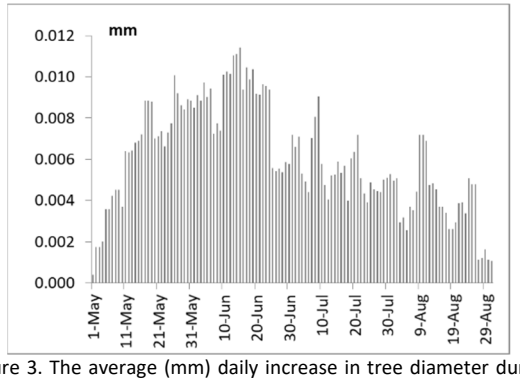

Figure 3. The average (mm) daily increase in tree diameter during the period from May to August in 1976-2013.

Weak statistically significant relationship (r = 0.35) links the tree growth in May with maximal air temperature of the same month. Meanwhile, correlation between precipitation amount and tree ring growth is statistically insignificant. At the beginning of warm season precipitation amount is less important for tree growth because the ground is usually saturated with water after snow melt and despite the lack of precipitation weather conditions can be favorable for vegetation if the air temperature is higher than the average. A close correlation between the air temperature in April and the tree growth in May was determined. The warmer first part of spring (which is largely predetermined by the temperature of April) leads to earlier start of tree growth. Therefore, for May growth rate the temperature of April has greater impact than the temperature of May. It was found that the last frost date also statistically significantly correlates with tree growth rate in May (r=-0.40).

According to our investigation results, the main factor which determines June-August tree growth fluctuations is precipitation amount. Since the amount of heat during these months is usually sufficient, a limiting factor becomes moisture availability for the wood formation. Another explanation of the precipitation impact on tree diameter changes is associated with tree swelling. In rainy periods trees swell and after that they shrink during following dry period. During the investigation period 7 cases were recorded (all in July and August) when the monthly changes in the median diameter of the trees was equal to 0 or even negative. During all of them a strong negative rainfall anomalies were observed.

We analyzed the short term changes of tree growth according to the measurements carried out every three days. The cases with median tree diameter increase of 0.1 mm or more within three days period were investigated. Total number of such cases was equal to 48. It was determined that such rapid growth is exclusively associated with heavy precipitation events. Precipitation amount during the five-day period prior to the measurement varied from 2 to 113 mm. Average value (35,1 mm) significantly exceeded the mean five-days precipitation sum in May-August (12 mm). Smaller than 12 mm precipitation amount was observed only five times and in all such cases it was recorded after a prolonged period without rain or with a very small amount of it. Thus, the rapid growth events can be explained by the recovery which follows the tree shrinkage in dry period.

We also investigated the cases when the decrease in tree diameters was observed during three-day periods. Total number of such cases was equal to 111. In 81 cases there weren't any precipitation during three days period prior to the measurements and in 101 cases precipitation amount was smaller than 3 mm.

5. Conclusions

The analysis shows a statistically significant positive tree growth trend in May-August. For tree diameter growth in May the thermal conditions of the entire spring season gain the largest impact, while in summer the precipitation amount is of decisive importance. During a warm spring tree vegetation starts earlier. Lack of precipitation in summer months can lead to soil moisture deficit and tree growth rate can decrease or even shrinkage of trees can start.

References

Vitas, A. 2011. Seasonal growth variations of pine, spruce, and birch recorded by band dendrometers in NE Lithuania, Baltic Forestry, 17(2), 197-204.

Bogino, S., Fernández Nieto, M. J. amd Bravo, F. (2009). Climate effect on radial growth of Pinus sylvestris at its southern and western distribution limits, Silva Fennica, 43(4), 609–623.

Seo, J-W., Eckstein, D., Jalkanen, R., Schmitt, U. (2011). Climatic control on intra- and inter-annual wood-formation dynamics of Scots pine in northern Finland. Environmental and Experimental Botany, 72, 422-431.

Long term impacts of societal and climatic changes on nutrient loading to the Baltic Sea

Marianne Zandersen[1], Sampo Pihlainen[2], Kari Hyytiäinen[2], Hans Estrup Andersen[1], Mohamed Jabloun[6], Erik Smedberg[3], Bo Gustafsson[3], Alena Bartosova[4], Hans Thodsen[1], H.E. Markus Meier[5,4], Sofia Saraiva[4,7], Jørgen E. Olesen[1], Dennis Swaney[3], Michelle McCrackin[3]

[1] Aarhus University, Denmark (mz@envs.au.dk)
[2] University of Helsinki, Finland
[3] Stockholm University, Sweden
[4] Swedish Meteorological and Hydrological Institute, Sweden
[5] Leibniz-Institute for Baltic Sea Research Warnemünde (IOW), Germany
[6] University of Nottingham, UK
[7] University of Lisbon, Portugal

1. A vulnerable ecosystem

The Baltic Sea is a vulnerable ecosystem that is greatly influenced by human activities and the climatic system due to a combination of natural conditions and multiple, interacting anthropogenic pressures. Excessive nutrient loading is one of the main pressures altering the state of the Baltic Sea. Policy-makers and stakeholders around the riparian countries can benefit from a systematic exploration of how alternative global developments in climate and socio-economic factors are likely to affect the amount of nutrient loading to the Baltic Sea in the long term. Such load projections can be used for estimating the additional nutrient abatement efforts needed to reach the goals of marine protection, such as under HELCOM BSAP.

2. Nutrient Scenarios

We develop long-term quantitative scenarios of nutrient loading under different combinations of RCPs and SSPs over the period 2010-2100. The SSPs include the pathways *Sustainability* (SSP1), *Middle of the Road* (SSP2), *Fragmentation* (SSP3), and *Fossil-fuelled development* (SSP5); RCPs cover *intermediate scenario* (RCP4.5) and *very high GHG emissions* (RCP8.5). The analysis accounts for all major sources of nitrogen and phosphorus from non-point source loading (i.e. agricultural load, loads from forest and background loading), point source loading (i.e. load from wastewater treatment plants) and the atmospheric deposition. The impacts of inventory uncertainty and structural uncertainty are addressed for scenarios.

Quantitative assumptions of drivers of nutrient emissions are developed based on an extension of the SSP narratives to the Baltic Sea and applied in a spatially explicit model framework combining agricultural management and land use, wastewater treatment levels and scale, and atmospheric deposition based on sectoral developments. Climate impacts are integrated via the HYPE riverine flow model, altering nutrient loads from land compared to no climate change.

3. Results

Results show that nutrient loads overall are on a declining trend for SSP1, SSP2, SSP3 but increase for SSP5 with respect to both nitrogen and phosphorus loads. With sustainable development and moderate climate change (SSP1/RCP4.5), N loads could be halved and P loads decrease to around 60% of the current level by the end of the century. In a fossil-fuelled world (SSP5) and extreme climate change (RCP8.5) the nutrient loads would increase by around 25% from the current level, necessitating substantial policy efforts in nutrient abatement.

Non-point sources are the biggest contributor to the external nutrient loading of the Baltic Sea. Furthermore, their share of the total load will increase over time for all climate and socioeconomic scenarios considered. Point source loading of both N and P will decrease, but for different reasons for different SSPs. Main determinants include technological development and urbanization (SSP1 and SSP2), investments in treatment technology, (SSP1, SSP2 and SSP5), and decreasing population (SSP3).

Topic G

Regional Climate System Modelling

Evaluation of the ERA-20C data using surface observations in the Hardanger Glacier, Norway

Bhuwan C. Bhatt[1] and Asgeir Sorteberg[1]

[1] Geophysical Institute (University of Bergen) and Bjerknes Center for Climate Research, Bergen, Norway (Bhuwan.Bhatt@gfi.uib.no)

1. Introduction

The Hardanger Glacier is one of the meteorological data-sparse regions in Norway. Few of the available observation stations are placed in valley bottoms, which lack information on the glacier meteorology and climate. The erroneous observations are often reported due to the under-catchment of snow in wintertime. A high-resolution reanalysis data can be proven useful, enabling a number of climatic processes to be studied. Reanalysis data cover a long duration. Here we provide an evaluation of ERA-20C against observations and thus we correct ERA-20C data.

The surface variables from the reanalysis are surface air temperature, wind speed, humidity, rainfall, snowfall. The purpose of correcting reanalysis over the glacier is to feed them to 1D snow model or to WRF-snow coupled modeling system to be implemented in near future.

2. Method

The station data from the Finse station, which is nearby the Hardanger Glacier are available from 1969 to 2016 on a 6-hourly basis. We use Finse station observation to correct ERA-20C data. We use distribution mapping method (Sorteberg et. al. 2014) to correct datasets. This method potentially correct all moments of the statistical distribution. We combined Normal and General Pareto distribution for surface air temperature data. The Gamma and Gumbel distributions were considered for the rainfall and wind, respectively.

3. Results

Here we present results from the air temperature only (Fig. 1). This shows a comparison between the raw data (blue color crosses) and the corrected data (green color crosses), in the form of Q-Q plot. One can note that there is good improvement in the ERA20C temperature.

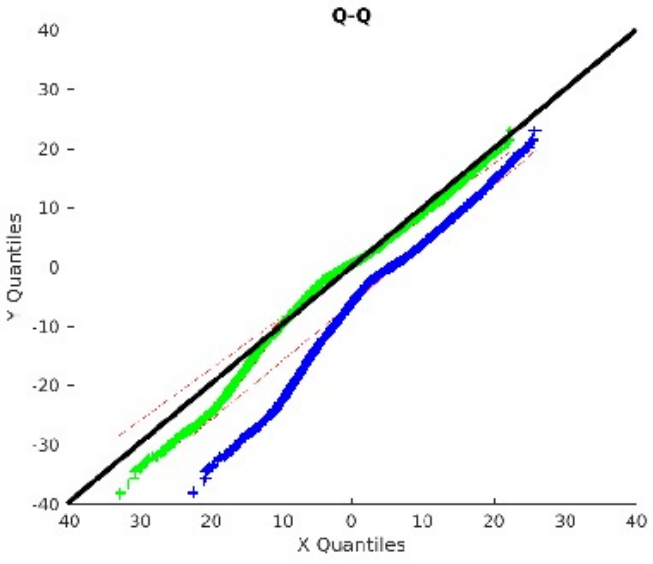

Figure 1. Q-Q plot for the surface air temperature.

Figure 2 shows the trends in both datasets, station observation from the Finse station and corrected ERA-20C data show a similar trend.

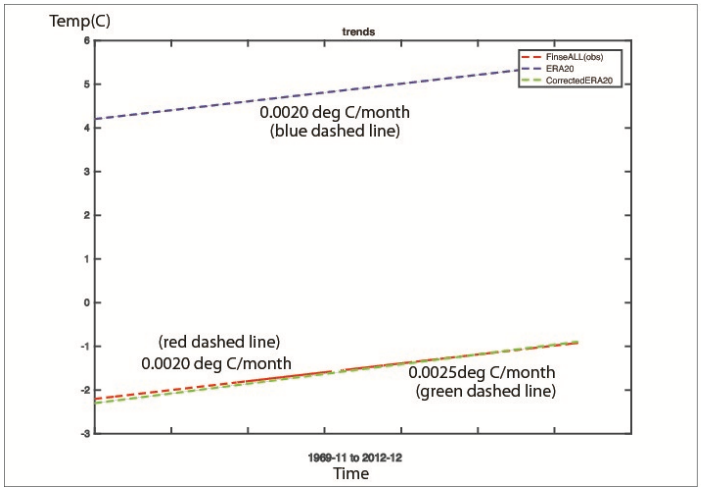

Figure 2. Trends in raw and corrected surface air temperature datasets. Refer to the legend box in the graph.

4. Summary

Bias correction is important, distribution mapping allows all the information in both observation and reanalysis to be taken into consideration. The bias correction improved the Reanalysis towards the observation. We aim to use these data in WRF snow coupled modeling.

Acknowledgements

This research work was carried out under the Evoglac project supported by the research council of Norway.

References

Sorteberg. A. et al (2014) Evaluation of distribution mapping based bias correction methods, NCCS report, No. 1, folk.uib.no/gbsag/Publications/Sorteberg_NCCS_2014.pdf

Evaluation of a regional climate system model for the Baltic Sea region

Sandra-Esther Brunnabend[1], Manja Placke[1], Claudia Frauen[1], Florian Börgel[1], Martin Schmidt[1], Thomas Neumann[1], and H. E. Markus Meier[1]

[1] Leibniz Institute for Baltic Sea Research Warnemuende, Rostock, Germany (Sandra.Brunnabend@io-warnemuende.de)

1. Introduction

The semi-enclosed Baltic Sea is located in Northern Europe and accommodates a complex marine ecosystem. To investigate impacts of past and future climate change on this marine ecosystem, regional climate system models are needed as variations in local air-sea interactions are not resolved in the coarse resolution global climate models and are neglected in uncoupled ocean and atmosphere models. In addition, only sparse long-term observations exist and provide only limited information about long-term changes in the ecosystem of the Baltic Sea.

For these reasons, a regional climate system model is under development to study the Baltic Sea and the impacts of past and future climate variations on its ecosystem. In this study, we present the concept of a first version of the IOW Regional Climate System Model (IOW-RCSM) which includes an online coupling between atmosphere and ocean over the Baltic Sea region. Here, we focus on the model evaluation. Especially the fluxes between atmosphere and ocean are analyzed and compared with observations and reanalyses data sets.

2. Coupled Model System

The IOW-RCSM will include different component models regarding atmosphere, ocean, sea-ice, hydrology, and the ecosystem in the Baltic Sea region.

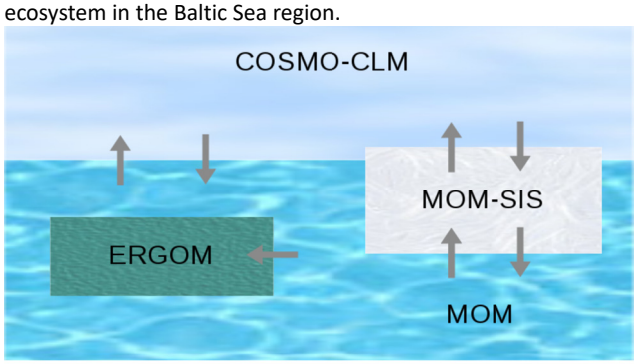

Figure 1. Schematic diagram of the current version of the IOW-RCSM for the Baltic Sea region.

The first version of the IOW-RCSM (Figure 1) couples the COSMO-CLM atmosphere model (Rockel et al., 2008, EURO-CORDEX domain) to the Modular Ocean Model (MOM-5, Griffies, 2012) over the Baltic Sea. The model COSMO-CLM has a horizontal grid resolution of 25 km and the model MOM 8nm (about 14.8 km). The hourly online exchange of the fluxes between the atmospheric and ocean components of the coupled model is performed using the OASIS3-MCT coupler (Valcke et al., 2015).

The current coupled model system includes no hydrology model. Instead, data from the HELCOM assessments (www.helcom.fi) is used as prescribed river runoff to the Baltic Sea. At the open ocean boundary in the Kattegat (in the ocean component), the same boundary conditions (sea surface height from a statistical model; climatological temperature and salinity data sets) as in Neumann et al., (2017) are applied. The ERA-Interim reanalysis data (Dee et al., 2011) are used as boundary conditions for the atmosphere and ocean model.

3. Coupling

The used OASIS3-MCT library provides routines for the exchange of data between the atmosphere and ocean components and routines for the interpolation of data from one model grid to the other. The model components run with their own executable, while the coupler organizes the single MPI (Message Passing Interface) environment. Within the COSMO-CLM model, an interface to the coupler is available (Will et al., 2017) that has been adapted for the coupling to MOM-5. The coupling interface within MOM-5 has been implemented.

The MOM-5 model already contains the thermodynamic/dynamic sea-ice model SIS (Winton, 2000; Hunke and Dukowicz, 1997), which is used in this version of the coupled model system. Additionally, MOM-5 provides a coupling to the biogeochemical model ERGOM (Neumann, 2009; Neumann et al., 2017), which reasonably simulates the biogeochemical processes in the Baltic Sea, including the phosphorus and nitrogen cycle, three phytoplankton groups and a dynamically developing zooplankton variable. In addition, the oxygen development and the biogeochemical processes are coupled (Neumann et al., 2017).

The two-way coupling process (Figure 2) has a coupling time step of one hour and sends sea surface temperature and sea-ice area fraction from the ocean to the atmospheric component. The heat and freshwater fluxes, as well as wind velocities and sea level pressure, are calculated by the atmospheric component and are sent to the ocean component. The initialization of the coupling fields are provided by atmosphere- and ocean-only simulations.

4. Model Evaluation

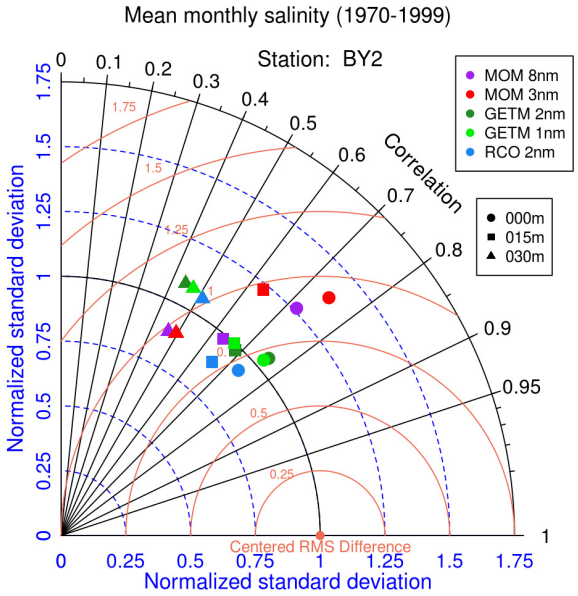

Figure 3. Comparison of monthly mean salinity over 30 years, simulated with the uncoupled model MOM-5 and with other ocean-only models and observations in the Arkona basin. The Taylor Diagram shows the correlation, RMS difference, and the normalized standard deviation. Observations are provided by the BED – Baltic Environmental Database at Baltic Nest Institute, Stockholm, http://nest.su.se/bed . (Placke et al., 2018, in prep.)

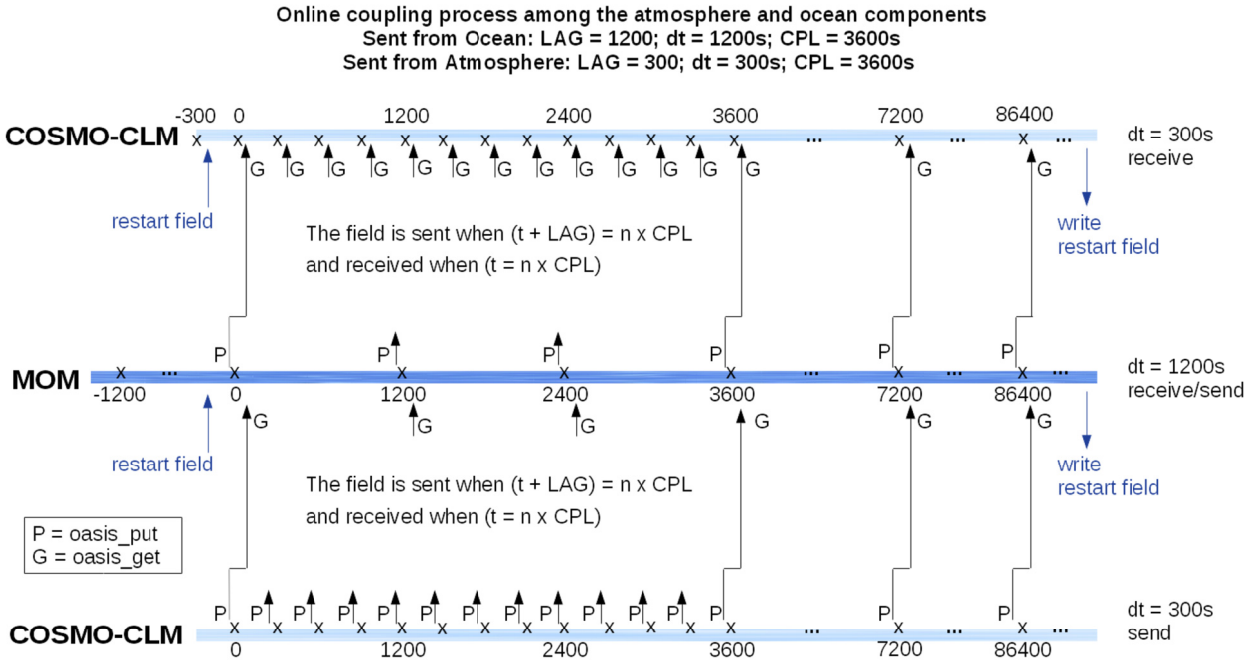

Figure 2: Schematic diagram of the coupling process between the atmosphere and ocean model component

We aim to perform a simulation using the coupled model for the ERA-Interim period from 1979 up to present in order to analyze its general performance and stability. The load balancing of the coupled components is optimized using the lucia tool, which is made available with the OASIS3-MCT coupler. The interpolation error of the exchanged fields are evaluated.

The model results will be compared with corresponding uncoupled simulations and observations (Figure 3). The added-value of the coupled model system as well as the capability of the coupled model system to realistically simulate the air-sea fluxes will be assessed by comparing model results of an uncoupled and coupled simulation to observations.

References

Dee, D. P., Uppala, S. M., Simmons, A. J., Berrisford, P., Poli, P., Kobayashi, S., Andrae, U., Balmaseda, M. A., Balsamo, G., Bauer, P., Bechtold, P., Beljaars, A. C. M., van de Berg, L., Bidlot, J., Bormann, N., Delsol, C., Dragani, R., Fuentes, M., Geer, A. J., Haimberger, L., Healy, S. B., Hersbach, H., Hólm, E. V., Isaksen, L., Kållberg, P., Köhler, M., Matricardi, M., McNally, A. P., Monge-Sanz, B. M., Morcrette, J.-J., Park, B.-K., Peubey, C., de Rosnay, P., Tavolato, C., Thépaut, J.-N. and Vitart, F. (2011), The ERA-Interim reanalysis: configuration and performance of the data assimilation system. Q.J.R. Meteorol. Soc., 137: 553–597. doi: 10.1002/qj.828.

Griffies, S.M. ,(2012), Elements of the Modular Ocean Model (MOM). GFDL Ocean, Group Technical Resport No. 7, NOAA/Geophysical Fluid Dynamics Laboratory, 618pp..

Hunke, E. C. and Dukowicz, J. K. (1997), An elastic-viscous-plastic model for sea ice dynamics, Journal of Physical Oceanography, 27(9): 1849–1867, doi: 10.1175/1520-0485(1997)027<1849:AEVPMF>2.0.CO;2.

Hunke, E. C., Lipscomb, W. H., Turner, A. K., and Jeffery, N., Elliott, S. M. (2013), CICE: the Los Alamos Sea Ice Model, Documentation and Software, Version 5.0. Los Alamos National Laboratory Tech. Rep. LA-CC-06-012.

Neumann, T. (2009), Climate-change effects on the Baltic Sea ecosystem: A model study, Journal of Marine Systems, 81, 213-224, doi: 10.1016/j.jmarsys.2009.12.001.

Neumann, T., Radtke, H., and Seifert, T., (2017), On the importance of Major Baltic Inflows for oxygenation of the central Baltic Sea, Journal of Geophysical Research: Oceans, 122, doi: 10.1002/2016JC012525.

Placke, M., Meier, H.E.M. , Gräwe, U., Neumann, T., and, Liu, Y. (2018), Long-term mean circulation of the Baltic Sea as represented by various ocean circulation models, (in prep.)
Rockel, B., Will, A., Hense, A. eds., (2008), Special issue Regional climate modelling with COSMO-CLM (CCLM), Met. Z., Vol. 17, ISSN 0941-2948.

Valcke, S., Craig, T., Coquart, L. , (2015), OASIS3-MCT User Guide, OASIS3-MCT 3.0, Technical Report, TR/CMGC/ 15/38, CERFACS/CNRS SUC URA No 1875, Toulouse, France.

Will, A., Akhtar, N., Brauch, J., Breil, M., Davin, E., Ho-Hagemann, H. T. M., Maisonnave, E., Thürkow, M., and Weiher, S., (2017), The COSMO-CLM 4.8 regional climate model coupled to regional ocean, land surface and global earth system models using OASIS3-MCT: description and performance. Geoscientific Model Development, 10:1549–1586, doi:10.5194/gmd-10-1549-2017.

Winton, M., (2000), A reformulated three-layer sea ice model, Journal of Atmospheric and Ocean Technology, 17, 525-531, doi: 10.1175/1520-0426(2000)017<0525:ARTLSI>2.0.CO;2.

Acknowledgments

The model development, simulations and validation were performed with resources provided by the North-German Supercomputing Alliance (HLRN). COSMO-CLM is the community model of the German regional climate research jointly further developed by the CLM-Community.

Do we know more about climate change than during PRUDENCE?

Ole Bøssing Christensen[1], M. A. D. Larsen[2], M. Drews[2], M. Stendel[1] and J. H. Christensen[3]

[1] Research and Development, Danish Meteorological Institute, Denmark (obc@dmi.dk)
[2] Management Engineering, Danish Technical University, Denmark
[3] Niels Bohr Institute, University of Copenhagen, Denmark

1. Introduction

For a couple of decades, a string of projects have focused on creating coordinated RCM simulations over Europe. Here we will be looking at simulations according to several emission scenarios from FP5 PRUDENCE (2001-2004; SRES A2 and B2), FP6 ENSEMBLES (2004-2009; SRES A1B) and two resolutions (50km and 12km; RCP4.5 and RCP8.5) from WCRP CORDEX, specifically Euro-CORDEX (since 2012). Simulations have increased their standard resolution from 50km (PRUDENCE) to about 12km (Euro-CORDEX) and from time slice simulations (PRUDENCE) to transient experiments (ENSEMBLES and CORDEX); from one driving model and emission scenario (PRUDENCE) to several (Euro-CORDEX).

How has the overall picture of state-of-the-art regional climate change projections changed over this period? By scaling with global temperature change we can compare the projected signals of European climate change focusing on temperature and precipitation. Both robust common results and changes through the project generations will be pointed out.

2. Results

In Figure 1 simulated annual temperature change per degree of global warming is depicted for the various projects and compared to a corresponding observed value from the CRU TS dataset for the period 1901-2016.

In Figure 2 the general tendency is for the intra-ensemble spread to decrease with the project sequence, however, new aspects of spread can turn up, which did not exist in earlier projects.

Several aspects of average climate change do become more robust with the more modern models, larger ensembles, and higher resolution of the most recent projects. However, this tendency is partly cancelled by the fact that PRUDENCE basically only used two different driving GCMS.

An analysis of intra-ensemble standard deviation and of pattern-based Empirical Orthogonal Functions (EOFs) shows clear characteristics of the individual projects. Some examples are:

-PRUDENCE summer precipitation change over the Baltic area is unrealistic for several models, which is also seen in the model spread. The reason for this has been identified as an unrealistic construction of sea surface temperature for one driving model.

ENSEMBLES summer temperature change has a very large spread, probably connected to soil parameterization

-For CORDEX, large model differences turn up for precipitation, especially during summer, in areas with land-sea contrast like the Adriatic Croatian coast and the European North Sea coast.

The presentation will go into more detail with these and other features; EOF analysis results will also be presented.

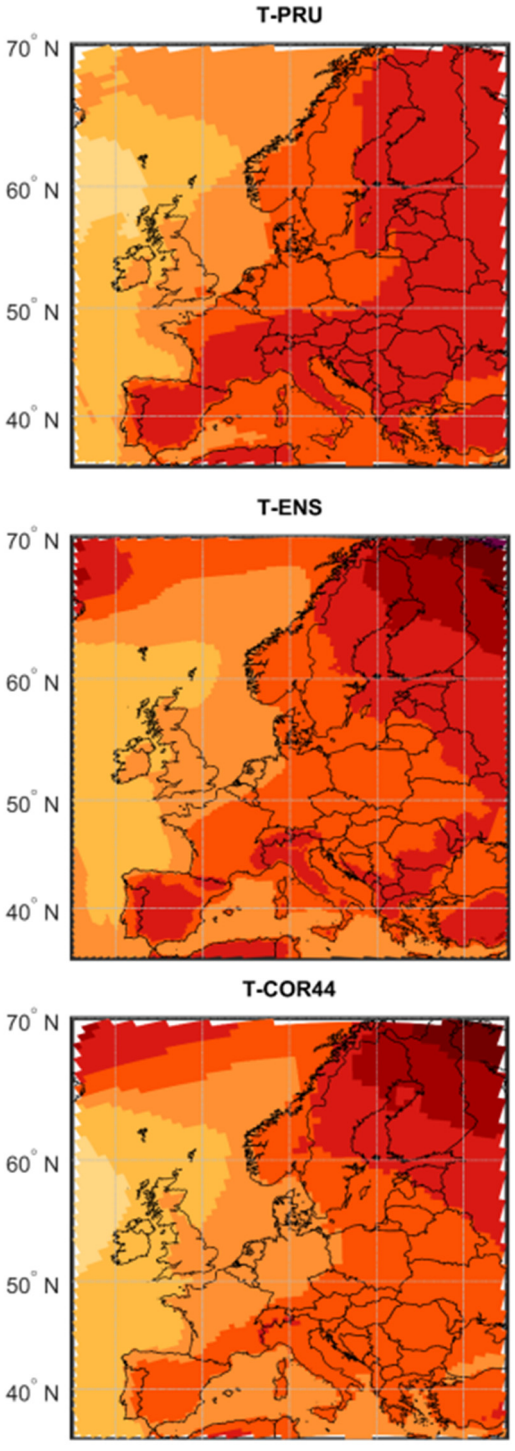

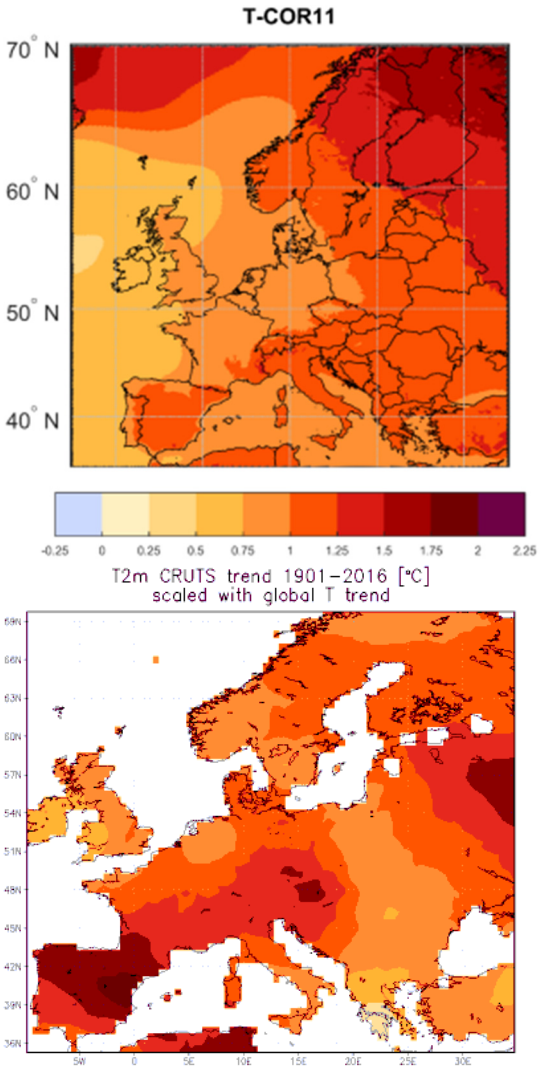

Figure 1 Ensemble average temperature change for Europe per degree of global warming. Annual averages for PRUDENCE, ENSEMBLES, CORDEX 44km and CORDEX 11km simulations; observed temperature change per degree global warming from observations 1901-2016.

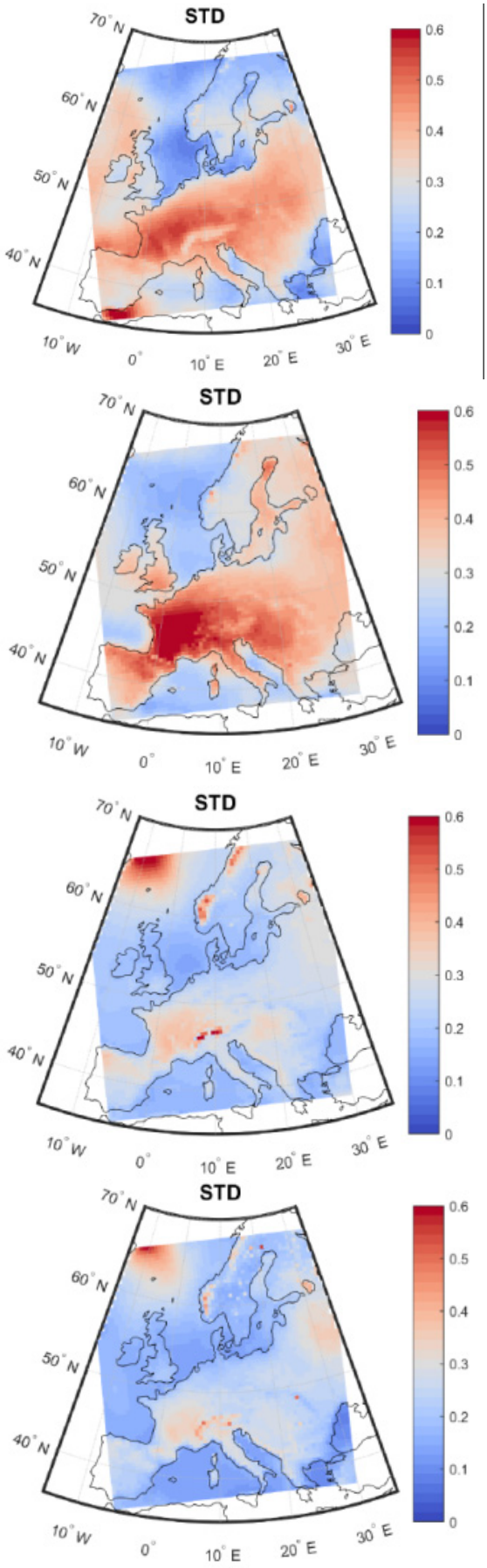

Figure 2 Ensemble standard deviation of temperature change for PRUDENCE, ENSEMBLES, CORDEX 44km and CORDEX 11km simulations during summer (JJA) in degrees per degree of global warming.

Projected Changes in Baltic Sea Upwelling in Climate Change Scenarios

Christian Dieterich [1], Matthias Gröger [1], Semjon Schimanke [1], Lars Arneborg [1] and H. E. Markus Meier [2,1]

[1] Swedish Meteorological and Hydrological Institute, Norrköping, Sweden (christian.dieterich@smhi.se)

[2] Leibniz Institute for Baltic Sea Research, Warnemünde, Germany

1. Introduction

Climate change scenarios with global circulation models (GCMs) do not represent regional processes adequately enough to permit an analysis of regional effects of possible changes in the Baltic Sea region. Dynamical downscaling with regional climate models (RCMs) allow for a consistent projection of climate change in the Baltic Sea region and for a closer look at regional phenomena like coastal upwelling. Upwelling in the Baltic Sea has been identified to play a potential role for the algae bloom forecast, fisheries, weather prediction and tourism (Lehmann and Myrberg, 2008). Sea surface temperature in the Baltic Sea is expected to increase between 1 and 4 degrees depending on the Representative Concentration Pathways (RCPs) and on the season. An analysis of Lehmann et al. (2012) has shown that the upwelling frequency in the upwelling regions along the southeastern Swedish coast has increased by up to 30% within the period 1990 to 2009. We aim to verify whether upwelling will occur more frequently under projected changes of the regional climate during this century.

2. Methods

To this end we ran an ensemble of scenarios with the SMHI coupled atmosphere-ice-ocean model RCA4-NEMO (Wang et al., 2013). The ensemble consists of three different RCP scenarios from five different GCMs. This yields a number of different trajectories for the possible evolution of the climate in the Baltic Sea region. The GCMs that are applied on the open boundaries of the atmosphere and the ice-ocean model together with the RCPs are listed in Table 1.

Experiment	RCP8.5	RCP4.5	RCP2.6
MPI-ESM-LR	1961 - 2099	1961 - 2099	1961 - 2099
EC-EARTH	1961 - 2099	1961 - 2099	1961 - 2099
GFDL-ESM2M	1961 - 2099	1961 - 2099	1961 - 2099
HadGEM2-ES	1961 - 2099	1961 - 2099	1961 - 2099
IPSL-CM5A-MR	1961 - 2099	1961 - 2099	

Table 1. Ensemble of RCP scenario experiments conducted with RCA4-NEMO.

RCA4-NEMO consists of the RCA4 atmosphere model in a model domain covering the Northeast Atlantic and Europe and the NEMO-Nordic setup for the North Sea and Baltic Sea (Dieterich et al., 2013). RCA4-NEMO is a fully coupled atmosphere-ice-ocean model, where the different components are coupled every 3 hours using the Oasis3 coupler. The coupler does exchange the surface temperatures of open water and sea ice together with the ice fraction and ice albedo to the atmosphere model. From the atmosphere the ice-ocean model receives the momentum fluxes and pressure at the surface, the shortwave and non-solar heat fluxes and the freshwater fluxes due to the evaporation - precipitation. For the experiments discussed here the river discharge was prescribed using results from an E-HYPE simulation driven by a downscaled ERA-interim reanalysis (Donnelly et al., 2016). To approximate the expected increase in river discharge in the Bothnian Sea and the Bothnian Bay an artificial trend of 10% per century has been added for the years 2008 - 2099 to the climatological seasonal cycle derived from the E-HYPE simulation.

3. Results

The modeled changes in sea surface temperature are not uniformly distributed in the Baltic Sea. The summer SST in the middle and at the end of the century changes most pronounced in those areas that have been identified as typical upwelling areas by Bychkova et al. (1988).

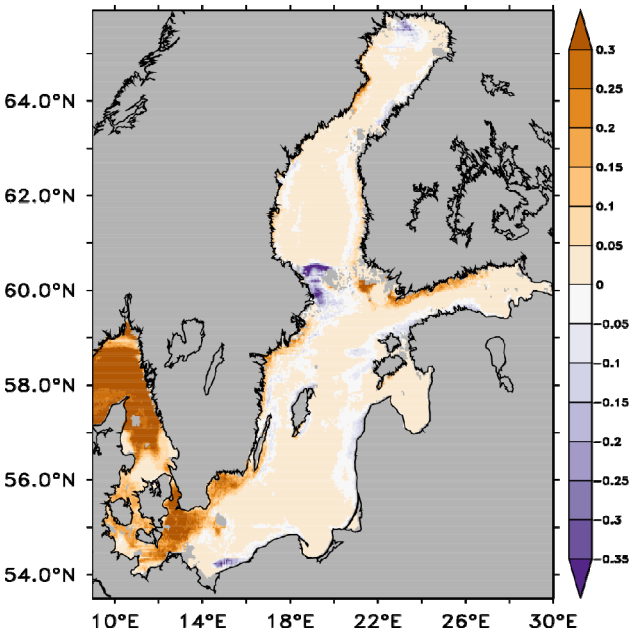

Figure 1. Changes in upwelling frequency [1] between the far future (2070 to 2099) and the recent past (1970 to 1999) for the RCP8.5 ensemble median. Values of 0.2 and above are significant and represent a change of 20%.

There is a tendency for the upwelling areas along the Swedish south and east coasts and the Finish south coast to produce more frequent upwelling (Figure 1). In the middle of the century the SST has increased by 1 degree on average. In the upwelling areas that are favored by strong westerlies the SST has actually decreased compared to the reference period. On the eastern side of the Baltic Sea and on the Estonian coast of the Gulf of Finland SST increased more rapidly than on average and those upwelling areas seem to have been weakened. The same principal picture emerges towards the end of the century although the SST signals of the upwelling areas are masked somewhat on the backdrop of the overall increase in SST of 2 degrees.

References

A. Lehmann, K. Myrberg (2008) Upwelling in the Baltic Sea - A review, J.~Mar. Systems, 74, Supplement, pp. S3-S12

A. Lehmann, K. Myrberg, K. Höflich (2012) A statistical approach to coastal upwelling in the Baltic Sea based on the analysis of satellite data for 1990-2009, Oceanologia, 54, 3, pp. 369-393

S. Wang, C. Dieterich, R. Döscher, A. Höglund, R. Hordoir, H.E.M. Meier, P. Samuelsson, S. Schimanke (2015) Development and evaluation of a new regional coupled atmosphere-ocean model in the North Sea and Baltic Sea, Tellus A, 67, 24284

C. Dieterich, S. Schimanke, S. Wang, G. Väli, Y. Liu, R. Hordoir, L. Axell, A. Höglund, H.E.M. Meier (2013) Evaluation of the SMHI coupled atmosphere-ice-ocean model RCA4_NEMO, SMHI-Report, RO 47, pp. 76

C. Donnelly, J. C. M. Andersson, B. Arheimer (2016) Using flow signatures and catchment similarities to evaluate the E-HYPE multi-basin model across Europe, Hydrological Sciences Journal, 61, 2, pp. 255-273.

I. Bychkova, S. Viktorov, D. Shumakher (1988) A relationship between the large-scale atmospheric circulation and the origin of coastal upwelling in the Baltic, Meteorologiya i Gidrologiya, 10, pp. 91-98.

Assessment of Different Wind Products as Forcing for Baltic Sea Ocean Models

Claudia Frauen[1], Ulf Gräwe[1] and H. E. Markus Meier[1]

[1] Leibniz Institute for Baltic Sea Research Warnemünde, Rostock, Germany (claudia.frauen@io-warnemuende.de)

1. Introduction

The Baltic Sea is a semi-enclosed sea in Northern Europe with a complex marine ecosystem. Due to its relative shallowness the mean circulation of the Baltic Sea is strongly influenced by the atmospheric conditions. Also its salinity and oxygen concentration strongly depend on the atmospheric conditions since the occurrence of Major Baltic Inflows (MBIs), which are responsible for transporting saline and oxygen-rich waters from the North Sea into the central Baltic Sea and therefore play an important role for the Baltic Sea ecosystem, are strongly driven by the local wind.

In order for ocean models to realistically simulate the state of the Baltic Sea high quality atmospheric forcing datasets are needed. Since there are no long-term observational datasets with high spatial and temporal resolution, we rely on reanalyses. However, even the resolution of most state-of-the-art reanalysis datasets, like for example ERA-Interim (Dee et al., 2011), is still too coarse to drive high-resolution regional ocean models. Therefore, regional climate models are used to perform a downscaling of the global reanalyses. The aim of this study is to compare different wind products and to assess their quality for the use as forcing for Baltic Sea ocean models.

2. Wind Products

For this study three different wind products have been used. The first dataset is a RCA downscaling (Samuelsson et al., 2011) of the ERA40 global reanalysis (Uppala et al., 2005). Since it is known that RCA underestimates the wind strength, the data has been corrected using the gustiness of the wind (Höglund et al., 2009, Meier et al., 2011). The other two datasets are coastDat2 (Geyer, 2014) and coastDat3 (Geyer, 2017, personal communication), both regional downscalings of the global reanalysis products NCEP/NCAR reanalysis 1 (Kalnay et al., 1996) (coastDat2) and ERA-Interim (coastDat3) with spectral nudging to enforce the observed large-scale circulation.

Even though huge efforts have been made to provide reliable high resolution atmospheric forcing datasets, there remain still large uncertainties especially regarding the quality of the wind fields. Substantial differences exist between the different datasets. To estimate their realism, they were compared to wind measurements from 28 automatic stations along the Swedish coast for the period 1996-2008 (Höglund et al., 2009). The observations are available as hourly 10-minutes averages while coastDat2 and coastDat3 have an hourly resolution and RCA3-ERA40 only 3-hourly. For comparison daily averages for all datasets have been computed. To compare the station-based observations to the gridded reanalysis datasets, the nearest grid point away from land has been manually selected for each station.

3. Assessment

Looking at the mean statistics over all stations one can see clear differences between the different datasets. With regard to the mean wind speed coastDat2 and coastDat3 are very close to observations while RCA-ERA40 clearly underestimates it (Table 1). In the zonal direction all reanalyis datasets show mean westerly winds close to observations. In the meridional direction they all show mean southerly winds, although weaker than observed (not shown).

	Obs.	cD2	cD3	RCA3-ERA40
mean	5.806	5.943	6.042	5.183
std	2.676	2.886	2.868	2.673
mean diff.	-	0.137	0.237	-0.622
RMSD	-	1.861	1.649	2.258

Table 1. Mean statistics of the total wind speed over all stations for the period 1996-2008 for the observations, coastDat2, coastDat3, and RCA3-ERA40. Unit [m/s].

With slight deviations this also holds true for the individual stations. Exemplary the mean annual cycles of the wind speed at two of the stations are presented in Figure 1. At Landsort on the central Baltic coast and Måseskär on the coast of the Skagerrak RCA3-ERA40 continuously underestimates the mean wind speed throughout the whole year. CoastDat2 is closer to the observations but also still underestimates the mean wind speed at these stations and coastDat3 is closest to the observations and especially in winter agrees well with them.

4. Impact on ocean model simulations

To study the impact of different atmospheric forcing datasets on Baltic Sea ocean model simulations experiments were performed with the General Estuarine Transport Model (GETM) for the North and Baltic seas (Gräwe et al., 2015). In the first simulation the model was driven by coastDat2. Since it is known that coastDat2 has a cold bias in winter and accordingly a bias in humidity a bias correction has been performed. In coastDat3 these biases have been strongly reduced and thus no bias correction was needed.

Figure 2a shows the time series of monthly mean salinity at 225m depth at the station Gotland deep (BY15) of the two simulations compared to observations from the BED database (Gustafsson and Rodriguez Medina, 2011). It can be seen that the GETM model performs well with both atmospheric forcings and especially the timing of the MBIs is well captured. During the stagnation period in the 1980s and in the recent period the simulation forced by coastDat3 performs better and is very close to the observations while in the 1990s the simulation forced by

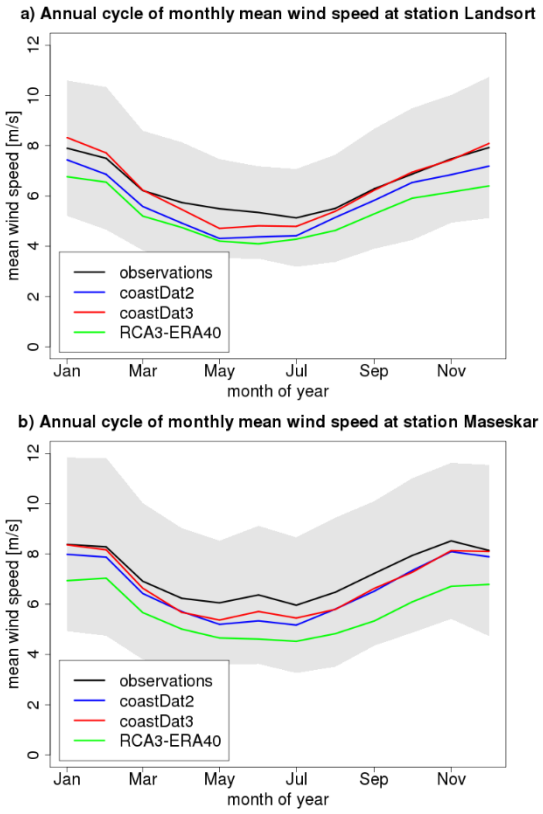

Figure 1. Annual cycle of monthly mean wind sped at the stations a) Landsort at the central Baltic coast and b) Måseskär at the coast of the Skagerrak for the observations (black), coastDat2 (blue), coastDat3 (red), and RCA3-ERA40 (green). The solid lines indicate the monthly mean and the grey shading indicates ±1 observed standard deviation. Unit: [m/s].

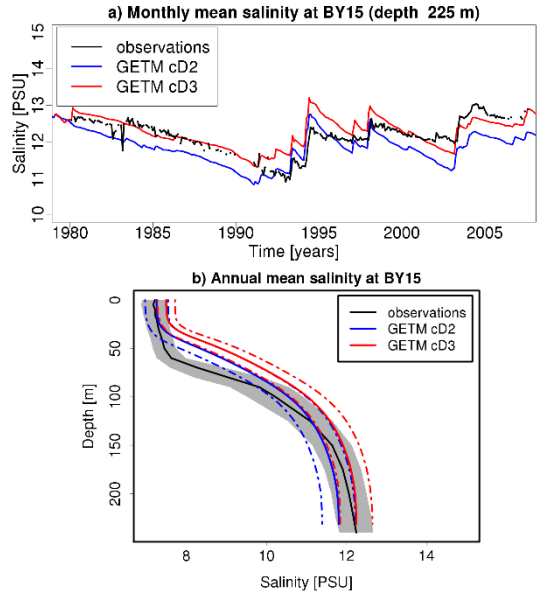

Figure 2. a) Monthly mean salinity at 225m depth at Gotland Deep (BY15) for observations from the BED database (black), the GETM coastDat2 run (blue), and the GETM coastDat3 run (red) and b) mean vertical profiles of salinity from the different datasets at Gotland Deep (BY15) for the period 1980-2007.

coastDat2 performs better. However, looking at the vertical salinity profile at BY15 one can see that the halocline is too shallow in both simulations, especially in the one driven by coastDat3 (Fig. 2b).

5. Conclusion

All three atmospheric forcing datasets compare well with the observations from the Swedish stations, but coastDat2 and coastDat3 are much closer. Even though the wind speed has been corrected in RCA3-ERA40 it is still underestimated. The differences between coastDat2 and coastDat3 are small in terms of the overall wind statistics but vary for different locations.

In experiments with the GETM model it can be seen that the choice of atmospheric forcing has an impact on the simulations. Despite the bias correction in temperature and humidity for coastDat2 and GETM being tuned with the coastDat2 dataset, the GETM simulation forced by coastDat3 also performs comparably well.

The results presented here show that huge improvements have been made in the quality of atmospheric forcing datasets. An assessment like the one presented here can help to select the best atmospheric forcing datasets to drive Baltic Sea ocean models.

References

Dee, D. P., Uppala, S. M., Simmons, A. J., Berrisford, P., Poli, P., Kobayashi, S., Andrae, U., Balmaseda M. A. et al. (2011) The ERA-Interim reanalysis: confguraton and performance of the data assimilaton system, Q.J.R. Meteorol. Soc., 137: 553–597

Geyer, B. (2014) High-resolution atmospheric reconstruction for Europe 1948–2012: coastDat2, Earth Syst. Sci. Data, 6, 147-164

Gräwe, U., P. Holtermann, K. Klingbeil, and H. Burchard (2015) Advantages of vertically adaptive coordinates in numerical models of stratified shelf seas, Ocean Modelling, 92, pp. 56-68

Gustafsson, B.G. and Rodriguez Medina, M. (2011): Validation data set compiled from Baltic Environmental Database, (Version 2, January 2011), Baltic Nest Institute Technical Report No. 2, ISBM: 978-86655-3.

Höglund, A., Meier, M., Broman, B., & Kriezi, E. (2009) Validation and correction of regionalised ERA-40 wind fields over the Baltic Sea using the Rossby Centre Atmosphere model RCA3, Rap. Oceanogr. No. 97, SMHI, Norrkoping (2009), p. 29

Kalnay, E., Kanamitsu, M., Kistler, R., Collins, W., Deaven, D., Gandin, L., Iredell, M. et al. (1996) The NCEP/NCAR 40-year reanalysis project, Bulletin of the American Meteorological Society, 77(3), pp.437-471

Meier, H. M., Höglund, A., Döscher, R., Andersson, H., Löptien, U., & Kjellström, E. (2011) Quality assessment of atmospheric surface fields over the Baltic Sea from an ensemble of regional climate model simulations with respect to ocean dynamics, Oceanologia, 53, 193-227

Samuelsson, P., Jones, C.G., Willén, U., Ullerstig, A., Gollvik, S., Hansson, U.L.F., Jansson, C. et al. (2011) The Rossby Centre Regional Climate model RCA3: model description and performance, Tellus A, 63(1), pp.4-23

Uppala, S. M., KÅllberg, P. W., Simmons, A. J., Andrae, U., Bechtold, V. D. C., Fiorino, M., Gibson, J. K. et al. (2005), The ERA-40 re-analysis, Q.J.R. Meteorol. Soc., 131: 2961–3012

High resolution discharge simulations over Europe and the Baltic Sea catchment

Stefan Hagemann[1], Tobias Stacke[2] and Ha T.M. Ho-Hagemann[1]

[1] Institute of Coastal Research, Helmholtz-Zentrum Geesthacht, Germany (stefan.hagemann@hzg.de)
[2] Max Planck Institute for Meteorology, Hamburg, Germany

1. Introduction

Discharge (or river runoff) is closing the water cycle between atmosphere, land and ocean. Hence, in a coupled atmosphere-ocean model, the discharge is the interface between the land surface hydrology and the ocean, and thus an integral part of the coupled system. For global applications of a discharge model within a fully coupled general circulation model (GCM) or an Earth System Model (ESM), a grid resolution of 0.5° is usually sufficient. The same applies for regional applications where the main objective is an adequate representation of the mean monthly discharge of large rivers. If smaller catchments are of interest or the representation of daily discharge, then higher resolutions are required for appropriate simulation of discharge. Consequently, to prepare high resolution discharge simulations over Europe and the Baltic sea catchment within a regional coupled system model, we further developed a well established discharge model, the HD model, to be globally applicable at 5 Min. resolution. This study shows first results in comparison with available observations over Europe and the Baltic Sea catchment.

2. The HD model

The hydrological discharge (HD) model (Hagemann and Dümenil 1998; Hagemann and Dümenil Gates 2001) is used in this study for the calculation of river runoff. The HD model has already been used for many years in the global Earth System Model (ESM) MPI-ESM (Giorgetta et al. 2013) and its predecessor ECHAM5/MPIOM (Roeckner et al. 2003; Jungclaus et al. 2006), but was also recently implemented into the regional ESMs ROM (Sein et al. 2015) and RegCM-ES (Sitz et al. 2017) as well as the regional climate model REMO-MPIOM (Elizalde 2011). Currently the HD model is being implemented into the regional coupled system model GCOAST of Helmholtz-Zentrum Geesthacht. The HD model was designed to run on a fixed global regular grid of 0.5° horizontal resolution, and it uses a pre-computed river channel network to simulate the horizontal transport of water within model watersheds. Originally, the HD model used a daily time step, but some refinements made during the MPI-ESM development allow sub-daily time steps, e.g. hourly.

Figure 1 shows the structure of the HD model. It separates the lateral water flow into the three flow processes of overland flow, baseflow, and riverflow. Overland flow and baseflow are both represented by a single linear reservoir, and riverflow is represented by a cascade of five equal linear reservoirs. Overland flow represents the fast flow component within a grid box and uses surface runoff as input. Baseflow represents the slow flow component within a grid box and is fed by drainage from the soil (or subsurface runoff) and the inflow from other grid boxes contributes to river flow. The sum of the three flow processes is equal to the total outflow from a grid box. The model parameters are functions of the topography gradient between grid boxes, the slope within a grid box, the grid box length, the lake area, and the wetland fraction of a particular grid box. The model input fields of surface runoff and drainage resulting from the various climate or land surface model resolutions are, therefore, interpolated to the HD grid before being fed into the HD model.

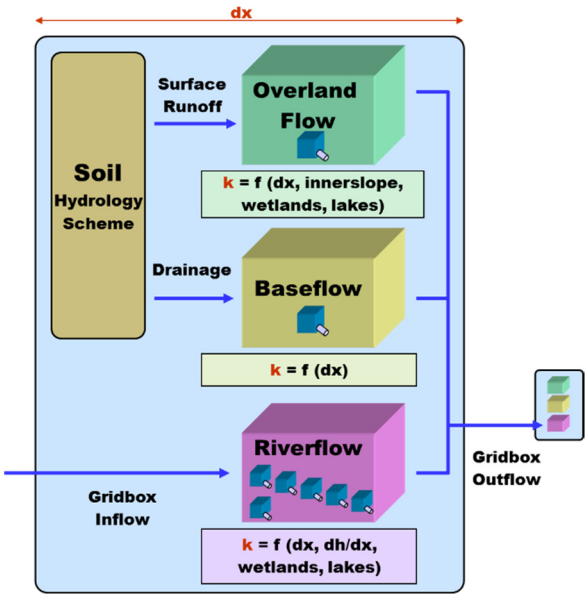

Figure 1. The HD model structure. The figure was designed by S. Kotlarski (pers. comm. 2006).

3. Model improvements

The HD model has been adapted to run on a regular grid of 5-Min. horizontal resolution, which corresponds to an average grid box size of 8-9 km. For the initial development application of the 5-Min. version, a regional domain over Europe was chosen that covers the land areas between -11°W to 69°E and 27°N to 72°N. River directions and digital elevation data were provided by Bernhard Lehner (pers. comm., 2014) and were derived from the Hydrosheds (http://hydrosheds.cr.usgs.gov/index.php) database and from the Hydro1K dataset for areas north of 60°N (https://lta.cr.usgs.gov/HYDRO1K). Lake fractions are taken from the European Space Agency (ESA) Land Cover Climate Change Initiative (LC_CCI) for epoch 2010 (version 2.0.7; available at http://maps.elie.ucl.ac.be/CCI/viewer/) and wetland fractions from the LSP2 dataset (Hagemann 2002). To adapt the HD model parameters used at 0.5° resolution to the higher resolution, global scaling factors were applied to retention coefficients of each of the three flow processes. Thus, during this development step, no river specific parameter adjustments were conducted. In a second step, river flow velocities of the main stream grid boxes were corrected using an automated procedure for

those rivers where sufficient daily observations were available for the most downstream gauge and where a lag was indicated between simulated and observed discharge.

4. First results

In order to generate input fields for the HD model, we forced the land surface scheme JSBACH (vs. 3 + frozen soil physics; Ekici et al. 2014) at 0.5° with WATCH forcing data (Weedon et al. 2011) to generate daily input fields of surface runoff and drainage. Then, these data were spatially interpolated to the European 5-Min. domain using conservative remapping and fed into the HD model. The simulation period of the reference run with no river specific adjustments is 1979-2003. For a second simulation with the adjustments of main stream flow velocities for some rivers, we used a restart file from the reference simulation and run the HD model from 1999-2003. To regard some potential spin-up, the evaluation shown in Figure 2 covers only the years 2000-2003.

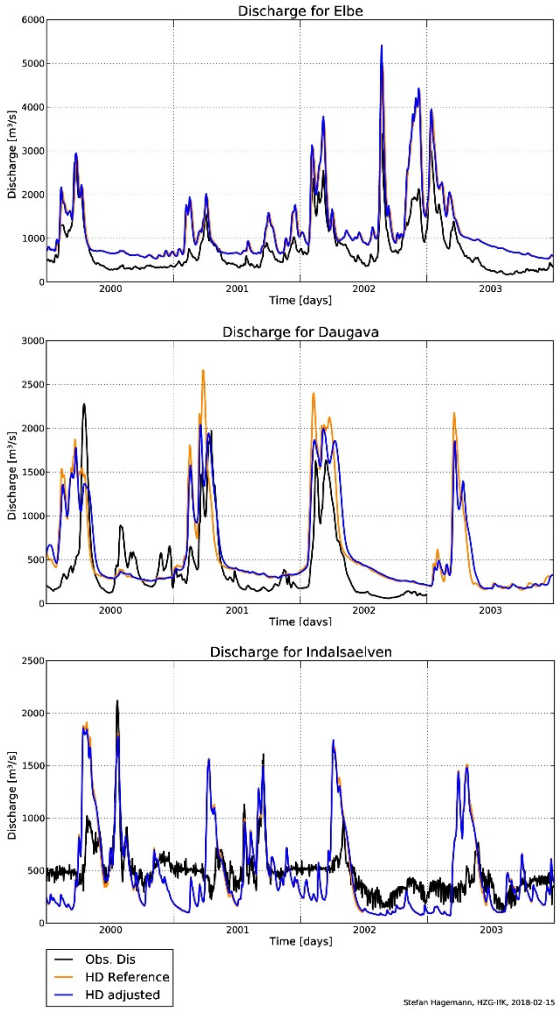

Figure 2. Simulated and observed discharges during 2000-2003 for selected catchments.

For many rivers, the main peaks are more or less captured, such as, e.g., for the Elbe (Fig. 2, upper panel). Thus, the main stream flow velocities were only adjusted for a few rivers. Here, a prominent example is the Daugava (Fig. 2, middle panel). In Scandinavia, especially in Sweden, many rivers are regulated. As this regulation is not regarded in the HD model, its effects can generally not be simulated. A typical example is given for the Indalsaelven (Fig. 2, lower panel). On the one hand, strong snow melt induced discharge peaks in spring are simulated, but only weak indications of such peaks occur in the observed time series. On the other hand, there is only little variation in the observed low flow time periods, while there is variability and generally lower discharge in the simulations. This can be interpreted as extractions of water during the snowmelt season and supply of the stored water during low flow periods. It can be noted that rainfall induced discharge peaks outside the snowmelt season are rather well captured by the HD model.

References

Ekici, A., C. Beer, S. Hagemann, J. Boike, M. Langer and C. Hauck (2014) Simulating high latitude permafrost regions by the JSBACH terrestrial ecosystem model, Geosci. Model Dev., 7, 631-647, doi:10.5194/gmd-7-631-2014.

Elizalde, A. (2011). The water cycle in the Mediterranean Region and the impacts of climate change. Phd-Thesis, University of Hamburg, Hamburg. Berichte zur Erdsystemforschung, 103, doi:10.17617/2.1216556

Giorgetta, M. et al. (2013) Climate and carbon cycle changes demo 1850 to 2100 in MPI-ESM simulations for the Coupled Model Intercomparison Project phase 5, J. Adv. Model. Earth Syst., 5, 572–597

Hagemann S (2002) An improved land surface parameter dataset for global and regional climate models. Max Planck Institute for Met. Rep 336, MPI for Meteorology, Hamburg, Germany.

Hagemann, S. and L. Dümenil (1998) A parametrization of the lateral waterflow for the global scale, Clim. Dyn., 14, 17–31, doi:10.1007/s003820050205

Hagemann, S. and L. Dümenil Gates (2001) Validation of the hydrological cycle ECMWF and NCEP reanalyses using the MPI hydrological discharge model, J. Geophys. Res. D Atmos., 106, 1503–1510, doi:10.1029/2000JD900568

Jungclaus, J. H.,M. Botzet, H. Haak,N.Keenlyside, J.-J. Luo,M. Latif, J. Marotzke, U. Mikolajewicz, and E. Roeckner (2006), Ocean circulation and tropical variability in the coupled model ECHAM5/MPIOM, J Clim., 19, 3952–3972

Roeckner, E., et al. (2003), The atmospheric general circulation model ECHAM5. Part I:Model description, Max Planck Institute for Meteor. Rep. 349, MPI for Meteorology, Hamburg, Germany.

Sein, D.V., U. Mikolajewicz, M. Gröger, I. Fast, W. Cabos, J.G. Pinto. S. Hagemann, T. Semmler, A. Izquierdo and D. Jacob (2015) Regionally coupled atmosphere-ocean-sea ice-marine biogeochemistry model ROM: 1. Description and validation, J. Adv. Model. Earth Syst., 7, 268–304

Sitz, L. E., F. Di Sante, R. Farneti, R. Fuentes-Franco, E. Coppola, L. Mariotti, M. Reale, G. Sannino, M. Barreiro, R. Nogherotto, G. Giuliani, G. Graffino, C. Solidoro, G. Cossarin, and F. Giorgi (2017) Description and evaluation of the Earth System Regional Climate Model (Reg CM-ES), J. Adv. Model. Earth Syst., 9, 1863–1886, doi:10.1002/2017MS000933.

Weedon, G.P., S. Gomes, P. Viterbo, W.J. Shuttleworth,E.O. Blyth H. Österle, J.C. Adam, N. Bellouin, O. Boucher and M. Best (2011) Creation of the WATCH forcing data and its use to assess global and regional reference crop evaporation over land during the twentieth century. J Hydrometeor 12:823–848. doi:10.1175/2011JHM1369.1.

The BALTIC and NORTH SEAS CLIMATOLOGY (BNSC) - a comprehensive, observation-based data product of atmospheric and hydrographic parameters

Iris Hinrichs[1], Annika Jahnke-Bornemann[1], Viktor Gouretski[1], Axel Andersson[2], Birgit Klein[3], Remon Sadikni[1], Nils Schade[3], Detlef Stammer[1] and Birger Tinz[2]

[1] CEN, University of Hamburg, Hamburg, Germany (iris.hinrichs@uni-hamburg.de)
[2] German Meteorological Service [Deutscher Wetterdienst (DWD)], Hamburg, Germany
[3] Federal Maritime and Hydrographic Agency, Hamburg, Germany

1. Overview

The BNSC data product presented here was created in cooperation between the University of Hamburg (UHH), the Federal Maritime and Hydrographic Agency [Bundesamt für Seeschifffahrt und Hydrographie (BSH)] and the German Meteorological Service [Deutscher Wetterdienst (DWD)]. The goal was, on the one hand, to update the KLIWAS climatology for the North Sea (see Sadikni et al. (2013), Bersch et al. (2014), Sadikni et al. (2018)) and, on the other hand, to extend it to the Baltic Sea. Observations from the DWD's Marine Data Centre (GZS) for the atmospheric part and from several different sources (e.g. WOD13, ICES, DOD) for the hydrographic part form the basis. A thorough quality control and reduction of the temporal sampling error as well as spatial and temporal averaging were applied to the observations, yielding time series of gridded fields of atmospheric and hydrographic parameters in the region of the Baltic Sea, the North Sea and the adjacent regions of the North Atlantic.

The BNSC data product can be used to directly study climate variability but also holds the chance to validate climate simulations by regional numerical models, which makes it a valuable reference data sett. The BSNC will be made freely and publicly available via the website of UHH's Integrated Climate Data Center (ICDC, http://icdc.cen.uni-hamburg.de).

2. Atmospheric part

The atmospheric subset of the BNSC consists of time series of monthly mean gridded fields of near surface variables: 2m air temperature, air pressure at sea level and 2m dew point temperature on a horizontal 1°x1° grid. Climatological mean values are provided as well: The main climatology incorporates observations from 1950-2015; additionally, four 30-year climatologies with differing time frame were created and corresponding statistical parameters are provided. Table 1 gives an overview of the available atmospheric variables of the BNSC and their temporal structuring.

The methods used for creation of the BNSC's atmospheric part are described in detail by Sadikni et al. (2018). Exemplarily for all three atmospheric parameters, the climatological monthly mean air pressure is displayed in Figure 1 for February and August (upper row). Additionally, the corresponding statistical parameters "number of observations" and "standard deviation" (lower two rows) are shown. Not shown, but also provided in the data product is the number of neighboring boxes used for creation of temporal mean values.

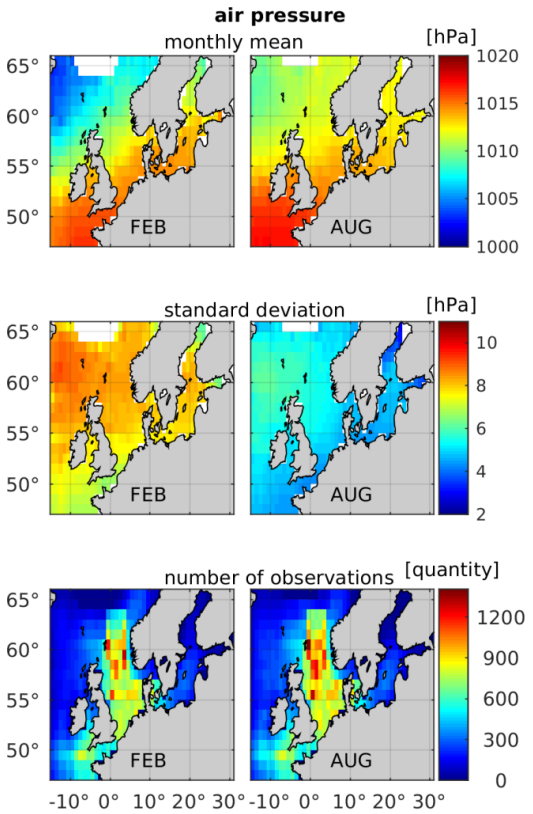

Figure 1. 1950-2015: Monthly mean air pressure at sea level with corresponding statistical variables, exemplarily for 2 of the 12 months and one of the parameters of the atmospheric BSNC data product

variable	temporal structuring
2 m air temperature (°C)	time series 1950-2015, 30-year climatologies, climatology 1950-2015
2 m dew point temperature (°C)	
air pressure at sea level (hPa)	

Table 1. Atmospheric BNSC data product. The statistical parameters provided with each variable are monthly mean, standard deviation, number of observations, number of neighboring boxes

3. Hydrographic part

The hydrographic part of the BNSC comprises the variables water temperature and salinity on 105 depth levels with non-linearly decreasing distances for the time interval 1873-2015. The horizontal resolution differs from the one used in the atmospheric part and is 0.25° in zonal as well as in meridional direction.

Monthly and annual mean fields (example, see Figure 2) are provided as well as decadal monthly mean fields for

six consecutive decades starting in 1956 (example, see Figure 3). Empty grid cells due to a lack of observations characterize those fields. To create homogenous fields, the method of objective analysis was applied to the fields of decadal means (for an example, see

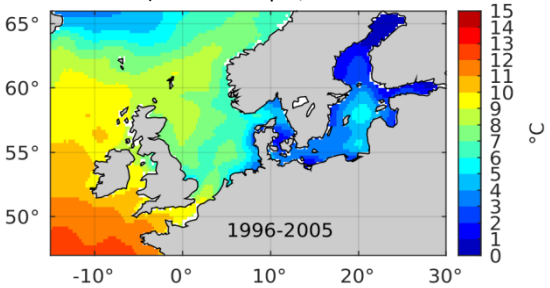

Figure 4). Table 2 gives an overview of variables and temporal/spatial structuring.

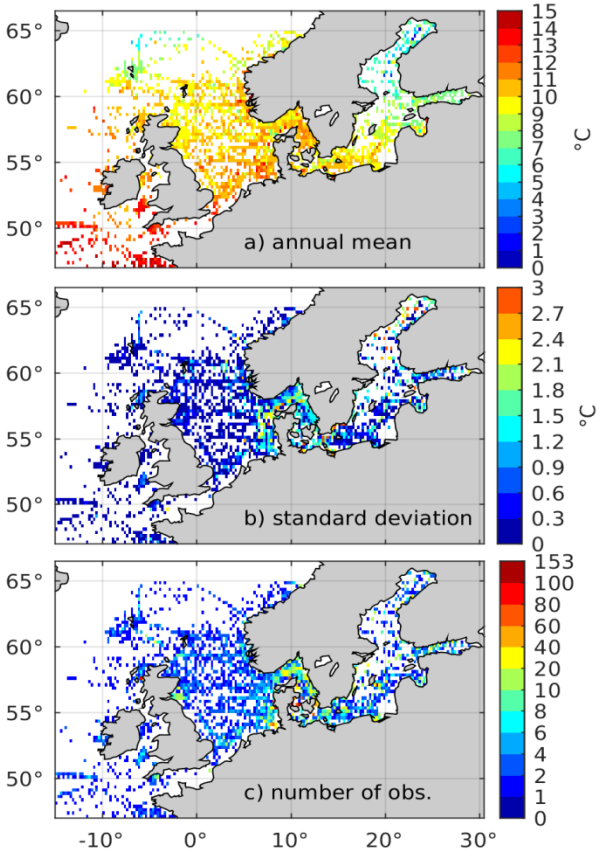

Figure 2. Exemplarily for the annual mean fields of the hydrographic BNSC data product: box average, annual mean surface temperature for year 2000 with corresponding standard deviation and number of observation

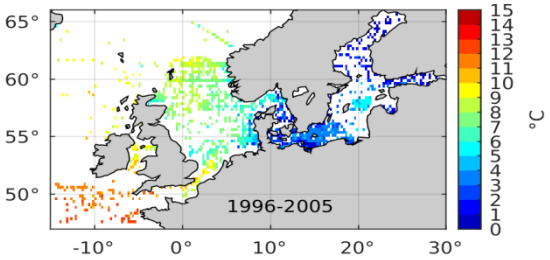

Figure 3. JANUARY, water temperature at surface, decadal mean as box averages for the decade 1996-2005

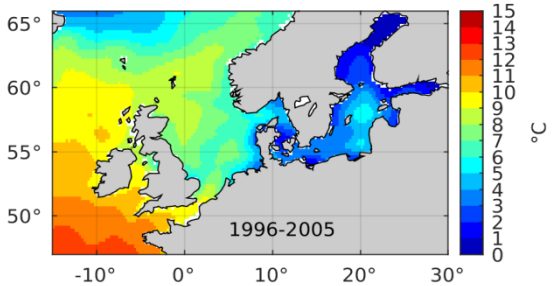

Figure 4. JANUARY, temperature at surface: interpolated decadal monthly mean for the decade 1996-2005

variable	temporal and spatial structuring
water temperature (°C)	box averages 1873-2015, monthly and annual mean
salinity (PSU)	decadal box averages, monthly mean decadal monthly mean, optimally interpolated

Table 2. Hydrographic BNSC data product: Temporal and spatial structuring of variables

4. Comparison with other data products

The BNSC introduced here shows good agreement with several different data products: The ERA-Interim Reanalysis product (Dee et a., 2011) for the atmospheric part; the hydrographic subset was compared to two independent sources of in situ data, the KLIWAS data product (Bersch et al. 2014), the BALTIC ATLAS (Feistel et al. 2005) and the Baltic Sea Physical Reanalysis Product (Axell et al., 2016)

5. Availability of data product

The data product will soon be made freely and publicly available via the website of UHH's Integrated Climate Data Center (ICDC, http://icdc.cen.uni-hamburg.de).

References

Axell, L. and Y. Liu, 2016: Application of 3-D ensemble variational data assimilation to a Baltic Sea reanalysis 1989-2013, Tellus A, 68, 24220, http://dx.doi.org/10.3402/tellusa.v68.24220.

Bersch, M.; Gouretski, V.; Sadikni, R.; Hinrichs, I. (2014). KLIWAS North Sea Climatology of Hydrographic Data (Version 1.1). World Data Center for Climate (WDCC) at DKRZ. http://cera-www.dkrz.de/WDCC/ui/Compact.jsp?acronym=KNSC_hyd_v1.1

Dee, D. P., et al. (2011), The ERA-Interim reanalysis: configuration and performance of the data assimilation system, Quarterly Journal of the Royal Meteorological Society, 137(656), 553-597.

Feistel, R., S. Feistel, G. Nausch, J. Szaron, E. Łysiak-Pastuszak, and G. Ærtebjerg (2008), BALTIC: Monthly Time Series 1900–2005, in State and Evolution of the Baltic Sea, 1952–2005, edited, pp. 311-336, John Wiley & Sons, Inc.

Sadikni, R., N.H. Schade, A. Andersson, A. Jahnke-Bornemann, I. Hinrichs, L. Gates, B. Tinz, and D. Stammer, 2018: The KLIWAS North Sea Climatology. Part I: Processing of the Atmospheric Data. J. Atmos. Oceanic Technol., 35, 111–126, https://doi.org/10.1175/JTECH-D-17-0044.1

Sadikni, R.; Bersch, M.; Jahnke-Bornemann, A.; Hinrichs, I.; (2013): KLIWAS North Sea Climatology of Meteorological Data (Version 1.0); World Data Center for Climate (WDCC). doi:10.1594/WDCC/KNSC_met_v1.0

Implementing surface wave effects into an ocean general circulation model of the Baltic Sea: A semi-empirical type wave model approach.

Katharina Höflich[1] and Andreas Lehmann[1]

[1] GEOMAR Helmholtz Centre for Ocean Research Kiel, Germany (khoeflich@geomar.de)

1. Motivation

Air-sea coupling in ocean general circulation models is usually parametrized in terms of a drag coefficient that only approximates momentum and energy fluxes in terms of a local wind speed (e.g. Babanin et al., 2012). The actual drag, however, cannot be described by a simple coefficient because it is determined by the physics of the boundary layer and the state of the surface wave field, which depends upon wind speed, duration and distance over which the wind has acted (e.g. Young, 1999). Surface waves are the "gearbox" between ocean and atmosphere, improving model performance from increasing consistency in the description of upper ocean dynamics critically depends upon implementation of wave effects into the model physics (Ardhuin et al., 2005).

2. Related Work

Efforts to couple wave-related processes into a regional ocean general circulation model of the Baltic Sea and North Sea have been untertaken by Alari et al. (2016) and Staneva et al. (2017) based on utilizing a spectral wave model. Inclusion of the Stokes-Coriolis term, the sea state dependent momentum flux, and turbulent energy transfer by breaking waves improved the simulation of sea-surface temperature, mixed layer depths, coastal upwelling filaments, as well as storm surges and the vertical current structure during extreme forcing. In Tuomi et al. (2018) consideration of the Stokes drift, the net mass transport associated with the surface wave field, was demonstrated to improve the prediction of a drifter pathway.

3. Goals

This study aims at reaching a more coherent description of upper ocean dynamics by one-way coupling of atmosphere and ocean based on the state of the wind-driven surface wave field. The goal is to achieve an improved simulation of Baltic Sea hydrography and circulation without operation of a computationally intense state-of-the-art spectral wave model. To this end, a semi-empirical type approach is implemented.

4. Methods

The ocean general circulation model at the basis of this study is the Baltic Sea Ice Ocean Model introduced in Lehmann (1995) based on the free-surface Brian-Cox-Semter model (Killworth et al., 1991). The current model setup (e.g. Lehmann et al., 2014) includes a dynamic-thermodynamic sea-ice model (Lehmann and Hinrichsen, 2000) and an advanced k-e turbulence closure model (Lehmann et al., 2002). Surface boundary conditions are provided by ERA-interim reanalysis data (Dee et al., 2011) and 10 m winds are calculated from geostrophic winds according to the local sea level pressure gradient and a directional roughness reduction at the land-ocean interface (Bumke et al., 1998). The sea state is calculated from the semi-empirical growth formulas presented in Schmager et al. (2008, and references therein) which estimate significant waveheight and period from known properties of the meteorological forcing, namely wind speed, direction and duration. Validation of calculated wave heights against in-situ wave buoy measurements is shown in Figure 1, where both the spatial (compare with spectral wave model results by e.g. Tuomi et al., 2011) and temporal agreement (see correlation coefficients) is found to be satisfactorily.

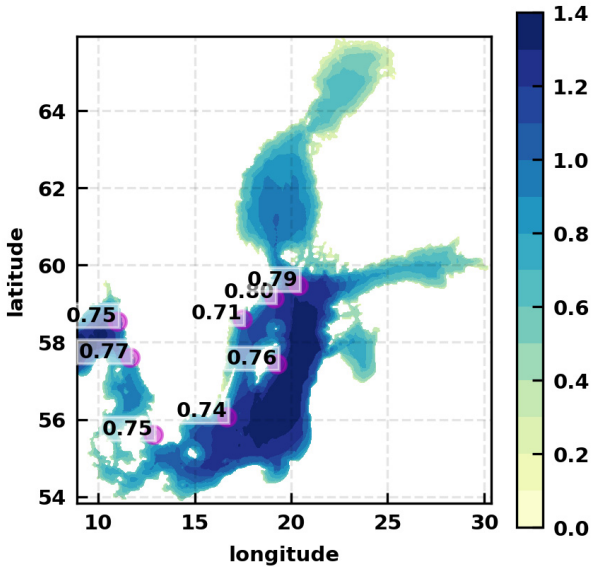

Figure 1. Average significant wave heights in m for the year 1986 calculated from the semi-empirical type wave model presented in Schmager et al. (2008, and references therein). Magenta dots indicate locations of in-situ wave measurements by the Swedish Meteorological and Hydrological Institute. Temporal correlation with estimated 3-hourly wave heights is shown in the boxes.

5. Outlook

Preliminary results regarding the implementation of the Stokes drift and the sea state dependent momentum flux based on the semi-empirical type wave model are presented. General limitations and the applicability of the approach are discussed.

References

Alari, V., Staneva, J., Breivik, O., Bidlot, J., Mogensen, K., Janssen, P. (2016) Surface wave effects on water temperature in the Baltic Sea: simulations with the coupled NEMO-WAM model. Ocean Dynamics, 66

Ardhuin, F., Jenkins, A. D. , Hauser, D., Reniers, A., Chapron, B. (2005), Waves and operational oceanography: Toward a coherent description of the upper ocean, Eos Trans. AGU, 86(4), pp. 37–40

Babanin, A. V., Onorato, M. and Qiao, F. (2012) Surface waves and wave-coupled effects in lower atmosphere and upper ocean, Journal of Geophysical Research, 117, C00J01

Bumke, K., Karger, U., Hasse, L., Niekamp, K. (1998) Evaporation over the Baltic Sea as an example of a semi-enclosed sea. Contributions to Atmospheric Physics, 71(2), pp. 249–261

Killworth, P. D., Webb, D. J., Stainforth, D., Paterson, S. M. (1991) The Development of a Free-Surface Bryan–Cox–Semtner Ocean Model. Journal of Physical Oceanography, 21(9), pp. 1333-1348

Lehmann, A. (1995) A three-dimensional baroclinic eddy-resolving model of the Baltic Sea. Tellus A, 47(5), pp. 1013-1031

Lehmann, A., Hinrichsen, H.-H. (2000) On the thermo-haline variability of the Baltic Sea. Journal of Marine Systems, 25(3–4), pp. 333–357

Lehmann, A., Hinrichsen, H. H. (2002) Water, heat and salt exchange between the deep basins of the Baltic Sea, Boreal Environment Research, 7(4), pp.405-415
Schmager, G., Fröhle, P., Schrader, D., Weisse, R., Müller-Navarra, S. (2008) Sea State, Tides, in State and Evolution of the Baltic Sea, 1952-2005: A Detailed 50-Year Survey of Meteorology and Climate, Physics, Chemistry, Biology, and Marine Environment, John Wiley & Sons, Inc., Hoboken, NJ, USA
Staneva, J., Alari, V., Breivik, Ø., Bidlot, J.-R., Mogensen, K. (2017) Effects of wave-induced forcing on a circulation model of the North Sea. Ocean Dynamics, 67(1), pp. 81–101
Tuomi, L., Kahma, K., Pettersson, H. (2011) Wave hindcast statistics in the seasonally ice-covered Baltic Sea. Boreal Environment Research, 16, pp. 451-472
Tuomi, L., Vähä-Piikkiö, O., Alenius, P., Björkqvist, J. V., Kahma, K. K. (2018) Surface Stokes drift in the Baltic Sea based on modelled wave spectra, Ocean Dynamics, 68(1), pp. 17–33
Young, I. (1999) Wind Generated Ocean Waves, Elsevier Ocean

Different methods to handle seasonal ice cover in wave modeling

Riikka Marjamaa[1], Laura Tuomi[1], Jan-Victor Björkqvist[1], Hedi Kanarik[1], Jouni Vainio[1] and Robinson Hordoir[2]

[1] Finnish Meteorological Institute, Helsinki, Finland (riikka.marjamaa@fmi.fi)

[2] Swedish Meteorological and Hydrological Institute, Norrköping, Sweden

1. Introduction

The Baltic Sea has seasonal ice cover; even in the mildest winters there is ice in the Bothnian Bay and in the eastern Gulf of Finland. The ice cover interacts with the surface waves in several ways. The ice field affects the propagation and the growth of the surface waves. The short waves are fast attenuated by the ice field. Long waves can propagate further into the ice field and alter the distribution of sea ice as well as cause fragmentation. Wave growth is also affected by the ice field. The fetch over which the waves grow changes as the waves start to grow from the edge of the ice field instead of the shoreline. This has a significant effect on the wave climate especially in the small enclosed or semi-enclosed basins (Tuomi 2011).

2. Handling ice in wave model

Wave models can handle ice cover in different ways. A threshold value can be determined for the ice concentration within a wave model grid point after which the point is excluded from calculation. Alternatively the ice concentration in a wave model grid point can be dealt as a grid obstruction which reduces the amount of wave energy propagated between the wave model grid points (Tolman 2003). This method has previously been successfully implemented to attenuate wave energy due to unresolved islands in order to improve the quality of the WAM-model results in the coastal archipelagos of the northern Baltic Sea (Tuomi 2014).

3. Materials and methods

We use the third generation wave model WAM to simulate the Baltic Sea wave fields over four ice seasons in 2008-2012 with 1 NM resolution. We use daily ice charts compiled from satellite observations from FMI's Ice Service and modeled ice cover from SMHI's Nemo-Nordic model. Two different methods to handle ice will be studied: 1) a fixed threshold of 30 % ice concentration and 2) a grid obstruction method up to 70% ice concentration after which wave energy is set to zero.

4. Preliminary results

The four ice winters studied differ in severity. The severity classification is based on the maximum extent of the ice cover from the winters 1960-61 to 2009-10. The winter of 2010-11 has been classified severe, while 2009-10 and 2011-12 were average and 2008-09 was mild. The differences in wave statistics using the different ice handling methods are relatively small. Typically, the monthly mean significant wave height using grid obstruction method is 1 -15cm higher than with the 30% threshold method and the differences are concentrated to areas near the edge of the ice. However, in individual cases the differences may be significant and thus important for operational wave forecasts.

References

Tuomi, L., Kahma, K. K., and Pettersson, H. (2011) Wave hindcast statistics in the seasonally ice-covered Baltic Sea, Boreal Environment Research, 16, 451-472

Tolman, H. L. (2003) Treatment of unresolved islands and ice in wind wave models, Ocean modelling, 5, 219-231

Tuomi, L., Pettersson, H., Fortelius, C., Tikka, K., Björkqvist, J.-V., and Kahma, K. K. (2014) Wave modelling in archipelagos, Coastal Engineering, 83, 205-220

Assessment of ocean circulation models for their applicability in the Baltic Sea

Manja Placke[1], H.E. Markus Meier[1,2], Ulf Gräwe[1], Thomas Neumann[1] and Ye Liu[2]

[1] Department of Physical Oceanography and Instrumentation, Leibniz Institute for Baltic Sea Research, Rostock, Germany (manja.placke@io-warnemuende.de)
[2] Department of Research and Development, Swedish Meteorological and Hydrological Institute, Norrköping, Sweden

1. Introduction

State-of-the-art ocean circulation models are in general developed for different purposes like for instance shallow sea applications or large-scale ocean simulations. However, their scopes of application often go beyond the envisaged usage which makes assessments of models together with observational data inevitable. Also, the application of several different ocean models in the same area raises the question of how good physical conditions and processes are reproduced and if the models are suitable for further investigations in that area.

In the present study, we will analyze the applicability of three ocean circulation models in the Baltic Sea. These models are the General Estuarine Transport Model (GETM; see, e.g., Burchard and Bolding (2002), Gräwe et al. (2015)), the Rossby Centre Ocean model (RCO; see, e.g., Killworth et al. (1991), Meier et al. (2003)) and the Modular Ocean Model (MOM; see, e.g., Pacanowksi and Griffies (2000), Griffies (2004)). We will not perform an intercomparison of these models as for instance their setups, grid resolutions, and atmospheric and hydrological forcing are different.

The assessment contains the investigation of their long-term capability to simulate the evolution, variability, and vertical profiles of temperature and salinity at representative monitoring stations. Furthermore, the mean circulation and volume transports for the entire Baltic Sea as well as current velocities through selected transects are analyzed. The model data is validated with observations from the Baltic Environmental Database (BED) as well as with measurements by Acoustic Doppler Current Profilers (ADCP; see, e.g., Krüger (2000)).

2. Investigated areas and methods

The assessment of temperature and salinity as simulated by the three models is performed at representative monitoring stations in the southern, central, and northern Baltic Sea. Hence, different influences by salt water inflows, insolation, and flow conditions are covered. The model simulations are considered together with observations over the whole depth range at the stations Arkona Basin, Bornholm Deep, Gotland Deep, Gulf of Finland, Bothnian Sea, and Bothnian Bay. Their locations are illustrated in Figure 1.

The mean circulation and volume transports are analyzed for the whole Baltic Sea and current velocities are investigated at different transects from the models. For the validation of currents, ADCP measurements are considered near the stations Arkona Basin and Gotland Deep at particular depths.

Methods for evaluation cover for instance statistical time series analyses at different depths including Taylor diagrams which combine standard deviation, Pearson correlation coefficient, and root mean square difference. Furthermore, cost functions are calculated which consider principally means and standard deviations of simulations and observations.

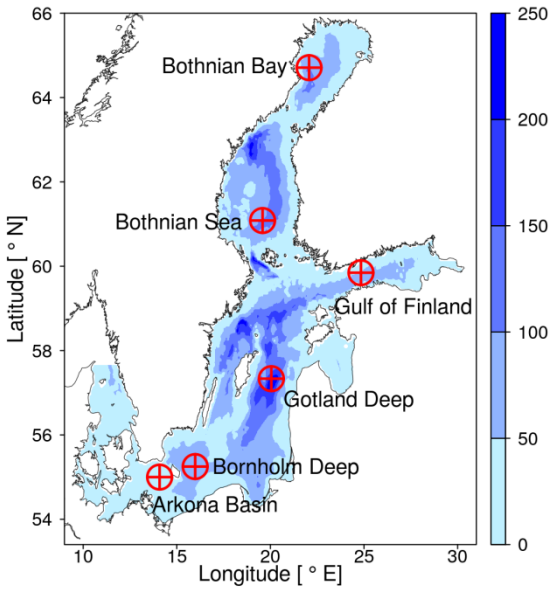

Figure 1. The Baltic Sea bathymetry as simulated by RCO and the locations of six representative monitoring stations for our assessment.

3. Preliminary results

The investigations of temperature, salinity, current velocities and volume transports are predominantly done for a period of 30 years from 1970 through 1999. The temporal evolution, variability as well as vertical profiles of temperature and salinity at six representative monitoring stations are simulated most realistically by the model RCO, especially when it is used in an assimilation / reanalysis setup. The models GETM and MOM simulate partly a thermocline which lies closer to the sea surface than in RCO and in the observations from the BED validation dataset. But overall, the mean vertical temperature profiles of GETM and MOM lie well within the standard deviation of the observations.

Salinity is well reproduced by GETM except for the northern monitoring stations where the simulations deviate stronger from the BED validation dataset. This is also emphasized by lower correlations and worse cost function values. For MOM, the mean salinity near the sea surface is overestimated at the southern stations and underestimated at the northern stations. Hence, statistics for salinity simulations by MOM reveal partly poor results at some depths at a variety of stations.

Furthermore, the mean wind-driven circulation and depth-integrated volume transport is evaluated for the

entire Baltic Sea from the three models. In principle, the surface velocity is strongest in the Kattegat and volume transports maximize in the Gotland Basin. The strongest currents and volume transports are simulated by GETM, the weakest ones by MOM. The deviations between MOM and RCO are smaller than those between GETM and RCO.

The investigation of current velocities and flows through different transects in the Baltic Sea clarifies the structure of the simulated circulations in horizontal and vertical direction. The currents through the transects reveal stronger deviations between results from RCO and GETM than for RCO and MOM. Absolute numbers of volume transports through selected transects are in good accordance for the three models.

As no comprehensive current measurements are available for the entire Baltic Sea, zonal and meridional current velocities are validated at two monitoring stations where ADCPs are deployed. Hence, the quality of the simulated model currents can be estimated at least for these regions. The simulated model means lie predominantly well within the standard deviation of the observations. An exception are the meridional current velocities near Gotland Deep which are underestimated by all models.

References

BED – Baltic Environmental Database at Baltic Nest Institute, Stockholm, http://nest.su.se/bed

Burchard, H., Bolding, K. (2002) GETM – a general estuarine transport model, Scientific documentation, Tech. Rep. EUR 20253 EN, European Commission

Gräwe, U., Holtermann, P., Klingbeil, K., Burchard, H. (2015) Advantages of vertically adaptive coordinates in numerical models of stratified shelf seas, Ocean Modelling, 92, 56–68, doi:10.1016/j.ocemod.2015.05.008

Griffies, S.M. (2004) Fundamentals of Ocean Climate Models, Princeton University Press, Princeton, NJ

Killworth, P.D., Webb, D.J., Stainforth, D., Paterson, S.M. (1991) The development of a free-surface Bryan-Cox-Semtner ocean model, J. Phys. Oceanogr., 21, 1333–1348, doi:10.1175/1520-0485(1991)021<1333:TDOAFS>2.0.CO;2

Krüger, S. (2000) Basic shipboard instrumentation and fixed automatic stations for monitoring in the Baltic Sea, in: El-Hawary, Ferial (Ed.), The Ocean Engineering Handbook, CRC Press LLC, N.W. Corporate Blvd. Boca Raton, FL 33431, U.S.A., p. 52

Meier, H.E.M., Döscher, R., Faxén, T. (2003) A multiprocessor coupled ice-ocean model for the Baltic Sea: Application to salt inflow, J. Geophys. Res., 108(C8), 3273, doi: 10.1029/2000JC000521

Pacanowski, R.C., and Griffies, S.M. (2000) MOM 3.0 manual. Tech. rep., Geophysical Fluid Dynamics Laboratory

Copernicus regional reanalysis for Europe

Semjon Schimanke[1], Per Undén[1], Martin Ridal[1], Ludvig Isaksson[1], Lisette Edvinson[1]

[1] Swedish Meteorological and Hydrological Institute (SMHI), Norrköping, Sweden (Semjon.schimanke@smhi.se)

1. Introduction

We are going to present a Copernicus Climate Change service which might be of interest for many researchers working in Europe. The service aims to produce and deliver a regional reanalysis (RRA) for Europe. The service is implemented in several steps. First, a system developed in the FP7 pre-operational UERRA project (www.uerra.eu) will be used to update the existing RRA in near real time. In combination with the RRA produced already in the pre-operational project, the service will offer a consistent RRA from 1961 to near real time. For instance, when the conferences will be hold in June 2018 data will be available until April 2018. A more detailed description of the C3S service can be found on its homepage: https://climate.copernicus.eu/copernicus-climate-change-service-regional-reanalysis-europe

2. Model system

The UERRA reanalysis system builds on the HARMONIE system cycle 38h1.1. HARMONIE is basically a script framework that allows for different physics packages, surface schemes and data assimilation schemes. The ALADIN synoptic scale physics scheme was used together with a three dimensional variational data assimilation (3D-Var) scheme including only conventional observations and an optimal interpolation (OI) assimilation scheme for the surface observations.

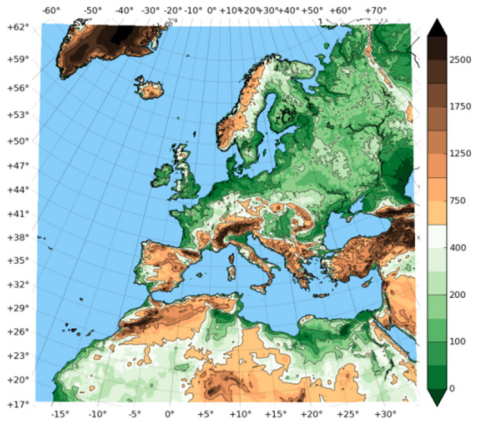

Figure 1. The orography is shown over land whereas ocean points are shown in blue. The entire model domain of the UERRA system is highlighted.

The UERRA system is setup with a horizontal resolution of 11km and covers entire Europe (Fig 1). Herewith, the model domain consists of 565x565 grid points.

3. Available data

As mentioned in the introduction, the service produces operational updates of a RRA for Europe. In February 2018, we had data from Jan 1961 – Nov 2017 and until the onset of the conference we expect to continue the data set until April 2018. Over the entire period, the RRA is available with hourly resolution at 11km.

The list of available parameters is long and comprises all standard parameters as well as relevant essential climate variables, e.g. temperature, wind, precipitation, radiation, pressure, etc. The data is available for 24 pressure levels (1000-10hPa), 11 height levels (15-500m) and close to the surface (0, 2, 10m). In total, the amount of data which is available is 6.5 TB. All this data is freely available through the ECMWF archive MARS.

In our presentation, we will explain what data is available and how it might be used. Here, we will even go through the shortcomings of the data set and explain how to deal with them.

4. Comparison with global ERA products

The aim of the service is to provide a better reanalysis for Europe than it is available from global reanalysis products. Consequently, we will compare our product with ERA-interim (~80km resolution), which is also used at the lateral boundary.

Figure 2 shows a comparison of 2m-temperature for our product and ERA-interim against observations. We see that the bias of our product is smaller than for ERA-interim at most forecasts lengths. Also, the standard deviation is smaller highlighting the superior quality of the regional product compared to the global reanalysis.

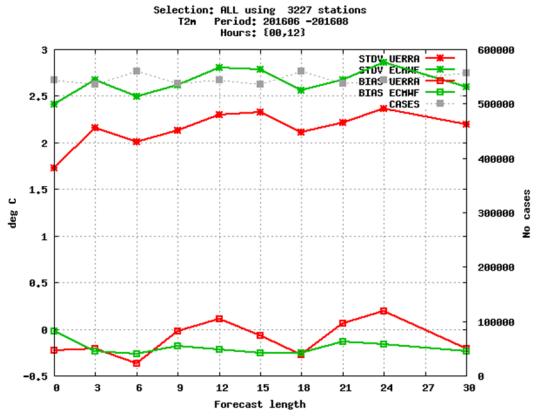

Figure 2. Bias and standard deviation of the UERRA system (red) and ERA-interim (green).

Climate Change in Estonia – warmer weather patterns or more warm weather patterns?

Mait Sepp[1], Piia Post[2] and Merily Lakson[1]

[1] Department of Geography, University of Tartu, Tartu, Estonia (mait.sepp@ut.ee)
[2] Institute of Physics, University of Tartu, Tartu, Estonia

1. Introduction

In comparison to the global average, the climate in the Baltic Sea region, including in Estonia, has been warming particularly fast. During the last half-century, the yearly average temperature in Estonia has risen about 2 °C (BACC Author Team II 2015).

From synoptic climatology's point of view, a question arises. Is this warming caused by changes in the frequency of weather patterns or by the characteristics of weather patterns, i.e. has warmer weather started accompanying those weather patterns (Beck et al. 2007).

2. Data and Methods

In the present study, changes in frequency of weather patterns belonging to twelve classifications, and changes in air temperature accompanying these types during the period of 1966-2015 were analysed. The daily temperature anomalies of three Estonian weather stations (Jõhvi, Türi, Vilsandi) were used for the analysis. According to Huth et al. (2015) classifications used here have the best correlations with the air temperature in Baltic Sea region. The software package cost733class (Philipp et al. 2014) and the air pressure data from NCEP/NCAR reanalysis (Kalnay et al. 1996) was used for calculating classifications.

Classifications with nine types were used in the analysis. Weather types of different classifications were compared to each other on the basis of the similar movement direction of air masses. The types were divided into 'warm' and 'cold' for a given season according to temperature anomalies. Changes in time series were analysed using linear trends ($p<0.05$).

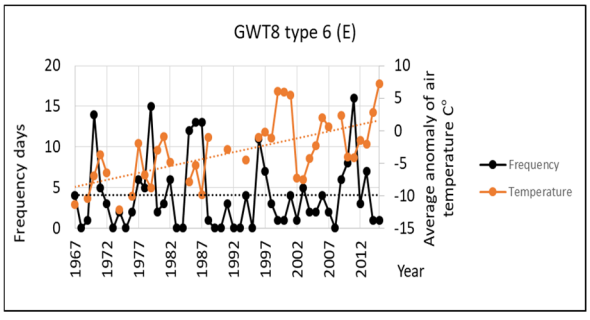

Figure 1. Changes in frequency and in winter (period of 1966-2016) air temperature anomalies accompanying classification GWT8 type 6. This weather pattern representing an air flow from the east.

3. Results

Trend analysis show that there are only a few statistically significant changes in the frequency of circulation types. The major changes have taken place in spring – the frequency of E and NE flow types has decreased and the frequency related to NW types has increased. However, there is increasing trend in practically all temperatures accompanying circulation types. A particularly great warming has taken place in winter 'cold' types. For example, air temperatures accompanying E types in winter have risen approximately 5 degrees (Figure 1).

References

BACC Author Team II (2015) Second Assessment of Climate Change for the Baltic Sea Basin. Springer Open Access.

Beck C, Jacobeit J, Jones PD. (2007) Frequency and within-type variations of large scale circulation types and their effects on low-frequency climate variability in Central Europe since 1780. Int. J. Clim., Vol. 27, pp 473-491

Huth, R., Beck C. and M. Kučerová (2015) Synoptic-climatological evaluation of the classifications of atmospheric circulation patterns over Europe Int. J. Climatol., DOI: 10.1002/joc.4546

Kalnay, E., Kanamitsu, M., Kistler, R., Collins, W., Deaven, D., Gandin, L., Iredell, M., Saha, S., White, G., Woollen, J., Zhu, Y., Leetmaa, A., Reynolds, R., Chelliah, M., Ebisuzaki, W., Higgins, W., Janowiak, J., Mo, K. C., Ropelewski, C., Wang, J., Jenne, R., and Joseph, D. (1996): The NCEP/NCAR 40-Year Reanalysis Project, B. Am. Meteorol. Soc., 77, pp. 437–472

Philipp, A., Beck, C., Huth, R., Jacobeit, J. (2014) Development and comparison of circulation type classifications using the COST 733 dataset and software, Int. J. of Clim. Vol. 36, pp. 2673–2691

Author Index

International Baltic Earth Secretariat Publications

ISSN 2198-4247

No. 1 Programme, Abstracts, Participants. Baltic Earth Workshop on ”Natural hazards and extreme events in the Baltic Sea region”. Finnish Meteorological Institute, Dynamicum, Helsinki, 30-31 January 2014. International Baltic Earth Secretariat Publication No. 1, 33 pp, January 2014.

No. 2 Conference Proceedings of the 2nd International Conference on Climate Change - The environmental and socio-economic response in the Southern Baltic region. Szczecin, Poland, 12-15 May 2014. International Baltic Earth Secretariat Publication No. 2, 110 pp, May 2014.

No. 3 Workshop Proceedings of the 3rd International Lund Regional-Scale Climate Modelling Workshop ”21st Century Challenges in Regional Climate Modelling”. Lund, Sweden, 16-19 June 2014. International Baltic Earth Secretariat Publication No. 3, 391 pp, June 2014.

No. 4 Programme, Abstracts, Participants. Baltic Earth - Gulf of Finland Year 2014 Modelling Workshop ”Modelling as a tool to ensure sustainable development of the Gulf of Finland-Baltic Sea ecosystem”. Finnish Environment Institute SYKE, Helsinki, 24-25 November 2014. International Baltic Earth Secretariat Publication No. 4, 27 pp, November 2014.

No. 5 Programme, Abstracts, Participants. A Doctoral Students Conference Challenges for Earth system science in the Baltic Sea region: From measurements to models. University of Tartu and Vilsandi Island, Estonia, 10 - 14 August 2015. International Baltic Earth Secretariat Publication No. 5, 66 pp, August 2015.

No. 6 Programme, Abstracts, Participants. International advanced PhD course on Impact of climate change on the marine environment with special focus on the role of changing extremes. Askö Laboratory, Trosa, Sweden, 24 - 30 August 2015 International Baltic Earth Secretariat Publication No. 6, 61 pp, August 2015.

No. 7 Programme, Abstracts, Participants. HyMex-Baltic Earth Workshop ”Joint regional climate system modelling for the European sea regions”, ENEA, Rome, Italy, 5- 6 November 2015. International advanced PhD course on Impact of climate change on the marine International Baltic Earth Secretariat Publication No. 7, 103 pp, October 2015.

No. 8 Programme, Abstracts, Participants. A PhD seminar in connection with the Gulf of Finland Scientific Forum: "Exchange process between the Gulf of Finland and other Baltic Sea basins". Tallinn, Estonia, 19 November 2015. International Baltic Earth Secretariat Publication No. 8, 27 pp, November 2015

No. 9 Conference Proceedings. 1st Baltic Earth Conference. Multiple drivers for Earth system changes in the Baltic Sea region. Nida, Curonian Spit, Lithuania, 13 - 17 June 2016. International Baltic Earth Secretariat Publication No. 9, 222 pp, June 2016

No. 10 Programme, Abstracts, Participants. Baltic Earth Workshop on ”Coupled atmosphere-ocean modeling for the Baltic Sea and North Sea”, Leibniz Institute for Baltic Sea Research Warnemünde, Germany, 7- 8 February 2017. International Baltic Earth Secretariat Publication No. 10, 24 pp, February 2017

No. 11 Baltic Earth Science Plan 2017. International Baltic Earth Secretariat Publication No. 11, 28 pp, February 2017

No. 12 Programme, Abstracts, Participants. MedCORDEX-Baltic Earth-COST Workshop ”Regional Climate System Modelling for the European Sea Regions”. Universitat de les Illes Baleares, Palma de Mallorca, Spain, 14 - 16 March 2018, International Baltic Earth Secretariat Publication No. 12, 96 pp, March 2018.

No. 13 Conference Proceedings. 2nd Baltic Earth Conference. The Baltic Sea in Transition. Helsingør, Denmark, 11 - 15 June 2018. International Baltic Earth Secretariat Publication No. 13, 216 pp, June 2018

For a list of International BALTEX Secretariat Publications (ISSN 1681-6471), see www.baltex-research.eu/publications

International Baltic Earth Secretariat Publications
ISSN 2198-4247